TESTING THE BOUNDARIES OF NOVEL FRIEDEL-CRAFTS-TYPE METHODOLOGIES INSPIRED BY *N*-HETEROAROMATIC MEDICINAL TARGETS

A Dissertation
Presented to
The Academic Faculty

by

Evelyn Shaye Ligon

In Partial Fulfillment
of the Requirements for the Degree
Doctor of Philosophy in the
School of Chemistry & Biochemistry

Georgia Institute of Technology
May 2019

TESTING THE BOUNDARIES OF NOVEL FRIEDEL-CRAFTS-TYPE METHODOLOGIES INSPIRED BY *N*-HETEROAROMATIC MEDICINAL TARGETS

Approved by:

Dr. Stefan France, Advisor
School of Chemistry & Biochemistry
Georgia Institute of Technology

Dr. Joseph Sadighi
School of Chemistry & Biochemistry
Georgia Institute of Technology

Dr. M.G. Finn
School of Chemistry & Biochemistry
Georgia Institute of Technology

Dr. Simon Blakey
Department of Chemistry
Emory University

Dr. David Collard
School of Chemistry & Biochemistry
Georgia Institute of Technology

Date Approved: March 19, 2019

This thesis is dedicated to my maternal grandparents. From a young age, they encouraged my love of science and prayed tirelessly over me as I pursued my education. Shortly after I began graduate school, they went to be with God, and their absence is keenly felt as I reach this significant milestone in my life.

To Elmer and Barbara Rumminger, in loving memory

ACKNOWLEDGEMENTS

There are so many people without whose support, encouragement, and tough love I would not have embarked on this journey at Georgia Tech and carried on to complete my PhD. First, to Dr. Chris Waidner, my undergraduate advisor at Wofford College. He was the true catalyst to my professional development when he challenged me to rise above the bare minimum and prove myself as a chemist. That was only the beginning of the advice and guidance he offered me throughout my undergraduate career, including his attempts to convince me to pursue an MD/PhD. (He ultimately approved my decision to pursue "just" my PhD.) I am so thankful to him and to the rest of the chemistry faculty at Wofford who made the third floor of Milliken Building my home away from home and always left their office doors open.

To Jan Patton and Gregory Pullen, fellow Wofford alumni who have gone on to pursue their own careers in chemistry. It has made such a difference having close friends that share my passion for chemistry. Their enthusiasm and support for my research is gratefully accepted and reciprocated.

To Dr. Allison Tolbert, a fellow Wofford alumna and recent Georgia Tech graduate who facilitated my first visit to Georgia Tech. Because of her, I was introduced to my future thesis advisor, for which I am eternally grateful.

To Dr. Stefan France, "Boss," who may not realize just how influential our first meeting was toward my decision to attend Georgia Tech. I knew so little about graduate school when we met, and the fact that he personally took the time to walk me through his

group's research and to offer me advice at the start of the application process gave me hope that I would find my place for the next five years. I am so thankful that he kept in touch throughout my search, gave me the chance to join a group with supportive coworkers and inspiring research, and encouraged me to apply for the SMART fellowship. Even beyond cultivating a positive research environment, he has been understanding and accommodating toward all the curveballs of life that grad school can't deflect. I am deeply moved by his care for the wellbeing of everyone in our lab, and I will never forget the support he offered in a time of sorrow when my grandparents passed away, and in a time of great joy when I got married. Dr. France is a phenomenal boss, and I hope he recognizes how much we as students appreciate and respect him.

To my lab mates, past and present. I especially thank Dr. George Ward, who was the most amazing mentor a fledgling graduate student could ask for and has become a close friend in the process. This last semester has been an adjustment without his physical presence in the lab, yet he has still made time to answer my questions *via* email and encourage me in the home stretch. To Kym Osborne-Benthaus, it meant more to me than I realized having another girl in the lab, and I've missed the easy camaraderie we shared during those three years as bench mates. To Dr. Corey Williams, who was always the positive energy and ray of sunshine that buoyed my spirits when chemistry was frustrating, as well as a vast font of knowledge on any topic (chemistry or otherwise). To them and to Rebecca Key, Marchello Cavitt, Joel Aponte-Guzmán, Cynthia Martin, Ray Shenje, and Matthew Sandridge, I am forever grateful for their leadership and endless support, and answered my questions unceasingly. To Meghan Benda, Doris Chen, Gabriel Faura, Ariel

Parker, Liz Jones, Nima Ronaghi, and Shaoren Yuan, it has been a genuine pleasure working alongside them and witnessing them flourish as chemists.

To my two undergraduate assistants, Peyton Cleary and Nya Dawson. Both contributed tireless, high-quality work toward my research projects and were joys to mentor.

To the scientists that I've had the opportunity to collaborate with through the SMART program. I am grateful for their mentorship and their tolerating the quirks of a synthetic organic chemist in a highly methodical analytical chemistry lab.

To the friends I've made at Georgia Tech, who have offered intellectual insight and moral support throughout: Breanne Hamlett, Osiris Martinez-Guzman, Eric Drew, Abe Jordan, David Fialho, and Sandy Pitelli. It's been a tough five years, but these people have made the effort both worth it and workable as we found that balance between research and quality time.

To my faith community at North Avenue, who made my first two years of graduate school less daunting and more fulfilling. Especial thanks to John and Jenn Washburn, Beth McKinnon Raver, Rachel Lovins, and Rev. Jeff Meyers, and to honorary members Tom and Yupar Merriam. I am blessed to have dear friends whom I can trust implicitly and who I know will always go out of their way to help when there's a crisis.

To my family, who have offered unending and overwhelming support for my decision to attend graduate school. My parents, Rich and Adrienne Maris, have encouraged my curiosity and intellect from the day I was born and inspired me to "dream big" when it

came to my eventual vocation. They've seen the best of times and the worst of times as I've navigated my new life in Atlanta, and I'm grateful to them for frequently making the trip down from Greenville to give me that emotional boost (and, importantly, food) that would get me through the next few weeks. My sister, Kathleen, is one of the few people I communicate with daily, and her uplifting texts often pierce through the haze of work frustrations and help me find that optimism to carry on. My brothers, Greg and Jackson, have always come in at the crucial moment and been an insulating presence to give me space from my overworked brain. To my late maternal grandparents, Elmer and Barbara Rumminger, and to my paternal grandparents, Bob and Gizella Maris, I am thankful for the interest they've shown in my education and career and for their constant prayers for energy, drive, and peace of mind.

To my new family, who have shown such an active interest in and enthusiasm for my work. Randy and Jeannie Ligon, my parents-in-law, opened their arms and their home to me without reservations and always make a point to ask insightful questions about my research. For their support and their understanding toward the many long weekends spent writing on their back patio, I am deeply grateful. Mary Catherine, my new sister, has given me the opportunity to review fundamental chemistry concepts through tutoring her in organic chemistry, as well as offered me a fun outlet away from the lab through shopping and fashion.

Finally, to my husband, George Ligon. This man has supported my goals and dreams even before I began applying to graduate programs. He celebrated with me when I received my first acceptance letter and my fellowship offer from Georgia Tech, and offered himself as a sounding board while I tried to decide where to attend graduate school. He has

been there for me every time that graduate school felt too challenging and was often the push and voice of reason I needed to press on. He encouraged me to apply for the SMART program, even though it meant locking us into four extra years in Atlanta and restricting his initial career options. He dealt with my unpredictable schedule and long nights in the lab, and drove long distances sometimes every weekend to make our relationship work. Most recently, he committed to a two-hour commute every day so that we could get married while we were finishing school. How can I say thank you enough for all the sacrifices George has made, the steadiness he's offered me through the hardest times, and the excitement he's shown at even the smallest successes I've achieved? Because of him, my pursuit of a graduate degree and my future career in chemistry are more fulfilling than I could've imagined. So, to George Ligon, I say: Thank you. I love you.

TABLE OF CONTENTS

LIST OF TABLES

LIST OF FIGURES

LIST OF SCHEMES

LIST OF SYMBOLS AND ABBREVIATIONS

$(COCl)_2$	oxalyl chloride
$[Au(PPh_3)]NTf_2$	chloro(triphenylphosphine)gold(I) bis(trifluoromethylsulfonyl)imide
[O]	oxidation
1,10-phen.	1,10-phenanthroline
1,2-DBE	1,2-dibromoethane
^{13}C	carbon-13
^{19}F	fluorine-19
^{1}H	proton
2,6-lut.	2,6-lutidine
2°	secondary
3°	tertiary
Ac	acetyl
Ac_2O	acetic anhydride
ACS	American Chemical Society
Ag_2CO_3	silver(I) carbonate
Ag_2O	silver(I) oxide
$AgBF_4$	silver(I) tetrafluoroborate
AgOTf	silver(I) trifluoromethanesulfonate
$Al(OTf)_3$	aluminum(III) trifluoromethanesulfonate
$AlCl_3$	aluminum(III) trichloride

amu	atomic mass unit
aq.	aqueous
Ar	aryl
ArMgBr	arylmagnesium bromide
ArN_3	aroyl azide
$B(OH)_2$	boronic acid
BCl_3	boron trichloride
$Bi(OTf)_3$	bismuth(III) trifluoromethanesulfonate
Bn	benzyl
BnBr	benzyl bromide
BnOH	benzyl alcohol
Boc	*tert*-butyloxycarbonyl
Boc_2O	di-*tert*-butyl dicarbonate
$Ca(NTf_2)_2$	calcium bis(trifluoromethanesulfonimide)
cat.	catalytic
CH_3	methyl
cm^{-1}	wavenumber
Comins's reagent	*N*-(5-chloro-2-pyridyl)bis(trifluoromethanesulfonimide)
conc.	concentration
COSY	homonuclear correlation spectroscopy
Cs_2CO_3	cesium carbonate
CSA	Controlled Substances Act

$Cu(OTf)_2$	copper(II) trifluoromethanesulfonate
CuI	copper(I) iodide
d.r.	diastereomeric ratio
D-A	donor-acceptor
DACP	donor-acceptor cyclopropane
DBU	1,8-diazabicyclo[5.4.0]undec-7-ene
DCC	dicyclohexylcarbodiimide
DCE	1,2-dichloroethane
DCM	dichloromethane
DEA	Drug Enforcement Administration
DEPT	Distortion Enhancement by Polarization Transfer
DHF	dihydrofuran
DIBAL-H	diisobutylaluminum hydride
DIPEA	diisopropylethylamine (Hünig's base)
DMAP	4-dimethylaminopyridine
DMF	dimethylformamide
DMSO	dimethylsulfoxide
DMSO-*d6*	deuterated dimethylsulfoxide
DMTP	dimethylterephthalate
DOS	diversity-oriented synthesis
EAS	electrophilic aromatic substitution
EDCI	*N*-ethyl-*N*′-(3-dimethylaminopropyl)carbodiimide

EDG	electron-donating group
ee	enantiomeric excess
EI	electrospray ionization
equiv.	equivalent(s)
Et	ethyl
Et_2O	diethyl ether
Et_3N	triethylamine
EtOAc	ethyl acetate
eV	electron volts
EWG	electron-withdrawing group
F-C	Friedel-Crafts
$FeCl_3$	iron(III) chloride
FTIR	Fourier transform infrared
g	gram
$Ga(OTf)_3$	gallium(III) trifluoromethanesulfonate
$GaCl_3$	gallium(III) chloride
GC	gas chromatography
h	hour
H_2	molecular hydrogen
H_2O	water
H_2O_2	hydrogen peroxide
H_2SO_4	sulfuric acid

HBTU	(2-(1*H*-benzotriazol-1-yl)-1,1,3,3-tetramethyluronium hexafluorophosphate
HCl	hydrochloric acid
HepG-2	liver hepatocellular carcinoma
HRAM-MS	high-resolution accurate-mass mass spectrometry
HSQC	heteronuclear single quantum coherence spectroscopy
HWE	Horner-Wadsworth-Emmons
Hz	Hertz
ImH	1*H*-imidazole
$In(OTf)_3$	indium(III) trifluoromethanesulfonate
$InCl_3$	indium(III) cloride
IPA	isopropanol
i-PrMgCl	isopropylmagnesium chloride
i-PrMgCl.LiCl	isopropylmagnesium chloride lithium chloride salt, Turbo Grignard
IR	infrared
IUPAC	International Union of Pure and Applied Chemistry
K_2CO_3	potassium carbonate
$K_4[Fe(CN)_6]$	potassium ferrocyanide
KH	potassium hydride
KOH	potassium hydroxide
KO*t*-Bu	potassium *tert*-butoxide
kV	kilovolts
LC	liquid chromatography

LDA	lithium diisopropylamide
LG	leaving group
LHMDS	lithium hexamethyldisilazide
$LiAlH_4$	lithium aluminum hydride
LiBr	lithium bromide
LiCl	lithium chloride
$LiOH{\cdot}H_2O$	lithium hydroxide monohydrate
L_n	ligand
M	metal
m	*meta*
m/z	mass-to-charge
MAD	methylaluminum bis(2,6-di-*tert*-butyl-4-methylphenoxide)
MCR	multicomponent reaction
MDR	multidrug resistance
Me	methyl
Me_3Al	trimethylaluminum
MeCN	acetonitrile
Meldrum's acid	2,2-dimethyl-1,3-dioxane-4,6-dione
MeOH	methanol
mesyl	methanesulfonyl
mg	milligram
$Mg(OTf)_2$	magnesium trifluoromethanesulfonate

Mg^0	magnesium metal
$MgBr_2 \cdot OEt_2$	magnesium bromide ethyl etherate
$MgSO_4$	magnesium sulfate
MHz	mega-Hertz
min	minutes
mL	milliliter
mm	millimeters
mmol	millimole
$Mn(OAc)_3 \cdot 2H_2O$	manganese(III) acetate dihydrate
mol	mole
mol%	mole percent
MOM	methoxymethyl
MS	mass spectrometry
Ms	methanesulfonate
MSD	mass selective detector
Mukaiyama's reagent	2-chloro-1-methylpyridinium iodide
N	nitrogen
N.D.	not determined
N.R.	no reaction
N_2	molecular nitrogen
Na_2CO_3	sodium carbonate
Na_2SO_4	sodium sulfate

NaCl	sodium chloride
NaH	sodium hydride
$NaHCO_3$	sodium bicarbonate
NaHMDS	sodium hexamethyldisilazide
$NaIO_4$	sodium periodate
NaOH	sodium hydroxide
n-Bu	*n*-butyl
n-Bu_4NHSO_4	tetrabutylammonium hydrogensulfate
n-Bu_4NPF_6	tetrabutylammonium hexafluorophosphate
n-BuLi	*n*-butyllithium
n-BuOH	butanol
NH_3	ammonia
NH_4Cl	ammonium chloride
Ni(DPPP)Cl_2	[1,3-bis(diphenylphosphino)propane]dichloronickel(II)
NIST	National Institute of Standards and Technology
NMO	*N*-methylmorpholine *N*-oxide
NMR	nuclear magnetic resonance
NO_2	nitro
Ns	nitrobenzenesulfonyl
Nu	nucleophile
o	*ortho*
O_2	molecular oxygen

OsO_4	osmium tetroxide
p	*para*
p-ABSA	*p*-acetamidobenzenesulfonyl azide
PBr_3	phosphorus tribromide
$Pd(TFA)_2$	palladium(II) trifluoroacetate
Pd/C	palladium on carbon
$Pd_2(dba)_2$	bis(dibenzylideneacetone)palladium(0)
PFK	perfluorokerosene
PG	protecting group
Ph	phenyl
$PhB(OH)_2$	phenylboronic acid
PhLi	phenyllithium
PhMe	toluene
PhMgBr	phenylmagnesium bromide
$PhNTf_2$	*N*-phenylbistrifluoromethanesulfonimide
PMP	*p*-methoxyphenyl
PPh_3	triphenylphosphine
ppm	part(s) per million
prep-TLC	preparative thin-layer chromatography
psi	pounds per square inch
Pyr	pyridine
q-NMR	quantitative nuclear magnetic resonance

quant.	quantitative
R	alkyl group
r.t.	room temperature
ref.	reference
R_f	retention factor
$Rh_2(esp)_2$	bis[rhodium(α,α,α′,α′-tetramethyl-1,3-benzenedipropionic acid)]
ROC	ring-opening cyclization
$Sc(OTf)_3$	scandium(III) trifluoromethanesulfonate
$SiPhMe_2$	dimethylphenylsilyl
SM	starting material
$Sn(OTf)_2$	tin(II) trifluoromethanesulfonate
$SnCl_4$	tin(IV) tetrachloride
solv.	solvent
T	temperature
T. corymbosa	*Tabernaemontana corymbosa*
TBAI	tetrabutylammonium iodide
TBD	to be determined
TBDPS	*tert*-butyldiphenylsilyl
TBHP	*tert*-butyl hydrogen peroxide
TBS	*tert*-butyldimethylsilyl
t-BuOH	*tert*-butanol
t-BuOOBz	*tert*-butyl peroxybenzoate

temp.	temperature
Tf_2NH	trifluoromethanesulfonimide
Tf_2O	trifluoromethanesulfonic anhydride
TFA	trifluoroacetic acid
TfOH	trifluoromethanesulfonic acid
THF	tetrahydrofuran
THI	5,6,7,8-tetrahydroindolizine
$TiCl_4$	titanium(IV) tetrachloride
TLC	thin-layer chromatography
TMEDA	tetramethylenediamine
TMS	trimethylsilyl
TMSI	trimethylsilyl iodide
TMSOTf	trimethylsiliyl trifluoromethanesulfonate
tosyl	*p*-toluenesulfonyl
triflate	trifluoromethanesulfonate
triflimide	trifluoromethanesulfonimide
Ts	*p*-toluenesulfonate
TSE	2-(trimethylsilyl)ethyl
TsN_3	*p*-toluenesulfonyl azide
TsOH	*p*-toluenesulfonic acid
$TsOH{\cdot}H_2O$	*p*-toluenesulfonic acid monohydrate
UHPLC	ultra-high pressure liquid chromatography

UV	ultraviolet
wt%	weight percent
X	some atom (assigned)
$Yb(OTf)_3$	ytterbium(III) trifluoromethanesulfonate
$Zn(OTf)_2$	zinc(II) trifluoromethanesulfonate
$ZnCl_2$	zinc(II) chloride
Δ	reflux
μL	microliter
μmol	μmol

SUMMARY

Methodology development is an essential pursuit to enable the synthesis of pharmaceutically-relevant targets. The emergent concept of privileged scaffolds has provided a framework for focused synthetic methodology development toward polycyclic heteroaromatic compounds with inherent and important bioactivities. This thesis explores novel applications of the Friedel-Crafts reaction toward three medicinal compounds and their privileged scaffolds: flubromazepam, a 1,4-benzodiazepine; tronocarpine, a tetrahydro-7,11-methanoazocino[1,2-*a*]indole; and rhazinicine, a tetrahydroindolizine. Several 1,4-benzodiazepine positional isomers were synthesized and characterized for the first time. Additionally, significant advances in knowledge were accomplished toward the reactivity and stereochemical behavior of donor-acceptor bicyclo[3.1.0]hexanes, an understudied class of DACPs, in intramolecular ring-opening cyclizations, and a novel formal [3+2] cycloaddition of a C5-substituted D-A oxabicyclo[3.1.0]hexane was demonstrated.

CHAPTER 1. INTRODUCTION

1.1 Organic Synthesis and Privileged Scaffolds

Organic synthetic methodology development exists in a synergetic relationship with molecular targets, both natural and synthetic, that benefit our society. For instance, many pharmaceutical and some agrochemical targets are inspired by bioactive compounds isolated from nature, i.e. natural products. The discovery of novel natural products with significant bioactivities (e.g. antimalarial, antibacterial) not only offers alternatives to currently available therapies, but fundamentally broadens chemical understanding of how molecular scaffolds impart potency. Inspiration and application are therefore in a healthy equilibrium that continually fuels new research (Figure 1-1).

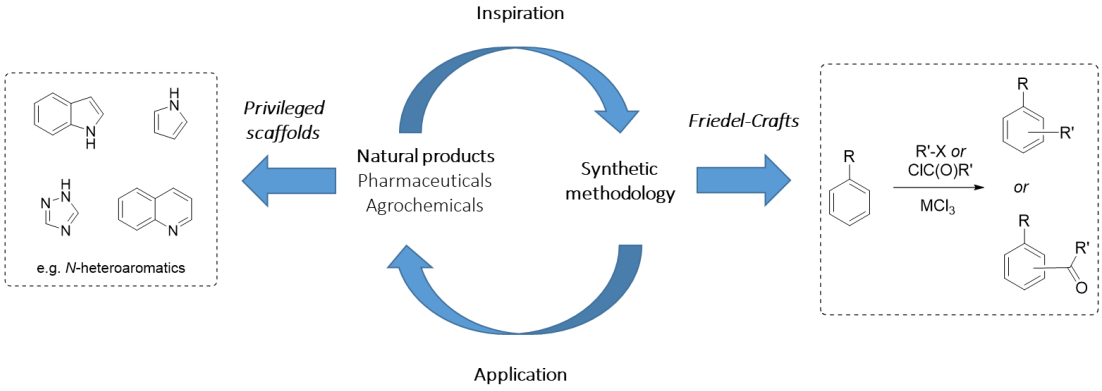

Figure 1-1: Synergistic relationship between natural products and synthetic methodology.

Over the last twenty years, general trends have been established to further guide drug discovery and relevant synthetic methodology development, to culminate in the concept of "privileged scaffolds" in medicinal targets[1]. One of the most prevalent structural features encompassed by privileged scaffolds is polycyclic, heteroaromatic core structures,

especially nitrogen-containing cores (e.g. indoles, pyrroles, quinolines, anilines).[2] This more focused approach has inspired novel strategies and enabled efficient techniques to synthesize and evaluate vast libraries of compounds for biological survey,[3] such as diversity-oriented synthesis (DOS),[4] late-stage C-H functionalization[5] and directed cross-coupling,[6] multicomponent reactions (MCRs),[7] and cascade transformations.[8]

1.2 The Friedel-Crafts Reaction: A Tool for Synthetic Organic Chemists

1.2.1 Fundamentals of the Friedel-Crafts Reaction

Among classic but extraordinarily powerful organic transformations to access densely functionalized heteroaromatic scaffolds is the Friedel-Crafts (F-C) reaction.[9] Found in every introductory organic chemistry textbook, this reaction is categorically an electrophilic aromatic substitution (EAS), whereby an arene is functionalized with an alkyl or acyl substituent. Regioselectivity for this transformation is largely dictated by electronic influences from any substituents already present on the arene. Electron-donating groups (EDGs, e.g. alkyl, aryl, alcohol, amino) promote EAS first at an open *para* position and next at an open *ortho* position (Figure 1-2a); EDGs, for this reason, are referred to as *ortho/para* directors for this class of chemistry. Electron-withdrawing groups (EWGs, e.g. acyl, nitro, halo), on the other hand, are *meta* directors (Figure 1-2b). Furthermore, EDGs are considered EAS-activating and EWGs, EAS-deactivating.

The classic F-C reaction employs Lewis acids such as aluminum(III) trichloride ($AlCl_3$) to activate the acylating or alkylating agent, usually an acyl chloride or an alkyl halide, respectively. To demonstrate the mechanism, Figure 1-2c shows a general F-C acylation with an EDG-substituted arene, and Figure 1-2d, a general F-C alkylation with

an EWG-substituted arene. The reaction begins with halogen abstraction from the acylating/alkylating agent by a Lewis acid catalyst, generating an acylium ion or a carbocatioin, respectively. This positively charged intermediate is then trapped by the aromatic partner, resulting in a σ-complex, in which the positive charge is delocalized throughout the ring. Deprotonation by the abstracted halide promotes rearomatization of the arene.

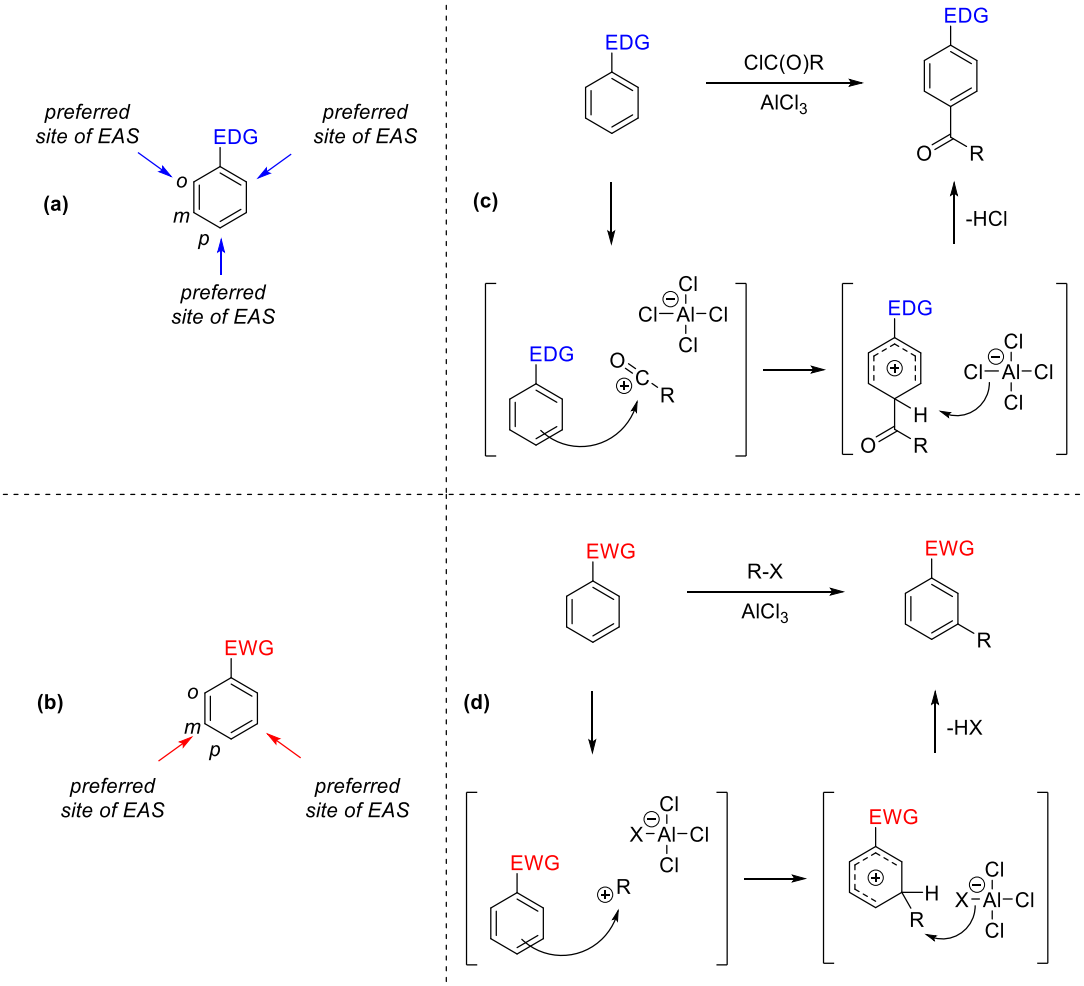

Figure 1-2: (a) Regioselectivity for EDG-subsitutent arenes. (b) Regioselectivity for EWG-substituted arenes. (c) Mechanism of F-C acylation with an *ortho/para* director. (d) Mechanism of F-C alkylation with a *meta* director.

These electronic effects have important implications. First, predicting the regiochemical outcome of a Friedel-Crafts reaction is rather straightforward, but at the cost of limiting what regioisomers are accessible by this method. Second, if sufficient acylating/alkylating agent is available, this reaction is susceptible to over-substitution, especially for electron-rich arenes; in the case of alkylation, the arene becomes even more activated for EAS. Third, lower yields are expected for EWG-substituted arenes due to the electron-poorness of the system.

1.2.2 The Friedel-Crafts Reaction Nearly a Century-and-a-Half Later

Despite these drawbacks, the F-C reaction has seen many important advances since its appearance in 1877, especially in the context of total synthesis[10]. One significant application is intramolecular Friedel-Crafts-type reactions (so defined as long as the basic mechanistic pathway is followed) in cascade reactions, which are intricately designed, one-pot transformations that rely on the interplay between compatible reactive moieties within a molecule. The result is a highly convergent manipulation strategy that facilitates the synthesis of vast combinatorial libraries for biological assay, often from commercially or readily available starting materials. Examples of cascade processes employing Friedel-Crafts include but are certainly not limited to Pictet-Spengler (Scheme 1-1),[11] Michael-type additions (Scheme 1-2),[12] and Prins-type cyclizations (Scheme 1-3).[13]

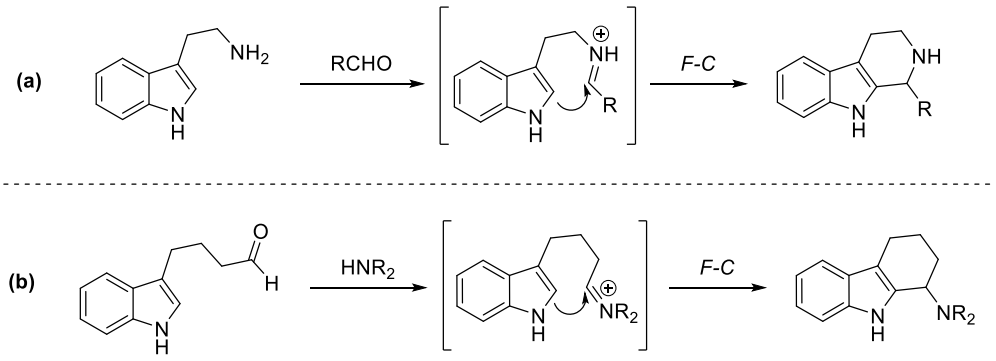

Scheme 1-1: Representative example of Pictet-Spengler cascade. (a) Classic Pictet-Spengler. (b) Exocyclic Pictet-Spengler from Hansen, *et al*.

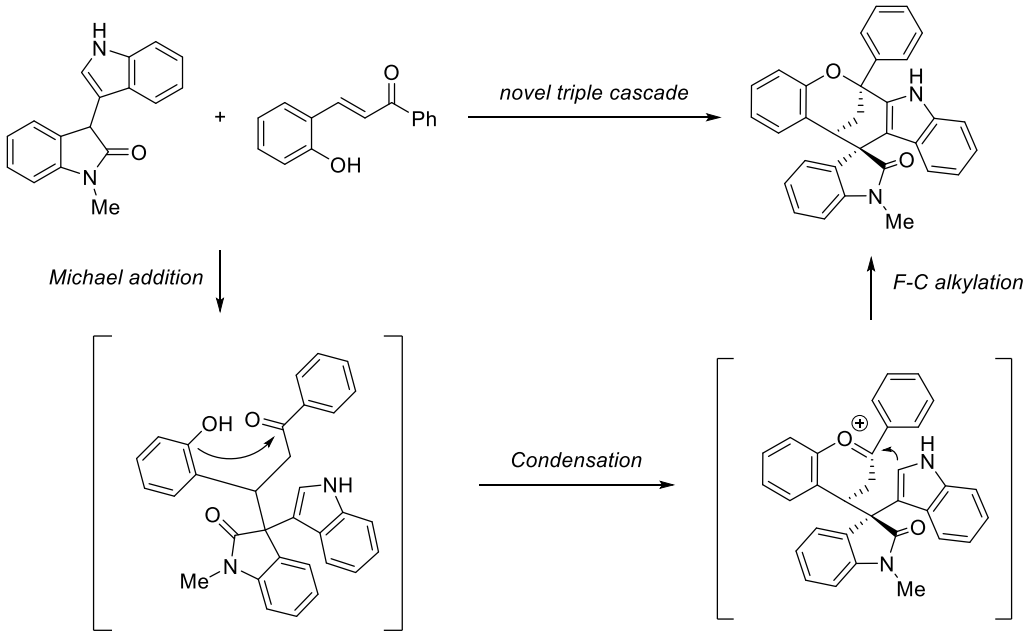

Scheme 1-2: Novel Michael addition/condensation/F-C alkylation cascade from Wang, *et al*.

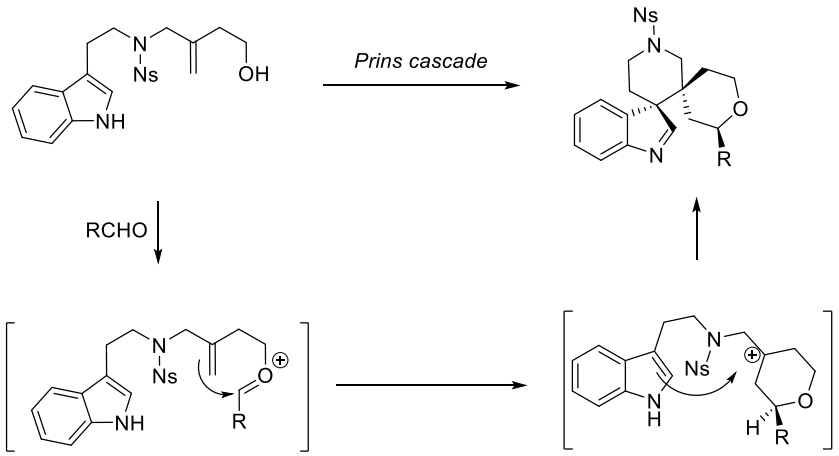

Scheme 1-3: Prins cyclization/F-C alkylation cascade from Reddy, *et al.*

With the advent of Friedel-Crafts-type reactions, cascade or otherwise, alternatives to classic acyl chloride and alkyl halide reagents have emerged. Acylating agents range from classic carboxylic acid derivatives, ketenes, and nitriles, to even more recent examples including twisted amides (Szostak)[14] and aroyl triflates generated *in situ* from commercial aryl iodides and CO_2 (Arndtsen).[15] Alkylating agents, too, constitute a vast scope of reagents, from alkynes and alkenes to epoxides, carboxylic acid derivatives, ethers and sulfides, and even alkanes with the advent of C-H functionalization strategies.

Other mechanistic pathways, too, have been established for Friedel-Crafts beyond EAS. For instance, acyl iodides have been employed as partners for photochemical F-C acylation (Szostak),[16] and aryldiazonium borohydrides were successful in effecting radical F-C acylation (Yadav).[17] Douglas, in a recent publication, also demonstrated a regioselective F-C acylation *meta* to EDGs using sterically bulky salicylate esters,[18] which is an important complement to classic F-C reactions.

1.3 This Thesis: Featured *N*-Heteroaromatic Products

This dissertation will showcase novel methodology development guided by the principles of the Friedel-Crafts reaction and inspired by three bioactive targets: flubromazepam, tronocarpine, and rhazinicine (Figure 1-3). The unique features of these compounds' molecular scaffolds presented diverse challenges in the pursuit of their total syntheses. These structural features and previously published strategies toward accessing them will be described in Chapter 1, whereas my hypotheses and synthetic attempts toward each target will be detailed in individual chapters. Potential applications of the Friedel-Crafts reaction will be highlighted when relevant.

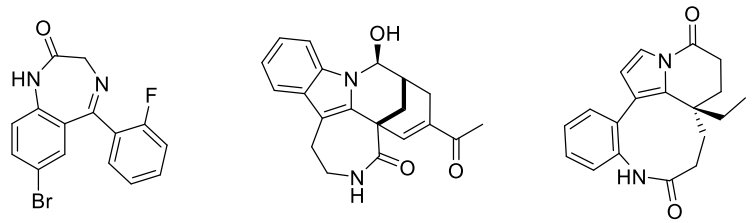

Flubromazepam Tronocarpine Rhazinicine

Figure 1-3: Featured bioactive synthetic and natural products.

1.4 Flubromazepam: A Synthetic Benzodiazepine

Flubromazepam (IUPAC name: 7-bromo-5-(2-fluorophenyl)-1,3-dihydro-2*H*-benzo[*e*][1,4]diazepin-2-one) belongs to a class of bioactive compounds known as benzodiazepines. In general, benzodiazepines are highly effective pharmaceutical remedies for anxiety, seizures, insomnia, and opiate and alcohol withdrawals,[19] and the core benzodiazepine scaffold is considered privileged.[2b]

The syntheses of benzodiazepines including flubromazepam were extensively studied by Sternbach and co-workers in the early 1960s.[20] By their published method, *para*-

substituted anilines underwent classic Friedel-Crafts acylations with *ortho*-substituted benzoyl chlorides to form the 2-aminobenzophenone synthetic precursors to benzodiazepines.[20c] (Note: Several 2-aminobenzophenone preparations relied on *N*-acetyl or -tosyl starting materials and/or employed aluminum(III) chloride rather than zinc(II) chloride.) Then, one of two pathways was pursued: 1) a stepwise annulation with 2-haloacetyl halide (X = Cl, Br) to prepare the intermediary 2-haloacetamidobenzophenone, followed by treatment of ammonia to promote the imination; or 2) a one-pot annulation effected by glycine ethyl ester hydrochloride in refluxing (Scheme 1-4).[20d]

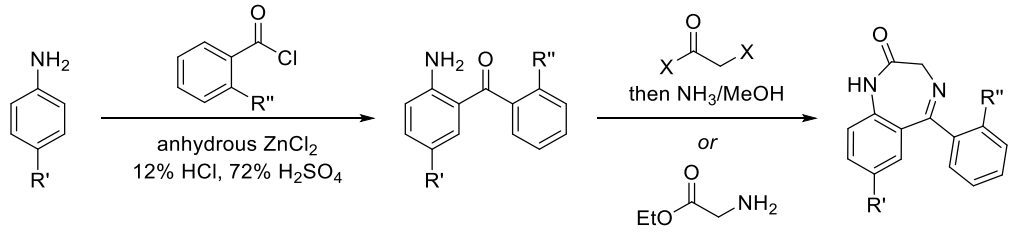

Scheme 1-4: Sternbach method to prepare benzodiazepines.

Though myriad benzodiazepines were successfully prepared by Sternbach using this method, the scope was generally limited to products originating from anilines with electron-withdrawing *para* substituents. This is unsurprising: given the synergistic substitution preferences of Friedel-Crafts acylations, 4-EWG-substituted anilines would facilitate acylation *ortho* to the amine, which is essential to enable synthesis of the benzodiazepine scaffold (Figure 1-4).[21] These preferences are in stark contrast to the expected undesired acylations that would predominate with the 2- or 3-substituted anilines in the pursuit of novel benzophenone regioisomers. Thus, 2-aminobenzophenones with bromo, chloro, and nitro substituents *para* to the amino group are highly accessible,[20b] and there are few benzodiazepines with differing substitution patterns as a result. (Observed

exceptions to this rule from Sternbach's work were often products of anilines with electron-donating *meta* substituents, also favored by Friedel-Crafts chemistry.)

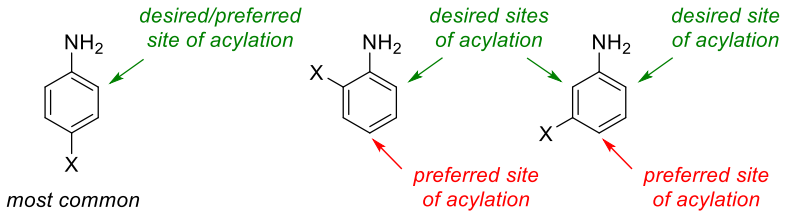

Figure 1-4: Anticipated outcomes for Friedel-Crafts acylations of EWG-substituted anilines.

This limitation of classic Friedel-Crafts reactivity has led to a gap of knowledge surrounding the biological and analytical properties of benzodiazepine targets with varying substitution patterns. There are alternative approaches to F-C acylation that circumvent the regioselectivity issues for benzophenone synthesis, which will be discussed in Chapter 2, but these methodologies have largely not followed through with the syntheses of the corresponding benzodiazepines. Moreover, these novel methods often do not tolerate the bromo and/or nitro substituents characteristic of more potent pharmaceutical benzodiazepines. Therefore, there is an opportunity to exploit and further develop advances in Friedel-Crafts chemistry, such as chelation-assisted F-C acylation, to access novel benzodiazepine isomers.

1.5 Tronocarpine and Rhazininicine

In contrast to synthetic benzodiazepines like flubromazepam, which benefit from classic Friedel-Crafts acylation conditions, the two natural products described herein, tronocarpine and rhazinicine, represent significant opportunities to advance novel intramolecular Friedel-Crafts-type methodologies, specifically ring-opening cyclizations employing donor-acceptor cyclopropanes (DACPs). Therefore, a case will first be made

for DACPs as a powerful tool, both as a synthon and in the context of Friedel-Crafts-type methodologies, before discussing the bioactivities of and previous synthetic attempts toward tronocarpine and rhazinicine.

1.5.1 Donor-Acceptor Cyclopropanes

As a synthon, cyclopropane benefits from inherent strain—both angular and torsional—and high *p*-character. These characteristics lend cyclopropane alkene-like reactivity[22] and enable C—C bond cleavage to result in a transitory 1,3-dipole, which can subsequently perform *homo*-enolate, *homo*-conjugate, or cycloaddition chemistry (Figure 1-5).[10g] This bond cleavage may be facilitated by the incorporation of electron-donating (e.g. $–CH_3$, –Ph) and electron-withdrawing (e.g. $–NO_2$, $-CO_2R$) substituents onto vicinal carbons, resulting in a DACP.

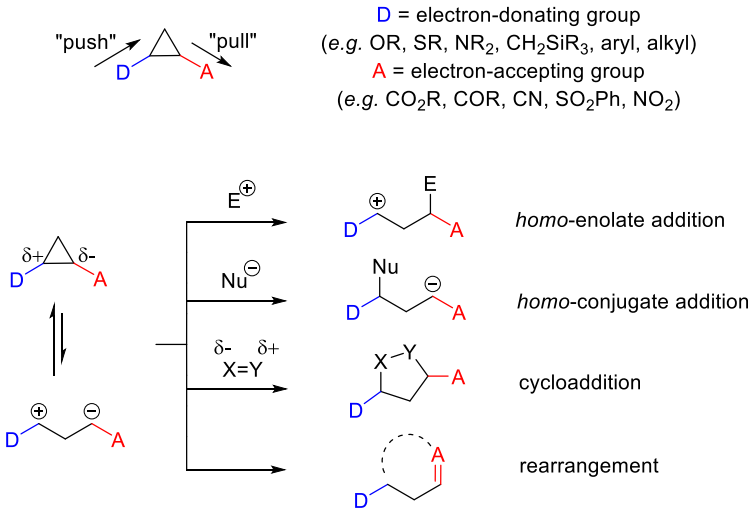

Figure 1-5: Donor-acceptor cyclopropane reactivity.

It has been validated computationally that DACPs benefit from the polarized bond between the donor and acceptor carbons, which lowers the activation barrier for bond

cleavage. Additionally, the carbanion charge can be delocalized into the acceptor substituent, and the donor substituent contributes stabilizing electron density, making the carbocation more localized and persistent.[23] Thus, reactivity increases as more donor and acceptor groups are added (to the benefit or detriment of the desired transformation), and the identities of these substituents also tune the energetics of the system (Figure 1-6). Significantly, incorporation of an additional (geminal) acceptor group increases the binding ability of DACPs to Lewis acids, which further facilitates ring-opening as well as enables catalytic activation.

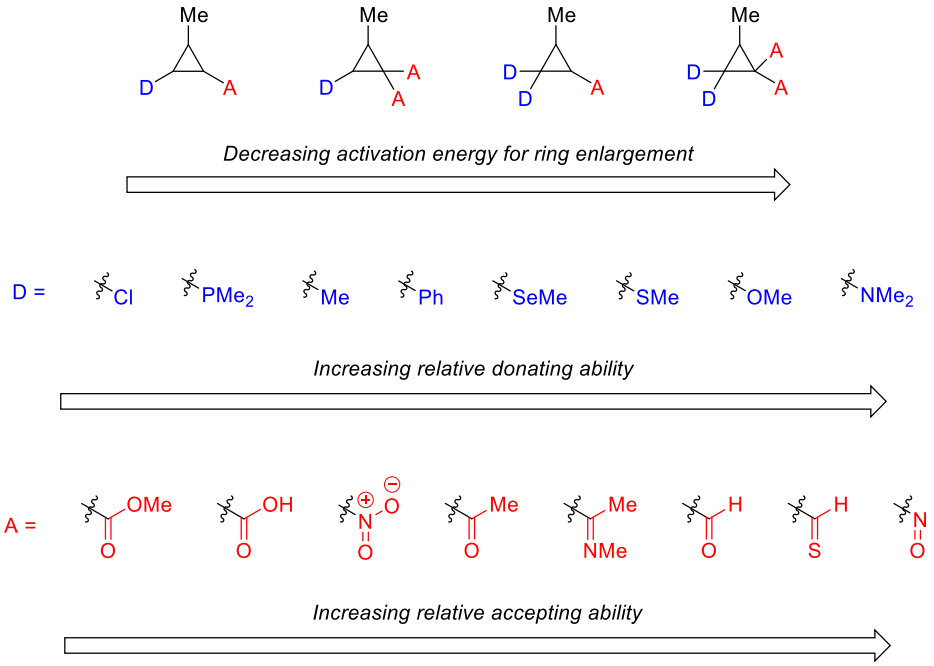

Figure 1-6: Substituent effects on DACP reactivity.

DACPs were first reviewed by Reißig in 1988,[24] with a key focus on their synthesis. The first DACP was prepared from Michael-type nucleophilic attack of a donor group onto an acceptor-bearing allylic halide, followed by ring-closing and displacement of the halide.[25] There have been many synthetic strategies demonstrated since then;[26] however, a

broadly applied method derives DACPs from cyclopropanation reactions of donor-substituted olefins with acceptor-substituted α-diazo compounds (i.e. carbene precursors), typically in the presence of copper- or rhodium-based catalysts.

Research toward developing intramolecular reactions of DACPs was pioneered by Stork and Grieco primarily as a method for Michael-type cyclizations afforded by olefin/aryl attack onto D-A cyclopropyl ketones (Scheme 1-5).[27] The authors demonstrated acid-promoted syntheses of fused di-cyclohexanes, with the methyl substituent and the ketone serving as donor and acceptor, respectively.

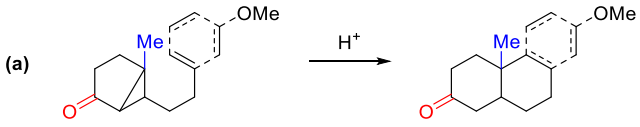

Scheme 1-5: Michael-type cyclizations of D-A cyclopropyl ketones.

Another early method showcases the ring-opening of 1,2-dialkoxy-3-ketylcyclopropanes followed by oxidation and aldol-type condensation to cyclopentenones, established by Wenkert.[28] Similarly, intramolecular ring-opening cyclizations of DACPs onto their ester acceptor substituents yield dihydrofuran derivatives[29] as well as γ-butyrospirolactones[30] in certain cases; if the elimination route is available, substituted, fully unsaturated furans are the preferred product. Notably, too, Reißig demonstrated that DACPs with diene and dienophile substituents can perform intramolecular Diels-Alder reactions to yield fused bicyclic derivatives with reasonably good diastereoselectivity (d.r. = 6:1).[31]

The France group has made valuable contributions in the field of intramolecular ring-opening cyclizations of DACPs, particularly toward the formal *homo*-Nazarov cyclization (Scheme 1-6). In contrast to the traditional Nazarov cyclization of divinyl

ketones to cyclopentenones (Scheme 1-6a),[32] the classic formal *homo*-Nazarov reaction employs alkenyl cyclopropyl ketones and results in cyclohexenone products (Scheme 1-6b). Early reports of this reaction required high temperatures and (super-)stoichiometric quantities of Bronsted acid, with limited applications.[33] In 2009, Waser was the first to demonstrate this transformation catalytically, using 20 mol% of tosic acid.[34] Then, in 2010, France and co-workers harnessed the synthetic utility of DACPs by introducing an additional acceptor group, an ester, *beta* to the ketone. The system afforded effective coordination to a Lewis acid and greater stabilization of the dipolar intermediate following ring-opening. These characteristics allowed for milder conditions, high selectivity, and high yields, resulting in a much more efficient *homo*-Nazarov cyclization (Scheme 1-6c).[35]

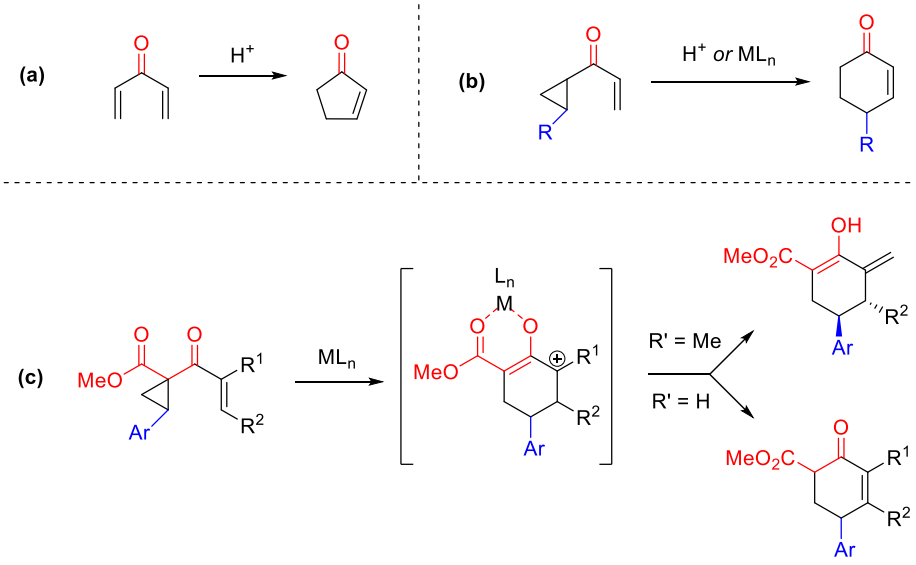

Scheme 1-6: (a) Traditional Nazarov cyclization. (b) *Homo*-Nazarov cyclization. (c) *Homo*-Nazarov cyclization of a DACP with an additional acceptor group developed by France.

This reactivity was quickly expanded to aromatic and heteroaromatic products. In 2011, France and co-workers demonstrated the intramolecular Friedel-Crafts-type ring-opening cyclization of DACPs tethered to substituted arenes and various heterocycles (e.g.

pyrrole, indole, furan, benzofuran, thiophene) at the 2- and 3-positions (Scheme 1-7a),[36] as well as an analogous cyclization onto *N*-acylindoles to construct the hydropyrido[1,2-*a*]indole core (Scheme 1-7b).[37]

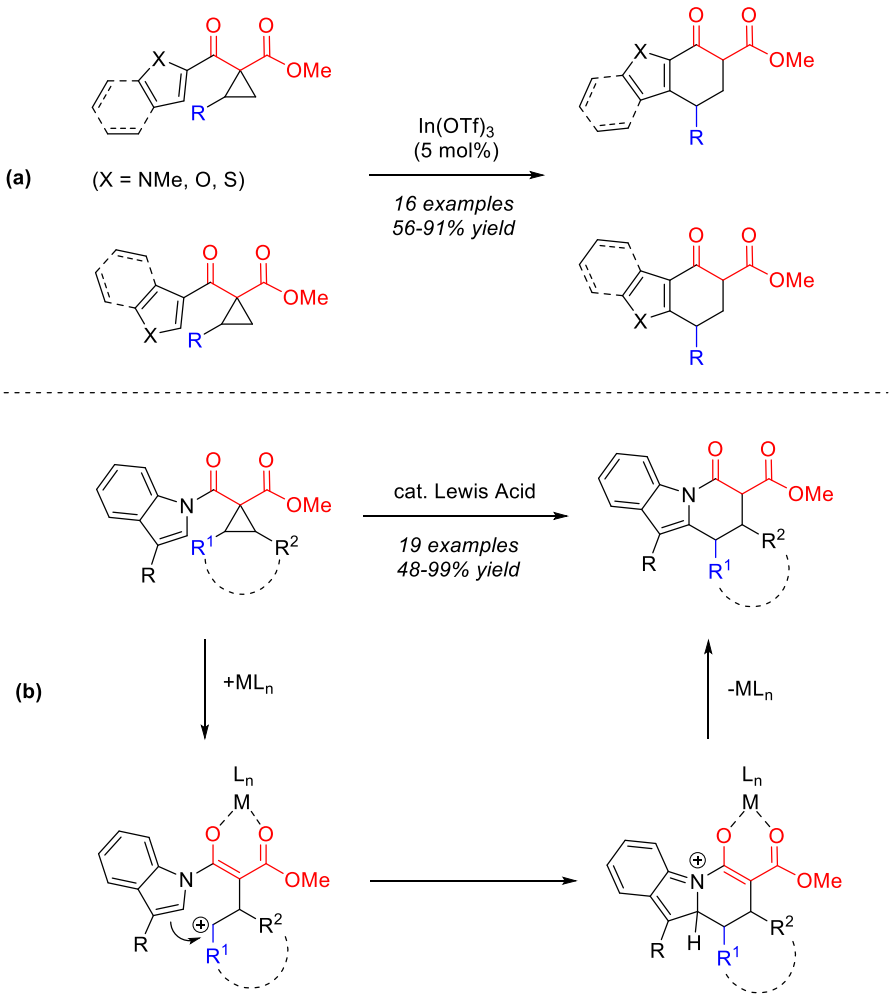

Scheme 1-7: (a) Intramolecular F-C-type ROC of C2- and C3-heteroaromatic-tethered DACPs. (b) Intramolecular F-C-type ROC of *N*-acyl indole-tethered DACPs and mechanism.

These and further applications of formal *homo*-Nazarov-type[38] and Friedel-Crafts-type[39] reactions—including the total synthesis of deethyleburnamonine (Scheme 1-8)[40] and a tandem cyclopropanation-ring-opening cyclization in continuous flow[41]—represent important advances in the field with respect to facile construction of polycyclic

heteroaromatic scaffolds in natural products, as well as the incorporation of functionality where previous methods had not succeeded.

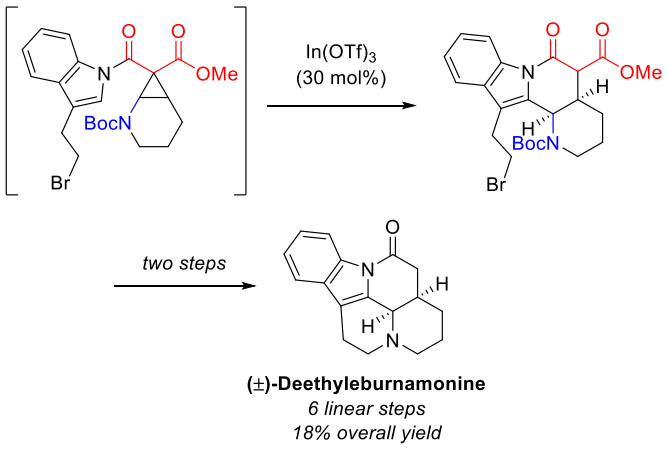

Scheme 1-8: Concise total synthesis to deethyleburnamonine.

A comprehensive review from the France group describes intramolecular ring-opening cyclizations of donor-acceptor cyclopropanes through 2013.[10g] More recent intramolecular examples include Nishii's stereoretentive intramolecular ring-opening cyclization of various aryl-tethered DACPs in the presence of superstoichiometric $TiCl_4$;[42] Trushkov's synthesis of 2,3-dihydrobenzo[*b*]furans and -thiophenes under $MgBr_2 \cdot OEt_2$ catalysis;[43] and Wang's $Yb(OTf)_3$-mediated intramolecular [4+3] cycloadditions to form various hydroazulenes (bicyclo[5.3.0]decanes),[44] among others.[45]

Intermolecular Friedel-Crafts-type reactions of DACPs have also been shown. As a representative example, in 2001, Kerr published the first application of intermolecular ring-opening cyclizations of DACPs to form heteroaromatic tricycles in the pursuit of indole alkaloid natural products (Scheme 1-9).[46] This reaction is of particular relevance to tronocarpine.

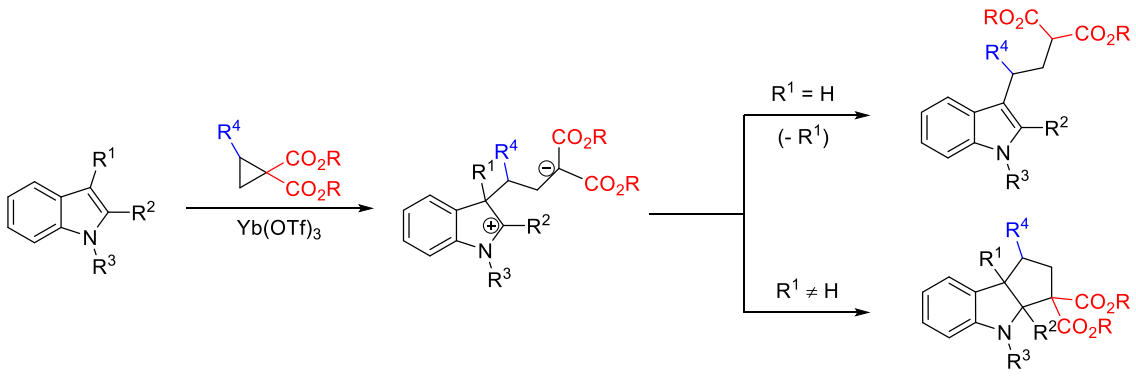

Scheme 1-9: Kerr's intermolecular ring-opening cyclization toward indole-containing tricycles.

1.5.2 Tronocarpine

Tronocarpine is a chippiine-type indole alkaloid isolated from *T. corymbosa* in 2000.[47] Though its bioactivity is currently unknown, its structural similarities to the chippiine indole alkaloids shown in Figure 1-7 suggest cytotoxic or anticancer activity.[48] Like most natural products in this family, tronocarpine has a pentacyclic scaffold containing a tryptamine core and a bridged azabicyclo[3.3.1]nonane moiety. Unlike other chippiines, however, tronocarpine has a seven-membered lactam bound to the bridgehead carbon of the bicyclic moiety.

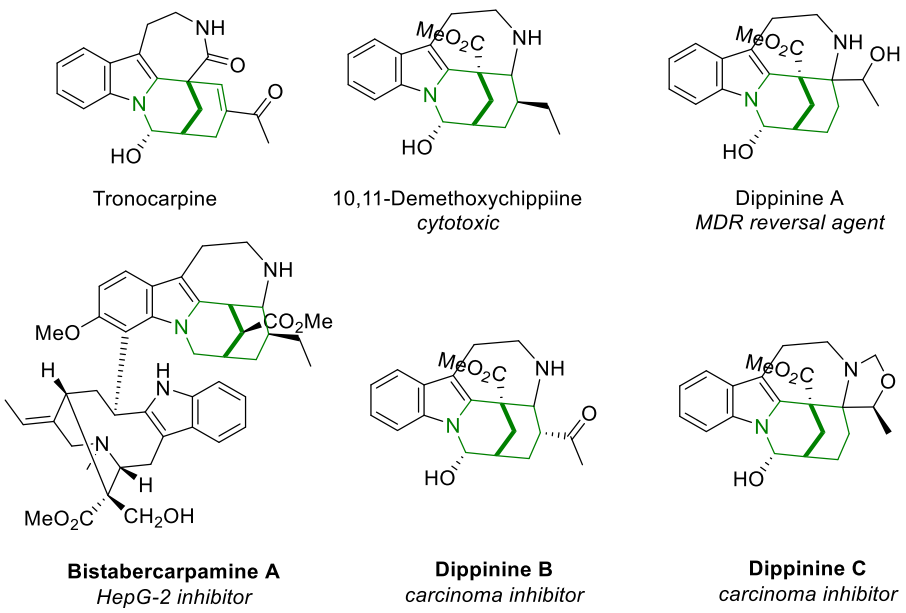

Figure 1-7: Tronocarpine and related chippiine analogues.

Synthetically, tronocarpine is an important target because it should be the most readily accessible in its class and may reasonably serve as a precursor to the rest of the chippiines through a Michael addition/rearrangement (Scheme 1-10). Additionally, elucidating the bioactivity of tronocarpine is dependent upon its total synthesis, as its relatively low abundance in nature hinders biological assay.

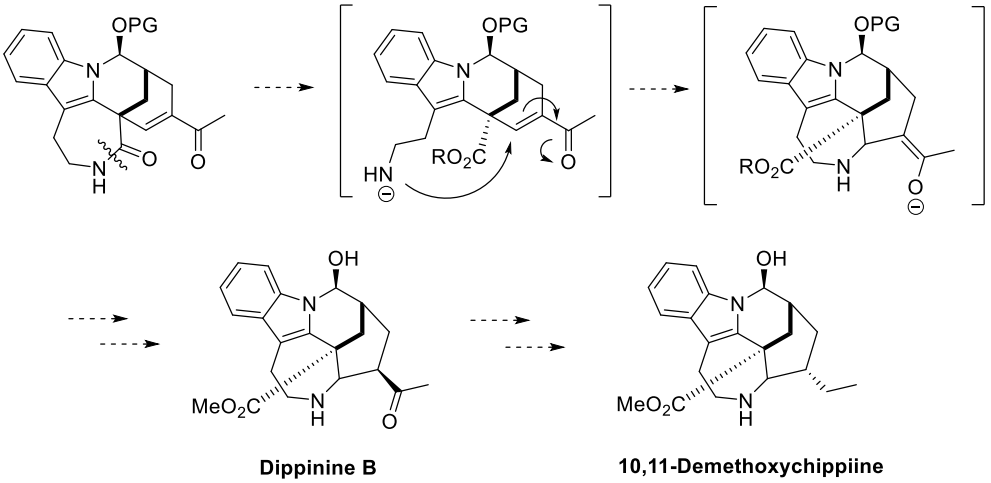

Scheme 1-10: Proposed preparation of dippinine B and 10,11-demethoxychippiine from tronocarpine.

There have been several published attempts toward the total synthesis of tronocarpine, but none have achieved the final target. Despite this, researchers have generally succeeded in accessing four rings of the pentacyle. The first publication attributed to this effort actually preceded discovery of tronocarpine: in 1995, Mahboobi and coworkers showcased the syntheses of various tetracyclic frameworks from 2-malonyl indoles, albeit in low yields (6 steps, < 6%) (Scheme 1-11).[49] Their key intermediate was a 3-(2-nitrovinyl)-2-dimethylmalonyl indole which could then undergo Michael-type additions to cyclize at the indole *N*. Oxidation of the alcohol, hydrogenation of the vinyl moiety, reduction of the nitro group, and acid-mediated condensation afforded the final lactam-containing tetracycle.

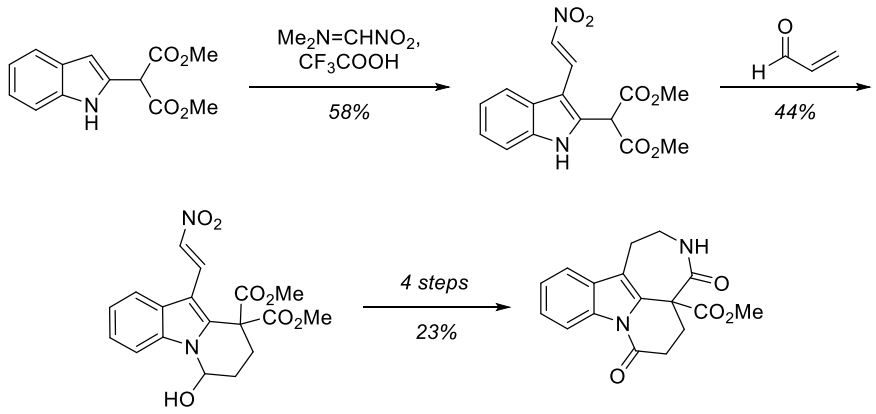

Scheme 1-11: Mahboobi's synthesis of the lactam-containing tetracycle in tronocarpine.

The next study would not be until 2006, when Magolan and Kerr published a concise synthesis the identical compound in three steps and 20% overall yield from 1*H*-indole-3-acetonitrile (Scheme 1-12).[50] After *N*-acylation with 2-methoxycarbonyl-pentanedioic acid chloride, their synthesis featured a Mn-mediated radical cyclization to generate the tricycle, followed by reduction over Raney Ni to afford the seven-membered lactam.

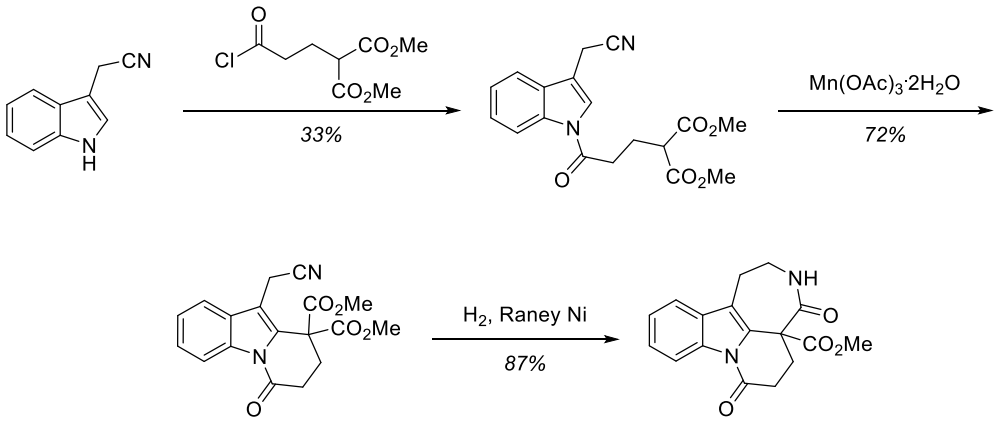

Scheme 1-12: Magolan and Kerr's synthesis of the lactam-containing tetracycle in tronocarpine.

Miranda and coworkers demonstrated an additional synthesis of this tetracycle in 2009 (Scheme 1-13).[51] Their overall strategy was similar to Mahboobi's, but their first step

showcased a radical oxidative xanthate addition to a protected tryptamine to result in the 2-malonyl indole. Subsequent cyclization, deprotection, and lactamization afforded the desired tetracycle, for a yield of 32% over four total steps.

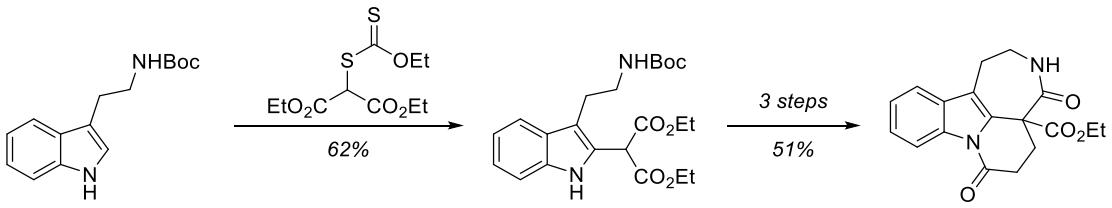

Scheme 1-13: Miranda's synthesis of the lactam-containing tetracycle in tronocarpine.

Further syntheses to access this tetracyclic skeleton include work from Hájícek,[52] and from Nidhiry and Prasad.[53]

The first successful synthesis of the bridged bicycle-containing tetracycle was also performed in 2009 by Sapeta and Kerr (Scheme 1-14).[54] Their methodology relied upon a stepwise [3+3] annulation of an indole-tethered donor-acceptor cyclopropane and 2-(chloromethyl)-3-trimethylsilyl-1-propene, and they accomplished this tetracycle in 6 steps with 31% overall yield.

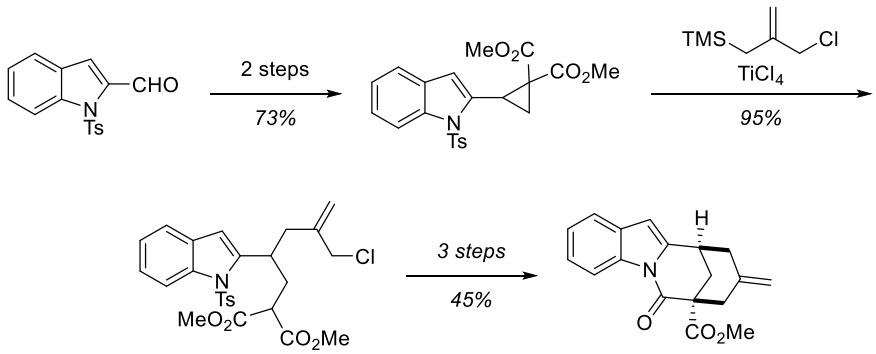

Scheme 1-14: Sapeta and Kerr's synthesis of the bridged bicycle-containing tetracycle in tronocarpine.

Finally, in one notable example, Martínez and coworkers achieved the entire pentacyclic skeleton in 2014 (Scheme 1-15).[48b] Building upon previous research with Miranda, after C2-addition of the malonyl xanthate, they incorporated additional functionality in their annulation step, which ultimately enabled them to generate the fifth ring through a Dieckmann condensation. Unfortunately, even in this case, the lack of useful functional handles in the final compound prevented the completion of the total synthesis.

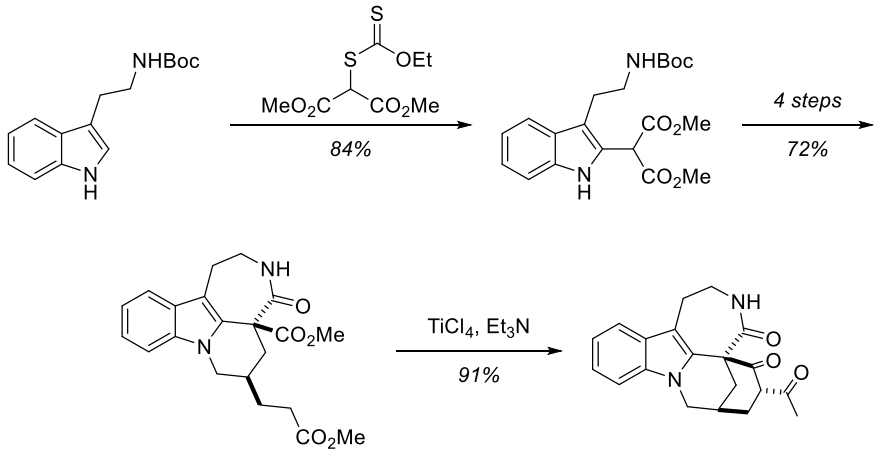

Scheme 1-15: Martínez's synthesis of the pentacyclic scaffold of tronocarpine.

At this time, there have been no further published synthetic studies regarding tronocarpine, and its bioactivity remains unknown. The key limitation seems to be construction of the bridged bicyclic moiety under conditions tolerant of synthetic handles necessary to complete final functionalizations. A novel intramolecular ring-opening cyclization to afford this scaffold may be the avenue to achieve a total synthesis of tronocarpine for the first time.

1.5.3 Rhazinicine

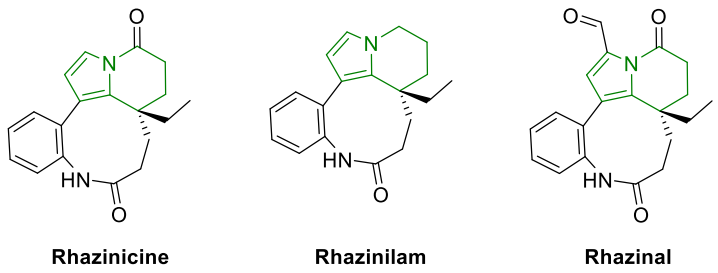

Figure 1-8: Rhazinicine and analogues.

Compared with tronocarpine, synthetic efforts toward rhazinicine and related compounds have been much more fruitful. From the Aspidosperma alkaloid family, rhazinicine is a tetracyclic 5,6,7,8-tetrahydroindolizine (THI) that has been identified as a potential antitumor agent (Figure 1-8). THIs in general can be prepared through reduction reactions of indolizines;[55] pyrrolidine annulations;[56] and [3+3]-cycloadditions,[57] and synthetic analogues rhazinilam[58] and rhazinal[59] have been achieved by these methods.

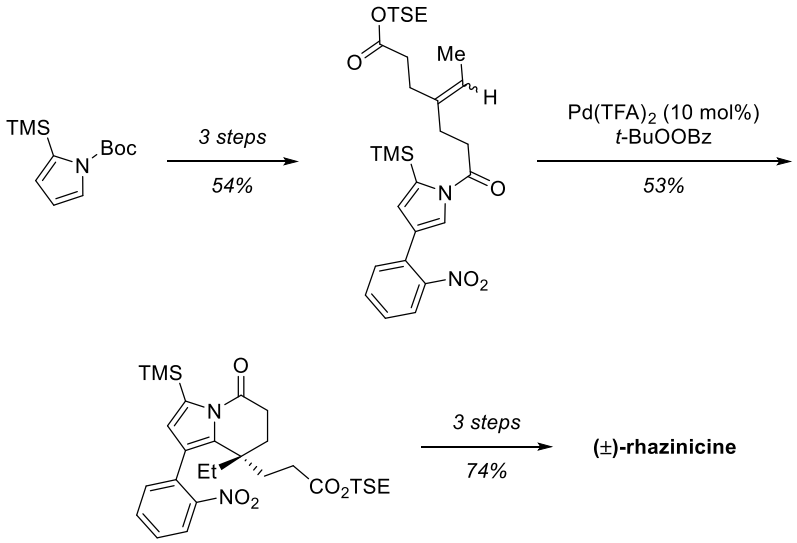

Scheme 1-16: Gaunt's total synthesis of rhazinicine.

This pyrrole alkaloid natural product has two reported total syntheses. First, in 2008, Gaunt performed a high-yielding albeit racemic total synthesis of rhazinicine through a regioselective C-H arylation dictated by the Boc protecting group, then a Suzuki coupling to form the THI core (Scheme 1-16, 21% yield over 8 steps).[60] Then, in 2013, Tokuyama developed an enantioselective total synthesis of (-)-rhazinicine (Scheme 1-17, 9% yield over 14 steps).[61] His synthesis featured a gold(I)-catalyzed cascade cyclization employing $[Au(PPh_3)]NTf_2$[62] to afford the THI core in a single step, with complete retention of stereochemistry. Significantly, his synthesis was also free of protecting groups, making his route greener and more expedient.[63]

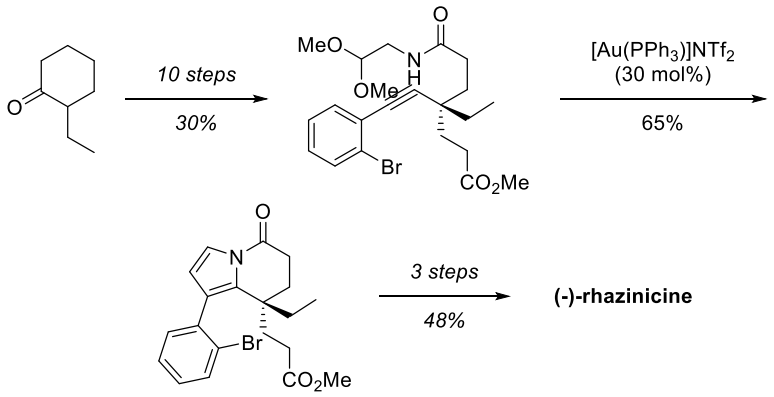

Scheme 1-17: Tokuyama's total synthesis of (-)-rhazinicine.

The structural similarities of the THI core to the hydropyrido[1,2-*a*]indole core found in indole alkaloids prompted a study to further develop the intramolecular Friedel-Crafts ring-opening cyclization of *N*-acyl DACPs to include pyrrole-based scaffolds. Pyrroles generally do not behave as predictably as other heterocycles,[64] so this would represent an important advancement in the field of *N*-heterocyclic synthetic methods.

1.6 Thesis Outline

This thesis proposes novel Friedel-Crafts-inspired methodologies to access the *N*-heteroaromatics featured: flubromazepam, tronocarpine, and rhazincine. Hypotheses and synthetic strategies will be outlined; experimental troublehooting will be discussed in detail; and advances in known synthetic methods will be highlighted.

Chapter 2 will cover various efforts toward the syntheses of variably halogen-substituted benzodiazepines, using the positional isomers of flubromazepam as a model. Chapter 3 will discuss the characterization data acquired for each of these positional isomers and offer recommendations for analytical differentiation.

Chapter 4 will outline methodology development toward intramolecular ring-opening cyclizations of C5-substituted donor-acceptor bicyclo[3.1.0]hexanes, inspired by the bridged bicyclic moiety of tronocarpine. Chapter 5 will survey an analogous class, C6-substituted donor-acceptor bicyclo[3.1.0]hexanes, and showcase an interesting stereochemical outcome of a model ring-opening cyclization. Chapter 6 will discuss synthetic attempts toward the total syntheses of rhazinicine and tronocarpine.

Chapter 7 will offer conclusions and future outlook for each research project herein.

1.7 References

(1) (a) Carson, C.A.; Kerr, M.A. Heterocycles from cyclopropanes: applications in natural product synthesis. *Chem. Soc. Rev.* **2009**, *38*, 3051-3060. (b) Kim, J.; Kim, H.; Park, S.B. Privileged Structures: Efficient Chemical "Navigators" toward Unexplored Biologically Relevant Chemical Spaces. *J. Am. Chem. Soc.* **2014**, *136*, 14629-14638. (c) Doveston, R.; Marsden, S.; Nelson, A. Towards the

realisation of lead-oriented synthesis. *Drug Discovery Today* **2014**, *18*, 813-819. (d) Garcia-Castro, M.; Zimmermann, S.; Sankar, M.G.; Kumar, K. Scaffold Diversity Synthesis and Its Application in Probe and Drug Discovery. *Angew. Chem. Int. Ed.* **2016**, *55*, 7586-7605. (e) Kalaria, P.N.; Karad, S.C.; Raval, D.K. A review on diverse heterocyclic compounds as the privileged scaffolds in antimalarial drug discovery. *Eur. J. Med. Chem.* **2018**, *158*, 917-936.

(2) Verma, A.; Yadav, M.; Giridhar, R.; Prajapati, N.; Tripathi, A.; Saraf, S. Nitrogen Containing Privileged Structures and their Solid Phase Combinatorial Synthesis. *Comb. Chem. High Throughput Screen.* **2013**, *16*, 345-393. (b) Kaur, N. An insight into medicinal and biological significance of privileged scaffold: 1,4-benzodiazepine. *Int. J. Pharma. Bio. Sci.* **2013**, *4*, 318. (c) Martin, S.F. Chapter Three - Strategies for the Synthesis of Alkaloids and Novel Nitrogen Heterocycles. *Adv. Heterocycl. Chem.* **2013**, *110*, 73-117. (d) Zhao, J.; Zhang, Q. Recent advances in directed intramolecular C(sp^3)-H amination reactions for construction of aza-heterocycles. *Huaxue Xuebao* **2015**, *73*, 1235-1244. (e) Patil, S.S.; Dandagvhal, K.R. Indole - an interesting scaffold in drug discovery. *Int. J. Res. Pharm. Chem.* **2016**, *6*, 301-311. (f) Gharpure, S.J.; Nanda, L.N. Application of oxygen/nitrogen substituted donor-acceptor cyclopropanes in the total synthesis of natural products. *Tetrahedron Lett.* **2017**, *58*, 711-720.

(3) Grabowski, K.; Baringhaus, K.-H.; Schneider, G. Scaffold diversity of natural products: inspiration for combinatorial library design. *Nat. Prod. Rep*. **2008**, *25*, 892-904.

(4) (a) Burke, M.D.; Schreiber, S.L. A Planning Strategy for Diversity-Oriented Synthesis. *Angew. Chem. Int. Ed.* **2003**, *43*, 46-58. (b) Grabowski, K.; Baringhaus, K.-H.; Schneider, G. Scaffold diversity of natural products: inspiration for combinatorial library design. *Nat. Prod. Rep*. **2008**, *25*, 892-904. (c) Cordier, C.; Morton, D.; Murrison, S.; Nelson, A.; O'Leary-Steele, C. Natural products as an inspiration in the diversity-oriented synthesis of bioactive compound libraries. *Nat. Prod. Rep*. **2008**, *25*, 719-737. (d) Shaw, J.T. Naturally diverse: highlights in versatile synthetic methods enabling target- and diversity-oriented synthesis. *Nat. Prod. Rep*. **2009**, *26*, 11-26. (e) Galloway, W.R.; Isidro-Ilobet, A.; Spring, D.R. Diversity-oriented synthesis as a tool for the discovery of novel biologically active small molecules. *Nature Comm.* **2010**, *1*, 80. (f) Serba, C.; Winssinger, N. Following the Lead from Nature: Divergent Pathways in Natural Product Synthesis and Diversity-Oriented Synthesis. *Eur. J. Org. Chem.* **2013**, *2013*, 4195-4214. (g) Sen, S.; Prabhu, G.; Bathula, C.; Hati, S. Diversity-Oriented Asymmetric Synthesis. *Synthesis* **2014**, *46*, 2099-2121. (h) Maier, M.E. Design and synthesis of analogues of natural products. *Org. Biomol. Chem.* **2015**, *13*, 5302-5343. (i) Pavlinov, I.; Gerlacha, E.M.; Aldrich, L.N. Next generation diversity-oriented synthesis: a paradigm shift from chemical diversity to biological diversity. *Org. Biomol. Chem.* **2019**, *17*, 1608-1623.

(5) (a) Campbell, M.G.; Ritter, T. Late-stage formation of carbon-fluorine bonds. *Chem. Rec.* **2014**, *14*, 482-491. (b) Cernak, T.; Dykstra, K.D.; Tyagarajan, S.; Vachal, P.; Krska, S.W. The medicinal chemist's toolbox for late stage functionalization of drug-like molecules. *Chem. Soc. Rev.* **2016**, *45*, 546-576. (c)

Parasram, M.; Gevorgyan, V. Silicon-Tethered Strategies for C-H Functionalization Reactions. *Acc. Chem. Res.* **2017**, *50*, 2038-2053. (d) Yerien, D.E.; Barata-Vallejo, S.; Postigo, A. Difluoromethylation Reactions of Organic Compounds. *Chem. Eur. J.* **2017**, *23*, 14676-14701. (e) Lu, X.; He, S.-J.; Cheng, W.-M.; Shi, J. Transition-metal-catalyzed C-H functionalization for late-stage modification of peptides and proteins. *Chin. Chem. Lett.* **2018**, *29*, 1001-1008. (f) White, M.C.; Zhao, J. Aliphatic C-H Oxidations for Late-Stage Functionalizations. *J. Am. Chem. Soc*. **2018**, *140*, 13988-14009.

(6) (a) Kuranaga, T.; Sesoko, Y.; Inoue, M. Cu-mediated enamide formation in the total synthesis of complex peptide natural products. *Nat. Prod. Rep.* **2014**, *31*, 514-532. (b) Heravi, M.M.; Hashemi, E.; Nazari, N. Negishi coupling: an easy progress for C-C bond construction in total synthesis. *Mol. Divers.* **2014**, *18*, 441-472. (c) Standley, E.A.; Tasker, S.Z.; Jensen, K.L.; Jamison, T.F. Nickel Catalysis: Synergy between Method Development and Total Synthesis. *Acc. Chem. Res.* **2015**, *48*, 1503-1514. (d) Sivanandan, S.T.; Shaji, A.; Ibnusaud, I.; Seechurn, C.C.; Colacot, T.J. Palladium-Catalyzed α-Arylation Reactions in Total Synthesis. *Eur. J. Org. Chem*. **2015**, *2015*, 38-49. (e) Zweig, J.E.; Kim, D.E.; Newhouse, T.R. Methods Utilizing First-Row Transition Metals in Natural Product Total Synthesis. *Chem. Rev.* **2017**, *117*, 11680-11752. (f) Heravi, M.M.; Mohammadkhani, L. Recent applications of Stille reaction in total synthesis of natural products. *J. Organometal. Chem.* **2018**, *869*, 106-200. (g) Prendergast, A.M.; McGlacken, G.P. Transition Metal Mediated C-H Activation of 2-Pyrones, 2-Pyridones, 2-Coumarins and 2-Quinolones. *Eur. J. Org. Chem.* **2018**, *2018*, 6068-6082.

(7) (a) Sunderhaus, J.D.; Martin, S.F. Applications of Multicomponent Reactions to the Synthesis of Diverse Heterocyclic Scaffolds. *Chem. Eur. J.* **2009**, *15*, 1300-1308. (b) Ganem, B. Strategies for Innovation in Multicomponent Reaction Design. *Acc. Chem. Res.* **2009**, *42*, 463-472. (c) Erdmann, N.; Philipps, A.R.; Atodiresei, I.; Enders, D. An Asymmetric Organocatalytic Quadruple Cascade Initiated by a Friedel–Crafts-Type Reaction with Electron-Rich Arenes. *Adv. Synth. Catal*. **2013**, *355*, 847-852. (d) Hall, D.G.; Rybak, T.; Verdelet, T. Multicomponent Hetero-[4 + 2] Cycloaddition/Allylboration Reaction: From Natural Product Synthesis to Drug Discovery. *Acc. Chem. Res.* **2016**, *49*, 2489-2500. (e) Ilich, A.; Ibarra, A. I.-J.; González-Zamora, E. Synthesis of polyheterocycles via multicomponent reactions. *Org. Biomol. Chem*. **2018**, *16*, 1402-1418.

(8) (a) Grondal, C.; Jeanty, M.; Enders, D. Organocatalytic cascade reactions as a new tool in total synthesis. *Nature Chem.* **2010**, *2*, 167-178. (b) Lu, L.-Q.; Chen, J.-R.; Xiao, W.-J. Development of Cascade Reactions for the Concise Construction of Diverse Heterocyclic Architectures. *Acc. Chem. Res.* **2012**, *45*, 1278-1293. (c) Gao, F.; Zhou, Y.; Liu, H. Recent Advances in the Synthesis of Heterocycles via Gold-catalyzed Cascade Reactions: A Review. *Curr. Org. Chem.* **2017**, *21*, 1530-1566.

(9) (a) Friedel, C.; Crafts, J.M. *Compt. Rend*. **1877**, *84*, 1392–1395. (b) Olah, G.A. Friedel-Crafts and Related Reactions. Interscience Publishers, **1964**. (c) Roberts, R.M.; Khalaf, A.A. Friedel-Crafts alkylation chemistry: a century of discovery. *Volume 10 of Studies in Organic Chemistry*. Dekker: University of

Michigan, **1984**. (d) Catalytic Assymmetric Friedel-Crafts Alkylations in Total Synthesis. Ed. Bandini, M.; Umani-Ronchi, A. Wiley VCH, **2009**. (e) Campbell, J.A. "Asymmetric Friedel-Crafts Reactions: Past to Present." *Name Reactions for Carbocyclic Ring Formations*. Wiley; 1 edition (**2010**). p. 600-674.

(10) (a) Bandini, M.; Emer, E.; Tommasi, S.; Umani-Ronchi, A. Innovative catalytic protocols for the ring-closing Friedel-Crafts-type alkylation and alkenylation of arenes. *Eur. J. Org. Chem.* **2006**, *2006*, 3527-3544. (b) Chen, M.; Fan, H.; Li, X. Applications of intramolecular Friedel-Crafts cyclization reaction in chemical synthesis of benzo-fused ring systems. *Huaxue Yanjiu* **2010**, *21*, 106-112. (c) Nachtsheim, B.J. Catalytic Asymmetric Friedel–Crafts Alkylations in Total Synthesis. *Belstein J. Org. Chem.* **2010**, 6. (d) Bandini, M.; Umani-Ronchi, A.; Blay, G.; Pedro, J.R; Vila, C. Catalytic Asymmetric Friedel–Crafts Alkylations, **2009**, p.223-270 (e) Maltsev, O.V. Beletskaya, I.P.; Zlotin, S.G. Organocatalytic Michael and Friedel–Crafts reactions in enantioselective synthesis of biologically active compounds. *Russ. Chem. Rev.* **2011**, *80*, 1067-1113. (f) Dell'Acqua, M.; Facoetti, D.; Pirovano, V.; Abbiati, G.; Rossi, E. Recent advances in gold catalyzed inter- and intramolecular functionalization of heteroaromatic compounds. *Targets in Heterocyclic Systems* **2011**, *15*, 86-139. (g) Cavitt, M.A.; Phun, L.H.; France, S. Intramolecular donor-acceptor cyclopropane ring-opening cyclizations. *Chem. Soc. Rev.* **2014**, *43*, 804-818. (h) Sánchez-Roselló, M.; Aceña, J.L.; Simón-Fuentes, A.; del Pozo, C. A general overview of the organocatalytic intramolecular aza-Michael reaction. *Chem. Soc. Rev.* **2014**, *43*, 7430-7453. (i) Sun, D.; Li, B.; Lan, J.; Huang, Q.; You, J. Chelation-assisted Pd-catalysed *ortho*-selective oxidative C–H/C–H

cross-coupling of aromatic carboxylic acids with arenes and intramolecular Friedel–Crafts acylation: one-pot formation of fluorenones. *Chem. Commun.* **2016**, *52*, 3635-3638. (j) Nemoto, T.; Hamada, Y. Synthesis of Spirocyclic and Fused Cyclic Compounds by Transition-Metal-Catalyzed Intramolecular Friedel-Crafts-Type Reactions of Phenol Derivatives. *Synlett* **2016**, *27*, 2301-2313. (k) Das, S.K. Recent Advances in the Intramolecular Reactions of Epoxides with Arenes and Heteroarenes. *Asian J. Org. Chem.* **2017**, *6*, 243-256. (l) Heravi, M.M.; Zadsirjan, V.; Saedi, P.; Momeni, T. Applications of Friedel–Crafts reactions in total synthesis of natural products. *RSC Adv.* **2018**, *8*, 40061-40163. (m) Heydari, M.; Heravi, M.M. Organometal-catalyzed asymmetric Friedel-Crafts reactions. *J. Organometal. Chem.* **2019**, *879*, 78-138.

(11) (a) Wang, S.; Chai, Z.; Zhou, S.; Wang, S.; Zhu, W.; Wei, Y. A Novel Lewis Acid Catalyzed [3 + 3]-Annulation Strategy for the Syntheses of Tetrahydro-β-Carbolines and Tetrahydroisoquinolines. *Org. Lett.* **2013**, *15*, 2628-2631. (b) Yokosaka, T.; Kanehira, T.; Nakayama, H.; Nemoto, T.; Hamada, Y. Synthesis of fused-tricyclic indole derivatives through an acid-promoted skeletal rearrangement. *Tetrahedron* **2014**, *70*, 2151-2160. (c) Hansen, C.L.; Ohm, R.G.; Olsen, L.B.; Ascic, E.; Tanner, D.; Nielsen, T.E. Catalytic Enantioselective Synthesis of Tetrahydocarbazoles and Exocyclic Pictet–Spengler-Type Reactions. *Org. Lett.* **2016**, *18*, 5990-5993. (d) Khunnawutmanotham, N.; Sahakitpichan, P.; Chimnoi, N.; Techasakul, S. Efficient One-Pot Synthesis of Tetrahydronaphtho[2,1-*f*]isoquinolines by Using Domino Pictet–Spengler/Friedel–Crafts-Type Reactions. *Eur. J. Org. Chem.* **2017**, *2017*, 6434-6440.

(12) (a) Cao, Y.J.; Cheng, H.G.; Lu, L.Q.; Zhang, J.J.; Cheng, Y.; Chen, J.R.; Xiao, W.J. Organocatalytic Multiple Cascade Reactions: A New Strategy for the Construction of Enantioenriched Tetrahydrocarbazoles. *Adv. Synth. Catal*. **2011**, *353*, 617-623. (b) Pan, J.; Wang, Y.; Chen, S.; Zhang, X.; Wang, Y.; Zhou, Z. Stereocontrolled construction of 2-(3-indolyl)chromane scaffolds via organocatalyzed cascade Michael addition-hemiketalization followed by Friedel-Crafts alkylation reaction. *Tetrahedron* **2016**, *72*, 240-246. (c) Guo, J.; Bai, X.; Wang, Q.; Bu, Z. Diastereoselective Construction of Indole-Bridged Chroman Spirooxindoles through a TfOH-Catalyzed Michael Addition-Inspired Cascade Reaction. *J. Org. Chem.* **2018**, 83, 7, 3679-3687. (d) Lee, S. G.; Sin, S.; Kim, S.; Kim, S.G. Lewis acid-catalyzed Friedel-Crafts/Michael cascade reaction of *N*,*N*-dialkyl-3-vinylanilines with *N*-tosylaziridines for the stereoselective synthesis of highly functionalized tetrahydroisoquinolines. *Tetrahedron Lett*. **2018,** *59*, 1480-1483.

(13) Chandrashekhar, R.; Vemulapalli, S.P.B.; Sridhar, B.; Reddy, B.V.S Stereoselective Construction of Spiro-Indolenine Frameworks through a Prins/Friedel–Crafts Cyclization Cascade Reaction. *Eur. J. Org. Chem*. **2018**, *2018*, 1693–1698.

(14) (a) Liu, Y.; Meng, G.; Liu, R.; Szostak, M. Sterically-controlled intermolecular Friedel–Crafts acylation with twisted amides via selective N–C cleavage under mild conditions. *Chem. Commun.* **2016**, *52*, 6841-6844. (b) Liu, C.; Szostak, M. Twisted Amides: From Obscurity to Broadly Useful Transition-Metal-

Catalyzed Reactions by N-C Amide Bond Activation. *Chem. Eur. J.* **2017**, *23*, 7157-7173

(15) Kinney, R.G.; Tjutrins, J.; Torres, G.M.; Jiabao Liu, N.J.; Kulkarni, O.; Arndtsen, B.A. A general approach to intermolecular carbonylation of arene C–H bonds to ketones through catalytic aroyl triflate formation. *Nature Chem*. **2018**, *10*, 193-198.

(16) (a) Smith, D.B.; Cox, G.; Gilbert, A. *J. Chem. Soc. D* **1971**, 914. (b) Voronkov, M.G.; Vlasova, N.N.; Vlasov, A.V.; Grigor´eva, O.Y. *Dokl. Chem. (Engl. Transl.)* **2010**, *435*, 294; (c) Vlasova, A.V. *Russ. Chem. Bull., Int. Ed.* **2013**, *62*, 1945.

(17) Tripathi, S.; Singh, S.N.; Yadav, L.D.S. Metal-free efficient cross coupling of aromatic aldehydes with aryldiazonium tetrafluoroborates using DTBP as a radical initiator. *Tetrahedron Lett.* **2015**, *56*, 4211.

(18) Serratore, N.A.; Anderson, C.B.; Frost, G.B.; Hoang, T.-G.; Underwood, S.J.; Gemmel, P.M.; Hardy, M.A.; Douglas, C.J. Integrating Metal-Catalyzed C–H and C–O Functionalization To Achieve Sterically Controlled Regioselectivity in Arene Acylation. *J. Am. Chem. Soc*. **2018**, *140*, 10025-10033.

(19) (a) Schmitz A. Benzodiazepine use, misuse, and abuse: A review. *Ment. Health Clin*. **2016**, *6*, 120-126. (b) Griffin, C. E.; Kaye, A. M.; Bueno, F. R.; Kaye, A. D. Benzodiazepine pharmacology and central nervous system-mediated effects. *Ochsner J*. **2013**, *13*, 214-23. (c) Cascade, E.; Kalali, A. H. Use of benzodiazepines in the treatment of anxiety. *Psychiatry* **2008**, *5*, 21–22. (d) Nordqvist, J. (**2018**, January 5). "The benefits and risks of benzodiazepines." *Medical News Today*.

Retrieved from https://www.medicalnewstoday.com/articles/262809.php. (e) The emergence of new psychoactive substance (NPS) benzodiazepines: A review. *Drug Test Anal.* **2018**, *10*, 37–53; (f) Wick, J. The History of Benzodiazepines. *Consult. Pharm.* **2013**, *28*, 538-548; (g) Miller, N. S.; Gold, M. S. Benzodiazepines: Reconsidered. *Adv. Alcohol Subst. Abuse* **1990**, *8*, 67-84. (h) "Drug Fact Sheet: Benzodiazepines." **2017** Edition. Drug Enforcement Administration, https://www.dea.gov/sites/default/files/sites/getsmartaboutdrugs.com/files/publications/DoA_2017Ed_Updated_6.16.17.pdf#page=59.

(20) (a) Sternbach, L.H.; Reeder, E. Quinazolines and 1,4-Benzodiazepines. IV. Transformations of 7-Chloro-2-methylamino-5-phenyl-3H-1,4-benzodiazepine 4-Oxide. *J. Org. Chem.* **1961**, *26*, 4936-4941. (b) Bell, S.C.; Sulkowski, T.S.; Gochman, C.; Childress, S.J. 1,3-Dihydro-2H-1,4-benzodiazepine-2-ones and Their 4-Oxides. *J. Org. Chem*. **1962**, *27*, 562-566. (c) Sternbach, L.H.; Fryer, R.I.; Metlesics, W.; Reeder, E.; Sach, G.; Saucy, G.; Stempel, A. Quinazolines and 1,4-Benzodiazepines. V. *o*-Aminobenzophenones. *J. Org. Chem*. **1962**, *27*, 3781-3788. (d) Sternbach, L.H.; Fryer, R.I.; Metlesics, W.; Reeder, E.; Sach, G.; Saucy, G.; Stempel, A. Quinazolines and 1,4-Benzodiazepines. VI. Halo-, Methyl-, and Methoxy-substituted 1,3-Dihydro-5-phenyl-2H-1,4-benzodiazepin-2-ones. *J. Org. Chem*. **1962**, *27*, 3788-3796. (e) Reeder, E.; Nutley; Sternbach, L.H. US3136815, **1964**. (f) Cook. J.M.; Huang, Q.; He, X.; Li, X.; Yu, J.; Han, D. WO 03/082832 A2, **2003**.

(21) Sahu, K. B.; Banerjee, M.; Ghosh, S.; Maity, A.; Mondal, S.; Paira, R.; Hazra, A.; Karmakar, S.; Samanta, A.; Mondal, N. B. I_2 catalyzed Friedel–Crafts

alkylation reaction of substituted anilines with ninhydrin: formation of novel products and their antimicrobial evaluation. *Med. Chem. Res*. **2013**, *22,* 2023-2037.

(22) Anslyn, E.V.; Dougherty, D.A. "Strain and Stability." *Modern Physical Organic Chemistry*. University Science Books: **2006,** p. 100.

(23) Schneider, T.F.; Werz, D.B. Ring-Enlargement Reactions of Donor−Acceptor-Substituted Cyclopropanes: Which Combinations are Most Efficient? *Org. Lett.* **2011**, *13*, 1848-1851.

(24) Reißig, H.-U. Donor-acceptor-substituted cyclopropanes: Versatile building blocks in organic synthesis. *Top. Curr. Chem.* **1988**, *144*, 73-135.

(25) Rambaud, R. *Bull. Soc. Chim. Fr*. **1938**, 1552.

(26) (a) Yu, M.; Pagenkopf, B.L. Recent advances in donor–acceptor (DA) cyclopropanes. *Tetrahedron* **2005,** *61*, 321-347. (b) Bos, M.; Poisson, T.; Pannecoucke, X.; Charette, A.B.; Jubault, P. Recent Progress Toward the Synthesis of Trifluoromethyl- and Difluoromethyl-Substituted Cyclopropanes. *Chem. Eur. J.* **2017**, *23*, 4950-4961. (c) Tomilov, Y.V.; Menchikov, L.G.; Novikov, R.A.; Ivanova, O.A.; Trushkov, I.V. Methods for the synthesis of donor-acceptor cyclopropanes. *Russ. Chem. Rev*. **2018**, *87*, 201-250. (d) Dian, L.; Marek, I. Asymmetric Preparation of Polysubstituted Cyclopropanes Based on Direct Functionalization of Achiral Three-Membered Carbocycles. *Chem. Rev.* **2018,** *118*, 8415-8434.

(27) (a) Stork, G.; Marx, M. Six-membered rings via olefin participation in the opening of acylcyclopropanes. *J. Am. Chem. Soc.* **1969**, *91*, 2371-2373. (b) Stork, G.; Gregson, M. Aryl participation in concerted cyclization of cyclopropyl ketones.

J. Am. Chem. Soc. **1969**, *91*, 2373-2374. (c) Stork, G.; Grieco, P.A. Olefin participation in the acid-catalyzed opening of acylcyclopropanes. III. Formation of the bicyclo[2.2.1]heptane system. *J. Am. Chem. Soc.* **1969**, *91*, 2407-2408. (d) Stork, G.; Grieco, P.A. Olefin participation in the acid-catalyzed opening of acylcyclopropanes. IV. Cyclization of 5-methyl-6-endo-(trans-3-pentenyl)bicyclo(3.1.0)hexan-2-one. *Tetrahedron Lett.* **1971**, *12*, 1807-1810. (e) Grieco, P.A.; Finkelhor, R.S. Studies on the acid-catalyzed opening of non-rigid acylcyclopropanes: a dramatic solvent effect. A route to the bicyclo[2.2.1]heptane ring system. *Tetrahedron Lett.* **1974**, *15*, 527-530.

(28) Wenkert, E., Greenberg, R. S., Raju, M. S. Oxocyclopentenol syntheses. *J. Org. Chem*. **1985**, *50*, 4681-4685.

(29) Abdallah, H., Grée, R., Carrié, R. Synthese et reactivite d'oxycyclopropanes electrophiles. *Tetrahedron* **1985**, *41*, 4339-4346.

(30) Wenkert, E., Alonso, M. E., Buckwalter, B. L., Chou, K. J. A method of synthesis of β-methylfurans and α-methylene and β-methylene γ-lactones. Two menthofuran syntheses. *J. Am. Chem. Soc.* **1977**, *99*, 4778-4782.

(31) Zschiesche, R., Grimm, E. L., Reissig, H.-U. Intramolecular Diels–Alder Reactions with Methyl 2-Trimethylsiloxy-2-vinylcyclopropanecarboxylates as Key Building Blocks. *Angew. Chem. Int. Ed. Engl.* **1986**, *25*, 1086-1087.

(32) (a) Nazarov, I.N.; Zaretskaya, I.I. Acetylene derivatives, XVII. Hydration of hydrocarbons of the divinylacetylene series. *Izv. Akad. Nauk. SSSR, Ser. Khim*. **1941**, 211. (b) Pellissier, H. Recent developments in the Nazarov process. *Tetrahedron* **2005**, *61*, 6479-6517. (c) Frontier, A. J.; Collison, C. The Nazarov

cyclization in organic synthesis. Recent advances. *Tetrahedron* **2005**, *61*, 7577. (d) Tius, M. A. Some New Nazarov Chemistry. *Eur. J. Org. Chem.* **2005**, *2005*, 2193-2206. (e) Nakanishi, W.; West, F. G. Advances in the Nazarov cyclization. *Curr. Opin. Drug Discovery Dev.* **2009**, *12*, 732-751.

(33) Tsuge, O.; Kanemasa, S.; Otsuka, T.; Suzuki, T. Synthesis and Acid-Catalyzed Ring Opening of 1-Alkenyl Cyclopropyl Ketones. *Bull. Chem. Soc. Jpn.* **1988**, *61*, 2897-2908.

(34) De Simone, F.; Andres, J.; Torosantucci, R.; Waser, J. Catalytic Formal Homo-Nazarov Cyclization. *Org. Lett.* **2009**, *11*, 1023-1026.

(35) Patil, D.V.; Phun, L.H.; France, S. Indium-Catalyzed Homo-Nazarov Cyclizations of Alkenyl Cyclopropyl Ketones. *Org. Lett.* **2010**, *12*, 5684-5687.

(36) Phun, L.H.; Patil, D.V.; Cavitt, M.A.; France, S. A catalytic homo-Nazarov cyclization protocol for the synthesis of heteroaromatic ring-fused cyclohexanones. *Org. Lett.* **2011**, *13*, 1952-1955.

(37) Patil, D.V.; Cavitt, M.A.; Grzybowski, P.; France, S. An efficient synthesis of hydropyrido [1,2-*a*]indole-6(7H)-ones via an In(III)-catalyzed tandem cyclopropane ring-opening/Friedel–Crafts alkylation sequence. *Chem. Commun.* **2011**, *47*, 10278-10280.

(38) (a) Williams, C.W.; Shenje, R.; France, S. Catalytic, Interrupted Formal Homo-Nazarov Cyclization with (Hetero)arenes: Access to α-(Hetero)aryl Cyclohexanones. *J. Org. Chem.* **2016**, *81*, 8253-8267. (b) Sandridge, M.J.; France, S. Calcium-Catalyzed, Dehydrative, Ring-Opening Cyclizations of Cyclopropyl Carbinols Derived from Donor–Acceptor Cyclopropanes. *Org. Lett.* **2016**, *18*,

4218-4221. (c) Martin, M.C.; Shenje, R.; France, S. The Catalytic, Formal Homo-Nazarov Cyclization as a Template for Diversity-Oriented Synthesis. *Isr. J. Chem.* **2016**, *56*, 499-511. (d) Martin, M.C.; Sandridge, M.J.; Williams, C.W.; Francis, Z.A.; France, S. Dehydrative Nazarov-type electrocyclizations of alkenyl (hetero)aryl carbinols via calcium catalysis: Access to cyclopenta[*b*]thiophenes and indene derivatives. *Tetrahedron* **2017**, *73*, 4093-4108.

(39) (a) Patil, D.V.; Cavitt, M.A.; France, S. Diastereoselective Intramolecular Friedel-Crafts Cyclizations of Substituted Methyl 2-(1H-Indole-1-Carbonyl)acrylates: Efficient Access to Functionalized 1*H*-Pyrrolo[1,2-*a*]indoles. *Org. Lett.* **2011**, *13*, 5820-5823. (b) Patil, D.V.; Cavitt, M.A.; Grzybowski, P.; France, S. A general intramolecular Friedel–Crafts approach to functionalized pyrrolo[3,2,1-*ij*]quinolin-4-ones. *Chem. Commun*. **2012**, *48*, 10337-10339.

(40) Patil, D.V.; Cavitt, M.A.; France, S. DIASTEREOSELECTIVE SYNTHESIS OF (±)-DEETHYLEBURNAMONINE USING A CATALYTIC CYCLOPROPANE RING-OPENING/FRIEDEL-CRAFTS ALKYLATION STRATEGY. *Heterocycles* **2012**, *84*, 1363-1373.

(41) Aponte-Guzman, J.; Shenje, R.; Huang, Y.; Woodham, W.; Saunders, S.R.; Mostaghimi, S.; Flack, K.; Pollet, P.; Eckert, C.; Liotta, C.; France, S. A Tandem, Bicatalytic Continuous Flow Cyclopropanation-Homo-Nazarov-Type Cyclization. *Ind. Eng. Chem. Res.* **2015**, *54*, 9550-9558.

(42) Takada, S.; Takaki, N.; Yamada, K.; Nishii, Y. A formal homo-Nazarov cyclization of enantioenriched donor–acceptor cyclopropanes and following

transformations: asymmetric synthesis of multi-substituted dihydronaphthalenes. *Org. Biomol. Chem*. **2017**, *15*, 2443-2449.

(43) Ivanova, O.A.; Andronov, V.A.; Vasin, V.S.; Shumsky, A.N.; Rybakov, V.B.; Voskressensky, L.G.; Trushkov, I.V. Expanding the Reactivity of Donor–Acceptor Cyclopropanes: Synthesis of Benzannulated Five-Membered Heterocycles via Intramolecular Attack of a Pendant Nucleophilic Group. *Org. Lett.* **2018**, *20*, 7947-7952.

(44) Zhang, C.; Tian, J.; Ren, J.; Wang, Z. Intramolecular Parallel [4+3] Cycloadditions of Cyclopropane 1,1-Diesters with [3]Dendralenes: Efficient Construction of [5.3.0]Decane and Corresponding Polycyclic Skeletons. *Chem. Eur. J.* **2017**, *23*, 1231-1236.

(45) Dawande, S.G.; Harode, M.; Kalepu, J.; Katukojvala, S. Ag(I)-catalyzed intramolecular transannulation of enynone tethered donor–acceptor cyclopropanes: a new synthesis of 2,3-dihydronaphtho[1,2-*b*]furans. *Chem. Commun.* **2016**, *52*, 13699-13701.

(46) (a) England, D.B.; Kuss, T.D.O.; Keddy, R.G.; Kerr, M.A. Cyclopentannulation of 3-Alkylindoles: A Synthesis of a Tetracyclic Subunit of the Kopsane Alkaloids. *J. Org. Chem.* **2001**, *66*, 4704-4709. (b) Kerr, M.A.; Keddy, R.G. The annulation of 3-alkylindoles with 1,1-cyclopropanediesters. *Tetrahedron Lett.* **1999**, *40*, 5671–5675.

(47) Kam, T.-S.; Sim, K.-M.; Lim, T.-M. Tronocarpine, a novel pentacyclic indole incorporating a seven-membered lactam moiety. *Tetrahedron Lett*. **2000**, *41*, 2733-2736.

(48) (a) Kam, T.-S.; Sim, K.-M.; Pang, H.S.; Koyano, T.; Hayashi, M.; Komiyama, K. Cytotoxic effects and reversal of multidrug resistance by ibogan and related indole alkaloids. *Bioorg. Med. Chem. Lett.* **2004**, *14*, 4487-4489. (b) Torres-Ochoa, R.O.; Reyes-Gutiérrez, P.E.; Martínez, R. Synthesis of the Pentacyclic Framework of the Alkaloid Tronocarpine. *Eur. J. Org. Chem*. **2014**, *2014*, 48-52. (c) Ma, K.; Wang, J.-S.; Luo, J.; Yang, M.-H.; Yao, H.-Q.; Sun, H.-B.; Kong, L.-Y. Bistabercarpamines A and B, first vobasinyl-chippiine-type bisindole alkaloid from *Tabernaemontana corymbosa*. *Tetrahedron Lett.* **2014**, *55*, 101-104. (d) Ma, K.; Wang, J.-S.; Luo, J.; Yang, M.-H.; Kong, L. Tabercarpamines A–J, Apoptosis-Inducing Indole Alkaloids from the Leaves of *Tabernaemontana corymbosa. J. Nat. Prod*. **2014**, *77*, 1156-1163.

(49) Mahboobi, S.; Burgemeister, T.; Kastner, F. Synthese von Carbazolderivaten, 1. Mitt.: Über die Reaktion von 3-(2-Nitroethenyl)indol-2-malonestern mit *Michael*-Akzeptoren. *Arch. Pharm.* **1995**, *328*, 29-38.

(50) Magolan, J.; Kerr, M. Expanding the Scope of $Mn(OAc)_3$-Mediated Cyclizations: Synthesis of the Tetracyclic Core of Tronocarpine. *Org. Lett*. **2006**, *8*, 4561-4564.

(51) Reyes-Gutiérrez, P.E.; Torres-Ochoa, R.O.; Martínez, R.; Miranda, L.D. Synthesis of azepino[4,5-*b*]indolones via an intermolecular radical oxidative substitution of N-Boc tryptamine. *Org. Biomol. Chem*. **2009**, *7*, 1388-1396.

(52) Hájícek, J. Recent developments in syntheses of the post-secodine indole alkaloids. Part III: Rearranged alkaloid types. *Collect. Czechoslov. Chem. Commun*. **2011**, *76*, 2023-2083.

(53) Nidhiry, J.E.; Prasad, K.R. Synthesis of Azepino[4,5-*b*]indolones by an Intramolecular Cyclization of -Unsaturated Tryptamides. *Synlett* **2014**, *25*, 2585-2590.

(54) Sapeta, K.; Kerr, M.A. Synthesis of Cyclohexanes via [3 + 3] Hexannulation of Cyclopropanes and 2-Chloromethyl Allylsilanes. *Org. Lett*. **2009**, *11*, 2081-2084.

(55) Teodoro, B.V.M.; Correia, J.T.M.; Coelho, F. Selective Hydrogenation of Indolizines: An Expeditious Approach To Derive Tetrahydroindolizines and Indolizidines from Morita–Baylis–Hillman Adducts. *J. Org. Chem*. **2015**, *80*, 2529-2538.

(56) Capomolla, S.S.; Lim, N.-K.; Zhang, H. Single-Step Synthesis of 5,6,7,8-Tetrahydroindolizines via Annulation of 2-Formylpiperidine and 1,3-Dicarbonyl Compounds. *Org. Lett*. **2015,** *17*, 3564-3567.

(57) Ghosh, S.K.; Buchanan, G.S.; Long, Q.A.; Wei, Y.; Al-Rashid, Z.F.; Sklenicka, H.M.; Hsung, R.P. Aza- and carbo-[3+3] annulations of *exo*-cyclic vinylogous amides and urethanes. Synthesis of tetrahydroindolizidines and an unexpected formation of hexahydroquinolines. *Tetrahedron* **2008**, *64*, 883-893.

(58) (a) Ratcliffe, A.H.; Smith, G.F.; Smith, G.N. The synthesis of rhazinilam. *Tetrahedron Lett*. **1973**, *14*, 5179-5184. (b) Johnson, J.A.; Sames, D. C−H Bond Activation of Hydrocarbon Segments in Complex Organic Molecules: Total Synthesis of the Antimitotic Rhazinilam. *J. Am. Chem. Soc*. **2000**, *122*, 6321-6322. (c) Johnson, J.A.; Li, N.; Sames, D. Total Synthesis of (−)-Rhazinilam: Asymmetric C−H Bond Activation via the Use of a Chiral Auxiliary. *J. Am. Chem.*

Soc. **2002**, *124*, 6900-6903. (d) Magnus, P.; Rainey, T. Concise synthesis of (±)-rhazinilam. *Tetrahedron* **2001**, *57*, 8647-8651. (e) Banwell, M.G.; Beck, D.A.S.; Willis, A.C. Enantioselective total syntheses of the alkaloids (−)-rhazinal, (−)-rhazinilam, (−)-leuconolam and (+)-*epi*-leuconolam. *ARKIVOC* **2006**, *3*, 163-174. (f) Bowie, A.L., Jr.; Hughes, C.C.; Trauner, D. Concise Synthesis of (±)-Rhazinilam through Direct Coupling. *Org. Lett.* **2005**, *7*, 5207-5209. (g) Liu, Z.; Wasmuth, A.S.; Nelson, S.G. Au(I)-Catalyzed Annulation of Enantioenriched Allenes in the Enantioselective Total Synthesis of (−)-Rhazinilam. *J. Am. Chem. Soc.* **2006**, *128*, 10352-10353.

(59) (a) Banwell, M.G.; Edwards, A.J.; Jolliffe, K.A.; Smith, J.A.; Hamel, E.; Verdier-Pinard, P. Total synthesis of (±)-rhazinal, an alkaloidal spindle toxin from *Kopsia teoi*. *Org. Biomol. Chem*. **2003**, *1*, 296-305. (b) Bowie, A.L., Jr.; Trauner, D. Total Synthesis of (±)-Rhazinal Using Novel Palladium-Catalyzed Cyclizations. *J. Org. Chem*. **2009**, *74*, 1581-1586. (c) Sui, X.; Zhu, R.; Li, G.; Ma, X.; Gu, Z. Pd-Catalyzed Chemoselective Catellani *Ortho*-Arylation of Iodopyrroles: Rapid Total Synthesis of Rhazinal. *J. Am. Chem. Soc.* **2013**, *135*, 9318-9321.

(60) (a) Beck, E.M.; Hatley, R.; Gaunt, M.J. *Angew. Chem. Int. Ed.* **2008**, *47*, 3004-3007. (b) Beck, E.M.; Grimster, N.P.; Hatley, R.; Gaunt, M.J. Mild Aerobic Oxidative Palladium (II) Catalyzed C−H Bond Functionalization: Regioselective and Switchable C−H Alkenylation and Annulation of Pyrroles. *J. Am. Chem. Soc.* **2006**, *128*, 2528-2529.

(61) Sugimoto, K.; Toyoshima, K.; Nonaka, S.; Kotaki, K.; Ueda, H.; Tokuyama, H. Protecting-Group-Free Total Synthesis of (−)-Rhazinilam and (−)-

Rhazinicine using a Gold-Catalyzed Cascade Cyclization. *Angew. Chem. Int. Ed.* **2013**, *52*, 7168-7171.

(62) Mézailles, N.; Ricard, L.; Gagosz, F. Phosphine Gold(I) Bis-(trifluoromethanesulfonyl)imidate Complexes as New Highly Efficient and Air-Stable Catalysts for the Cycloisomerization of Enynes. *Org. Lett.* **2005**, *7*, 4133–4136.

(63) Young, I.S.; Baran, P.S. Protecting-group-free synthesis as an opportunity for invention. *Nature Chem.* **2009**, *1*, 193–205.

(64) Schmuck, C.; Rupprecht, D. The Synthesis of Highly Functionalized Pyrroles: A Challenge in Regioselectivity and Chemical Reactivity. *Synthesis* **2007**, *20*, 3095-3110.

CHAPTER 2. SYNTHESIS OF FLUBROMAZEPAM POSITIONAL ISOMERS FOR FORENSIC ANALYSIS

2.1 Designer Benzodiazepines: A Growing Problem in Forensics

Benzodiazepines constitute a large class of pharmaceutical compounds that exhibit sedative, depressant, and relaxant properties.[1-4] Phenazepam (**1**), for instance, is currently obtainable in most states as a research chemical self-prescribed for insomnia, anxiety, and opiate withdrawal (Figure 2-1).[5,6] Though still prescribed for medicinal purposes, many benzodiazepines, such as diazepam (Valium®, **2**) and alprazolam (Xanax®, **3**), have become federally controlled under Schedule IV due to their abuse and addiction potential.[7] As a result, designer benzodiazepines have entered the recreational market as legal alternatives to Schedule IV benzodiazepines since the early 2010s. Among them, flubromazepam (**4**), its triazole counterpart flubromazolam (**5**), and etizolam (**6**), a structurally similar triazolothienobenzodiazepine, were listed in the most recent annual Drug Enforcement Administration (DEA) Emerging Threat Report as the benzodiazepine designer drugs most frequently seized and analyzed in the United States.[8]

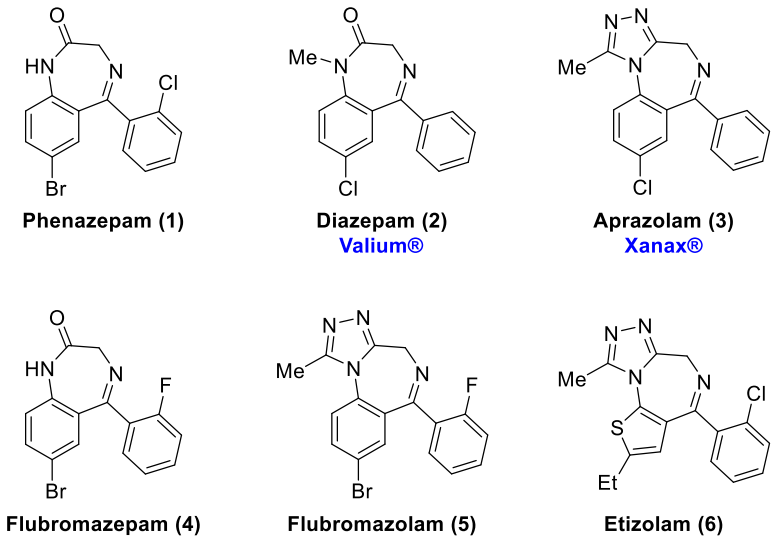

Figure 2-1: Representative pharmaceutical benzodiazepines.

2.1.1 Positional Isomers and the Federal Analogue Act

An understudied class of designer benzodiazepines is the positional isomers of federally controlled parent benzodiazepines. Positional isomers have identical core structures to their parents but differ by the placement of one or two atoms or substituents. Because of these close structural similarities, positional isomers are expected to exhibit similar physiological effects to their parents, making them prime candidates for technically legal alternatives. The Federal Analogue Act,[9] which is part of the Controlled Substances Act (CSA) of 1971,[10] allows entire classes of "substantially similar" compounds to become controlled in one broad sweep.[7a,11] The analogue rule applies only to Schedule I and Schedule II substances, however, so Schedule IV benzodiazepines, including their positional isomers, are processed individually as distinct substances.

At the time of this research, analytical reference data are not readily available to differentiate between many illicit benzodiazepines and their corresponding positional isomers. An important question was raised: if positional isomers of known benzodiazepine

drugs enter the recreational market as technically legal alternatives to their federally controlled parents, will current forensic methods rapidly identify and accurately differentiate between them?

2.1.2 Flubromazepam: A Model for Positional Isomer Synthesis

To address this deficiency, flubromazepam (**4**) was targeted for synthesis and characterization for two primary reasons. First, recent incidents have made flubromazepam a candidate for future scheduling, and its current uncontrolled status facilitates unrestricted research. Second, from a synthetic perspective, flubromazepam has twelve possible positional isomers (including the parent), which maximizes the available chemical space for synthetic, analytical, and biological survey.

Despite its recent appearance in forensic cases, flubromazepam (**4**) was first prepared and studied by Sternbach and co-workers in the early 1960s (Scheme 2-1).[12] By their published method, *p*-bromoaniline (**7a**) undergoes a Friedel-Crafts acylation with *o*-fluorobenzoyl chloride (**8a**) to form the 2-aminobenzophenone **9aa**.[12b] Then, a two-step annulation sequence is employed involving 2-bromoacetyl bromide (**10**) to first prepare the 2-bromoacetamidobenzophenone intermediate, followed by treatment with ammonia and heat to promote ring closure through imine formation.[12c]

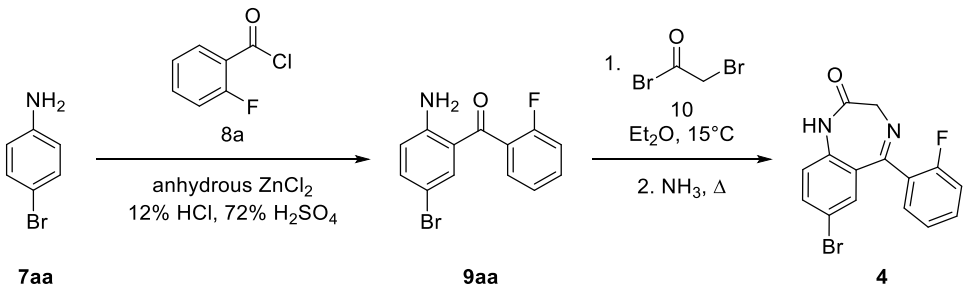

Scheme 2-1: Sternbach synthesis of flubromazepam (4).

Flubromazepam was fully characterized by Moosmann and co-workers in 2013,[13] and initial biological studies showed that it has anticonvulsant properties and an elimination half-life of 100 hours.[14] Incidents involving flubromazepam include three hospitalizations from acute exposure in the last four years in the US,[15] thirty-three in Sweden between 2012-2015,[16] and a severe case of poisoning from **4** mixed with synthetic opioid U-47700 which resulted in severe brain damage followed by patient death.[13,17] Additionally, in certain military cases, on-duty personnel in possession of the drug have been convicted of violating operational readiness, which is an important threat to national security.[18]

As a side note, flubromazolam (**5**), which was first reported in 2016 and is directly prepared from **4** (Scheme 2-2), has exhibited even more potent effects.[19] The synthesis of flubromazolam from flubromazepam was first published in 1976 as a two-step, one-pot annulation to install the triazole moiety.[20] The benzodiazepine reacts first with di-4-morpholinylphosphinic chloride at the amide oxygen atom, then acetylhydrazide is introduced to eliminate the activated oxygen, and finally self-condensation occurs to close the ring.[12a]

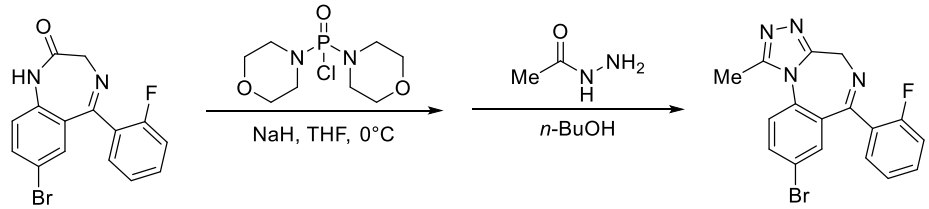

4 5

Scheme 2-2: Synthesis of flubromazolam (5) from flubromazepam (4).

Though various benzodiazepines were successfully prepared by Sternbach, the scope was generally limited to products originating from anilines with electron-

withdrawing *para*-substituents, as discussed in Chapter 1. Thus, 2-aminobenzophenones with bromo, chloro, and nitro substituents *para* to the amino group are highly accessible,[21] which explains the greater abundance of their corresponding benzodiazepines on the recreational drug market and thus in forensic cases.

Preparative methods for positional isomers of benzodiazepines, on the other hand, are limited in the scientific literature. That being said, there have been additional methods devised to access the crucial 2-aminobenzophenone core that do not proceed by a Friedel-Crafts pathway and could thus facilitate the syntheses of benzodiazepines with previously unobserved substitutions.

2.1.3 Alternative Routes to the Benzophenone Precursors to Benzodiazepines

The earliest example of a non-Friedel-Crafts synthesis of benzophenones was from Lothrop and Goodwin in 1943[22] (though their interest in 2-aminobenzophenones was as a template for fluorene derivatives). Through double *N*-acetylation of various 2-aminobenzoic acids, they first prepared a 3,1,4-benzoxaz-4-one, then achieved aryl Grignard addition followed by acidification to cleave the *N*-acetate (Scheme 2-3). Overall yields for this sequence were generally low (e.g. 14% over 3 steps for R' = H, R" = Me).

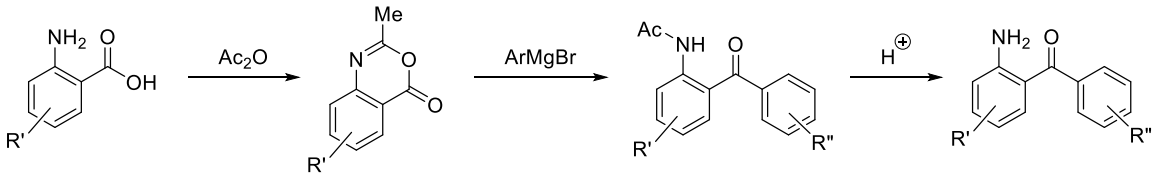

Scheme 2-3: Lothrop and Goodwin's synthesis of 2-aminobenzophenones.

Additional literature approaches that will be explored later in this chapter include: directed oxidative coupling of anilines and benzaldehydes; Sugasawa coupling of anilines

and benzonitriles; decarboxlative coupling of phenylglyoxylic acids and phenylboronic acids; phenyllithiate addition onto Weinreb benzamides; and oxidative rearrangements of 3-hydroxy-3-phenyloxindoles. However, though these studies have investigated and demonstrated efficient routes to various benzodiazepine precursors,[23,24] most fall short of at least one of three important criteria: 1) they do not showcase precursors with substitution patterns that would lead to positional isomers of the more common parents; 2) they do not tolerate halo- and nitro-substituted benzodiazepines most frequently surveyed in forensic cases; and 3) they have failed to follow through in the actual preparation of the corresponding benzodiazepine products. Consequently, the characterization data to accompany these benzodiazepines, both analytical and biological, are nonexistent.

To address this gap in knowledge, I set out to develop a uniform synthetic method that would enable access to the positional isomers of flubromazepam (Scheme 2-4).[25] An ideal synthesis would employ commercially available precursors and tolerate a variety of substituents and substitution patterns. This chapter outlines a generalized approach to access the twelve possible positional isomers of flubromazepam by developing a complementary approach to the substituted benzophenones that bypasses the issues associated with Friedel-Crafts regioselectivity. Both successful and unsuccessful approaches will be described, culminating in access to nine of the twelve isomers. Further attempts to the remaining three isomers, one of which has proven promising in initial studies, will also be detailed. Additionally, an ancillary goal was the synthesis of the corresponding flubromazolams, which is currently ongoing. This study serves as a proof of concept while establishing a roadmap for synthesizing and characterizing the isomers of additional benzodiazepines of interest.

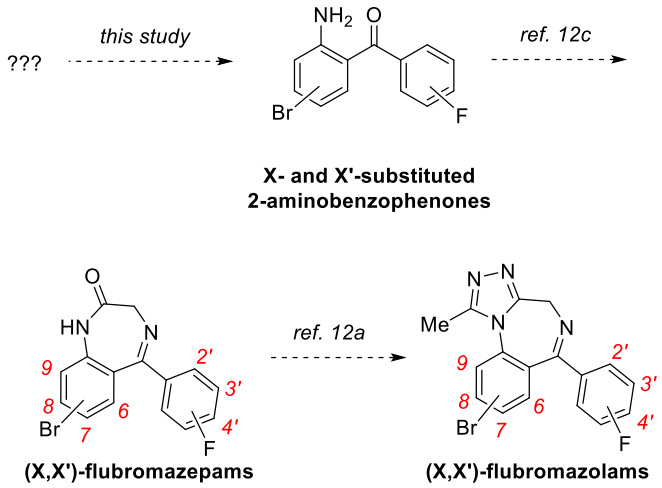

Scheme 2-4: Synthetic roadmap to flubromazepam and flubromazolam positional isomers.

2.2 Retrosynthetic Analysis

For the proposed synthesis of the positional isomers of flubromazepam, three different approaches are outlined in the retrosynthetic analysis shown in Scheme 2-5. The initial goal was to mimic chelation-assisted Friedel-Crafts acylation as a complementary approach to the classic Friedel-Crafts reaction observed in benzodiazepine literature. However, it was determined early on that Friedel-Crafts-type pathways were not the ideal method, as will be discussed throughout the chapter.

In Approach 1, an oxidative cross-coupling of bromoanilines **7** with fluorobenzaldehydes **11** was envisioned to access the 2-aminobenzophenones **9**. Approach 2 explored the potential of decarboxylative cross-coupling reactions between bromoisatins **12** (*via* its hydrolysis products, X-bromo-2-(2-aminophenyl)-2-oxoacetates) and fluorophenylboronic acids **13**. Finally, Approach 3 targeted benzophenones **9** via acylation of X'-fluorophenyllithiums **15** with the Weinreb 2-aminobenzamides **14**.

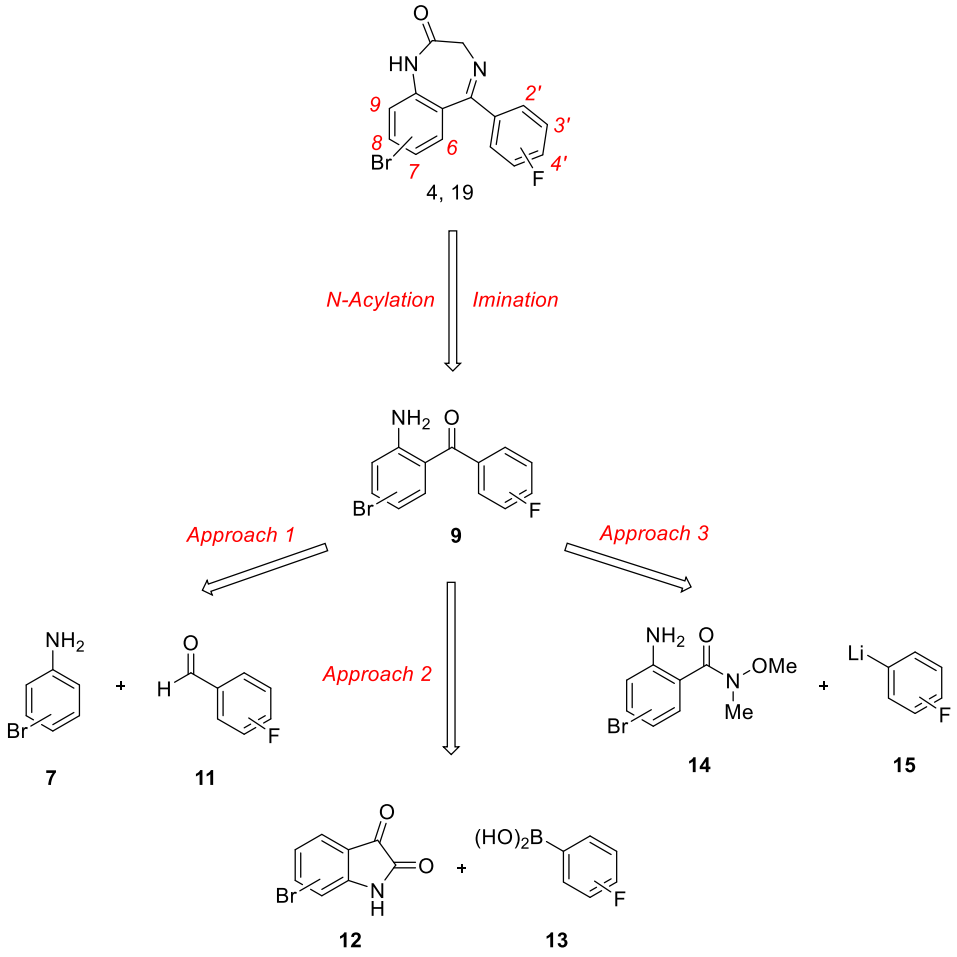

Scheme 2-5: Retrosynthetic analysis for the synthesis of flubromazepam isomers.

2.3 Approach 1: Oxidative Coupling

2.3.1 Pd-Catalyzed Oxidative Coupling

Initial attempts to access the functionalized benzophenones explored a Pd-catalyzed oxidative C-H bond coupling of acetanilides and aldehydes that was reported by Li and Kwong (Scheme 2-6a).[25] This strategy was appealing due to the commercial availability of each of the bromoanilines and fluorobenzaldehydes. The acetyl substituent serves as a directing group for the *ortho* C-H functionalization to access the desired benzophenones. Moreover, if successful, this strategy would be particularly appealing

since two distinct sets of regioisomeric cross-coupling adducts (**17ba-17bc** and **17da-17dc**) should be accessible from reactions with 3-bromoacetanilide (**16b**), which would streamline isomer synthesis (Scheme 2-6b).

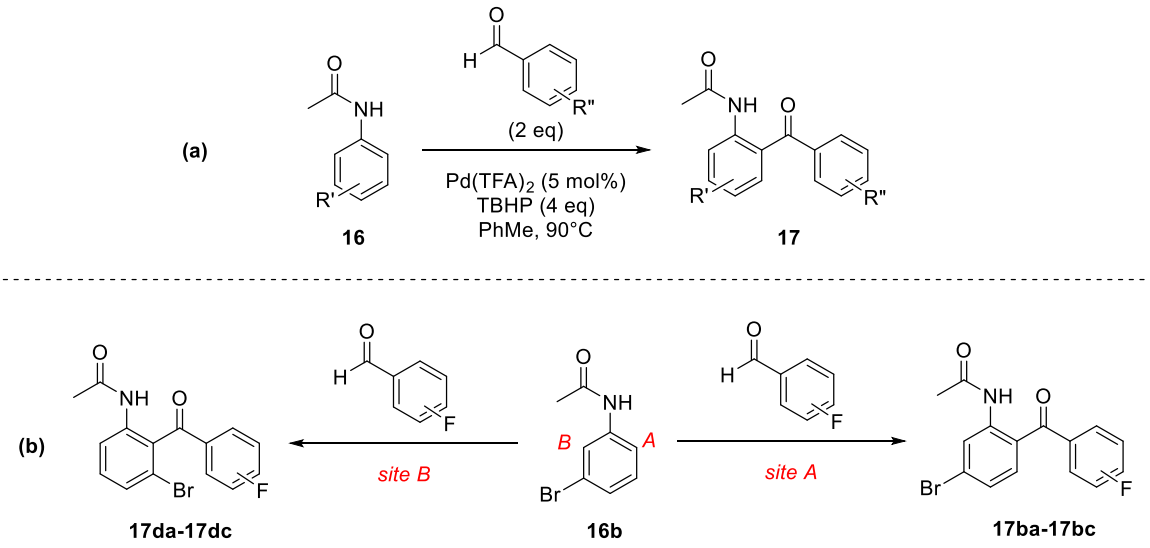

Scheme 2-6: (a) Li and Kwong's oxidative coupling of acetanilides and aldehydes; (b) Proposed divergent coupling of 3-bromoacetanilide.

As a starting point, 4-bromoaniline **7a** was acetylated with acetic anhydride then separately treated with 2, 3, or 4-fluorobenzaldehyde (**11a**, **11b**, or **11c**) under the published conditions (Scheme 2-7). Although the protocol boasted a tolerance for both amino- and halo-substituted arenes, early attempts toward these cross-coupling reactions afforded complex mixtures and trace amounts of isolated product by preparatory TLC. These setbacks led to a short optimization study to probe the effects of solvent and atmosphere on the reaction system (Table 2-1).

The reaction was first tested on the *para*-bromo acetanilide, as only one EAS product was expected from this precursor, under nitrogen atmosphere (entry 1). However, a closer review of the Supporting Information revealed that the reaction performed better under air. Wishing to conserve starting material, the reaction was repeated open to air with

simple aniline and benzaldehyde as coupling partners (entry 2). The unsubstituted model system greatly outperformed its halogenated counterpart, which made me optimistic that the atmosphere was the primary issue. Wishing to improve the yield further, solvent effects were evaluated, since toluene was the preferred reaction solvent. The TBHP solution in nonane was subjected to a solvent exchange, only to result in comparable yield (entry 3). Increasing the loading of TBHP, in contrast, was a detriment (entry 4).

Table 2-1: Optimization of Pd-catalyzed oxidative coupling.

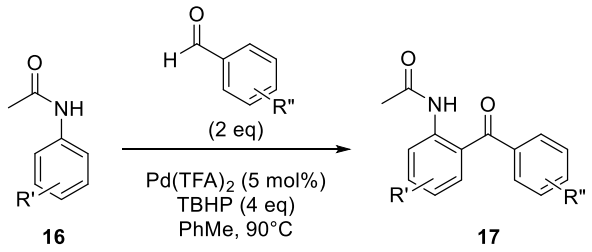

Entry	R', R''	TBHP Solution	Atmosphere	Yield
1	4-Br, 2-F	5.5 M/Nonane	Nitrogen	6%
2	H, H	5.5 M/Nonane	Air	48%
3	H, H	4.13 M/Toluene	Air	43%
4	H, H	4.13 M/Toluene	Air	29%[a]

[a] Used 6 equiv. TBHP.

These conditions were then re-applied to the desired halogenated starting materials (Scheme 2-7). In each case, however, the reactions continued to give a complex mixture of products, and isolated yields of the desired benzophenones **17** remained low (8-12%). These results were partially attributed to deactivation of the substitution reaction from the bromine substituent. Not to be deterred, since the ultimate goal was successful preparation of the flubromazepam isomers, a test reaction with 3-bromoacetanilide **16b** was attempted to probe the hypothesized generation of two desired regioisomers. Unfortunately, this

reaction gave low yields of only one regioisomer of the benzophenone, signifying that all twelve fluobromazepam isomers would not be accessible by this route.

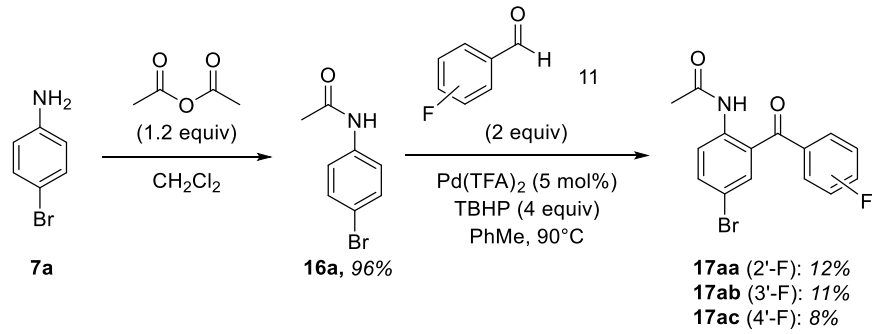

Scheme 2-7: Attempted Pd-catalyzed oxidative cross-couplings between *N*-acetyl-4-bromoaniline (7a) and fluorobenzaldehydes 11.

Despite this disappointment, sufficient amounts of material (~10-20 mg) were isolated from the 4-bromoacetanilide reactions to attempt the syntheses of three flubromazepam isomers; namely, the (7,2')-, (7,3')-, and (7,4')-isomers. Based on previous benzodiazepine syntheses through Friedel-Crafts acylation, these three isomers were already expected to be the most accessible by distributors, as the fluorine substitution would likely not drastically affect reaction outcomes. Thus, it was appealing to obtain the corresponding characterization data early in the project.

From the 2-acetamido-4-bromo-X'-fluorobenzophenones **17aa**-**ac**, acid-promoted *N*-deprotection was attempted, followed by annulation of the crude product using glycine ethyl ester *via* an alternative Sternbach method (Scheme 2-8).[26] No desired product could be isolated as only a trace amount of each isomer was detected by ^{1}H NMR. Ultimately, this approach was deemed inviable to access the isomers.

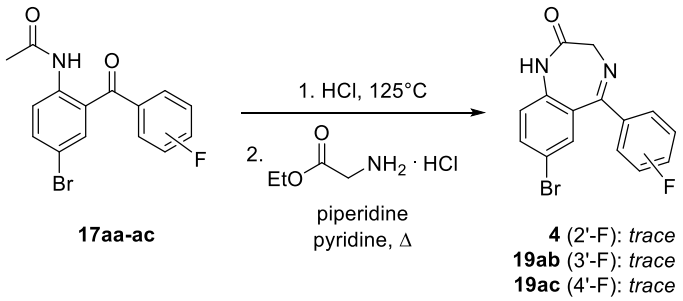

Scheme 2-8: Attempted endgame to (7,X')-flubromazepams.

2.3.2 Sugasawa Coupling

As a last-ditch effort in using the bromoanilines, an alternative directed *ortho*-C-H functionalization approach was envisioned involving Sugasawa coupling[27] of 3-bromoaniline with 4-fluorobenzonitrile in the presence of BCl_3 and $AlCl_3$ (Scheme 2-9).[28] As in Scheme 2-6, we anticipated that the use of 3-bromoaniline in the Sugasawa reaction would give a mixture of the regiosiomeric benzophenones. However, the reaction afforded 22% of **9bc** as the only benzophenone isomer.

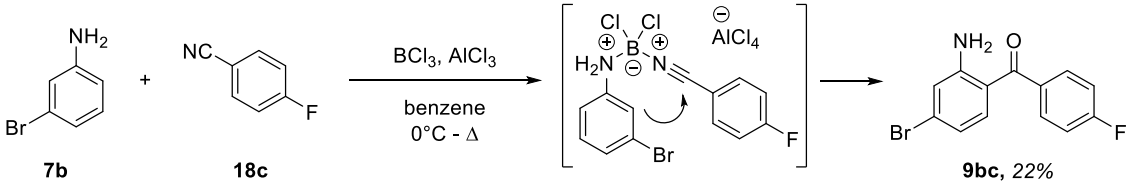

Scheme 2-9: Attempted Sugasawa coupling.

Hypothesizing that the coupling could be directed to the desired acylation site by blocking the preferred site, the reaction was tested again with 2,5-dibromoaniline **31** (Scheme 2-10). Unfortunately, a complex mixture of products resulted, and none of them appeared to be the desired **32c** by ^{1}H NMR.

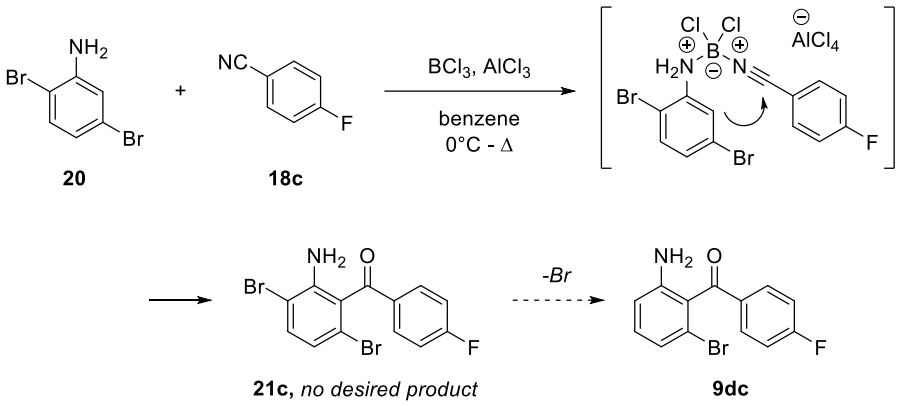

Scheme 2-10: Attempted Sugasawa coupling with the preferred site blocked.

2.4 Approach 2: Decarboxylative Coupling

Changing tactics, we were inspired by the work of Qi and co-workers[29] who demonstrated a silver-catalyzed decarboxylative acylation of phenylglyoxylic acids **22** with phenylboronic acids **23** to afford substituted benzophenones **24** (Scheme 2-11). The authors particularly highlighted the method's tolerance for both halo- and amino-substituted phenylglyoxylic acids and boronic acids. Employing (2-amino-X-bromophenyl)glyoxylic acids would set the isomer substitution pattern at the beginning of the synthesis, thus simplifying purification and characterization throughout the sequence.

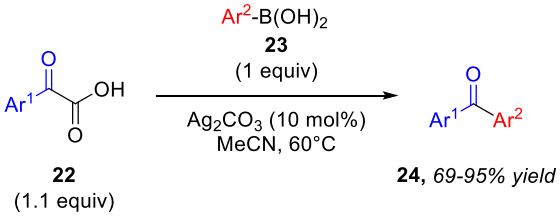

Scheme 2-11: Qi's glyoxylic acid decarboxylative cross-coupling.

However, given that (2-amino-5-bromophenyl)glyoxylic acid **25a** is the only commercially-available isomer, the synthesis of the remaining glyoxylic acids presented a challenge. To address this, 4-, 5-, 6-, and 7-bromoisatins (**12a-d**) were explored as

precursors to the glyoxylic acids, as each bromoisatin is commercially available and should be readily hydrolyzed to generate the glyoxylic acid salt.

Starting with a model system, the saponification of unsubstituted isatin (**12e**) was evaluated in the presence of KOH or NaOH in various loadings and temperatures (Table 2-2); conversion was determined by crude ^{1}H NMR. In general, increasing the loading of hydroxide base saw a correlating increase in yield, with a plateau beyond 2 equiv. (entries 1-4). Increasing temperature did not have a drastic impact on yield (entries 5-6, 8), but changing the cation from K to Na showed marked improvement (entries 7-8). Thus, the optimal conditions were stirring the isatin at room temperature in 2 equiv of 30% aqueous NaOH to readily afford the ring-opened 2-aminophenylglyoxylate salt (**25e**) with 76% conversion (entry 7).[30]

Table 2-2: Optimization of isatin conversion to 2-aminophenylglyoxylate salt.

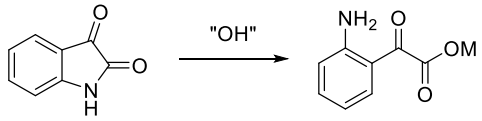

12e **25e**

Entry	Base (equiv)[a]	Solvent (conc, T)	Conversion[b]
1	KOH (1.3)	MeOH (2.5 M, r.t.)	30%
2	KOH (1.6)	MeOH (1 M, r.t.)	52%
3	KOH (2.0)	MeOH (1 M, r.t.)	74%
4	KOH (2.5)	MeOH (1 M, r.t.)	72%
5	KOH (1.6)	MeOH (1 M, 50°C)	57%
6	KOH (2.0)	MeOH (1 M, 50°C)	65%
7	NaOH (2.0)	MeOH (1 M, r.t.)	76%
8	NaOH (2.0)	MeOH (1 M, 50°C)	74%

[a] 30% aqueous solution. [b] Determined conversion by ^{1}H NMR of crude reaction mixture.

Next, we attempted to acidify the 2-aminophenylglyoxylate salt to the corresponding 2-aminophenylglyoxylic acid for the subsequent decarboxylative coupling (Scheme 2-12). It was soon found, however, that acidic workup (to pH 3) drove the reaction predominantly back to isatin (Table 2-3, entries 1-3).

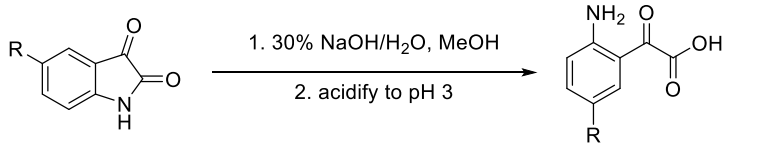

12e (R = H)
12a (R = Br)

25e: *no desired product*
25a: *inseparable mixture*

Scheme 2-12: Attempted isatin saponification-acidification sequence.

Hypothesizing that an electron-withdrawing substituent might hinder this process by making the amine less nucleophilic, the saponification-acidification sequence was attempted with **12a** (entry 4), but mixtures of glyoxylic acid and isatin were obtained. Methods to separate the acid from the isatin by either chromatography (flash or preparative), extraction, or recrystallization failed. Next, the preparations of various glyoxylate salts were attempted (entries 6-14) to employ directly in the decarboxylative cross coupling reaction. The sodium and lithium salts were prepared by isatin treatment with either NaOH or LiOH. The potassium salt was prepared using K_2CO_3. Finally, since the cross-coupling procedure is catalyzed by Ag(I) salts, the silver glyoxylate salt was generated from Ag_2O or Ag_2CO_3. Of these, only two salts were successfully obtained (entry 10: Na; entry 11: Li).

Table 2-3: Test preparations and isolations of 2-aminophenylglyoxylic acids and 2-aminophenylglyoxylate salts.

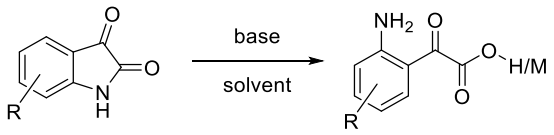

12 25

Entry	R	Base (equiv)	Solvent (conc, T)	Yield
1	H	NaOH (2)[a]	MeOH (1 M, r.t.)	3%[b,c]
2	H	NaOH (2)[a]	MeOH (1 M, r.t.)	(Not isolated)[c,d]
3	H	NaOH (2)[a]	MeOH (1 M, r.t.)	(Not isolated)[c,e]
4	5-Br	NaOH (2)[a]	MeOH (1 M, r.t.)	(Not isolated)[c,e]
5	H	NaOH (2)[a]	MeOH (1 M, r.t.)	(Not isolated)[c,f]
6	H	Ag_2O (1)	THF (1 M, r.t.)	No reaction
7	H	Ag_2O (1)	DMSO (1 M, r.t.)	No reaction
8	H	Ag_2O (1)	DMF (1 M, r.t.)	No reaction
9	H	NaOH (2)	MeOH (0.3 M, Δ)	No reaction
10	H	NaOH (2)[a]	MeOH (1 M, r.t.)	94% (77% pure)[g,h]
11	H	$LiOH{\cdot}H_2O$ (2)[a]	MeOH (1 M, r.t.)	98% (66% pure)[g,h]
12	H	NaOH (1)[a]	MeOH (1 M, r.t.)	No reaction
13	H	K_2CO_3 (1)	H_2O (0.2 M, Δ)	No desired product[g,h]
14	H	Ag_2CO_3 (1)	H_2O (0.2 M, Δ)	No desired product[g,h]

[a] 30% aqueous solution. [b] Attempted to purify on silica. [c] Product reverted to starting material. [d] Collected organic layer crude. [e] Attempted an acid/base extraction. [f] Extracted with minimal MeCN in attempts to separate starting material from product. [g] Concentrated the aqueous layer to collect the glyoxylate salt. [h] Analyzed by q-NMR (DMTP internal standard).

These two salts were then subjected to the cross coupling conditions with the unsubstituted phenylboronic acid (**26**) (Scheme 2-13). In both cases, no desired products were detected.

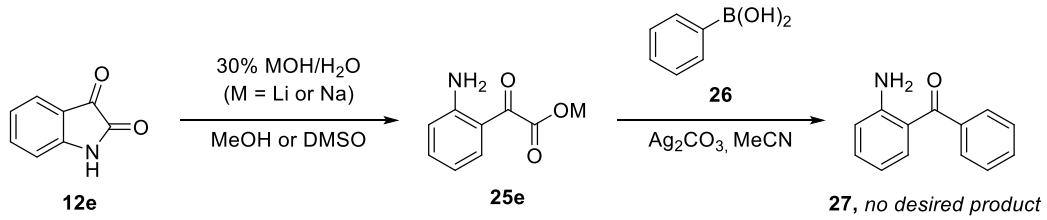

Scheme 2-13: Unsuccessful decarboxylative coupling using glyoxylate salts.

In a final attempt to effect cross-coupling, several *N*-protection protocols were evaluated with hopes of stabilizing the glyoxylic acid for isolation (Table 2-4). Methyl chloroformate and di-*tert*-butyl dicarbonate (Boc_2O) protections were unproductive (entries 1-3), but a two-step protection-saponification protocol employing ethyl chloroformate and Na_2CO_3 afforded the desired glyoxylic acid **28** in high yield (entry 4).[31] Unfortunately, the subsequent cross coupling of **12e** with 2-fluorophenylboronic acid (**13a**) did not give any observable products (Scheme 2-14).

Table 2-4: Test preparations of *N*-acyl 2-aminophenylglyoxylic acids.

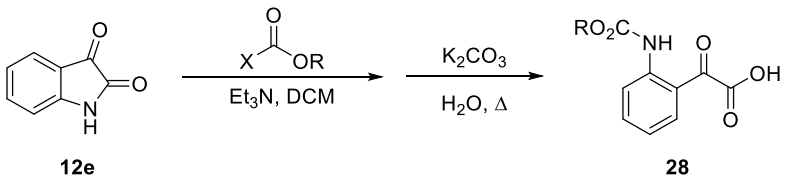

Entry	XCO_2R	Yield
1	$ClCO_2Me$	4%
2	$ClCO_2Me$	20%[a]
3	Boc_2O	No reaction
4	$ClCO_2Et$	88%[b]

[a]Kept reaction mixture cold during workup and washed precipitate with cold solvents. [b]Used Na_2CO_3.

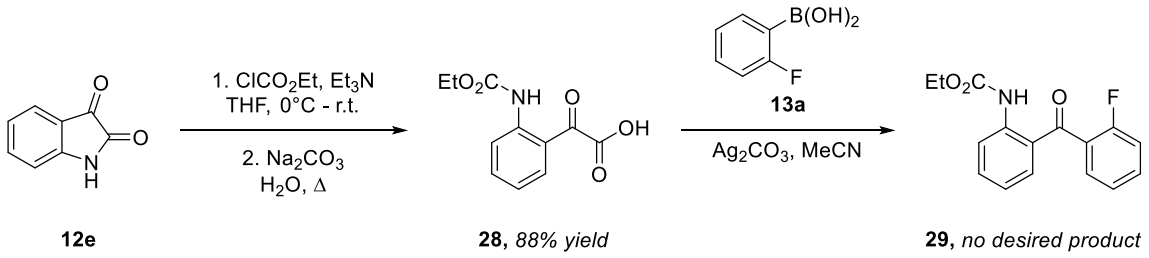

Scheme 2-14: Failed coupling of *N*-protected glyoxylic acid 28.

2.5 Approach 3: Benzoylation of Fluoro-substituted Phenyllithiums

Following the failed cross-coupling approaches, an alternative strategy was undertaken involving benzoylation of fluoro-substituted phenyl anions **15** (Grignards or lithiates) with 2-amino-X-bromo-*N*-methoxy-*N*-methylbenzamides **14** (Scheme 2-15).

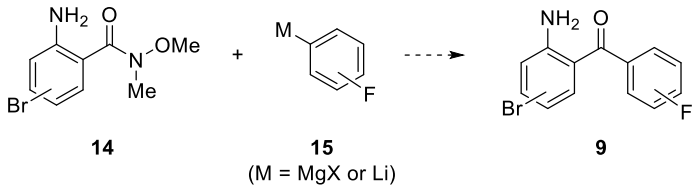

Scheme 2-15: Proposed benzoylation strategy.

2.5.1 Synthesis of the Weinreb Amide Precursors

Preparation of each Weinreb amide involved a two-step sequence starting from a bromo-substituted isatin **12a-d** (Scheme 2-16). Isatins **12** were treated with hydrogen peroxide under strongly basic conditions to produce 2-amino-X-bromobenzoic acids **31a-d**,[32] which were collected in moderate to high yields as the hydrochloride salts after acidification. Amidation of **31a-d** with *N*,*N'*-dimethylhydroxylamine hydrochloride was then effected in the presence of HBTU[33] and *N*-methylmorpholine to give Weinreb amides **14a-c** in moderate to high yields. Unfortunately, obtaining **14d** proved particularly troublesome. Though crude NMR validated its formation, **14d** was inseparable from the

complex mixture that was formed. In hopes of still accessing the desired benzophenone isomer, the crude mixture of **14d** was taken forward.

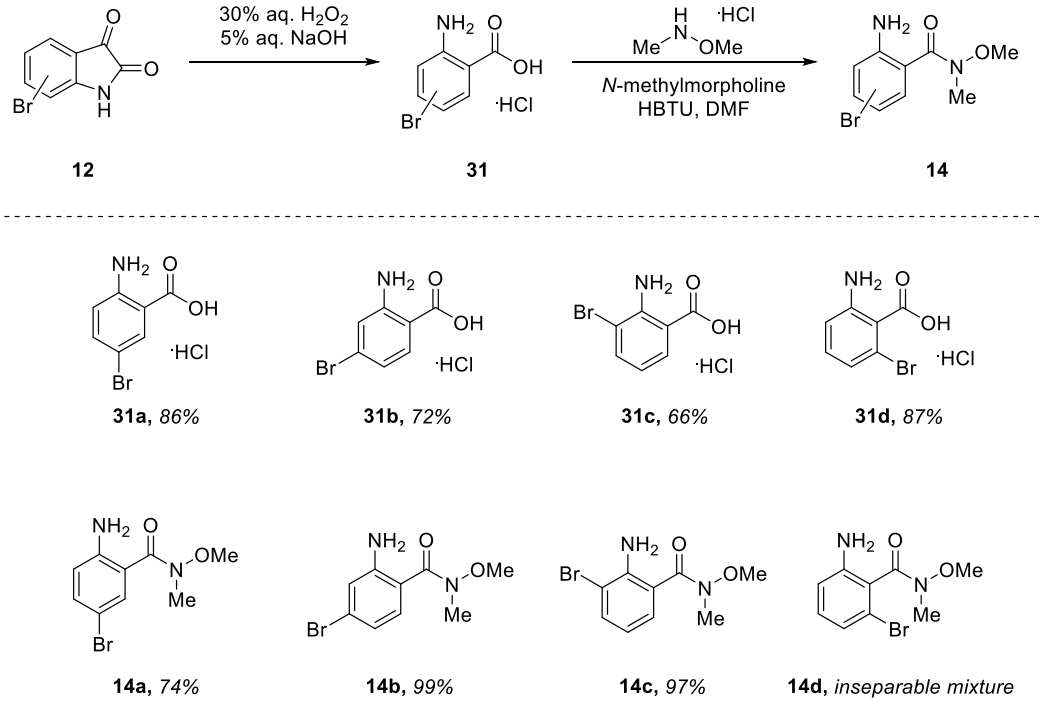

Scheme 2-16: Two-step synthesis to prepare 2-amino-X-bromobenzoic acids 28a-d and Weinreb amides 14a-d from bromoisatins 12a-d.

2.5.2 Optimizing the Benzophenone Synthesis

Next, the conditions for benzophenone formation were explored (Table 2-5). Initial test reactions between amides **14a-c** and phenylmagnesium bromide were promising (entries 1-3).[34] However, *in situ* preparation of the fluorophenyl magnesium bromides from the various fluoro-substituted bromobenzenes gave inconsistent results (entries 4-7). Several reagents for magnesium-halogen exchange were tested, including Turbo Grignard[35] (*i*-PrMgCl·LiCl), with no success. Next, lithium-halogen exchange was examined as a potential protocol. Gratifyingly, a test reaction between **14c** and

phenyllithium afforded the 2-aminobenzophenone in 43% yield (entry 8); this result served as proof of concept to continue forward with lithium-halogen exchange.

Table 2-5: Optimization of Grignard addition to 2-aminobenzamides.

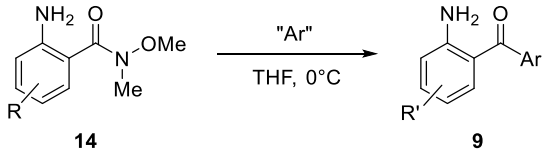

14 **9**

Entry	R	"Ar" source	Yield
1	H	PhMgBr (3 M/Et_2O)	22%
2	3-Br	PhMgBr (3 M/Et_2O)	42%
3	4-Br	PhMgBr (3 M/Et_2O)	53%
4	H	Bromobenzene (2.5 equiv), Mg (7.5 equiv), THF (1 M, 60°C), 2 h	Trace
5	H	Bromobenzene (2.5 equiv), Mg (7.5 equiv), 1,2-DBE (cat.), THF (1 M, 60°C), 2 h	Trace
6	N/A[a]	1-Bromo-2-fluorobenzene (1 equiv), iPrMgCl (1 eq, 2 M/THF), 0°C, 1 h	No desired product
7	N/A[a]	1-Bromo-2-fluorobenzene (1 equiv), iPrMgCl·LiCl (1 eq, 1.3 M/THF), 0°C, 1 h	No desired product
8	3-Br	PhLi (1.9 M/THF)	46%

[a] Control experiment to test Grignard formation. After 1 h, quenched with H_2O and analyzed by ^1H NMR.

Lithiation of 1-bromo-4-fluorobenzene (**32c**) was attempted first, and treatment with *n*-butyllithium proceeded smoothly at -78 ˚C (Scheme 2-17).[36] Upon transferring a solution of the Weinreb amide **14a** dropwise *via* syringe to the lithiate solution, the desired 2-amino-3-bromo-4'-fluorobenzophenone (**9ac**) was formed, and ultimately isolated, in 78% yield. This order of addition was crucial to ensure that the lithiate did not thermally degrade.

Having succeeded with **32c**, the same approach was first applied to accessing the benzophenone isomers containing the 4'-fluoro substituent. Addition of the lithiate to

amides **14b** and **14c** gave the desired benzophenones **9bc** and **9cc** in 49% and 62% yield, respectively. Next, the lithium-halogen exchange reactions of 1-bromo-3-fluorobenzene **32b** were conducted. The reactions generated the respective benzophenone isomers (**9ab**, **9bb**, and **9cb**) in 60%, 55%, and 63% yield.

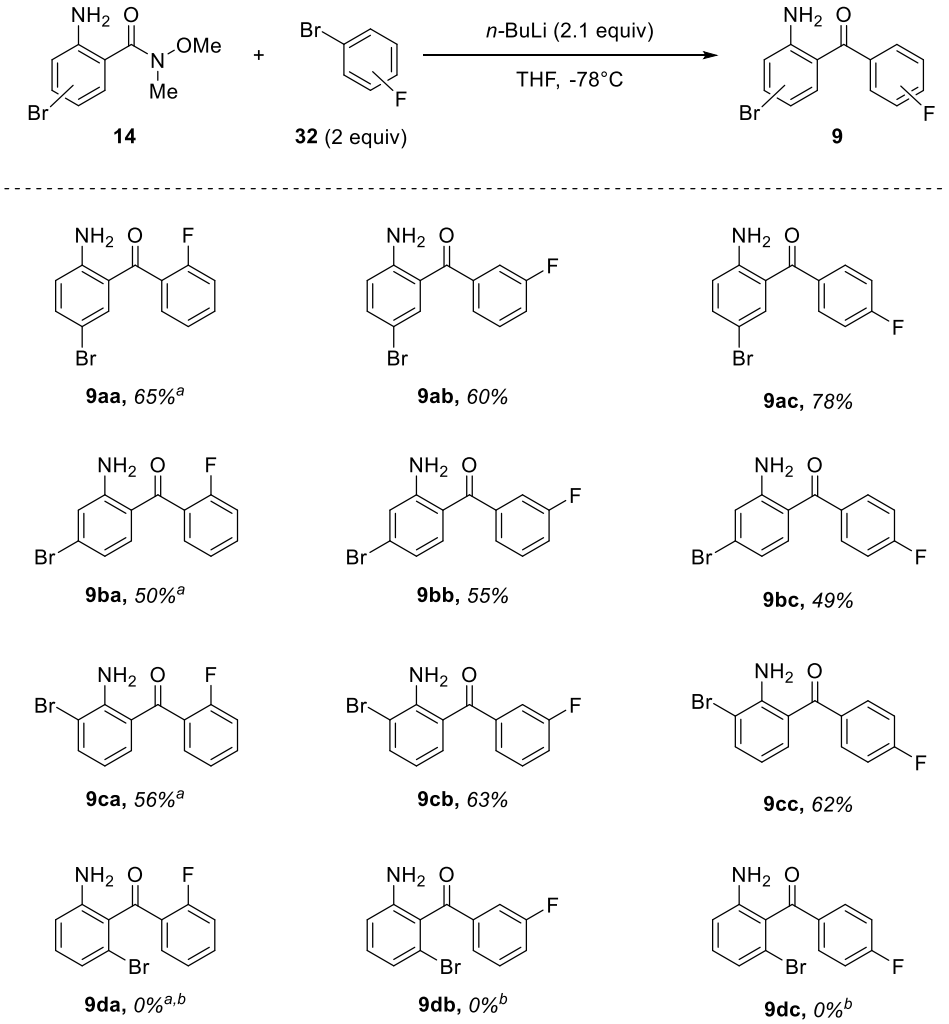

Scheme 2-17: Synthesis of 2-amino-X-bromobenzophenones 9 via benzoylation.

For 1-bromo-2-fluorobenzene **32a**, lithiation was not successful at -78˚C as the lithiate appeared to degrade as immediately as it was formed. A quick literature search

revealed that lithiation of **32a** could be accomplished at temperatures as low as -110˚C, so the reaction was attempted again at -100 ˚C. The corresponding benzophenone precursors **9aa**, **9ba**, and **9ca** were afforded with yields of 65%, 50%, and 56%, respectively.

The yields for this synthetic transformation were modest due to the nucleophilic attack of the Weinreb amide by *n*-butyllithium, forming an *n*-butyl phenone adduct (**33**, Scheme 2-18). A test reaction with *t*-butyllithium to promote lithium-halogen exchange and reduce nucleophilic activity of the lithiating agent gave a lower yield along with a number of uncharacterized side products. When this approach failed, the reaction was monitored carefully at 15-minute time intervals. It was found that halting the reaction after 30 minutes gave the optimal yield and prevented formation of **33**, while attempting to increase the yield by stirring for 45 minutes allowed this side reaction to occur.

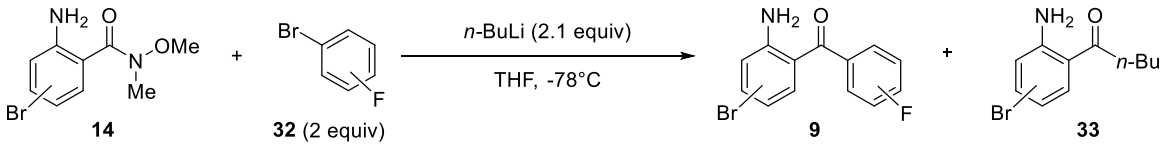

Scheme 2-18: Generation of *n*-butyl phenome by-product.

Unfortunately, applying any of the reaction conditions to the crude mixture of **14d** failed to deliver the desired benzophenones. It is hypothesized that the purification issues with **14d**, the steric hindrance at the site of nucleophilic addition, and potential cross lithium-halogen exchange may have prevented the transformation from occurring.

2.5.3 Synthesis of the Flubromazepam Isomers from the Prepared Benzophenones

With nine of the twelve possible benzophenone precursors in hand, the conversions to the desired flubromazepam positional isomers were performed using the known literature procedures (Scheme 2-19). For each benzophenone, *N*-acylation was first

effected using 2-bromoacetyl bromide. Subsequently, the crude product was dissolved in 7M ammonia in methanol and stirred overnight to afford the parent flubromazepam (**4**) and eight other positional isomers **19**. Most yields were modest (32-77%), though isomers **19ab** and **19cc** were isolated with lower yields (< 20%) than expected. This chemistry was not further optimized, however, as sufficient quantities of each positional isomer were isolated for analysis.

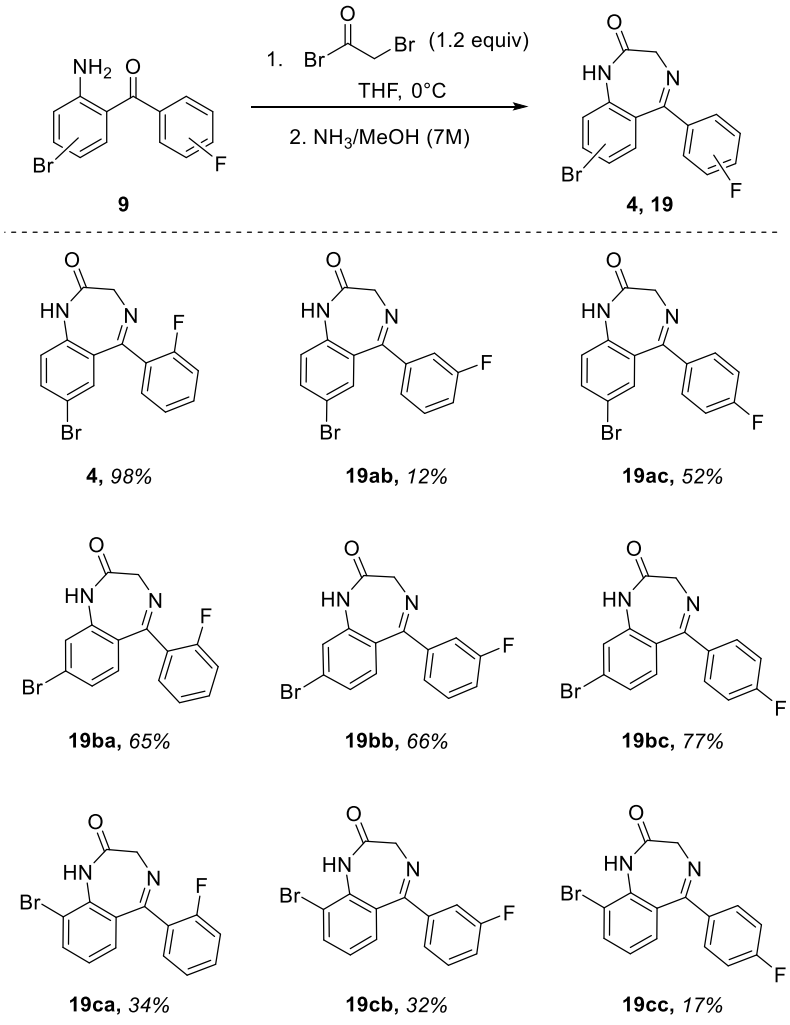

Scheme 2-19: Synthesis of flubromazepam positional isomers.

2.6 Further Efforts Toward the Elusive Benzophenones

With nine of the twelve positional isomers of flubromazepam in hand, and with the considerable difficulty of accessing benzophenones **9da-dc** (precursors to the three (6,X')-flubromazepam isomers (**19da-dc**), there was some debate over whether these three elusive isomers were worth pursuing. The primary argument for their synthesis was the obvious benefit of building up a complete dataset for forensic comparison; the offered counterargument was that, if their synthesis was so challenging to effect in a well-equipped synthetic organic chemistry laboratory, then these isomers would be the least likely targets for potential distributors. In the end, there was one alternative route based on literature precedent that hadn't been incorporated into the original synthetic plan but displayed promise on paper: oxidative rearrangement of 4-bromo-3-(X-fluorophenyl)-3-hydroxyoxindoles (**34a-c**), from the direct 3-arylation of 4-bromoisatin (**12d**).

As a starting point, 4-bromoindole (**35**) was also considered as a precursor, as we envisioned that **35** could be readily accessed through reduction of **12d**. This search led us to recent work from Kim and co-workers, who demonstrated a cesium carbonate-mediated oxidative rearrangement of 2-arylindoles **36** to 2-aminobenzophenones **37** (Scheme 2-20a).[37] Through their mechanistic studies, they proposed that the rearrangement must proceed from a 3-hydroxyoxindole intermediate; and indeed, in one example, they demonstrated formation of by-product 3-phenyl-3-hydroxyoxindole **38**, subjected it to the oxidative conditions, and achieved the desired 2-aminobenzophenone **27** in 75% yield (Scheme 2-20b).

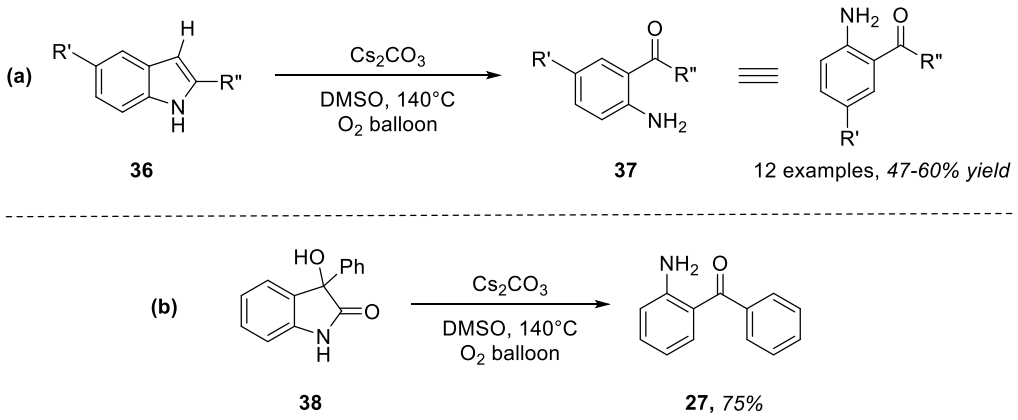

Scheme 2-20: (a) Kim's oxidative rearrangement of 2-arylindoles to 2-aminobenzophenones; (b) Isolated example of 3-hydroxy-3-phenyloxindole 33 rearrangement to 2-aminobenzophenone 25.

This work, though promising, demonstrated a limited scope of only 5-substituted indole precursors and no bromine or fluorine atom substitutions. An analogous rearrangement from Lee and co-workers,[36] however, showcased tolerance of bromine with the substrate 7-bromo-3-hydroxy-3-phenyloxindole (**39**) when potassium ferrocyanide ($K_4[Fe(CN)_6]$) was employed as the reaction mediator (Scheme 2-21). Though they did not report the yield for this particular substrate (**40**), a similar compound [7-chloro-3-hydroxy-3-(2-tolyl)oxindole] was achieved at a reported 89% yield.

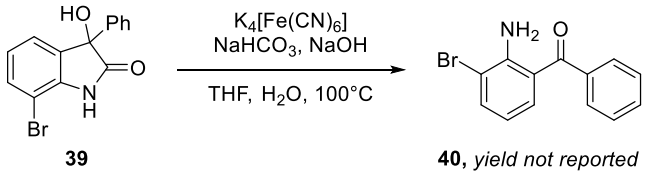

Scheme 2-21: Oxidative rearrangement by potassium ferrocyanide from 7-bromo-3-hydroxy-3-phenyloxindole 34 to 2-amino-3-bromobenzophenone 35.

Anxious to effect this rearrangement toward a 4-bromooxindole precursor, 3-arylation methods were evaluated. The most straightforward method, a direct Grignard addition, was achieved readily with **12e** in the presence of phenylmagnesium bromide

(Scheme 2-22);[38] unfortunately, this same method applied to **12d** resulted primarily in degradation products.

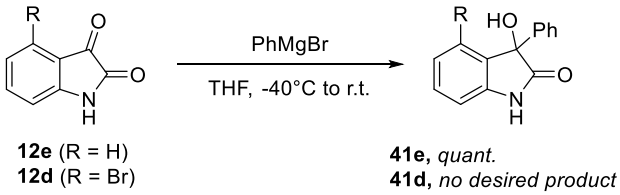

12e (R = H)
12d (R = Br)

41e, *quant.*
41d, *no desired product*

Scheme 2-22: 3-Arylation of isatins 12e and 12d with PhMgBr.

Next, different transition metal-catalyzed methods were considered. Highly prevalent in recent literature were various rhodium-catalyzed 3-arylations with phenylboronic acids,[39] but the catalysts and ligands employed in these studies were very specific and not generalizable, and there was concern that extensive (and expensive) optimization would delay efficient access to these targets.

A more promising route from Zhang and co-workers showcased a milder, copper(II)-mediated 3-arylation of isatins **42**,[40] also using phenylboronic acids (**23**) as the coupling partner (Scheme 2-23a). Compared to rhodium-based methods, this work was optimized with low loadings of copper(II) triflate [$Cu(OTf)_2$] catalyst and 1,10-phenanthroline ligand (5 mol% and 10 mol%, respectively), as well as lithium hydroxide monohydrate ($LiOH{\cdot}H_2O$) to facilitate addition of the boronic acid. All of these reagents are inexpensive and very shelf-stable. Even more importantly, the authors showcased one high-yielding (86%) example of 3-arylation onto 4-bromo-*N*-(*n*-butyl)isatin (**44**) (Scheme 2-23b).

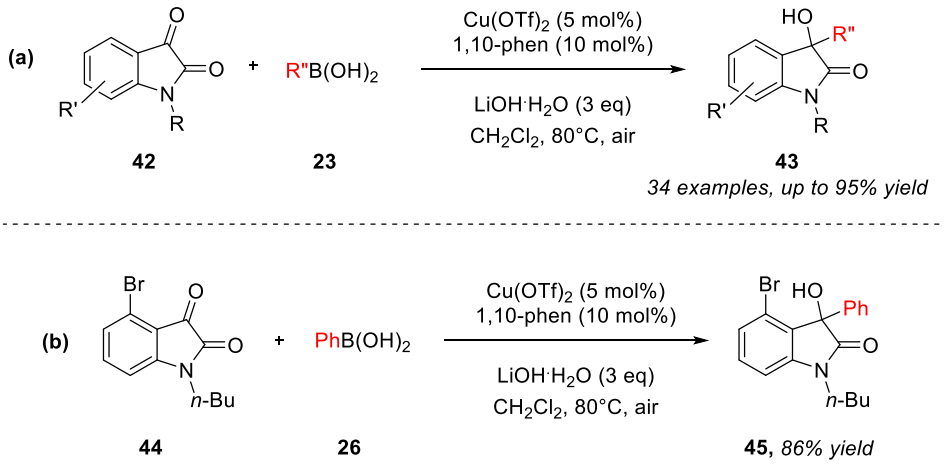

Scheme 2-23: (a) Zhang's Cu-mediated 3-arylation of substituted isatins; (b) Example of successful $PhB(OH)_2$ 36 coupling with 4-bromo-*N*-(*n*-butyl)isatin 37.

To assess this transformation, 4-bromoisatin (**12d**) was first protected with a benzyl group to form *N*-benzyl-4-bromoisatin (**46**, 86% yield);[41] benzyl was chosen over *n*-butyl to facilitate deprotection later. Then, selecting 4-fluorophenylboronic acid (**13c**) as the coupling partner to minimize any potential steric hindrances, **46** was subjected to the prescribed conditions (Scheme 2-24). Pleasingly, the desired product **47c** was afforded after 48 hours in 82% yield, which is on par with the literature example. Steps remaining to access the benzophenone core are deprotection by hydrogenolysis to afford **48c**, then the oxidative rearrangement to **9dc**. This synthesis will be replicated with 2- and 3-fluorophenylboronic acids (**13a-b**), as well, to access benzophenones **9da-db**.

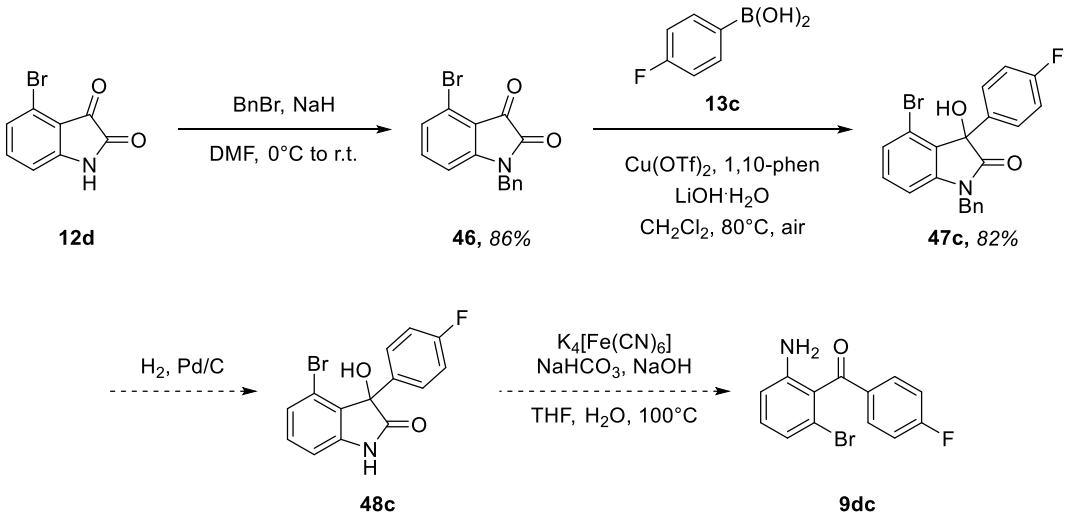

Scheme 2-24: Progress toward synthesis of benzophenones 9da-dc by 3-arylation of *N*-benzyl-4-bromoisatin 39 and subsequent oxidative rearrangement.

Armed with the knowledge that the three elusive isomers were within reach, the crucial rearrangement was tested on 3-hydroxy-3-phenyloxindole **38** (Scheme 2-25), which is much more readily accessible since the Grignard addition proceeds quantitatively and in a single step. A single test reaction afforded **27** in 21% isolated yield. While there is certainly room for optimization, the low yield may be partially attributed to solubility issues encountered with the literature conditions; and practically speaking, the set-up is more facile than the cesium carbonate method. Significantly, the fact remains that sufficient quantities of desired benzophenone may be isolated to carry forward to the flubromazepam isomers.

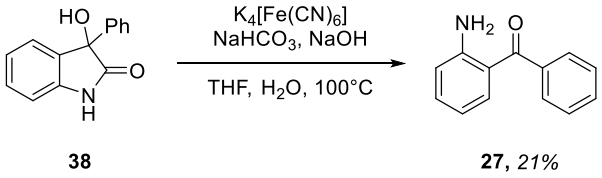

Scheme 2-25: Successful test reaction to prepare 27 from 38 with potassium ferrocyanide.

2.7 Summary

In this study, nine of the twelve positional isomers of flubromazepam were successfully synthesized. The synthetic route developed was a three-step saponification, amidation, and lithiate addition and has not been used previously to access the 2-amino-X-bromo-X'-fluorobenzophenone precursors to the flubromazepam positional isomers. Alternative approaches to synthesize the final three flubromazepam isomers were also explored, and the route to effect 3-arylation of *N*-benzyl-4-bromoisatin has proven promising. The chemical characterization data acquired from this study will be made available to forensic scientists. This method may be adapted to synthesize and characterize other benzodiazepines of interest.

2.8 Experimental Details

2.8.1 General Information

Chromatographic purification was performed via flash chromatography with Silicycle SiliaFlash P60 silica gel (40-63 μm) or preparative thin-layer chromatography (prep-TLC) with Analtech silica gel F254 (1000 μm) plates and solvents indicated as eluent with 0.1-0.5 bar pressure. For quantitative flash chromatography, technical grades solvents were utilized. Analytical thin-layer chromatography (TLC) was also used to separate and purify reaction products using Silicycle SiliaPlate TLC silica gel F254 (250 μm) TLC glass plates. Products on the TLC plates were visualized under UV light (254 nm).

Proton, carbon, and fluorine nuclear magnetic resonance spectra (^{1}H NMR, ^{13}C NMR, and ^{19}F NMR, respectively) were recorded on a Bruker 500 MHz spectrometer. The solvent resonances were used the internal standards (^{1}H NMR: $CDCl_3$ at 7.26 ppm, DMSO-

d$_6$ at 3.50 ppm; ^{13}C NMR: $CDCl_3$ at 77.0 ppm, DMSO-d_6 at 39.5 ppm; ^{19}F NMR: locked to $CDCl_3$ or DMSO-*d*$_6$). MestReNova (v. 11.0) was used to analyze NMR spectra. ^{1}H NMR data are reported as follows: chemical shift (ppm), multiplicity (s = singlet, d = doublet, dd = doublet of doublets, dt = doublet of triplets, ddd = doublet of doublet of doublets, t = triplet, m = multiplet, br = broad), coupling constants (Hz), and integration. High-resolution accurate mass-mass spectrometry (HRAM-MS) was performed using a ThermoFisher Q-Exactive Plus Mass Spectrometer. Samples were first separated using a ThermoFisher Vanquish Ultra-high pressure liquid chromatograph (UHPLC). Thermo QualBrowser (Xcalibur 4.1.31.9) was employed for data processing, including integrations and background subtractions. Infrared (IR) spectra were recorded using a Spectra Analysis DiscovIR-GC coupled with an Agilent 7890A Gas Chromatograph. Data were processed in Grams (version 9.1) for baseline correction and exported to Microsoft Excel for plotting. The IR bands were characterized as broad (br), weak (w), medium (m), and strong (s).

2.8.2 Procedures for Approach 1

*2-Amino-N-(4-bromophenyl)acetamide (**16a**).* Following the published procedure from Fagnou:[43] In a flame-dried flask under nitrogen atmosphere, **7a** (500 mg, 2.907 mmol) was stirred with acetic anhydride (0.33 mL, 3.488 mmol) in anhydrous CH_2Cl_2 (7.3 mL) at room temperature. After 16 h, the reaction was quenched with saturated aqueous Na_2CO_3. The aqueous layer was extracted three times with CH_2Cl_2, then the combined organic layers were dried over anhydrous magnesium sulfate, filtered through celite under reduced pressure, and concentrated by rotary evaporation. Compound **16a** was collected (25% EtOAc/hexanes, R_f = 0.07) without further purification as a white solid (609.1 mg, 97% yield). ^{1}H NMR (300 MHz, $CDCl_3$) δ 7.42 (d, *J* = 2.2 Hz, 4H), 2.18 (s, 3H).

General Procedure for the Oxidative Coupling. Following the published procedure:[26] In a dry flask open to air, **16a** (75 mg, 0.350 mmol) and $Pd(TFA)_2$ (5.8 mg, 0.0175 mmol) were dissolved in anhydrous toluene (0.7 mL). After 5 min, X'-fluorobenzaldehyde **11** (0.07 mL, 0.700 mmol) and TBHP (0.34 mL, 1.40 mmol, 4.13 M solution in toluene) were added, then the reaction was heated at 90 ˚C and stirred for 24 h. After cooling to room temperature, the reaction was quenched with saturated aqueous K_2CO_3. The aqueous layer was extracted three times with EtOAc, then the combined organic layers were dried over anhydrous Na_2SO_4, filtered through celite under reduced pressure, and concentrated by rotary evaporation. Compound **17** was isolated by silica prep-TLC.

*2-Acetamido-5-bromo-2'-fluorobenzophenone (**17aa**)*. The general decarboxylative coupling procedure was followed using **11a** (0.07 mL, 0.700 mmol). The product **17aa** was isolated by silica prep-TLC (25% EtOAc/hexanes, R_f = 0.37) to afford a yellow solid (14.8 mg, 12% yield). ^{1}H NMR (500 MHz, $CDCl_3$) δ 11.17 (s, 1H), 8.68 (d, *J* = 9.1 Hz, 1H), 7.67 (dd, *J* = 9.0, 2.3 Hz, 1H), 7.61 – 7.55 (m, 2H), 7.48 – 7.44 (m, 1H), 7.30 (td, *J* = 7.5, 1.0 Hz, 1H), 7.21 (ddd, *J* = 9.6, 8.4, 1.0 Hz, 1H), 2.26 (s, 3H). ^{13}C NMR (126 MHz, $CDCl_3$) δ 195.86, 169.36, 159.54 (d, *J* = 253.0 Hz), 140.13, 138.07, 135.96 (d, *J* = 2.1 Hz), 133.64 (d, *J* = 8.3 Hz), 130.24 (d, *J* = 2.3 Hz), 126.78 (d, *J* = 14.4 Hz), 124.49 (d, *J* = 3.6 Hz), 123.91, 122.62, 116.60 (d, *J* = 21.4 Hz), 114.56, 25.48. ^{19}F NMR (471 MHz, $CDCl_3$) δ -111.61 (dtd, *J* = 9.8, 7.1, 6.3, 3.6 Hz). HRAM-MS (EI) m/z $[M+H]^+$ Calcd for $C_{15}H_{12}BrFNO_2$ 336.0030; Found 336.0025.

*2-Acetamido-5-bromo-3'-fluorobenzophenone (**17ab**)*. The general decarboxylative coupling procedure was followed using **11b** (0.07 mL, 0.700 mmol). The

product **17ab** was isolated by silica prep-TLC (10% EtOAc/hexanes, R_f = 0.30) to afford a yellow oil (13.1 mg, 11% yield). ^{1}H NMR (500 MHz, $CDCl_3$) δ 10.55 (s, 1H), 8.55 (d, *J* = 9.0 Hz, 1H), 7.67 (dd, *J* = 9.0, 2.5 Hz, 1H), 7.62 (d, *J* = 2.4 Hz, 1H), 7.50 (td, *J* = 7.9, 5.3 Hz, 1H), 7.48 – 7.38 (m, 2H), 7.33 (tdd, *J* = 8.2, 2.7, 1.2 Hz, 1H), 2.22 (s, 3H). ^{13}C NMR (126 MHz, $CDCl_3$) δ 196.81 (d, *J* = 2.2 Hz), 169.06, 162.48 (d, *J* = 249.4 Hz), 139.81 (d, *J* = 6.4 Hz), 139.45, 137.22, 135.25, 130.26 (d, *J* = 7.8 Hz), 125.66 (d, *J* = 3.1 Hz), 124.33, 123.39, 120.01 (d, *J* = 21.4 Hz), 116.54 (d, *J* = 22.7 Hz), 114.59, 25.24. ^{19}F NMR (471 MHz, $CDCl_3$) δ -110.96 (td, *J* = 8.6, 5.5 Hz). HRAM-MS (EI) m/z $[M+H]^+$ Calcd for $C_{15}H_{12}BrFNO_2$ 336.0030; Found 336.0025.

2-Acetamido-5-bromo-4'-fluorobenzophenone ***(17ac)***. The general decarboxylative coupling procedure was followed using **11c** (0.07 mL, 0.700 mmol). The product **17ac** was isolated by silica prep-TLC (10% EtOAc/hexanes, R_f = 0.33) to afford a yellow solid (9.4 mg, 8% yield). ^{1}H NMR (500 MHz, $CDCl_3$) δ 10.44 (s, 1H), 8.52 (d, *J* = 9.0 Hz, 1H), 7.79 – 7.72 (m, 3H), 7.66 (dd, *J* = 9.0, 2.3 Hz, 1H), 7.61 (d, *J* = 2.4 Hz, 1H), 7.23 – 7.18 (m, 2H), 2.21 (s, 3H). ^{13}C NMR (126 MHz, $CDCl_3$) δ 196.55, 169.01, 165.65 (d, *J* = 255.8 Hz), 139.14, 136.83, 135.00, 133.96 (d, *J* = 3.1 Hz), 132.62 (d, *J* = 9.4 Hz), 124.94, 123.51, 115.86 (d, *J* = 21.8 Hz), 114.62, 25.20. ^{19}F NMR (471 MHz, $CDCl_3$) δ -104.32 (tt, *J* = 8.3, 5.4 Hz). HRAM-MS (EI) m/z $[M+H]^+$ Calcd for $C_{15}H_{12}BrFNO_2$ 336.0030; Found 336.0023.

General Deprotection Procedure of N-Acetylbenzophenones. In a flask equipped with a stir bar and a condenser under nitrogen atmosphere, 2-acetamido-X-bromo-X'-fluorobenzophenone **17** (14.8 mg, 0.0440 mmol) was stirred with hydrochloric acid (0.15 mL, 37 wt% H_2O) at 125 ˚C. After 3 h, the reaction was cooled to 0 ˚C, diluted with EtOAc,

and quenched with saturated aqueous $NaHCO_3$. The aqueous layer was extracted three times with EtOAc, then the combined organic layers were washed with H_2O, dried over anhydrous Na_2SO_4, filtered through celite under reduced pressure, and concentrated by rotary evaporation.

General Glycine Ethyl Ester Annulation Procedure. The crude deprotection product was re-dissolved in pyridine (0.09 mL) in a flask equipped with a stir bar and a condenser under nitrogen atmosphere, then stirred at reflux with glycine ethyl ester hydrochloride (18.4 mg, 0.132 mmol) and piperidine (1 drop) for 15 h. The reaction mixture was concentrated by rotary evaporation, then diluted with CH_2Cl_2. The organic layer was washed with H_2O, dried over anhydrous $MgSO_4$, filtered through celite under reduced pressure, and concentrated by rotary evaporation.

*Flubromazepam (**4**) from 2-acetamido-5-bromo-2'-fluorobenzophenone **17aa***. The general deprotection and annulation procedures were followed using (14.8 mg, 0.0440 mmol) in 0.15 mL of HCl (37 wt% H_2O), then glycine ethyl ester hydrochloride (18.4 mg, 0.132 mmol) and piperidine (1 drop) in 0.09 mL of pyridine. Compound **4** was not isolated.

*(7,3')-Isomer (**19ab**) from 2-acetamido-5-bromo-3'-fluorobenzophenone **17ab***. The general deprotection and annulation procedures were followed using **17ab** (13.1 mg, 0.0390 mmol) in 0.13 mL of HCl (37 wt% H_2O), then glycine ethyl ester hydrochloride (16.3 mg, 0.117 mmol) and piperidine (1 drop) in 0.08 mL of pyridine. Compound **19ab** was not isolated.

*(7,4')-Isomer (**19ac**) from 2-acetamido-5-bromo-4'-fluorobenzophenone **17ac***. The general deprotection and annulation procedures were using **17ac** (9.3 mg, 0.0277 mmol) in

0.09 mL of HCl (37 wt% H_2O), then glycine ethyl ester hydrochloride (11.6 mg, 0.0831 mmol) and piperidine (1 drop) in 0.3 mL of pyridine. Compound **19ac** was not isolated.

Sugasawa Procedure: Modified from the published procedure:[28] To a flame-dried flask under nitrogen equipped with a stir bar was added BCl_3 (0.76 mL, 0.755 mmol, 1 M solution in CH_2Cl_2). After cooling to 0 ˚C, **17b** (100 mg, 0.581 mmol) was added dropwise, followed by $AlCl_3$ (100.7 mg, 0.755 mmol), **18c** (140.7 mg, 1.162 mmol), and anhydrous benzene (1.2 mL). The reaction was heated to 80 ˚C for 12 hours then cooled back to 0˚C. HCl (2.5 mL, 1 M solution) was added, then the nitrogen line was removed and the reaction was warmed to 80˚C for 30 min. After cooling to room temperature, the aqueous layer was extracted three times with CH_2Cl_2, then the combined organic layers were washed with saturated aqueous NaCl, dried over $MgSO_4$, filtered through celite under reduced pressure, and concentrated by rotary evaporation. After purification by silica prep-TLC, benzophenone **9bc** was afforded as a yellow solid (38.5 mg, 22% yield) along with unreacted starting materials.

2.8.3 Procedures for Approach 2

Standard Isatin Ring-opening Procedure: In a round-bottom flask, a 30% KOH/H_2O (or 30% NaOH/H_2O) solution was prepared. MeOH was added, then isatin was added and dissolved. After 24 h, the reaction was brought to pH ~3 with 1 M HCl, then the aqueous layer was extracted with EtOAc and the combined organic extracts were dried over anhydrous Na_2SO_4, filtered through celite under reduced pressure, and concentrated.

*(2-Ethoxycarbonylaminophenyl)glyoxylic Acid (**28**).* Following the published procedure from Kraus and Guo:[32] In a flame-dried flask under nitrogen equipped with a stir bar, **12e** (500 mg, 3.398 mmol) was dissolved in dry tetrahydrofuran (8.5 mL), then

Et_3N (0.66 mL, 4.757 mmol) was added. After stirring for 30 min, the reaction was cooled to 0 ˚C, and ethyl chloroformate (0.33 mL, 3.398 mmol) was added slowly. The reaction was allowed to warm to room temperature. After 45 min, Na_2CO_3 (540.2 mg, 5.097 mmol) and H_2O (8.5 mL) were added and the reaction was heated to reflux. After 1 h, the reaction was cooled to 0 ˚C and the solution pH adjusted to 1-2 with 0.5 M HCl. The aqueous layer was extracted three times with Et_2O. The combined organic layers were washed once with H_2O, then dried over anhydrous Na_2SO_4, filtered through celite under reduced pressure, and concentrated by rotary evaporation. The product **28** was isolated by silica column chromatography (10% MeOH/CH_2Cl_2, R_f = 0.06) to afford a yellow solid (670.8 mg, 88% yield). ^{1}H NMR (500 MHz, DMSO-d_6) δ 10.82 (s, 1H), 8.20 (d, *J* = 8.3 Hz, 1H), 7.73 (d, *J* = 7.6 Hz, 1H), 7.63 (t, *J* = 7.8 Hz, 1H), 7.15 (t, *J* = 7.3 Hz, 1H), 4.16 (q, *J* = 7.1 Hz, 2H), 1.25 (t, *J* = 7.1 Hz, 3H). ^{13}C NMR (126 MHz, DMSO) δ 197.02, 166.83, 153.06, 141.04, 134.99, 133.47, 122.00, 119.01, 118.64, 60.99, 14.35. HRAM-MS (EI) m/z $[M-H]^-$ Calcd for $C_{11}H_{10}NO_5$ 236.0564; Found 236.0561. HRAM-MS (EI) m/z $[M-H]^-$ Calcd for $C_{11}H_{10}NO_5$ 236.0564; Found 236.0561.

2.8.4 Procedures for Approach 3

*General Saponification Procedure for the Synthesis of 2-Amino-X-bromobenzoic Acids **31***. Following the published procedure,[34] X-bromoisatin **12** (1.00 g, 4.42 mmol) was charged to a round-bottom flask equipped with a stir bar. NaOH (5% H_2O, 22 mL) was added, and the solution was warmed to 50 ˚C. Then, H_2O_2 (30 wt%/H_2O, 1.1 mL, 11.06 mmol) was added in one shot. After 30 min stirring, the solution was brought to pH ~ 4 with 1 M HCl. The product **31** was collected under reduced pressure on a Buchner funnel, rinsed with cold water, and used without further purification as the hydrochloride salt.

*2-Amino-5-bromobenzoic acid (**31a**)*. The general saponification procedure was followed using **12a** (1.00 g, 4.424 mmol). After workup and purification (10% MeOH/CH_2Cl_2, R_f = 0.55), compound **31a** was afforded as an off-white solid (957.1 mg, 86% yield). ^{1}H NMR (500 MHz, DMSO-d_6) δ 7.74 (d, *J* = 2.5 Hz, 1H), 7.34 (dd, *J* = 8.9, 2.5 Hz, 1H), 6.73 (d, *J* = 8.8 Hz, 1H). ^{13}C NMR (126 MHz, DMSO-d_6) δ 168.4, 150.6, 136.1, 132.8, 118.7, 111.1, 104.5. GC-FTIR ν_{max} (cm^{-1}): 3500, 3384, 3010, 2885, 1671, 1615, 1584, 1549, 1482, 1424, 1316, 1291, 1231, 1161, 689. HRAM-MS (EI) m/z: $[M+H]^+$ Calcd. for $C_7H_7BrNO_2$ 215.96547; Found 215.96517.

*2-Amino-4-bromobenzoic acid (**31b**)*. The general saponification procedure was followed using **12b** (1.00 g, 4.424 mmol). After workup and purification (10% MeOH/CH_2Cl_2, R_f = 0.59), compound **31b** was afforded as an off-white solid (799.8 mg, 72% yield). ^{1}H NMR (500 MHz, DMSO-d_6) δ 7.59 (d, *J* = 8.5 Hz, 1H), 6.97 (d, *J* = 2.0 Hz, 1H), 6.64 (dd, *J* = 8.5, 2.0 Hz, 1H). ^{13}C NMR (126 MHz, DMSO-d_6) δ 168.9, 152.5, 133.1, 127.34, 118.1, 117.3, 108.8. GC-FTIR ν_{max} (cm^{-1}): 3502, 3384, 2908, 2717, 1667, 1609, 1580, 1547, 1482, 1428, 1312, 1237, 1156, 1094, 899. HRAM-MS (EI) m/z: $[M+H]^+$ Calcd. for $C_7H_7BrNO_2$ 215.96547; Found 215.96523.

*2-Amino-3-bromobenzoic acid (**31c**)*. The general saponification procedure was followed using **12c** (1.00 g, 4.424 mmol). After workup and purification (10% MeOH/CH_2Cl_2, R_f = 0.62), compound **31c** was afforded as an off-white solid (594.3 mg, 66% yield). ^{1}H NMR (500 MHz, DMSO-d_6) δ 7.78 (dd, *J* = 8.0, 1.6 Hz, 1H), 7.63 (dd, *J* = 7.8, 1.5 Hz, 1H), 6.74 (s, 1H), 6.52 (t, *J* = 7.9 Hz, 1H). ^{13}C NMR (126 MHz, DMSO-d_6) δ 169.0, 147.8, 137.12, 131.0, 115.8, 111.8, 109.5. GC-FTIR ν_{max} (cm^{-1}): 3489 (s), 3369 (s), 2998 (br), 2863 (br), 2719 (m), 2638 (m), 1667 (s), 1607 (s), 1576 (s), 1543 (s), 1449, 1418,

1314, 1264, 1244, 1059, 746, 692. HRAM-MS (EI) m/z: $[M+H]^+$ Calcd. for $C_7H_7BrNO_2$ 215.9655; Found 215.9652.

*2-Amino-6-bromobenzoic acid (**31d**)*. The general saponification procedure was followed using **12d** (1.00 g, 4.424 mmol), with the following modification: after bringing the solution to pH ~ 4, compound **31d** (10% MeOH/CH_2Cl_2, R_f = 0.07) was extracted into EtOAc, dried over anhydrous Na_2SO_4, filtered through celite under reduced pressure, and concentrated by rotary evaporation to afford a red solid (970.6 mg, 87% yield). ^{1}H NMR (500 MHz, DMSO-d_6) δ 7.00 – 6.96 (m, 1H), 6.76 (dd, J = 7.7, 1.0 Hz, 1H), 6.70 (dd, J = 8.2, 1.0 Hz, 1H). ^{13}C NMR (126 MHz, DMSO-d_6) δ 168.1, 148.4, 131.4, 120.1, 119.8, 118.7, 114.8. GC-FTIR ν_{max} (cm^{-1}): 3492, 3382, 3377, 3334, 3008, 2910, 2607, 1673, 1613, 1584, 1553, 1462, 1420, 1385, 1293, 1256, 1235, 1161, 1127, 885, 799, 774, 689. HRAM-MS (EI) m/z $[M+H]^+$ Calcd for $C_7H_7BrNO_2$ 215.96547; Found 215.96533.

*General Amidation Procedure for the Synthesis of 2-Amino-X-bromo-N-methoxy-N-methylbenzamides **14.*** Following the published procedure:[35] To a flame-dried round-bottom flask equipped with a stir bar and under inert nitrogen atmosphere were charged 2-amino-X-bromobenzoic acid hydrochloride **31** (1 equiv) and *N*-methoxy-*N*-methylamine hydrochloride (1.5 equiv). Anhydrous DMF (0.2 M) was added at room temperature with stirring, then *N*-methylmorpholine (4.5 equiv) and HBTU (1.5 equiv) were added. After 18 h, the mixture was poured onto water in a separatory funnel. The aqueous layer was extracted three times with EtOAc. The combined organic extracts were dried over anhydrous Na_2SO_4, filtered through celite under reduced pressure, and concentrated by rotary evaporation. The product **14** was isolated by alumina flash chromatography (25% EtOAc/hexanes).

*2-Amino-5-bromo-N-methoxy-N-methylbenzamide (**14a**)*. The general amidation procedure was followed using **31a** (1.11 g, 4.38 mmol), *N*-methoxy-*N*-methylamine hydrochloride (641 mg, 6.57 mmol), *N*-methylmorpholine (2.2 mL, 19.7 mmol), and HBTU (2.49 g, 6.57 mmol) in 22 mL of anhydrous DMF. Compound **14a** was isolated by alumina flash chromatography (25% EtOAc/hexanes, R_f = 0.10) as an orange solid (1.10 g, 97% yield). ^{1}H NMR (500 MHz, $CDCl_3$) δ 7.50 (d, *J* = 2.3 Hz, 1H), 7.26 (dd, *J* = 8.6, 2.3 Hz, 1H), 6.59 (d, *J* = 8.6 Hz, 1H), 4.67 (s, 2H), 3.59 (s, 3H), 3.34 (s, 3H). ^{13}C NMR (126 MHz, $CDCl_3$) δ 168.5, 145.9, 134.1, 131.6, 118.6, 118.2, 108.2, 61.3, 33.9. GC-FTIR ν_{max} (cm^{-1}): 3456, 3354, 3245, 2971, 2935, 1617, 1582, 1488, 1424, 1403, 1383, 1302, 1262, 1210, 1158, 1113, 1084, 1057, 997, 978, 903, 891, 829, 820, 770, 745, 689. HRAM-MS (EI) m/z: $[M+H]^+$ Calcd for $C_9H_{12}BrN_2O_2$ 259.00767; Found 259.00768.

*2-Amino-4-bromo-N-methoxy-N-methylbenzamide (**14b**)*. The general amidation procedure was followed using **31b** (1.14 g, 4.53 mmol), *N*-methoxy-*N*-methylamine hydrochloride (662 mg, 6.79 mmol), *N*-methylmorpholine (2.2 mL, 20.4 mmol), and HBTU (2.58 g, 6.79 mmol) in 23 mL of anhydrous DMF. Compound **14b** was isolated by alumina flash chromatography (25% EtOAc/hexanes, R_f = 0.16) as a red oil (1.16 g, 99% yield). ^{1}H NMR (500 MHz, $CDCl_3$) δ 7.26 (d, *J* = 8.4 Hz, 1H), 6.86 (d, *J* = 1.9 Hz, 1H), 6.79 (dd, *J* = 8.3, 1.9 Hz, 1H), 4.79 (s, 2H), 3.56 (s, 3H), 3.33 (s, 3H). ^{13}C NMR (126 MHz, $CDCl_3$) δ 169.2, 148.3, 130.7, 125.5, 119.7, 119.1, 115.5, 61.2, 33.9. GC-FTIR ν_{max} (cm^{-1}): 3454, 3352, 3242, 2971, 2935, 1615, 1578, 1489, 1476, 1459, 1418, 1383, 1318, 1287, 1262, 1215, 1173, 1148, 1071, 995, 976, 903, 860, 804, 760, 721, 689. HRAM-MS (EI) m/z: $[M+H]^+$ Calcd for $C_9H_{12}BrN_2O_2$ 259.00767; Found 259.00726.

*2-Amino-3-bromo-N-methoxy-N-methylbenzamide (**14c**).* The general amidation procedure was followed using **31c** (1.83 g, 7.233 mmol), *N*-methoxy-*N*-methylamine hydrochloride (1.06 g, 10.9 mmol), *N*-methylmorpholine (3.6 mL, 32.6 mmol), and HBTU (4.12 g, 10.9 mmol) in 36 mL of anhydrous DMF. Compound **14c** was isolated by alumina flash chromatography (25% EtOAc/hexanes, R_f = 0.29) as a light red oil (1.39 g, 74% yield). ^{1}H NMR (500 MHz, $CDCl_3$) δ 7.47 (dd, *J* = 7.9, 1.5 Hz, 1H), 7.32 (dd, *J* = 7.7, 1.5 Hz, 1H), 6.57 (t, *J* = 7.8 Hz, 1H), 5.13 (s, 2H), 3.57 (s, 3H), 3.35 (s, 3H). ^{13}C NMR (126 MHz, $CDCl_3$) δ 169.1, 144.2, 134.5, 128.4, 118.1, 117.2, 110.7, 61.3, 34.1. GC-FTIR ν_{max} (cm^{-1}): 3446, 3355, 2979, 2935, 1611, 1578, 1549, 1453, 1420, 1383, 1306, 1252, 1210, 1171, 1152, 1067, 980, 791, 750, 733. HRAM-MS (EI) m/z: $[M+H]^+$ Calcd for $C_9H_{12}BrN_2O_2$ 259.00767; Found 259.00729.

*2-Amino-6-bromo-N-methoxy-N-methylbenzamide (**14d**, crude mixture).* The general amidation procedure was followed using **31d** (968 mg, 3.83 mmol), *N*-methoxy-*N*-methylamine hydrochloride (561 mg, 5.750 mmol), *N*-methylmorpholine (1.9 mL, 17.3 mmol), and HBTU (2.18 g, 5.75 mmol) in 19 mL of anhydrous DMF. Compound **14d** was not isolated. GC-FTIR ν_{max} (cm^{-1}): 3440, 3352, 3242, 2975, 2937, 1617, 1594, 1565, 1466, 1449, 1420, 1387, 1296, 1215, 1179, 1156, 1117, 1096, 1073, 1042, 984, 878, 781, 752, 708, 662. HRAM-MS (EI) m/z: $[M+H]^+$ Calcd for $C_9H_{12}BrN_2O_2$ 259.00767; Found 259.00751.

*General Lithiate Addition Procedure for the Syntheses of 2-Amino-X-bromo-Y'-fluorobenzophenones **9**.* In a flame-dried flask under nitrogen equipped with a stir bar, 1-bromo-X-fluorobenzene **32** (0.07 mL, 0.607 mmol) was dissolved in anhydrous THF (0.3 mL). The solution was cooled to either -78 ˚C or -100 ˚C, then *n*-butyllithium (0.23 mL,

0.578 mmol, 2.5 M solution in hexanes) was added slowly. In a separate flame-dried flask under nitrogen, 2-amino-X-bromo-*N*-methoxy-*N*-methylbenzamide **14** (75 mg, 0.289 mmol) was dissolved in anhydrous THF (1.2 mL) and cooled to either -78˚C or -100˚C. After the lithiate solution had been stirring for 1 h, the benzamide solution was added dropwise to it. The reaction was quenched after 15 min with saturated aqueous NH_4Cl and allowed to warm gradually to room temperature. The aqueous layer was extracted with EtOAc, then the combined organic layers were dried over Na_2SO_4, filtered through celite under reduced pressure, and concentrated by rotary evaporation. The product **9** was then isolated by silica flash chromatography.

*2-Amino-5-bromo-2'-fluorobenzophenone (**9aa**).* The general lithiate addition procedure was followed at -100 ˚C using **14a** (75 mg, 0.289 mmol) and **32a** (0.07 mL, 0.607 mmol). Compound **9aa** was isolated by silica flash chromatography (25% EtOAc/hexanes, R_f = 0.57) to afford a yellow solid (55.2 mg, 65% yield). ^{1}H NMR (500 MHz, $CDCl_3$) δ 7.50 (dddd, *J* = 8.3, 7.2, 5.2, 1.8 Hz, 1H), 7.43 – 7.38 (m, 2H), 7.36 (dd, *J* = 8.8, 2.4 Hz, 1H), 7.26 (s, 6H), 7.17 (ddd, *J* = 9.5, 8.3, 1.0 Hz, 1H), 6.63 (d, *J* = 8.8 Hz, 1H), 6.38 (s, 2H). ^{13}C NMR (126 MHz, $CDCl_3$) δ 194.3, 159.0 (d, *J* = 250.3 Hz), 149.9, 137.7, 136.1 (d, *J* = 2.1 Hz), 132.2 (d, *J* = 8.1 Hz), 129.7 (d, *J* = 3.2 Hz), 127.9 (d, *J* = 16.3 Hz), 124.3 (d, *J* = 3.6 Hz), 119.3, 118.8, 116.3 (d, *J* = 21.5 Hz), 106.7. ^{19}F NMR (471 MHz, $CDCl_3$) δ -113.31 – -113.39 (m). GC-FTIR ν_{max} (cm^{-1}): 3456, 3346, 1613, 1582, 1538, 1484, 1468, 1451, 1410, 1347, 1318, 1298, 1269, 1240, 1217, 1161, 1144, 1103, 1092, 949, 939, 893, 839, 822, 785, 760, 723, 689. HRAM-MS (EI) m/z: $[M+H]^+$ Calcd for $C_{13}H_{10}BrFNO$ 293.99243; Found 293.99252.

*2-Amino-5-bromo-3'-fluorobenzophenone (**9ab**)*. The general lithiate addition procedure was followed at -78 ˚C using **14a** (75 mg, 0.289 mmol) and **32b** (0.07 mL, 0.607 mmol). Compound **9ab** was isolated by silica flash chromatography (25% EtOAc/hexanes, R_f = 0.50) to afford a yellow solid (51.6 mg, 60% yield). 1H NMR (500 MHz, $CDCl_3$) δ 7.51 (d, *J* = 2.4 Hz, 1H), 7.46 (td, *J* = 7.9, 5.4 Hz, 1H), 7.40 – 7.36 (m, 2H), 7.33 (ddd, *J* = 9.0, 2.6, 1.5 Hz, 1H), 7.25 (tdd, *J* = 8.3, 2.6, 1.1 Hz, 1H), 6.65 (d, *J* = 8.8 Hz, 1H), 6.12 (s, 2H). ^{13}C NMR (126 MHz, $CDCl_3$) δ 196.3, 162.4 (d, *J* = 248.4 Hz), 149.9, 137.2, 135.9, 130.0 (d, *J* = 7.8 Hz), 124.8 (d, *J* = 3.1 Hz), 118.9, 118.8, 118.5 (d, *J* = 21.4 Hz), 115.9 (d, *J* = 22.5 Hz), 106.7. ^{19}F NMR (471 MHz, $CDCl_3$) δ -111.71 – -111.85 (m). GC-FTIR ν_{max} (cm^{-1}): 3467, 3350, 3070, 1634, 1611, 1584, 1538, 1472, 1437, 1408, 1314, 1298, 1271, 1250, 1202, 1161, 1119, 986, 968, 882, 870, 820, 814, 793, 774, 735, 704, 683, 656. HRAM-MS (EI) m/z: $[M+H]^+$ Calcd for $C_{13}H_{10}BrFNO$ 293.99243; Found 293.99206.

*2-Amino-5-bromo-4'-fluorobenzophenone (**9ac**)*. The general lithiate addition procedure was followed at -78 ˚C using **14a** (75 mg, 0.289 mmol) and **32c** (0.07 mL, 0.607 mmol). Compound **9ac** was isolated by silica flash chromatography (25% EtOAc/hexanes, R_f = 0.46) to afford a yellow solid (66.7 mg, 78% yield). 1H NMR (500 MHz, $CDCl_3$) δ 7.67 (dd, *J* = 8.7, 5.4 Hz, 2H), 7.51 (d, *J* = 2.4 Hz, 1H), 7.37 (dd, *J* = 8.9, 2.4 Hz, 1H), 7.17 (t, *J* = 8.6 Hz, 2H), 6.65 (d, *J* = 8.8 Hz, 1H), 6.01 (s, 2H). ^{13}C NMR (126 MHz, $CDCl_3$) δ 196.3, 164.8 (d, *J* = 252.8 Hz), 149.6, 136.9, 135.8, 135.4, 131.7 (d, *J* = 8.9 Hz), 119.4, 118.9, 115.5 (d, *J* = 21.8 Hz), 106.7. ^{19}F NMR (471 MHz, $CDCl_3$) δ -107.24 (tt, *J* = 8.4, 5.5 Hz). GC-FTIR ν_{max} (cm^{-1}): 3469, 3352, 1611, 1599, 1580, 1538, 1507, 1474, 1408, 1296, 1240, 1158, 1096, 1015, 951, 939, 897, 853, 820, 806, 783, 739, 716, 683. HRAM-MS (EI) m/z: $[M+H]^+$ Calcd for $C_{13}H_{10}BrFNO$ 293.99243; Found 293.99219.

*2-Amino-4-bromo-2'-fluorobenzophenone (**9ba**)*. The general lithiate addition procedure was followed at -100 ˚C using **14b** (75 mg, 0.289 mmol) and **32a** (0.07 mL, 0.607 mmol). Compound **9ba** was isolated by silica flash chromatography (25% EtOAc/hexanes, R_f = 0.54) to afford a yellow oil (42.8 mg, 50% yield). ^{1}H NMR (500 MHz, $CDCl_3$) δ 7.48 (dddd, *J* = 8.4, 7.2, 5.2, 1.8 Hz, 1H), 7.40 (ddd, *J* = 7.6, 6.8, 1.8 Hz, 1H), 7.24 (dd, *J* = 7.5, 1.0 Hz, 1H), 7.19 – 7.13 (m, 2H), 6.91 (d, *J* = 1.8 Hz, 1H), 6.69 (dd, *J* = 8.6, 1.9 Hz, 1H), 6.42 (s, 2H). ^{13}C NMR (126 MHz, $CDCl_3$) δ 194.7, 159.0 (d, *J* = 250.1 Hz), 151.7, 135.8 (d, *J* = 2.1 Hz), 132.0 (*d*, *J* = 8.2 Hz), 130.0, 129.7 (d, *J* = 3.4 Hz), 128.3, 128.2, 124.3 (d, *J* = 3.6 Hz), 119.2 (d, *J* = 15.7 Hz), 117.0, 116.1 (d, *J* = 21.6 Hz). ^{19}F NMR (471 MHz, $CDCl_3$) δ -113.35 (dddd, *J* = 9.4, 7.1, 4.0, 1.3 Hz). GC-FTIR ν_{max} (cm^{-1}): 3450, 3340, 1609, 1584, 1530, 1480, 1451, 1424, 1318, 1269, 1244, 1219, 1156, 1138, 1098, 1049, 1032, 934, 878, 851, 824, 758, 687. HRAM-MS (EI) m/z: $[M+H]^+$ Calcd. for $C_{13}H_{10}BrFNO$ 293.99243; Found 293.99240.

*2-Amino-4-bromo-3'-fluorobenzophenone (**9bb**)*. The general lithiate addition procedure was followed at -78 ˚C using **14b** (75 mg, 0.289 mmol) and **32b** (0.07 mL, 0.607 mmol). Compound **9bb** was isolated by silica flash chromatography (25% EtOAc/hexanes, R_f = 0.57) to afford a yellow oil (47.1 mg, 55% yield). ^{1}H NMR (500 MHz, $CDCl_3$) δ 7.43 (td, *J* = 7.9, 5.5 Hz, 1H), 7.37 (dt, *J* = 7.6, 1.3 Hz, 1H), 7.31 (ddd, *J* = 9.0, 2.7, 1.5 Hz, 1H), 7.27 (d, *J* = 8.6 Hz, 1H), 7.23 (tdd, *J* = 8.3, 2.7, 1.1 Hz, 1H), 6.93 (d, *J* = 1.9 Hz, 1H), 6.73 (dd, *J* = 8.6, 1.9 Hz, 1H), 6.19 (s, 2H). ^{13}C NMR (126 MHz, $CDCl_3$) δ 196.8, 162.4 (d, *J* = 248.0 Hz), 151.8, 141.7 (d, *J* = 6.3 Hz), 135.5, 129.9 (d, *J* = 7.9 Hz), 129.5, 124.7 (d, *J* = 2.9 Hz), 119.5, 119.0, 118.2 (d, *J* = 21.3 Hz), 116.3, 115.9 (d, *J* = 22.7 Hz). ^{19}F NMR (471 MHz, $CDCl_3$) δ -112.03 (td, *J* = 8.8, 5.5 Hz). GC-FTIR ν_{max} (cm^{-1}): 3460, 3344, 3070,

1607, 1584, 1532, 1480, 1439, 1424, 1314, 1271, 1250, 1208, 1154, 1117, 1096, 1049, 1003, 978, 965, 895, 837, 826, 806, 793, 764, 716, 698, 683, 662. HRAM-MS (EI) m/z: $[M+H]^+$ Calcd for $C_{13}H_{10}BrFNO$ 293.99243; Found 293.99214.

*2-Amino-4-bromo-4'-fluorobenzophenone (**9bc**)*. The general lithiation addition procedure was followed at -78 ˚C using **14b** (75 mg, 0.289 mmol) and **32c** (0.07 mL, 0.607 mmol). Compound **9bc** was isolated by silica flash chromatography (25% EtOAc/hexanes, R_f = 0.57) to afford a yellow solid (42.4 mg, 49% yield). ^{1}H NMR (500 MHz, $CDCl_3$) δ 7.65 (dd, *J* = 8.8, 5.4 Hz, 2H), 7.27 (d, 1H), 7.14 (t, *J* = 8.7 Hz, 2H), 6.93 (d, *J* = 1.9 Hz, 1H), 6.74 (dd, *J* = 8.5, 1.9 Hz, 1H), 6.09 (s, 2H). ^{13}C NMR (126 MHz, $CDCl_3$) δ 196.9, 164.6 (d, *J* = 252.5 Hz), 151.6, 135.7 (d, *J* = 3.2 Hz), 135.4, 131.6 (d, *J* = 8.8 Hz), 129.1, 119.4, 118.9, 116.8, 115.3 (d, *J* = 21.8 Hz). ^{19}F NMR (471 MHz, $CDCl_3$) δ -107.64 (tt, *J* = 8.4, 5.5 Hz). GC-FTIR ν_{max} (cm^{-1}): 3460, 3344, 3072, 1605, 1582, 1532, 1507, 1478, 1422, 1312, 1239, 1156, 1096, 1051, 1015, 949, 932, 874, 849, 808, 768, 729, 700, 679. HRAM-MS (EI) m/z: $[M+H]^+$ Calcd for $C_{13}H_{10}BrFNO$ 293.99243; Found 293.99223.

*2-Amino-3-bromo-2'-fluorobenzophenone (**9ca**)*. The general lithiate addition procedure was followed at -100 ˚C using **14c** (75 mg, 0.289 mmol) and **32a** (0.07 mL, 0.607 mmol). Compound **9ca** was isolated by silica flash chromatography (25% EtOAc/hexanes, R_f = 0.73) to afford a yellow solid (47.8 mg, 56% yield). ^{1}H NMR (500 MHz, $CDCl_3$) δ 7.61 (dd, *J* = 7.7, 1.5 Hz, 1H), 7.48 (dddd, *J* = 8.4, 7.2, 5.3, 1.9 Hz, 1H), 7.41 (td, *J* = 7.3, 1.8 Hz, 1H), 7.33 (ddd, *J* = 8.1, 2.5, 1.5 Hz, 1H), 7.24 (dd, *J* = 7.5, 1.0 Hz, 1H), 7.15 (ddd, *J* = 9.4, 8.3, 1.0 Hz, 1H), 6.97 (s, 2H), 6.49 (t, *J* = 7.9 Hz, 1H). ^{13}C NMR (126 MHz, $CDCl_3$) δ 194.8, 159.0 (d, *J* = 250.2 Hz), 148.0, 138.0, 134.1 (d, *J* = 1.8 Hz), 132.1 (d, *J* = 8.2 Hz), 129.7 (d, *J* = 3.2 Hz), 124.2 (d, *J* = 3.4 Hz), 119.0, 116.1 (d, *J*

= 21.5 Hz), 116.0, 111.0. ^{19}F NMR (471 MHz, $CDCl_3$) δ -113.17 – -113.23 (m). GC-FTIR ν_{max} (cm^{-1}): 3473, 3334, 1634, 1609, 1574, 1532, 1484, 1451, 1435, 1333, 1316, 1279, 1248, 1219, 1156, 1134, 1100, 1063, 1034, 939, 826, 752, 735, 727. HRAM-MS (EI) m/z: $[M+H]^+$ Calcd for $C_{13}H_{10}BrFNO$ 293.99243; Found 293.99220.

*2-Amino-3-bromo-3'-fluorobenzophenone (**9cb**)*. The general lithiate addition procedure was followed at -78 ˚C using **14c** (75 mg, 0.289 mmol) and **32b** (0.07 mL, 0.607 mmol). Compound **9cb** was isolated by silica flash chromatography (25% EtOAc/hexanes, R_f = 0.68) to afford a yellow solid (54.0 mg, 63% yield). ^{1}H NMR (500 MHz, $CDCl_3$) δ 7.62 (dd, *J* = 7.7, 1.5 Hz, 1H), 7.47 – 7.38 (m, 3H), 7.33 (ddd, *J* = 9.0, 2.6, 1.4 Hz, 1H), 7.26 – 7.21 (m, 1H), 6.68 (s, 2H), 6.52 (t, *J* = 7.9 Hz, 1H). ^{13}C NMR (126 MHz, $CDCl_3$) δ 196.8, 162.3 (d, *J* = 248.1 Hz), 147.9, 141.6, 137.6, 133.8, 129.9 (d, *J* = 7.9 Hz), 124.9 (d, *J* = 3.1 Hz), 118.5, 118.3 (d, *J* = 21.3 Hz), 116.1 (d, *J* = 22.6 Hz), 115.8, 111.1. ^{19}F NMR (471 MHz, $CDCl_3$) δ -112.08 (td, *J* = 8.8, 5.4 Hz). GC-FTIR ν_{max} (cm^{-1}): 3475, 3342, 3070, 1632, 1607, 1584, 1572, 1532, 1484, 1439, 1314, 1268, 1250, 1208, 1154, 1113, 1061, 970, 887, 874, 860, 826, 808, 789, 750, 718, 685, 656. HRAM-MS (EI) m/z: $[M+H]^+$Calcd for $C_{13}H_{10}BrFNO$ 293.99243; Found 293.99195.

*2-Amino-3-bromo-4'-fluorobenzophenone (**9cc**)*. The general lithiate addition procedure was followed at -78 ˚C using **14c** (75 mg, 0.289 mmol) and **32c** (0.07 mL, 0.607 mmol). Compound **9cc** was isolated by silica flash chromatography (25% EtOAc/hexanes, R_f = 0.68) to afford a yellow solid (52.7 mg, 62% yield). ^{1}H NMR (500 MHz, $CDCl_3$) δ 7.67 (dd, *J* = 8.8, 5.3 Hz, 2H), 7.61 (dd, *J* = 7.7, 1.5 Hz, 1H), 7.40 (dd, *J* = 8.0, 1.5 Hz, 1H), 7.15 (t, *J* = 8.6 Hz, 2H), 6.57 (s, 2H), 6.52 (t, *J* = 7.9 Hz, 1H). ^{13}C NMR (126 MHz, $CDCl_3$) δ 196.9, 164.7 (d, *J* = 252.9 Hz), 147.7, 137.2, 135.6 (d, *J* = 3.2 Hz), 133.5, 131.8 (d, *J* =

8.8 Hz), 119.0, 115.8, 115.3 (d, J = 21.9 Hz), 111.1. ^{19}F NMR (471 MHz, $CDCl_3$) δ -107.43 (tt, J = 8.5, 5.4 Hz). GC-FTIR ν_{max} (cm^{-1}): 3477, 3344, 3070, 1630, 1607, 1572, 1534, 1505, 1437, 1408, 1312, 1266, 1248, 1229, 1156, 1134, 1098, 1061, 1015, 953, 939, 851, 816, 799, 754, 733, 718, 691. HRAM-MS (EI) m/z: $[M+H]^+$ Calcd for $C_{13}H_{10}BrFNO$ 293.99243; Found 293.99211.

2.8.5 Procedures for the Syntheses of (X,X')-Flubromazepam Positional Isomers

N-Acylation Procedure. In a flame-dried flask under nitrogen and equipped with a stir bar, 2-amino-X-bromo-X'-fluorobenzophenone **9** (1 equiv) was dissolved in anhydrous THF (0.2 M) and cooled to 0 ˚C. 2-Bromoacetyl bromide (1.3 equiv) was added slowly. After stirring for 1 h, the reaction was quenched with water. The aqueous layer was extracted three times with EtOAc, then the combined organic layers were washed with NaOH (0.5 M solution in water), dried over anhydrous Na_2SO_4, filtered through celite under reduced pressure, and concentrated by rotary evaporation.

Imination Procedure. The crude *N*-acylation adduct was dissolved in NH_3 (0.08 M, 13 wt% in MeOH) and stirred for 18 h. After concentrating by rotary evaporation, the mixture was partitioned between Et_2O and H_2O. The aqueous layer was extracted three times with Et_2O, then the combined organic layers were dried over anhydrous Na_2SO_4, filtered through celite under reduced pressure, and concentrated by rotary evaporation. The product was isolated by silica prep-TLC (5% MeOH/CH_2Cl_2).

*(7,2')-Isomer (Parent compound): IUPAC name- 7-Bromo-5-(2-fluorophenyl)-1,3-dihydro-2H-benzo[e][1,4]diazepin-2-one (flubromazepam, **4**).* The general *N*-acylation and imination procedures were followed using **9aa** (86.6 mg, 0.294 mmol) and 2-bromoacetyl bromide (0.03 mL, 0.382 mmol) in 2.3 mL of THF, then 3.7 mL of NH_3 (13

wt% in MeOH). Compound **4** was isolated by silica prep-TLC (5% MeOH/CH_2Cl_2, R_f = 0.15) to afford an orange oil (98.6 mg, 98% yield). ^{1}H NMR (500 MHz, DMSO-d_6) δ 10.74 (s, 1H), 7.72 (dd, *J* = 8.7, 2.3 Hz, 1H), 7.57 (tdd, *J* = 7.4, 3.3, 1.4 Hz, 2H), 7.33 (t, *J* = 7.5 Hz, 1H), 7.26 (t, 1H), 7.21 (d, *J* = 2.3 Hz, 1H), 7.19 (d, *J* = 8.7 Hz, 1H), 4.20 (s, 2H). ^{13}C NMR (126 MHz, DMSO-d_6) δ 169.6, 165.1, 159.6 (d, *J* = 248.6 Hz), 137.8, 134.4, 132.4 (d, *J* = 8.5 Hz), 131.5 (d, *J* = 2.7 Hz), 131.3, 129.2, 127.1 (d, *J* = 12.3 Hz), 124.7 (d, *J* = 3.5 Hz), 123.3, 116.0 (d, *J* = 21.4 Hz), 114.7, 57.1. ^{19}F NMR (471 MHz, DMSO-d_6) δ -113.91 – -114.01 (m). GC-FTIR ν_{max} (cm^{-1}): 3217, 3116, 3074, 2958, 1690, 1615, 1576, 1482, 1451, 1385, 1350, 1325, 1258, 1231, 1219, 1103, 1088, 1013, 949, 822, 770, 754, 654. HRAM-MS (EI) m/z: $[M+H]^+$ Calcd for $C_{15}H_{11}BrFN_2O$ 333.00333; Found 333.00302.

*(7,3')-Isomer: IUPAC name- 7-bromo-5-(3-fluorophenyl)-1,3-dihydro-2H-benzo[e][1,4]diazepin-2-one (**19ab**).* The general *N*-acylation and imination procedures were followed using **9ab** (70.9 mg, 0.241 mmol) and 2-bromoacetyl bromide (0.03 mL, 0.313 mmol) in 1.2 mL of THF, then 3.0 mL of NH_3 (13 wt% in MeOH). Compound **19ab** was isolated by silica prep-TLC (5% MeOH/CH_2Cl_2, R_f = 0.15) to afford a yellow oil (14.6 mg, 12% yield). ^{1}H NMR (500 MHz, DMSO-d_6) δ 10.68 (s, 1H), 7.76 (dd, *J* = 8.7, 2.3 Hz, 1H), 7.49 (td, *J* = 8.0, 5.9 Hz, 1H), 7.39 – 7.31 (m, 3H), 7.22 (t, *J* = 8.7 Hz, 2H), 4.17 (s, 2H). ^{13}C NMR (126 MHz, DMSO-d_6) δ 170.0, 167.2 (d, *J* = 2.7 Hz), 162.0 (d, *J* = 244.4 Hz), 141.0 (d, *J* = 7.4 Hz), 139.1, 134.6, 132.5, 130.5 (d, *J* = 8.0 Hz), 127.7, 125.6 (d, *J* = 2.7 Hz), 123.5, 117.4 (d, *J* = 21.2 Hz), 115.6 (d, *J* = 22.8 Hz), 114.5, 57.1. ^{19}F NMR (471 MHz, DMSO-d_6) δ -112.83 (td, *J* = 9.4, 6.5 Hz). GC-FTIR ν_{max} (cm^{-1}): 3213, 3116, 3074, 2952, 2852, 1692, 1613, 1584, 1478, 1441, 1383, 1356, 1322, 1291, 1271, 1260, 1235,

1200, 1148, 1121, 1088, 1019, 980, 868, 841, 826, 793, 770, 746, 696, 679. HRAM-MS (EI) m/z: $[M+H]^+$ Calcd for $C_{15}H_{11}BrFN_2O$ 333.00333; Found 333.00284.

*(7,4')-Isomer: IUPAC name- 7-bromo-5-(4-fluorophenyl)-1,3-dihydro-2H-benzo[e][1,4]diazepin-2-one (**19ac**).* The general *N*-acylation and imination procedures were followed using **9ac** (122.4 mg, 0.416 mmol) and 2-bromoacetyl bromide (0.05 mL, 0.541 mmol) in 2.1 mL of THF, then 5.2 mL of NH_3 (13 wt% in MeOH). Compound **19ac** was isolated by silica prep-TLC (5% MeOH/CH_2Cl_2, R_f = 0.56) to afford a light orange solid (45.8 mg, 52% yield). ^{1}H NMR (500 MHz, DMSO-d_6) δ 10.65 (s, 1H), 7.76 (dd, *J* = 8.7, 2.3 Hz, 1H), 7.53 (dd, *J* = 8.7, 5.6 Hz, 2H), 7.36 (d, *J* = 2.3 Hz, 1H), 7.28 (t, *J* = 8.8 Hz, 2H), 7.21 (d, *J* = 8.7 Hz, 1H), 4.15 (s, 2H). ^{13}C NMR (126 MHz, DMSO-d_6) δ 170.4, 167.5, 163.7 (d, *J* = 248.4 Hz), 139.3, 135.4 (d, *J* = 2.9 Hz), 134.7, 132.8, 131.9 (d, *J* = 8.8 Hz), 128.2, 123.7, 115.6 (d, *J* = 21.7 Hz), 114.7, 57.2. ^{19}F NMR (471 MHz, DMSO-d_6) δ -110.68 (tt, *J* = 8.9, 5.7 Hz). GC-FTIR ν_{max} (cm^{-1}): 3213, 3120, 3074, 2950, 2946, 2848, 1690, 1611, 1597, 1569, 1507, 1482, 1408, 1383, 1347, 1322, 1287, 1258, 1233, 1194, 1158, 1131, 1098, 1015, 947, 843, 824, 772, 756. HRAM-MS (EI) m/z: $[M+H]^+$ Calcd for $C_{15}H_{11}BrFN_2O$ 333.00333; Found 333.00290.

*(8,2')-Isomer: IUPAC name- 8-bromo-5-(2-fluorophenyl)-1,3-dihydro-2H-benzo[e][1,4]diazepin-2-one (**19ba**).* The general *N*-acylation and imination procedures were followed using **9ba** (86.6 mg, 0.294 mmol) and 2-bromoacetyl bromide (0.03 mL, 0.382 mmol) in 2.3 mL THF, then 3.7 mL of NH_3 (13 wt% in MeOH). Compound **19ba** was isolated by silica prep-TLC (5% MeOH/CH_2Cl_2, R_f = 0.15) to afford an off-white fluffy solid (62.6 mg, 65% yield). ^{1}H NMR (500 MHz, DMSO-d_6) δ 10.72 (s, 1H), 7.58 – 7.52 (m, 2H), 7.42 (d, *J* = 2.0 Hz, 1H), 7.34 – 7.30 (m, 2H), 7.24 (ddd, *J* = 10.8, 8.7, 1.1

Hz, 1H), 7.06 (d, *J* = 8.5 Hz, 1H), 4.20 (s, 2H). ^{13}C NMR (126 MHz, DMSO-d_6) δ 169.7, 165.8, 159.7 (d, *J* = 248.7 Hz), 139.8, 132.3 (d, *J* = 8.2 Hz), 131.5 (d, *J* = 7.2 Hz), 127.3 (d, *J* = 12.8 Hz), 126.5, 125.9, 124.6 (d, *J* = 3.4 Hz), 124.4, 123.3, 116.0 (d, *J* = 21.4 Hz), 57.1. ^{19}F NMR (471 MHz, DMSO-d_6) δ -113.90 (dt, *J* = 12.0, 6.7 Hz). GC-FTIR ν_{max} (cm^{-1}): 3207, 3128, 3045, 2962, 1688, 1615, 1596, 1567, 1488, 1478, 1451, 1379, 1360, 1329, 1260, 1215, 1165, 1154, 1103, 1086, 1017, 951, 930, 874, 822, 768, 748, 721, 673. HRAM-MS (EI) m/z: $[M+H]^+$ Calcd for $C_{15}H_{11}BrFN_2O$ 333.00333; Found 333.00311.

*(8,3')-Isomer: IUPAC name- 8-bromo-5-(3-fluorophenyl)-1,3-dihydro-2H-benzo[e][1,4]diazepin-2-one (**19bb**).* The general *N*-acylation and imination procedures were followed using **9bb** (70.9 mg, 0.241 mmol) and 2-bromoacetyl bromide (0.03 mL, 0.313 mmol) in 1.2 mL of THF, then 3.0 mL of NH_3 (13 wt% in MeOH). Compound **19bb** was isolated by silica prep-TLC (5% MeOH/CH_2Cl_2, R_f = 0.19) to afford an off-white granular solid (62.5 mg, 66% yield). ^{1}H NMR (500 MHz, DMSO-d_6) δ 10.66 (s, 1H), 7.50 – 7.44 (m, 2H), 7.39 – 7.30 (m, 3H), 7.25 (dt, *J* = 7.7, 1.2 Hz, 1H), 7.21 (d, *J* = 8.4 Hz, 1H), 4.18 (s, 2H). ^{13}C NMR (126 MHz, DMSO-d_6) δ 170.0, 167.9 (d, *J* = 2.9 Hz), 161.9 (d, *J* = 244.3 Hz), 141.1 (d, *J* = 7.2 Hz), 141.0, 132.5, 130.4 (d, *J* = 8.3 Hz), 125.6 (d, *J* = 5.4 Hz), 124.9, 124.6, 123.5, 117.2 (d, *J* = 21.3 Hz), 115.6 (d, *J* = 22.8 Hz), 57.1. ^{19}F NMR (471 MHz, DMSO-d_6) δ -112.98 (td, *J* = 9.4, 6.1 Hz). GC-FTIR ν_{max} (cm^{-1}): 3213, 3124, 3099, 3078, 3043, 2962, 2848, 1690, 1611, 1594, 1565, 1476, 1443, 1379, 1358, 1323, 1298, 1271, 1229, 1206, 1146, 1123, 1086, 1022, 1003, 968, 943, 878, 841, 820, 793, 758, 735, 696, 656. HRAM-MS (EI) m/z: $[M+H]^+$ Calcd for $C_{15}H_{11}BrFN_2O$ 333.00333; Found 333.00272.

*(8,4')-Isomer: IUPAC name: 8-bromo-5-(4-fluorophenyl)-1,3-dihydro-2H-benzo[e][1,4]diazepin-2-one (**19bc**)*. The general *N*-acylation and imination procedures were followed using **9bc** (122.4 mg, 0.416 mmol) and 2-bromoacetyl bromide (0.05 mL, 0.541 mmol) in 2.1 mL of THF, then 5.2 mL of NH_3 (13% wt% in MeOH). Compound **19bc** was isolated by silica prep-TLC (5% MeOH/CH_2Cl_2, R_f = 0.15) to afford a yellow granular solid (71.2 mg, 77% yield). ^{1}H NMR (500 MHz, DMSO-d_6) δ 10.64 (s, 1H), 7.53 (dd, *J* = 8.7, 5.6 Hz, 2H), 7.44 (d, *J* = 2.0 Hz, 1H), 7.37 (dd, *J* = 8.4, 2.0 Hz, 1H), 7.26 (t, *J* = 8.8 Hz, 2H), 7.19 (d, *J* = 8.4 Hz, 1H), 4.15 (s, 2H). ^{13}C NMR (126 MHz, DMSO-d_6) δ 170.5, 168.2, 163.7 (d, *J* = 248.0 Hz), 141.3, 135.6 (d, *J* = 3.2 Hz), 132.8, 131.9 (d, *J* = 8.6 Hz), 125.8, 125.5, 124.8, 123.7, 115.5 (d, *J* = 21.8 Hz), 57.3. ^{19}F NMR (471 MHz, DMSO-d_6) δ -110.78 (tt, *J* = 8.8, 5.5 Hz). GC-FTIR ν_{max} (cm^{-1}): 3213, 3124, 2958, 2848, 1688, 1613, 1594, 1563, 1509, 1476, 1408, 1379, 1354, 1323, 1262, 1227, 1200, 1156, 1086, 1019, 951, 924, 874, 843, 816, 758, 743, 714, 694, 671. HRAM-MS (EI) m/z: $[M+H]^+$ Calcd for $C_{15}H_{11}BrFN_2O$ 333.00333; Found 333.00272.

*(9,2')-Isomer: IUPAC name- 9-bromo-5-(2-fluorophenyl)-1,3-dihydro-2H-benzo[e][1,4]diazepin-2-one (**19ca**)*. The general *N*-acylation and imination procedures were followed using **9ca** (86.6 mg, 0.294 mmol) and 2-bromoacetyl bromide (0.03 mL, 0.382 mmol) in 2.3 mL of THF, then 3.7 mL of NH_3 (13 wt% in MeOH). Compound **19ca** was isolated by silica prep-TLC (5% MeOH/CH_2Cl_2, R_f = 0.19) to afford a yellow oil (36.8 mg, 35% yield). ^{1}H NMR (500 MHz, DMSO-d_6) δ 9.98 (s, 1H), 7.89 (dd, *J* = 7.6, 1.7 Hz, 1H), 7.63 – 7.54 (m, 2H), 7.33 (td, *J* = 7.5, 1.1 Hz, 1H), 7.24 (ddd, *J* = 10.9, 8.2, 1.1 Hz, 1H), 7.16 (dd, *J* = 7.9, 1.7 Hz, 1H), 7.12 (t, *J* = 7.7 Hz, 1H), 4.18 (s, 2H). ^{13}C NMR (126 MHz, DMSO-d_6) δ 169.1, 165.7, 159.7 (d, *J* = 248.9 Hz), 135.8, 135.4, 132.4 (d, *J* = 8.4

Hz), 131.4 (d, *J* = 2.6 Hz), 130.6, 128.7, 127.2 (d, *J* = 12.2 Hz), 125.4, 124.7 (d, *J* = 3.5 Hz), 116.4, 116.0 (d, *J* = 21.4 Hz), 56.8. ^{19}F NMR (471 MHz, DMSO-d_6) δ -113.39 – -113.50 (m). GC-FTIR ν_{max} (cm^{-1}): 3367, 3309, 3305, 3296, 3284, 3280, 3272, 3224, 3213, 3205, 3195, 3168, 3137, 3122, 3105, 3074, 3043, 3025, 3012, 3000, 2989, 2981, 2956, 2885, 1694, 1615, 1592, 1557, 1486, 1472, 1457, 1453, 1414, 1320, 1258, 1239, 1225, 1212, 1185, 1136, 1103, 1036, 1015, 858, 822, 797, 766, 754, 739, 718. HRAM-MS (EI) m/z: $[M+H]^+$ Calcd for $C_{15}H_{11}BrFN_2O$ 333.00333; Found 333.00333.

*(9,3')-Isomer: IUPAC name: 9-bromo-5-(3-fluorophenyl)-1,3-dihydro-2H-benzo[e][1,4]diazepin-2-one (1**9cb**)*. The general *N*-acylation and imination procedures were followed using **9cb** (70.9 mg, 0.241 mmol) and 2-bromoacetyl bromide (0.03 mL, 0.313 mmol) in 1.2 mL of THF, then 3.0 mL of NH_3 (13 wt% in MeOH). Compound **19cb** was isolated by silica prep-TLC (5% MeOH/CH_2Cl_2, R_f = 0.26) to afford a gold oil (25.4 mg, 31% yield). ^{1}H NMR (500 MHz, DMSO-d_6) δ 9.66 (s, 1H), 7.92 (dd, *J* = 7.9, 1.4 Hz, 1H), 7.52 – 7.45 (m, 1H), 7.35 (d, *J* = 8.4 Hz, 2H), 7.30 (d, *J* = 7.9 Hz, 2H), 7.19 (t, *J* = 7.9 Hz, 1H), 4.17 (s, 2H). ^{13}C NMR (126 MHz, DMSO-d_6) δ 169.5, 167.7 (d, *J* = 2.7 Hz), 162.0 (d, *J* = 244.3 Hz), 140.9 (d, *J* = 7.3 Hz), 137.0, 135.6, 130.5 (d, *J* = 8.2 Hz), 129.9, 129.0, 125.6 (d, *J* = 2.7 Hz), 125.2, 117.4 (d, *J* = 21.1 Hz), 116.6, 115.5 (d, *J* = 22.8 Hz), 56.8. ^{19}F NMR (471 MHz, DMSO-d_6) δ -112.81 (td, *J* = 9.4, 6.1 Hz). GC-FTIR ν_{max} (cm^{-1}): 3367, 3209, 3139, 3076, 1696, 1613, 1584, 1474, 1459, 1443, 1412, 1314, 1271, 1240, 1229, 1202, 1185, 1148, 1119, 1080, 1019, 986, 920, 883, 868, 843, 801, 754, 737, 712, 679. HRAM-MS (EI) m/z: $[M+H]^+$ Calcd for $C_{15}H_{11}BrFN_2O$ 333.00333; Found 333.00336.

*(9,4')-Isomer: IUPAC name- 9-bromo-5-(4-fluorophenyl)-1,3-dihydro-2H-benzo[e][1,4]diazepin-2-one (**19cc**)*. The general *N*-acylation and imination procedures were followed using **9cc** (122.4 mg, 0.416 mmol) and 2-bromoacetyl bromide (0.05 mL, 0.541 mmol) in 2.1 mL of THF, then 5.2 mL of NH_3 (13 wt% in MeOH). Compound **19cc** was isolated by silica prep-TLC (5% MeOH/CH_2Cl_2, R_f = 0.26) to afford a gold film (25.0 mg, 18% yield). ^{1}H NMR (500 MHz, DMSO-d_6) δ 9.63 (s, 1H), 7.92 (dd, *J* = 7.9, 1.4 Hz, 1H), 7.58 (dd, *J* = 8.8, 5.6 Hz, 2H), 7.30 – 7.22 (m, 3H), 7.18 (t, *J* = 7.9 Hz, 1H), 4.14 (s, 2H). ^{13}C NMR (126 MHz, DMSO-d_6) δ 169.6, 167.7, 163.4 (d, *J* = 248.2 Hz), 137.0, 135.4, 135.0 (d, *J* = 2.9 Hz), 131.5 (d, *J* = 8.7 Hz), 129.9, 129.2, 125.1, 116.6, 115.3 (d, *J* = 21.8 Hz), 56.7. ^{19}F NMR (471 MHz, DMSO-d_6) δ -110.56 (tt, *J* = 8.8, 5.5 Hz). GC-FTIR ν_{max} (cm^{-1}): 3367, 3217, 3135, 3074, 1692, 1613, 1594, 1507, 1472, 1459, 1408, 1314, 1225, 1185, 1156, 1134, 1096, 1013, 843, 818, 797, 756, 737, 714, 681. HRAM-MS (EI) m/z: $[M+H]^+$ Calcd for $C_{15}H_{11}BrFN_2O$ 333.00333; Found 333.00336.

*2.8.6 Procedures for the Synthesis of 2-Amino-6-bromo-X'-fluorobenzophenones **9da-dc***

*3-Hydroxy-3-phenyloxindole (**38**)*. Following the published procedure from Stoltz:[38] In a flame-dried flask under N_2, **12e** (250 mg, 1.70 mmol) was dissolved in 17 mL of anhydrous THF. The solution was cooled to -40°C. PhMgBr (1.4 mL, 4.25 mmol, 3 M/Et_2O) was added, then the solution was allowed to warm to room temperature. After 1.5 hours, the reaction was quenched with 1 M HCl. The aqueous layer was extracted with Et_2O, and the combined organic extracts were dried over anhydrous Na_2SO_4, filtered through celite under reduced pressure, and concentrated by rotary evaporation. Compound **38** was isolated by silica flash chromatography (25% EtOAc/hexanes) in quantitative yield. NMR data were consistent with previously reported results.

*N-Benzyl-4-bromoisatin (**46**).* Following the published procedure from Zhao:[41] In a flame-dried flask under N_2, **12d** (500 mg, 2.21 mmol) was dissolved in anhydrous DMF (4.4 mL). The solution was cooled to 0°C, then NaH (97.3 mg, 2.43 mmol, 60% dispersion in mineral oil) was added in portions. After the color changed from orange to purple and the bubbling stopped, benzyl bromide (0.32 mL, 2.65 mmol) was added slowly; the reaction color changed again to reddish-brown. The reaction mixture was allowed to warm to room temperature. After stirring for an hour, 22 mL of H_2O were added to precipitate the product, which was filtered through a Buchner funnel and washed with cold hexanes. Compound **46** was collected as an orange solid (601.8 mg, 86% yield). NMR data were consistent with previously reported results.

*N-Benzyl-4-bromo-3-(4-fluorophenyl)-3-hydroxyoxindole (**47c**).* Following the published procedure from Kim:[37] To a sealed tube under air, **46** (100 mg, 0.316 mmol), **13c** (141.0 mg, 0.632 mmol), $Cu(OTf)_2$ (5.7 mg, 0.0158 mmol), 1,10-phenanthroline (5.7 mg, 0.0316 mmol), and $LiOH{\cdot}H_2O$ (39.8 mg, 0.948 mmol) were all combined in 3.2 mL of anhydrous CH_2Cl_2 and warmed to 80°C over 48 hours. Then, the reaction mixture was allowed to cool to room temperature, diluted with EtOAc, filtered through a plug of silica under reduced pressure using EtOAc as the eluent, and concentrated by rotary evaporation. After purification by silica flash chromatography (25% EtOAc/hexanes, R_f = 0.24), compound **47c** was afforded as a light brown solid (107.6 mg, 82% yield). ^{1}H NMR (500 MHz, $CDCl_3$) δ 7.38 – 7.35 (m, 2H), 7.31 (ddd, *J* = 12.5, 7.7, 5.9 Hz, 3H), 7.26 – 7.23 (m, 2H), 7.19 (dd, *J* = 8.3, 1.0 Hz, 1H), 7.15 (t, *J* = 7.9 Hz, 1H), 7.05 (t, *J* = 8.7 Hz, 2H), 6.76 (dd, *J* = 7.6, 1.1 Hz, 1H), 4.97 (d, *J* = 15.6 Hz, 1H), 4.80 (d, *J* = 15.7 Hz, 1H), 3.37 – 3.34 (m, 1H). ^{13}C NMR (126 MHz, $CDCl_3$) δ 175.45, 162.90 (d, *J* = 247.5 Hz), 144.82, 134.85,

133.51, 131.51, 129.48, 128.96, 127.99, 127.55 (d, J = 8.5 Hz), 127.27, 127.22, 119.97, 115.65 (d, J = 21.8 Hz), 108.80, 78.65, 44.14.

*2-Aminobenzophenone (**27**).* Following the published procedure from Lee:[36] In a round-bottom flask equipped with a condenser, $K_4[Fe(CN)_6]$ (487.4 mg, 1.15 mmol), $NaHCO_3$ (100.7 mg, 1.20 mmol), and NaOH (17.8 mg, 0.444 mmol) were dissolved in 4.4 mL of H_2O and stirred at 100°C. After 30 minutes, **34e** (100 mg, 0.444 mmol) in 1.6 mL of THF was added dropwise over 5 minutes, then stirred at 100°C overnight. Then, the reaction mixture was allowed to cool to room temperature and diluted with saturated aqueous $NaHCO_3$. The aqueous layer was extracted with EtOAc, then the combined organic layers were treated with activated charcoal, dried over anhydrous $MgSO_4$, filtered through celite under reduced pressure, and concentrated by rotary evaporation. After purification by silica flash chromatography (10% MeOH/CH_2Cl_2), compound **25** was afforded as a yellow solid (18.2 mg, 21% yield). NMR data were consistent with previously reported results.

2.9 Copies of NMR Spectra

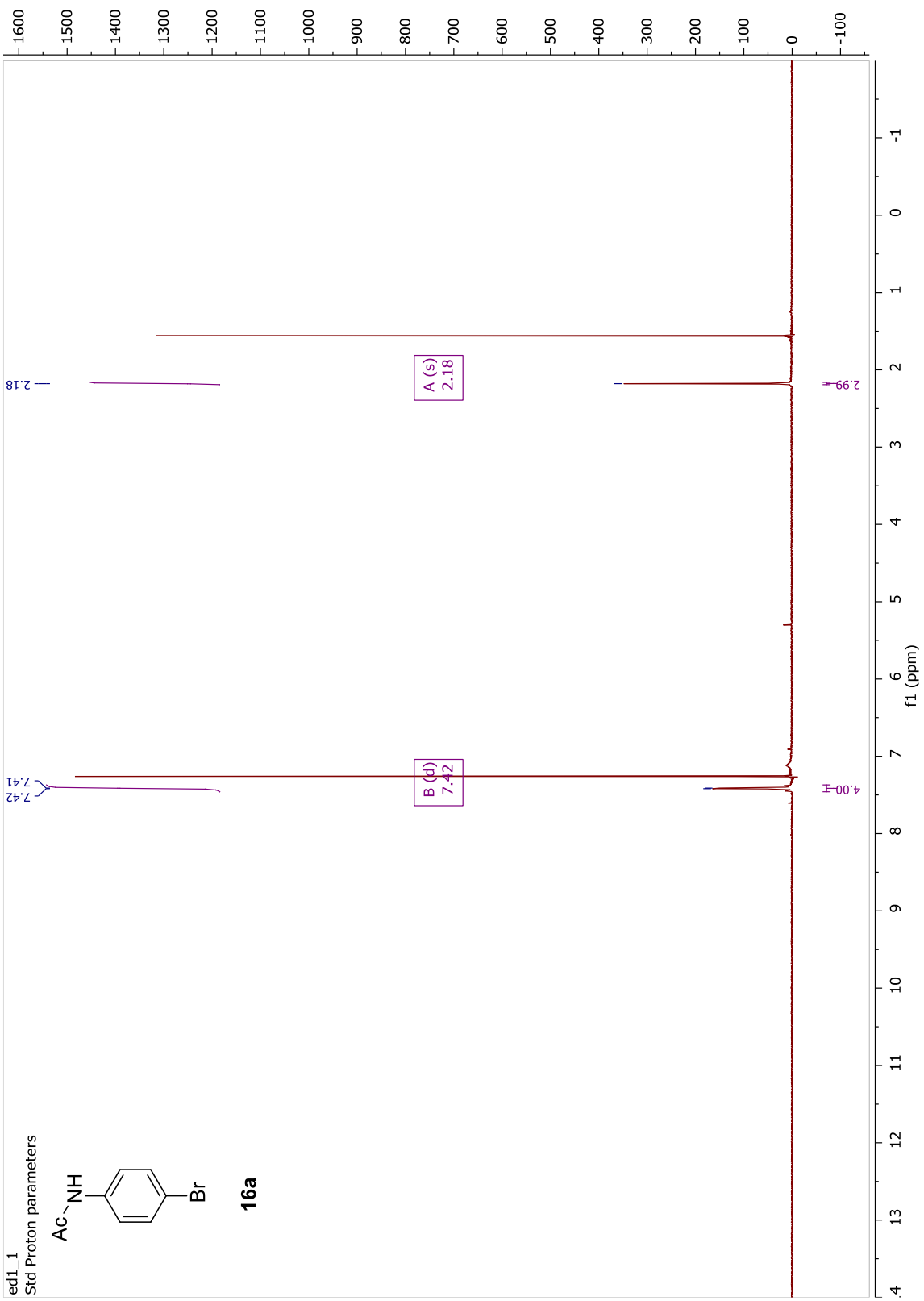
ed1_1
Std Proton parameters
Ac
NH
Br
16a
A (s)
2.18
B (d)
7.42
2.18
7.42
7.41
2.99
4.00
f1 (ppm)

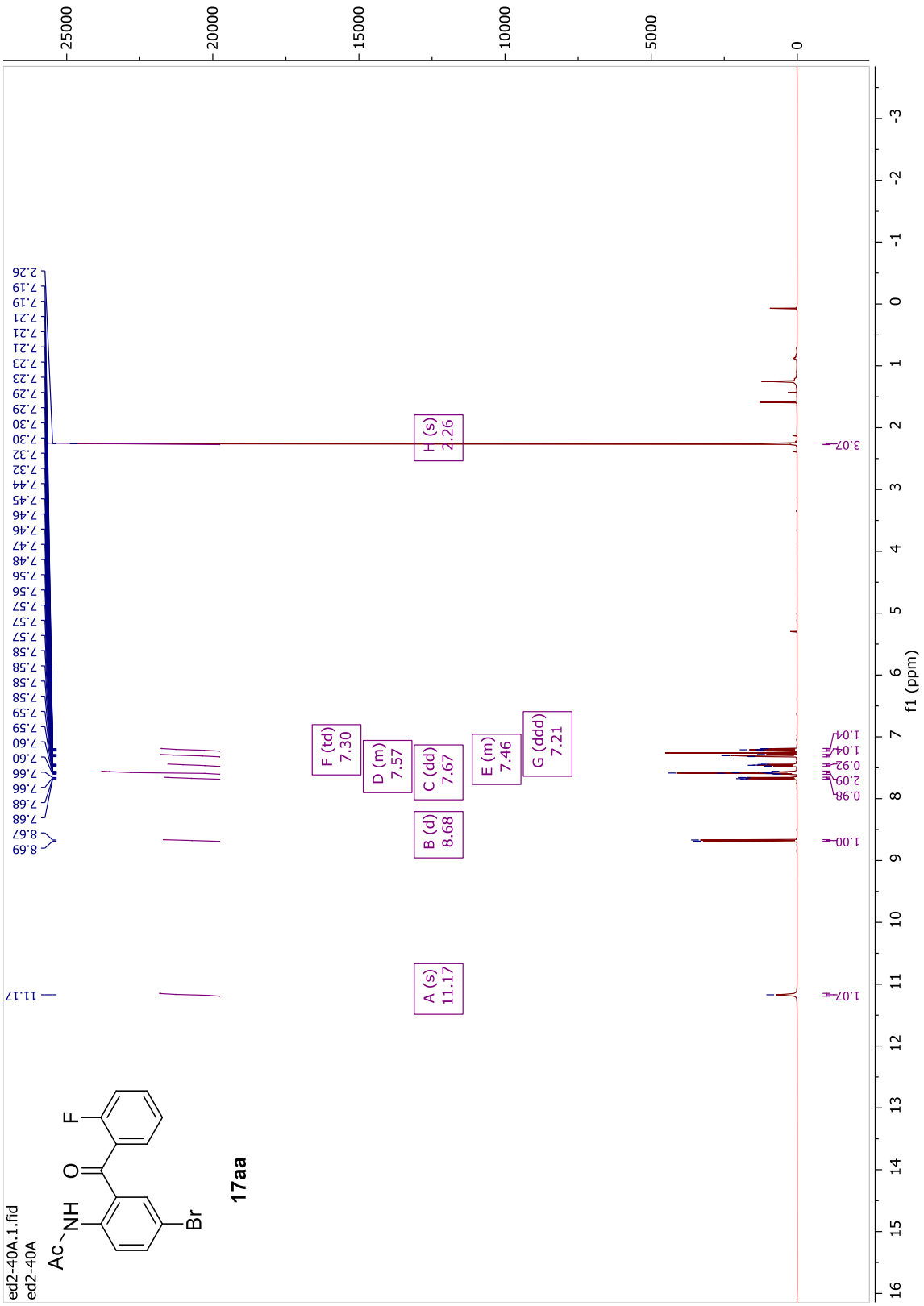
ed2-40A.1.fid
ed2-40A
17aa
A (s) 11.17
B (d) 8.68
C (dd) 7.67
D (m) 7.57
E (m) 7.46
F (td) 7.30
G (ddd) 7.21
H (s) 2.26
f1 (ppm)

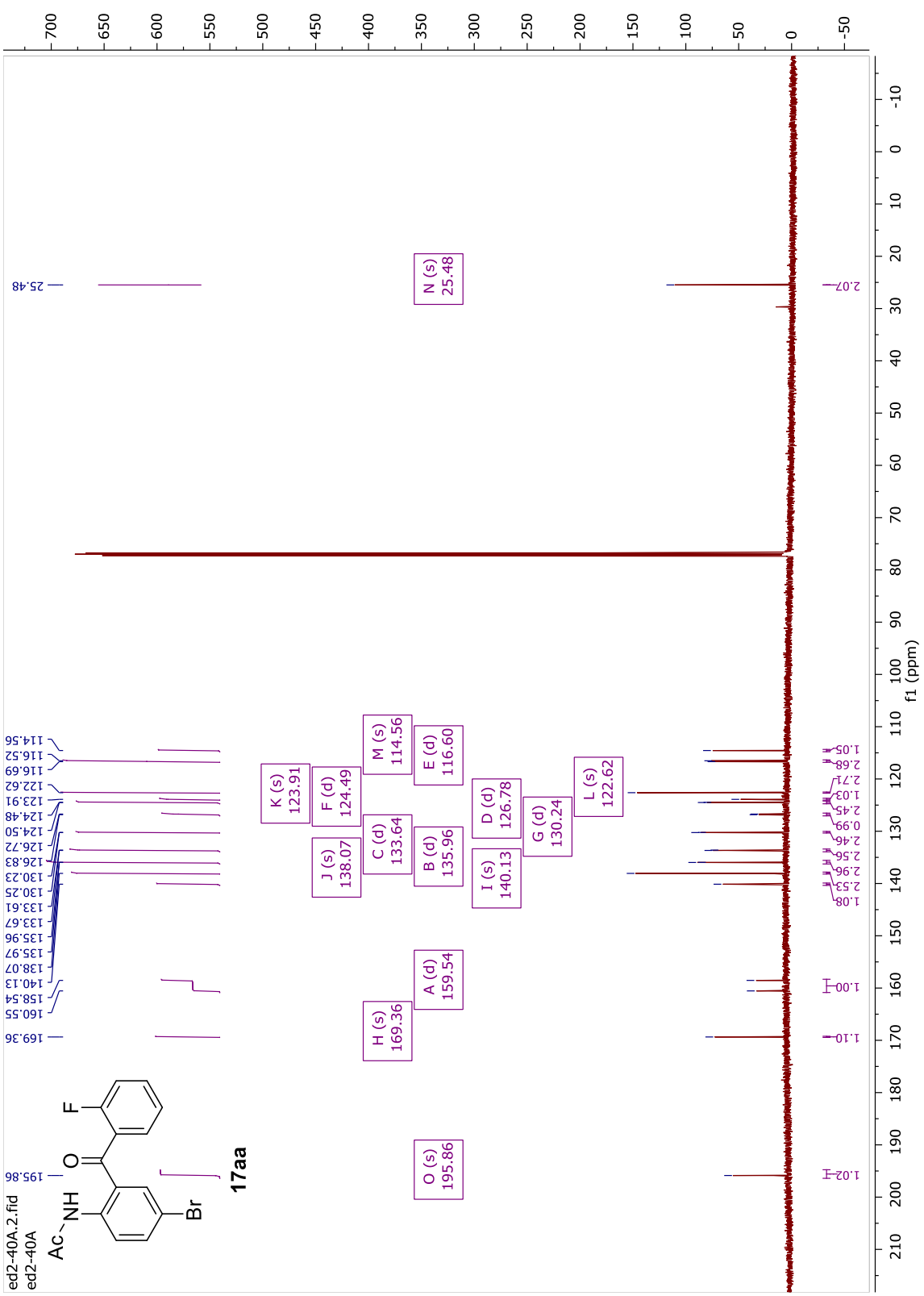
ed2-40A.2.fid
ed2-40A
17aa
f1 (ppm)
O (s) 195.86
H (s) 169.36
A (d) 159.54
I (s) 140.13
J (s) 138.07
C (d) 133.64
B (d) 135.96
D (d) 126.78
G (d) 130.24
L (s) 122.62
K (s) 123.91
F (d) 124.49
M (s) 114.56
E (d) 116.60
N (s) 25.48

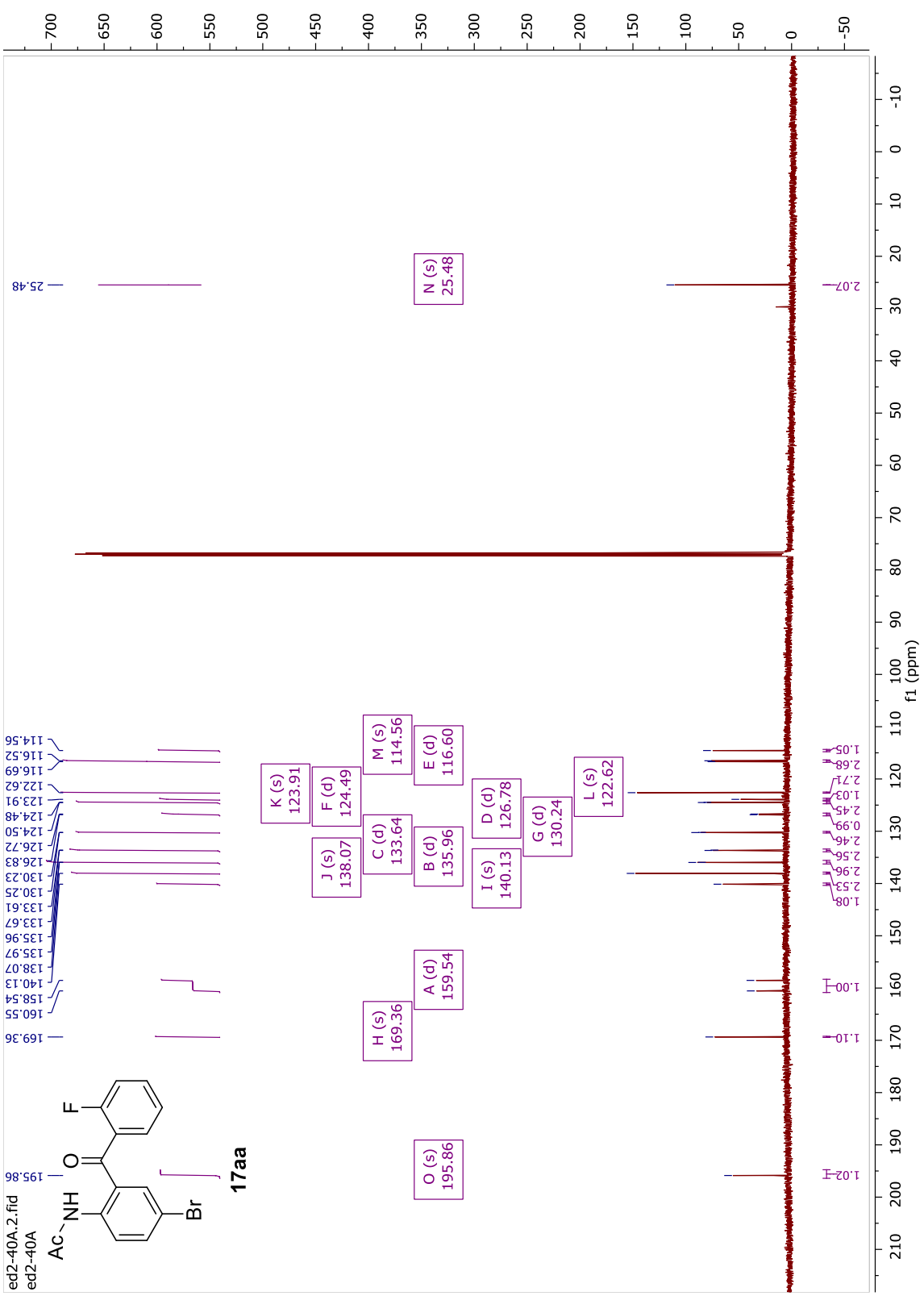
ed2-40A.2.fid
ed2-40A
17aa
f1 (ppm)
O (s) 195.86
H (s) 169.36
A (d) 159.54
I (s) 140.13
J (s) 138.07
C (d) 133.64
B (d) 135.96
D (d) 126.78
G (d) 130.24
L (s) 122.62
K (s) 123.91
F (d) 124.49
M (s) 114.56
E (d) 116.60
N (s) 25.48

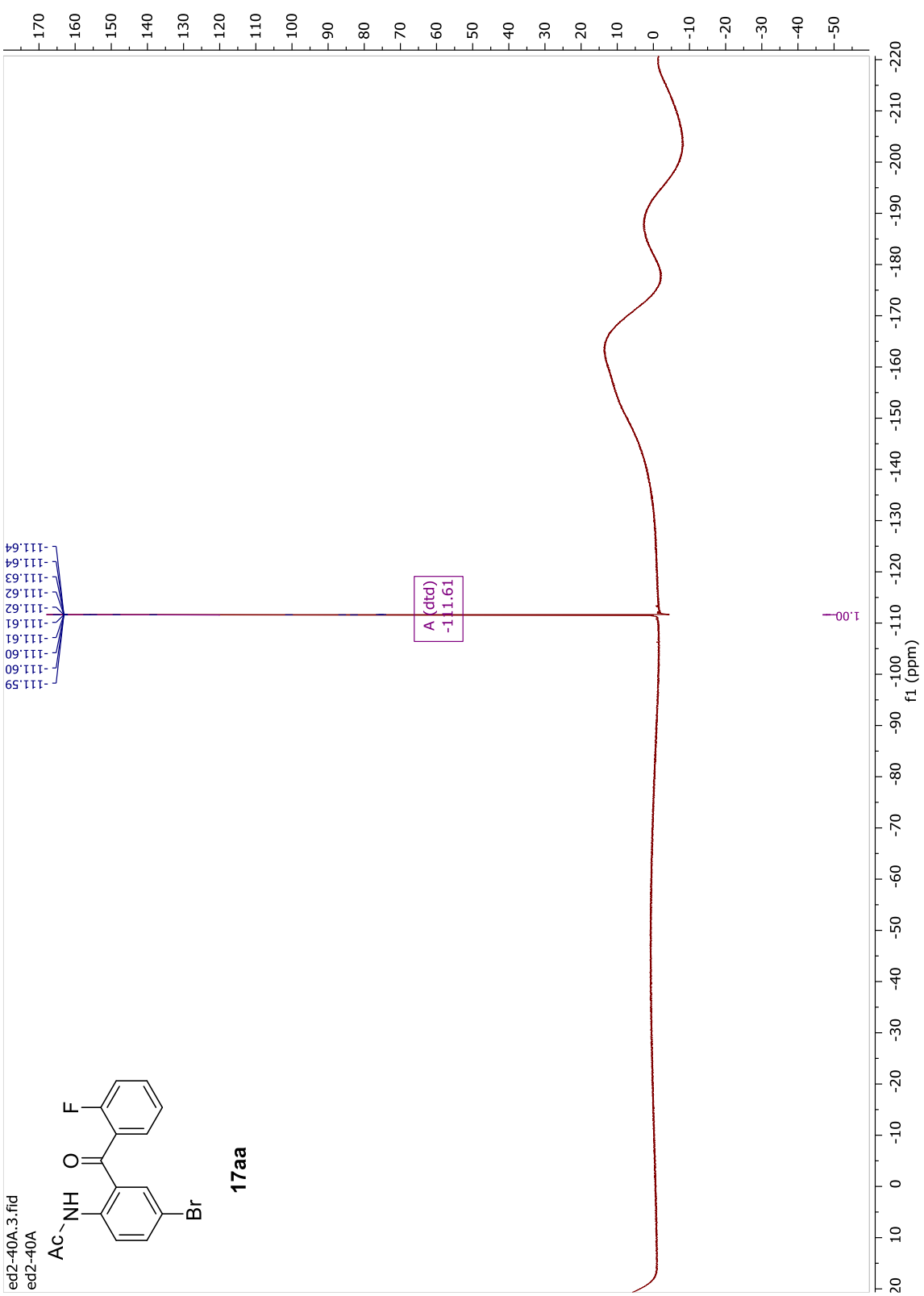
ed2-40A.3.fid
ed2-40A
17aa
A (dtd)
-111.61
f1 (ppm)

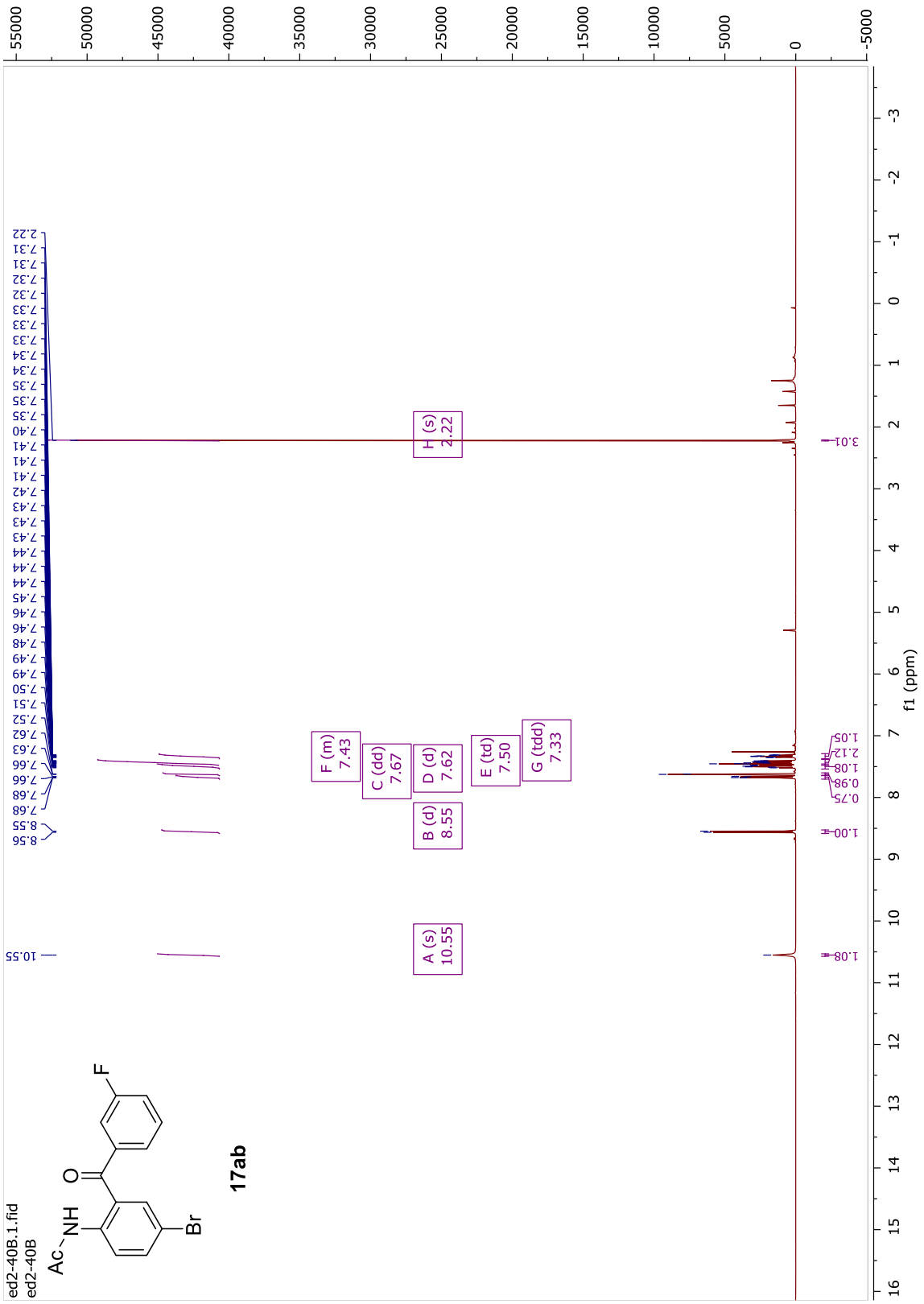
ed2-40B.1.fid
ed2-40B
17ab
A (s) 10.55
B (d) 8.55
C (dd) 7.67
D (d) 7.62
E (td) 7.50
F (m) 7.43
G (tdd) 7.33
H (s) 2.22
f1 (ppm)

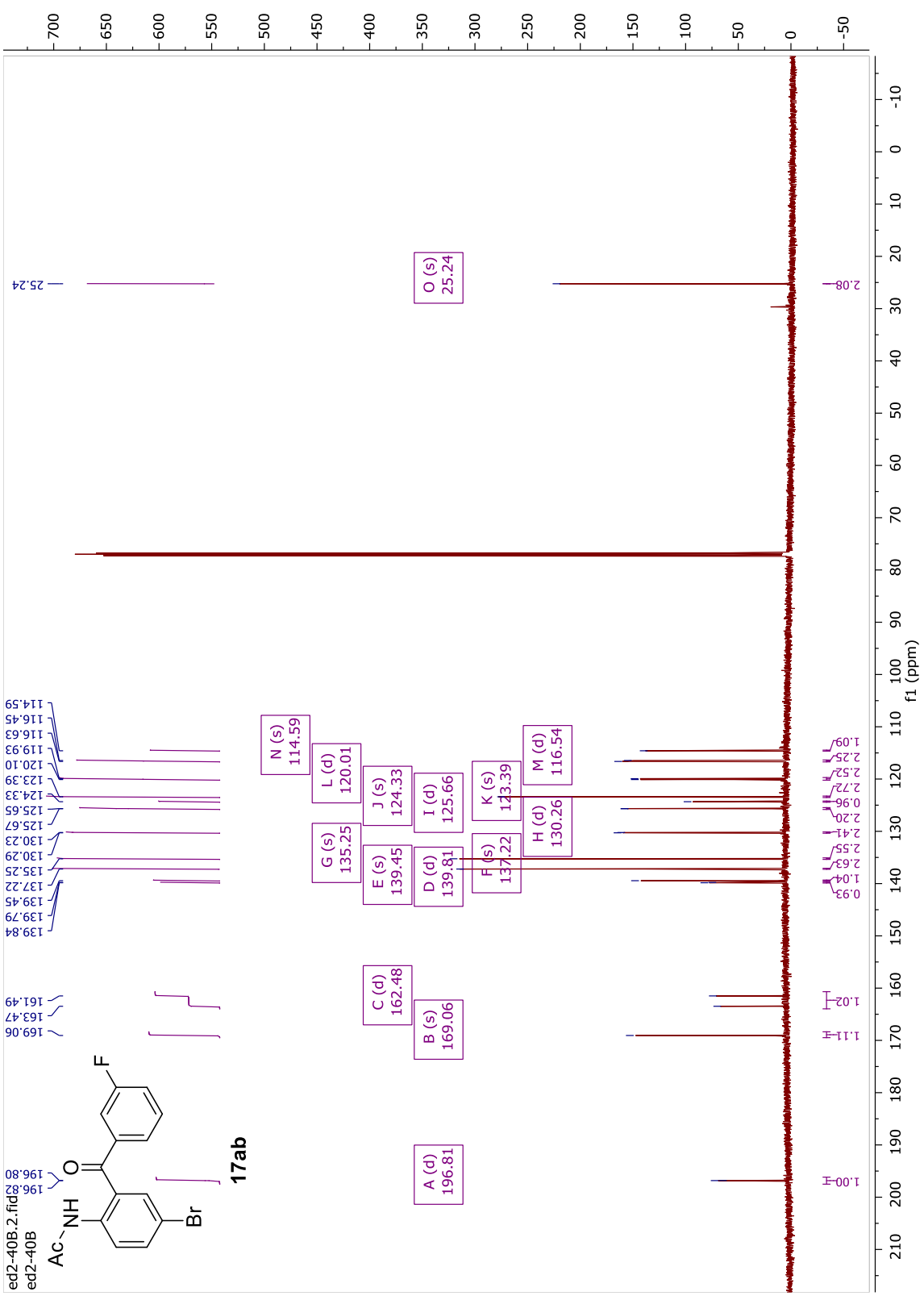
ed2-40B.2.fid
ed2-40B
17ab
f1 (ppm)

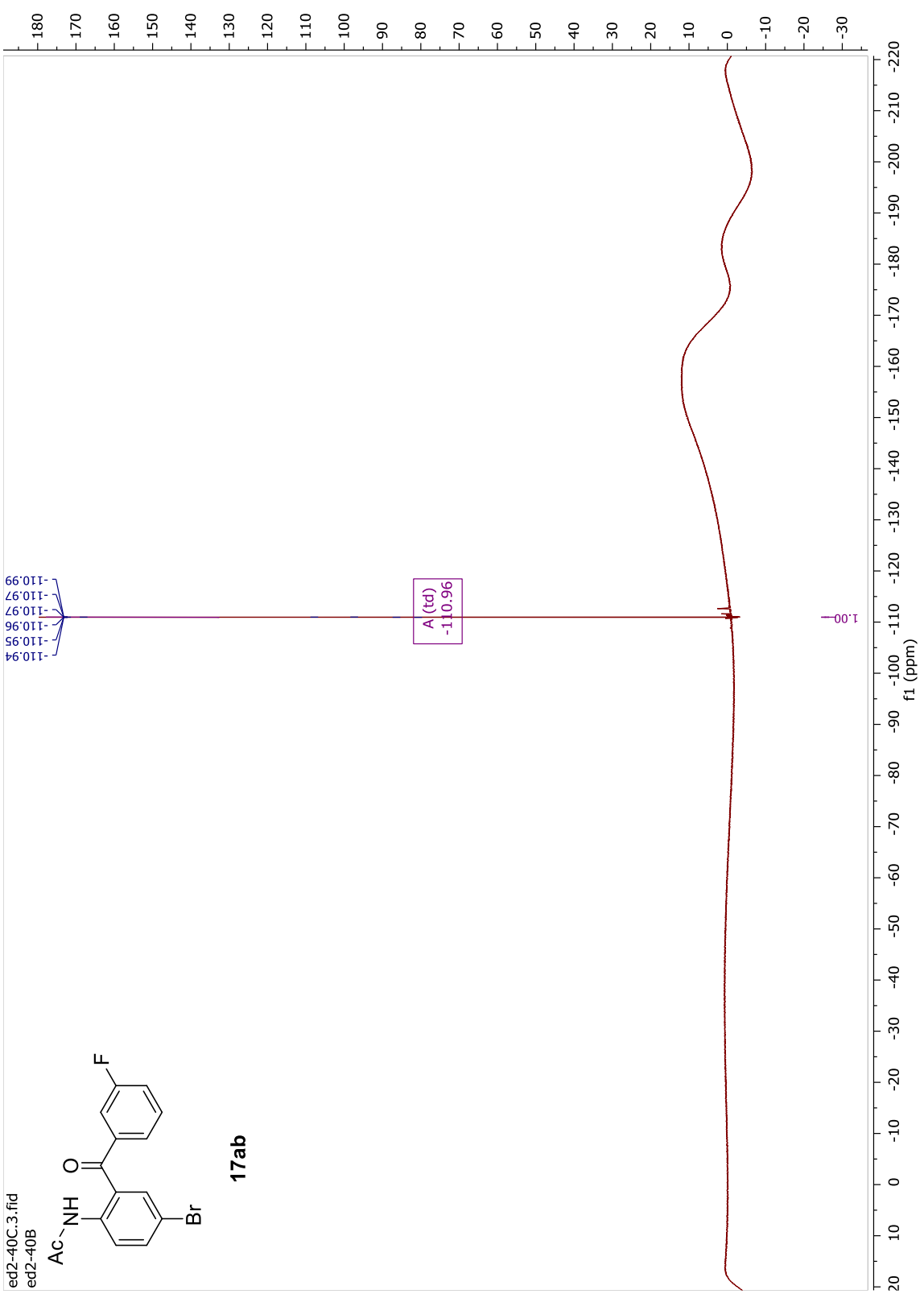
ed2-40C.3.fid
ed2-40B
17ab
A (td)
-110.96
-110.94
-110.95
-110.96
-110.97
-110.97
-110.99
1.00
f1 (ppm)

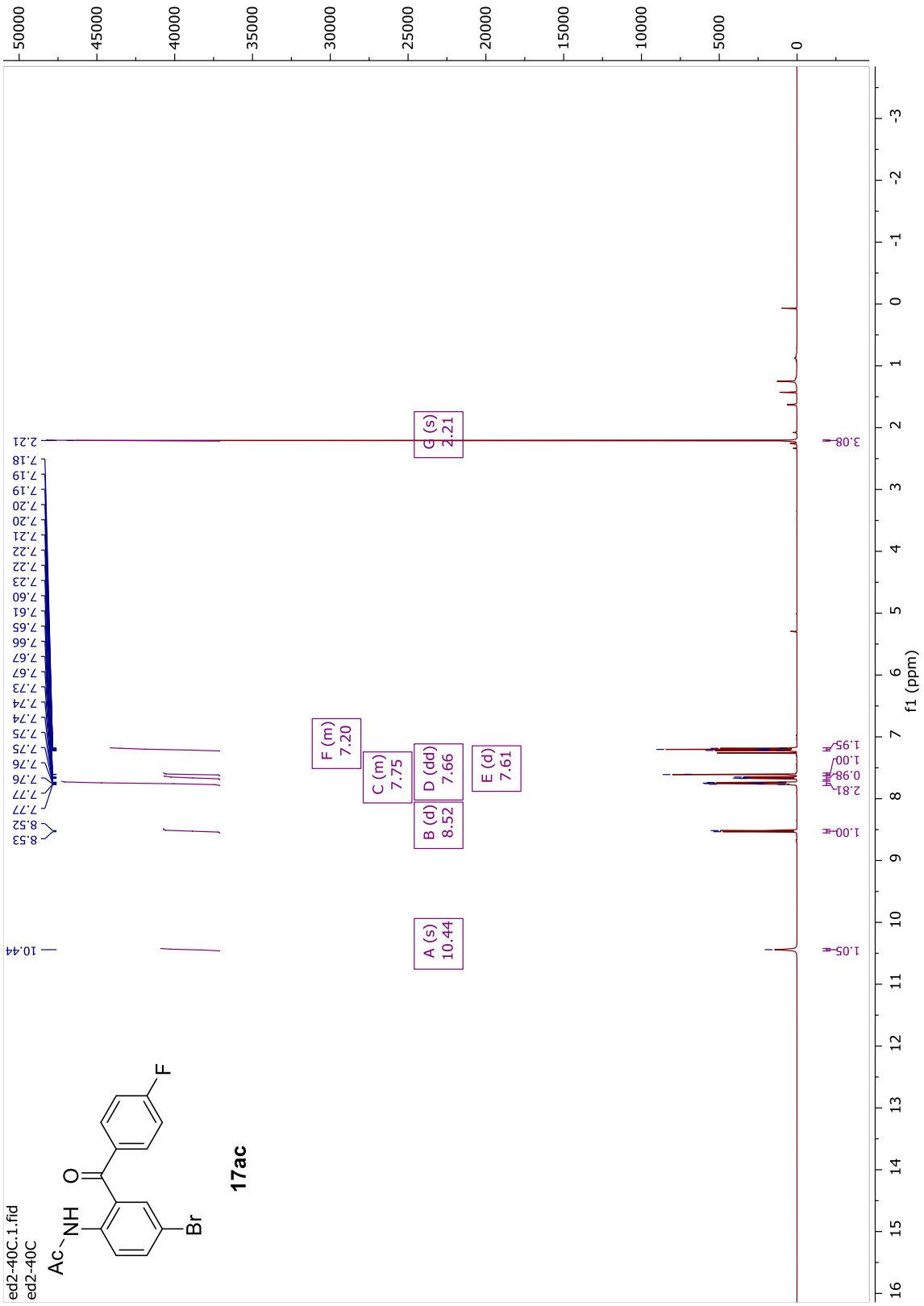
ed2-40C.1.fid
ed2-40C
17ac
Ac
NH
O
Br
F
A (s) 10.44
B (d) 8.52
C (m) 7.75
D (dd) 7.66
E (d) 7.61
F (m) 7.20
G (s) 2.21
f1 (ppm)

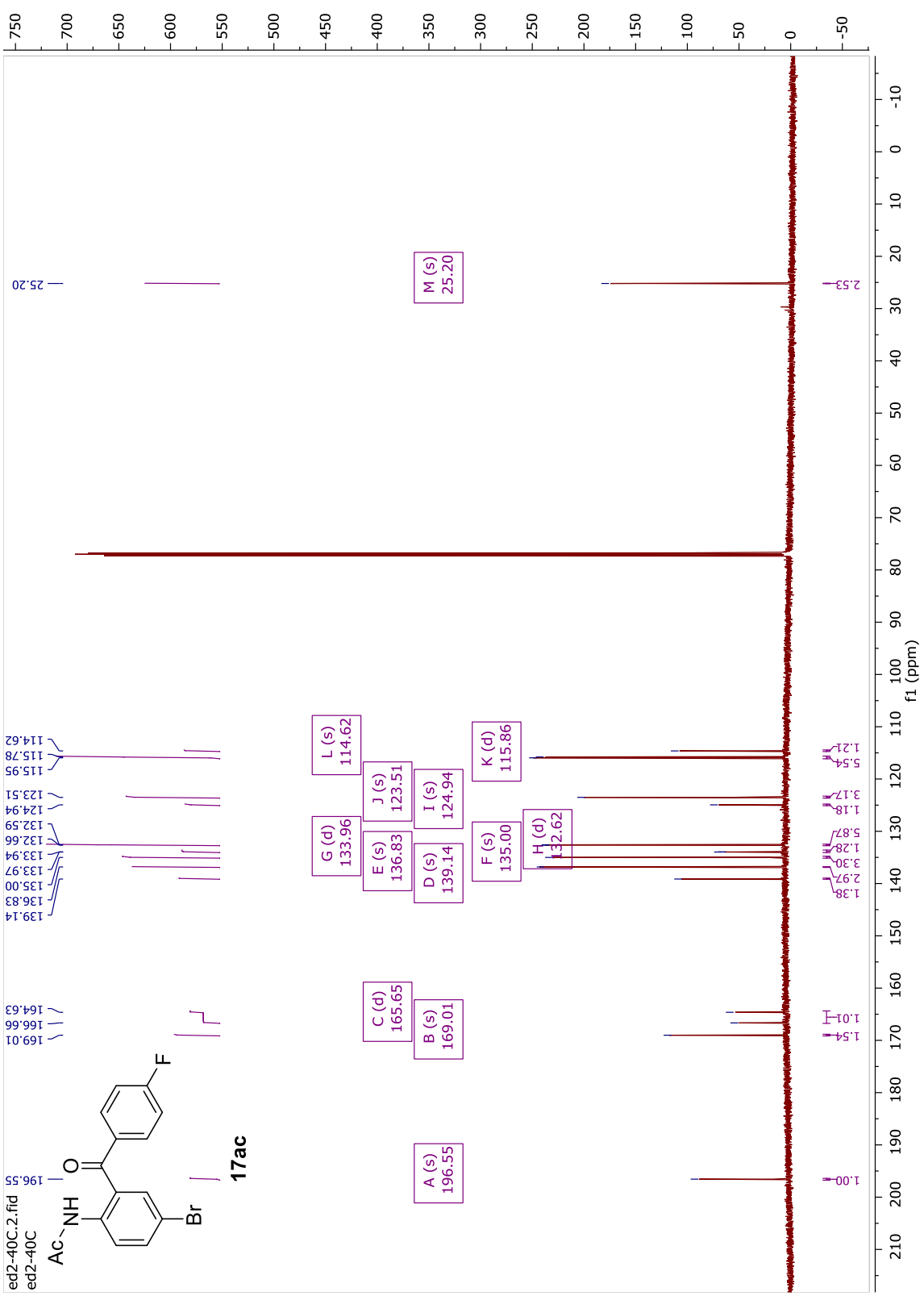
ed2-40C.2.fid
ed2-40C
17ac
A (s) 196.55
B (s) 169.01
C (d) 165.65
D (s) 139.14
E (s) 136.83
F (s) 135.00
G (d) 133.96
H (d) 132.62
I (s) 124.94
J (s) 123.51
K (d) 115.86
L (s) 114.62
M (s) 25.20
f1 (ppm)

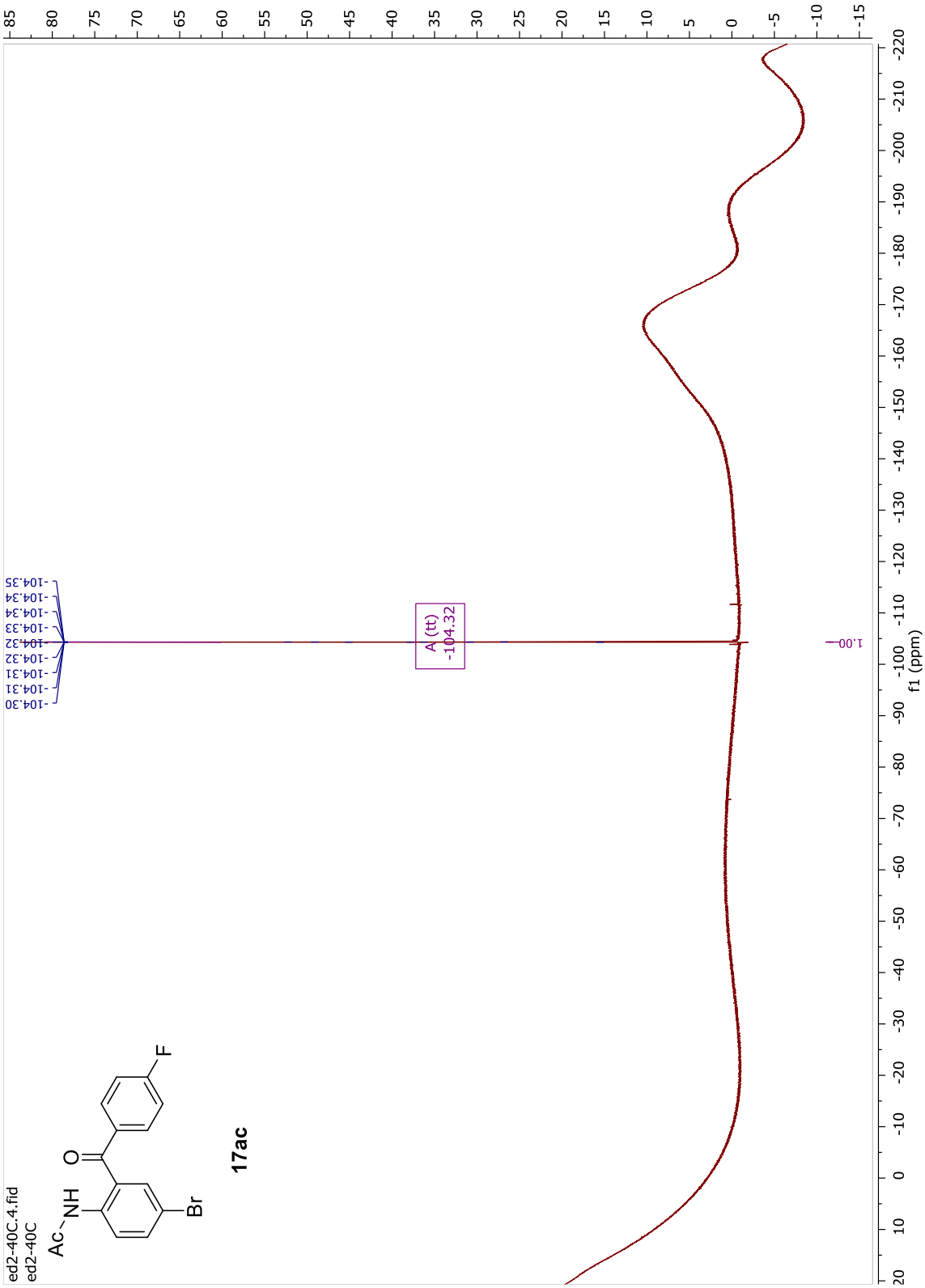
ed2-40C.4.fid
ed2-40C
17ac
A (tt)
-104.32
1.00
f1 (ppm)

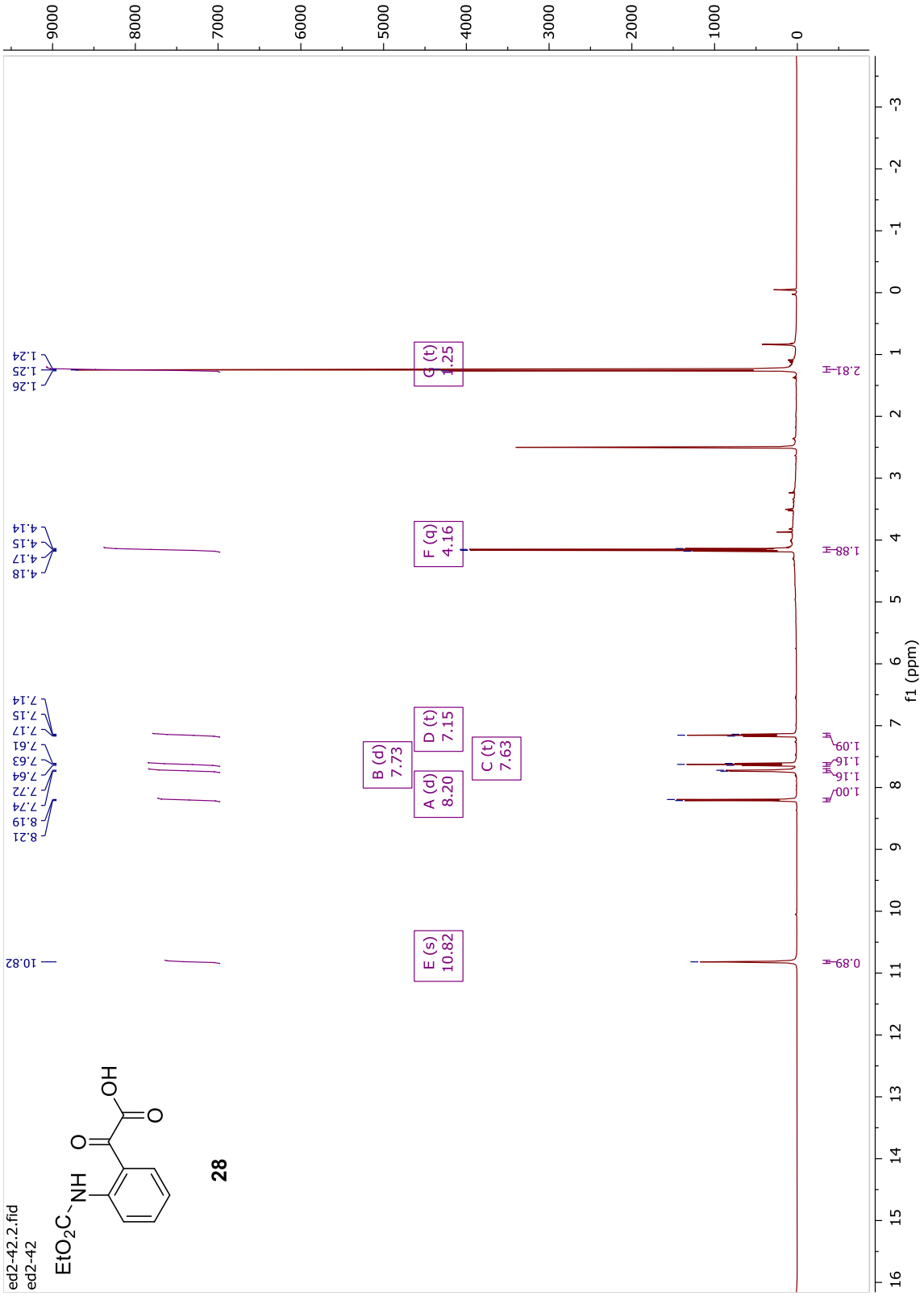
ed2-42.2.fid
ed2-42
28
EtO2C
NH
O
O
OH
O
10.82
8.21
8.19
7.74
7.72
7.64
7.63
7.61
7.17
7.15
7.14
4.18
4.17
4.15
4.14
1.26
1.25
1.24
E (s) 10.82
A (d) 8.20
B (d) 7.73
D (t) 7.15
C (t) 7.63
F (q) 4.16
G (t) 1.25
0.89
1.00
1.16
1.16
1.09
1.88
2.81
f1 (ppm)

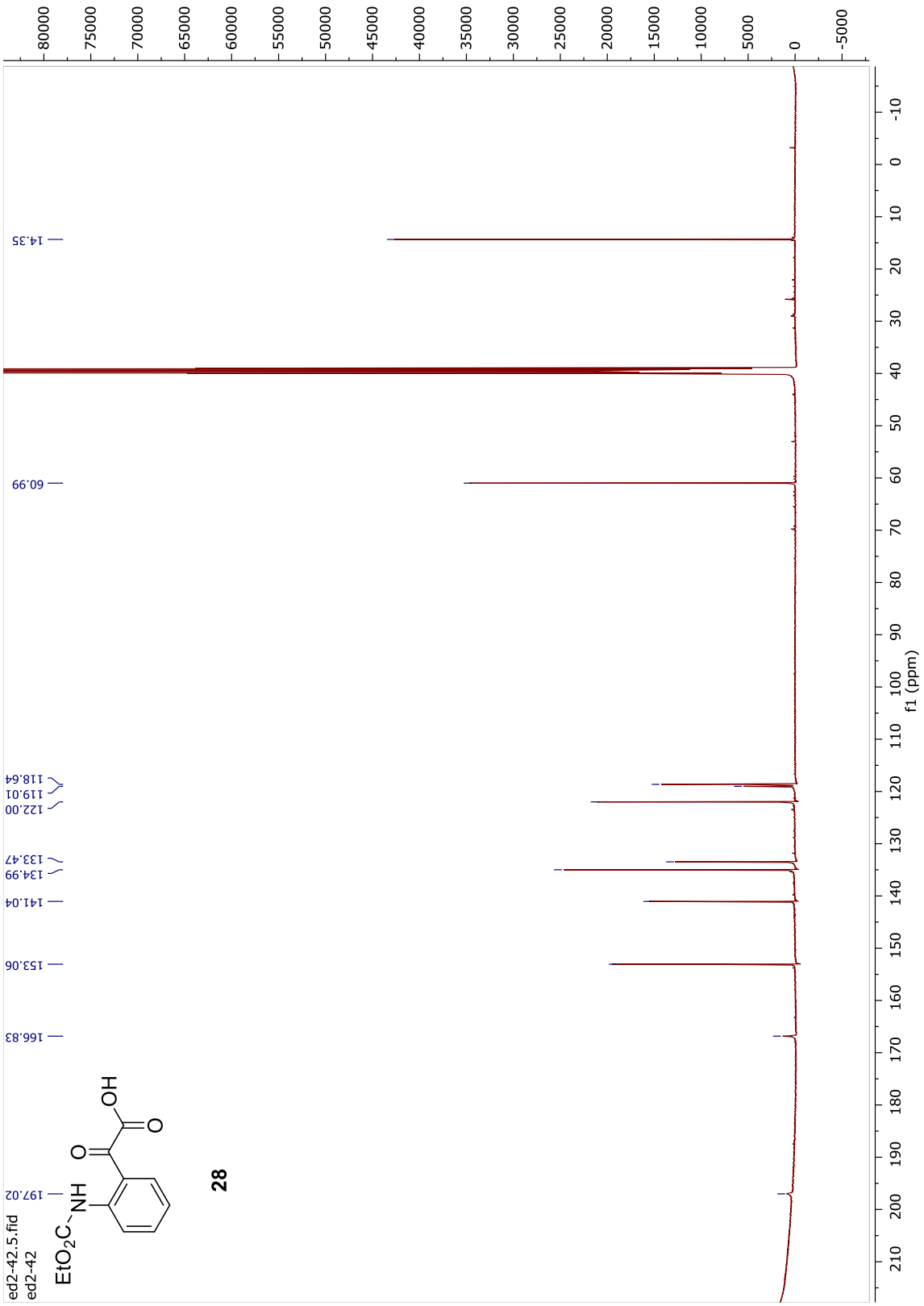
ed2-42.5.fid
ed2-42
28
14.35
60.99
118.64
119.01
122.00
133.47
134.99
141.04
153.06
166.83
197.02
f1 (ppm)

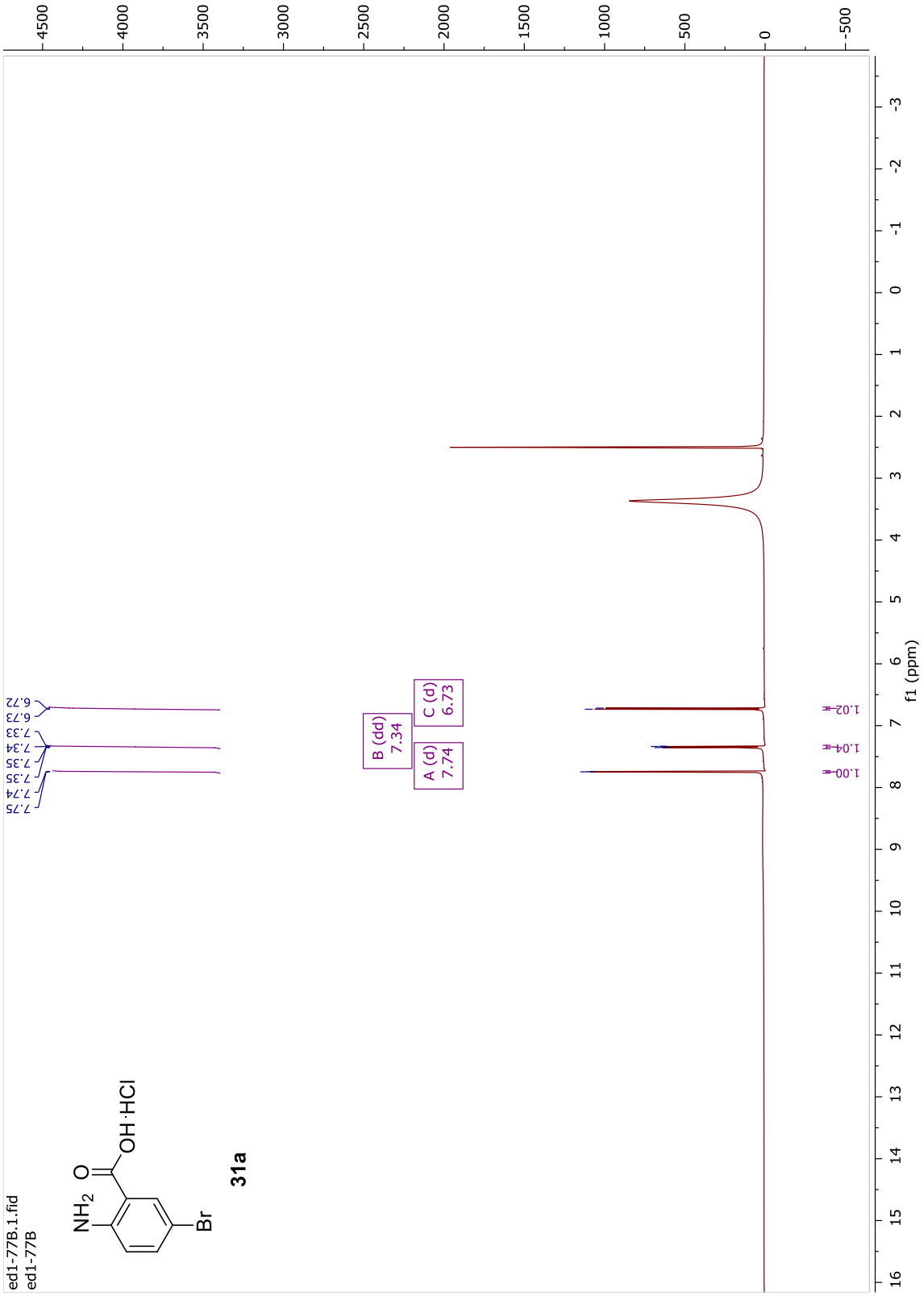
ed1-77B.1.fid
ed1-77B
31a
NH2
O
OH·HCl
Br
7.75
7.74
7.35
7.35
7.34
7.33
6.73
6.72
A (d)
7.74
B (dd)
7.34
C (d)
6.73
1.00
1.04
1.02
f1 (ppm)

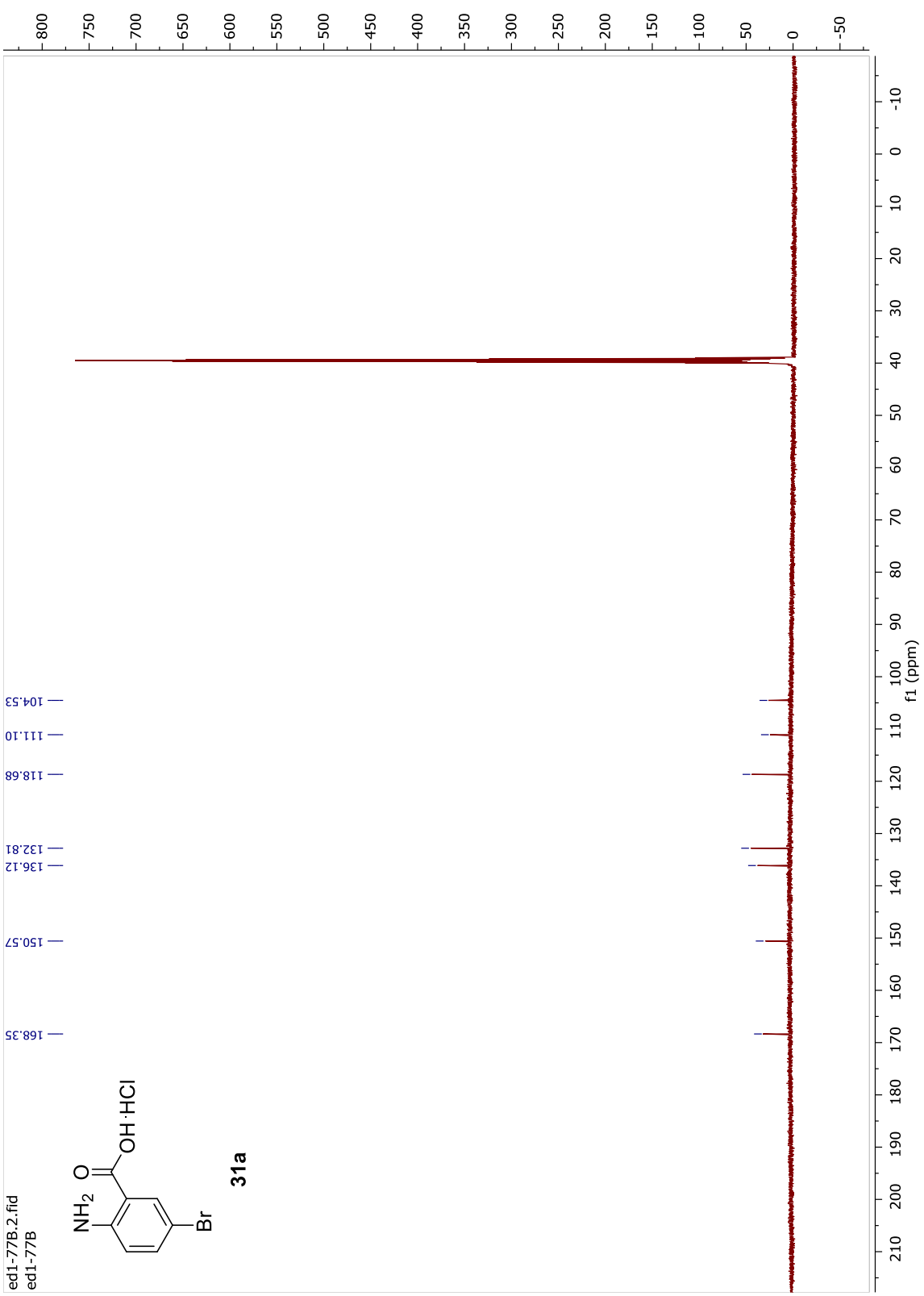
ed1-77B.2.fid
ed1-77B
31a
NH2
O
OH·HCl
Br
168.35
150.57
136.12
132.81
118.68
111.10
104.53
f1 (ppm)

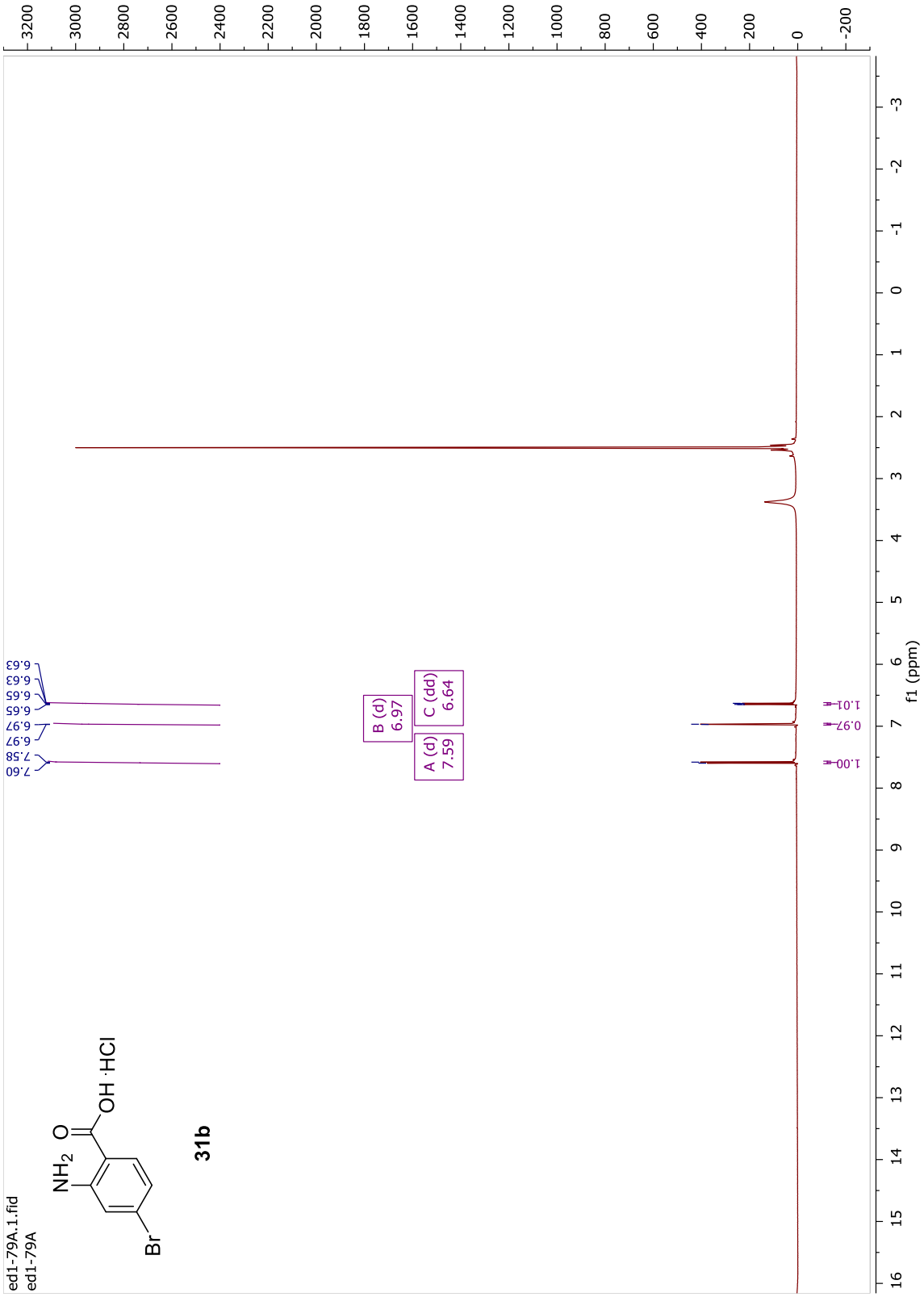
ed1-79A.1.fid
ed1-79A
31b
NH2
O
OH ·HCl
Br
7.60
7.58
6.97
6.97
6.65
6.65
6.63
6.63
A (d)
7.59
B (d)
6.97
C (dd)
6.64
1.00
0.97
1.01
f1 (ppm)

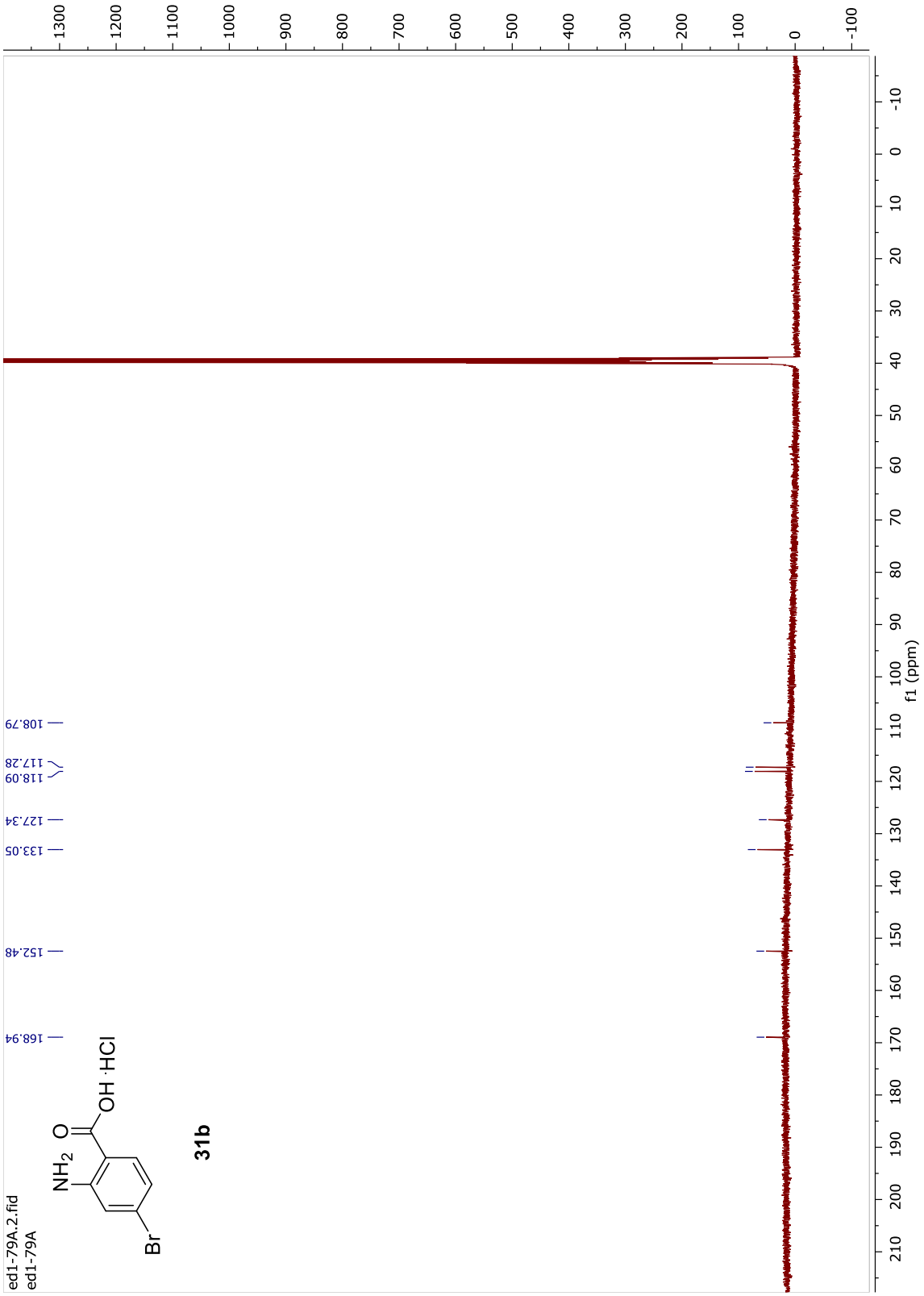
ed1-79A.2.fid
ed1-79A
31b
NH2
O
OH ·HCl
Br
168.94
152.48
133.05
127.34
118.09
117.28
108.79
f1 (ppm)

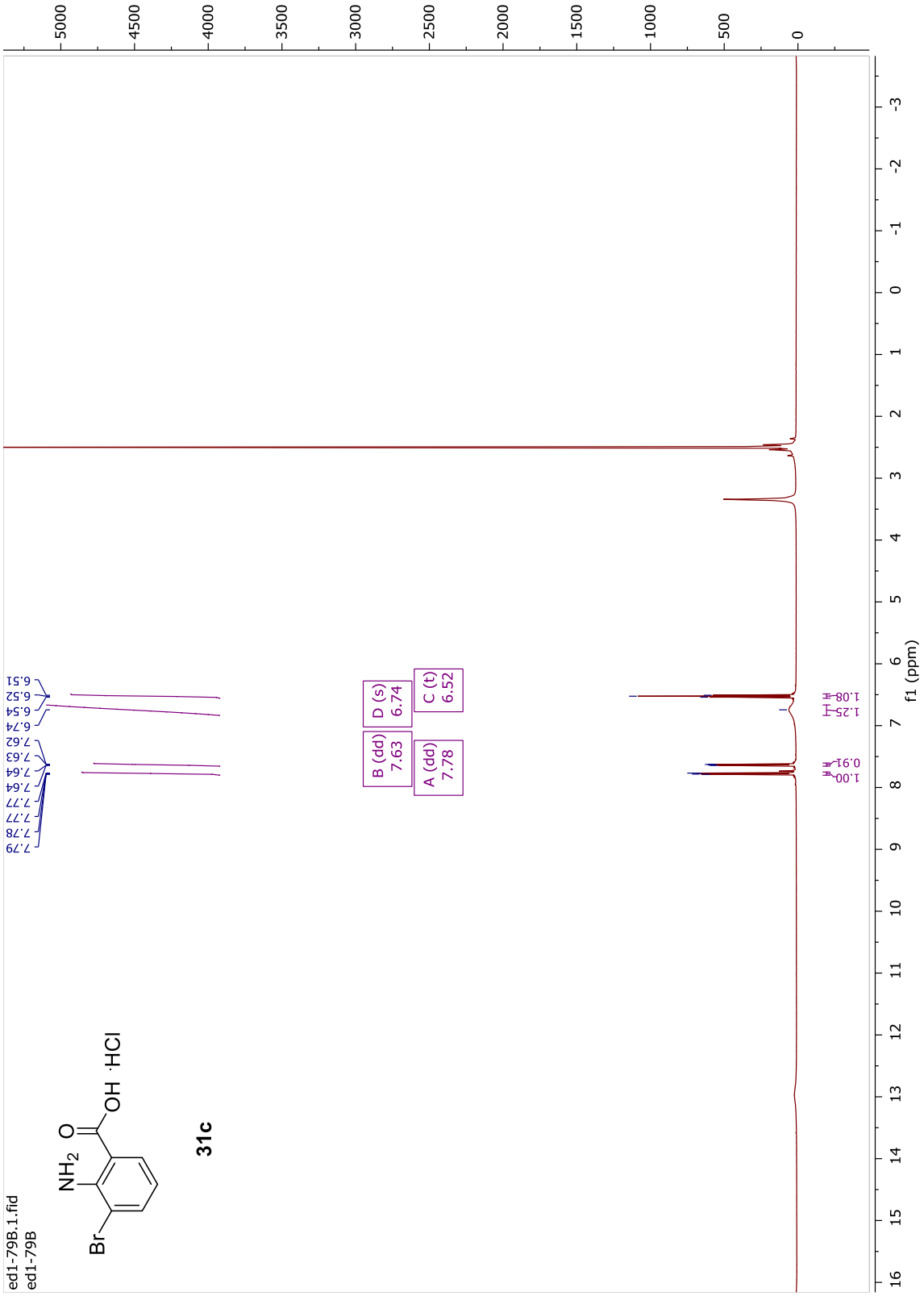
ed1-79B.1.fid
ed1-79B
31c
NH2
O
OH ·HCl
Br
B (dd) 7.63
D (s) 6.74
C (t) 6.52
A (dd) 7.78
1.00
0.91
1.25
1.08
f1 (ppm)

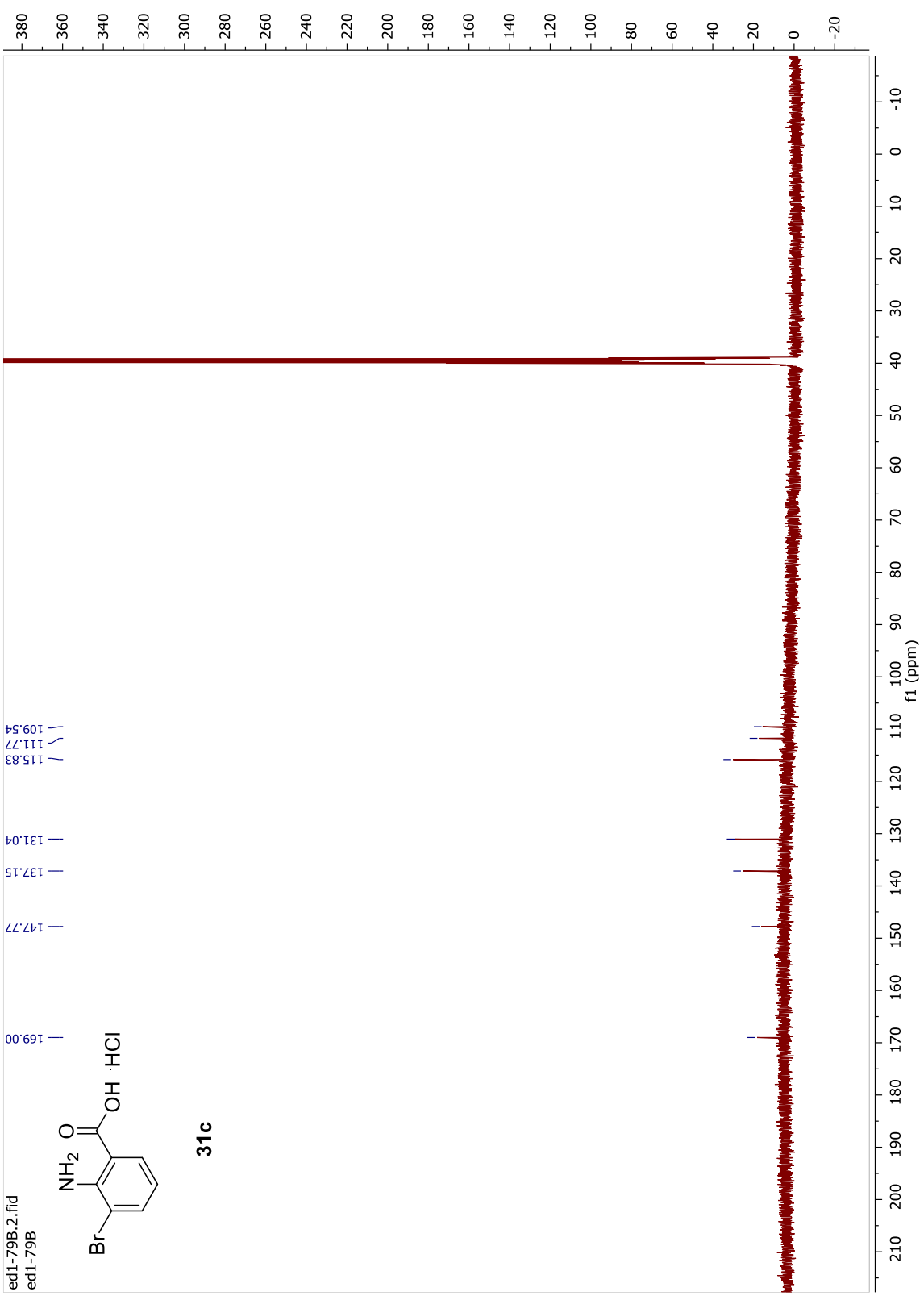
ed1-79B.2.fid
ed1-79B
31c
169.00
147.77
137.15
131.04
115.83
111.77
109.54
f1 (ppm)

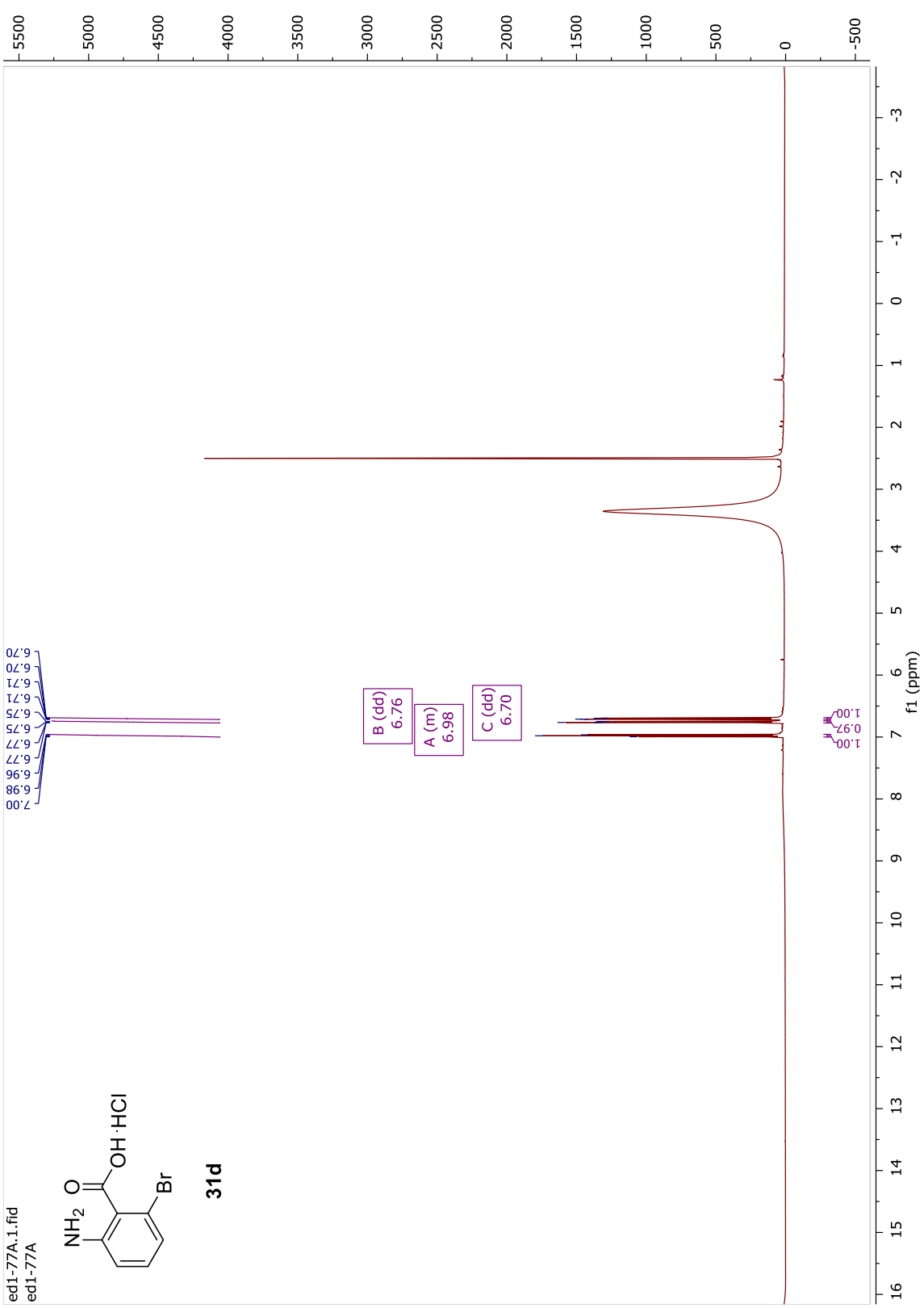
ed1-77A.1.fid
ed1-77A
31d
B (dd)
6.76
A (m)
6.98
C (dd)
6.70
1.00
0.97
1.00
f1 (ppm)

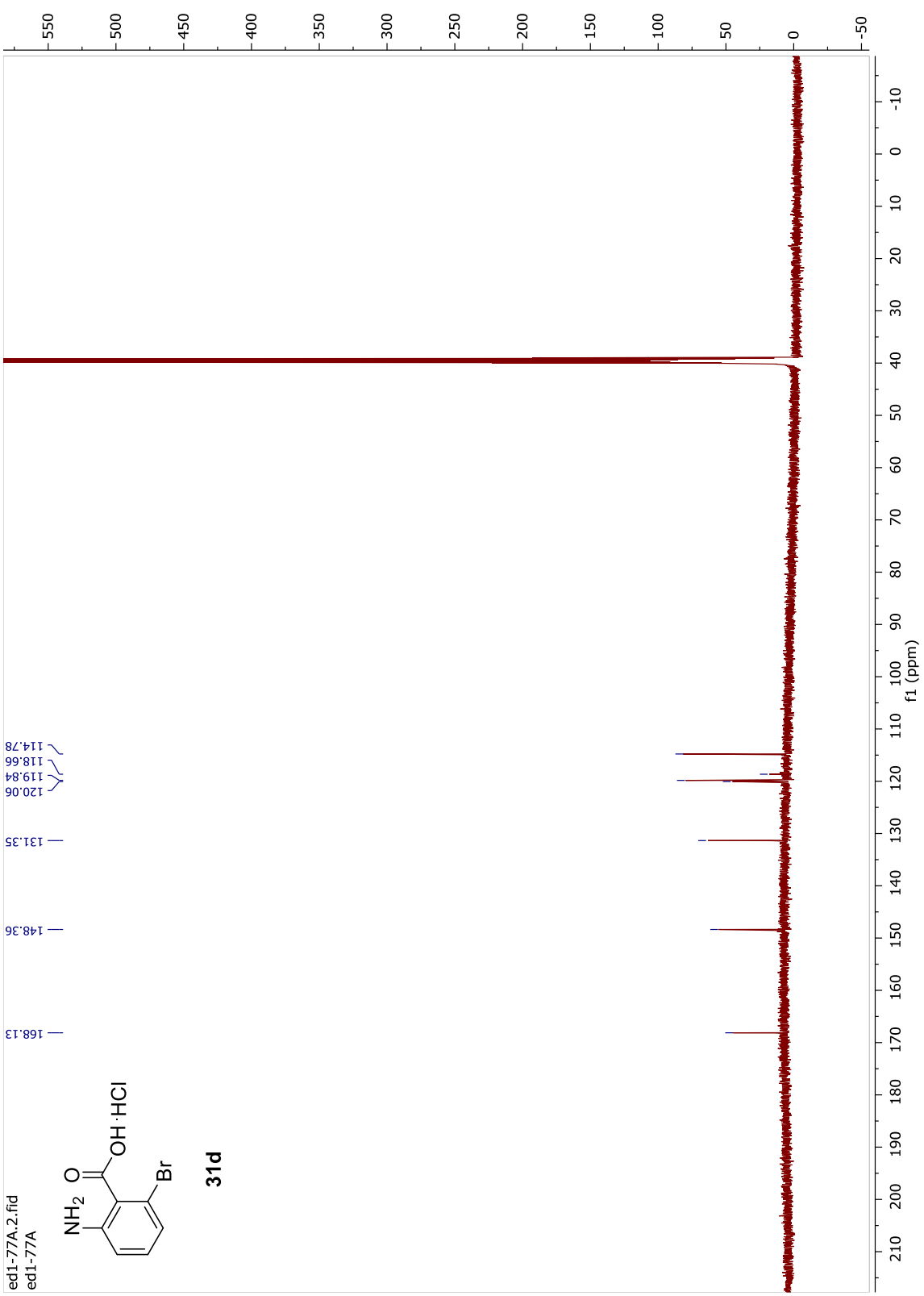
ed1-77A.2.fid
ed1-77A
31d
168.13
148.36
131.35
120.06
119.84
118.66
114.78
f1 (ppm)

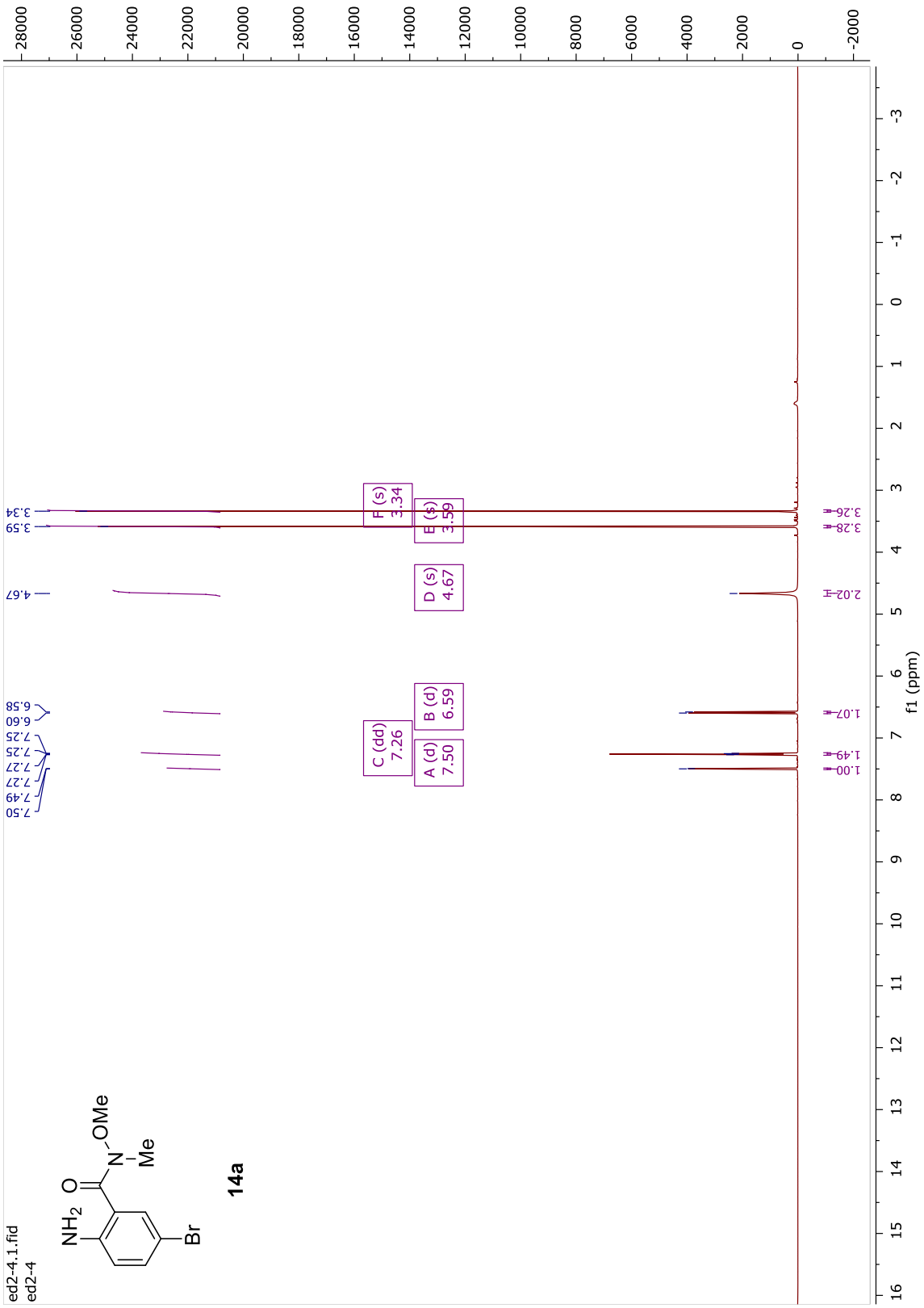
ed2-4.1.fid
ed2-4
14a
NH2
O
N
OMe
Me
Br
f1 (ppm)
A (d) 7.50
B (d) 6.59
C (dd) 7.26
D (s) 4.67
E (s) 3.59
F (s) 3.34
7.50
7.49
7.27
7.27
7.25
7.25
6.60
6.58
3.34
3.59
4.67
3.26
3.28
2.02
1.07
1.49
1.00

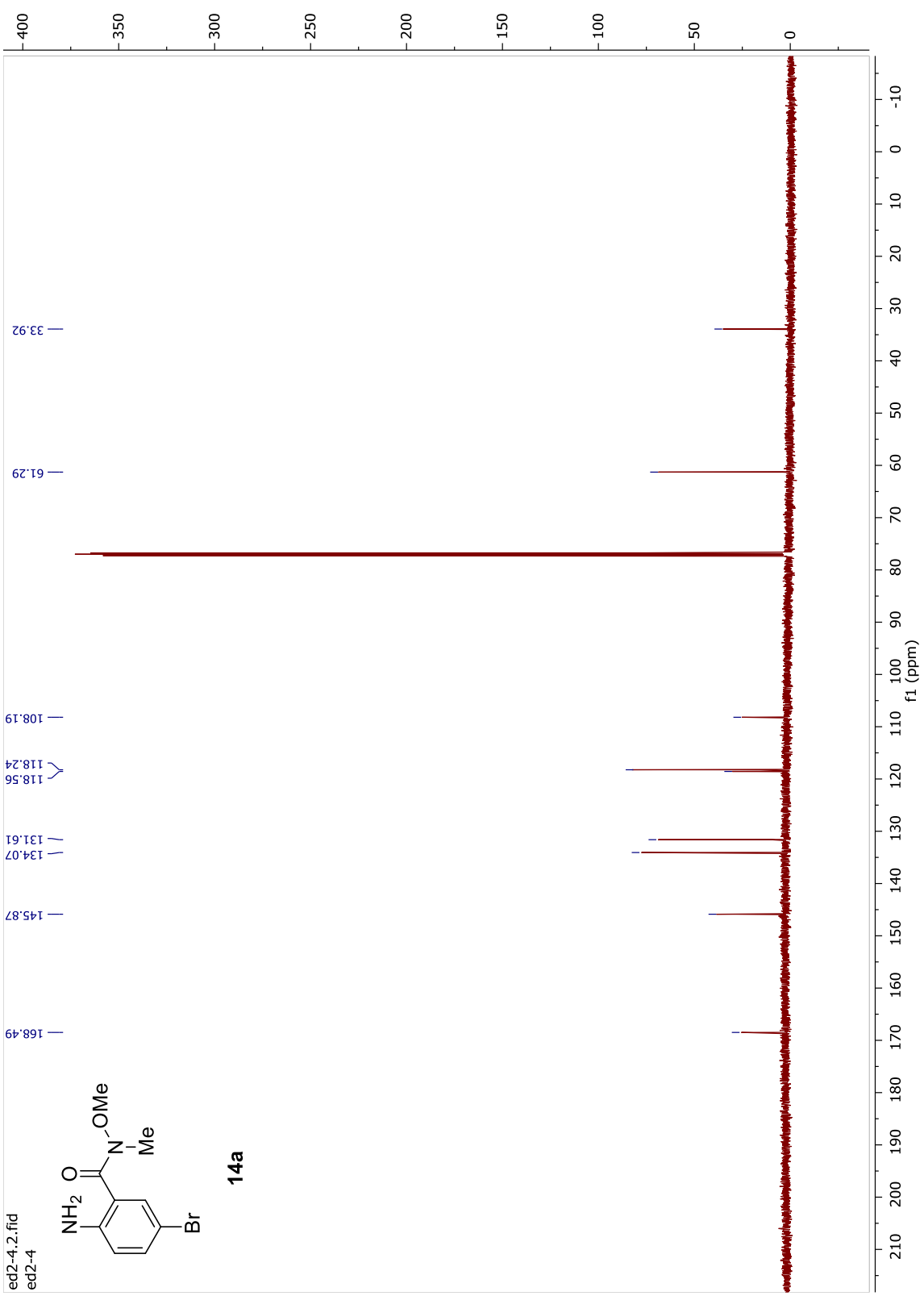
ed2-4.2.fid
ed2-4
14a
168.49
145.87
134.07
131.61
118.56
118.24
108.19
61.29
33.92
f1 (ppm)

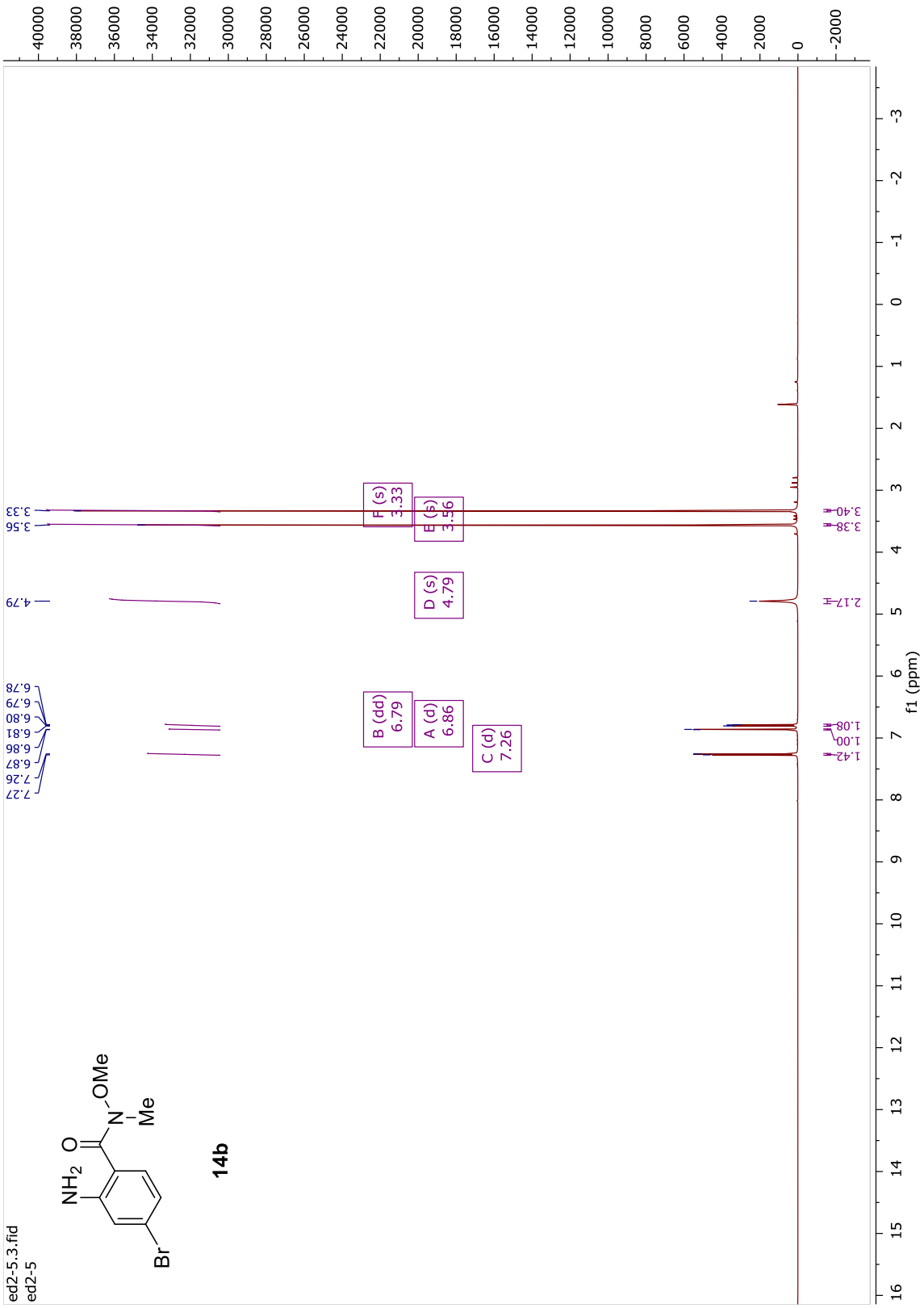
ed2-5.3.fid
ed2-5
14b
NH2
O
N
OMe
Me
Br
F (s)
3.33
E (s)
3.56
D (s)
4.79
B (dd)
6.79
A (d)
6.86
C (d)
7.26
3.33
3.56
4.79
6.78
6.79
6.80
6.81
6.86
6.87
7.26
7.27
3.40
3.38
2.17
1.08
1.00
1.42
f1 (ppm)

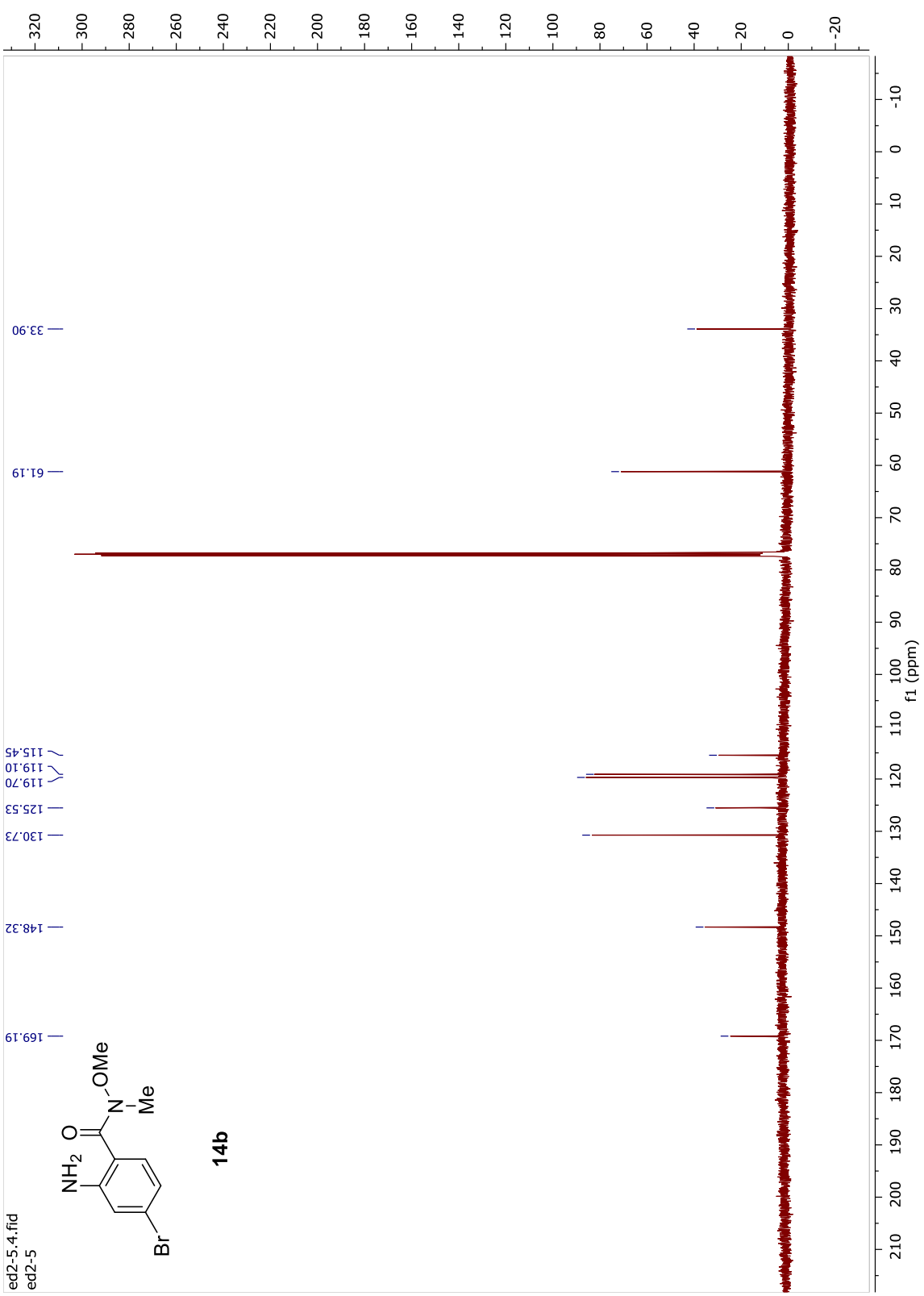
ed2-5.4.fid
ed2-5
14b
169.19
148.32
130.73
125.53
119.70
119.10
115.45
61.19
33.90
f1 (ppm)

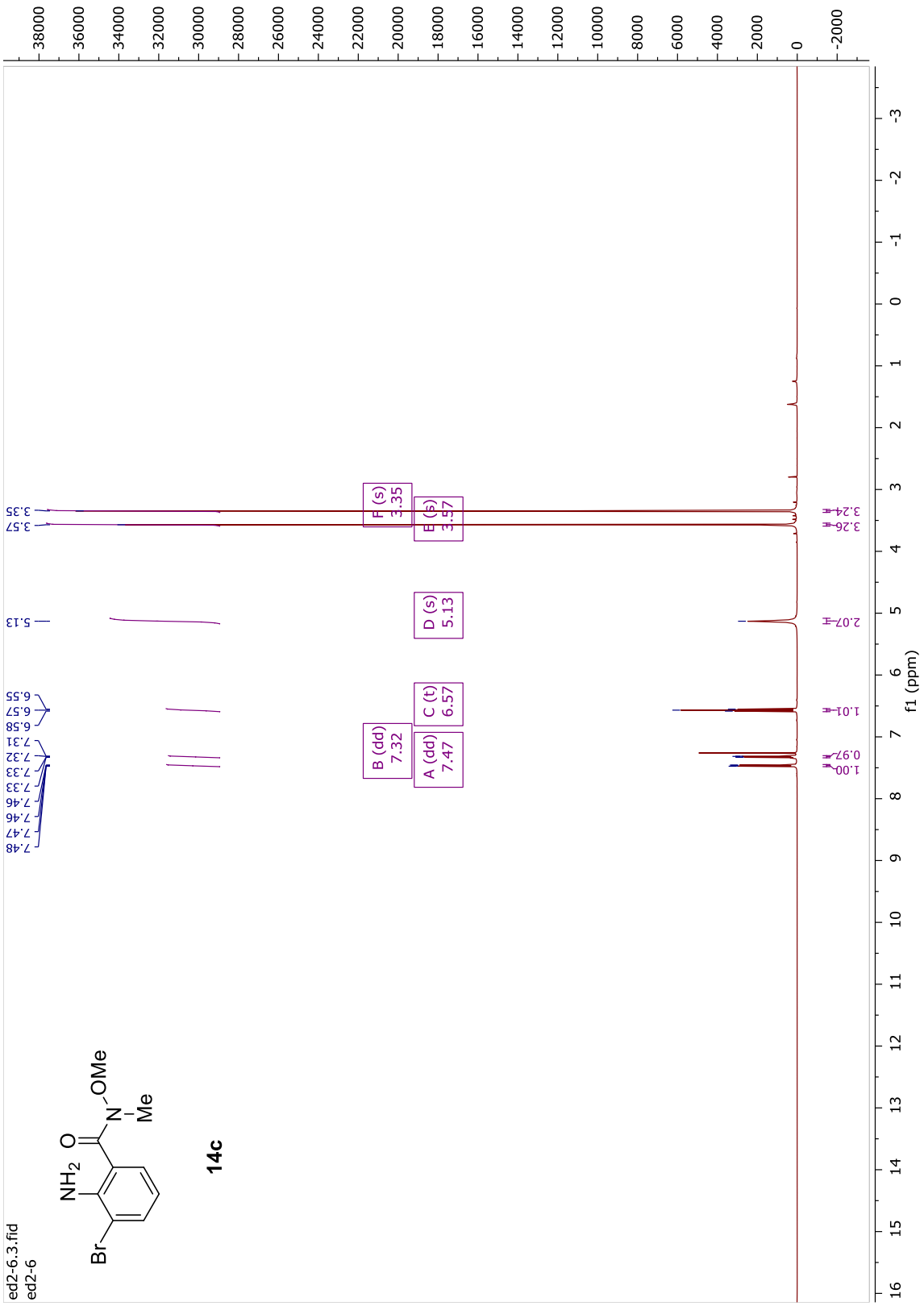
ed2-6.3.fid
ed2-6
14c
NH2
O
N
OMe
Me
Br
A (dd) 7.47
B (dd) 7.32
C (t) 6.57
D (s) 5.13
E (s) 3.57
F (s) 3.35
f1 (ppm)

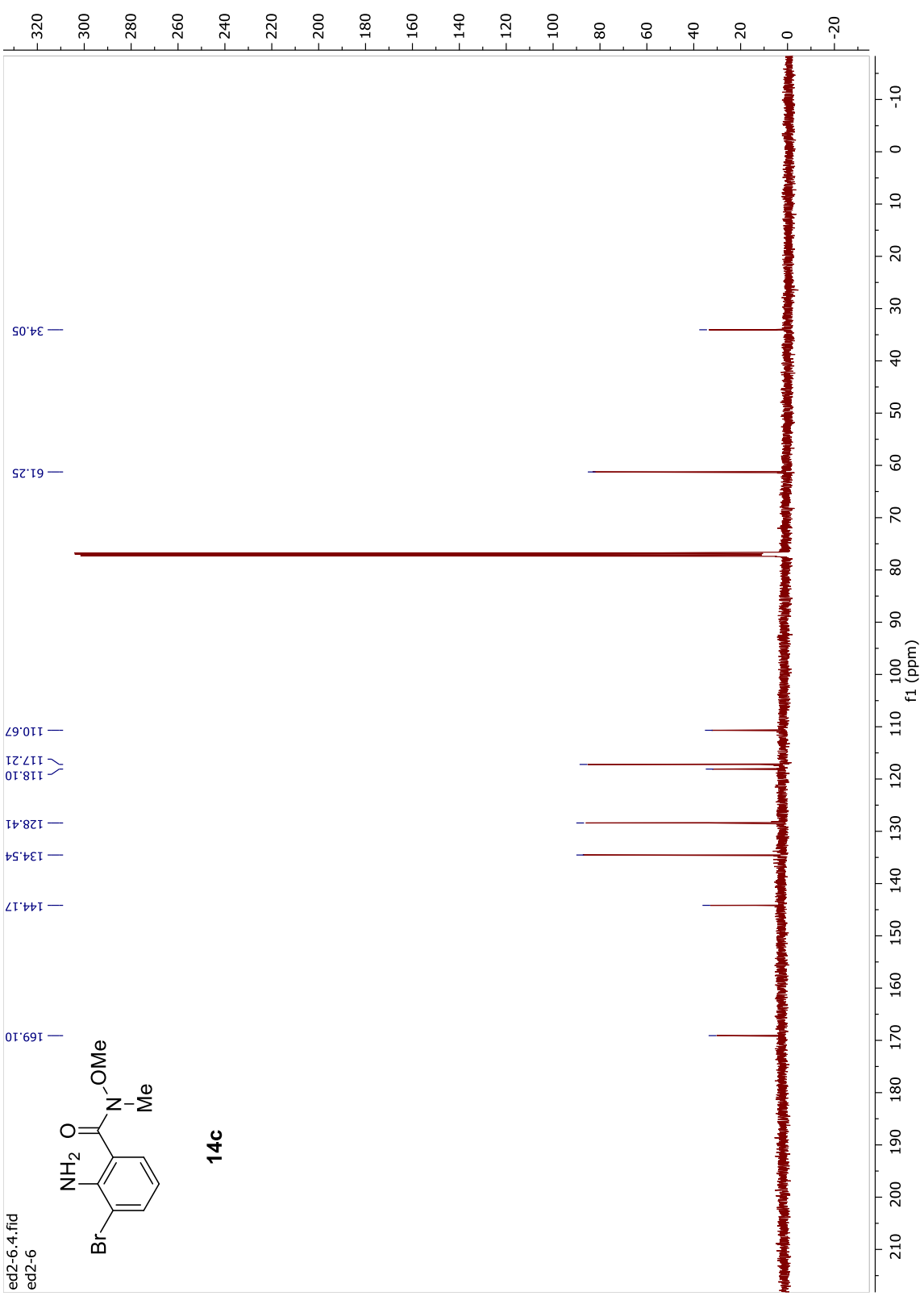
ed2-6.4.fid
ed2-6
14c
169.10
144.17
134.54
128.41
118.10
117.21
110.67
61.25
34.05
f1 (ppm)

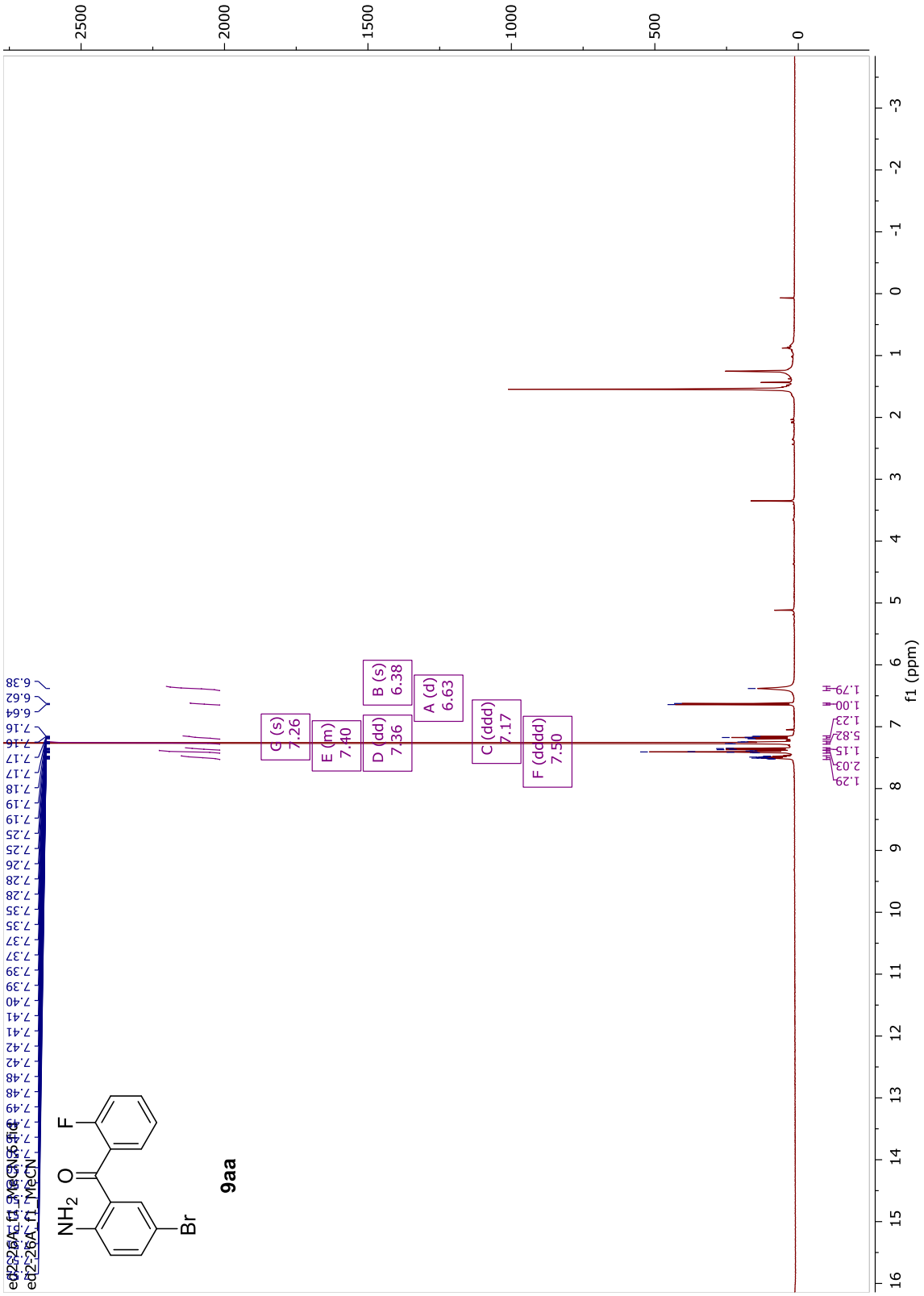
9aa
NH2
O
F
Br
D (s) 7.26
E (m) 7.40
D (dd) 7.36
B (s) 6.38
A (d) 6.63
C (ddd) 7.17
F (dddd) 7.50
f1 (ppm)

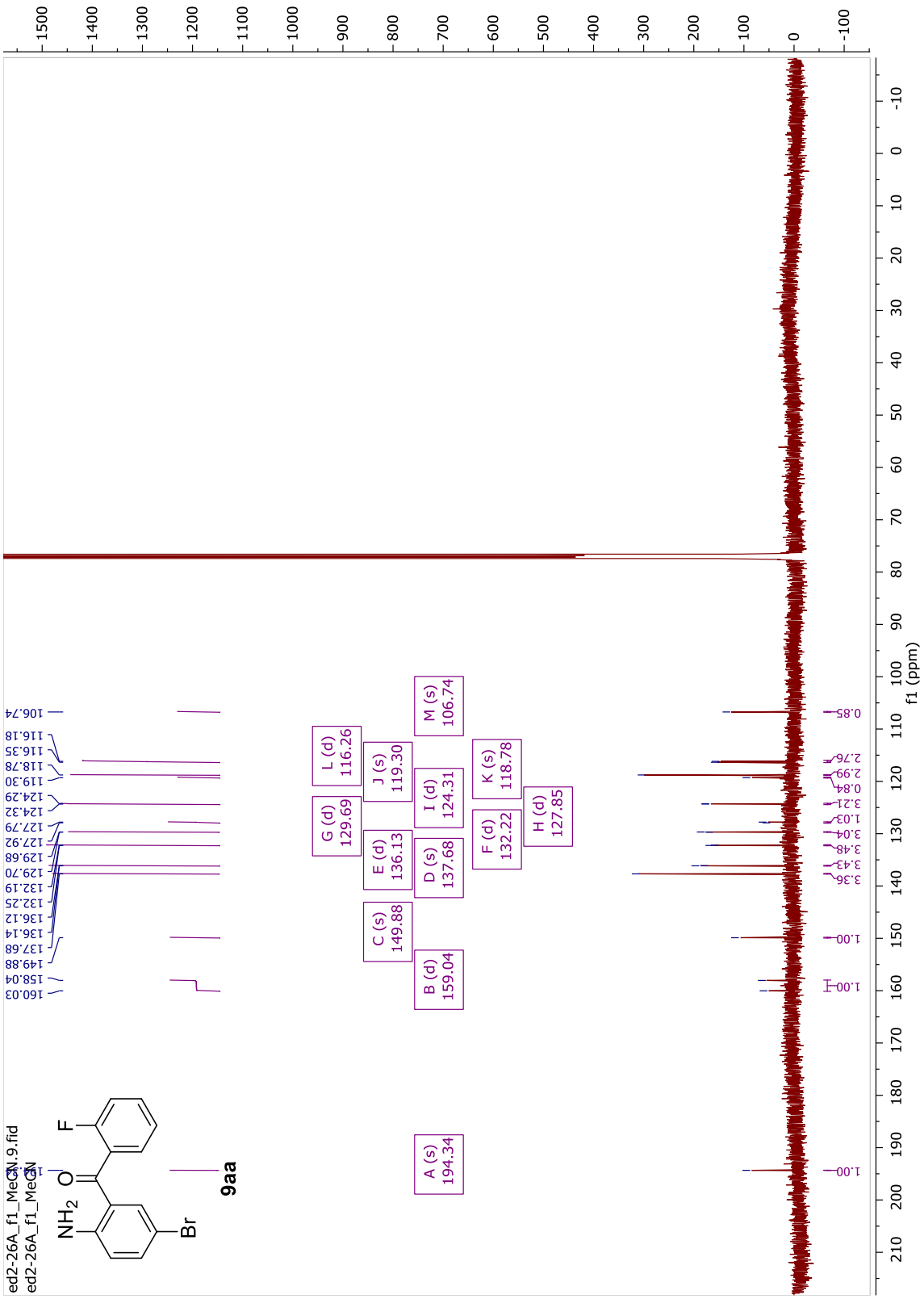
ed2-26A_f1_MeCN.9.fid
ed2-26A_f1_MeCN
9aa
A (s) 194.34
B (d) 159.04
C (s) 149.88
D (s) 137.68
E (d) 136.13
F (d) 132.22
G (d) 129.69
H (d) 127.85
I (d) 124.31
J (s) 119.30
K (s) 118.78
L (d) 116.26
M (s) 106.74
f1 (ppm)

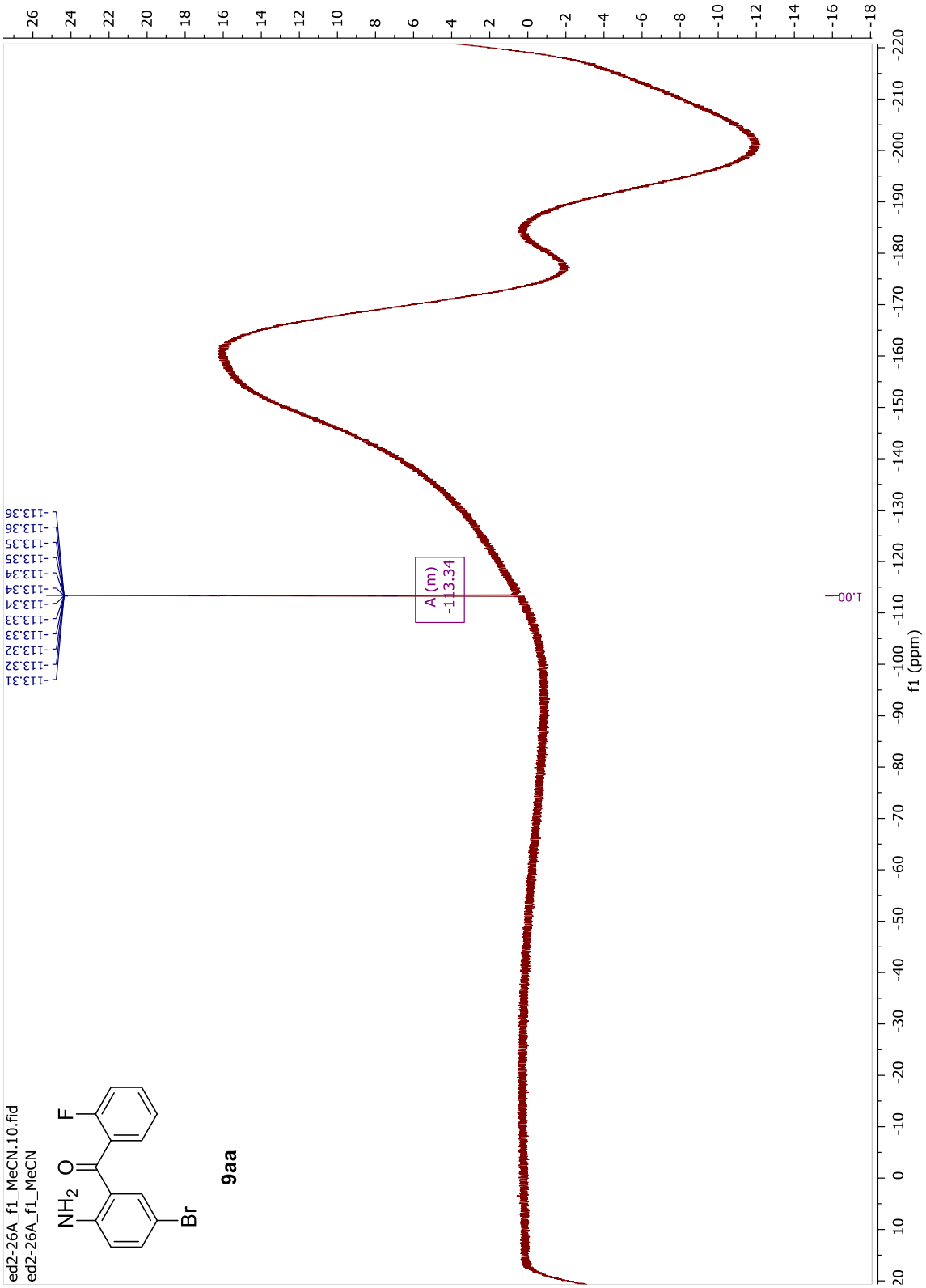
ed2-26A_f1_MeCN.10.fid
ed2-26A_f1_MeCN
9aa
A (m)
-113.34
f1 (ppm)

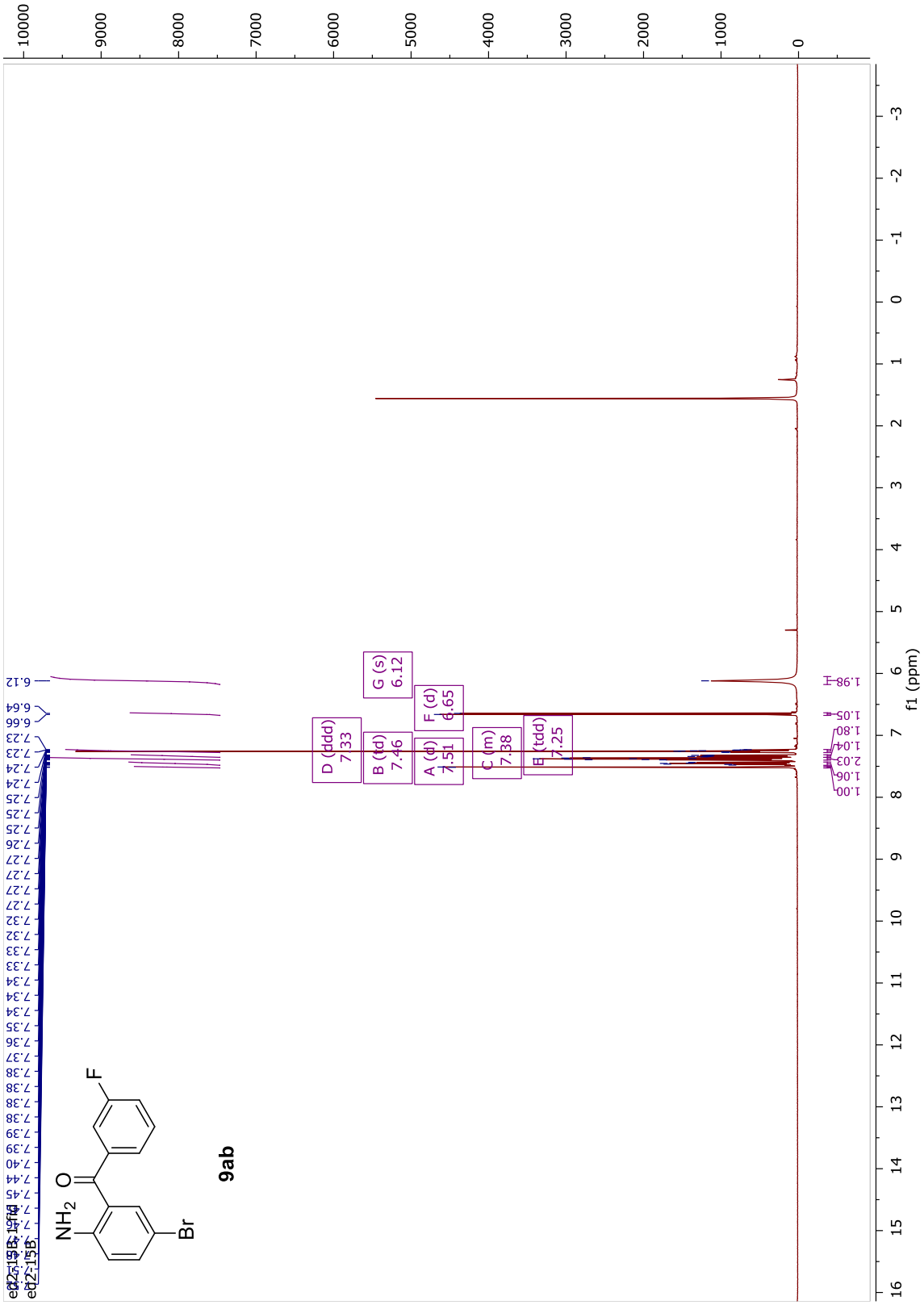
9ab
D (ddd) 7.33
B (td) 7.46
A (d) 7.51
C (m) 7.38
E (tdd) 7.25
F (d) 6.65
G (s) 6.12
f1 (ppm)

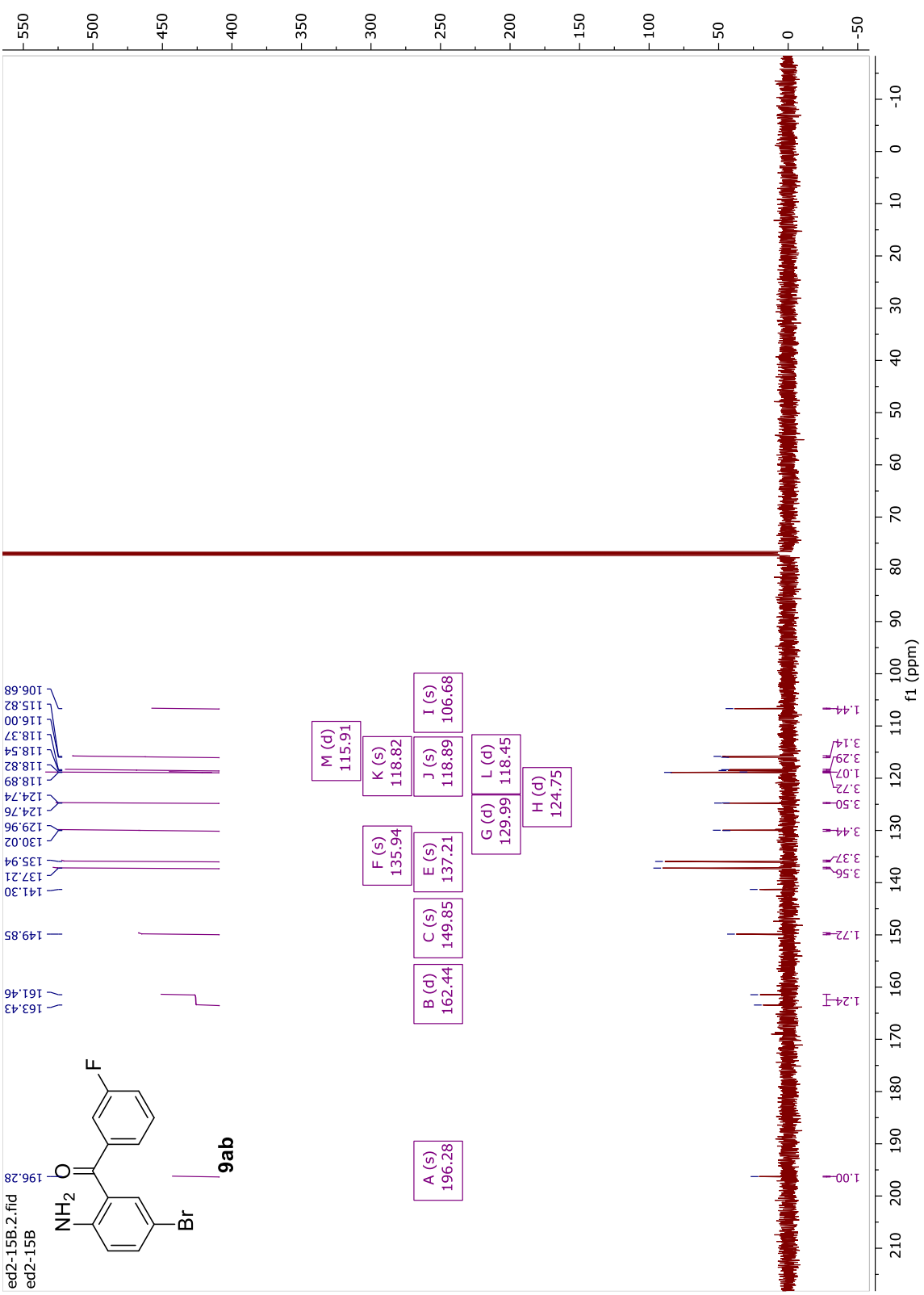
ed2-15B.2.fid
ed2-15B
9ab
A (s) 196.28
B (d) 162.44
C (s) 149.85
E (s) 137.21
F (s) 135.94
G (d) 129.99
H (d) 124.75
J (s) 118.89
K (s) 118.82
L (d) 118.45
M (d) 115.91
I (s) 106.68
f1 (ppm)

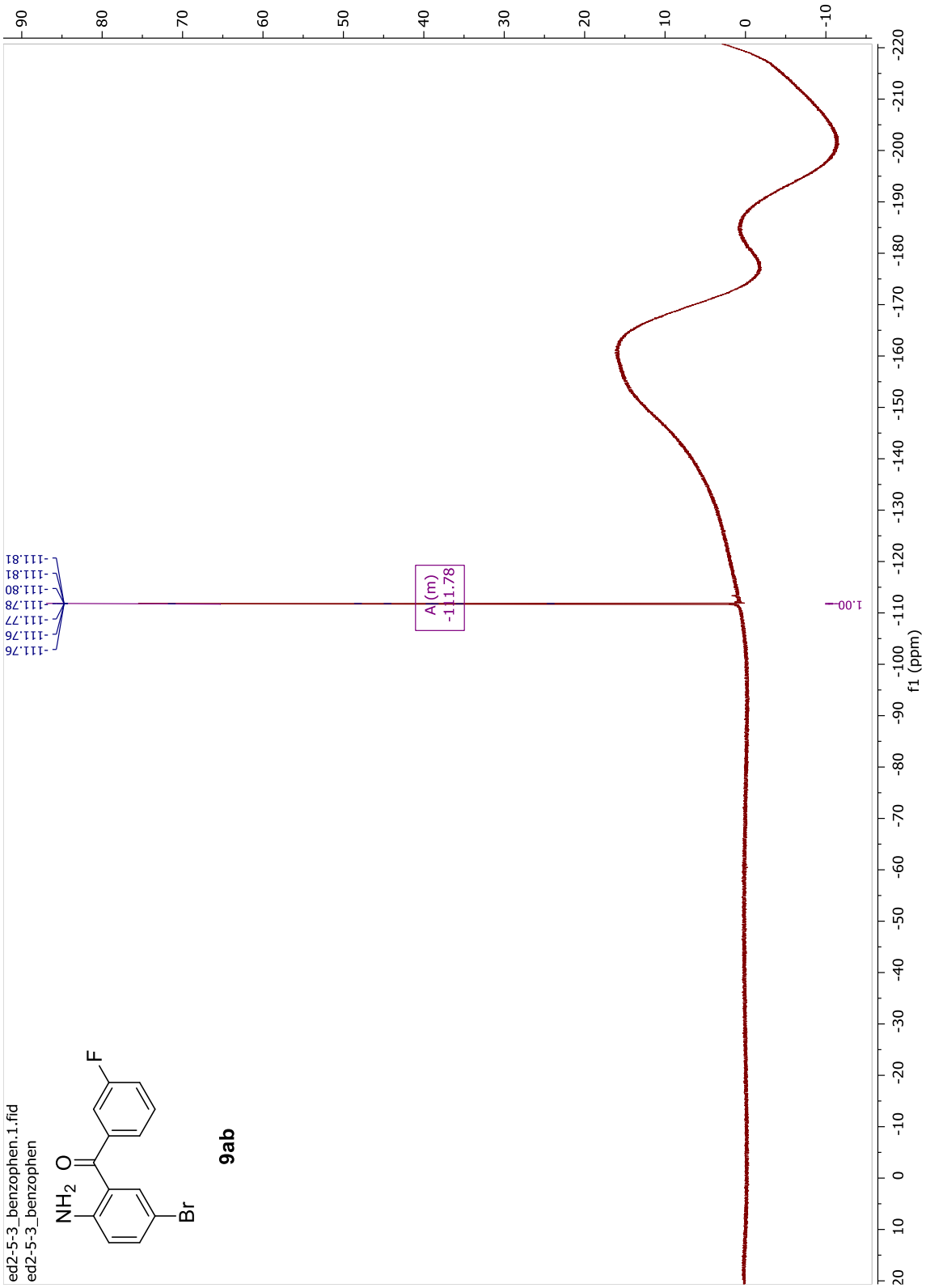
ed2-5-3_benzophen.1.fid
ed2-5-3_benzophen
9ab
A(m)
-111.78
-111.76
-111.76
-111.77
-111.78
-111.80
-111.81
-111.81
1.00
f1 (ppm)

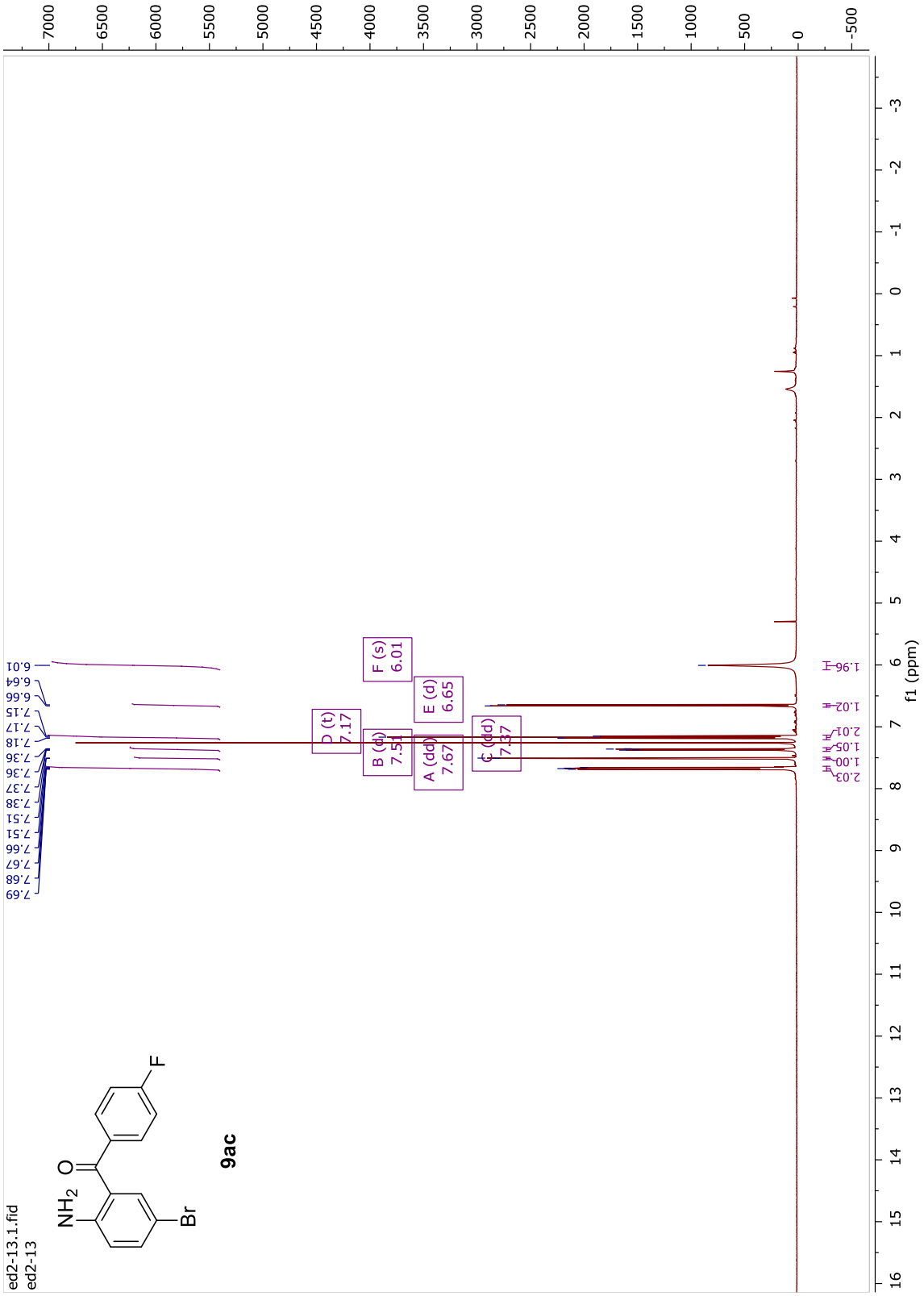
ed2-13.1.fid
ed2-13
9ac
NH2
O
F
Br
A (dd) 7.67
B (d) 7.51
C (dd) 7.37
D (t) 7.17
E (d) 6.65
F (s) 6.01
f1 (ppm)

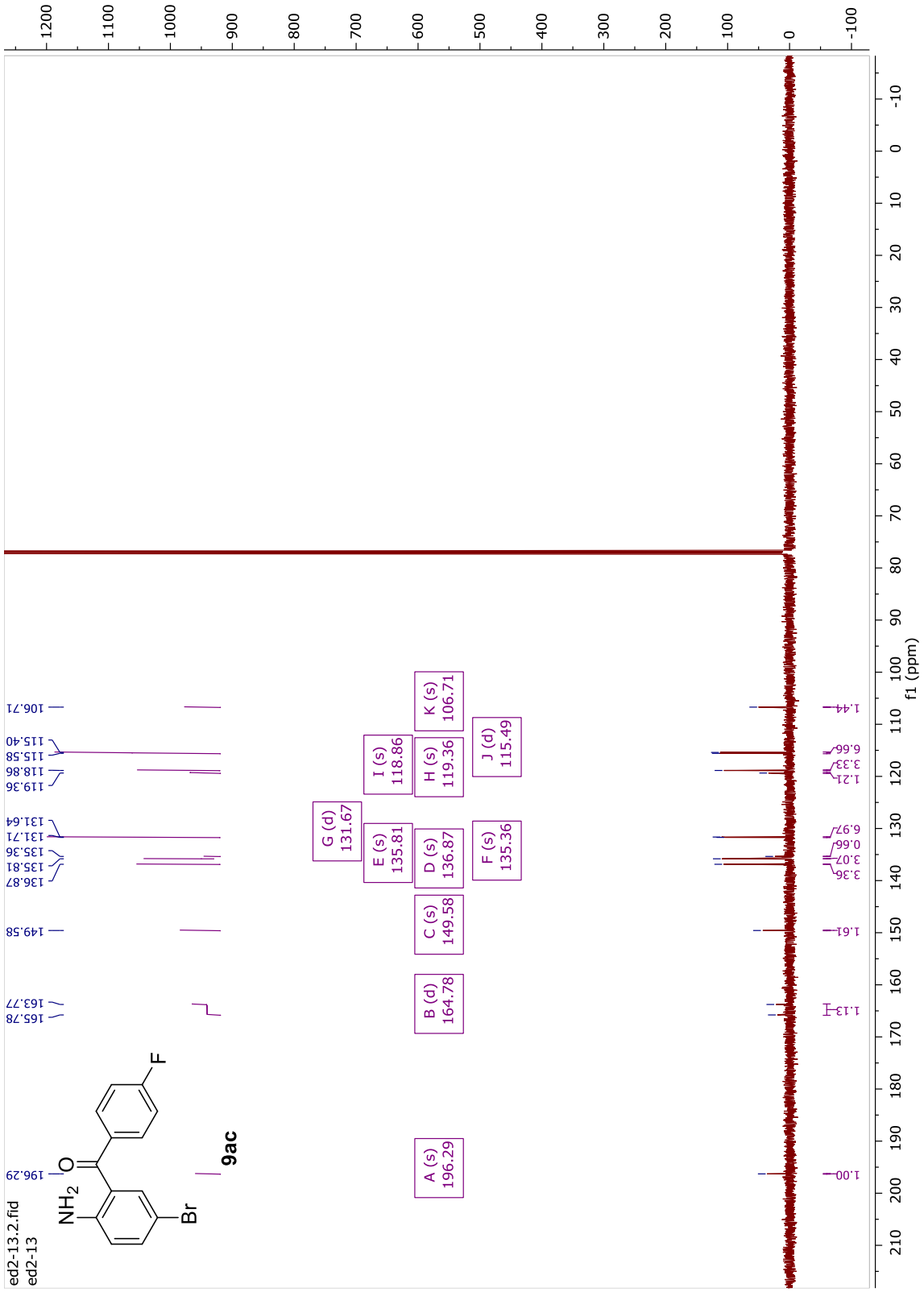
ed2-13.2.fid
ed2-13
9ac
A (s) 196.29
B (d) 164.78
C (s) 149.58
D (s) 136.87
E (s) 135.81
F (s) 135.36
G (d) 131.67
H (s) 119.36
I (s) 118.86
J (d) 115.49
K (s) 106.71
f1 (ppm)

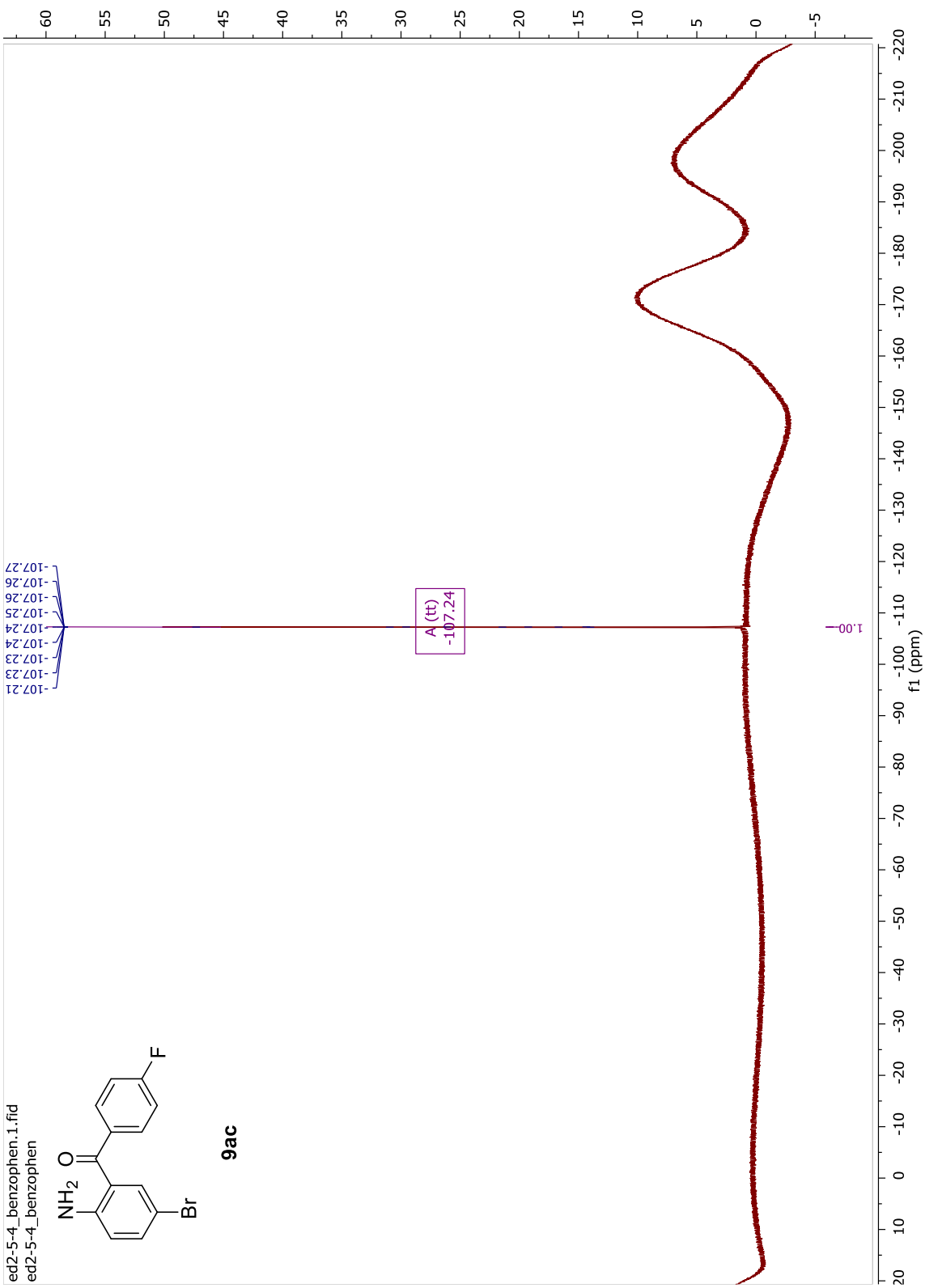
ed2-5-4_benzophen.1.fid
ed2-5-4_benzophen
9ac
A (tt)
-107.24
1.00
f1 (ppm)

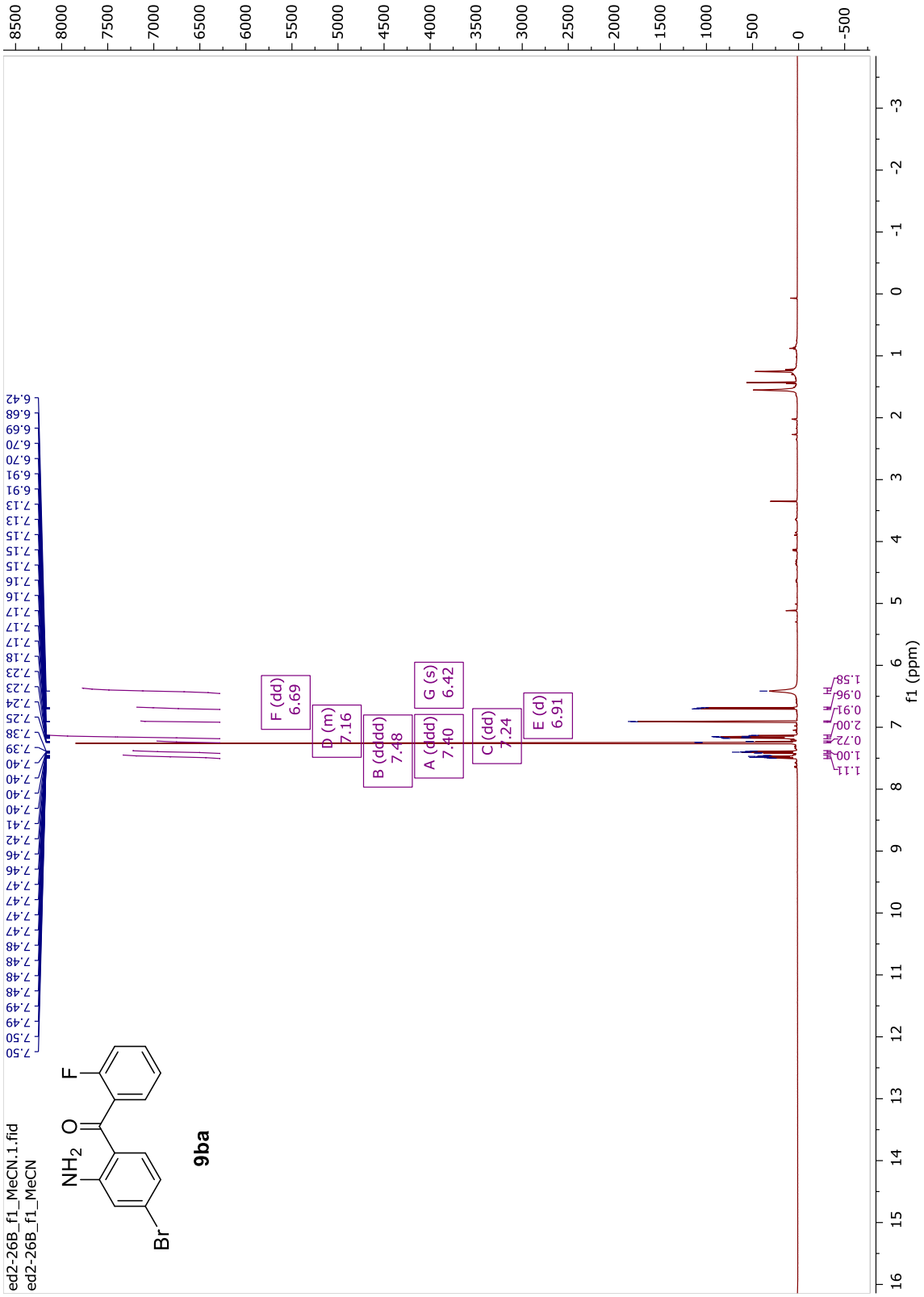
ed2-26B_f1_MeCN.1.fid
ed2-26B_f1_MeCN
9ba
F (dd) 6.69
D (m) 7.16
B (dddd) 7.48
A (ddd) 7.40
G (s) 6.42
C (dd) 7.24
E (d) 6.91
1.11
1.00
0.72
2.00
0.91
0.96
1.58
f1 (ppm)

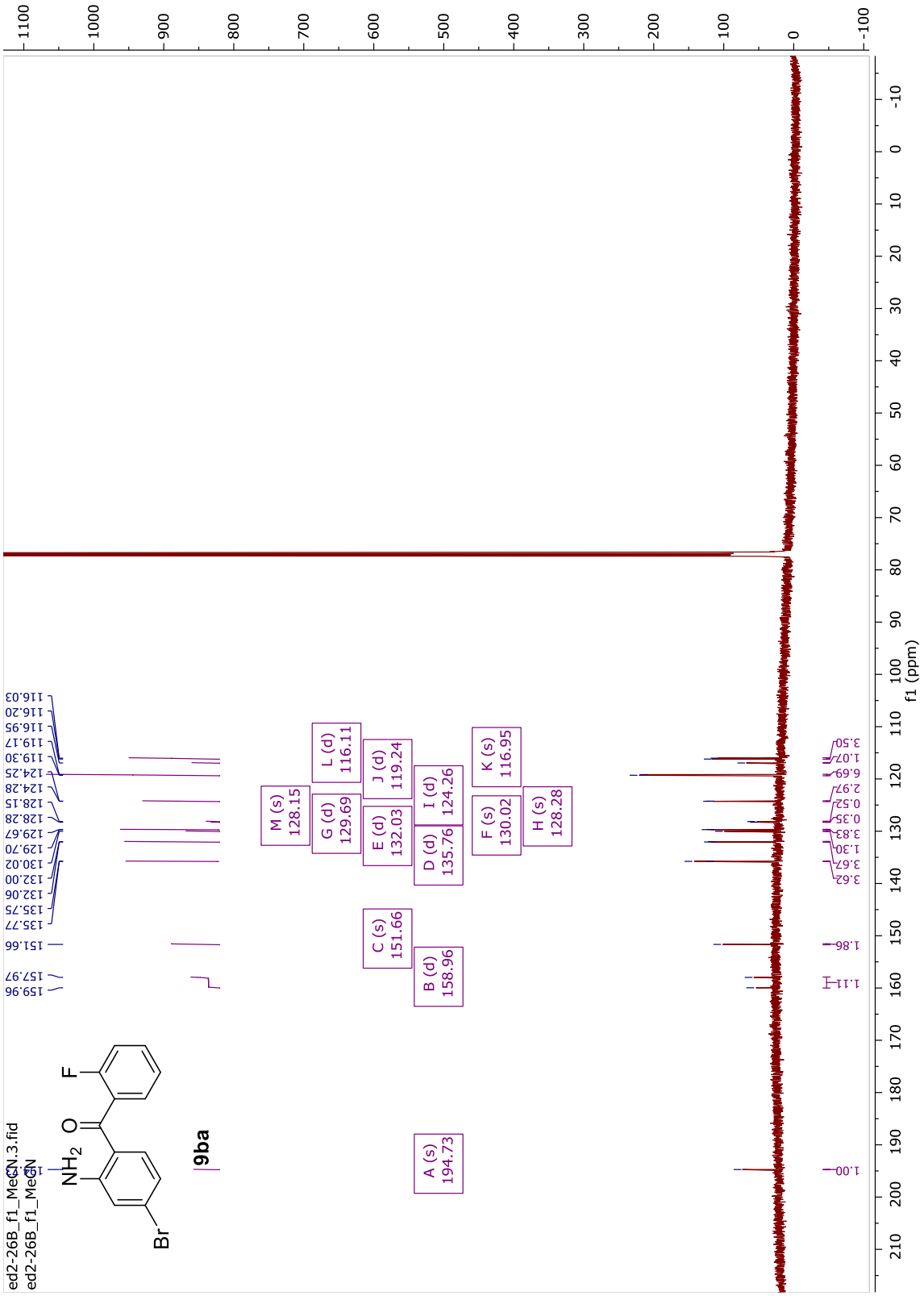
ed2-26B_f1_MeCN.3.fid
ed2-26B_f1_MeCN
9ba
A (s) 194.73
B (d) 158.96
C (s) 151.66
D (d) 135.76
E (d) 132.03
F (s) 130.02
G (d) 129.69
H (s) 128.28
I (d) 124.26
J (d) 119.24
K (s) 116.95
L (d) 116.11
M (s) 128.15
f1 (ppm)

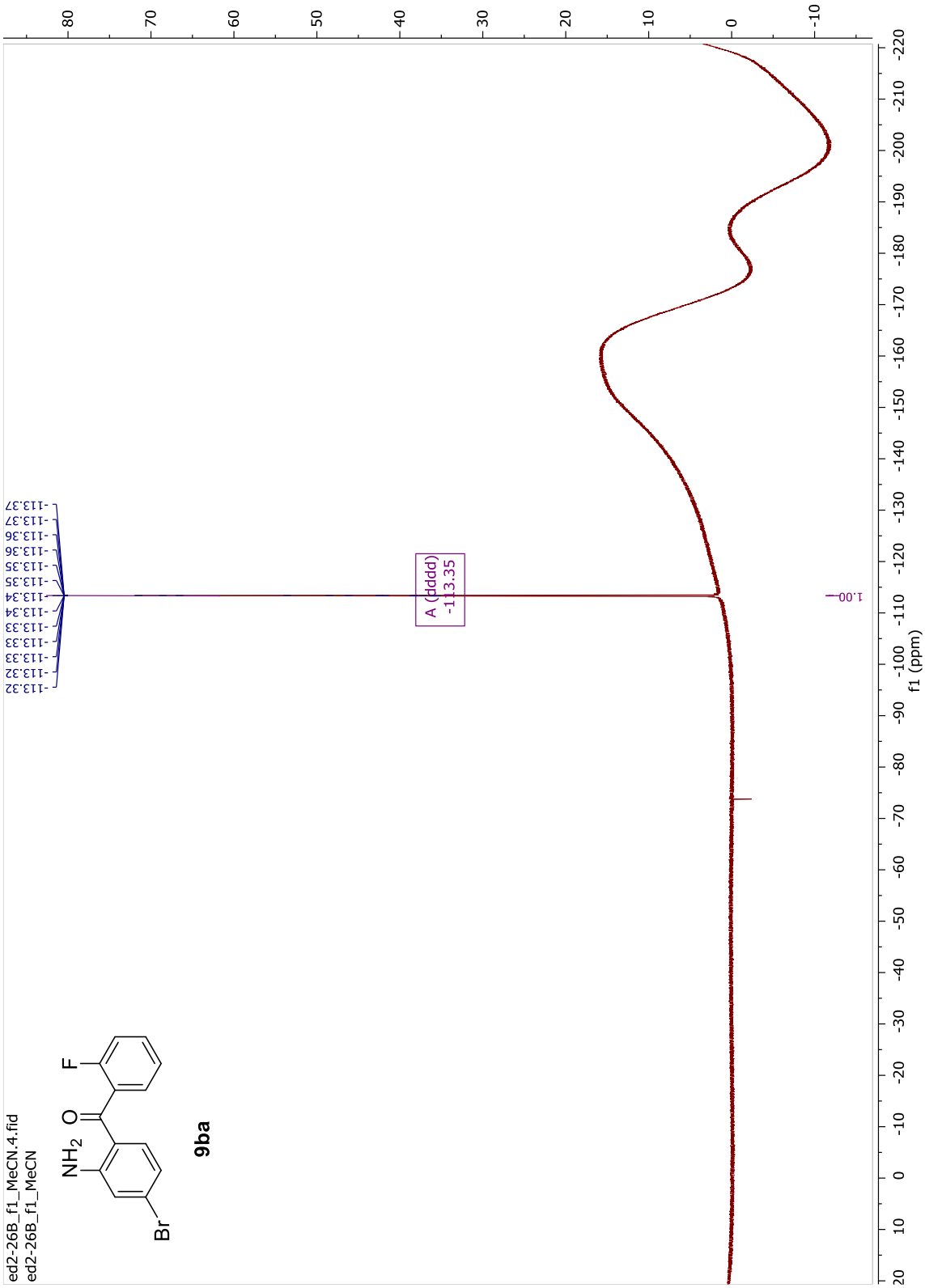
ed2-26B_f1_MeCN.4.fid
ed2-26B_f1_MeCN
9ba
A (dddd)
-113.35
1.00
f1 (ppm)

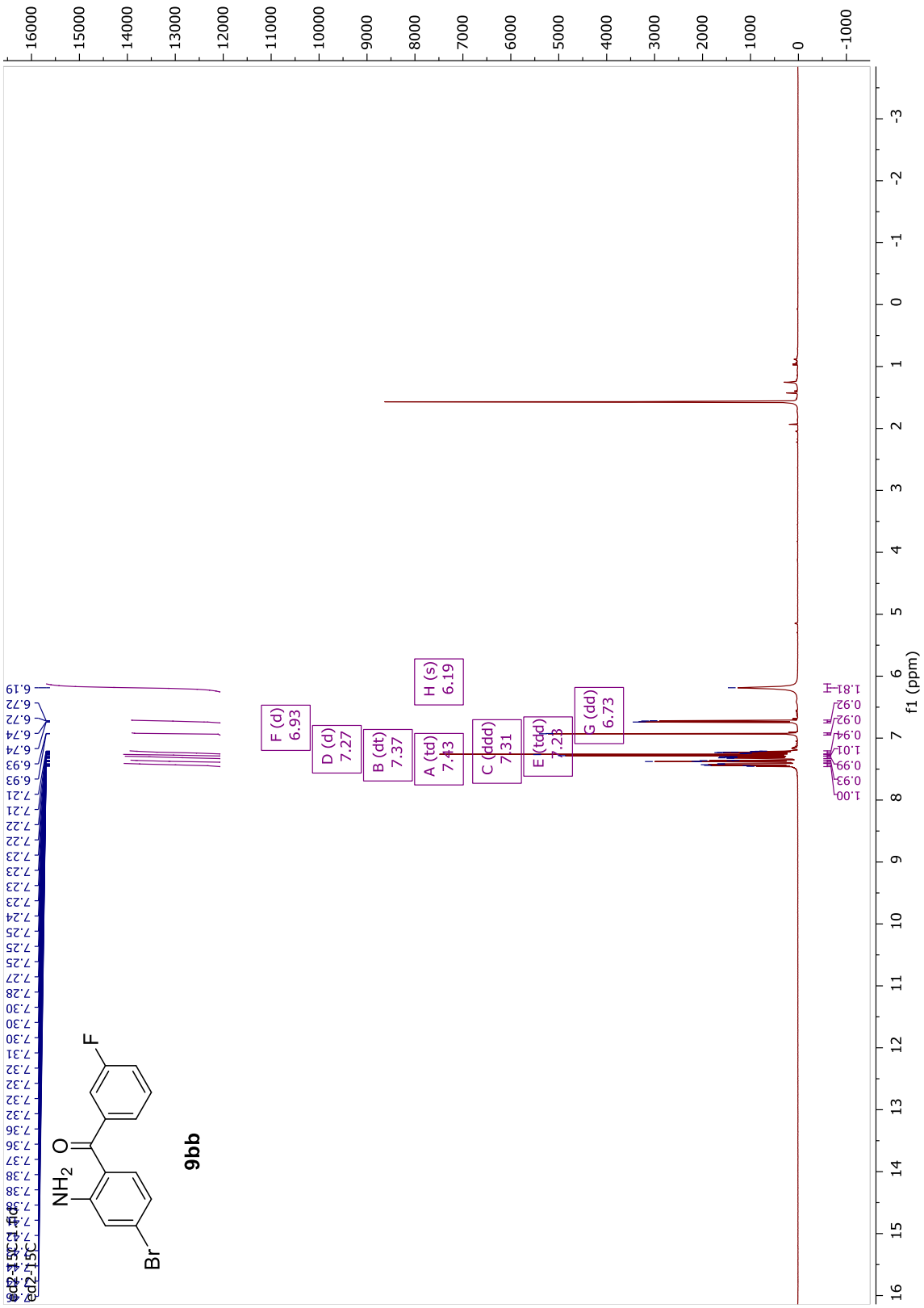
9bb
NH2
O
F
Br
F (d) 6.93
D (d) 7.27
B (dt) 7.37
A (td) 7.43
H (s) 6.19
C (ddd) 7.31
E (tdd) 7.28
G (dd) 6.73
f1 (ppm)

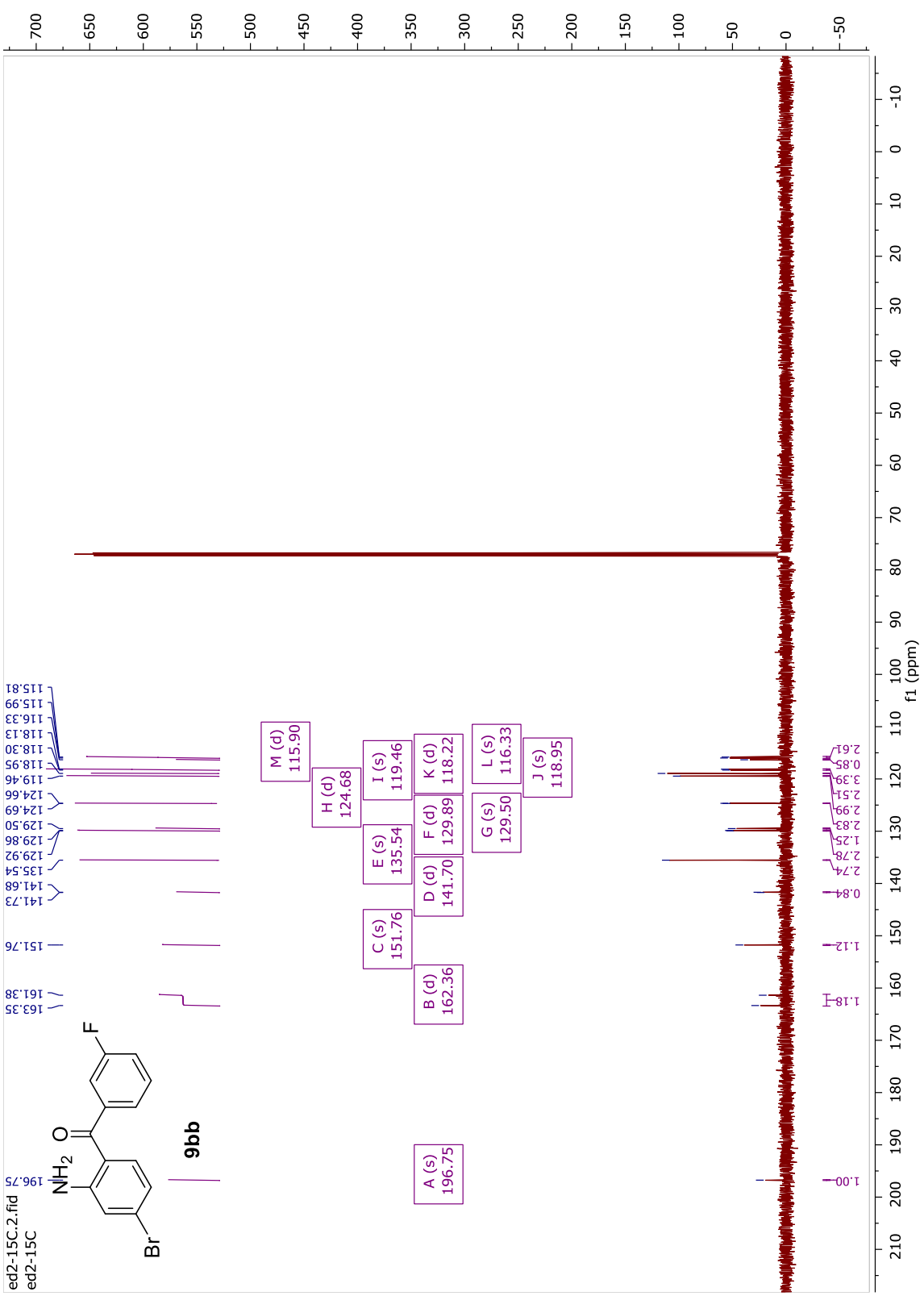
ed2-15C.2.fid
ed2-15C
9bb
A (s) 196.75
B (d) 162.36
C (s) 151.76
D (d) 141.70
E (s) 135.54
F (d) 129.89
G (s) 129.50
H (d) 124.68
I (s) 119.46
J (s) 118.95
K (d) 118.22
L (s) 116.33
M (d) 115.90
f1 (ppm)

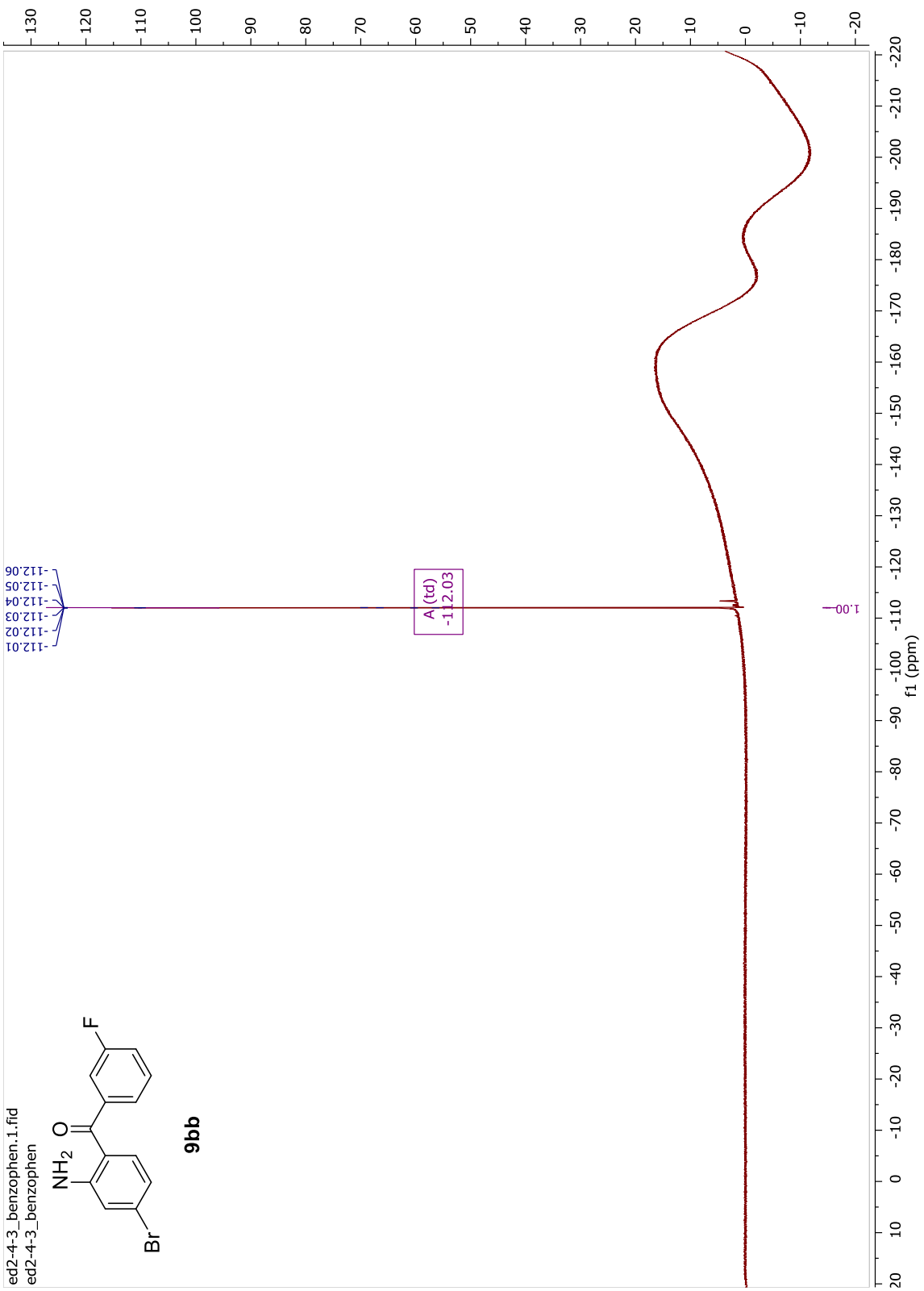
ed2-4-3_benzophen.1.fid
ed2-4-3_benzophen
9bb
A (td)
-112.03
1.00
f1 (ppm)

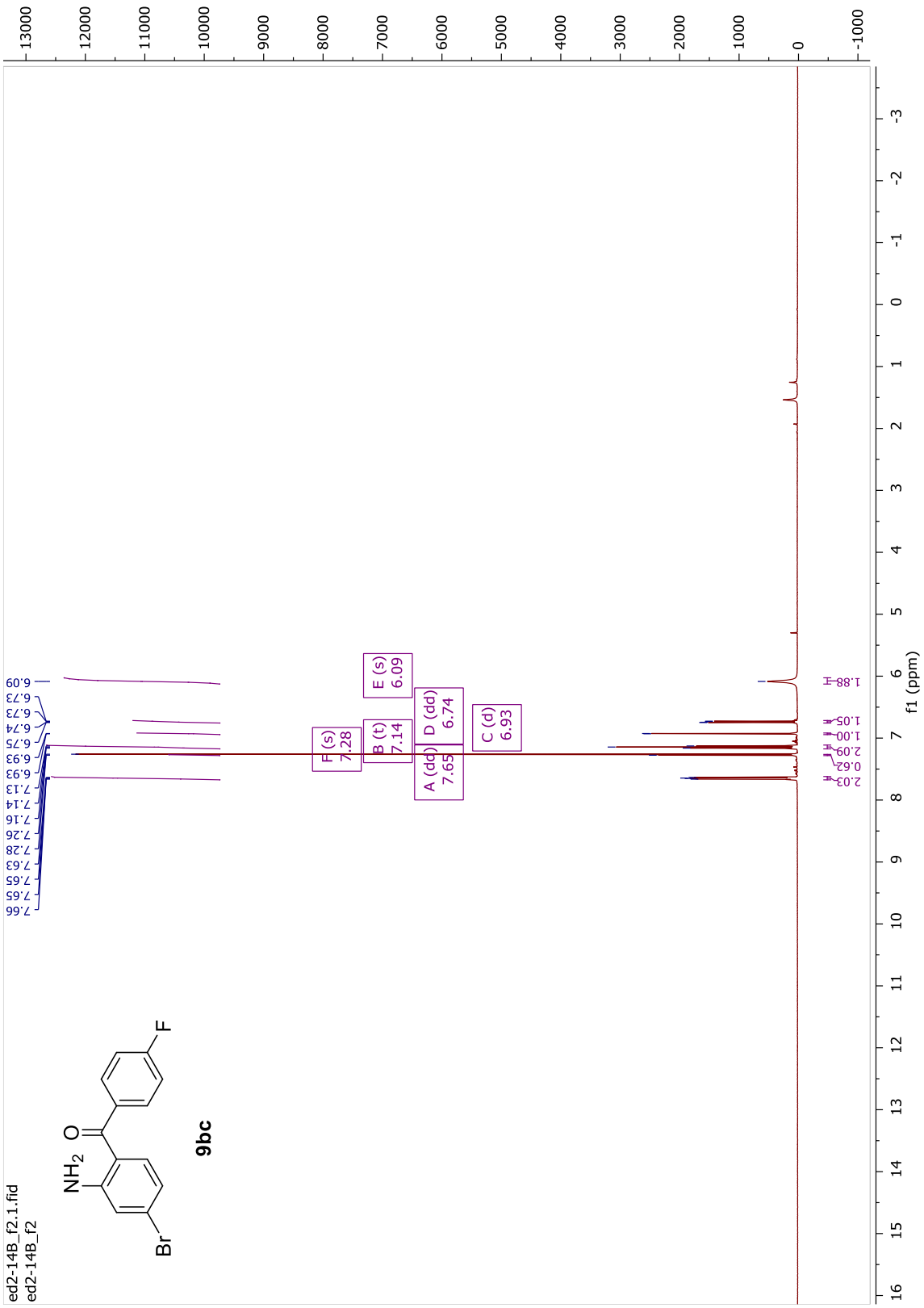
ed2-14B_f2.1.fid
ed2-14B_f2
9bc
NH2
O
F
Br
F (s) 7.28
B (t) 7.14
A (dd) 7.65
D (dd) 6.74
E (s) 6.09
C (d) 6.93
f1 (ppm)

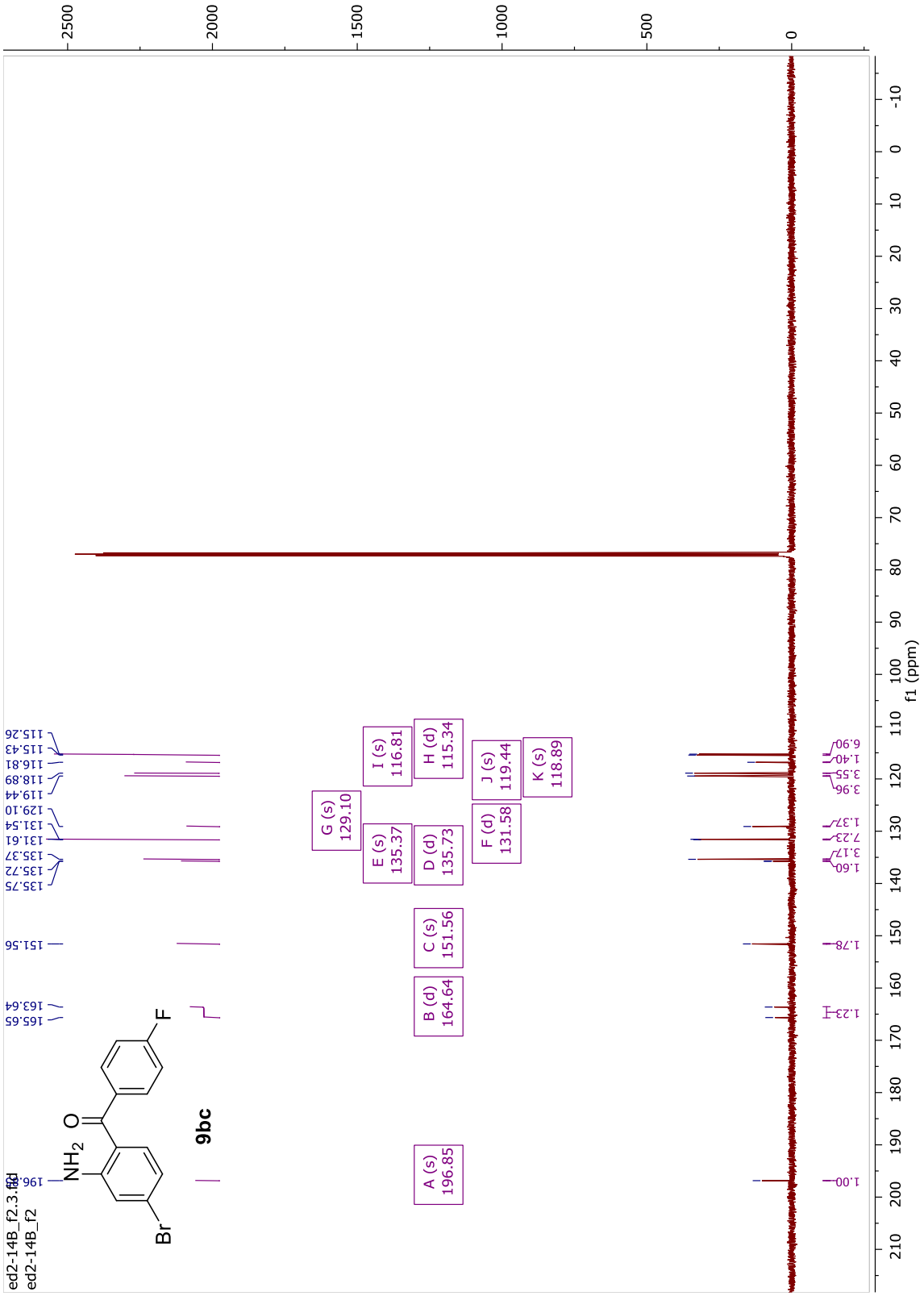
ed2-14B_f2.3.fid
ed2-14B_f2
9bc
A (s) 196.85
B (d) 164.64
C (s) 151.56
D (d) 135.73
E (s) 135.37
F (d) 131.58
G (s) 129.10
H (d) 115.34
I (s) 116.81
J (s) 119.44
K (s) 118.89
f1 (ppm)


ed2-4-4_benzophen.1.fid
ed2-4-4_benzophen
9bc
NH2
O
Br
F
A (tt)
-107.64
1.00
-107.61
-107.62
-107.63
-107.63
-107.64
-107.64
-107.65
-107.66
-107.67
f1 (ppm)

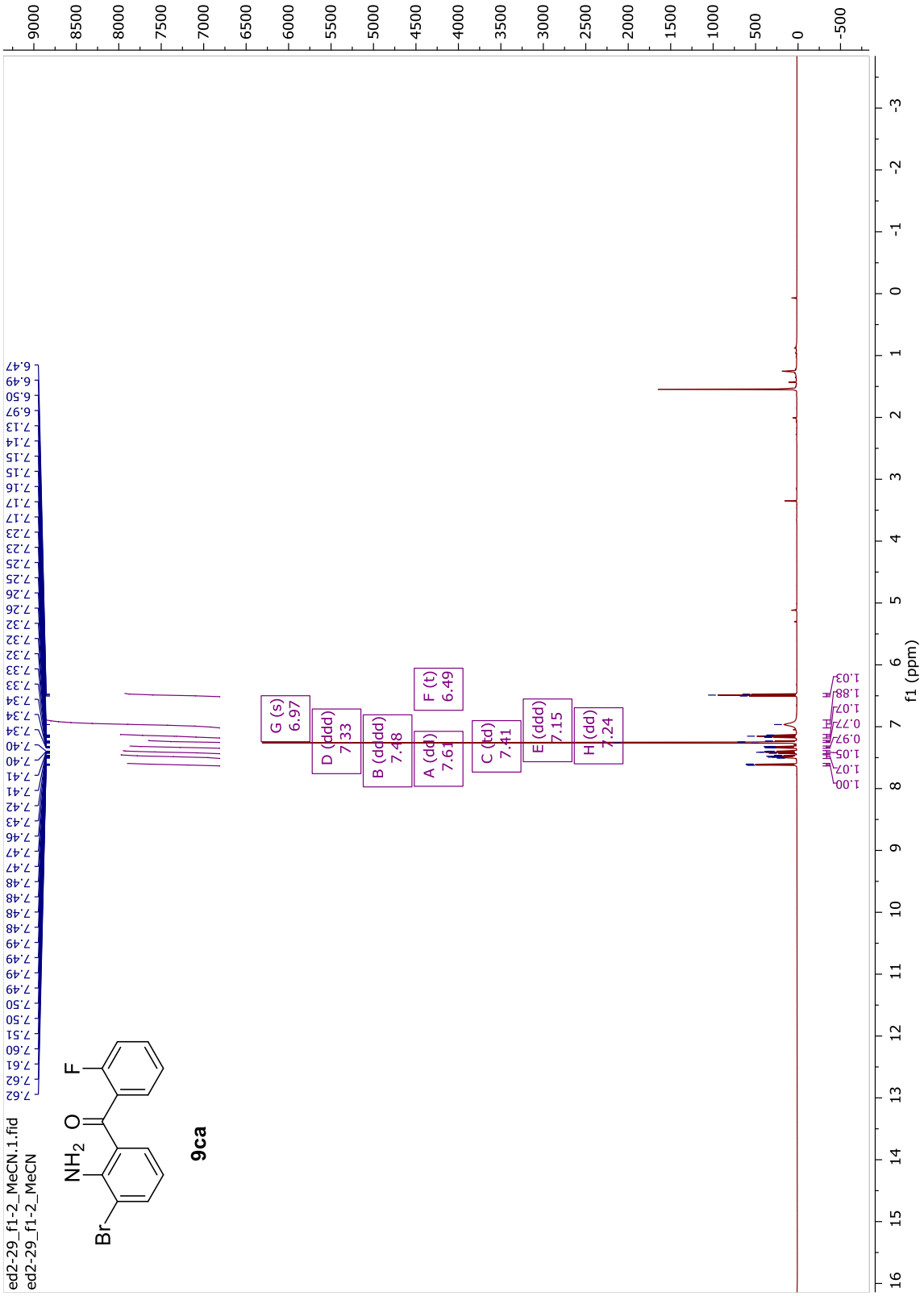
ed2-29_f1-2_MeCN.1.fid
ed2-29_f1-2_MeCN
9ca
G (s) 6.97
D (ddd) 7.33
B (dddd) 7.48
A (dd) 7.61
F (t) 6.49
C (td) 7.41
E (ddd) 7.15
H (dd) 7.24
f1 (ppm)

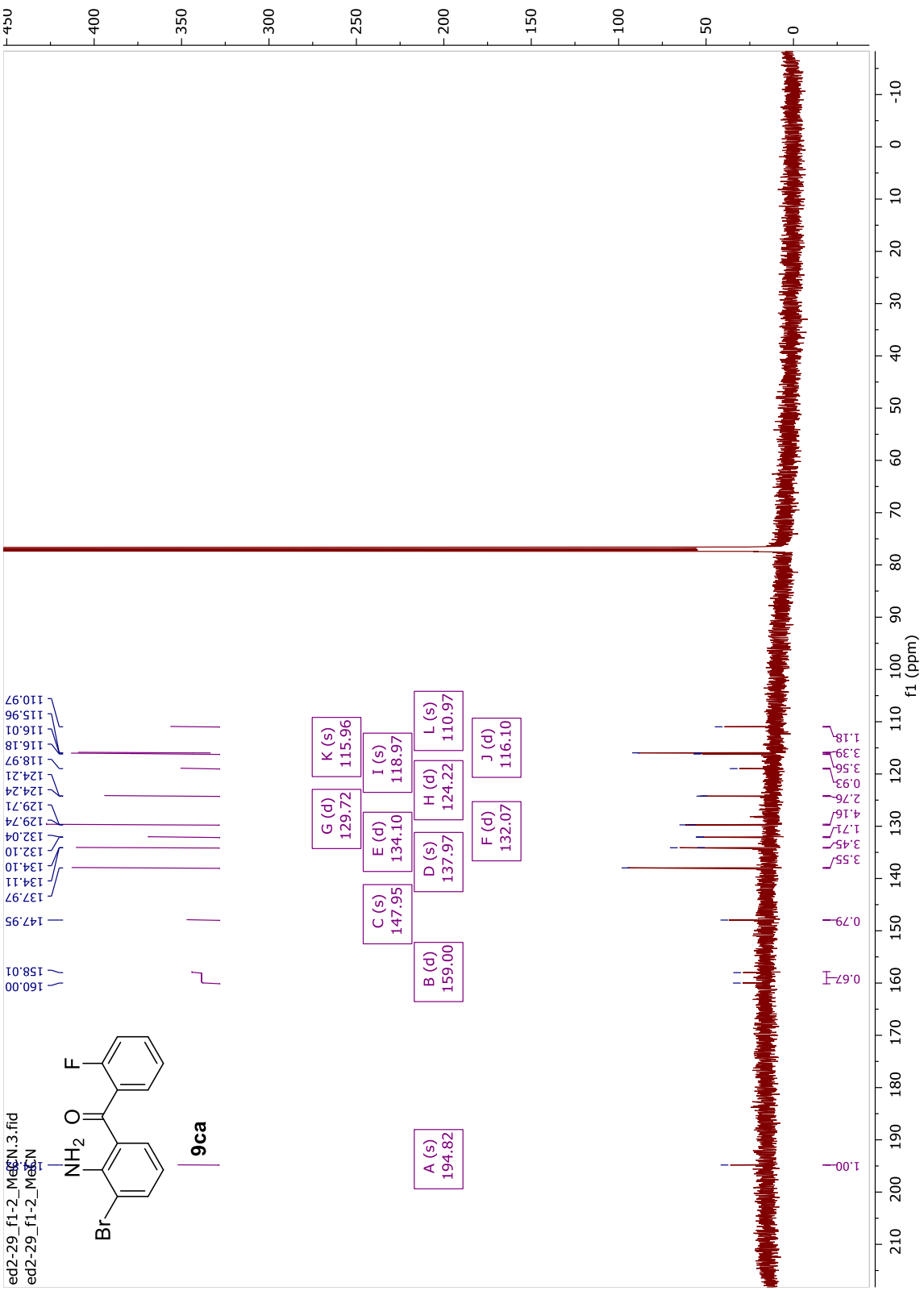
ed2-29_f1-2_MeCN.3.fid
ed2-29_f1-2_MeCN
9ca
A (s) 194.82
B (d) 159.00
C (s) 147.95
D (s) 137.97
E (d) 134.10
F (d) 132.07
G (d) 129.72
H (d) 124.22
I (s) 118.97
J (d) 116.10
K (s) 115.96
L (s) 110.97
f1 (ppm)

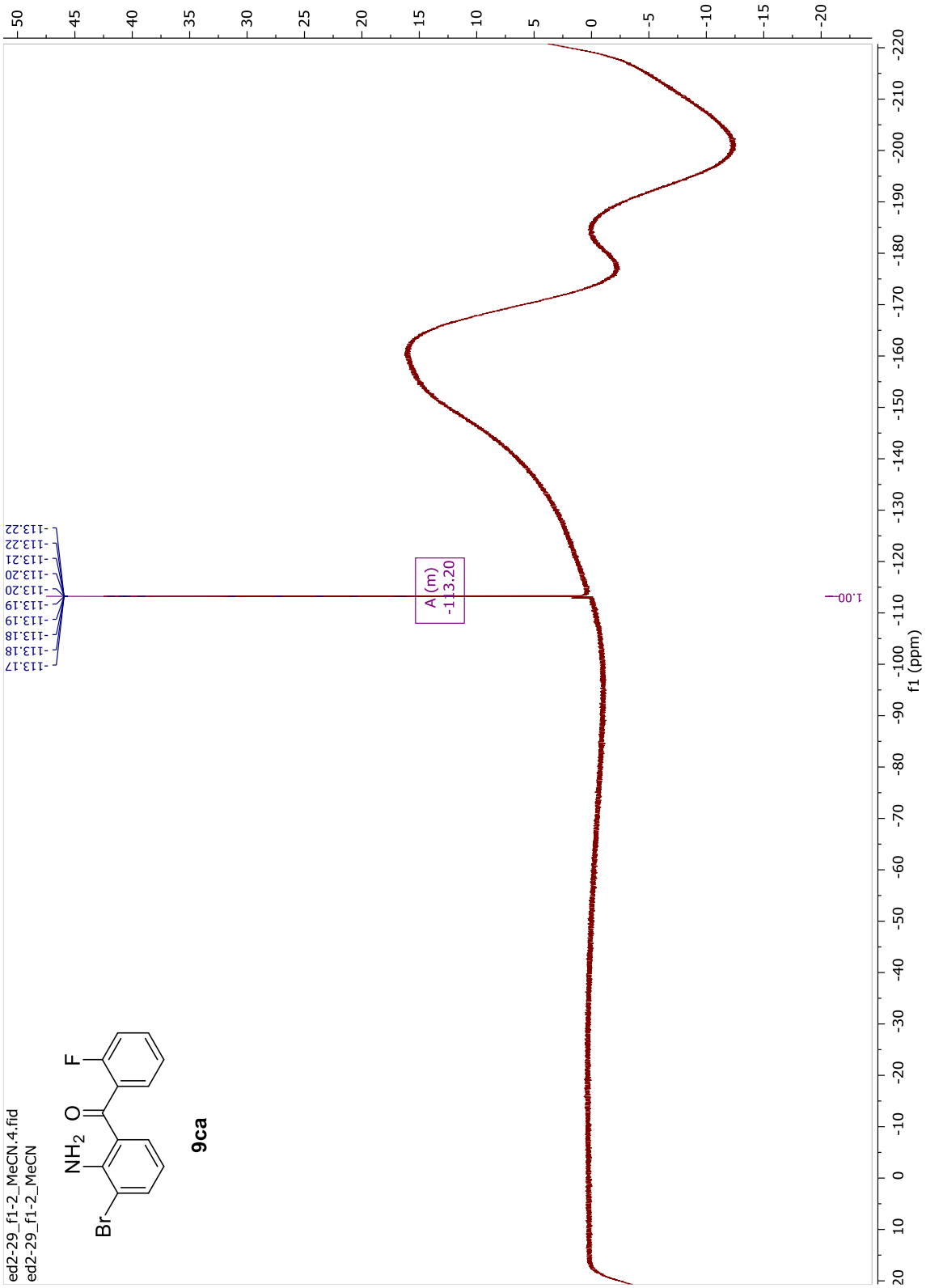
ed2-29_f1-2_MeCN.4.fid
ed2-29_f1-2_MeCN
9ca
A (m)
-113.20
f1 (ppm)

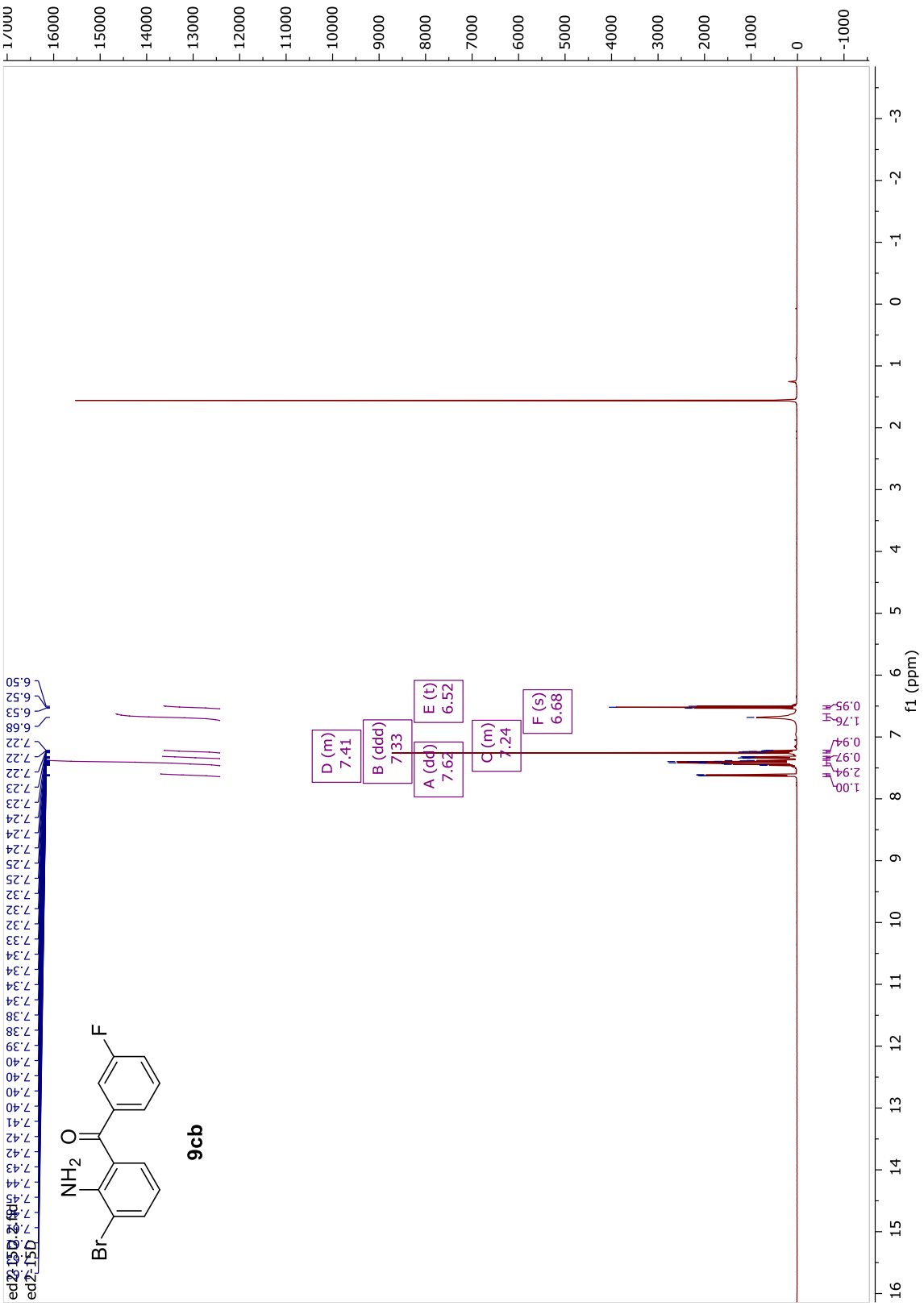
9cb
D (m) 7.41
B (ddd) 7.33
A (dd) 7.62
E (t) 6.52
C (m) 7.24
F (s) 6.68
f1 (ppm)

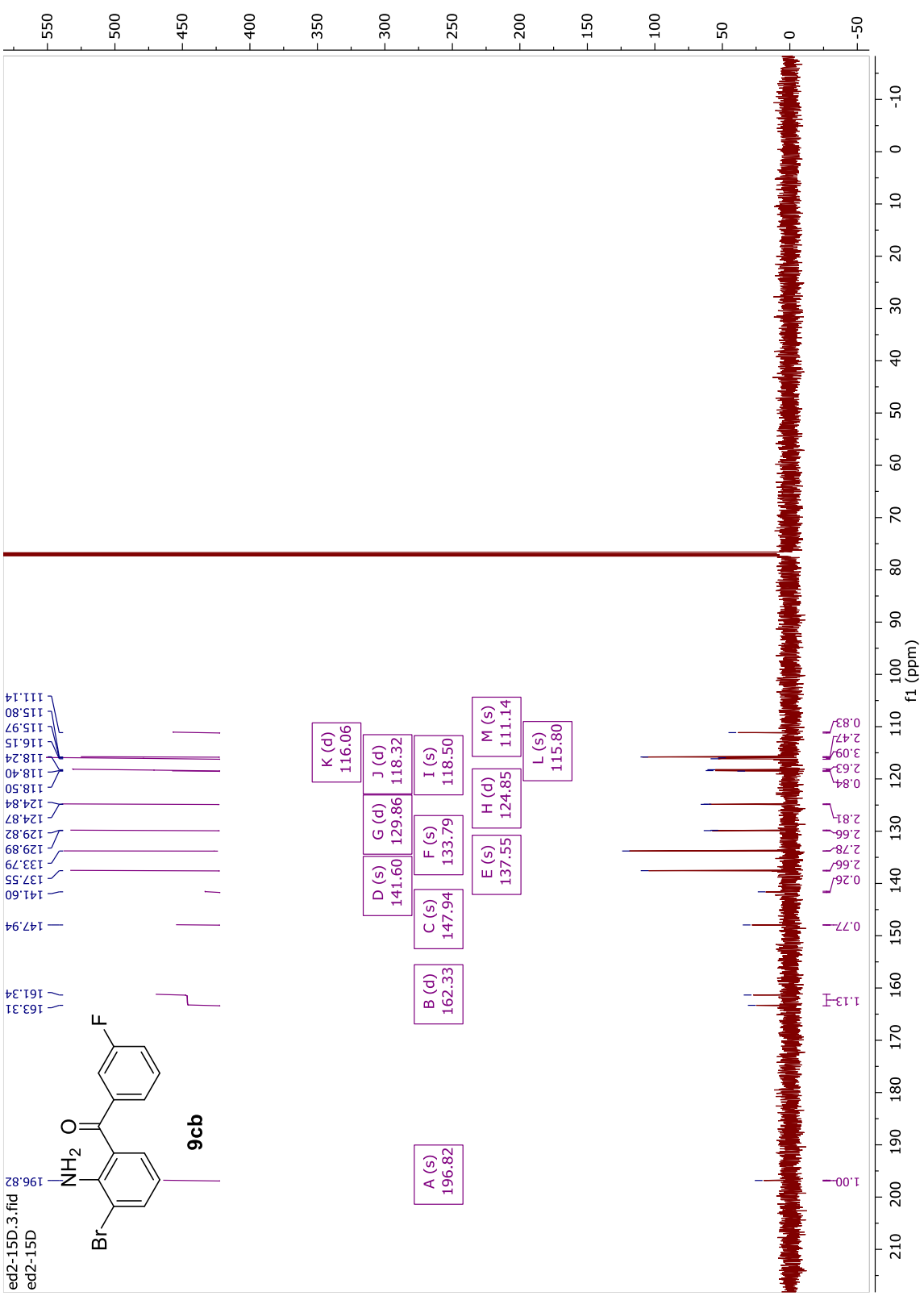
ed2-15D.3.fid
ed2-15D
9cb
f1 (ppm)
A (s) 196.82
B (d) 162.33
C (s) 147.94
D (s) 141.60
E (s) 137.55
F (s) 133.79
G (d) 129.86
H (d) 124.85
I (s) 118.50
J (d) 118.32
K (d) 116.06
L (s) 115.80
M (s) 111.14
196.82
163.31
161.34
147.94
141.60
137.55
133.79
129.89
129.82
124.87
124.84
118.50
118.40
118.24
116.15
115.97
115.80
111.14
1.00
1.13
0.77
0.26
2.66
2.78
2.66
2.81
0.84
2.63
3.09
2.47
0.83

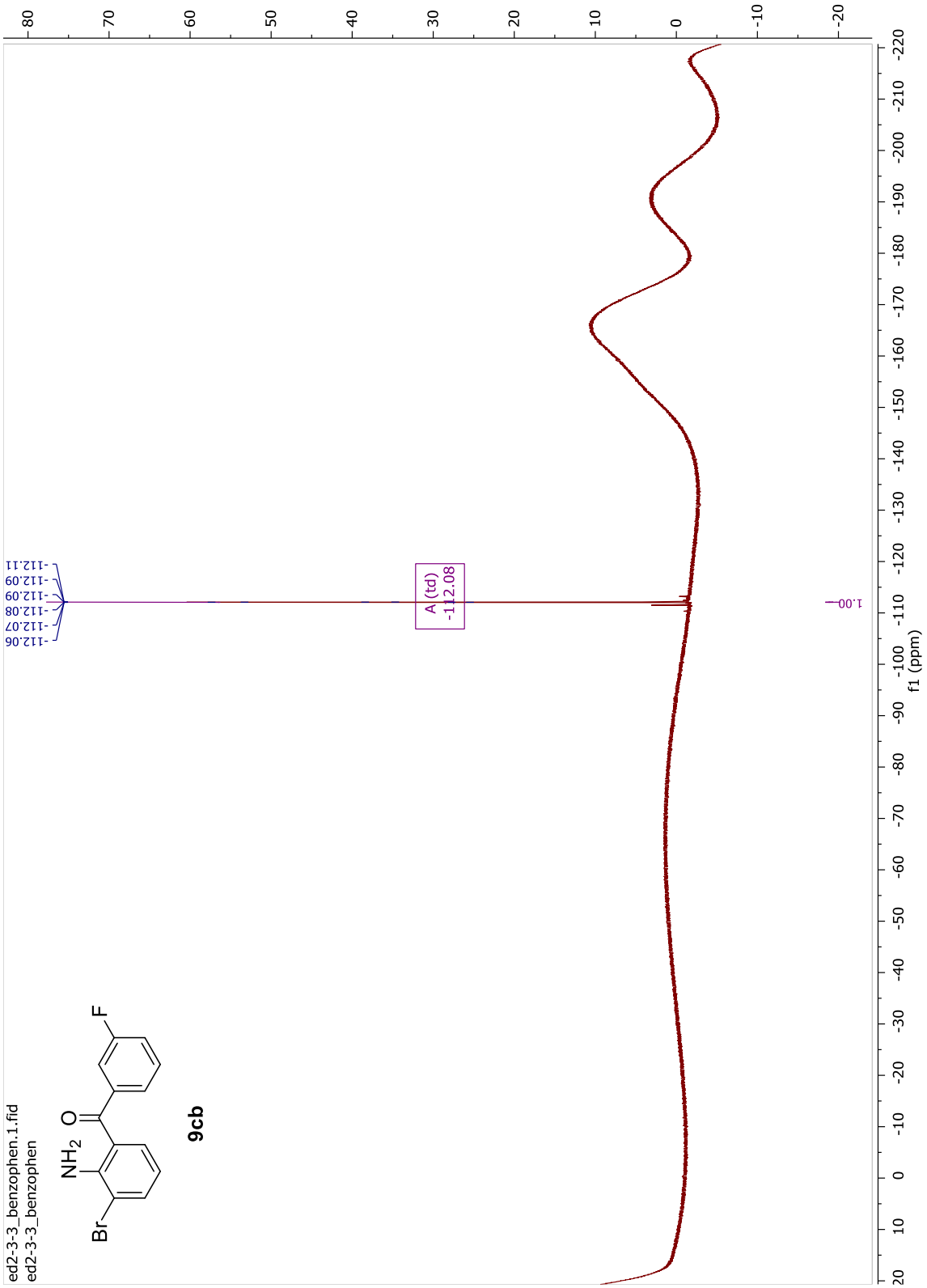
ed2-3-3_benzophen.1.fid
ed2-3-3_benzophen
9cb
A (td)
-112.08
-112.06
-112.07
-112.08
-112.09
-112.09
-112.11
1.00
f1 (ppm)

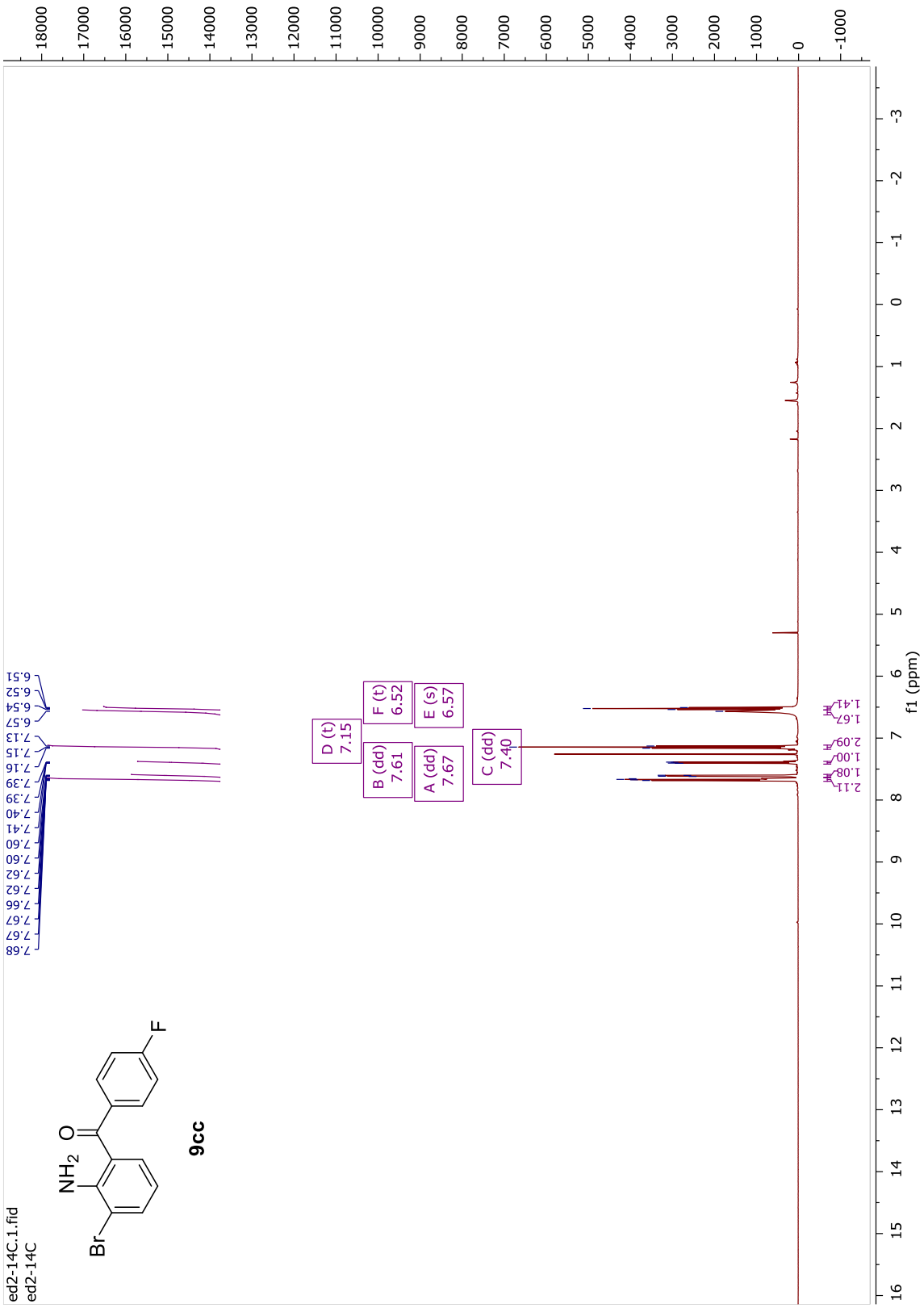
ed2-14C.1.fid
ed2-14C
9cc
NH2
O
Br
F
D (t)
7.15
B (dd)
7.61
A (dd)
7.67
F (t)
6.52
E (s)
6.57
C (dd)
7.40
f1 (ppm)

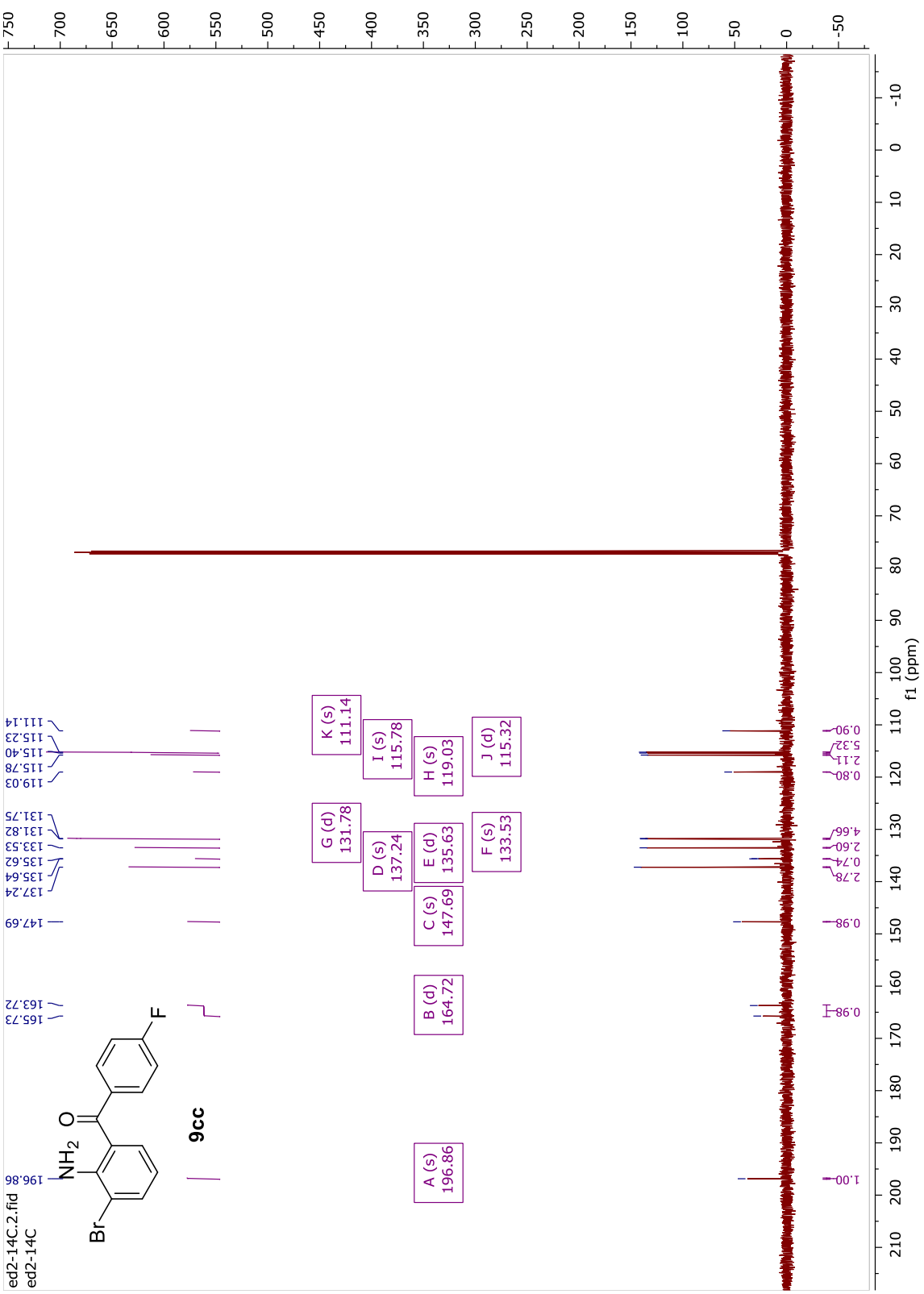
ed2-14C.2.fid
ed2-14C
9cc
A (s) 196.86
B (d) 164.72
C (s) 147.69
D (s) 137.24
E (d) 135.63
F (s) 133.53
G (d) 131.78
H (s) 119.03
I (s) 115.78
J (d) 115.32
K (s) 111.14
f1 (ppm)

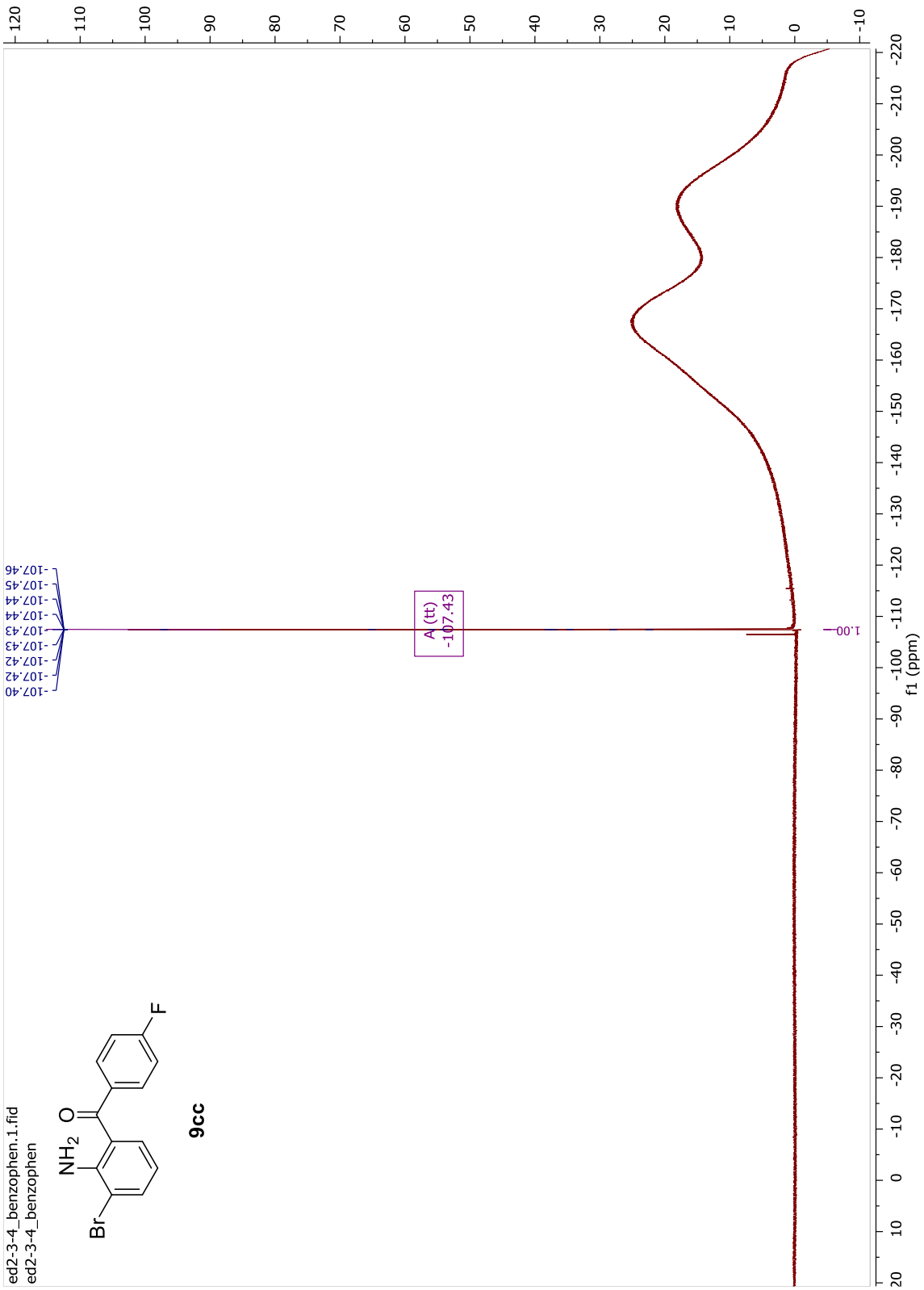
ed2-3-4_benzophen.1.fid
ed2-3-4_benzophen
9cc
A (tt)
-107.43
1.00
f1 (ppm)

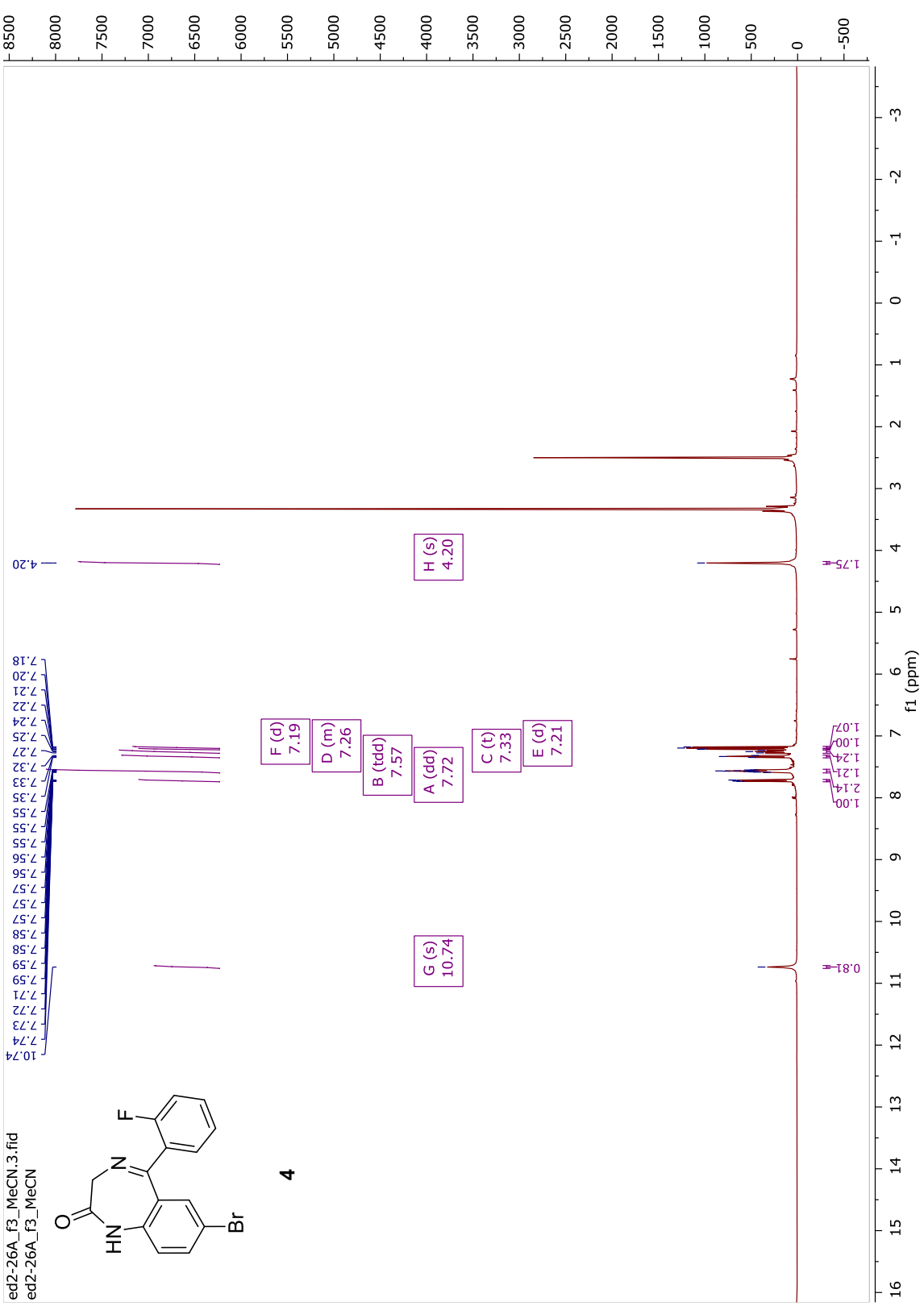
ed2-26A_f3_MeCN.3.fid
ed2-26A_f3_MeCN
4
F (d) 7.19
D (m) 7.26
B (tdd) 7.57
A (dd) 7.72
C (t) 7.33
E (d) 7.21
H (s) 4.20
G (s) 10.74
f1 (ppm)

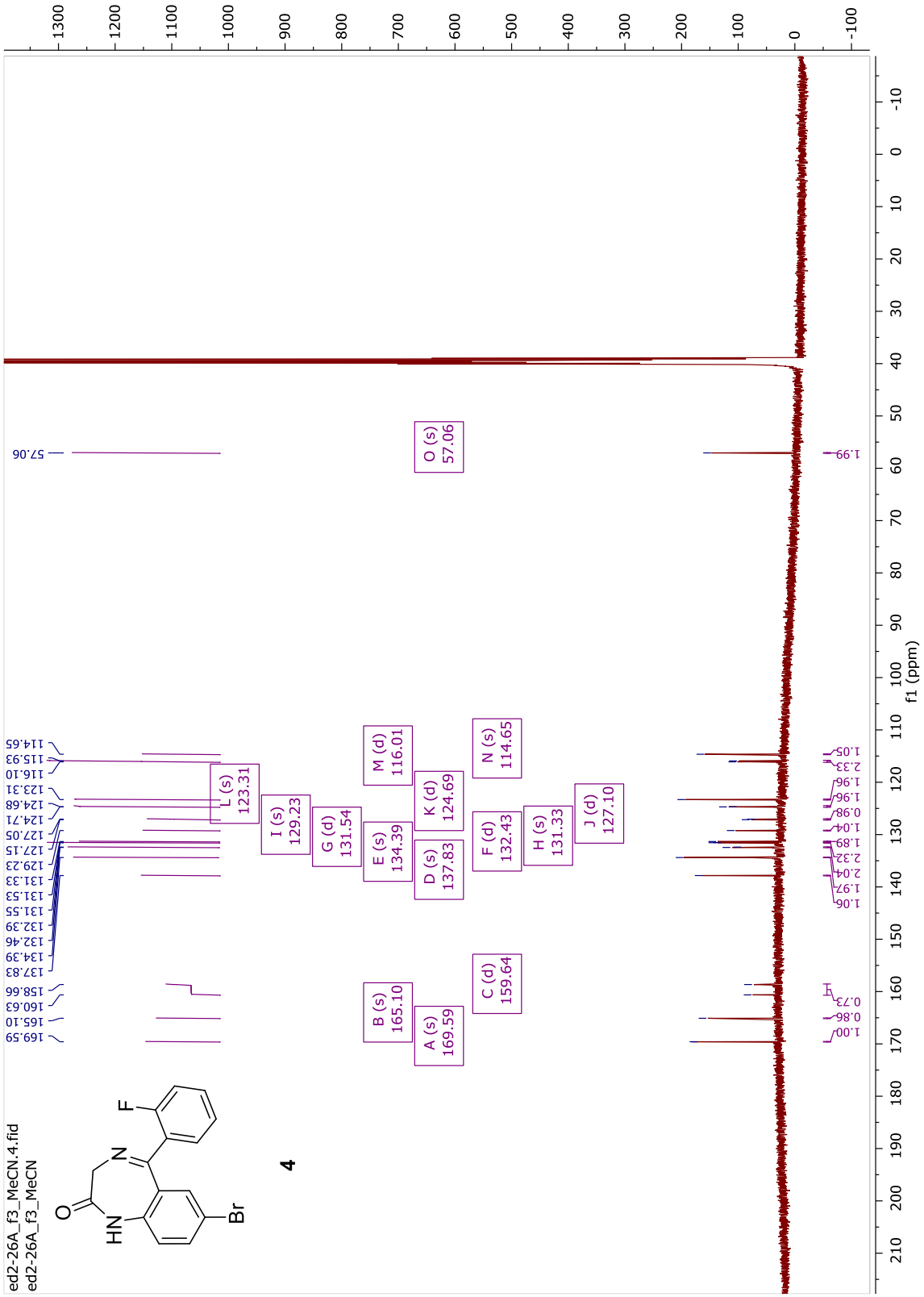
ed2-26A_f3_MeCN.4.fid
ed2-26A_f3_MeCN
4
A (s) 169.59
B (s) 165.10
C (d) 159.64
D (s) 137.83
E (s) 134.39
F (d) 132.43
G (d) 131.54
H (s) 131.33
I (s) 129.23
J (d) 127.10
K (d) 124.69
L (s) 123.31
M (d) 116.01
N (s) 114.65
O (s) 57.06
f1 (ppm)

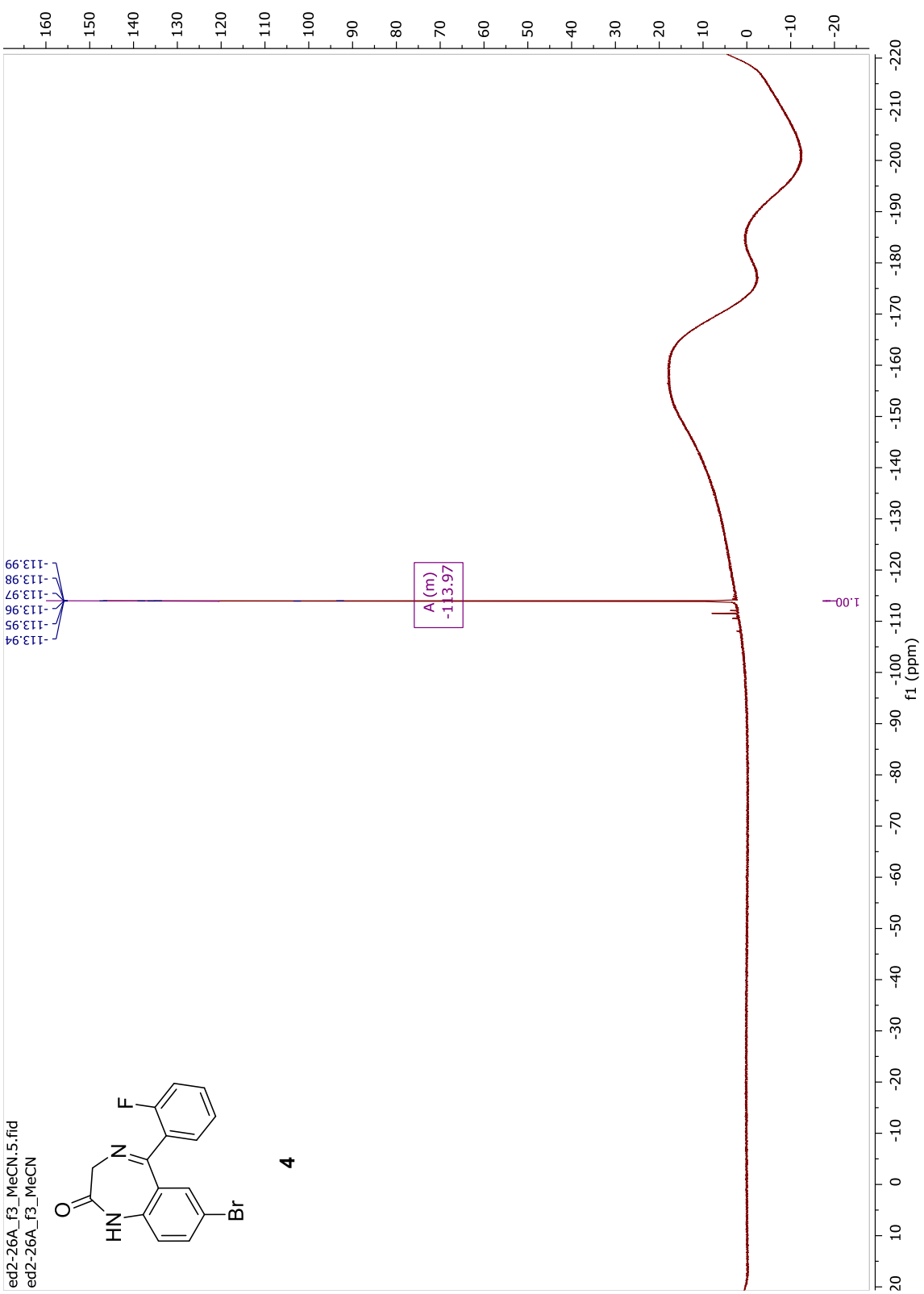
ed2-26A_f3_MeCN.5.fid
ed2-26A_f3_MeCN
4
A (m)
-113.97
-113.94
-113.95
-113.96
-113.97
-113.98
-113.99
1.00
f1 (ppm)

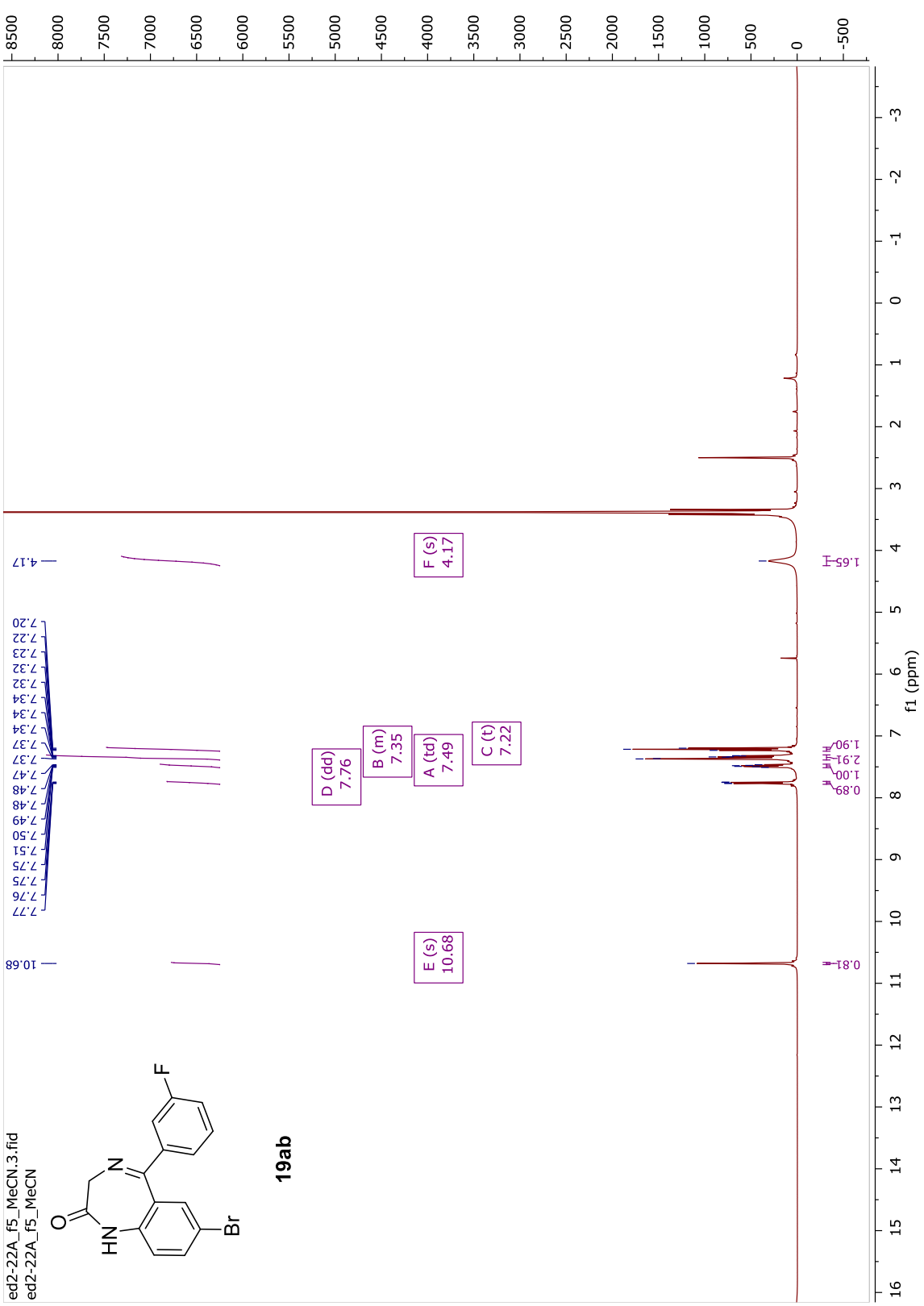
ed2-22A_f5_MeCN.3.fid
ed2-22A_f5_MeCN
19ab
F (s) 4.17
D (dd) 7.76
B (m) 7.35
A (td) 7.49
C (t) 7.22
E (s) 10.68
f1 (ppm)

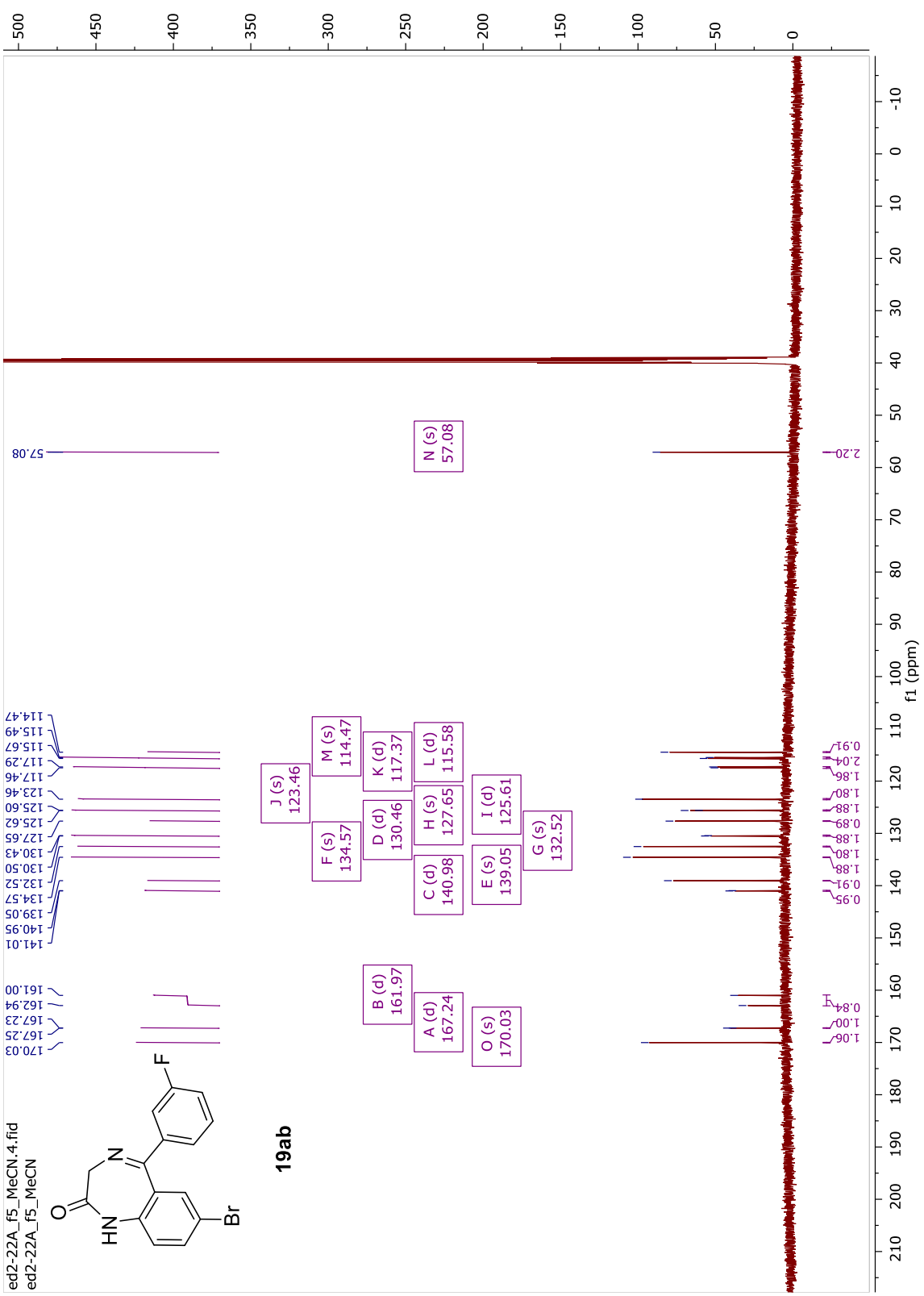
ed2-22A_f5_MeCN.4.fid
ed2-22A_f5_MeCN
19ab
f1 (ppm)
N (s) 57.08
A (d) 167.24
B (d) 161.97
C (d) 140.98
D (d) 130.46
E (s) 139.05
F (s) 134.57
G (s) 132.52
H (s) 127.65
I (d) 125.61
J (s) 123.46
K (d) 117.37
L (d) 115.58
M (s) 114.47
O (s) 170.03
57.08
2.20
0.84
1.06
1.00
0.95
0.91
1.88
1.80
0.89
1.88
1.80
1.88
1.80
2.04
0.91

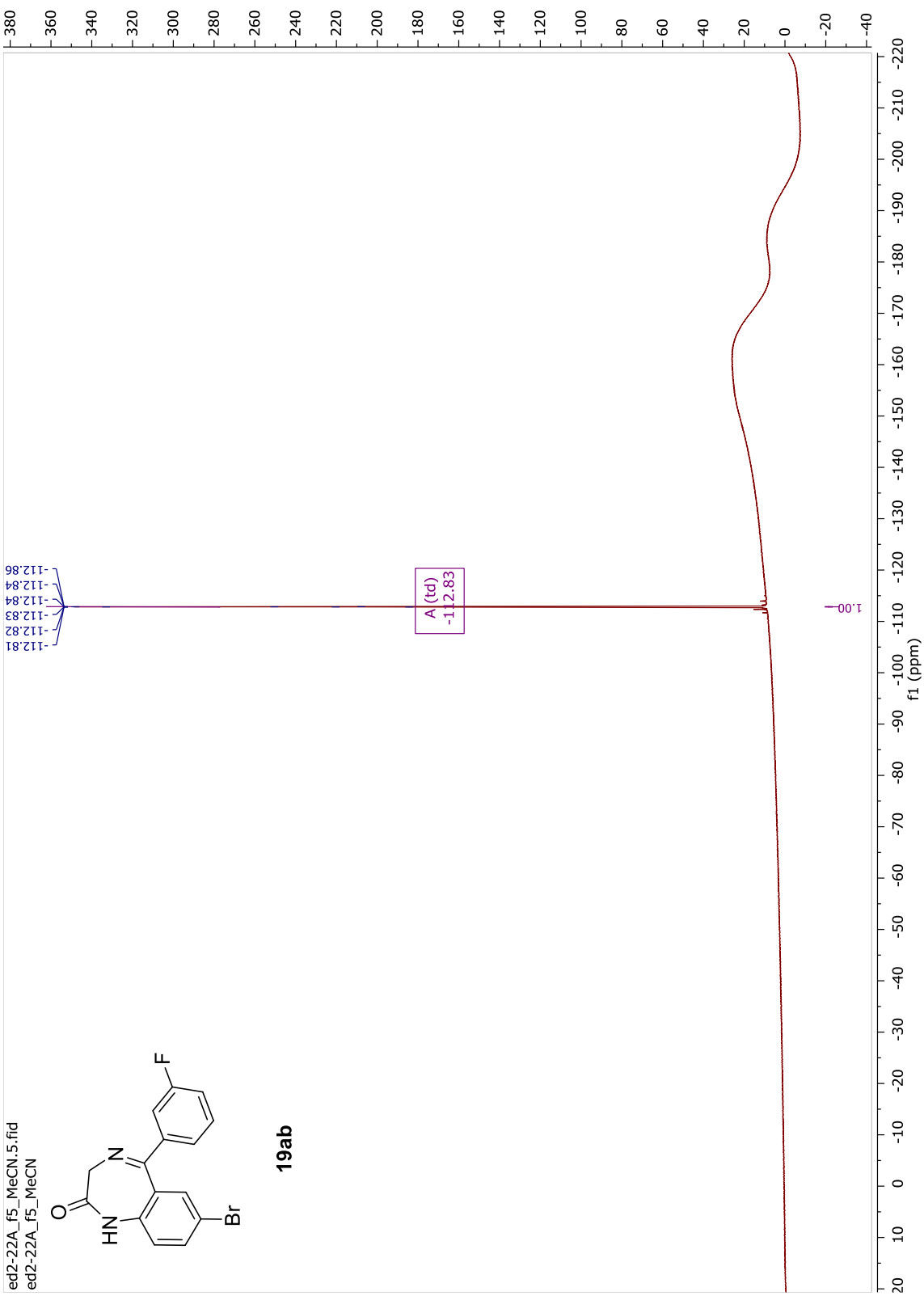
ed2-22A_f5_MeCN.5.fid
ed2-22A_f5_MeCN
19ab
A (td)
-112.83
1.00
f1 (ppm)

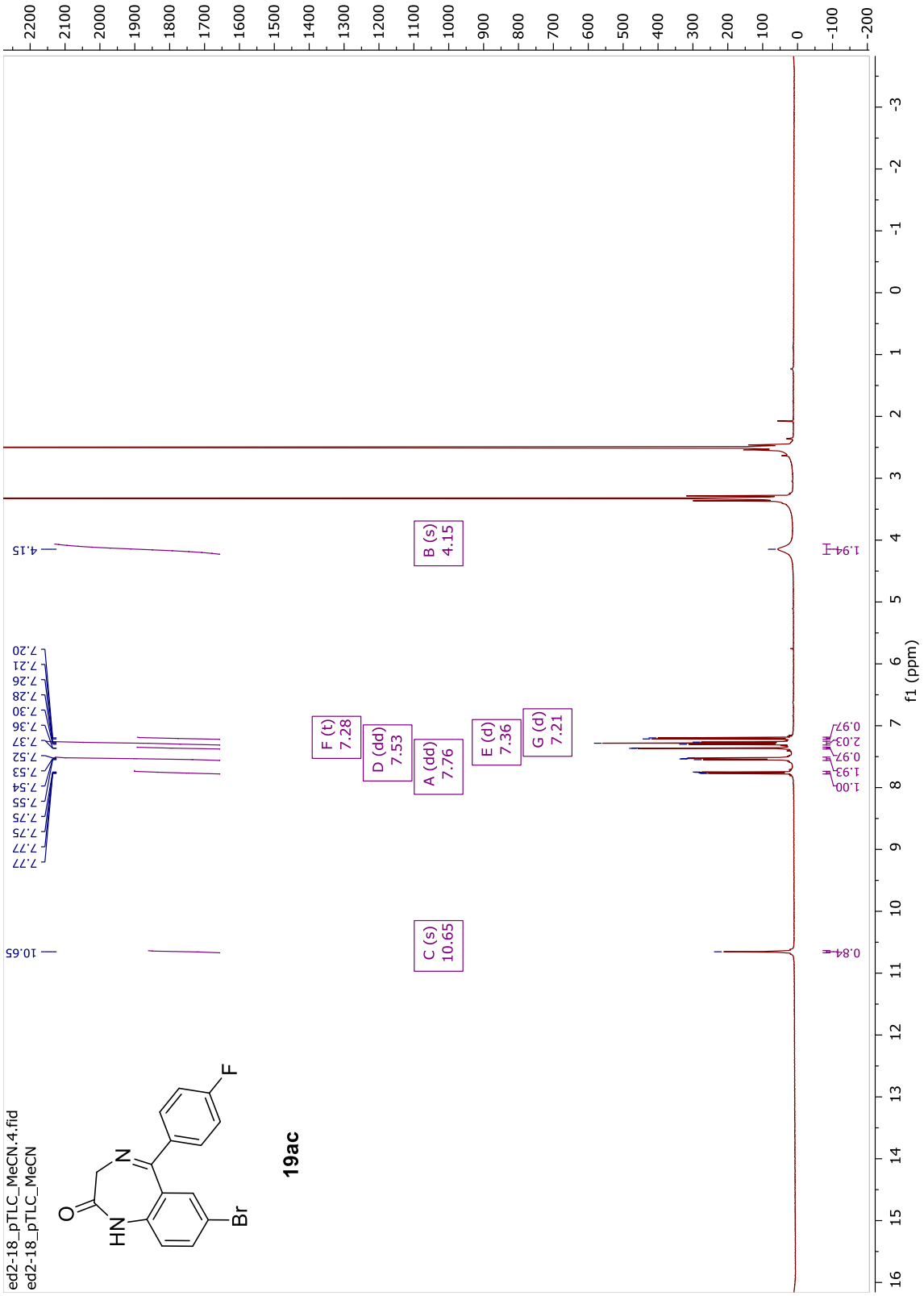
ed2-18_pTLC_MeCN.4.fid
ed2-18_pTLC_MeCN
19ac
F
Br
O
HN
N
C (s)
10.65
A (dd)
7.76
D (dd)
7.53
F (t)
7.28
E (d)
7.36
G (d)
7.21
B (s)
4.15
f1 (ppm)

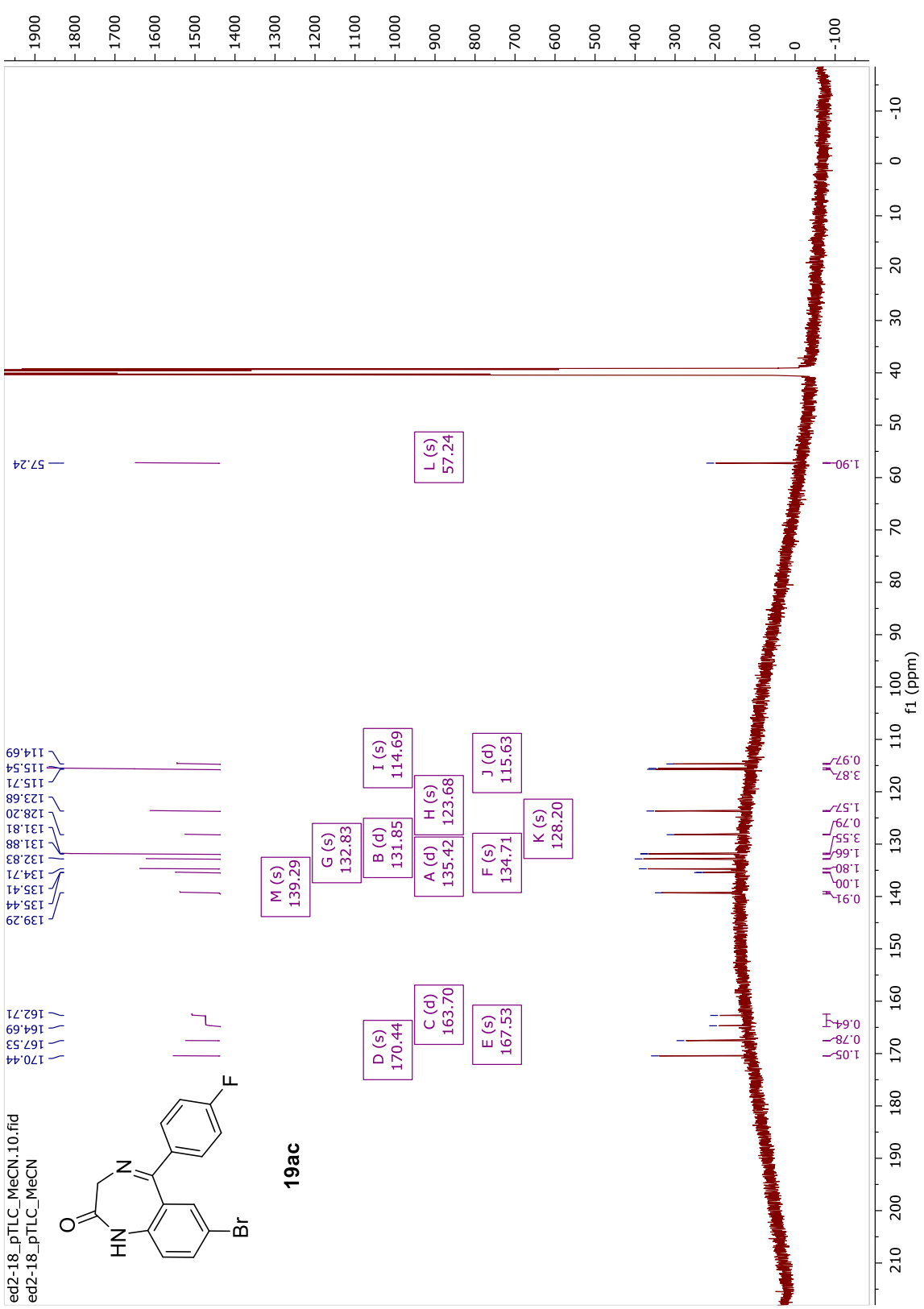
ed2-18_pTLC_MeCN.10.fid
ed2-18_pTLC_MeCN
19ac
F
Br
HN
O
N
170.44
167.53
164.69
162.71
139.29
135.44
135.41
134.71
132.83
131.88
131.81
128.20
123.68
115.71
115.54
114.69
57.24
D (s) 170.44
C (d) 163.70
E (s) 167.53
M (s) 139.29
G (s) 132.83
B (d) 131.85
A (d) 135.42
I (s) 114.69
H (s) 123.68
F (s) 134.71
J (d) 115.63
K (s) 128.20
L (s) 57.24
1.90
0.97
3.87
1.57
0.79
3.55
1.66
1.80
1.00
0.91
0.64
0.78
1.05
f1 (ppm)

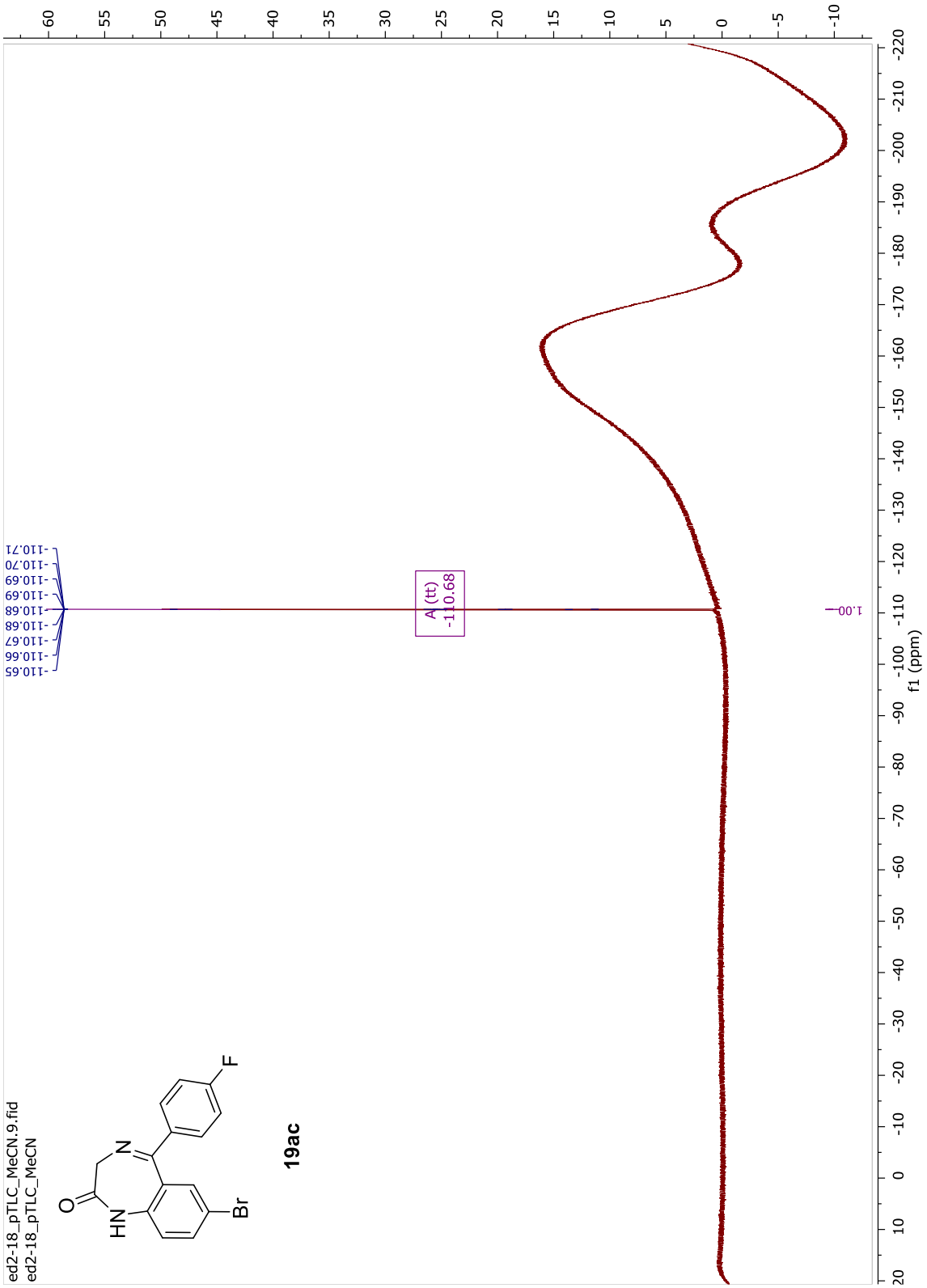
ed2-18_pTLC_MeCN.9.fid
ed2-18_pTLC_MeCN
19ac
A (tt)
-110.68
1.00
f1 (ppm)

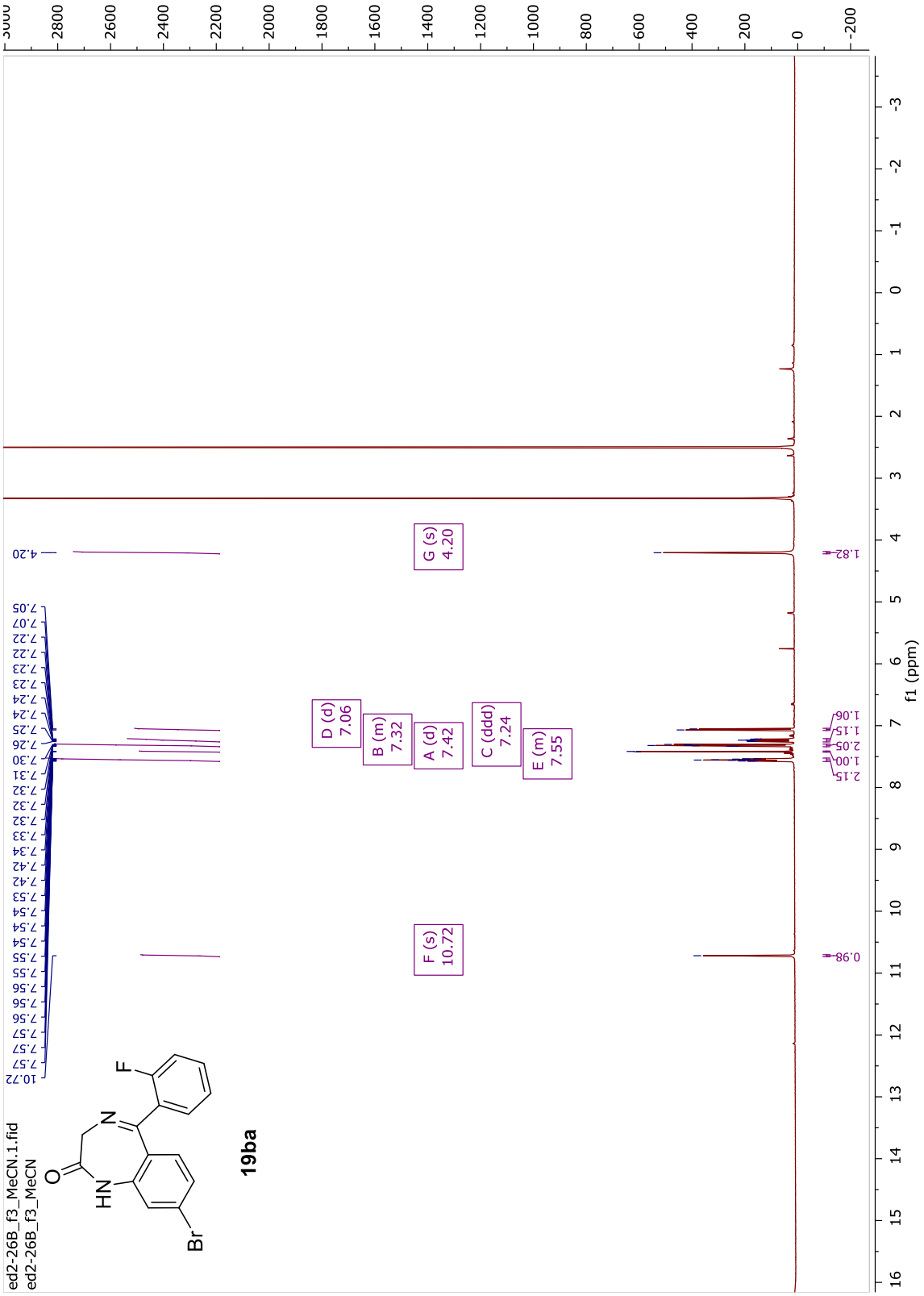
ed2-26B_f3_MeCN.1.fid
ed2-26B_f3_MeCN
19ba
F (s) 10.72
D (d) 7.06
B (m) 7.32
A (d) 7.42
C (ddd) 7.24
E (m) 7.55
G (s) 4.20
f1 (ppm)

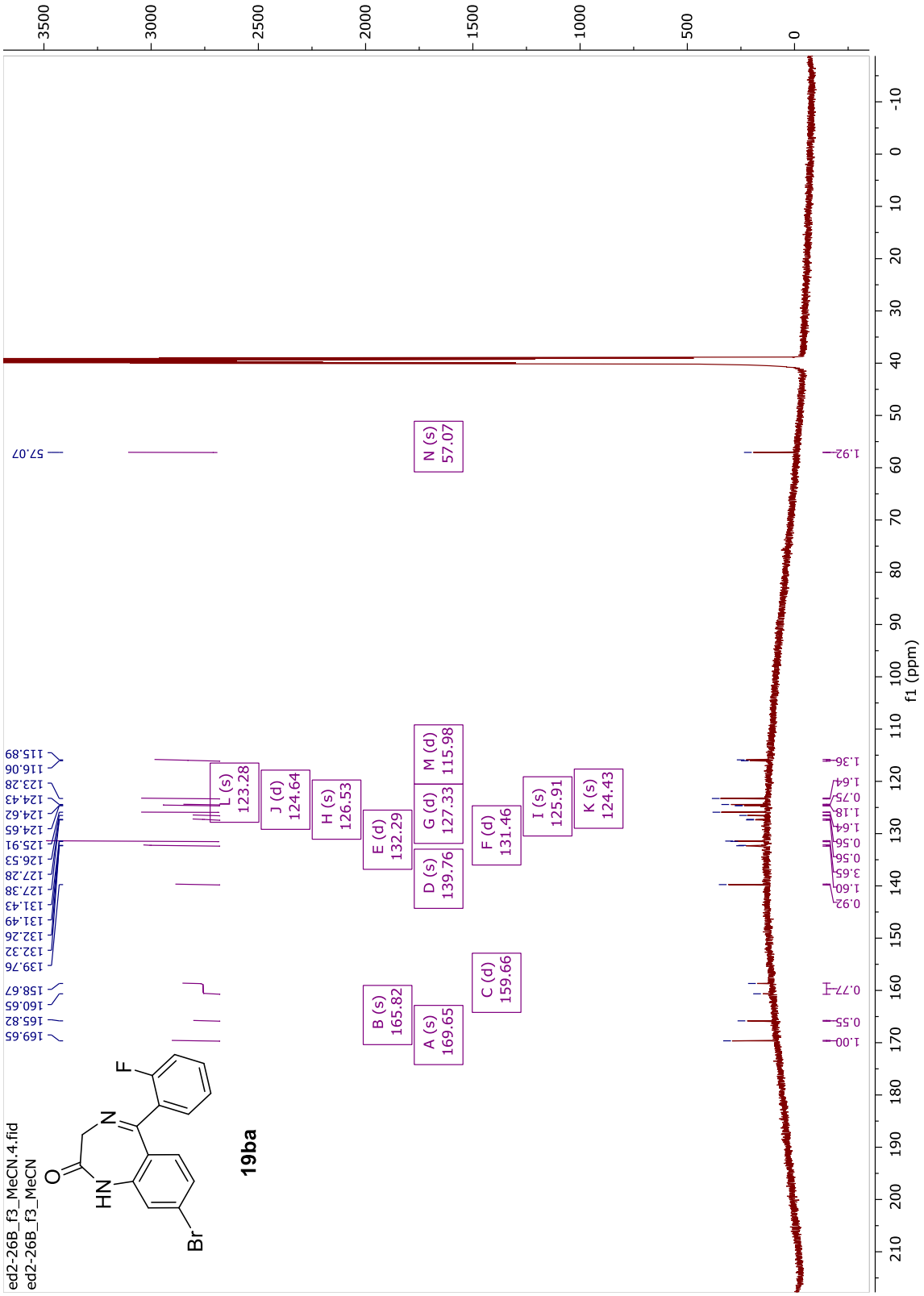
ed2-26B_f3_MeCN.4.fid
ed2-26B_f3_MeCN
19ba
A (s) 169.65
B (s) 165.82
C (d) 159.66
D (s) 139.76
E (d) 132.29
F (d) 131.46
G (d) 127.33
H (s) 126.53
I (s) 125.91
J (d) 124.64
K (s) 124.43
L (s) 123.28
M (d) 115.98
N (s) 57.07
f1 (ppm)

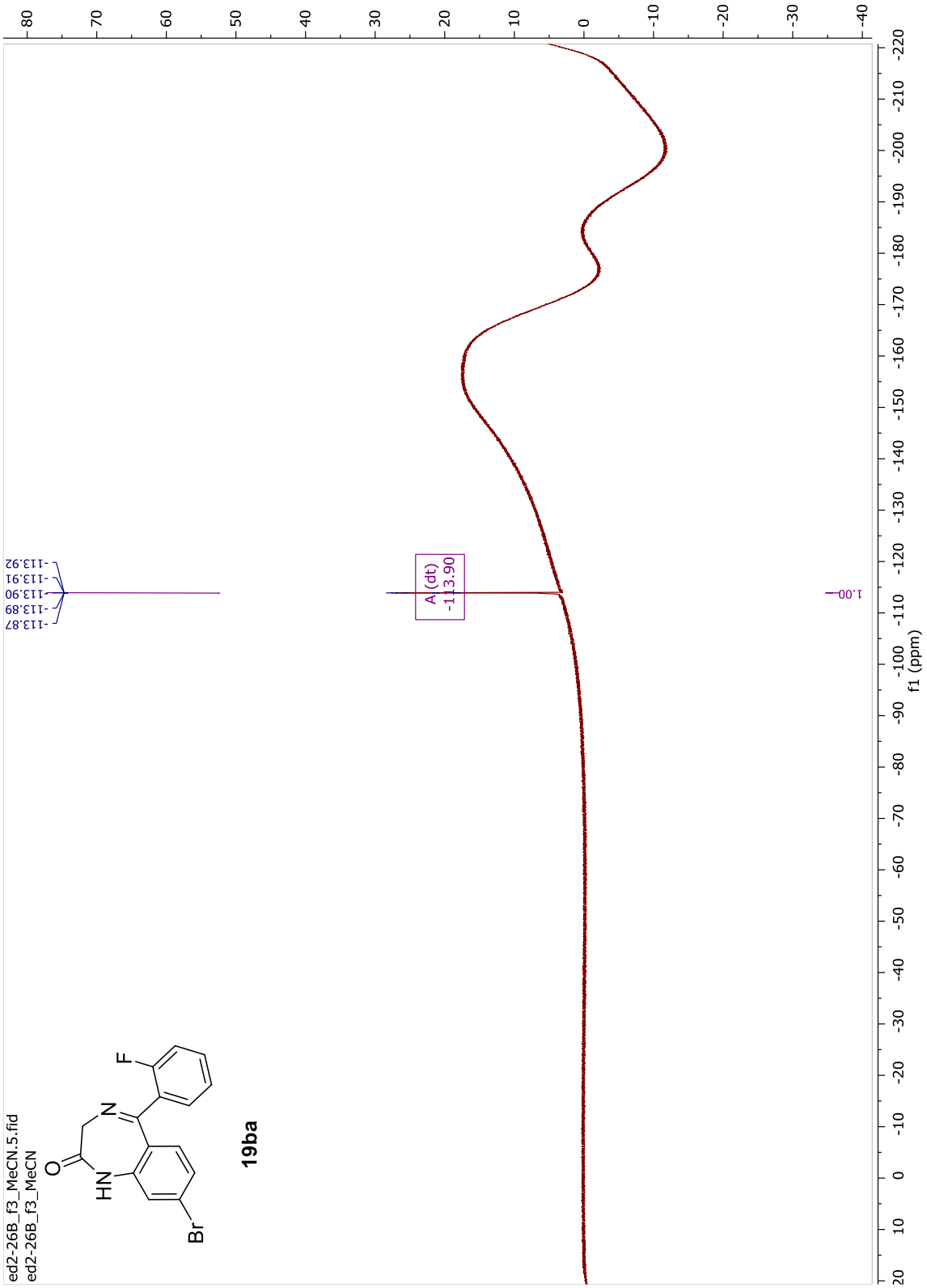
ed2-26B_f3_MeCN.5.fid
ed2-26B_f3_MeCN
19ba
A (dt)
-113.90
-113.87
-113.89
-113.90
-113.91
-113.92
1.00
f1 (ppm)

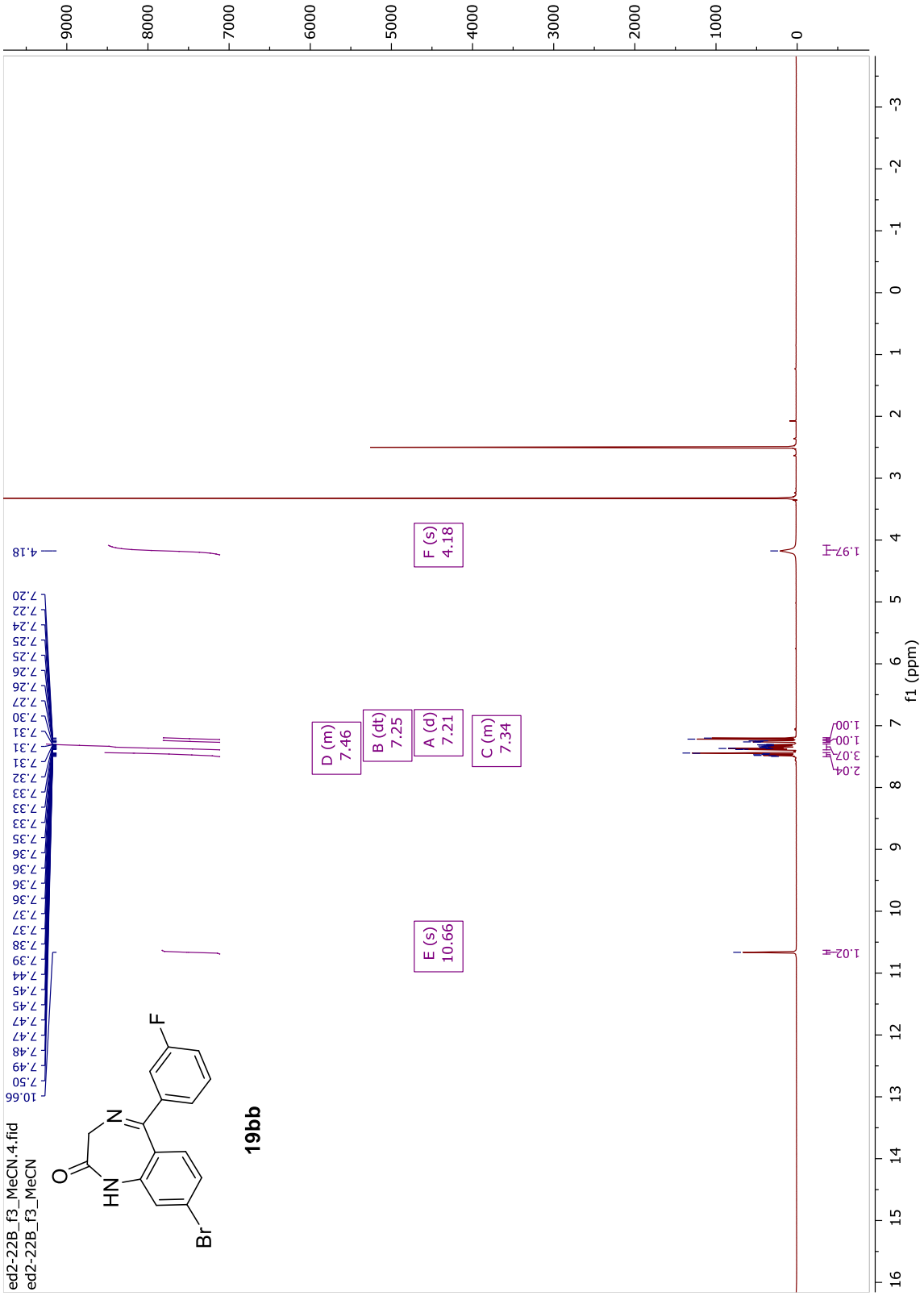
ed2-22B_f3_MeCN.4.fid
ed2-22B_f3_MeCN
19bb
F (s) 4.18
D (m) 7.46
B (dt) 7.25
A (d) 7.21
C (m) 7.34
E (s) 10.66
f1 (ppm)

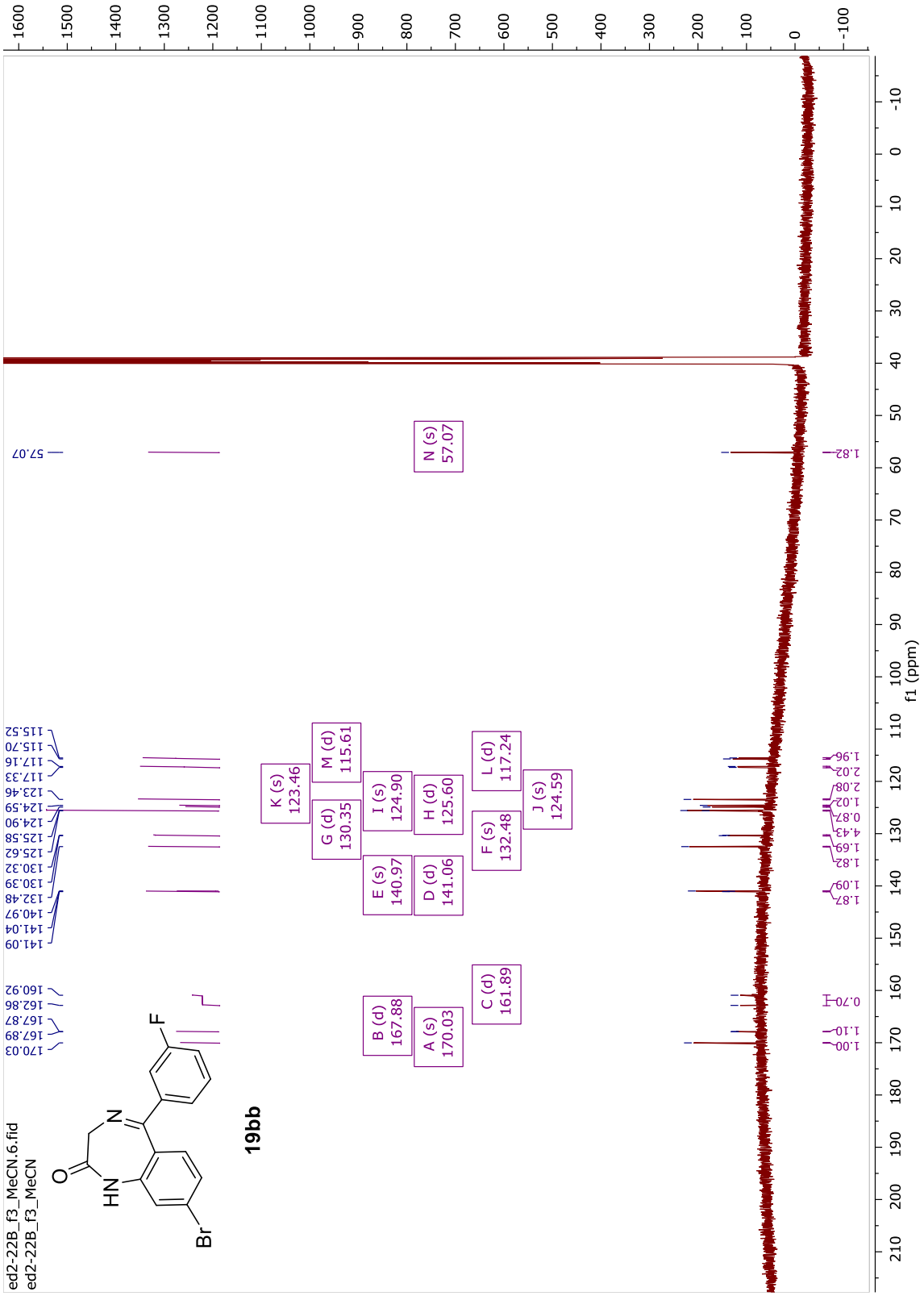
ed2-22B_f3_MeCN.6.fid
ed2-22B_f3_MeCN
19bb
f1 (ppm)
A (s) 170.03
B (d) 167.88
C (d) 161.89
D (d) 141.06
E (s) 140.97
F (s) 132.48
G (d) 130.35
H (d) 125.60
I (s) 124.90
J (s) 124.59
K (s) 123.46
L (d) 117.24
M (d) 115.61
N (s) 57.07
170.03
167.89
167.87
162.86
160.92
141.09
141.04
140.97
132.48
130.39
130.32
125.62
125.58
124.90
124.59
123.46
117.33
117.16
115.70
115.52
57.07
1.82
1.96
2.02
2.08
1.02
0.87
4.43
1.69
1.82
1.09
1.87
0.70
1.10
1.00
F
Br
HN
N
O

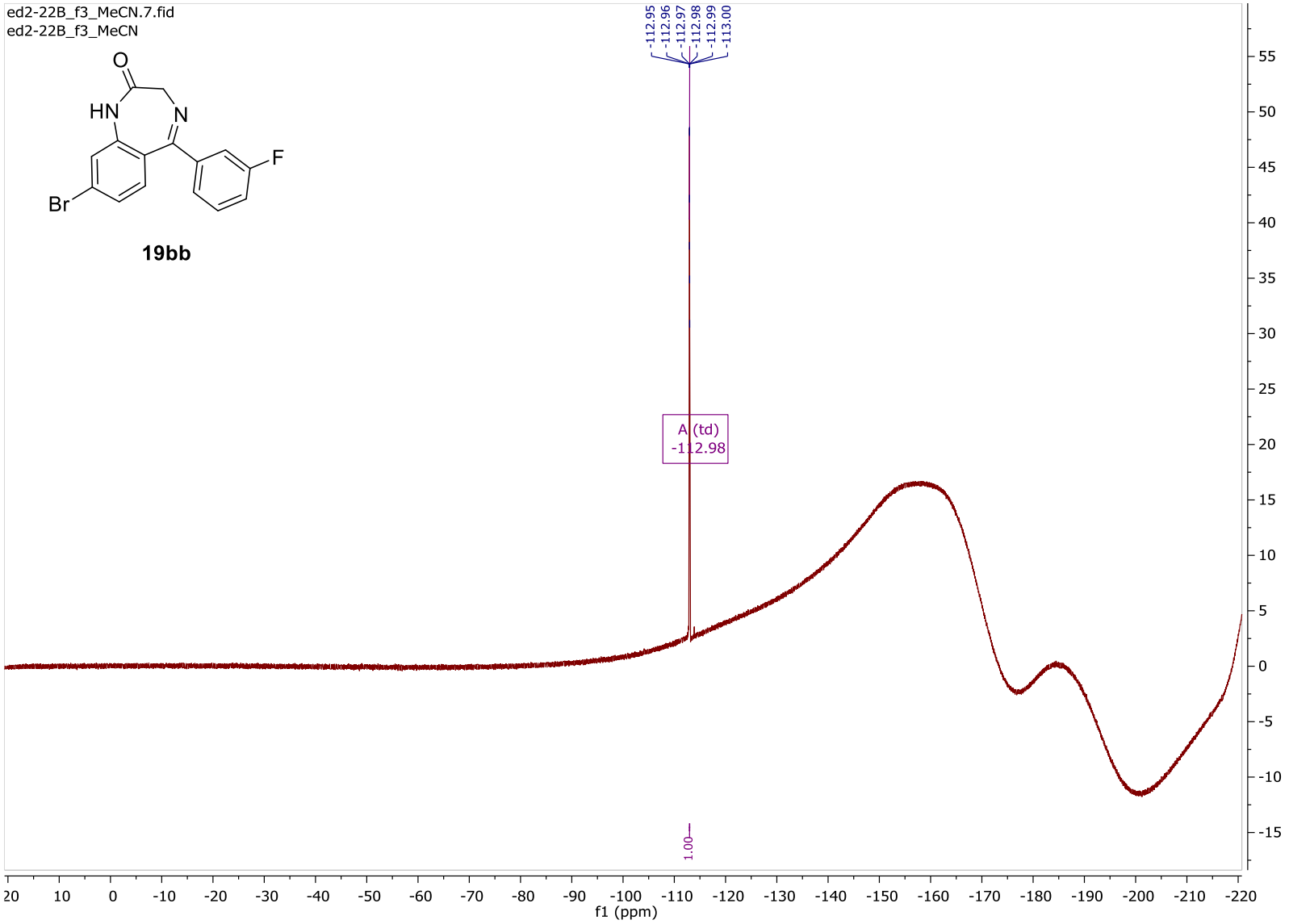
ed2-22B_f3_MeCN.7.fid
ed2-22B_f3_MeCN
O
HN
N
F
Br
19bb
-112.95
-112.96
-112.97
-112.98
-112.99
-113.00
A (td)
-112.98
1.00
f1 (ppm)

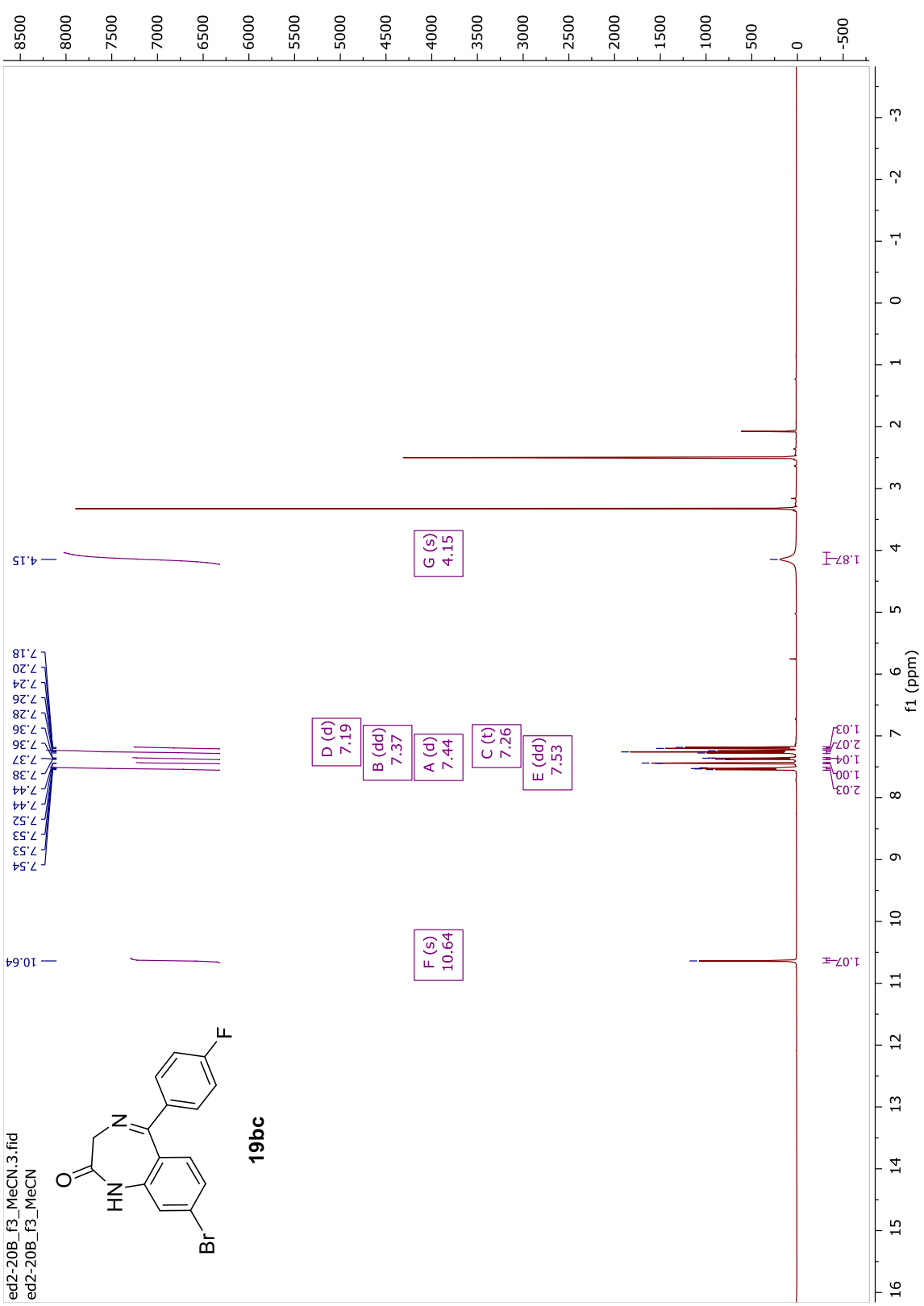
ed2-20B_f3_MeCN.3.fid
ed2-20B_f3_MeCN
19bc
F (s) 10.64
D (d) 7.19
B (dd) 7.37
A (d) 7.44
C (t) 7.26
E (dd) 7.53
G (s) 4.15
f1 (ppm)

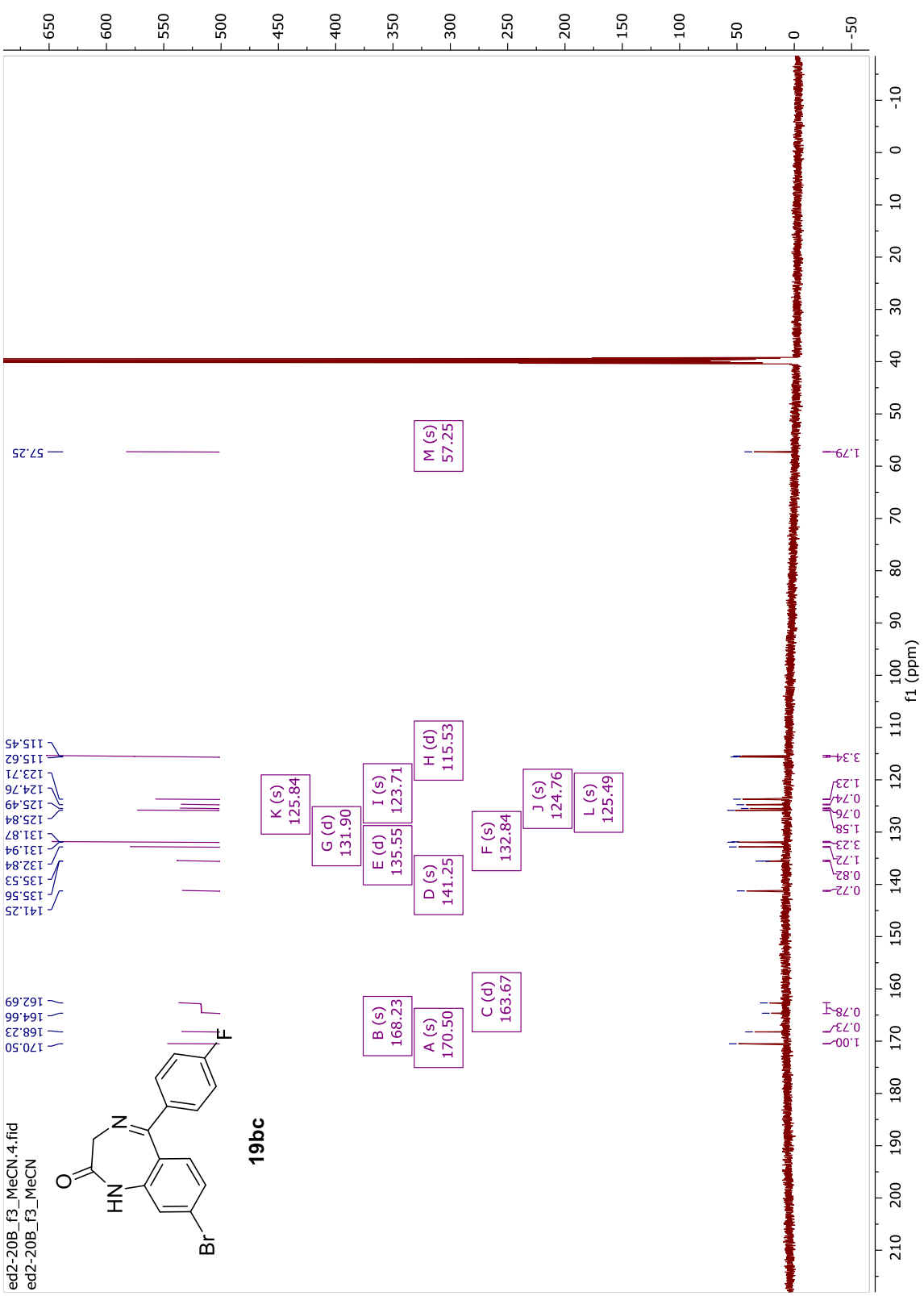
ed2-20B_f3_MeCN.4.fid
ed2-20B_f3_MeCN
19bc
f1 (ppm)
A (s) 170.50
B (s) 168.23
C (d) 163.67
D (s) 141.25
E (d) 135.55
F (s) 132.84
G (d) 131.90
H (d) 115.53
I (s) 123.71
J (s) 124.76
K (s) 125.84
L (s) 125.49
M (s) 57.25

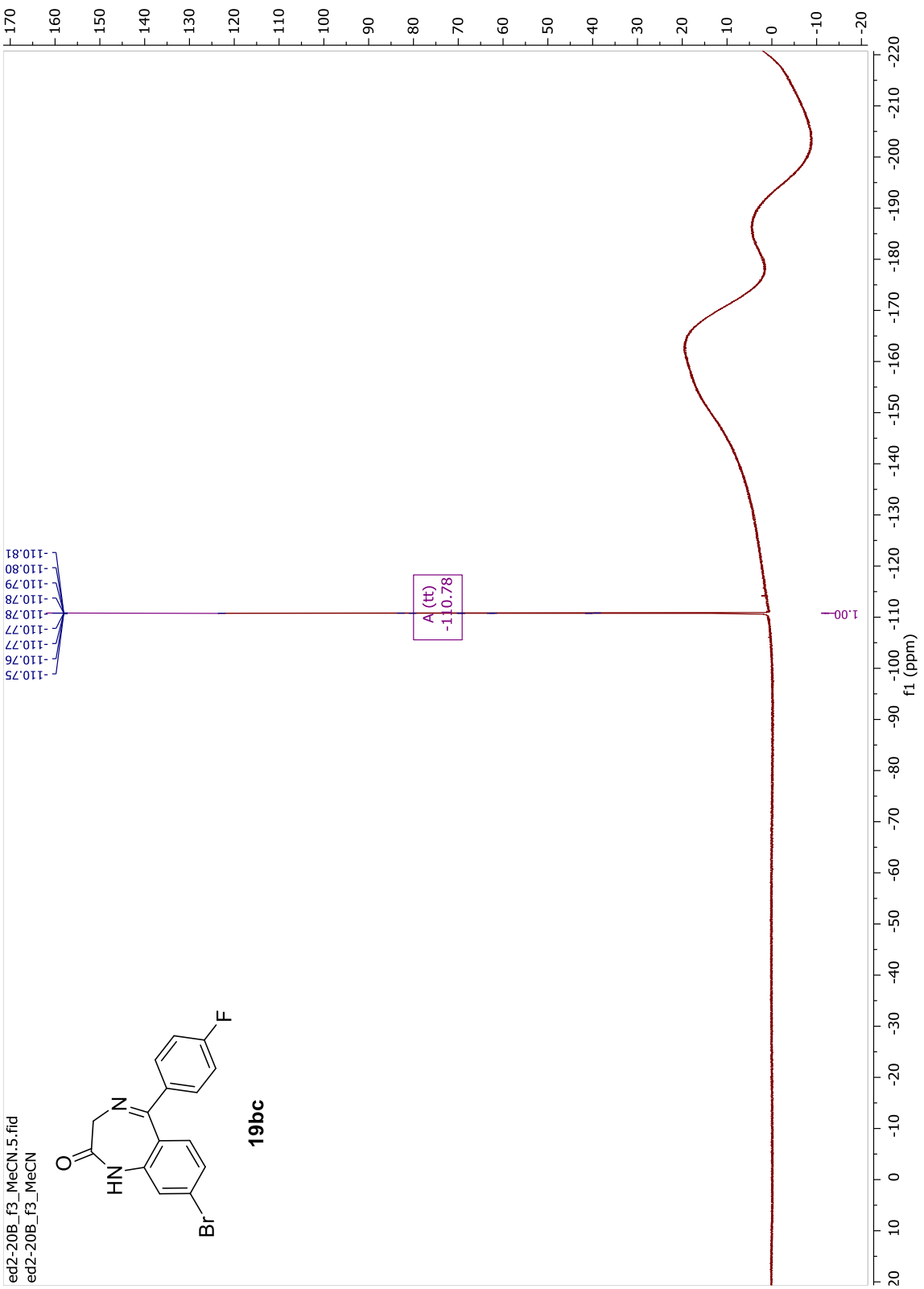
ed2-20B_f3_MeCN.5.fid
ed2-20B_f3_MeCN
19bc
A (tt)
-110.78
1.00
f1 (ppm)

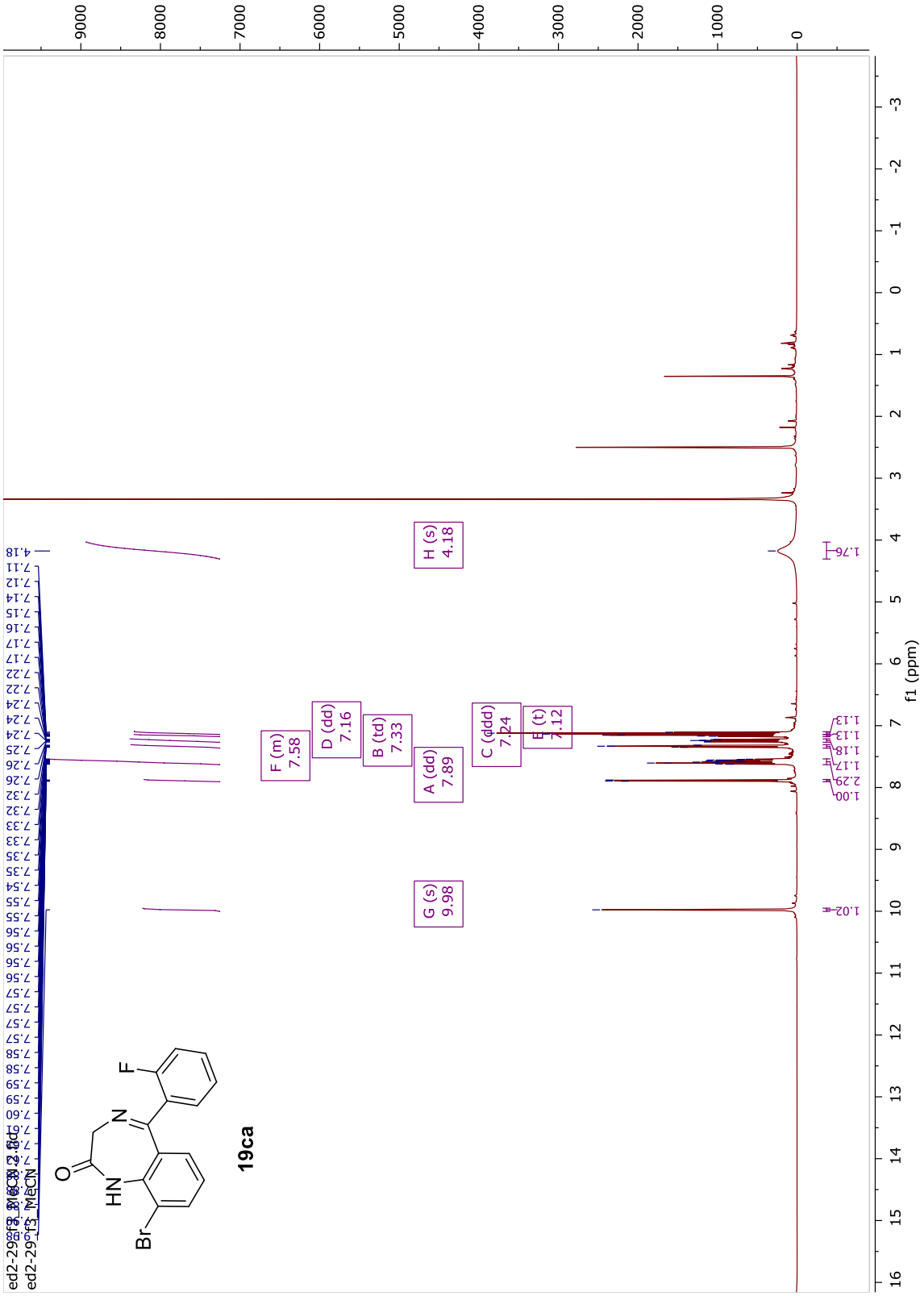
19ca
F (m) 7.58
D (dd) 7.16
B (td) 7.33
A (dd) 7.89
C (ddd) 7.24
E (t) 7.12
H (s) 4.18
G (s) 9.98
f1 (ppm)

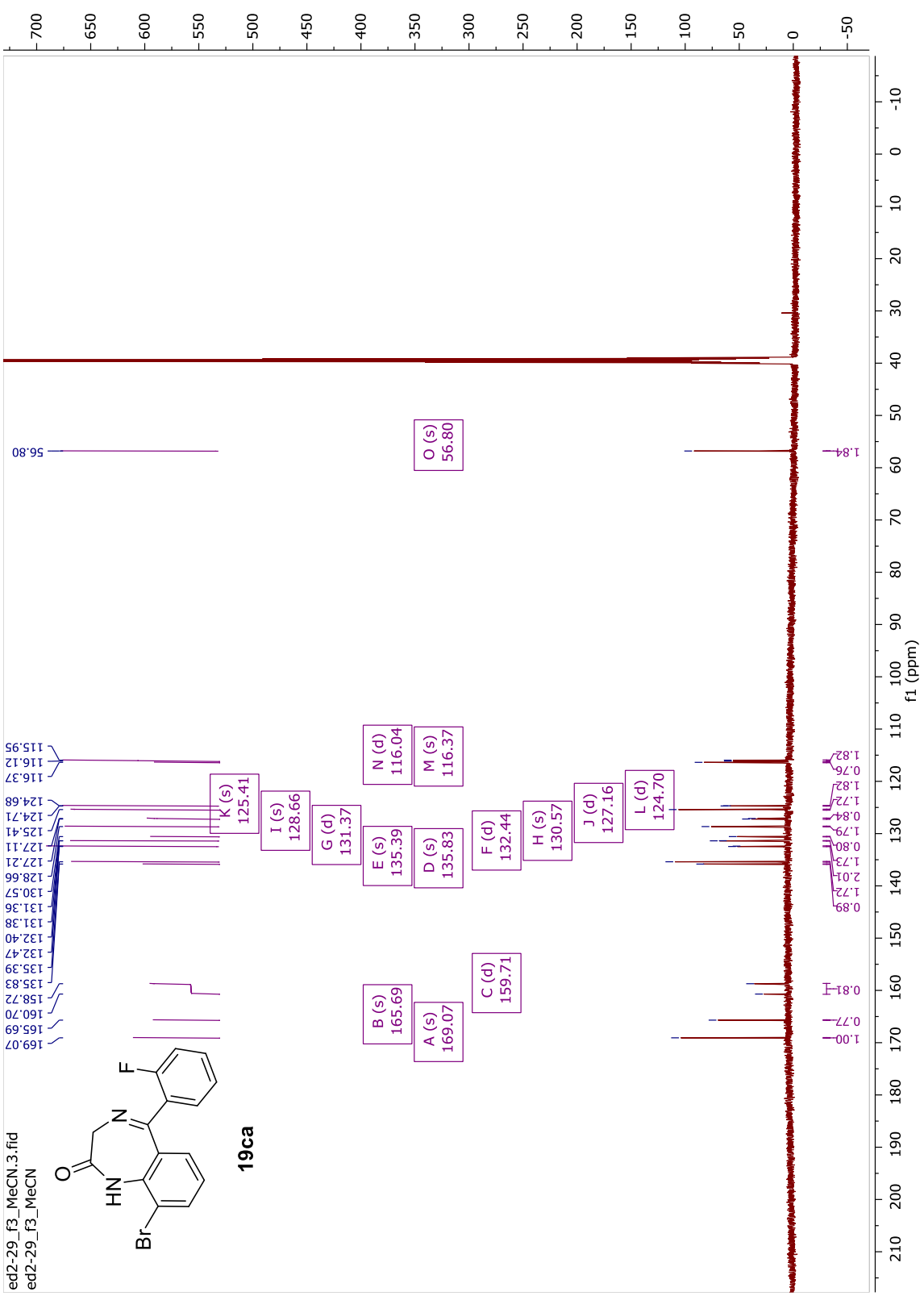
ed2-29_f3_MeCN.3.fid
ed2-29_f3_MeCN
19ca
f1 (ppm)
A (s) 169.07
B (s) 165.69
C (d) 159.71
D (s) 135.83
E (s) 135.39
F (d) 132.44
G (d) 131.37
H (s) 130.57
I (s) 128.66
J (d) 127.16
K (s) 125.41
L (d) 124.70
M (s) 116.37
N (d) 116.04
O (s) 56.80

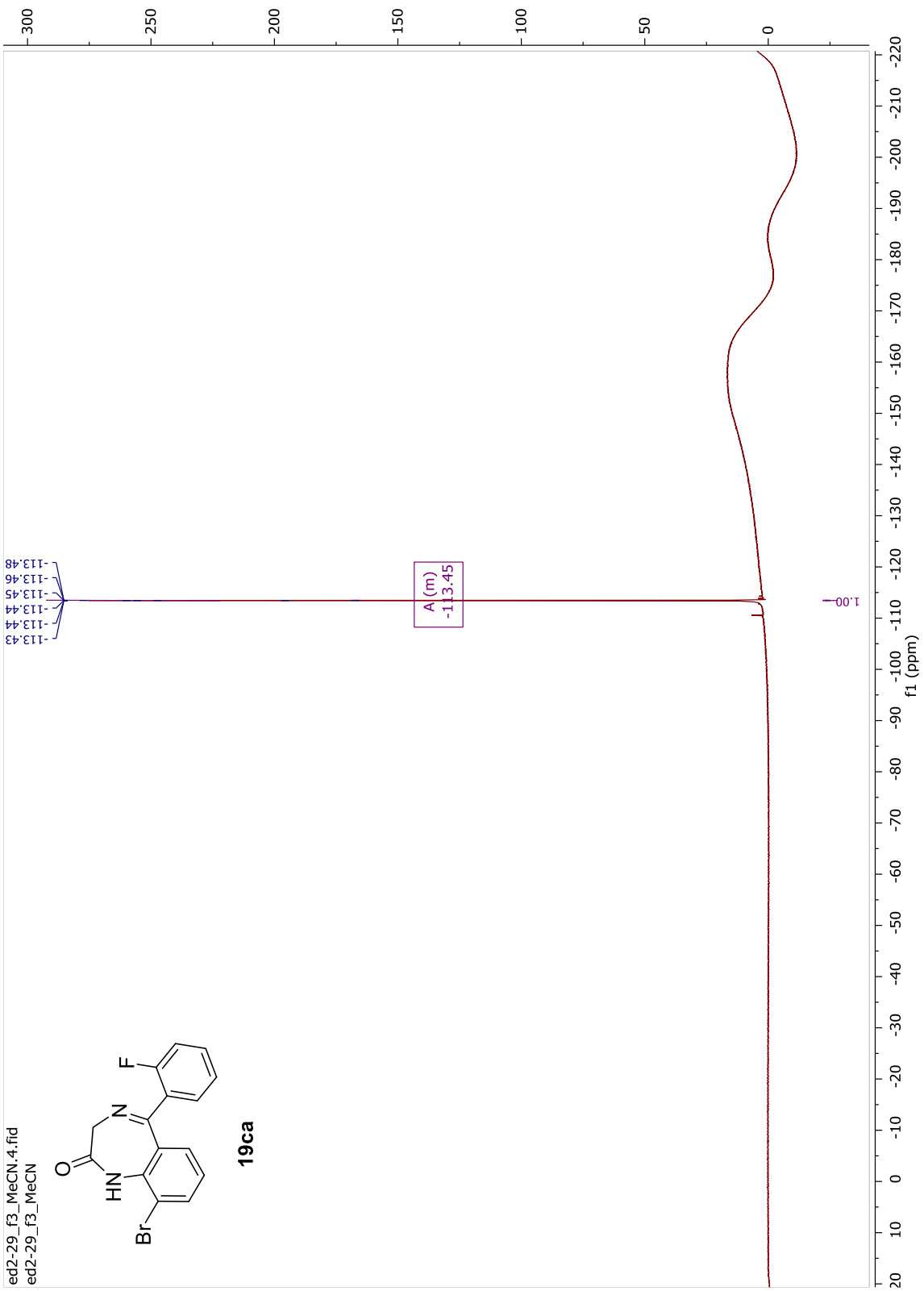
ed2-29_f3_MeCN.4.fid
ed2-29_f3_MeCN
19ca
A (m)
-113.45
1.00
f1 (ppm)

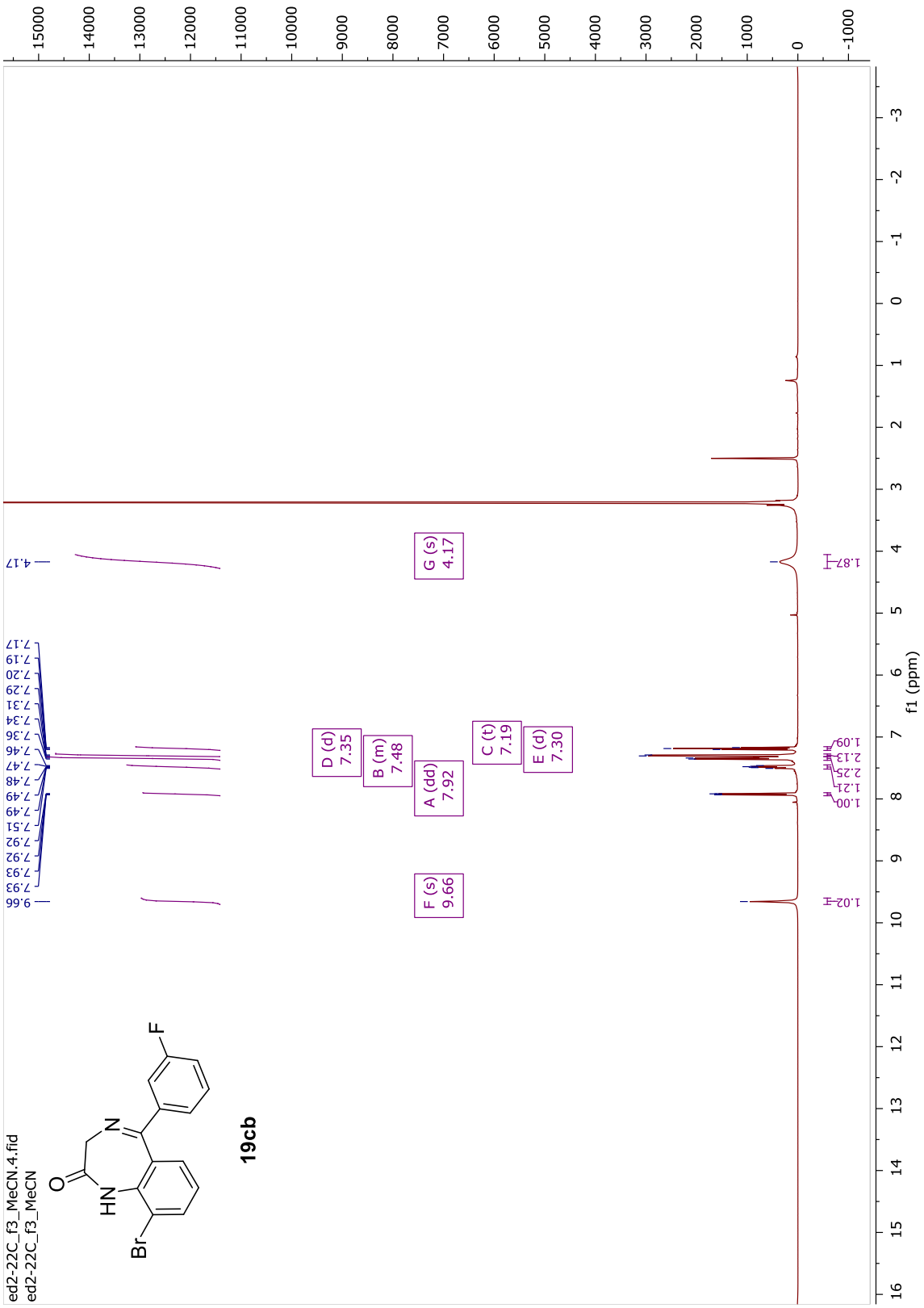
ed2-22C_f3_MeCN.4.fid
ed2-22C_f3_MeCN
19cb
F (s) 9.66
A (dd) 7.92
B (m) 7.48
D (d) 7.35
C (t) 7.19
E (d) 7.30
G (s) 4.17
f1 (ppm)

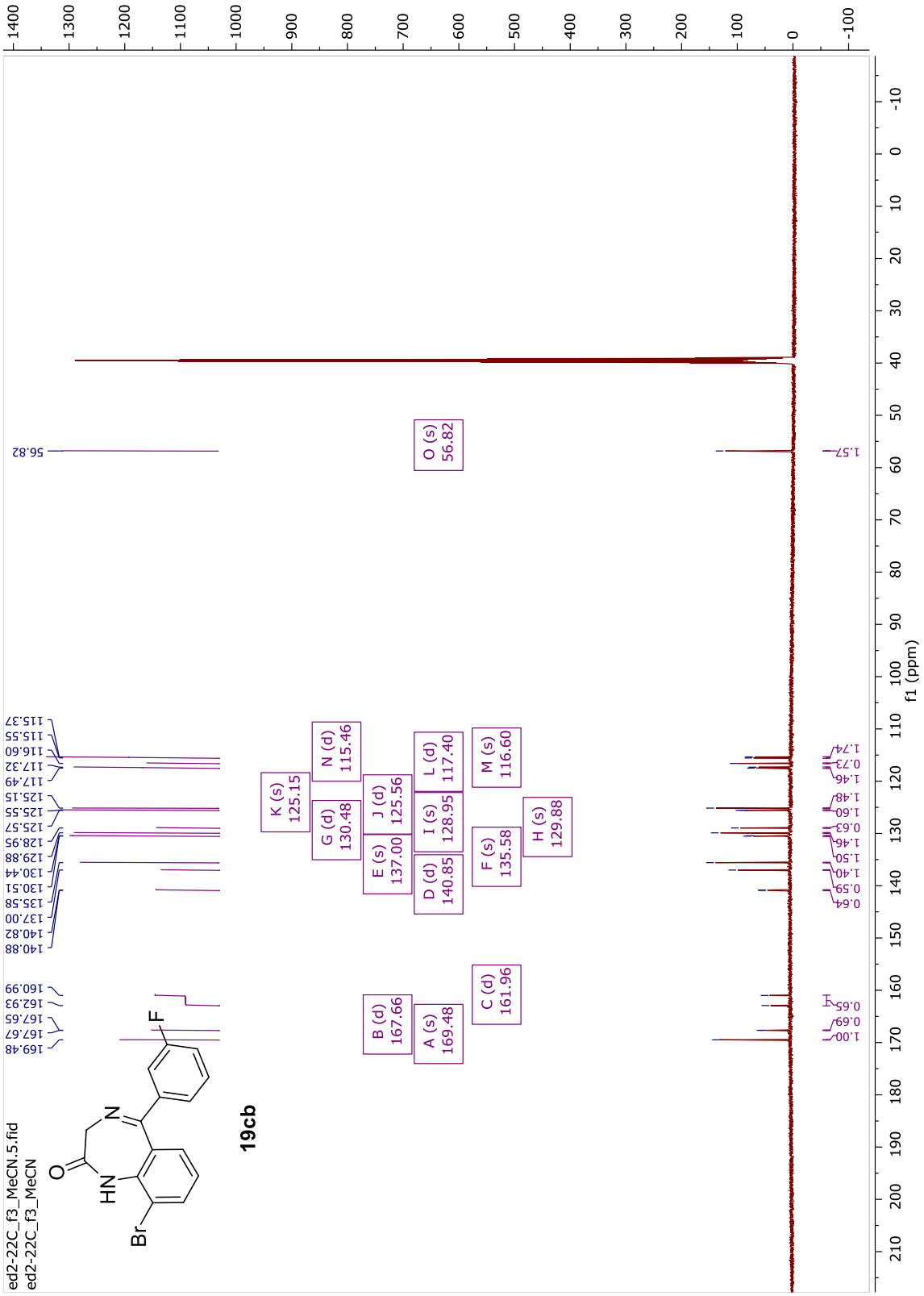
ed2-22C_f3_MeCN.5.fid
ed2-22C_f3_MeCN
19cb
f1 (ppm)
A (s) 169.48
B (d) 167.66
C (d) 161.96
D (d) 140.85
E (s) 137.00
F (s) 135.58
G (d) 130.48
H (s) 129.88
I (s) 128.95
J (d) 125.56
K (s) 125.15
L (d) 117.40
M (s) 116.60
N (d) 115.46
O (s) 56.82
Br
HN
O
N
F

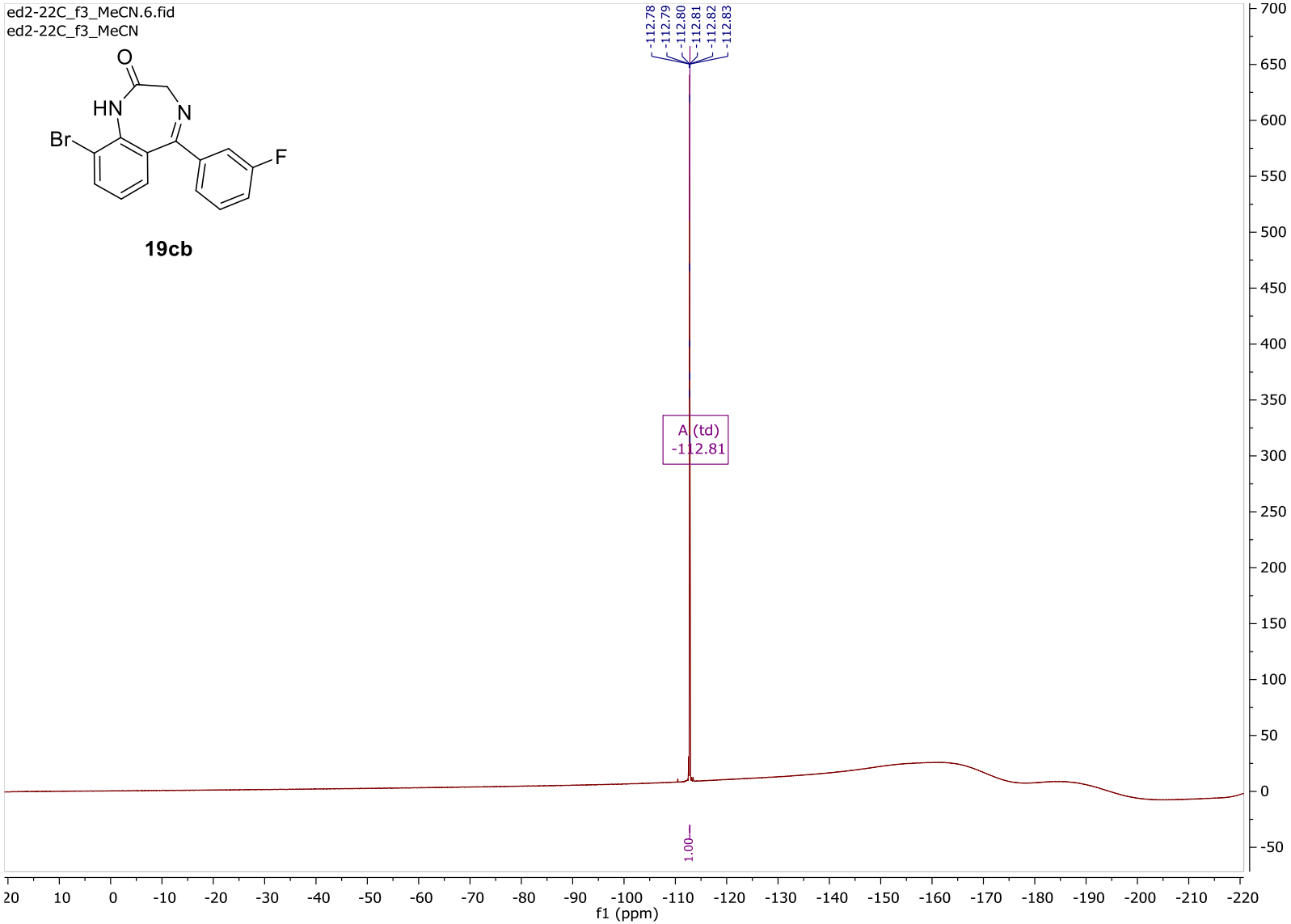
ed2-22C_f3_MeCN.6.fid
ed2-22C_f3_MeCN
O
HN
N
Br
F
19cb
-112.78
-112.79
-112.80
-112.81
-112.82
-112.83
A (td)
-112.81
1.00
f1 (ppm)

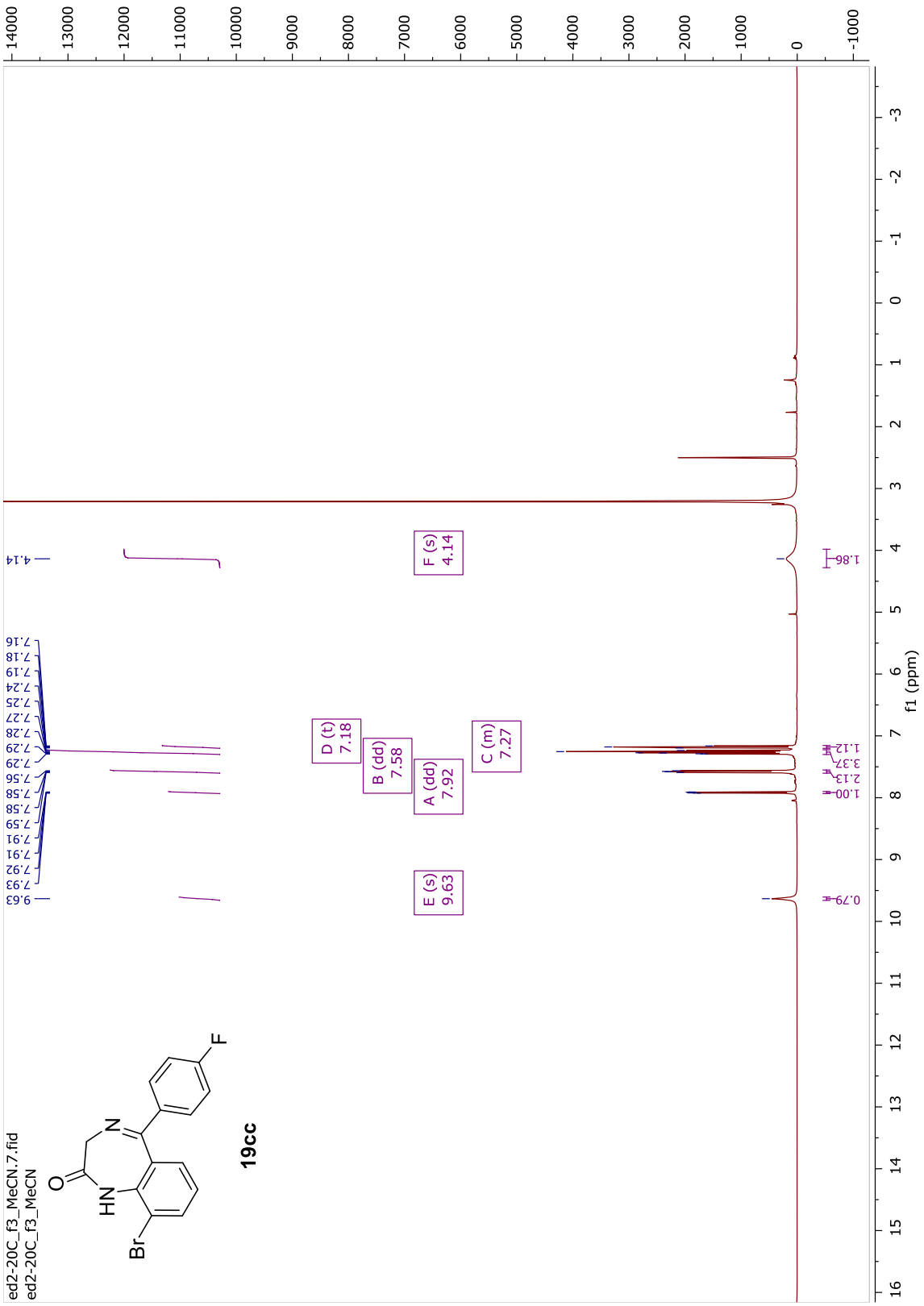
ed2-20C_f3_MeCN.7.fid
ed2-20C_f3_MeCN
19cc
F (s) 4.14
D (t) 7.18
B (dd) 7.58
A (dd) 7.92
C (m) 7.27
E (s) 9.63
f1 (ppm)

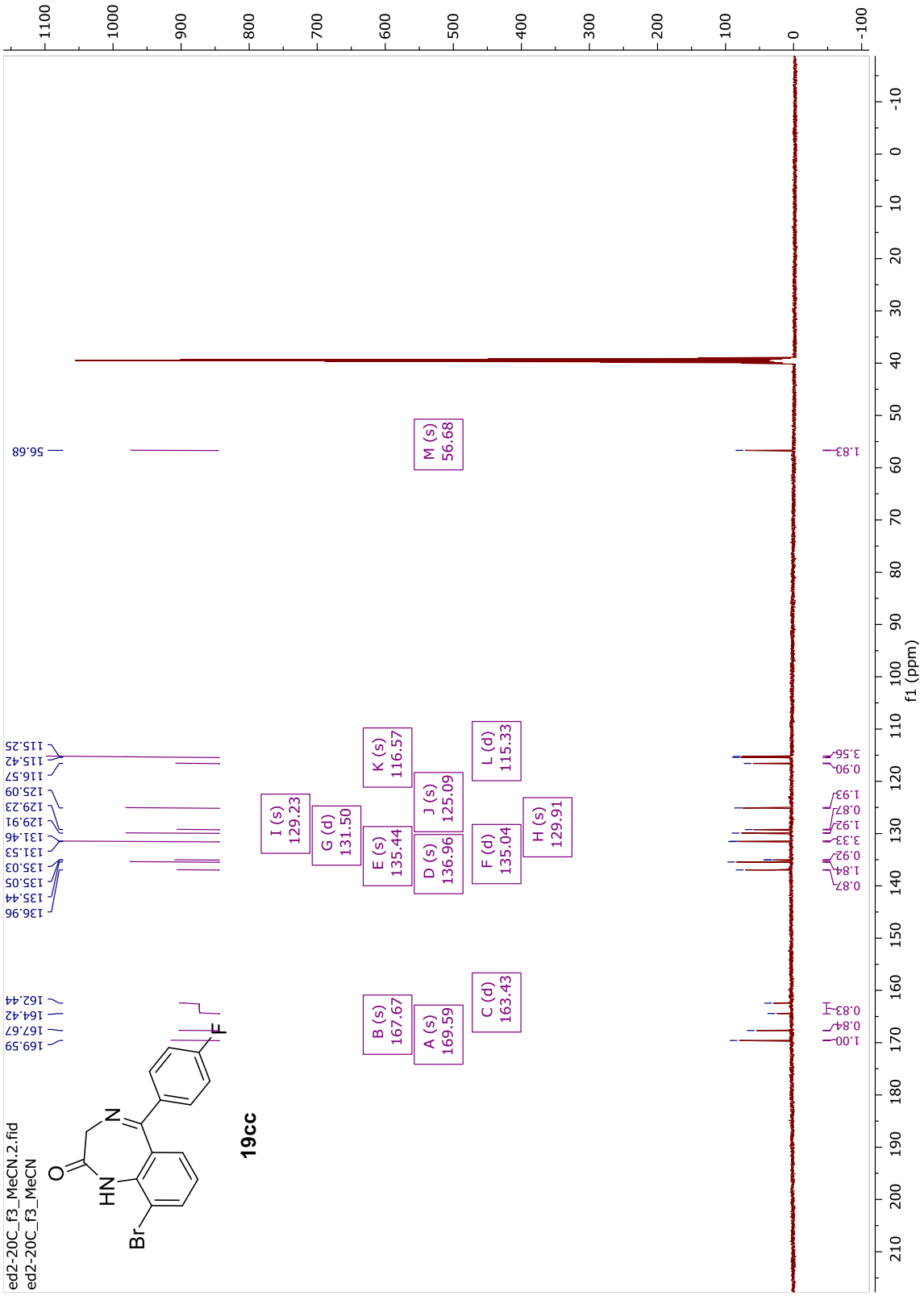
ed2-20C_f3_MeCN.2.fid
ed2-20C_f3_MeCN
19cc
f1 (ppm)
A (s) 169.59
B (s) 167.67
C (d) 163.43
D (s) 136.96
E (s) 135.44
F (d) 135.04
G (d) 131.50
H (s) 129.91
I (s) 129.23
J (s) 125.09
K (s) 116.57
L (d) 115.33
M (s) 56.68

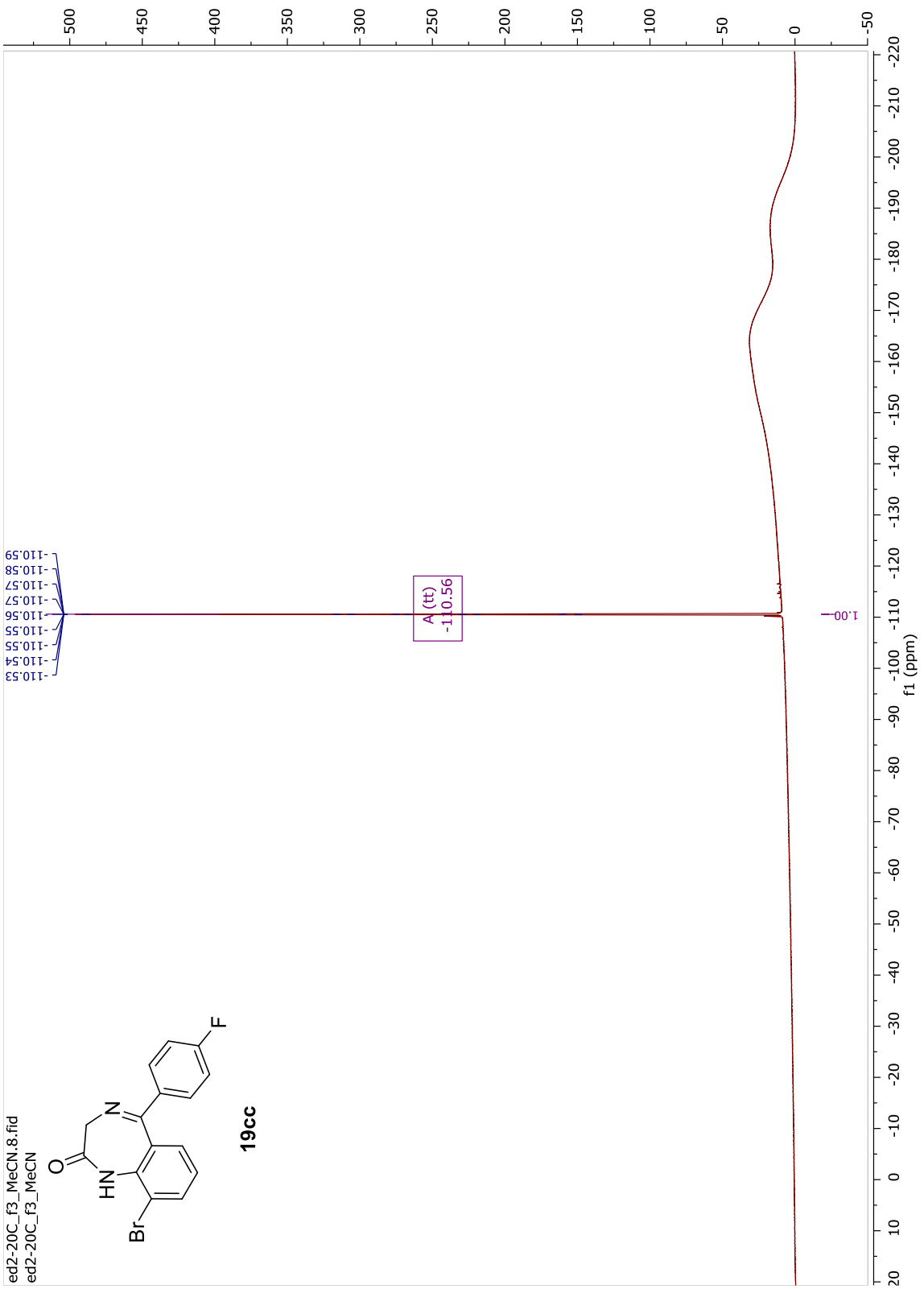
ed2-20C_f3_MeCN.8.fid
ed2-20C_f3_MeCN
19cc
A (tt)
-110.56
1.00
f1 (ppm)

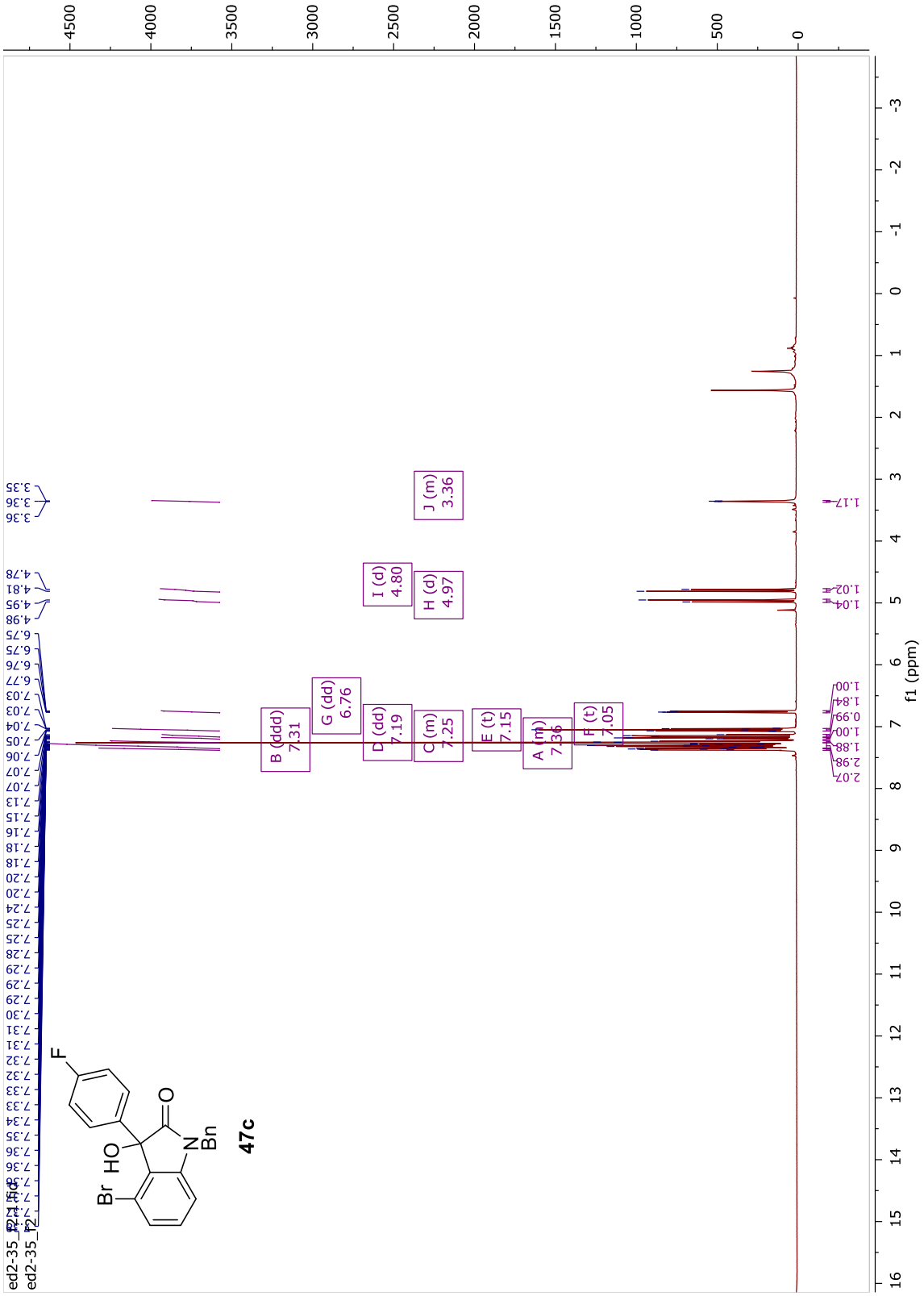
47c
B (ddd) 7.31
G (dd) 6.76
D (dd) 7.19
C (m) 7.25
E (t) 7.15
A (m) 7.36
F (t) 7.05
I (d) 4.80
H (d) 4.97
J (m) 3.36
f1 (ppm)

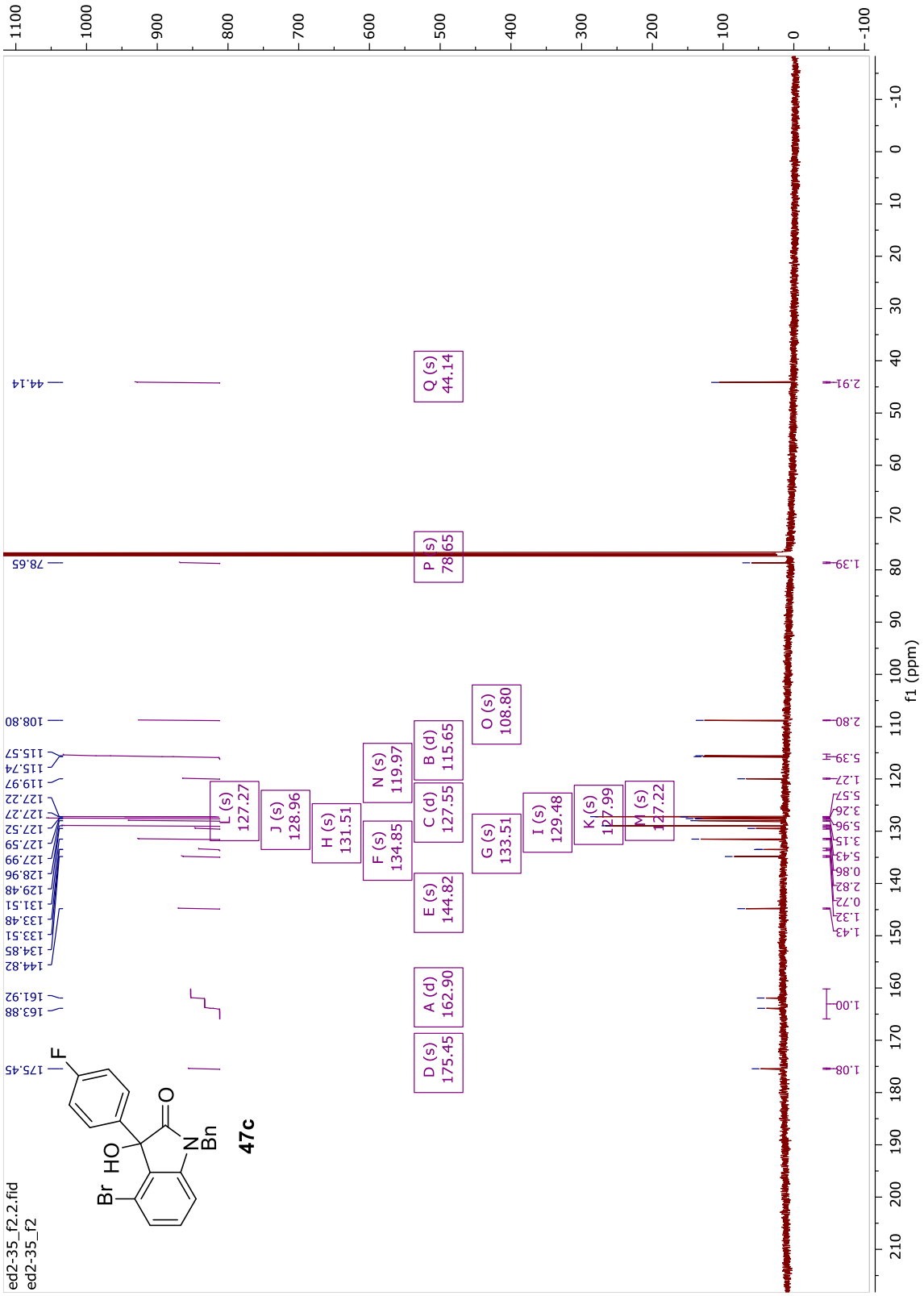
ed2-35_f2.2.fid
ed2-35_f2
47c
f1 (ppm)

2.10 References

(1) (a) Schmitz A. Benzodiazepine use, misuse, and abuse: A review. *Ment. Health Clin*. **2016**, *6*, 120-126. (b) Griffin, C. E.; Kaye, A. M.; Bueno, F. R.; Kaye, A. D. Benzodiazepine pharmacology and central nervous system-mediated effects. *Ochsner J*. **2013**, *13*, 214-23; (c) Cascade, E.; Kalali, A. H. Use of benzodiazepines in the treatment of anxiety. *Psychiatry* **2008**, *5*, 21–22.

(2) Nordqvist, J. (2018, January 5). "The benefits and risks of benzodiazepines." *Medical News Today*. Retrieved from https://www.medicalnewstoday.com/articles/262809.php.

(3) (a) The emergence of new psychoactive substance (NPS)benzodiazepines: A review. *Drug Test Anal*. **2018**, *10*, 37–53; (b) Wick, J. The History of Benzodiazepines. *Consult. Pharm*. **2013**, 28, 538-548; (c) Miller, N. S. ; Gold, M. S. Benzodiazepines: Reconsidered. *Adv. Alcohol Subst. Abuse* **1990**, *8*, 67-84.

(4) "Drug Fact Sheet: Benzodiazepines." 2017 Edition. Drug Enforcement Administration, https://www.dea.gov/sites/default/files/sites/getsmartaboutdrugs.com/files/publications/DoA_2017Ed_Updated_6.16.17.pdf#page=59.

(5) (a) Calcaterra, N. E.; Barrow, J. C. *ACS Chem. Neurosci*. **2014**, *5*, 253−260; (b) Oyemade, A. New uncontrolled benzodiazepine, phenazepam, emerging drug of abuse. *Innov. Clin. Neurosci.* **2012**, *9*, 10; (c) Maskell, P. D.; De Paoli, G.; Seetohul, L. N.; Pounder, D. J. Phenazepam: The drug that came in from the cold. *J. Forensic Leg. Med*. **2012**, *19*, 122-125.

(6) (a) “Phenazepam.” Updated 3 Nov 2018. https://drugs-forum.com/wiki/Phenazepam. (b) “Phenazepam: Legal Status.” Erowid, Updated 26 Feb 2016. https://www.erowid.org/pharms/phenazepam/phenazepam_law.shtml.

(7) a) 21 U.S.C. United States Code, 2012 Edition. Title 21 - FOOD AND DRUGS. CHAPTER 13 - DRUG ABUSE PREVENTION AND CONTROL. From the U.S. Government Printing Office, https://www.gpo.gov/fdsys/granule/USCODE-2011-title21/USCODE-2011-title21-chap13. b) “BENZODIAZEPINES.” Drug Enforcement Administration. Office of Diversion Control. Drug & Chemical Evaluation Section. Jan. 2013.

(8) Emerging Threat Report, Annual 2017. Drug Enforcement Administration: Special Testing and Research Laboratory. https://ndews.umd.edu/resources/dea-emerging-threat-reports.

(9) 21 U. S. C. § 813.

(10) Controlled Substances Act, U.S. Drug Enforcement Administration, https://www.dea.gov/druginfo/csa.shtml (last visited Jan. 22, 2017).

(11) Drug Enforcement Adminstration (DEA), Department of Justice. Definition of "positional isomer" as it pertains to the control of schedule I controlled substances. Final rule. *Fed Regist*. **2007**, *72*, 67850-2.

(12) (a) Reeder, E.; Nutley; Sternbach, L. H. Amino substituted benzophenone oximes and derivatives thereof. US3136815, 1964; (b) Sternbach, L. H.; Fryer, R. I.; Metlesics, W.; Reeder, E.; Sach, G.; Saucy, G.; Stempel, A. Quinazolines and 1,4-Benzodiazepines. VI. Halo-, Methyl-, and Methoxy-substituted 1,3-Dihydro-

5-phenyl-2H-1,4-benzodiazepin-2-ones. *J. Org. Chem*. **1962**, *27*, 3788; (c) Sternbach, L. H.; Fryer, R. I.; Metlesics, W.; Reeder, E.; Sach, G.; Saucy, G.; Stempel, A. Quinazolines and 1,4-benzodiazepines. V. o-Aminobenzophenones. *J. Org. Chem*. **1962**, *27*, 3781; (d) Sternbach, L. H.; Reeder, E. Quinazolines and 1,4-Benzodiazepines. IV. Transformations of 7-Chloro-2-methylamino-5-phenyl-3H-1,4-benzodiazepine 4-Oxide. *J. Org. Chem*. **1961**, *26*, 4936.

(13) Moosmann, B.; Huppertz, L. M.; Hutter, M.; Buchwald, A.; Ferlaino, S.; Auwärter, V. Detection and identification of the designer benzodiazepine flubromazepam and preliminary data on its metabolism and pharmacokinetics. *J. Mass. Spectrom*. **2013**, *48*, 1150-1159.

(14) Koch, K.; Auwarter, V.; Hermanns-Clausen, M.; Wilde, M.; Neukamm, M.A. Mixed intoxication by the synthetic opioid U-47700 and the benzodiazepine flubromazepam with lethal outcome: Pharmacokinetic data. *Drug Test. Anal*. **2018**, *10*, 1336-1341.

(15) Carpenter, J. E.; Murray, B. P.; Dunkley, C.; Kazzi, Z. N.; Gittinger, M. H. Designer benzodiazepines: a report of exposures recorded in the National Poison Data System, 2014-2017. *Clin. Toxicol*. **2018**, DOI: 10.1080/15563650.2018.1510502.

(16) Bäckberg, M.; Bergstrand, M.P.; Beck, O.; Helander, A. Occurrence and time course of NPS benzodiazepines in Sweden – results from intoxication cases in the STRIDA project. *Clin. Toxicol*. **2018**, DOI: 10.1080/15563650.2018.1506130.

(17) (a) Bergstrand, M.P.; Helander, A.; Hansson, T.; Beck, O. Detectability of designer benzodiazepines inCEDIA, EMIT II Plus, HEIA, and KIMS IIimmunochemical screening assays. *Drug Test. Anal*. **2017**, 9, 640-645; (b) O'Connor, L. C.; Torrance, H. J.; McKeown, D. A. *J. Anal. Toxicol*. **2016**, *40*, 159.

(18) (a) "Manual for Courts-Martial, United States." 1998 Ed. (b) "The Army Substance Abuse Program." 2012.

(19) (a) Huppertz, L. M.; Moosmann, B.; Auwärter, V. Flubromazolam- Basic pharmacokinetic evaluation of a highly potent designer benzodiazepine. *Drug. Test. Anal*. **2018**, *10*, 206-211; (b) Lukasik-Glebocka, M.; Sommerfeld, K.; Tezyk, A.; Zielinska-Psuja, B.; Panienski, P.; Zaba, C. Flubromazolam- A new life threatening designer benzodiazepine. *Clin. Toxicol*. **2016**, *54*, 66-68.

(20) (a) Ning, R.Y.; Fryer, R.I.; Madan, P.B.; Sluboski, B.C. Quinazolines and 1,4-Benzodiazepines. 76. Reactions of Some Di-4-morpholinylphosphinyloxy Imines. *J. Org. Chem.* **1976**, *41*, 2724-2727. (b) Cook, J.M.; Huang, Q.; He, X.-H.; Li, X.; Yu, J.; Han, D.-M.; Lelas, S.; McElroy, J.F. Anxiolytic Agents with Reduced Sedative and Ataxic Effects. WO 03/082832 A2, **2003**.

(21) Sahu, K. B.; Banerjee, M.; Ghosh, S.; Maity, A.; Mondal, S.; Paira, R.; Hazra, A.; Karmakar, S.; Samanta, A.; Mondal, N. B. I_2 catalyzed Friedel–Crafts alkylation reaction of substituted anilines with ninhydrin: formation of novel products and their antimicrobial evaluation. *Med. Chem. Res*. **2013**, *22*, 2023-2037.

(22) Lothrop, W.C.; Goodwin, P.A. A New Modification of the Ullmann Synthesis of Fluorene Derivatives. *J. Am. Chem. Soc.* **1943**, *65*, 363-367.

(23) (a) Cook, J. M.; Huang, Q.; He, X.; Li, X.; Yu, J.; Han, D. Preparation of benzodiazepines, in particular 1,4-benzodiazepines, as anxiolytic and anticonvulsant agents with reduced sedative and ataxic effects. Pub. No.: WO 2003082832 A2. 2003; (b) Bell, S. C.; Sulkowski, T. S.; Gochman, C.; Childress, S. J. 1,3-Dihydro-2H-1,4-benzodiazepine-2-ones and Their 4-Oxides. *J. Org. Chem*. **1962**, *27*, 562. (c) For a recent review of synthetic approaches toward 1,4-benzodiazepines, see: Kaur, N.; Kishore, D. Synthetic strategies applicable in the synthesis of privileged scaffold: 1,4-Benzodiazepine. *Synth. Commun*. **2014**, *44*, 1375-1413.

(24) For recent examples of strategic benzodiazepine syntheses: (a) Dondas, H. A.; Belveren, S.; Poyraz, S.; Grigg, R.; Kilner, C.; Ferrandiz-Saperas, M.; Selva, E.; Sansano, J. M. Design and synthesis of novel 1,4-benzodiazepine surrogates as potential CCKA and CCKB antagonists via palladium-catalyzed three-component cascade reactions. *Tetrahedron* **2018**, *74*, 6-11; (b) Khan, R.; Marsh, G.; Felix, R.; Kemmitt, P. D.; Baud, M. G. J.; Ciulli, A.; Spencer, J. Gram-Scale Laboratory Synthesis of TC AC 28, a High-Affinity BET Bromodomain Ligand. *ACS Omega* **2017**, *2*, 4328-4332; (c) Karaseva, T. L.; Likhota, E. B.; Krivenko, Ya. R.; Semibrat'ev, S. A.; Pavlovskii, V. I. Synthesis of New 7-bromo-5-(2'-chlorophenyl)-3-arylamino-1,2-dihydro-3H-1,4-benzodiazepine derivatives and their influence on appetite in rats. *Pharm. Chem. J.* **2017**, *51*, 258-261; (d) Ghelani, Satish M.; Naliapara, Yogesh T. Design, Synthesis, and Characterization of 1, 3-

disubstituted-1,4-benzodiazepine Derivatives. *J. Heterocycl. Chem*. **2016**, *53*, 1795-1800.

(25) The IUPAC name for the parent flubromazepam is **7**-Bromo-5-(**2**-fluorophenyl)-1,3-dihydro-2*H*-benzo[*e*][1,4]diazepin-2-one. In order to simply the discussion, we have established the following formalism based on the IUPAC name to represent each flubromazepam isomer: (X,X')-isomer, where X represents the position of the bromine atom and X' represents the position of the fluorine atom. Thus, the parent compound **4** may be designated as the (**7**,2')-isomer.

(26) Wu, Y.; Li, B.; Mao, F.; Li, X.; Kwong, F.Y. Palladium-Catalyzed Oxidative C–H Bond Coupling of Steered Acetanilides and Aldehydes: A Facile Access to *ortho*-Acylacetanilides. *Org. Lett*. **2011**, *13*, 3258-3261.

(27) Sternbach, L. H. 1,4-Benzodiazepines - Chemistry and Some Aspects of Structure-Activity Relationship. *Angew. Chem., Int. Ed*. 1971, *10*, 34−43.

(28) Sugasawa, T.; Toyoda, T.; Adachi M.; Sasakura, K. Aminohaloborane in organic synthesis. 1. Specific ortho substitution reaction of anilines. *J. Am. Chem. Soc*. **1978**, *100*, 4842-4852.

(29) (a) Claiborne, C. F.; Payne, L. J.; Boyce, R. J.; Sells, T. B.; Stroud, S. G.; Travers, S.; Vos, T. J.; Weatherhead, G. S. Compounds and methods for inhibiting mitotic progression. US2005/256102 A1, 2005; (b) Tabuchi, S.; Ito, H.; Sogabe, H.; Kuno, M.; Kinoshita, T.; Katumi, I.; Yamamoto, N.; Mitsui, H.; Satoh, Y. Dual CCK-A and CCK-B Receptor Antagonists (II). Preparation and Structure Activity Relationships of 5-Alkyl-9-methyl-1, 4-benzodiazepines and Discovery of FR208419. *Chem. Pharm. Bull*. **2000**, *48*, 1-15; (c) Douglas, A. W.; Abramson,

N. L.; Houpis, I. N.; Karady, S.; Molina, A.; Xavier, L. C.; Yasuda, N. In situ NMR spectroscopic studies of aniline ortho acylation ("sugasawa reaction"): The nature of reaction intermediates and Lewis acid influence on yield. *Tetrahedron Lett*. **1994**, *35*, 6807–6810.

(30) Cheng, K.; Zhao, B.; Qi, C. Silver-catalyzed decarboxylative acylation of arylglyoxylic acids with arylboronic acids. *RSC Adv*. **2014**, *4*, 48698-48702.

(31) Tsao, H.-W. Preparation of 2-trifluoromethyl cinchoninic acids. US4267333 A1, 1981.

(32) Kraus, G. A.; Guo, H. A direct synthesis of neocryptolepine and isocryptolepine. *Tetrahedron Lett*. **2010**, *51*, 4137-4139.

(33) HBTU = *N*,*N*,*N*′,*N*′-Tetramethyl-O-(1*H*-benzotriazol-1-yl)uronium hexafluorophosphate, O-(Benzotriazol-1-yl)-N,N,N′,N′-tetramethyluronium hexafluorophosphate. For a pertinent reference, see: Otsubo, N.; Okazaki, S.; Tsukumo, Y.; Iida, K.; Nakoji, M. PYRIMIDO-DIAZEPINONE COMPOUND. EP2708540 A1, 2014.

(34) Alanine, A.; Gobbi, L. C.; Kolczewski, S.; Luebbers, T.; Peters, J.-U.; Steward, L. (3,4-Dihydro-quinazolin-2-yl)-(2-aryloxy-ethyl)-amine. US2006/252779 A1, 2006.

(35) Maezaki, H.; Banno, Y.; Miyamoto, Y.; Moritoh, Y.; Asakawa, T.; Kataoka, O.; Takeuchi, K.; Suzuki, N.; Ikedo, K.; Kosaka, T.; Sasaki, M.; Tsubotani, S.; Tani, A.; Funami, M.; Yamamoto, Y.; Tawada, M.; Aertgeerts, K.; Yano, J.; Oi, S. Discovery of potent, selective, and orally bioavailable quinoline-

based dipeptidyl peptidase IV inhibitors targeting Lys554. *Bioorg. Med. Chem*. **2011**, *19*, 4482-4498.

(36) Gavai, A.V.; DeLucca, G.V.; O'Malley, D.; Gill, P.; Quesnelle, C.A.; Fink, B.E.; Zhao, Y.; Lee, F.Y. Bis(fluoroalkyl)alkanoylamino-1,4,-benzodiazepine compounds as Notch inhibitors and their preparation. WO 2014047372 A1, **2014**.

(37) Yu, J.; Moon, H.R.; Min, B.K.; Kim, J.N. 2-Arylindoles: A New Entry to Transition Metal-free Synthesis of 2-Aminobenzophenones. *Bull. Korean Chem. Soc.* **2016**, *37*, 893-897.

(38) Ma, S.; Han, X.; Krishnan, S.; Virgil, S.C.; Stoltz, B.M. Catalytic Enantioselective Stereoablative Alkylation of 3-Halooxindoles: Facile Access to Oxindoles with C3 All-Carbon Quaternary Stereocenters. *Angew. Chem. Int. Ed.* **2009**, *48*, 8037-8041.

(39) Selected examples: (a) Shintani, R.; Inoue, M.; Hayashi, T. Rhodium-Catalyzed Asymmetric Addition of Aryl- and Alkenylboronic Acids to Isatins. *Angew. Chem. Int. Ed.* **2006**, *45*, 3353-3356. (b) Toullec, P.Y.; Jagt, R.C.B.; de Vries, J.G.; Feringa, B.L.; Minnaard, A.J. Rhodium-catalyzed Addition of Phenylboronic Acids to Isatins: An Entry to Diversity in 3-Aryl-3-hydroxyoxindoles. *Org. Lett.* **2006**, *8*, 2715-2718. (c) Tan, J.; Kuang, Y.; Wang, Y.; Huang, Q.; Zhu, J.; Wang, Y. Axial Tri-*tert*-butylphosphane Coordination to $Rh_2(OAc)_4$: Synthesis, Structure, and Catalytic Studies. *Organometallics* **2016**, *35*, 3139-3147.

(40) Zhang, J.; Chen, J.; Ding, J.; Liu, M.; Wu, H. Copper-catalyzed Arylation of Indolin-2,3-ones with Arylboronic Acids. *Tetrahedron* **2011**, *67*, 9347-9351.

(41) Lu, S.; Poh, S.B.; Siau, W.-Y.; Zhao, Y. Kinetic Resolution of Tertiary Alcohols: Highly Enantioselective Access to 3-Hydroxy-3-Substituted Oxindoles. *Angew. Chem. Int. Ed.* **2013**, *52*, 1731-1734.

(42) Krasovskiy, A.; Krasovskaya, V.; Knochel, P. Mixed Mg/Li Amides of the Type $R_2NMgCl{\cdot}LiCl$ as Highly Efficient Bases for the Regioselective Generation of Functionalized Aryl and Heteroaryl Magnesium Compound. *Angew. Chem. Int. Ed*. **2006**, *45*, 2958–2961.

(43) Stuart, D. R.; Bertrand-Laperle, M.; Burgess, K. M. N.; Fagnou, K. Indole Synthesis via Rhodium Catalyzed Oxidative Coupling of Acetanilides and Internal Alkynes. *J. Am. Chem. Soc*. **2008**, *130*, 16474-16475.

CHAPTER 3. ANALYSIS OF FLUBROMAZEPAM POSITIONAL ISOMERS FOR FORENSIC DIFFERENTIATION

3.1 Purpose: Positional Isomer Differentiation

As discussed in Chapter 2, positional isomers of benzodiazepine drugs are nearly identical structurally and thus expected to exhibit similar bioactivity as their parent benzodiazepines, many of which are federally controlled. However, due to the technically legal status of various benzodiazepine isomers, as the analogue rule does not apply to benzodiazepines, they represent potentially attractive substitutes for drug abuse. In this study, flubromazepam, a recognized designer benzodiazepine since 2012, was targeted for synthesis and characterization due to its potential for federal scheduling and current legal status within the United States. Significantly, flubromazepam has twelve positional isomers including the parent drug, which opens up a broad chemical space for analytical study.

Nine of twelve positional isomers were successfully obtained for analysis (Figure 3-1), and the syntheses of the remaining three isomers are in progress. Then, the corresponding analytical reference spectra for each positional isomer of flubromazepam were collected. This chapter will discuss the structural identification and validation of synthesized flubromazepam isomers using liquid chromatography-high resolution accurate-mass mass spectrometry (LC-HRAM-MS) and proton, carbon, and fluorine nuclear magnetic resonance (^{1}H, ^{13}C, ^{19}F NMR). Then, the characterization data acquired using traditional forensic analytical techniques such as gas chromatography-mass

spectrometry (GC-MS), liquid chromatography-mass spectrometry (LC-MS), and gas chromatography-solid phase infrared spectroscopy (GC-IR) will be presented. From this data, an analytical roadmap may be developed to differentiate between each positional isomer of flubromazepam, and recommendations may be offered to forensic examiners to differentiate between benzodiazepine positional isomers without pre-existing reference data.

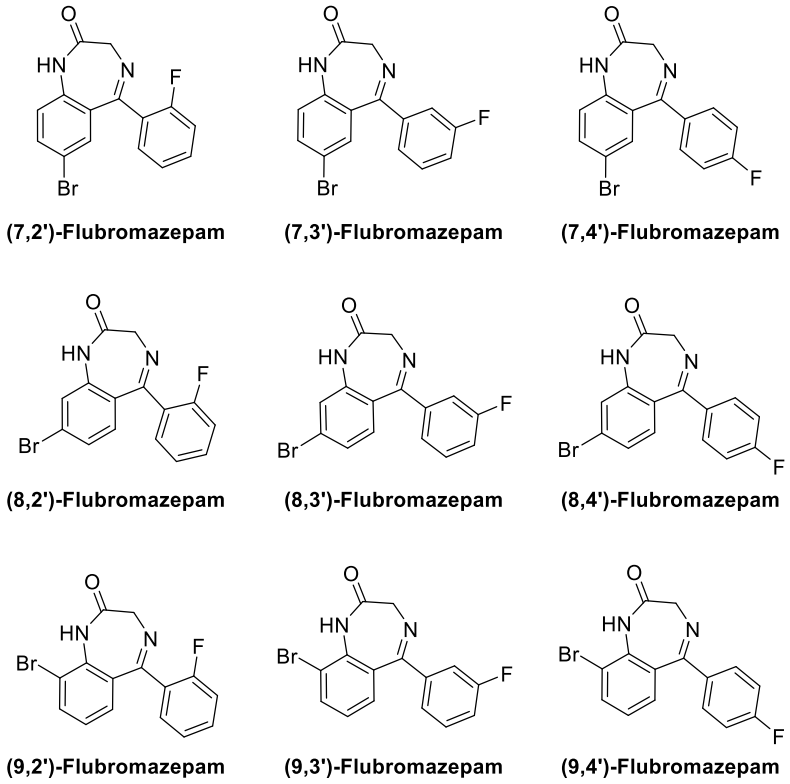

Figure 3-1: Nine successfully acquired flubromazepam isomers.

3.2 Discussion of Acquired Analytical Data

3.2.1 LC-HRAM-MS Results

Exact mass data were collected by LC-HRAM-MS for all flubromazepam targets and synthetic precursors as primary validation for the novel compounds. All molecular ion

peaks reported correspond to $[M+H]^+$ and exhibit the expected 1:1 $[M+H]^+/[M+2+H]^+$ isotope pattern indicative of the presence of a bromine atom. For flubromazepam $[M+H]^+$ (molecular formula: $C_{15}H_{11}BrFN_2O$), the calculated mass was 333.00333 amu, and experimental masses for every positional isomer fell within 2 ppm of this value (Table 3-1). For reference, the instrumental calibration allowed for up to 3 ppm error.

Table 3-1: LC-HRAMS Exact Mass Data for (X,X')-Flubromazepam Isomers

Isomer	Experimental Mass (amu)	Error (ppm)
(7,2')	333.00302	0.9
(7,3')	333.00284	1.5
(7,4')	333.00290	1.3
(8,2')	333.00311	0.7
(8,3')	333.00272	1.8
(8,4')	333.00272	1.8
(9,2')	333.00333	0.0
(9,3')	333.00336	0.1
(9,4')	333.00336	0.1
Calculated[a]	333.00333	N/A

[a] Calculated for $[M+H]^+$.

3.2.2 NMR Results

3.2.2.1 ^{1}H NMR

Like the exact mass data, ^{1}H and ^{13}C NMR served as primary validation methods for the identity of each flubromazepam positional isomer and all new precursor compounds. (Copies of NMR spectra may be found at the end of Chapter 2.) The ^{1}H NMR spectrum for parent flubromazepam agreed well with previously reported results (Table 3-2).[1]

Table 3-2: ^{1}H NMR Data for Parent Flubromazepam Compared to Literature

Literature Chemical Shift (ppm) (Multiplicity, Integration)[a]	Experimental Chemical Shift (ppm) (Multiplicity, Integration)[a]
10.74 (s, 1H)	10.73 (s, 1H) *(a)*
7.71, (dd, 1H)	7.72 (dd, 1H) *(b)*
7.52-7.59 (m, 2H)	7.53-7.60 (m, 2H) *(c)*
7.15-7.34 (m, 4H)	7.19-7.33 (m, 4H) *(d)*
4.20 (s, 2H)	4.20 (s, 2H) *(e)*

[a] Solvent: DMSO-d_6 (multiplicity: s = singlet; dd = doublet of doublets; m = undefined multiplet).

Furthermore, every flubromazepam isomer exhibited a sharp singlet between 9.0-11.0 ppm and a broad singlet between 4.1-4.3 ppm, corresponding to the NH and CH_2 protons, respectively. The aromatic regions (6.5-8.0 ppm) also showcased expected integrations of 7 aromatic protons total, *J* values consistent with *ortho* (proximal) and *meta* (long-distance) couplings, and splitting patterns dictated by changes in bromine and fluorine positioning on the benzene rings (Table 3-3). Significantly, these splitting patterns are unique to each isomer (Figure 3-2); thus, these results strongly suggest that ^{1}H NMR is useful for both structural validation and isomeric differentiation of benzodiazepine positional isomers in general.

Table 3-3: ^{1}H NMR Data for (X,X')-Flubromazepam Isomers

Isomer	Chemical Shift (ppm) (Multiplicity, *J* Value, Integration)[a]
(7,2') (parent)	10.74 (s, 1H), 7.72 (dd, *J* = 8.7, 2.3 Hz, 1H), 7.57 (tdd, *J* = 7.4, 3.3, 1.4 Hz, 2H), 7.33 (t, *J* = 7.5 Hz, 1H), 7.26 (t, 1H), 7.21 (d, *J* = 2.3 Hz, 1H), 7.19 (d, *J* = 8.7 Hz, 1H), 4.20 (s, 2H)
(7,3')	10.68 (s, 1H), 7.76 (dd, *J* = 8.7, 2.3 Hz, 1H), 7.49 (td, *J* = 8.0, 5.9 Hz, 1H), 7.39 – 7.31 (m, 3H), 7.22 (t, *J* = 8.7 Hz, 2H), 4.17 (s, 2H)
(7,4')	10.65 (s, 1H), 7.76 (dd, *J* = 8.7, 2.3 Hz, 1H), 7.53 (dd, *J* = 8.7, 5.6 Hz, 2H), 7.36 (d, *J* = 2.3 Hz, 1H), 7.28 (t, *J* = 8.8 Hz, 2H), 7.21 (d, *J* = 8.7 Hz, 1H), 4.15 (s, 2H)

(8,2')	10.72 (s, 1H), 7.58 – 7.52 (m, 2H), 7.42 (d, *J* = 2.0 Hz, 1H), 7.34 – 7.30 (m, 2H), 7.24 (ddd, *J* = 10.8, 8.7, 1.1 Hz, 1H), 7.06 (d, *J* = 8.5 Hz, 1H), 4.20 (s, 2H).
(8,3')	10.66 (s, 1H), 7.50 – 7.44 (m, 2H), 7.39 – 7.30 (m, 3H), 7.25 (dt, *J* = 7.7, 1.2 Hz, 1H), 7.21 (d, *J* = 8.4 Hz, 1H), 4.18 (s, 2H)
(8,4')	10.64 (s, 1H), 7.53 (dd, *J* = 8.7, 5.6 Hz, 2H), 7.44 (d, *J* = 2.0 Hz, 1H), 7.37 (dd, *J* = 8.4, 2.0 Hz, 1H), 7.26 (t, *J* = 8.8 Hz, 2H), 7.19 (d, *J* = 8.4 Hz, 1H), 4.15 (s, 2H)
(9,2')	9.98 (s, 1H), 7.89 (dd, *J* = 7.6, 1.7 Hz, 1H), 7.63 – 7.54 (m, 2H), 7.33 (td, *J* = 7.5, 1.1 Hz, 1H), 7.24 (ddd, *J* = 10.9, 8.2, 1.1 Hz, 1H), 7.16 (dd, *J* = 7.9, 1.7 Hz, 1H), 7.12 (t, *J* = 7.7 Hz, 1H), 4.18 (s, 2H)
(9,3')	9.66 (s, 1H), 7.92 (dd, *J* = 7.9, 1.4 Hz, 1H), 7.52 – 7.45 (m, 1H), 7.35 (d, *J* = 8.4 Hz, 2H), 7.30 (d, *J* = 7.9 Hz, 2H), 7.19 (t, *J* = 7.9 Hz, 1H), 4.17 (s, 2H)
(9,4')	9.63 (s, 1H), 7.92 (dd, *J* = 7.9, 1.4 Hz, 1H), 7.58 (dd, *J* = 8.8, 5.6 Hz, 2H), 7.30 – 7.22 (m, 3H), 7.18 (t, *J* = 7.9 Hz, 1H), 4.14 (s, 2H)

[a] Solvent: DMSO-d_6 (multiplicity: s = singlet; d = doublet; dd = doublet of doublets; ddd = doublet of doublets of doublets; dt = doublet of triplets; t = triplet; td = triplet of doublets; tdd = triplet of doublets of doublets; m = undefined multiplet).

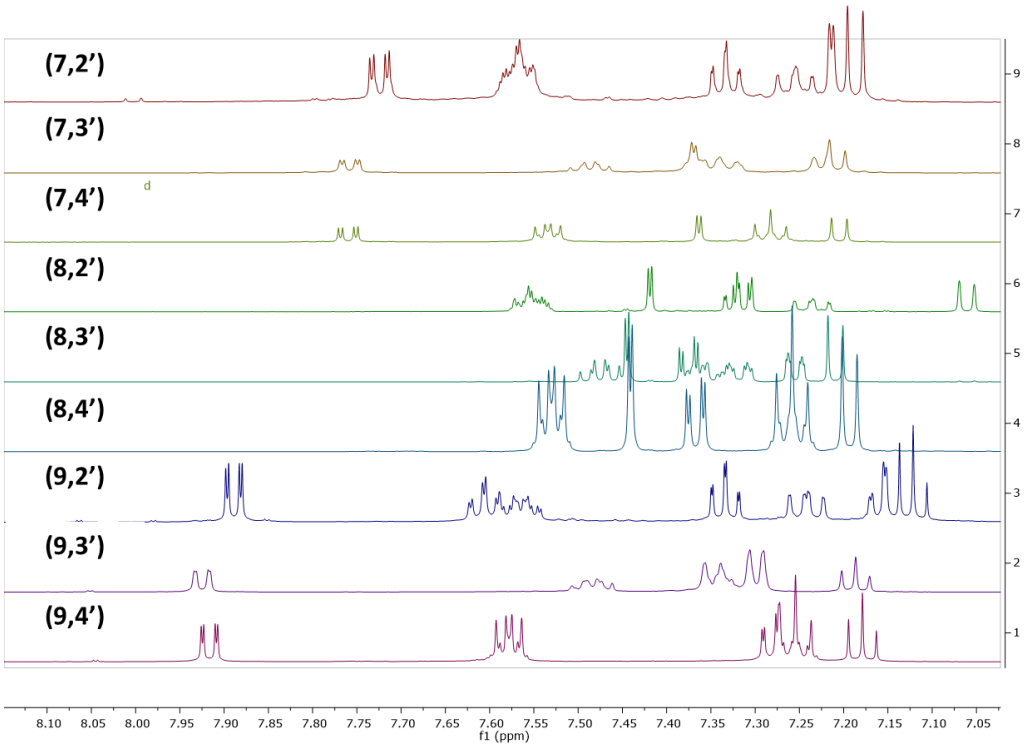

Figure 3-2: Overlay of (X,X')-flubromazepam positional isomer ^{1}H NMR spectra.

3.2.2.2 ^{13}C NMR

The ^{13}C NMR spectrum, though not previously reported in the literature for parent flubromazepam, is consistent with previous spectroscopic studies of fluorine-containing benzodiazepines.[2] Easily distinguishable functional groups include the amide carbonyl carbon (C=O), the imine carbon (C=N), and the lone aliphatic carbon (CH_2) at 169.59, 165.10, and 57.06 ppm, respectively (Figure 3-3).

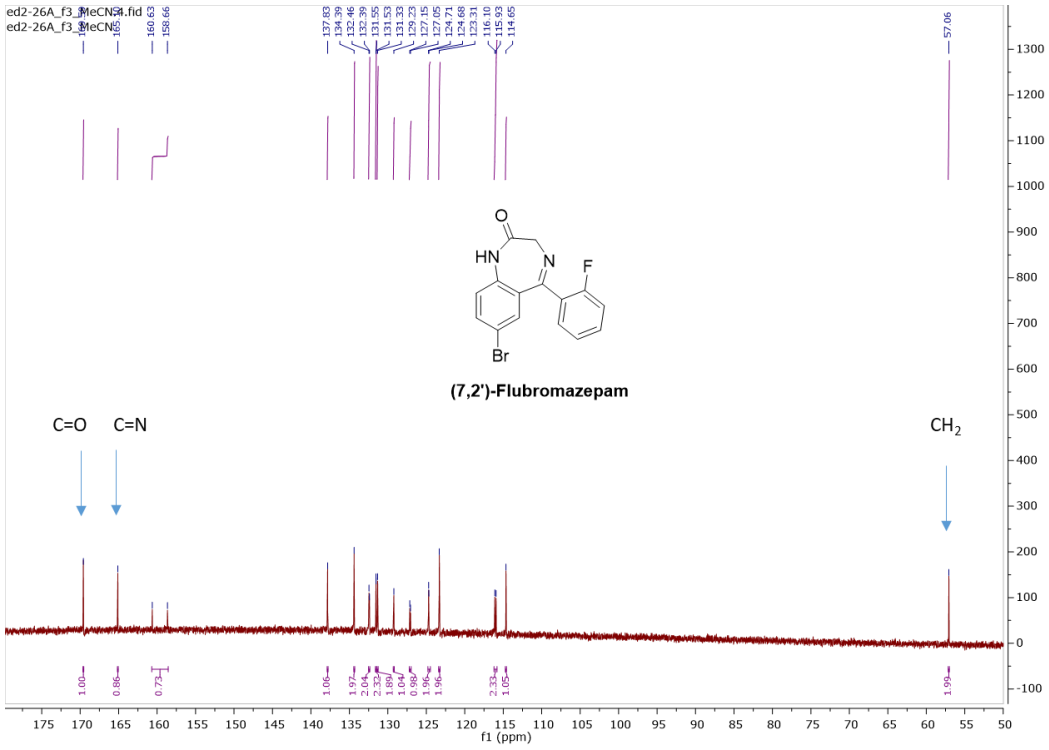

Figure 3-3: ^{13}C NMR spectrum for parent flubromazepam.

The remaining carbon atoms fall within the aromatic region (115-165 ppm) and exhibit additional peaks due to splitting from the fluorine atom (Table 3-4). As expected, the six aromatic carbons on the fluorine-containing phenyl ring are split into doublets, and the corresponding *J* values agree with previously reported *J* values for benzodiazepines with 2-fluoro substitutions. These trends hold across the spectra recorded for the novel

flubromazepam isomers, with some notable differences. First, only four aromatic carbon peaks split into doublets in the 4-fluoro targets due to symmetry. Second, and interestingly, doublet splitting was also observed in the 3-fluoro targets at the imine carbon, with a reasonable long-range splitting frequency of about 3 Hz.

Table 3-4: ^{13}C NMR Data for (X,X')-Flubromazepam Isomers

Isomer	Chemical Shift (ppm) (Multiplicity, *J* Value)[a]
(7,2') (parent)	169.59, 165.10, 159.64 (d, *J* = 248.6 Hz), 137.83, 134.39, 132.43 (d, *J* = 8.5 Hz), 131.54 (d, *J* = 2.7 Hz), 131.33, 129.23, 127.10 (d, *J* = 12.3 Hz), 124.69 (d, *J* = 3.5 Hz), 123.31, 116.01 (d, *J* = 21.4 Hz), 114.65, 57.06
(7,3')	170.03, 167.24 (d, *J* = 2.7 Hz), 161.97 (d, *J* = 244.4 Hz), 140.98 (d, *J* = 7.4 Hz), 139.05, 134.57, 132.52, 130.46 (d, *J* = 8.0 Hz), 127.65, 125.61 (d, *J* = 2.7 Hz), 123.46, 117.37 (d, *J* = 21.2 Hz), 115.58 (d, *J* = 22.8 Hz), 114.47, 57.08
(7,4')	170.44, 167.53, 163.70 (d, *J* = 248.4 Hz), 139.29, 135.42 (d, *J* = 2.9 Hz), 134.71, 132.83, 131.85 (d, *J* = 8.8 Hz), 128.20, 123.68, 115.63 (d, *J* = 21.7 Hz), 114.69, 57.24
(8,2')	169.65, 165.82, 159.66 (d, *J* = 248.7 Hz), 139.76, 132.29 (d, *J* = 8.2 Hz), 131.46 (d, *J* = 7.2 Hz), 127.33 (d, *J* = 12.8 Hz), 126.53, 125.91, 124.64 (d, *J* = 3.4 Hz), 124.43, 123.28, 115.98 (d, *J* = 21.4 Hz), 57.07
(8,3')	170.03, 167.88 (d, *J* = 2.9 Hz), 161.89 (d, *J* = 244.3 Hz), 141.06 (d, *J* = 7.2 Hz), 140.97, 132.48, 130.35 (d, *J* = 8.3 Hz), 125.60 (d, *J* = 5.4 Hz), 124.90, 124.59, 123.46, 117.24 (d, *J* = 21.3 Hz), 115.61 (d, *J* = 22.8 Hz), 57.07
(8,4')	170.50, 168.23, 163.67 (d, *J* = 248.0 Hz), 141.25, 135.55 (d, *J* = 3.2 Hz), 132.84, 131.90 (d, *J* = 8.6 Hz), 125.84, 125.49, 124.76, 123.71, 115.53 (d, *J* = 21.8 Hz), 57.25
(9,2')	169.07, 165.69, 159.71 (d, *J* = 248.9 Hz), 135.83, 135.39, 132.44 (d, *J* = 8.4 Hz), 131.37 (d, *J* = 2.6 Hz), 130.57, 128.66, 127.16 (d, *J* = 12.2 Hz), 125.41, 124.70 (d, *J* = 3.5 Hz), 116.37, 116.04 (d, *J* = 21.4 Hz), 56.80
(9,3')	169.48, 167.66 (d, *J* = 2.7 Hz), 161.96 (d, *J* = 244.3 Hz), 140.85 (d, *J* = 7.3 Hz), 137.00, 135.58, 130.48 (d, *J* = 8.2 Hz), 129.88, 128.95, 125.56 (d, *J* = 2.7 Hz), 125.15, 117.40 (d, *J* = 21.1 Hz), 116.60, 115.46 (d, *J* = 22.8 Hz), 56.82
(9,4')	169.59, 167.67, 163.43 (d, *J* = 248.2 Hz), 136.96, 135.44, 135.04 (d, *J* = 2.9 Hz), 131.50 (d, *J* = 8.7 Hz), 129.91, 129.23, 125.09, 116.57, 115.33 (d, *J* = 21.8 Hz), 56.68

[a] Solvent: DMSO-d_6 (multiplicity: d = doublet).

3.2.2.3 ^{19}F NMR

Similarly, no ^{19}F NMR spectrum was previously reported for parent flubromazepam. There are clear trends, however, across the ^{19}F NMR spectra for the positional isomers (Table 3-5). All (X,2') isomers exhibited multiplets in the -113.3 – -114.0 ppm range, only one of which, the (8,2') isomer spectrum, was well-resolved; while the (X,3') and (X,4') isomers manifested more resolved splitting patterns in the -112.8 – -113.0 and -110.5 – -110.8 ppm ranges, respectively. Although ^{13}C NMR has already been demonstrated as a diagnostic technique for fluorine substitution pattern, ^{19}F NMR is substantially more powerful for isomeric differentiation. Significantly, due to the similar natural abundances of proton and fluorine atoms, ^{19}F NMR acquisitions were achieved in shorter times (under a minute) and with greater resolution (471 MHz vs 126 MHz) than ^{13}C NMR.

Table 3-5: ^{19}F NMR Data for (X,X')-Flubromazepam Isomers

Isomer	Chemical Shift (ppm) (Multiplicity, *J* Value)
(7,2') (parent)	-113.91 – -114.01 (m)
(7,3')	-112.83 (td, *J* = 9.4, 6.5 Hz)
(7,4')	-110.68 (tt, *J* = 8.9, 5.7 Hz)
(8,2')	-113.90 (dt, *J* = 12.0, 6.7 Hz)
(8,3')	-112.98 (td, *J* = 9.4, 6.1 Hz)
(8,4')	-110.78 (tt, *J* = 8.8, 5.5 Hz)
(9,2')	-113.39 – -113.50 (m)
(9,3')	-112.81 (td, *J* = 9.4, 6.1 Hz)
(9,4')	-110.56 (tt, *J* = 8.8, 5.5 Hz)

[a] Solvent: DMSO-d_6 (multiplicity: m = multiplet, dt = doublet of triplets, td = triplet of doublets, tt = triplet of triplets.)

3.2.3 GC-MS Results

3.2.3.1 GC Retention Times

Retention times for flubromazepam positional isomers and corresponding synthetic precursors were reported from GC data following the method described in Section 3.5.3.3 (Table 3-6). Though GC retention time had initially been hypothesized as a distinguishing test for the identity of flubromazepam positional isomers, the retention times were resolved for only 65% of the nine positional isomers based on the 2% difference threshold allowed by the screening method (Table 3-7).

Table 3-6: GC Retention Times for (X,X')-Flubromazepam Isomers

Isomer	**(9,2')**	**(9,3')**	**(9,4')**	**(8,2')**	**(8,3')**	**(8,4')**	**(7,2') (parent)**	**(7,3')**	**(7,4')**
Retention Time (min)	7.610	7.699	7.716	7.969	8.093	8.116	7.887	8.075	8.087

Table 3-7: Percent Differences Between (X,X')-Flubromazepam Isomers Based on Retention Time

Isomer[a]	**(7,4')**	**(7,3')**	**(7,2')**	**(8,4')**	**(8,3')**	**(8,2')**	**(9,4')**	**(9,3')**	**(9,2')**
(9,2')	6.1%	5.9%	3.6%	6.4%	6.2%	4.6%	1.4%	1.2%	N/A
(9,3')	4.9%	4.8%	2.4%	5.3%	5.0%	3.4%	0.2%	N/A	1.2%
(9,4')	4.7%	4.5%	2.2%	5.1%	4.8%	3.2%	N/A	0.2%	1.4%
(8,2')	1.5%	1.3%	1.0%	1.8%	1.5%	N/A	3.2%	3.4%	4.6%
(8,3')	0.1%	0.2%	2.6%	0.3%	N/A	1.5%	4.8%	5.0%	6.2%
(8,4')	0.4%	0.5%	2.9%	N/A	0.3%	1.8%	5.1%	5.3%	6.4%
(7,2')	2.5%	2.4%	N/A	2.9%	2.6%	1.0%	2.2%	2.4%	3.6%
(7,3')	0.1%	N/A	2.4%	0.5%	0.2%	1.3%	4.5%	4.8%	5.9%
(7,4')	N/A	0.1%	2.5%	0.4%	0.1%	1.5%	4.7%	4.9%	6.1%

[a] Differentiation Threshold: ≥ 2.0%. (Green cells: ≥ 2.0%; orange cells: 1.0%-1.9%; red cells: < 1.0%; gray cells: duplicates or overlaps.)

However, the nine isomers evaluated were resolvable 80% of the time at a 1% threshold, which suggests that a new screening method could be developed to enable differentiation between benzodiazepine positional isomers. Moreover, an instrument with greater precision, or a different column, could allow for a lower threshold than 2% for differentiation.

3.2.3.2 EI Mass Spectral Data

The mass spectrum acquired by GC-MS for parent flubromazepam matched the NIST drug library reference and previously reported data by Moosmann, *et al*.[3] The expected molecular ion peak $M^{\cdot+}$ (chemical formula C15H10BrFN2O, 332 m/z) was present, as well as the $[M+2]^{\cdot+}$ peak (334 m/z) at nearly equivalent relative abundance correlating to the presence of a bromine atom. Mass spectra for the eight flubromazepam positional isomers also registered hits with ≥ 90% confidence against parent flubromazepam in the NIST drug library (Table 3-8). Major fragments included loss of CO, [M-28] and [M-26] (304 m/z and 306 m/z, respectively); loss of bromine, [M-79] (253 m/z); and loss of both CO and bromine [M-107] (223 m/z). Combined MS data are represented in Table 3-7; peaks were selected at ≥ 10% relative abundance based on recommendations from de Zeuww (Table 3-9) [4]. Copies of mass spectra may be found in Section 3.6.

Table 3-8: Combined MS Data for (X,X')-Flubromazepam Isomers

m/z	(7,2') parent	(7,3)	(7,4')	(8,2')	(8,3')	(8,4')	(9,2')	(9,3')	(9,4')
63	13%								
75	21%	19%	16%	14%	17%	15%	16%	23%	13%
76	13%							11%	
77	15%	11%		11%	10%		11%	12%	
81	11%								
85	15%	14%	14%	11%	11%	12%		14%	11%
89	11%								
95		11%			11%			11%	
98	11%								
99	13%	12%						12%	
102	30%	11%		17%			18%	12%	
103							12%		
104								10%	
107	11%								
109	10%								
112	18%	28%	21%	16%	15%	15%	13%	28%	17%
168	10%								
169	13%	13%	14%	11%	13%	13%	14%	19%	17%
170	15%	16%	15%	13%	15%	13%	11%	18%	15%
177	11%			11%					
182	12%	11%							
195	13%	12%	12%	10%	11%	11%	16%	19%	16%
196	15%	15%	15%	12%	15%	13%	15%	18%	18%
197	21%	23%	23%	18%	20%	21%	16%	21%	19%
198	12%	12%	11%					11%	
223	22%	28%	26%	17%	23%	22%	17%	25%	22%

224	15%	16%	15%	13%	14%	13%	14%	18%	17%
225	18%	21%	20%	13%	17%	17%	18%	24%	22%
252								11%	
253	11%	17%	19%	14%	18%	21%	12%	15%	18%
303	88%	77%	66%	63%	58%	53%	65%	74%	69%
304	90%	97%	100%	98%	100%	100%	60%	67%	83%
305	100%	100%	86%	94%	82%	71%	100%	100%	100%
306	89%	97%	94%	100%	100%	98%	57%	66%	77%
307	27%	28%	22%	25%	25%	20%	30%	33%	27%
313	21%			22%			25%		
315	23%			23%			28%		
331	68%	63%	57%	65%	63%	54%	74%	82%	85%
332	77%	75%	59%	55%	51%	44%	64%	66%	61%
333	66%	75%	65%	67%	69%	59%	85%	94%	90%
334	73%	72%	59%	53%	51%	41%	60%	67%	59%
335	14%	12%							

Table 3-9: Confidence Window for EI-MS Differentiation

Relative Intensity	Ion Abundance Precision
> 50 %	± 10 %
20 - 50 %	± 15 %
10 - 20 %	± 20 %
< 10 %	± 50 %

Unfortunately, due to these shared fragmentation patterns among flubromazepam isomers, mass spectrometry alone is likely not a suitable diagnostic for positional isomer differentiation. More rigorous statistical analysis will be required to determine if any individual diagnostic peaks based on relative abundance exist.

Interestingly, though, a key fragmentation pattern corresponding to the loss of fluorine, $[M-19]^{\cdot+}$ and $[M-17]^{\cdot+}$ (313 m/z and 315 m/z, respectively), is present at about 25% relative abundance for only the (X,2')-flubromazepam isomers; in contrast, for the other isomers, these peaks are present but at lower than 10% relative abundance, which is outside the recommended confidence window. Therefore, this mass spectrometry method could be employed to quickly gauge whether or not the fluorine atom is substituted at the 2' position.

3.2.4 GC-IR Results

Complete IR data for the flubromazepam are available in Section 3.7. Functional groups in the 4000-1600 cm^{-1} region were confidently assigned: the flubromazepam targets all exhibited a single N-H stretch with the amide formation, sp^2- and sp^3-C-H stretches as expected, and two strong peaks in the 1650-1550 cm^{-1} region corresponding to the amide C=O and imine C=N stretches.

Stretching and bending patterns were more distinctive in the fingerprint region of the IR based on the substitution patterns of the bromine and fluorine atoms on the two aromatic rings. More rigorous statistical analysis will be required, but it is interesting to note that isomers with the same bromine substitution but different fluorine substitution (and *vice versa*) display noticeable pattern similarities but have different spectra when taken as a whole (Figure 3-4). One highly evident example is the W-shape pattern from 1375-1320 cm^{-1} that is strong for the (7,3'), (7,4'), (8,3'), and (8,4') isomers, weak for the (7,2') and (8,2') isomers, and present in a simple V-shape around 1320 cm^{-1} for the (9,X') isomers.

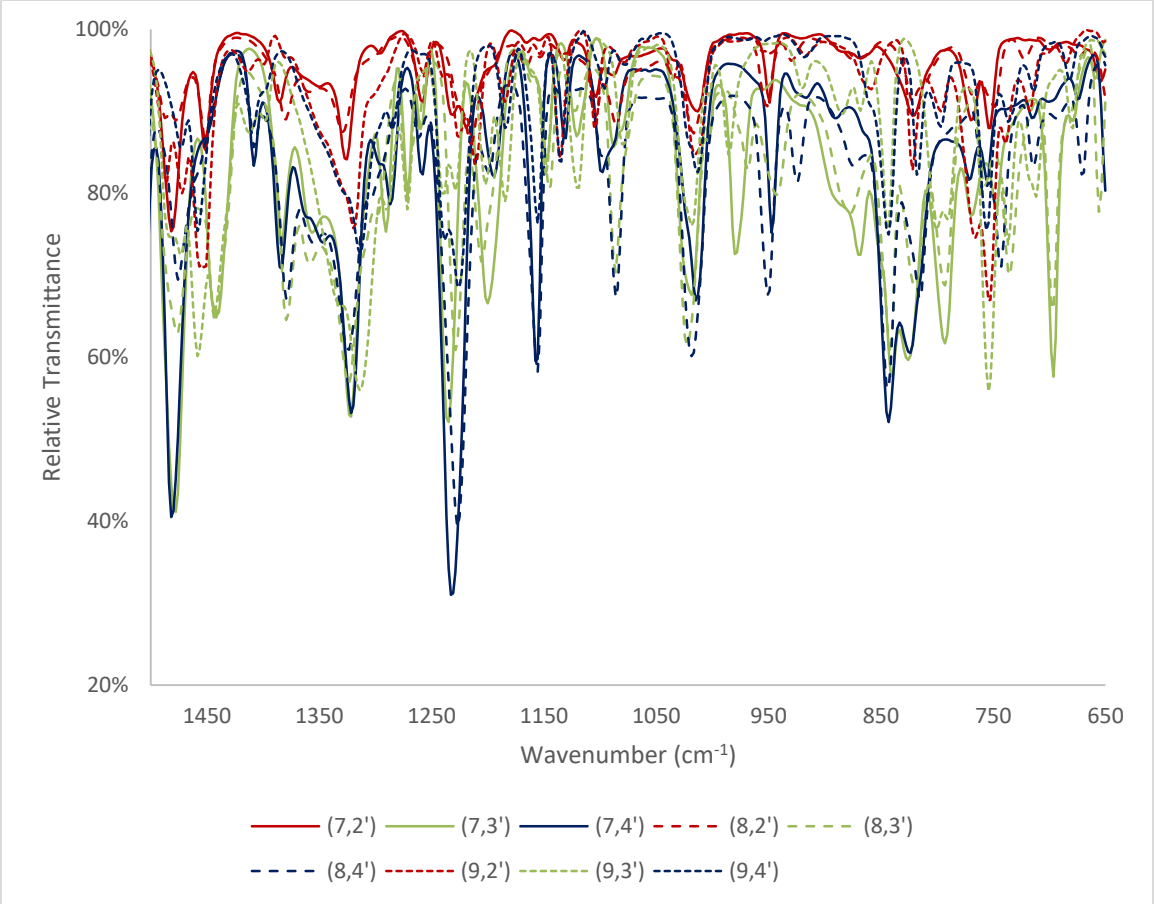

Figure 3-4: IR overlay for (X,X')-flubromazepam positional isomers.

3.3 Analytical Roadmap

Taking into account the characterization techniques available and results collected from the flubromazepam positional isomer standards, the following scheme may be recommended to distinguish between positional isomers.

First, GC-MS may be used as a baseline diagnostic for flubromazepam identity. The GC retention time (under the GC-MS Screen method described previously) should be within 7.6-8.1 minutes, and the mass spectrum should manifest a molecular ion peak of 332 m/z with a 1:1 $M^{\cdot+}$:$[M+2]^{\cdot+}$ pattern and a primary fragment at 304 m/z, also in a 1:1 $M^{\cdot+}$:$[M+2]^{\cdot+}$ pattern, corresponding to the loss of CO. Additionally, a specific diagnostic

for 315 m/z in a 1:1 $M^{\cdot+}$:$[M+2]^{\cdot+}$ pattern has been identified for (X,2')-flubromazepam isomers.

Next, IR is essential for determining isomeric identity. Primary differences between isomers are evident especially in the region from 1400-650 cm^{-1}. Direct comparison to standard reference data generated by this study is the most straightforward method to determine which isomer is present. It is possible also to choose representative peaks in one spectrum and compare manually to the other eleven isomer spectra to identify diagnostic peaks for a single isomer.

If IR should fail, or if the representative IR data is unavailable for the suspected isomer, NMR is a reliable method even without reference data, as it provides precise structural elucidation that isn't available with the other analytical techniques. With help from ^{13}C and ^{19}F NMR, which allow for confident assignment of the fluorine substitution, ^{1}H NMR may be employed to determine the exact bromine and fluorine substitutions on the ring based on multiplicity, coupling constant, and chemical shift.

3.4 Summary

In this study, characterization data were acquired for nine of the twelve possible positional isomers of flubromazepam. From these data sets, initial differentiation of the isomers was achieved, and an analytical roadmap was established. This roadmap may be employed in the future as a template to differentiate between positional isomers of additional benzodiazepines of interest.

3.5 Analytical Methods

3.5.1 Materials

1-Bromo-2-fluorobenzene (99% purity), 1-bromo-3-fluorobenzene (≥99% purity), 1-bromo-4-fluorobenzene (99% purity), hydrogen peroxide (30wt%/H_2O, ACS reagent), and *n*-butyllithium (2.5M/hexanes) were all purchased from Sigma-Aldrich. 3-Bromoisatin (>95% purity), 4-bromoisatin (98% purity), and 6-bromoisatin were purchased from Ark Pharm, Inc. 5-Bromoisatin (98% purity) and ammonia (7N/MeOH) were purchased from Acros Organics. *N,O*-Dimethylhydroxylamine hydrochloride (98% purity) was purchased from Oakwood Products. 2-(1*H*-Benzotriazol-1-yl)-1,1,3,3-tetramethyluronium hexafluorophosphate (HBTU, 98% purity) and 2-bromoacetylbromide (98% purity) were purchased from Alfa Aesar. Anhydrous dimethylformamide (DriSolv) and tetrahydrofuran (OmniSolv, unstabilized, HPLC/GC grade) were purchased from EMD Millipore. All reagents except for tetrahydrofuran were used directly without any additional purification. Tetrahydrofuran was distilled over sodium and benzophenone prior to use.

Solvents used for extraction and purification were: dichloromethane, diethyl ether, ethyl acetate, and hexanes, all ACS grade. Methanol (Optima grade) was purchased from Fisher Chemical and used to prepare GC and LC samples. For NMR analysis, deuterated dimethylsulfoxide (DMSO-d_6, 99.8% purity) was purchased from Acros Organics and deuterated chloroform ($CDCl_3$, 99.8% purity) was purchased from Cambridge Isotopic Laboratories, Inc.

Ammonium acetate buffer (15 mM, pH ~ 4 with acetic acid) was prepared for the polar LC mobile phase. Acetonitrile (Optima LC-MS grade) was purchased from Fisher Chemical and used for the non-polar LC mobile phase.

3.5.2 Sample Preparation

NMR samples were prepared at a concentration of 10mg/ml. Acid precursors and flubromazepam isomers were dissolved in deuterated dimethyl sulfoxide (DMSO-d_6); amide and benzophenone precursors were dissolved in deuterated chloroform ($CDCl_3$). Samples were prepared for GC-MS, GC-IR, and LC-MS from the NMR samples at a 1mg/ml concentration in MeOH.

3.5.3 Instrumental Methods

Flubromazepam targets and precursors were analyzed by liquid chromatography-high resolution accurate mass spectrometry (LC-HRAM-MSS) to determine exact mass, proton and carbon nuclear magnetic resonance ($^1H/^{13}C$ NMR) for structural validation, and subsequently analyzed by gas chromatography-mass spectrometry (GC-MS) and gas chromatography-infrared spectroscopy (GC-IR).

3.5.3.1 LC-HRAM-MS

A ThermoFisher Q-Exactive quadrupole Orbitrap tandem Mass Spectrometer (MSD) was coupled to a ThermoFisher Vanquish Liquid Chromatograph (LC) to determine the exact masses for the flubromazepam isomers. A sample volume of 10 μL was injected into the LC column at 35°C and a flow rate of 0.4 mL/min. Total run time was ten minutes. The mobile phase for the first 1.5 minutes was 3% acetonitrile (MeCN)/97% ammonium

acetate buffer, followed by a ramp up to 50% MeCN over 5 minutes. This mobile phase concentration was maintained for 1.5 minutes, then ramped down to 3% MeCN over 1 minute, followed by a 1-minute hold. The sample was transferred to the MSD via electrospray ionization in positive polarity mode, with a spray voltage of 3.5 kV and a capillary temperature of 350°C. The scanning range was 100-650 m/z, and the instrument calibrated for accuracy within 3 ppm. Thermo QualBrowser was employed for initial processing of exact mass data, including integrations and background subtractions. Molecular ion peaks were represented as $[M+H]^+$, and up to 5 decimal places were reported. Observed values were compared to values calculated by the QualBrowser software, and data were exported and plotted in Microsoft Excel 2010.

3.5.3.2 NMR

A Bruker 500-MHz spectrometer was used to record NMR data for the flubromazepam isomers. Locking, shimming, and tuning were performed automatically using the Bruker Topspin 3.2 software. Average spin speed per sample was 22 Hz. For ^{1}H NMR, sixteen scans at 3.28 seconds each were run. For ^{13}C NMR, which was proton-decoupled, up to 2048 scans at 3.28 seconds each were run, until the signal-to-noise ratio was at least 3:1. For ^{19}F NMR, which was proton-coupled, sixteen scans at 2.69 seconds each were run.

Deuterated dimethylsulfoxide [DMSO-d_6, $(CD_3)_2SO$] (^{1}H: 2.50 ppm; ^{13}C: 39.5 ppm) was employed as an internal resonance standard. NMR spectra were analyzed using MestreNova software (v. 11.0). Integration and peak picking were performed manually, and multiplet analysis and *J* value reporting were performed automatically on the selected peaks. ^{1}H NMR data are reported as follows: chemical shift (ppm), multiplicity (s = singlet,

d = doublet, t = triplet, m = multiplet, br = broad), coupling constants (Hz), and integration. ^{13}C NMR data are reported as proton-decoupled chemical shifts (ppm); when coupled to a fluorine atom, multiplicities (d = doublet) and coupling constants (Hz) are also reported. ^{19}F NMR data are proton-coupled and reported as follows: chemical shift (ppm), multiplicity (s = singlet, d = doublet, t = triplet, m = multiplet, br = broad), and coupling constants (Hz).

3.5.3.3 GC-MS

An Agilent 5977A quadrupole MSD coupled with an Agilent 7890B Gas Chromatograph (GC) was used to analyze the flubromazepam isomers. The GC inlet was heated to 250°C, and 1.0 µL of the sample was injected into a splitless, single taper, ultra-inert liner (Agilent 5190-2293) with a 100:1 split. Hydrogen carrier gas moved the vaporized sample at a flow rate of 1 ml/min onto a Restek Rxi-1ms column (13302, 20m x 180 um x 0.18 um) with initial oven temperature of 120°C. After a hold time of 2 minutes, temperature increased at a ramp rate of 25°C/min until oven temperature reached 300°C, followed by a 4-minute hold time. The sample was transferred through the MSD transfer line at 250°C, followed by electron impact ionization (70 eV). Data collection began after a solvent delay of 0.5 minutes. Total run time was 13.2 minutes. Data were exported from MassHunter Enhanced Data Analysis and plotted in Microsoft Excel 2010. Purity of each peak was validated by the Percent Report and Peak Purity features. Retention times were reported up to 3 decimal places, and the corresponding mass spectra were analyzed for major fragmentation patterns. Peaks with greater than or equal to 10% abundance relative to the base peak were considered. The confidence window employed for potential differentiation based on mass spectral relative abundance is shown in Table 3-9.

3.5.3.4 GC-IR

A Spectra Analysis DiscovIR-GC coupled with an Agilent 7890A GC was used to analyze the flubromazepam isomers. The GC inlet was heated to 250°C, and 1.0 µL of the sample was injected with a 2:1 split. Nitrogen carrier gas moved the vaporized sample (gas pressure: 25.36 psi) onto a 5ms column (5% diphenyl/95% dimethyl: 30m x 250 um x 0.25 um) with initial oven temperature of 120°C. After a hold time of 1 minute, temperature increased at a ramp rate of 25°C/min until oven temperature reached 290°C, followed by a 7.2-minute hold time. The sample was transferred through the IR transfer line at 250°C, then deposited onto a disk at -40°C to form a plasma. Disk spin speed was 3 mm/min. Total run time was 15 minutes. IR data were processed in Grams for baseline correction, then exported to Microsoft Excel 2010 for plotting. Peaks were selected for analysis by setting signal-to-noise at 10:1 relative to the total range and determining local minima. Manual de-selection was performed to remove duplicates or ill-defined humps from major peaks.

3.6 Copies of MS Data

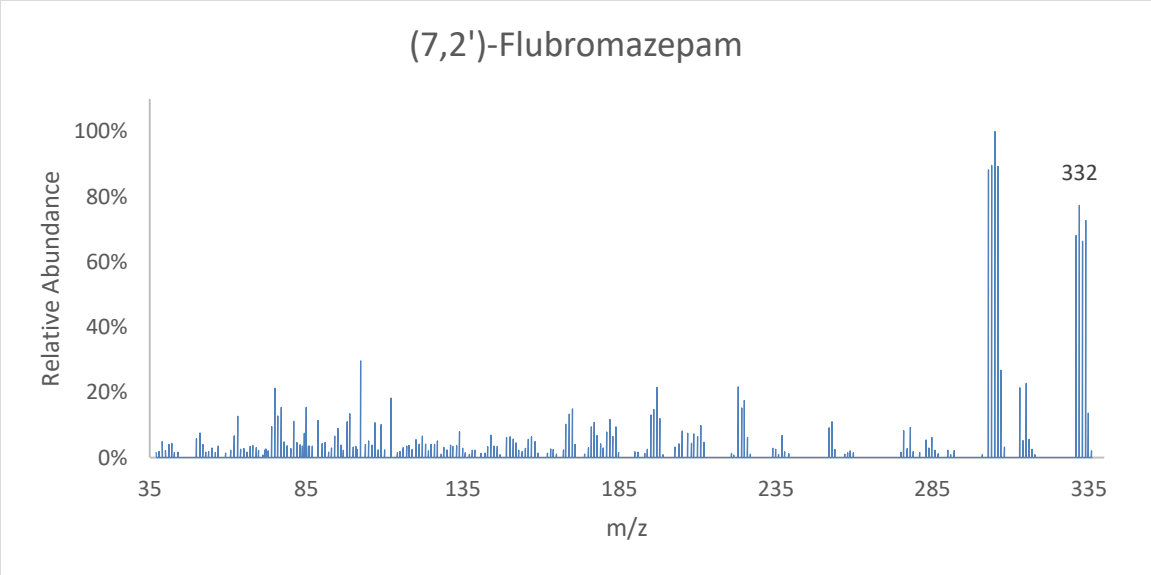

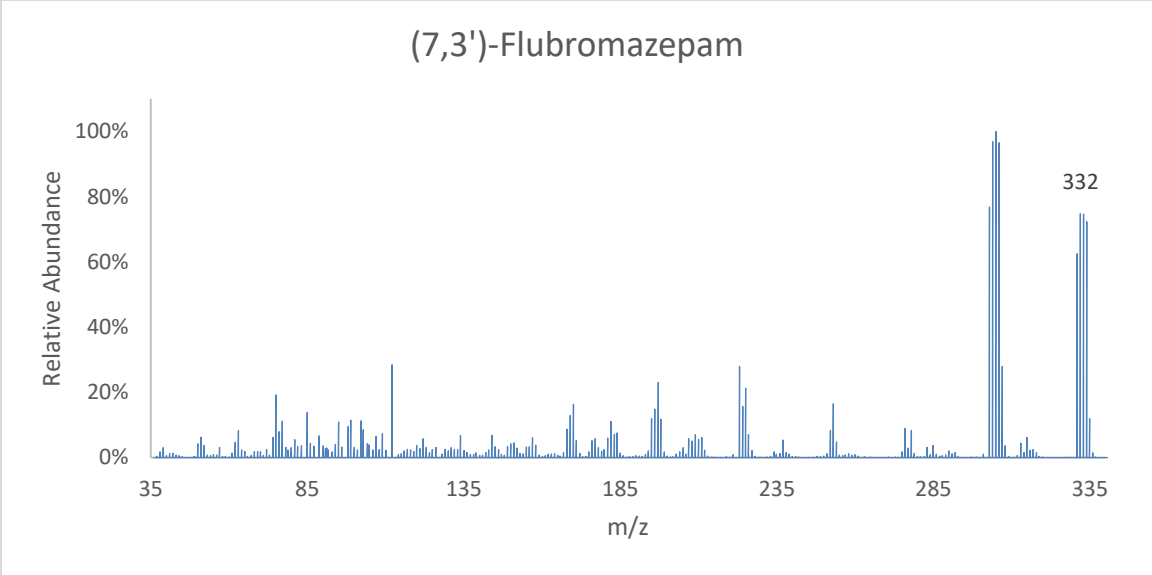
(7,3')-Flubromazepam
Relative Abundance
100%
80%
60%
40%
20%
0%
35
85
135
185
235
285
335
m/z
332

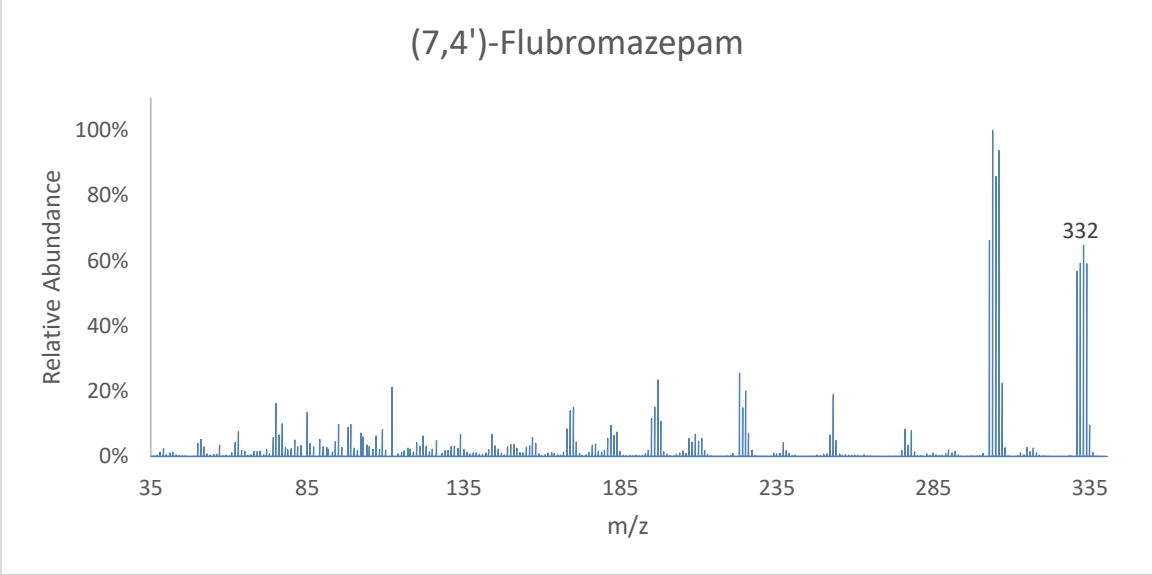
(7,4')-Flubromazepam
Relative Abundance
100%
80%
60%
40%
20%
0%
35
85
135
185
235
285
335
m/z
332

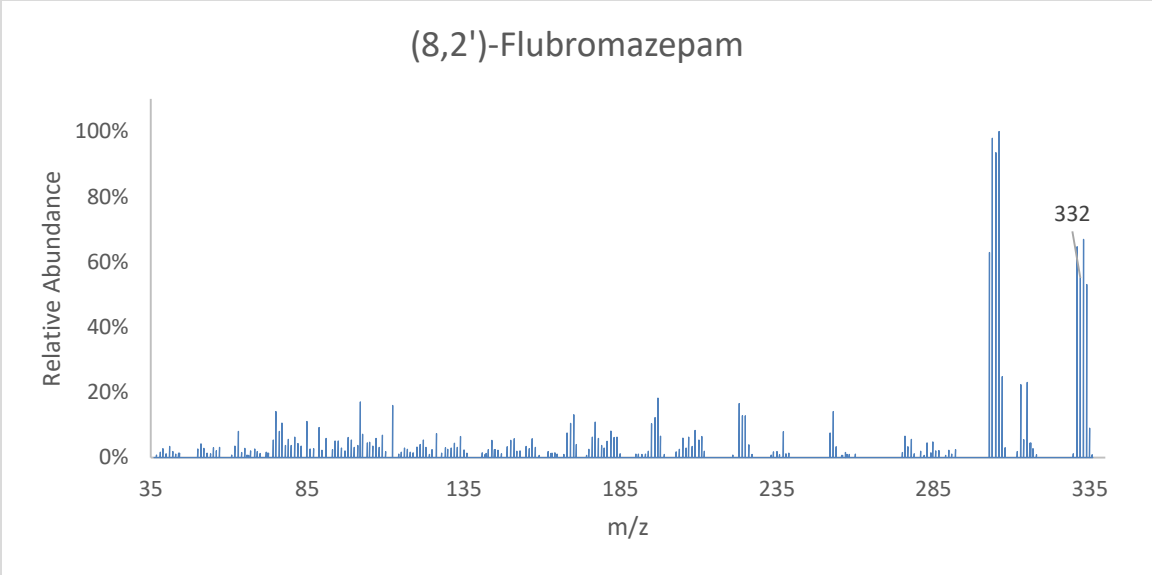
(8,2')-Flubromazepam
Relative Abundance
100%
80%
60%
40%
20%
0%
332
35
85
135
185
235
285
335
m/z

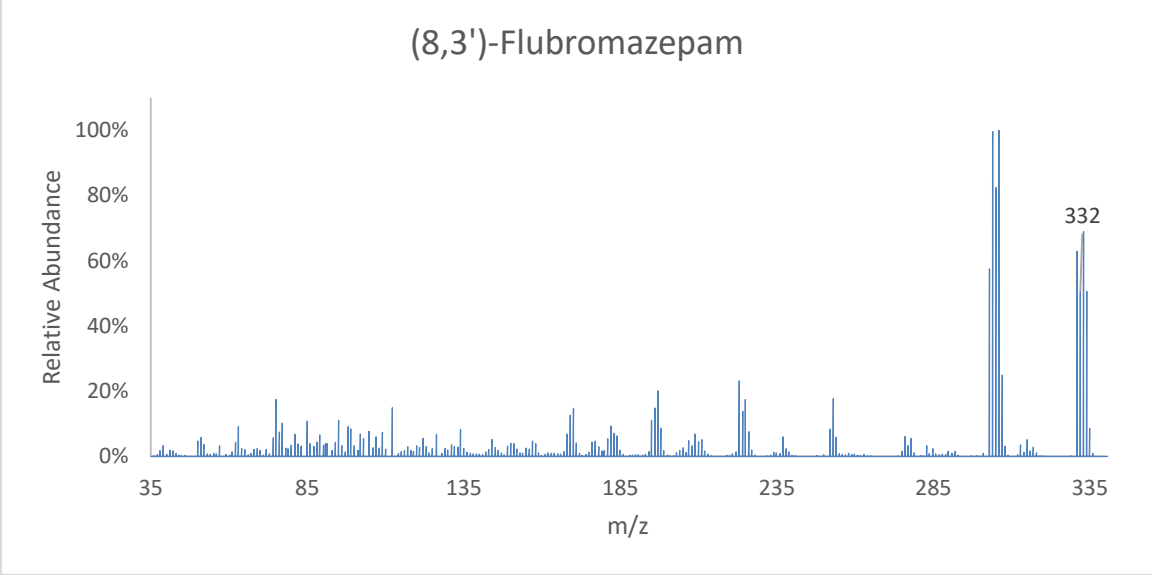
(8,3')-Flubromazepam
Relative Abundance
100%
80%
60%
40%
20%
0%
332
35
85
135
185
235
285
335
m/z

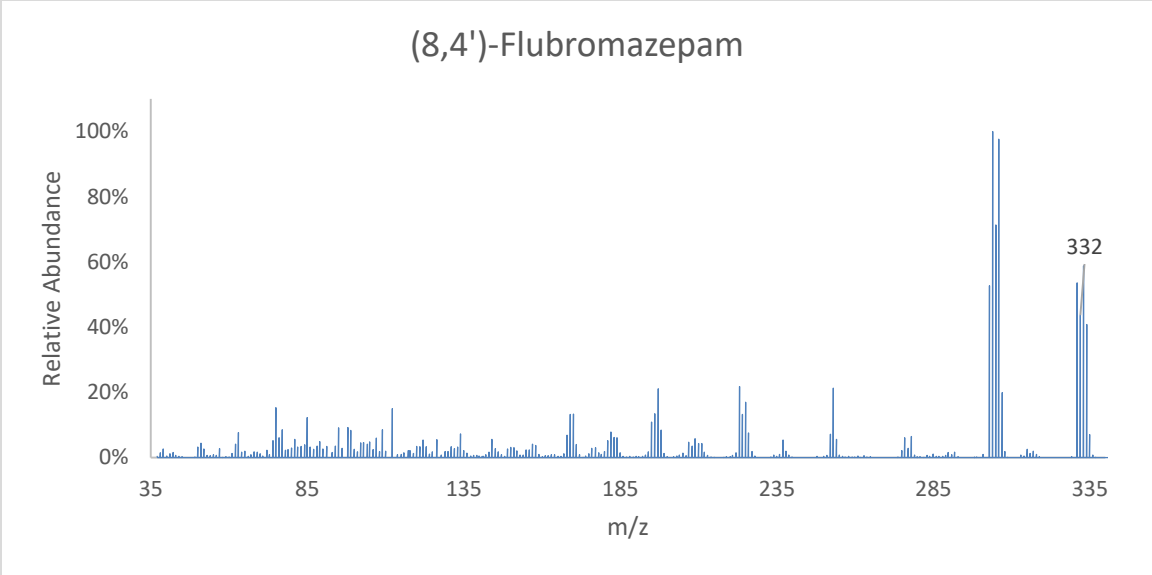
(8,4')-Flubromazepam
Relative Abundance
100%
80%
60%
40%
20%
0%
332
35
85
135
185
235
285
335
m/z

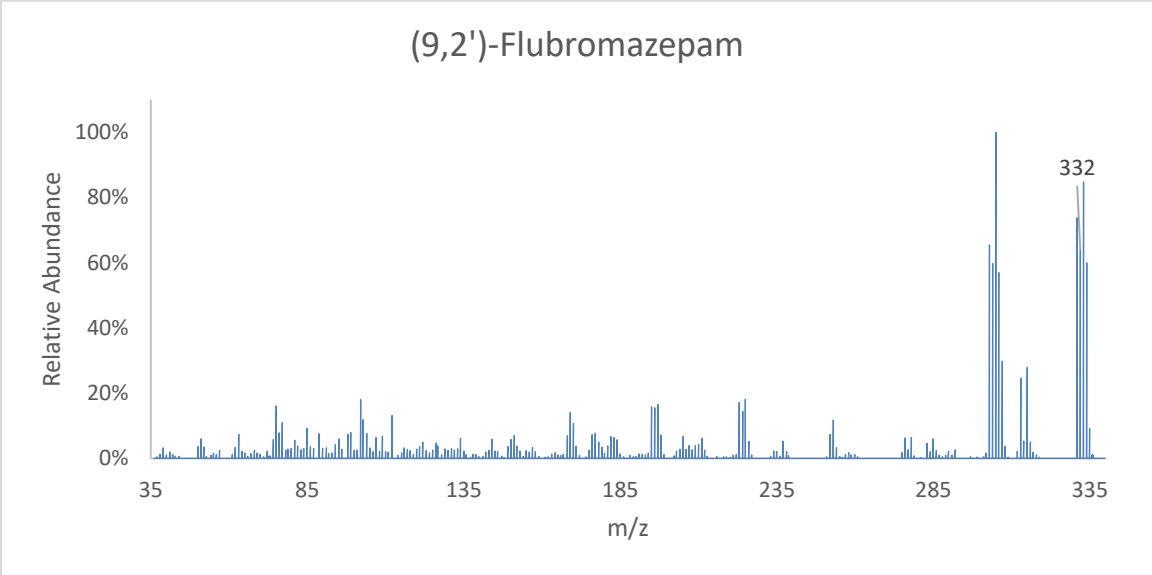
(9,2')-Flubromazepam
Relative Abundance
100%
80%
60%
40%
20%
0%
332
35
85
135
185
235
285
335
m/z

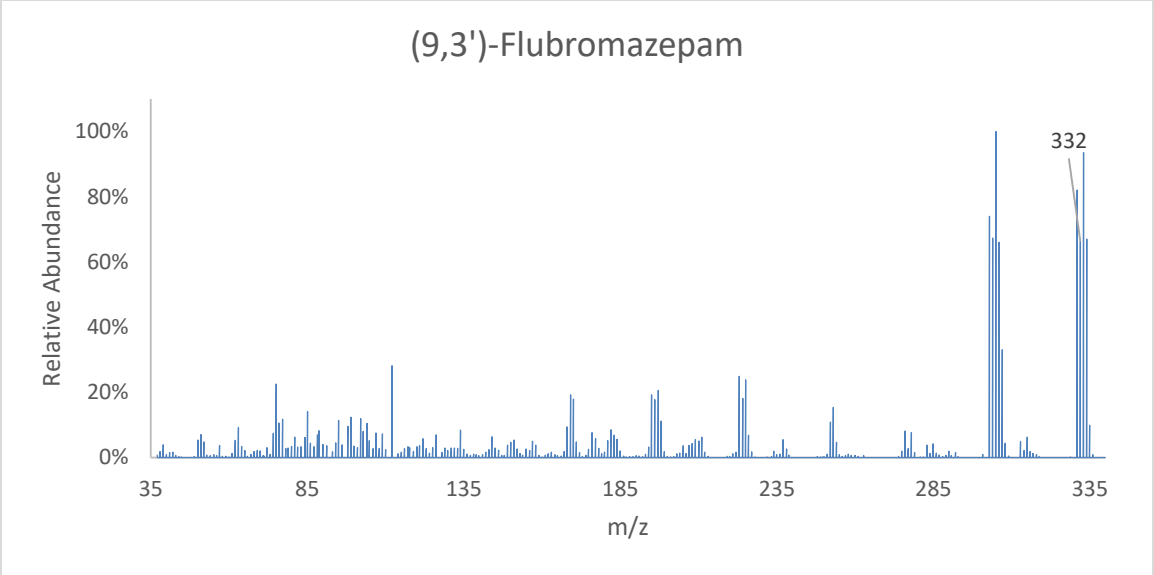
(9,3')-Flubromazepam
Relative Abundance
100%
80%
60%
40%
20%
0%
35
85
135
185
235
285
335
m/z
332

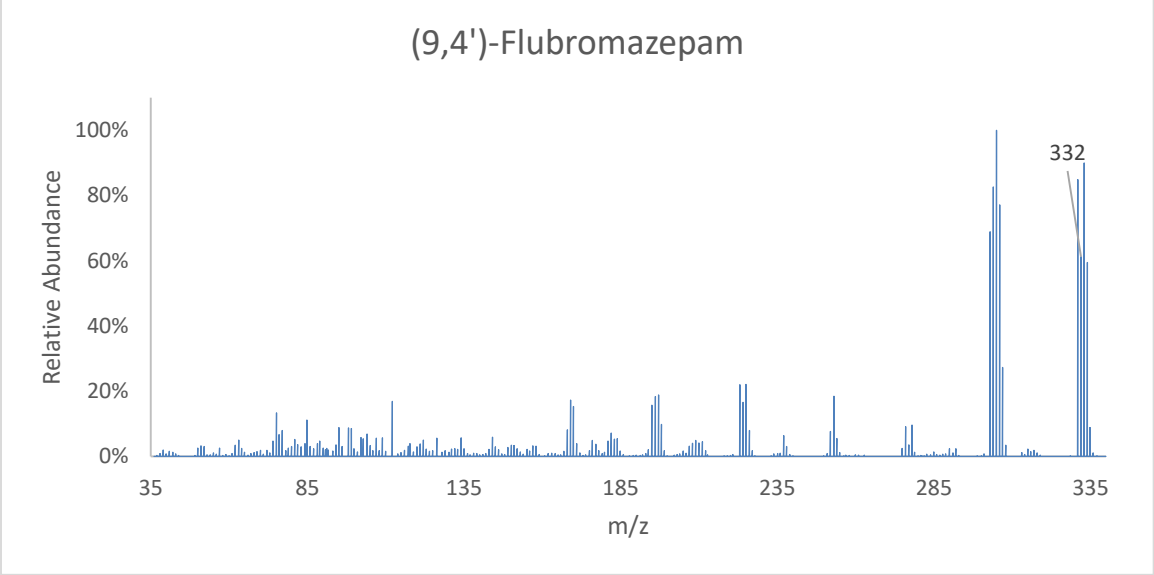
(9,4')-Flubromazepam
Relative Abundance
100%
80%
60%
40%
20%
0%
35
85
135
185
235
285
335
m/z
332

3.7 Copies of IR Data

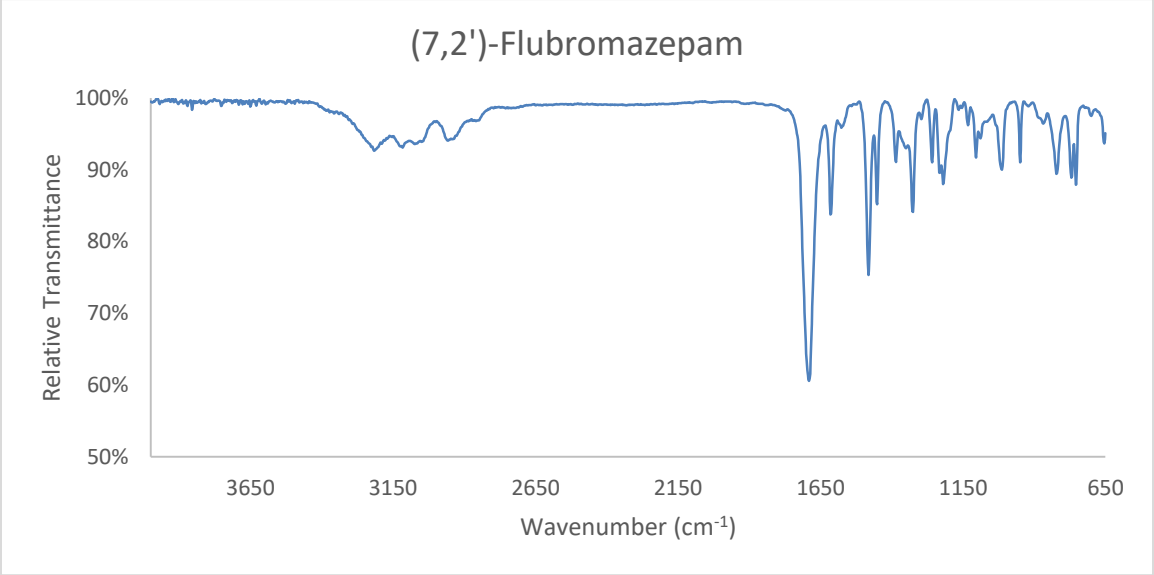

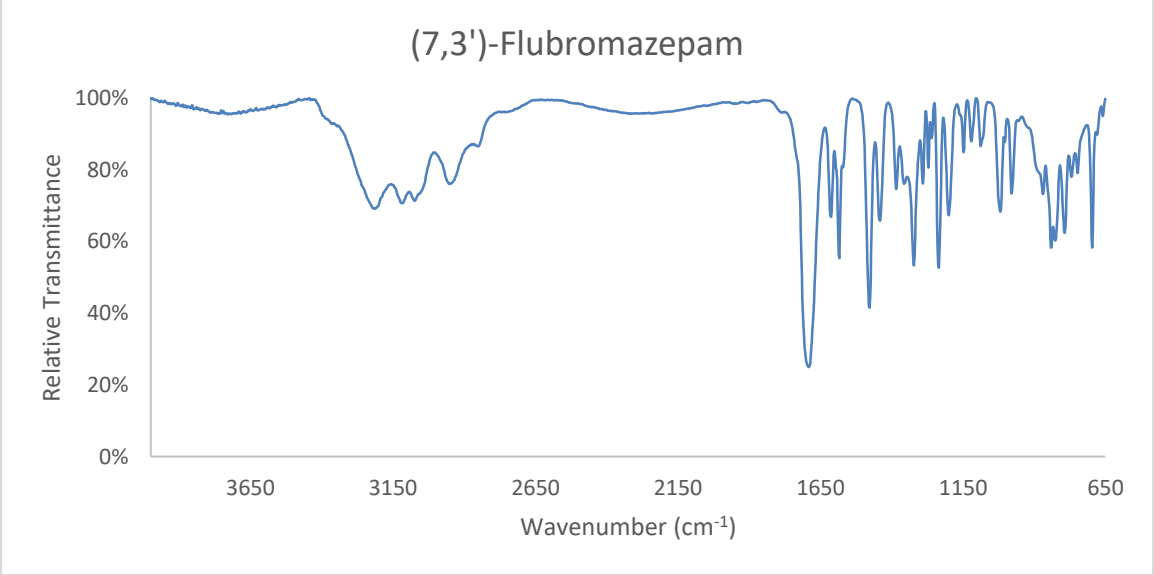

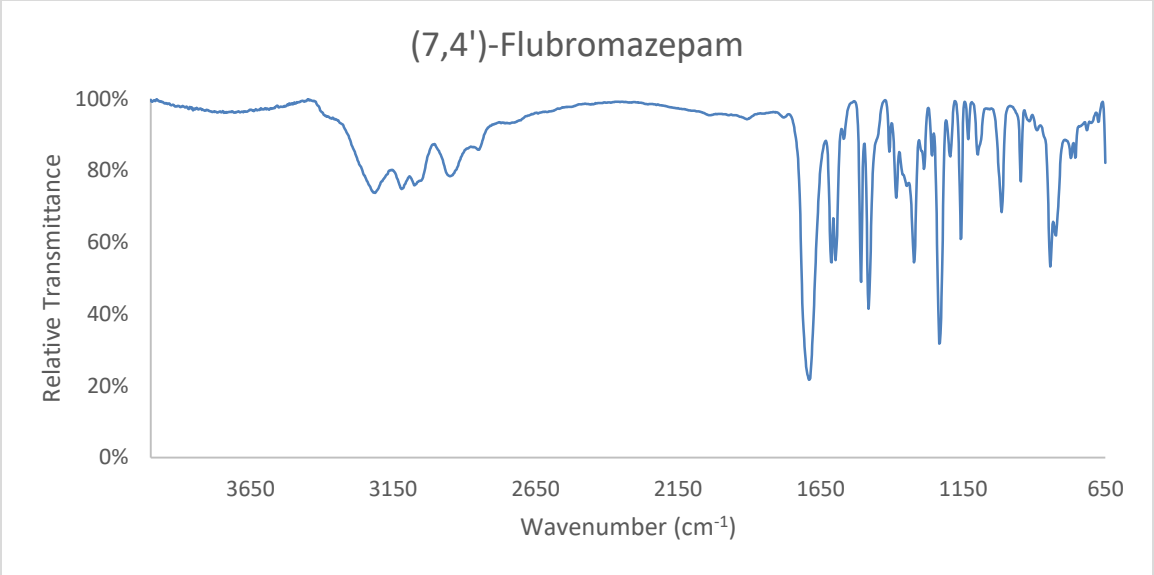
(7,4')-Flubromazepam
Relative Transmittance
100%
80%
60%
40%
20%
0%
3650
3150
2650
2150
1650
1150
650
Wavenumber (cm-1)

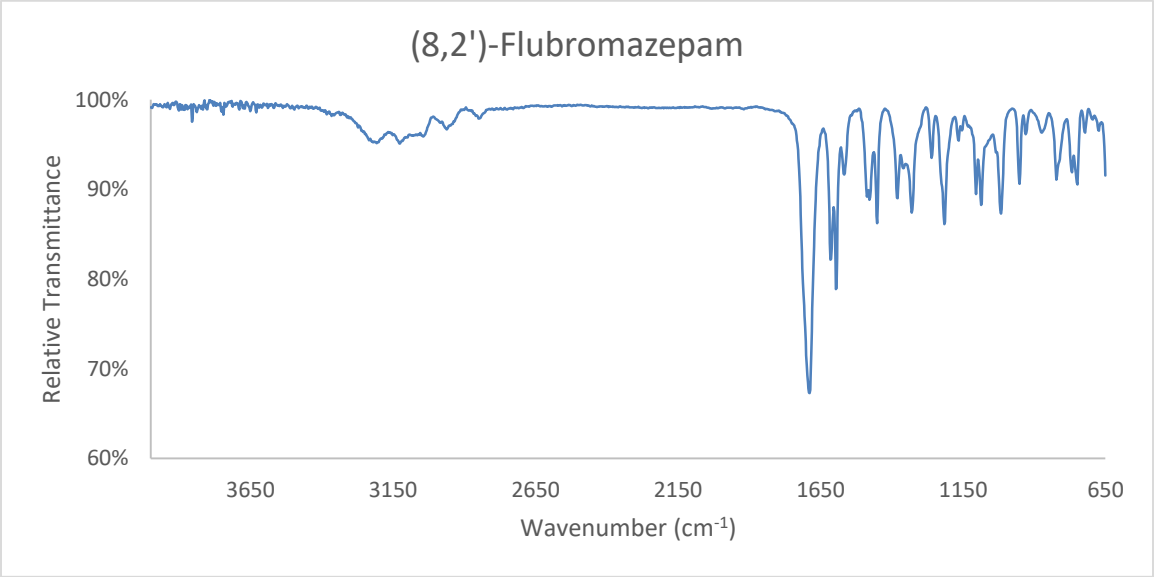
(8,2')-Flubromazepam
Relative Transmittance
100%
90%
80%
70%
60%
3650
3150
2650
2150
1650
1150
650
Wavenumber (cm-1)

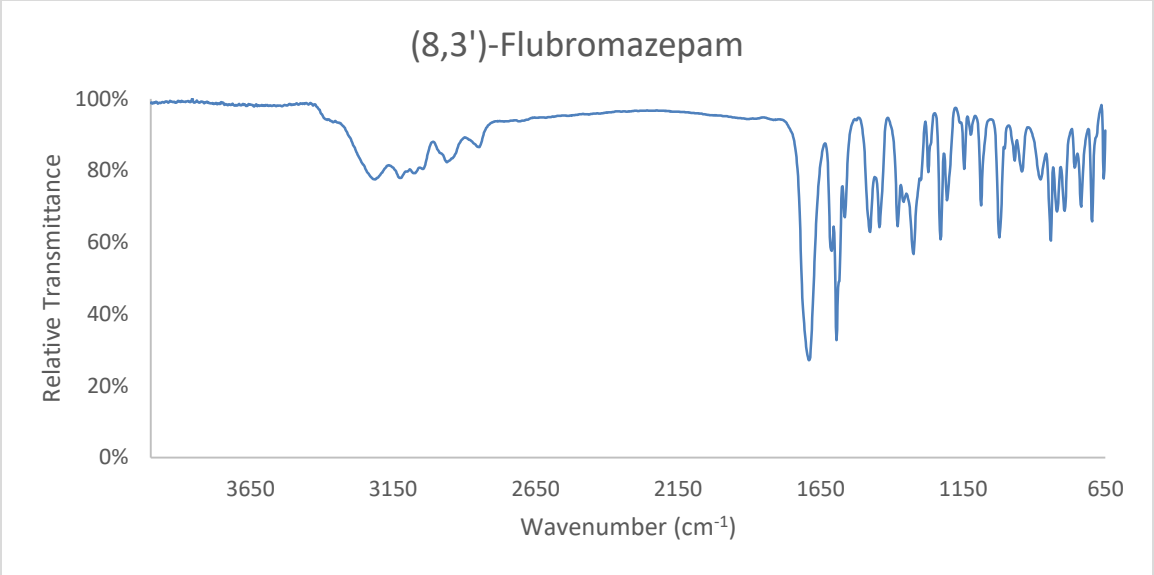
(8,3')-Flubromazepam
100%
80%
60%
40%
20%
0%
Relative Transmittance
3650
3150
2650
2150
1650
1150
650
Wavenumber (cm-1)

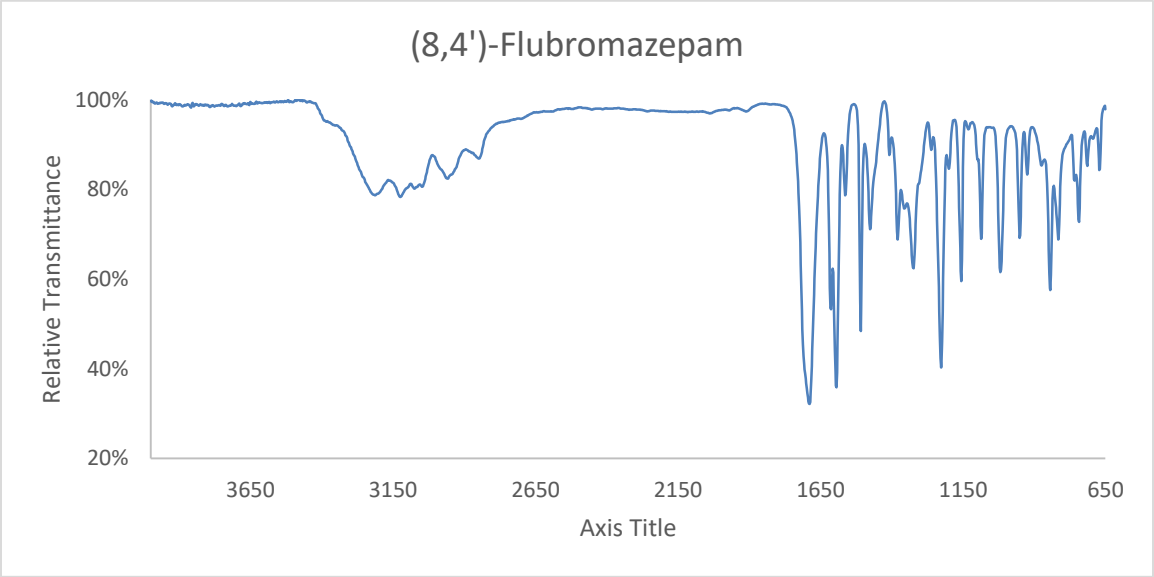
(8,4')-Flubromazepam
100%
80%
60%
40%
20%
Relative Transmittance
3650
3150
2650
2150
1650
1150
650
Axis Title

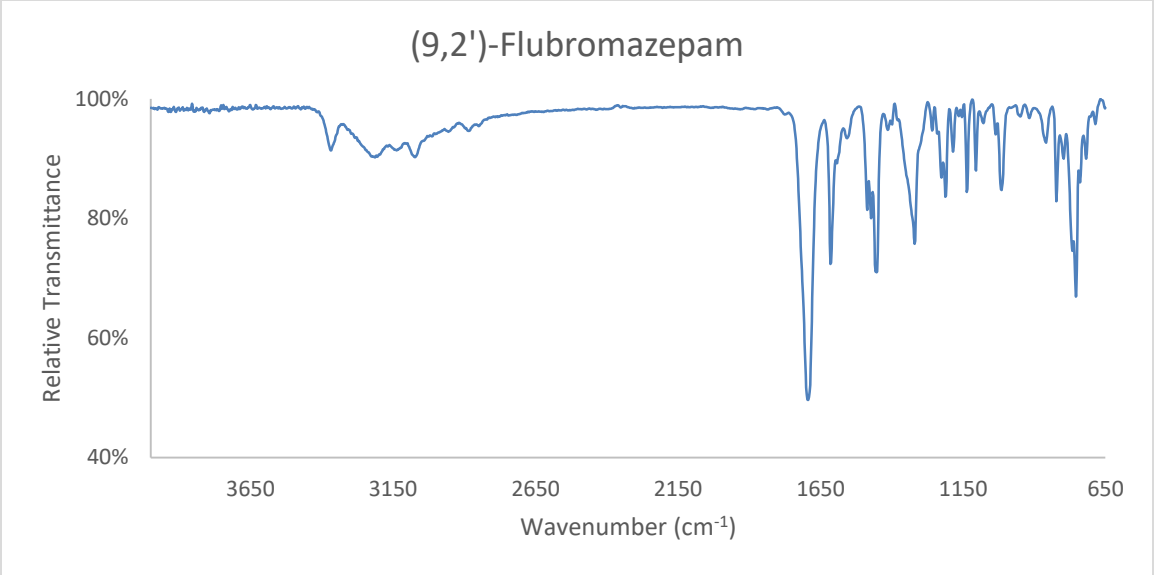
(9,2')-Flubromazepam
Relative Transmittance
100%
80%
60%
40%
3650
3150
2650
2150
1650
1150
650
Wavenumber (cm-1)

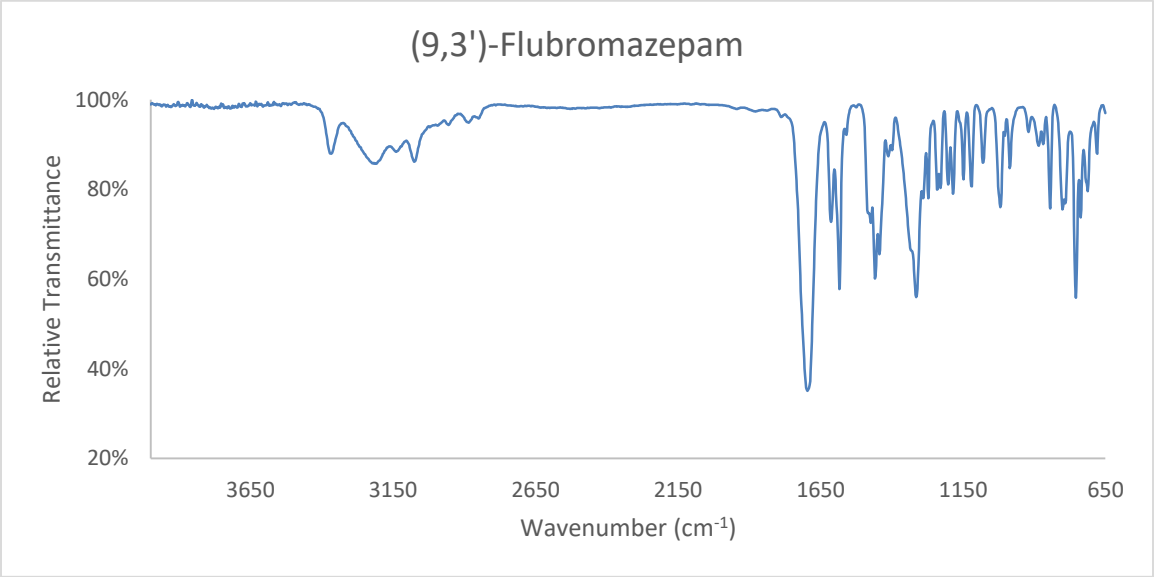
(9,3')-Flubromazepam
Relative Transmittance
100%
80%
60%
40%
20%
3650
3150
2650
2150
1650
1150
650
Wavenumber (cm-1)

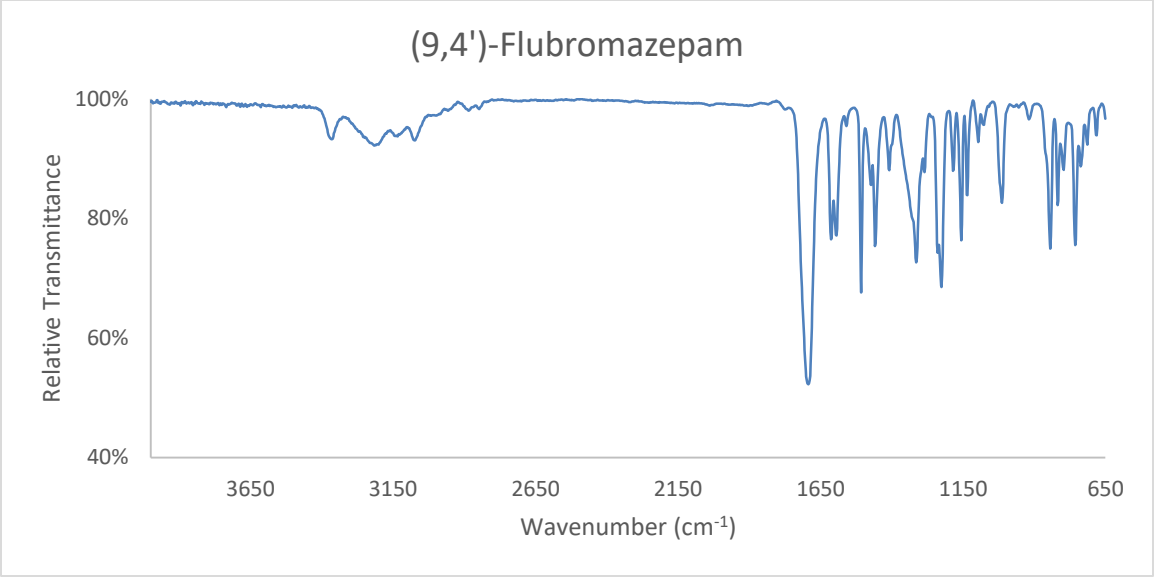

3.8 References

(1) Alberti, M.J.; Jung, D.K. Chemical Compounds. WO 2006/044753 A2, **2006**.

(2) Cortés Cortés, E.; Ebromares Martínez, I.; García Mellado, O. Synthesis and Spectral Properties of 7-Chloro-5-[(*o*- and *p*-R1)phenyl]-1-R2-3*H*-[1,4]benzodiazepin-2-ones. *J. Heterocyclic Chem.* **2002**, *39*, 1189-1193.

(3) Moosmann, B.; Huppertz, L. M.; Hutter, M.; Buchwald, A.; Ferlaino, S.; Auwärter, V. Detection and identification of the designer benzodiazepine flubromazepam and preliminary data on its metabolism and pharmacokinetics. *J. Mass. Spectrom*. **2013**, *48*, 1150-1159.

(4) de Zeeuw, R.A. Substance identification: the weak link in analytical toxicology. *J. Chromatogr. B* **2004**, *811*, 3-12.

CHAPTER 4. TOWARD AN INTRAMOLECULAR FRIEDEL-CRAFTS-TYPE RING-OPENING CYCLIZATION OF DONOR-ACCEPTOR C5-SUBSTITUTED BICYCLO[3.1.0]HEXANES

4.1 Donor-Acceptor Bicyclo[3.1.0]hexanes: An Understudied Class of DACPs

Donor-acceptor cyclopropanes (DACPs) have been showcased by the France lab and others as valuable synthons in ring-expansion chemistries to access complex, richly substituted hetero- and polycyclic frameworks found in important natural products.[1] Chapters 4 and 5 focus on recent efforts directed toward an understudied class of DACPs, donor-acceptor bicyclo[3.1.0]hexanes, as viable precursors to bioactive natural products containing fused or bridged bicyclic moieties. These compounds are essentially tethered DACPs, as the acceptor carbon is tethered to one of the vicinal carbons (C6 or C5; Scheme 4-1) by a three-atom linker.

In the left-hand reaction pathway, a donor-acceptor bicyclo[3.1.0]hexane with the electron-donating group situated at C6 results in a five-membered cyclic 1,3-dipole with an acyclic secondary carbocation upon ring-opening and a fused bicyclic scaffold upon cyclization. This transformation will be discussed in Chapter 5.

In the right-hand reaction pathway, a bicyclo[3.1.0]hexane with the electron-donating group situated at C5 results in a six-membered cyclic 1,3-dipole with an endocyclic tertiary carbocation upon ring-opening and a bridged bicyclic scaffold upon cyclization. A representative example of this latter scaffold is found in tronocarpine, which was a key part of the inspiration for this chapter.

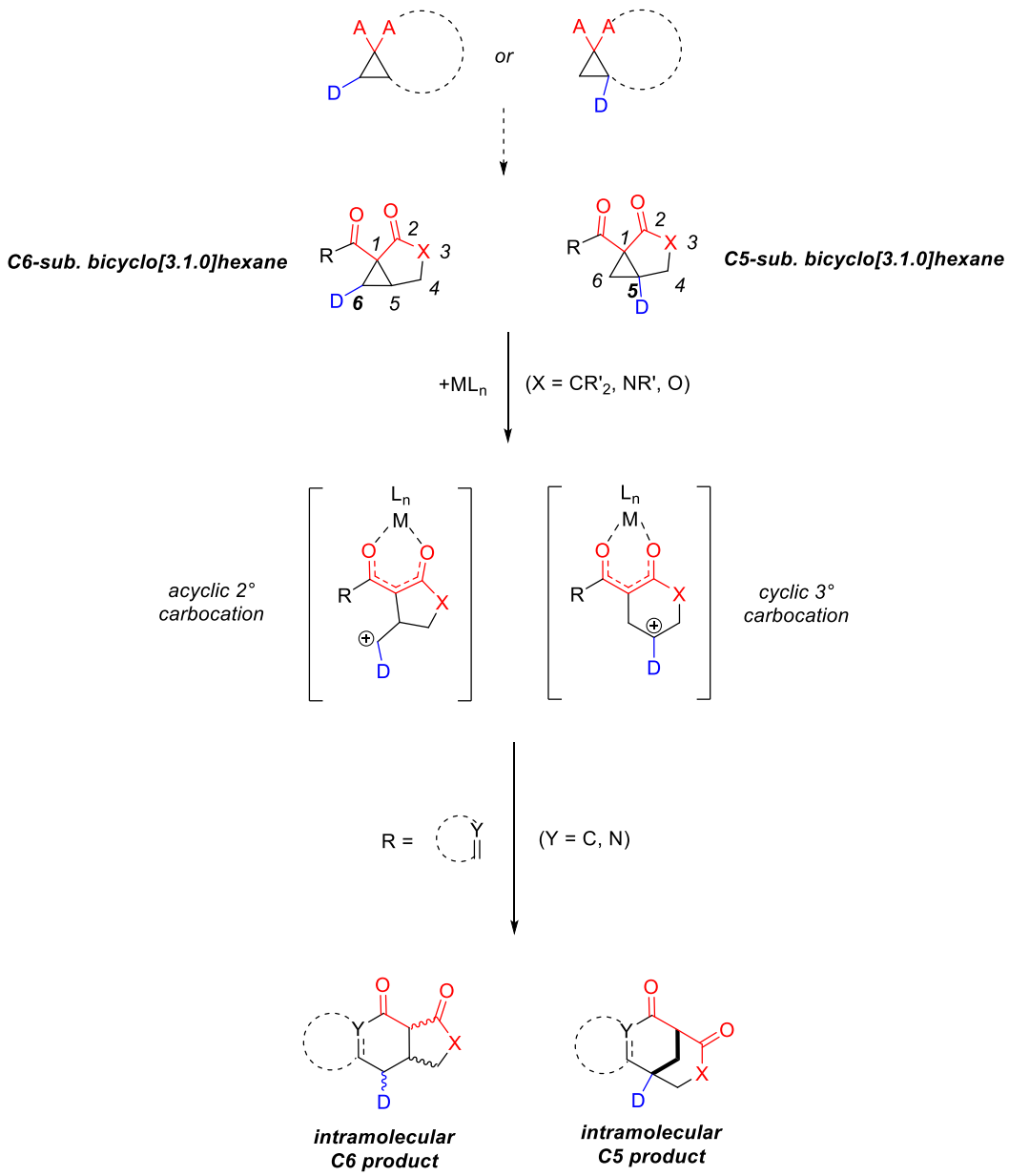

Scheme 4-1: Expected intramolecular reaction pathways of C6- and C5-substituted donor-acceptor bicyclo[3.1.0]hexanes.

Despite the undeniable utility of a one-step ring-opening cyclization to bridged bicyclic scaffolds, donor-acceptor bicyclo[3.1.0]hexanes have been showcased almost exclusively in applications to prepare ring-expanded fused bicycles (for representative examples, see Chapter 5). In fact, there are only two literature examples employing a C5-

substituted synthon. The first application was mentioned in Chapter 1 from Stork and Grieco (Scheme 4-2).[2] They showcased an intramolecular Michael-type addition of an anisole moiety onto a C5-methyl-substituted bicyclo[3.1.0]hexane to form a tricyclic scaffold, albeit fused rather than the desired bridged structure described above.

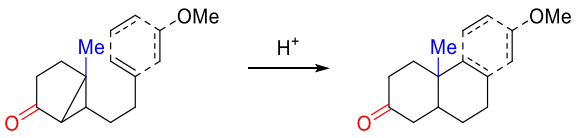

Scheme 4-2: Michael-type cyclizations of D-A cyclopropyl ketones.

The second example is an intermolecular application from Jiang and co-workers.[3] They presented a simple methyl-substituted donor-acceptor bicyclo[3.1.0]hexane that undergoes $SnCl_4$-catalyzed ring-opening, elimination, and acid-promoted isomerization to form an α,β-unsaturated cyclohexanone, which is further reacted in a Michael-type addition with 1,3,5-trimethoxybenzene (Scheme 4-3). This was the only example of this scaffold in the article, and this work was not probed further by the authors.

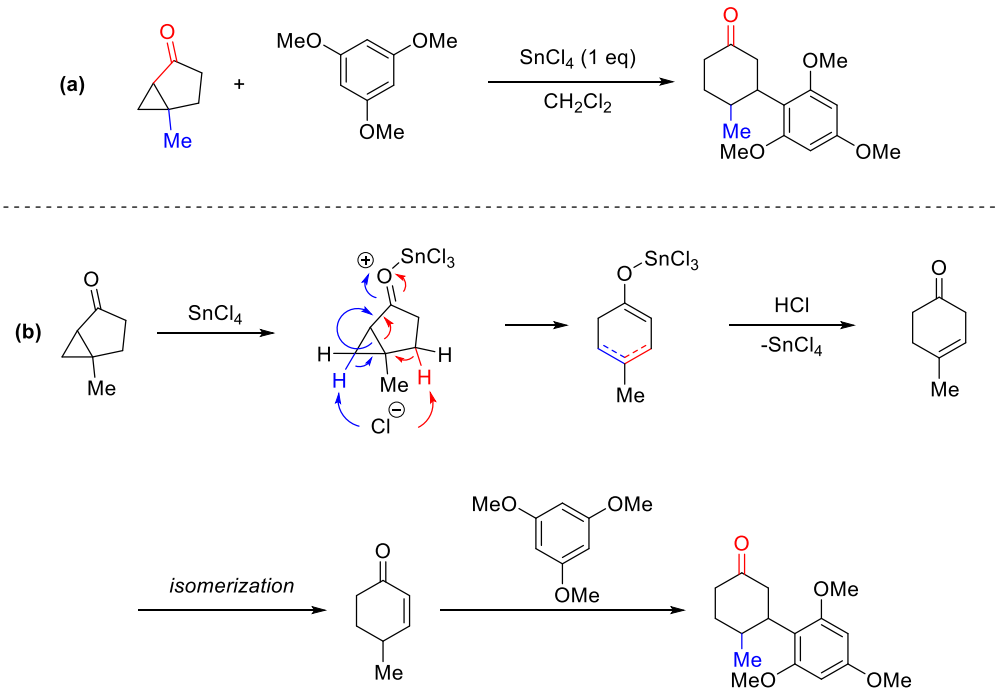

Scheme 4-3: (a) Jiang's example of $SnCl_4$-mediated D-A bicyclo[3.1.0]hexane ring-opening. (b) Mechanism proposed by the authors.

Nevertheless, these results do suggest that C5-substituted donor-acceptor bicyclo[3.1.0]hexanes may proceed by the polar ring-opening pathway described in Scheme 4-1. Whether a localized carbocation forms to be subsequently trapped, or a nucleophile is required to act as the driving force for ring-opening (as suggested by the example above), is a question that this study seeks to answer.

4.2 Hypothesis

With tronocarpine in mind, I hypothesized that the crucial bridged bicyclic moiety could be accessed through an intramolecular Friedel-Crafts-type ring-opening cyclization of heteroaromatic-tethered, C5-substituted donor-acceptor bicyclo[3.1.0]hexane. Using the *N*-acyl scaffold of tronocarpine as a model (as shown in Scheme 4-4), and following the previously established polar mechanism for intramolecular ring-opening cyclizations of *N*-

acyl-tethered DACPs, the bridgehead bond would cleave in the presence of a Lewis acid to form a localized tertiary carbocation, which would be trapped by the pendant indole to afford the bridged bicyclic moiety and be subsequently rearomatized. It should be noted that this proposed mechanism does not violate Bredt's rules, as it was shown by Wiseman and co-workers that a double bond is allowed at the bridgehead carbon in larger ring systems (i.e. 8+ atoms), which would allow for the enolate-type bicyclic intermediate.[4] This mechanism would be further applied to C2- and C3-tethered (benzo)furan and (benzo)thiophene scaffolds, as encompassed in Scheme 4-1.

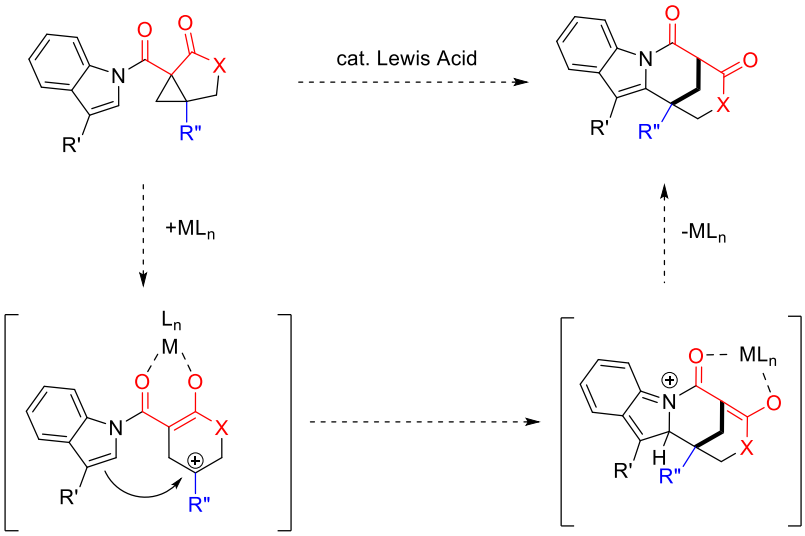

Scheme 4-4: Hypothesized intramolecular ring-opening cyclization to the tronocarpine core.

4.3 Model Systems for the Intramolecular Ring-opening Cyclization

From the outset of this research project, the plan was to establish the intramolecular ring-opening cyclization of an *N*-acyl indole-tethered D-A bicyclo[3.1.0]hexane, as a successfully developed method could subsequently be applied to the first total synthesis of tronocarpine. Thus, the first iterations of a proof-of-concept model all contain 3-methylindole as the heterocyclic nucleophile. Additional parameters to survey include

different heterocyclic nucleophiles such as benzofuran and thiophene; different acceptor groups such as ketone, ester, and amide; different donor groups, including a β-silane for its synthetic utility in Fleming-Tamao oxidations; and different ring sizes to probe entropic and stereochemical effects (Figure 4-1).

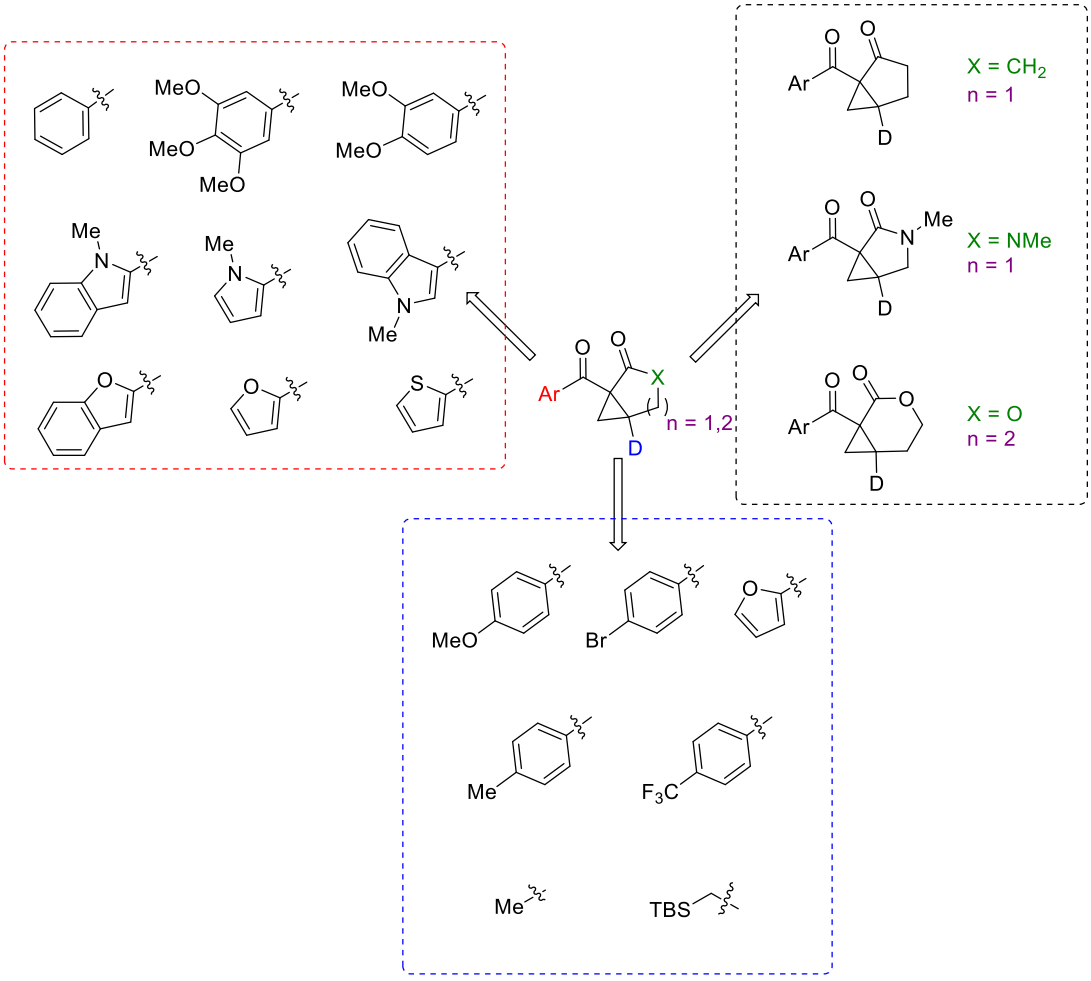

Figure 4-1: Envisioned substrate scope for C5-sub. D-A bicyclo[3.1.0]hexane template.

4.3.1 First Indole-tethered Model System

For the indole-tethered model, I initially envisioned a synthetic route that would install the indole moiety at the end of the synthesis. This approach would open the door to

synthesizing multiple bicyclo[3.1.0]hexane templates and pairing them with various heterocyclic nucleophiles to test the method's robustness, ultimately making the method more convergent. The general retrosynthetic analysis (Scheme 4-5) demonstrates the ring-opening cyclization adduct **49** that would arise from the *N*-acyl C5-substituted bicyclo[3.1.0]hexane **50**, after *N*-acylation of the methyl ester **51**. Intramolecular cyclopropanation would occur from the diazo alkene **52**; the diazo transfer would be effected following a nucleophilic addition of commercially available methyl acetoacetate (**53**) and allylic electrophile **54**, which may be prepared from allyl alcohol **55**.

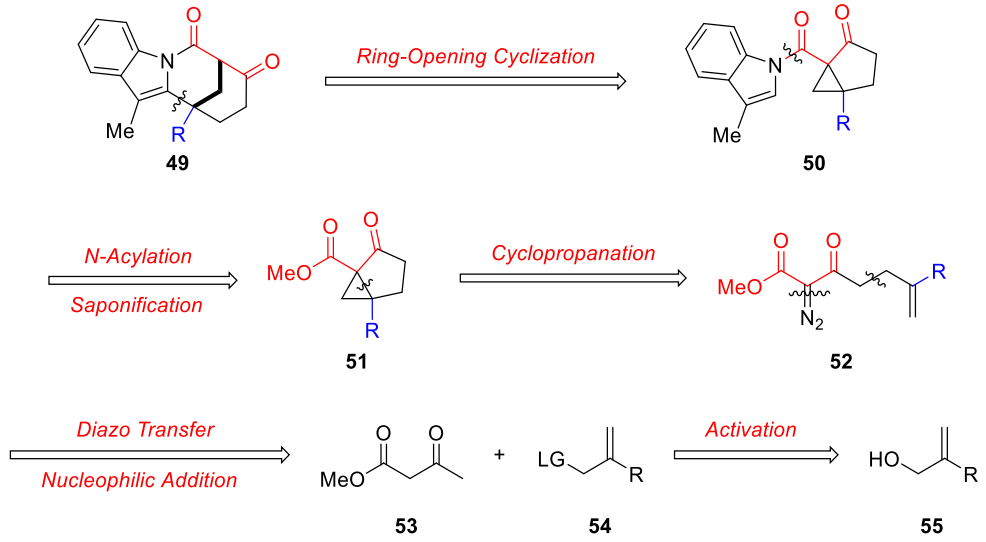

Scheme 4-5: General retrosynthetic analysis of tronocarpine model system.

The optimized synthetic route for the first indole-tethered model is shown below (Scheme 4-6) and will be discussed in the subsequent section. A silyl ether-protected β-alcohol was selected as the donor group, in hopes that this substituent would be donating enough to effect ring-opening and facilitate later access to the lactam carbonyl *via* deprotection and oxidation. Employing 2-methylene-1,3-propanediol (**56**) as the starting material, *tert*-butyldiphenylsilyl chloride (TBDPSCl) was selected as the protecting agent

for its UV activity (leading to enhanced visualization) and its stability under most conditions other than fluoride (deemed essential for maintaining this protecting group throughout the total synthesis). Mono-protection of **56** with TBDPSCl thus proceeded smoothly to form **55a** in 88% yield, with the remaining 12% constituting the di-protected adduct and unreacted starting material.

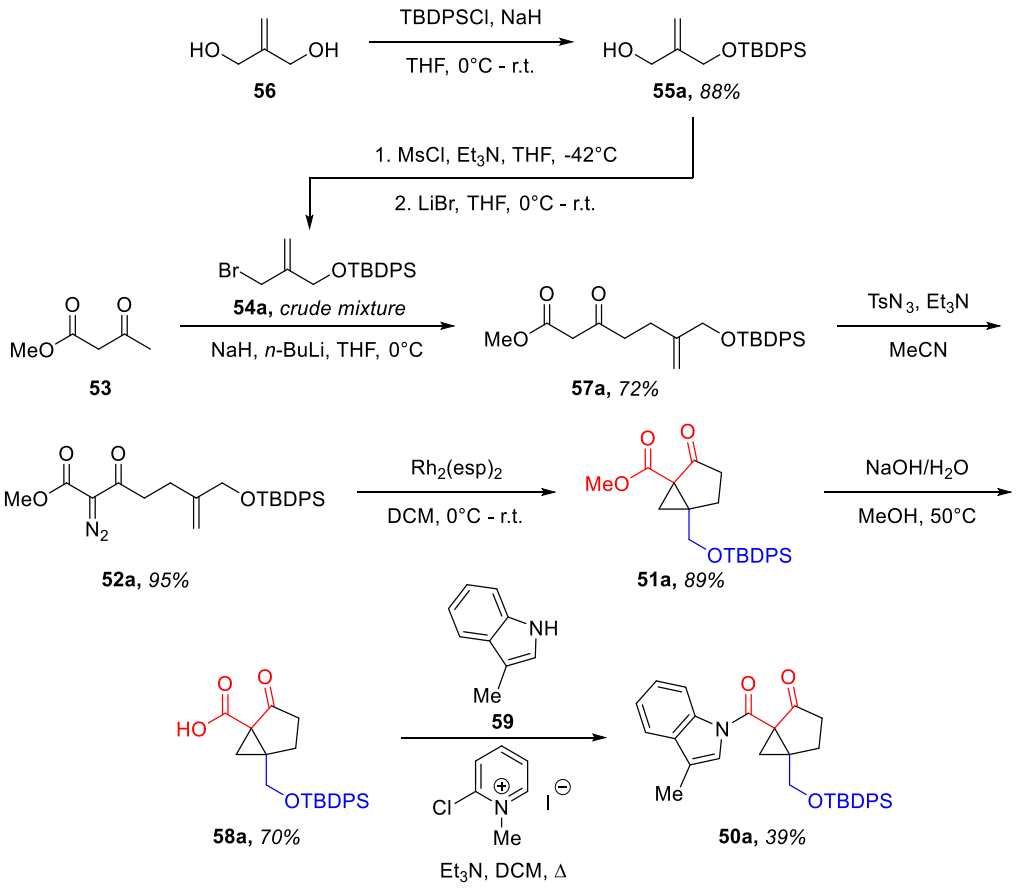

Scheme 4-6: Optimized synthesis of first tronocarpine model system.

Converting the second alcohol moiety to a suitable leaving group for nucleophilic attack required extensive optimization (Table 4-1). As a note, early experiments incorporated *tert*-butyldimethylsilane (TBS) as the alcohol protecting group due to its lower profile by proton NMR, as in entries 1-9, solely for the purpose of optimizations.

Leaving groups surveyed included tosyl (Ts), mesyl (Ms), bromide (Br), and iodide (I) for classic nucleophilic substitution chemistry, and acetate (Ac) for Tsuji-Trost chemistry.[5] It was determined after early attempts that purification by silica flash chromatography would be impossible due to the tendency for allylic groups to eliminate in acidic medium, so efforts were redirected toward protocols that afforded sufficiently clean adducts to take forward crude. Ultimately, the best protocol turned out to be a two-step, one-pot conversion of the alcohol first to a mesylate, then to a bromide (entry 15, 78% crude yield).

Table 4-1: Optimization of alcohol conversion to various leaving groups.

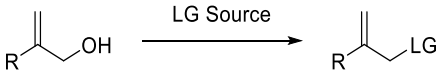

56 **54**

Entry	R	LG (equiv)	Base (equiv)	Additive (equiv)	Yield[a]
1	CH_2OTBS	TsCl (3)	Et_3N (4)	N/A	18 mg
2	CH_2OTBS	MsCl (3)	Et_3N (4)	N/A	trace
3	CH_2OTBS	TsCl (3)	Et_3N (4)	N/A	trace
4	CH_2OTBS	MsCl (1.5)	Et_3N (2)	N/A	trace
5	CH_2OTBS	I_2 (1.2)	ImH (1.3)	PPh_3 (1.15)	trace
6	CH_2OTBS	I_2 (1.2)	ImH (1.3)	PPh_3 (1.15)	trace
7	CH_2OTBS	TsCl (1)	Pyr (0.165M)	N/A	NR
8	CH_2OTBS	Ac_2O (1.2)	Pyr (2.3M)	N/A	31%
9	CH_2OTBS	Ac_2O (1.2)	Pyr (1M)	DMAP (0.1)	68%
10	CH_3	MsCl (1)	Et_3N (1.1)	DMAP (0.1)	28%
11	CH_3	MsCl (1.5)	Et_3N (2)	N/A	ND
12	CH_3	MsCl (2)	Et_3N (2)	LiBr (2.5)	ND
13	CH_3	CBr_4 (1.5)	N/A	PPh_3 (1.2)	25%
14	CH_3	LiBr (1.5)	Et_3N (2)	MsCl (1.5)	ND
15	H	LiBr (4)	Et_3N (2)	MsCl (1.5)	78%
16	$CH_2OTBDPS$	LiBr (4)	Et_3N (2)	MsCl (1.5)	65%
17	CH_3	PBr_3 (1)	N/A	N/A	NR

[a] NR = No reaction, ND = Not determined (i.e. complex mixture).

Next, conditions were evaluated to form the dienolate of methyl acetoacetate (**53**), which was essential to promote nucleophilic attack from the external (less acidic) ketone. Table 4-2 shows various attempts of nucleophilic attack onto commercially available electrophiles (benzyl bromide, allyl bromide, and methallyl bromide) promoted by various bases (sodium hydride, *n*-butyllithium, lithium hexamethyldisilazide, and lithium

diisopropylamide). Generally speaking, from these results, deprotonation required at least 3 equiv of base, and a lithium base alone, even at this loading, was ineffective toward forming the dienolate. Sodium hydride in 1.2-1.7 equivalents in conjunction with a similar loading of lithium base worked most cooperatively (entries 6-7).[6]

Table 4-2: Optimization of methylacetoacetate dienolate formation.

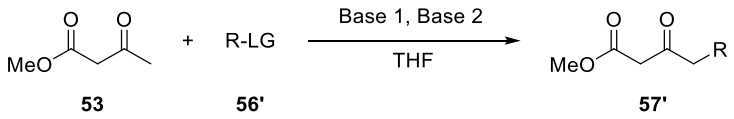

53 **56'** **57'**

Entry	Ester equiv	R-LG (equiv)	Base 1 (equiv)	Base 2 (equiv)	Result
1	1	BnBr (1)	NaH (1.1)	*n*-BuLi (1.1)	Complex mixture
2	1	BnBr (1)	NaH (1.1)	*n*-BuLi (1.1)	Complex mixture
3	1	BnBr (1)	LHMDS (2.2)	N/A	Complex mixture
4	1	allyl Br (1)	LHMDS (1.2)	NaH (1.2)	26%
5	1	allyl Br (1)	LDA (2.2)	N/A	No reaction
6	1.5	allyl Br (1)	NaH (1.7)	*n*-BuLi (1.6)	43%
7	1.1	allyl Br (1)	NaH (1.3)	*n*-BuLi (1.2)	35%
8	2	allyl Br (1)	NaH (2.5)	*n*-BuLi (2.5)	Complex mixture
9	1	methallyl Br (1.2)	NaH (1.5)	*n*-BuLi (1.5)	No reaction
10	1	methallyl Br (1.2)	NaH (1.5)	*n*-BuLi (1.5)	Complex mixture

Table 4-3 shows experiments in which the electrophile was first prepared and then subjected to nucleophilic conditions. (Tsuji-Trost protocols are included in this dataset, i.e. entries 1-2.) Among the combination protocols evaluated, it was determined that the optimal conditions were still the mesylation-bromination of the allylic alcohol starting material, then 1.5 equivalents of NaH followed by 1.5 equivalents of *n*-BuLi to form the

dienolate (Table 4-4, entry 13). These conditions greatly outperformed contrasting precedent for two full equivalents of a lithiate base such as LHMDS. This optimized protocol applied with **56a** afforded the desired precursor **57a** in 72% yield relative to **53**.

Table 4-3: Optimization of combined protocol (alcohol conversion to leaving group plus dienolate formation).

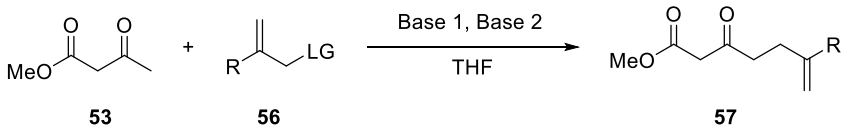

53 **56** **57**

Entry	R	LG Conditions	R-LG equiv	Ester equiv	Base 1 (equiv)	Base 2 (equiv)	Yield[a]
1[b]	CH_2OTBS	Ac_2O, DMAP, Pyr, 23°C	1	1	NaH (1.1)	*n*-BuLi (1.1)	NR
2[b]	CH_2OTBS	Ac_2O, DMAP, Pyr, 23°C	1	1	LHMDS (2.2)	N/A	ND
3	CH_2OTBS	MsCl, Et_3N, THF, -40°C	1	2	LHMDS (5)	N/A	ND
4	CH_2OTBS	MsCl, Et_3N, THF, -40°C	1	1	LHMDS (2.5)	N/A	ND
5	H	MsCl, Et_3N, DMAP, DCM, 23°C	1.5	2	NaH (2.5)	*n*-BuLi (2.5)	ND
6	CH_3	MsCl, Et_3N, DMAP, DCM, 23°C	1.5	2	NaH (2.5)	*n*-BuLi (2.5)	NR
7	CH_3	I_2, ImH, PPh_3, DCM, 23°C	1.5	2	NaH (2.5)	*n*-BuLi (2.5)	NR
8	CH_2OTBS	MsCl, Et_3N, DMAP, DCM, 0°C	1	1.5	NaH (2)	*n*-BuLi (2)	trace
9	CH_2OTBS	MsCl, Et_3N, DMAP, THF, 23°C	1	1.5	NaH (2)	*n*-BuLi (2)	NR
10	$CH_2OTBPDS$	MsCl, Et_3N, DMAP, THF, 23°C	1	1.5	NaH (2)	*n*-BuLi (2)	ND
11	$CH_2OTBPDS$	MsCl, Et_3N, DMAP, DCM, 23°C	1	1.5	NaH (2)	*n*-BuLi (2)	ND

12	$CH_2OTBPDS$	MsCl, Et_3N, DMAP, DCM, 23°C	1	1	NaH (1.5)	*n*-BuLi (1.5)	ND
13	$CH_2OTBPDS$	1. MsCl, Et_3N, THF, -42°C; 2. LiBr, THF, 0°C	2	1	NaH (1.5)	*n*-BuLi (1.5)	72%
14	$CH_2OTBPDS$	1. MsCl, Et_3N, THF, -42°C; 2. LiBr, THF, 0°C	1.7	1	NaH (1.5)	*n*-BuLi (1.5)	75%
15	$CH_2OTBPDS$	1. MsCl, Et_3N, THF, -42°C; 2. LiBr, THF, 0°C	1.7	1	NaH (1.5)	*n*-BuLi (1.5)	55%

[a] NR = No reaction, ND = Not determined (i.e. complex mixture). [b] Added $Pd_2(dba)_3$ and PPh_3.

In the process of optimizing the dienolate formation, it was hypothesized that a diazo transfer onto **53** could be performed before the nucleophilic addition step, thereby blocking the most acidic position and requiring only one equivalent of base to effect the transformation (Table 4-4). Unfortunately, every experiment led to either degradation of the diazo starting material or no reaction at all, so the synthesis was pushed forward with the optimized dienolate conditions.

Table 4-4: Test reactions for nucleophilic attack from a diazo precursor.

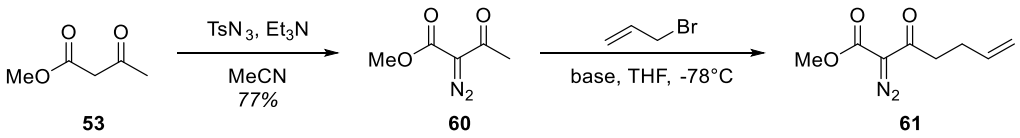

53 60 61

Entry	Bromide equiv	Base (equiv)	Result
1	1	LHMDS (1.5)	Complex mixture
2	1	LHMDS (1.5)	Degradation
3	1	LDA (1.5)	Degradation
4	1	NaH (2)	No reaction
5	1	Et_3N (2)	No reaction
6	1.5	Et_3N (2)	No reaction

Diazo transfer from **52a** proceeded without difficulty (95% yield), and the intramolecular cyclopropanation was similarly successful to afford **51a** (89% yield). Next, to incorporate the indole moiety, several conditions were evaluated. Saponification to the acid **58a** was feasible at 70% yield, but traditional preparations for the corresponding acid chloride were unsuccessful. Gratifyingly, *N*-acylation with 3-methylindole (**59**) was achievable in the presence of 2-chloro-1-methylpyridinium iodide (i.e. Mukaiyama's reagent)[7] to afford **50a** in a modest 39% yield.

Once the *N*-acylation was optimized and a suitable model for the eventual tryptamine-based system thus prepared, a short Lewis acid screen was conducted to test the intramolecular ring-opening cyclization (Scheme 4-7). Unfortunately, both $In(OTf)_3$ and $Al(OTf)_3$ afforded predominantly TBDPSOH and a slew of degradation products rather than desired cyclization adduct **49a**. These results were partially attributed to deprotection of the silyl group by the Lewis acid, despite the fact that TBDPS ought to have been

sufficiently stable,[8] and the β-silanol was deemed unsuitable as a donating group for this ring-opening cyclization.

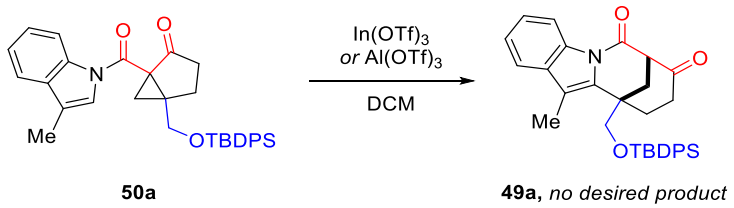

50a **49a,** *no desired product*

Scheme 4-7: Unsuccessful intramolecular ring-opening cyclization of first model system.

4.3.2 Second Indole-tethered Model System

Applying lessons learned from the first model system, the second model selected for evaluation traded the β-silanol for a simple phenyl donor group. Phenyl has been shown to be an effectively good donor not solely for its electron richness but also its improved ability over alkyl donors to stabilize the intermediary carbocation.[1a] Due to the close similarities between this model system and the previous one, the optimized conditions were expected to facilitate a more expedient synthesis of the final target (Scheme 4-8).

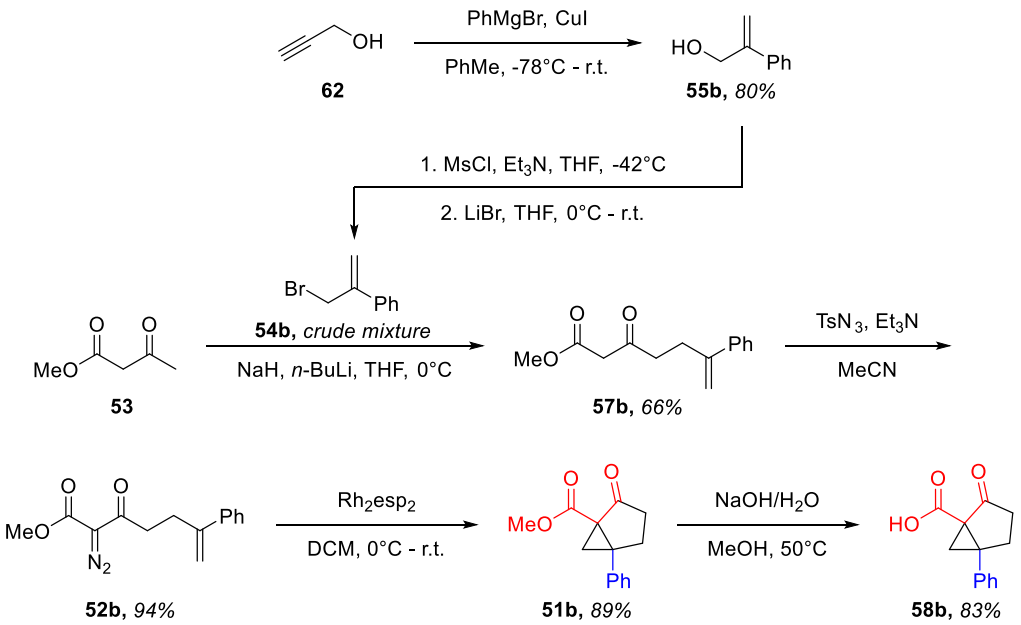

Scheme 4-8: Optimized synthesis for second tronocarpine model system.

To generate the allyl electrophile, propargyl alcohol (**61**) was treated with phenylmagnesium bromide and copper iodide in a Gilman reaction[9] to afford the allyl alcohol **55b** in 80% yield. After treatment with the same bromination conditions used previously to form **54b**, and after preparing the dienolate of methyl acetoacetate, nucleophilic addition to **57b** was readily achieved in 66% yield, followed by similar positive results for the diazo transfer to **52b**, cyclopropanation to **51b**, and saponification to **58b** (94%, 89%, and 83%, respectively).

At this stage of the model synthesis, however, it was quickly determined that bicyclo[3.1.0]hexane **58b** was incredibly susceptible to irreversible ring-opening elimination. Simply exposing **58b** to Mukaiyama's reagent, as optimized for the previous model system, led to various elimination and decarboxylation by-products, without showing any productive reactivity toward 3-methylindole (**59**); treatment with oxalyl chloride (i.e. Swern conditions) gave the same result (Scheme 4-9).

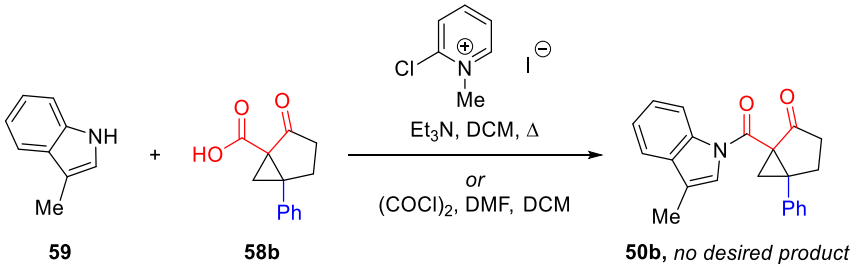

Scheme 4-9: Attempted amidation for second model system.

4.3.3 Third Indole-tethered Model System

Though disheartening, the apparent sensitivity of the bicyclo[3.1.0]hexane model precursor to ring-open in acidic medium was promising toward the ultimate goal, and it was hypothesized that installing the indole moiety earlier in the synthesis would both circumvent this issue and afford a system primed for intramolecular ring-opening cyclization. Initial test reactions probed the viability of performing a simple *N*-acylation on **59** and building up the alkene-containing side chain gradually (Scheme 4-10). Though formation of **63** proceeded readily in the presence of acetyl chloride, test reactions to append an additional ketone yielded no desired product and instead resulted in recovery of 3-methylindole.

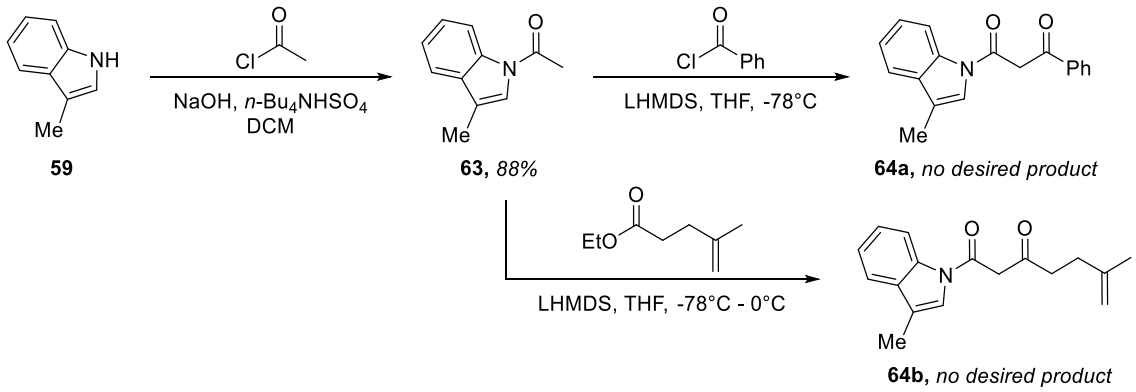

Scheme 4-10: Attempted model synthesis beginning with *N*-acylation of indole with acetyl chloride.

Then, a new model synthesis was envisioned in which the first step would be an addition of **59** and commercially available 2,2,6-trimethyl-4*H*-1,3-dioxin-4-one (**65**), essentially **53** masked as a ketal, to afford the *N*-acyl precursor. As shown in the new retrosynthetic analysis (Scheme 4-11), the key difference is that the bicyclo[3.1.0]hexane precursor would already be tethered to the indole nucleophile after the cyclopropanation step.

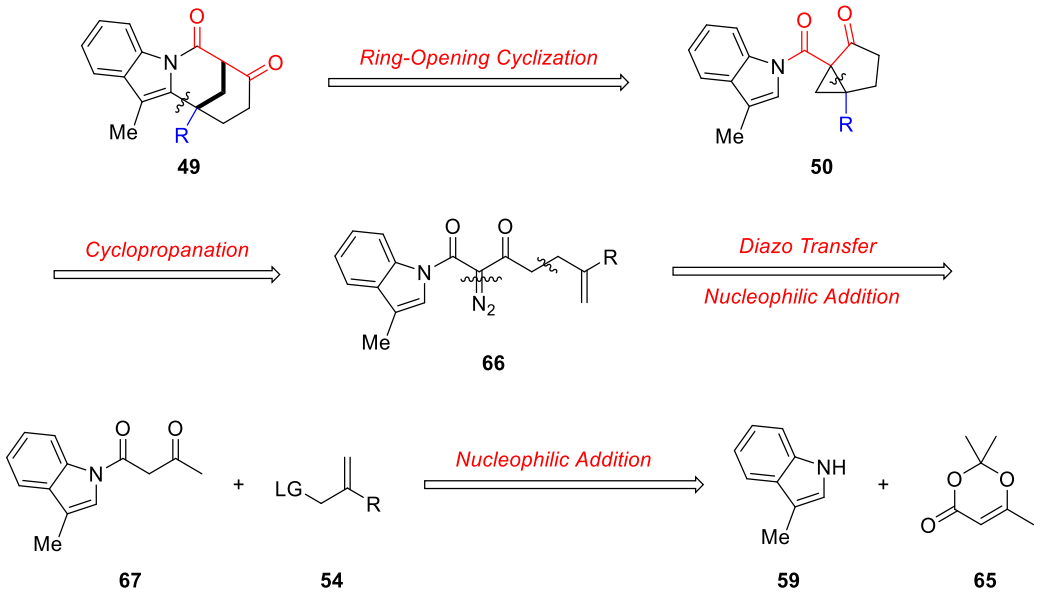

Scheme 4-11: Retrosynthetic analysis for third tronocarpine model system.

After a short optimization study, it was determined that the best conditions required stirring **59** and **65** overnight in refluxing toluene to afford β-ketoamide **67** (88% yield). The subsequent alkylation step to prepare **68**, however, proved challenging (Table 4-5). Previously optimized conditions for preparing the dienolate of **53** were, disappointingly, incompatible with **67** (entry 1). With this setback, a literature source suggested that employing a lithium based in greater than two equivalents and in the -20 to -15°C range should produce the dienolate with sufficient persistence and reactivity to perform

nucleophilic addition.[10] To evaluate these conditions, commercial methallyl bromide **54c** was selected as the electrophile to avoid having to prepare the allyl bromide for each test.

Several loadings of electrophile were surveyed in conjunction with LHMDS (entries 2-3). Despite increasing the concentration of **54c** to prevent loss of 3-methylindole, the yield did not improve beyond ~60%. Also surprisingly, subjecting these conditions to the prepared **54b** did not afford desired product (entry 4). After testing the effects of slow-addition of the base (entry 5) and a different cation (Na, entry 6), it was decided that the lowest effective loading of **54c** (1.5 equiv.) in conjunction with 2.5 equiv. LHMDS were the optimal conditions (entry 2, 59%).

Table 4-5: Optimization of nucleophilic addition for third tronocarpine model system.

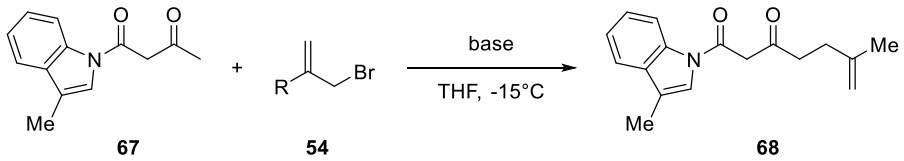

Entry	R (equiv)	Base (equiv)	Solvent (M, T)	Result
1	Ph (2)	NaH (1.5), *n*-BuLi (1.5)	THF (0.2M, 0°C)	No desired product
2	Me (1.5)	LHMDS (2.5)	THF (0.1M, -17°C)	59%
3	Me (2)	LHMDS (2.5)	THF (0.1M, -17°C)	61%
4	Me (4)	LHMDS (2.5)	THF (0.1M, -15°C)	59%
5	Ph (2)	LHMDS (2.5)	THF (0.1M, -15°C)	No desired product
6	Me (1.5)	LHMDS (2.5)	THF (0.1M, -15°C)	33%[a]
7	Me (1.5)	NaHMDS (2.5)	THF (0.1M, -15°C)	No reaction

[a] Slow-added LHMDS over 30 minutes.

The diazo transfer and cyclopropanation steps proceeded as expected to prepare **66a** (96%) and **50c** (87% yield), respectively. Therefore, the synthesis was completed in

four steps in 34% overall yield, a great improvement over previous model system syntheses (Scheme 4-12).

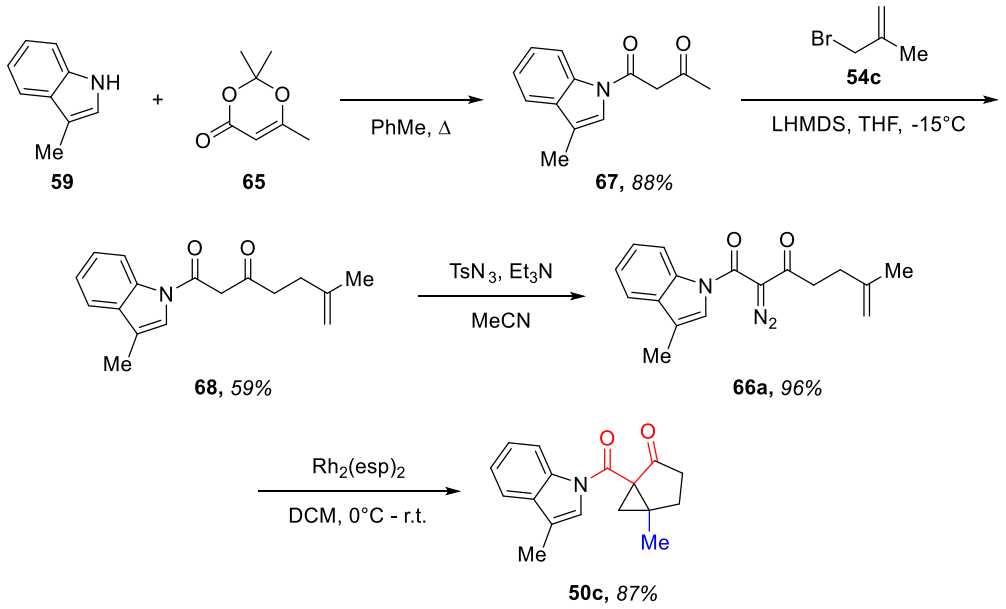

Scheme 4-12: Optimized synthesis of third tronocarpine model system.

Despite earlier lack of success with promoting nucleophilic attack from diazo compound **60**, it was desirous to improve the yield of the nucleophilic addition step as much as possible to facilitate large-scale synthesis. Two separate strategies were employed. First, nucleophilic addition directly from **65** was attempted (Table 4-6). Unfortunately, lithium and amine bases, even in the presence of activating agents, failed to deliver addition adduct **69**.

Table 4-6: Test reactions for direct nucleophilic addition of 2,2,6-trimethyl-4*H*-1,3-dioxin-4-one.

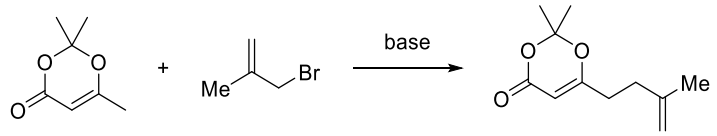

65 **54c** **69**

Entry	Allyl equiv	Base (equiv)	Additive (equiv)	Result
1	1.1	*n*-BuLi (1.1)	N/A	No desired product
2	1.1	Et_3N (1.1)	TMSOTf (1.1)	No desired product[a]
3	1.5	Et_3N (1.5)	TMSOTf (1.5)	No reaction
4	1.5	LDA (1.2)	N/A	No reaction
5	1.2	LDA (1.5)	TBAI (0.03)	No reaction

[a] Used BnBr instead of methallyl bromide.

Next, nucleophilic addition from **70**, the diazo transfer product of **67**, was endeavored (Table 4-7). A plethora of bases were employed, but in every case, there was either no desired product formed (entry 1), no reaction (entries 2-5), or degradation of starting material (entries 6-10). Activating agents attempted for adduct **70** also failed for this system (entries 11-12).

Table 4-7: Test reactions for direct nucleophilic addition of diazo precursor.

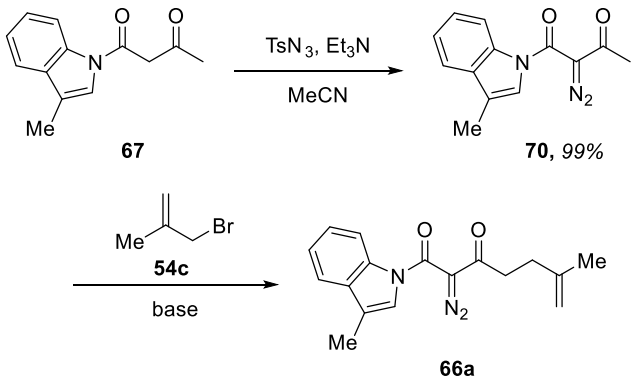

Entry	Allyl equiv	Base (equiv)	Result
1	1.2	LHMDS (1.5)	No desired product
2	1.2	DIPEA (1.5)	No reaction
3	1.2	Et_3N (1.5)	No reaction
4	1.2	ImH (1.5)	No reaction
5	1.2	2,6-lut. (1.5)	No reaction
6	1.2	LHMDS (1.5)	Degradation
7	1.2	DBU (1.5)	Degradation
8	1.2	KOtBu (1.5)	Degradation
9	1.2	NaH (1.5)	Degradation
10	1.5	LHMDS (2.5)	Degradation
11	1.5	Et_3N (1.1)	No reaction[a,b]
12	1.5	Et_3N (1.5)	No reaction[c]

[a] Used BnBr instead of methallyl bromide. [b] Added TMSOTf (1.1 equiv). [c] Added TMSOTf (1.5 equiv).

With a route to model system **50c** in hand, no further optimizations were pursued, and an extensive Lewis acid screen was conducted to test the intramolecular ring-opening cyclization to **49b** (Table 4-8, pathway **a**). Interestingly, the choice of catalyst counteranion affected the preferred reaction pathway. For metal triflates and bistriflimides, the preferred pathway was a ring-opening elimination (pathway **b**); whereas for metal chlorides, the

preferred pathway was not a ring-opening elimination, but accurate structural elucidation has proven challenging despite extensive NMR studies (pathway **d**). In one case, the major product resulted from a hydride shift of the intermediary carbocation (pathway **d**), though this result has not been replicated. Brønsted acids, in contrast, were ineffective catalysts for this reaction.

Table 4-8: Lewis acid screen for model intramolecular ring-opening cyclization.

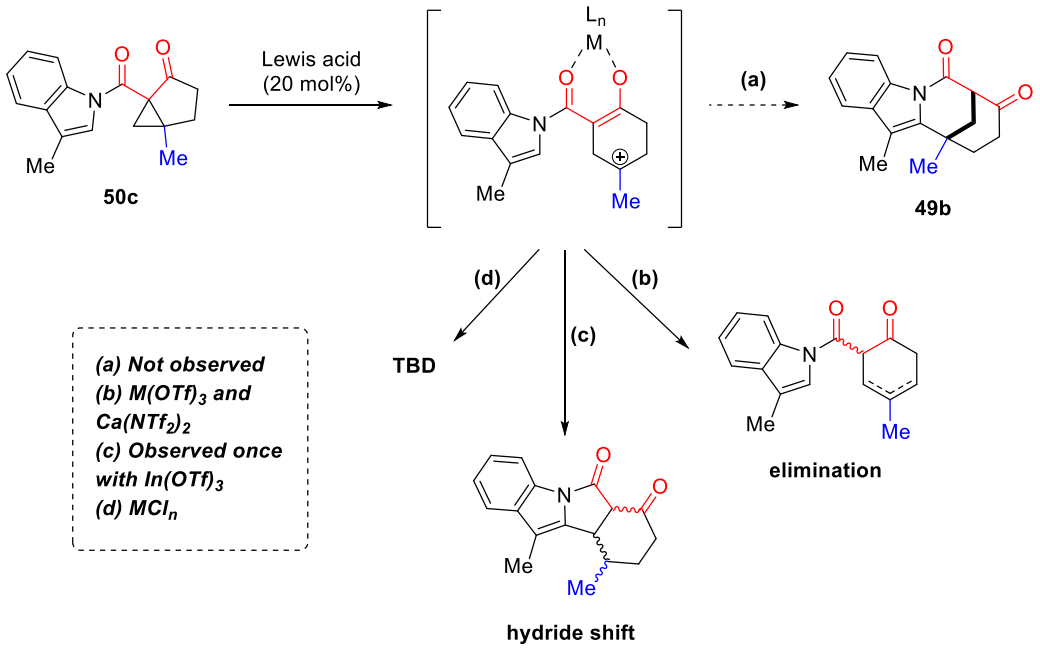

Entry	Lewis acid	Solvent	Temp.	Result/Notes
1	$In(OTf)_3$	DCM	r.t.	SM + 2.1mg **c**, messy reaction
2	$Sc(OTf)_3$	DCM	r.t.	Mostly **a**
3	$SnCl_4$	DCM	r.t.	Mostly **d**
4	$In(OTf)_3$	DCM	reflux	Complete after 1h, mostly **b**
5	$In(OTf)_3$	DCM	r.t.	Not complete after 22h, mostly **b**
6	$In(OTf)_3$	DCM	0°C	No reaction after 22h
7	$Ca(NTf_2)_2$/*n*-Bu_4NPF_6	DCM	r.t.	Mostly **a**
8	$Cu(OTf)_2$	DCM	r.t.	No reaction after 24 h

9	$In(OTf)_3$	MeCN	r.t.	No reaction after 23h
10	$In(OTf)_3$	MeCN	50°C	Mostly **a**, some degradation
11	$Al(OTf)_3$	DCM	r.t.	Complete after 4h, mostly **b**
12	$Ga(OTf)_3$	DCM	r.t.	Not complete after 21h, only SM + **b**
13	$Sc(OTf)_3$	DCM	r.t.	Not complete after 21h, only SM + **b**
14	$Yb(OTf)_3$	DCM	r.t.	No reaction after 21h
15	$Zn(OTf)_2$	DCM	r.t.	No reaction after 21h
16	$Mg(OTf)_2$	DCM	r.t.	No reaction after 21h
17	$Bi(OTf)_3$	DCM	r.t.	Mostly **a**
18	$SnCl_4$	DCM	r.t.	Mostly **d**
19	TFA	DCM	r.t.	No reaction after 48h
20	TsOH	DCM	r.t.	No reaction after 48h
21	TfOH	DCM	r.t.	Only **b** after 1h
22	Tf_2NH	DCM	r.t.	Not complete after 17h, only SM + **b**
23	$InCl_3$	DCM	r.t.	Not complete after 22h, mostly **d**
24	$InCl_3$	DCM	reflux	Only degradation after 6h
25	AgOTf	DCM	r.t.	No reaction after 24h
26	$AgBF_4$	DCM	r.t.	No reaction after 24h
27	$Bi(OTf)_3$, TFA	DCM	r.t.	After 19h, mostly **b** + degradation
28	$GaCl_3$	DCM	0°C-r.t.	Complete in 30 min, mostly **d**

Unfortunately, though the product outcomes support a ring-opening mechanism, none of the surveyed catalysts afforded the desired bridged bicyclic product **49b**, and additional treatment with a Brønsted acid failed to reprotonate the elimination product to drive the reaction toward cyclization.

4.3.4 Benzofuran-tethered Model System

Hypothesizing that 3-methylindole might not be the optimal nucleophile for testing this transformation, and that a β-ketoester might have better chelating ability than a β-

ketoamide (or a diketone, since the aromaticity of indole affords this amide more ketone-like character), a benzofuran-tethered oxabicyclo[3.1.0]hexane model system was prepared in short order from commercially available benzofuran-2-carboxylic acid (**71**) (Scheme 4-13). After converting **71** to its corresponding acid chloride, 2-phenylallyl acetate (**72**) was treated with LHMDS to promote nucleophilic attack onto the acid chloride, which afforded β-ketoester **73** in 65% yield. Next, diazo transfer to **74** was achieved with *p*-acetamidobenzenesulfonyl azide (*p*-ABSA)[11] in 95% yield, followed by intramolecular cyclopropanation to **75** at a modest 60% yield.

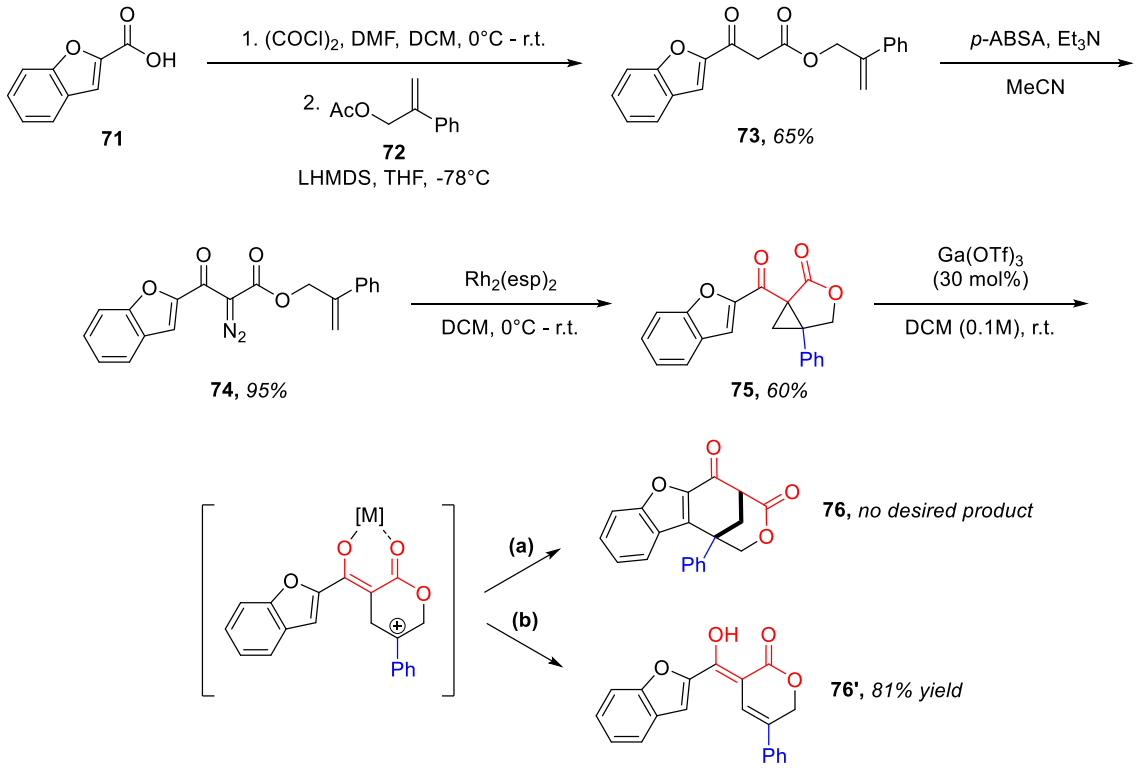

Scheme 4-13: Synthesis and testing of benzofuran-tethered oxabicyclo[3.1.0]hexane model system.

Subjecting this oxabicyclo[3.1.0]hexane model **75** to $Ga(OTf)_3$ afforded the same result as before, only more definitively: complete consumption of starting material after 2 hours to afford a single ring-opened elimination product **76'**. This result further supported

that the mechanism was proceeding as expected, but unfortunately, the desired product was not favored.

4.4 Troubleshooting the Intramolecular Ring-opening Cyclization

The propensity for the D-A bicyclo[3.1.0]hexane synthon to ring-open in acidic medium was incidental confirmation that a carbocation intermediate was being generated. Unfortunately, elimination appeared to be kinetically favored over Friedel-Crafts-type cyclization, especially when an enol could easily form, as in the benzofuran-tethered case.

With these limitations in mind, it was hypothesized that either the tertiary carbocation was too sterically hindered toward nucleophilic attack, or the carbonyl adjacent to the tethered heterocycle was making the system too rigid to access the carbocation. As the nature of the C5-subsituted donor-acceptor bicyclo[3.1.0]hexane scaffold necessitates formation of a tertiary carbocation, addressing the possible steric hindrance was functionally impossible. Thus, the rigidity of the system was targeted for alteration.

4.4.1 Decarbonylated Model Systems

Two syntheses were attempted to access model systems without the aforementioned carbonyl moiety. Beginning with the *N*-acyl system, **51b** was subjected to a universal reduction, which was effected quantitatively to yield **77** (Scheme 4-14). The next step was the selective conversion of the resulting primary alcohol to a suitable leaving group for nucleophilic displacement by **59**. Unfortunately, the mesylation-bromination conditions applied to earlier model syntheses were unsuccessful, and this reaction has not yet been probed further.

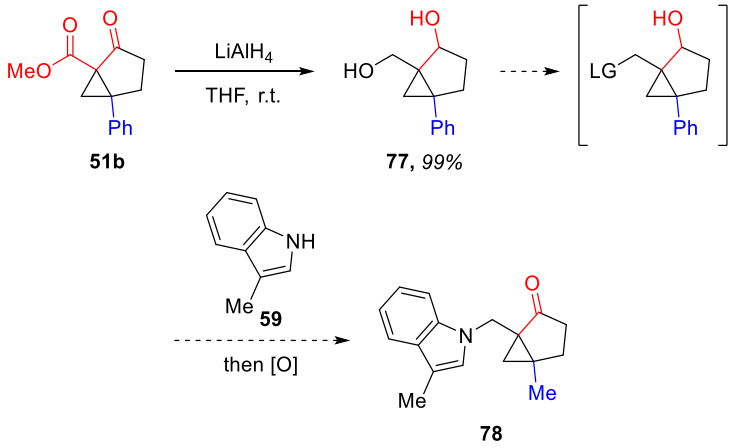

Scheme 4-14: Attempts toward an indole-tethered decarbonylated bicyclo[3.1.0]hexane model system.

Concurrently, efforts were directed toward the benzofuran-tethered system (Scheme 4-15). Acid **71** was first reduced to the alcohol **79** (51% yield), then converted to the bromide **80** in the presence of PBr_3.[12] Unfortunately, 2-(bromomethyl)benzofuran was inseparable from unreacted starting material by silica flash chromatography. Optimistic that the alcohol would not drastically hinder the next synthetic step, however, the bromide mass was estimated by ^{1}H NMR (93.7 mg out of 104.1 mg crude), and the mixture was carried forward.

Next, LHMDS-mediated nucleophilic addition was attempted with acetate **72**. Disappointingly, but perhaps due to the impure starting material, there was no evidence of desired product **81**. At this time, this reaction has not been optimized, but there are plans to attempt the mesylation-bromination sequence that was effective for the synthesis of allylic bromides. If successful, subsequent steps would include a NaH-mediated diazo transfer followed by cyclopropanation to afford the proposed benzofuran-based decarbonylated model system **82**.

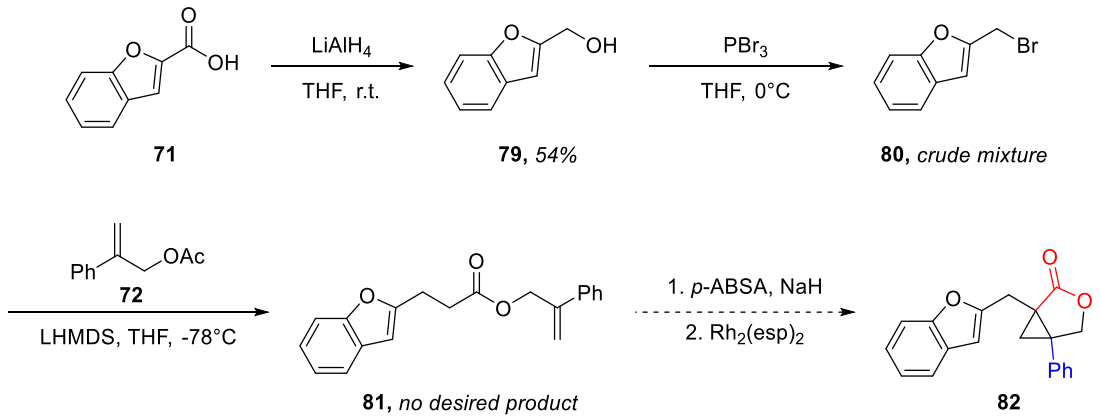

Scheme 4-15: Attempts toward a benzofuran-tethered decarbonylated oxabicyclo[3.1.0]hexane model system.

4.4.2 Ring-Expanded Model System

Although ring size was a parameter intended to evaluate later in the methodology development process, it was suggested that a ring-expanded model system might bring the tertiary carbocation into closer proximity to the heterocyclic nucleophile and reduce steric crowding at the carbocation. An indole-tethered oxabicyclo[4.1.0]heptane was therefore envisioned, beginning with readily available starting materials: 3-methylindole (**59**), Meldrum's acid (**83**),[13] and 2-methyl-1-buten-4-ol (**84**).

The initial reaction between **59** and **83** was tested in various solvents at their reflux temperatures (Table 4-9). It was quickly determined that stirring the two reagents in refluxing, anhydrous THF overnight provided acid **85** in the best yield (entry 1), as refluxing in higher-boiling solvents led to degradation of **83** (entries 2-3). Furthermore, increasing the loading of **59** added a driving force for the reaction (entry 4).

Table 4-9: Optimization of 3-methylindole *N*-acylation with Meldrum's acid.

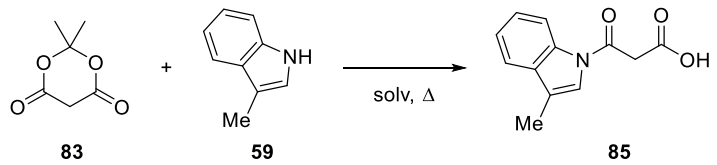

83 59 85

Entry	Meldrum's equiv	Indole equiv	Solvent	Yield
1	1	1	THF	50%
2	1	1	DCE	Degradation
3	1	1	MeCN	Degradation
4	1	1.5	THF	62%

Next, several esterification protocols were evaluated (Table 4-10). It was desirous to use the synthesized acid **85** in lower equivalents relative to the commercially available alcohol **84**. Unfortunately, these reaction attempts afforded no desired product (entries 1-3). Literature suggested an excess of acid under standard DCC coupling conditions, and gratifyingly, the ester **86** was achieved at 66% yield relative to the alcohol (entry 4).

Table 4-10: Optimization of 3-methyl-3-buten-1-ol esterification.

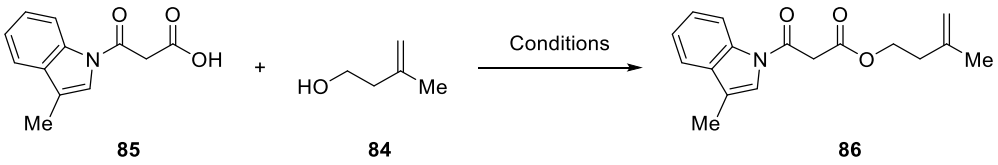

85 84 86

Entry	Acid equiv	Alcohol equiv	Conditions	Result
1	1	1.2	EDCI (1.3 equiv), DMAP (0.1 equiv)	No reaction
2	1	4	EtOC(O)Cl (1.3 equiv), Et_3N (1.2 equiv)	No desired product
3	1	1.2	DCC (1.1 equiv), DMAP (0.2 equiv)	No reaction
4	2.4	1	DCC (2 equiv), DMAP (0.1 equiv)	66%

Disappointingly, modest yields in these first two steps, coupled with requiring an excess **85** for the esterification, hampered preparation of sufficient quantities to push forward, and the proposed synthesis has yet to be completed (Scheme 4-16).

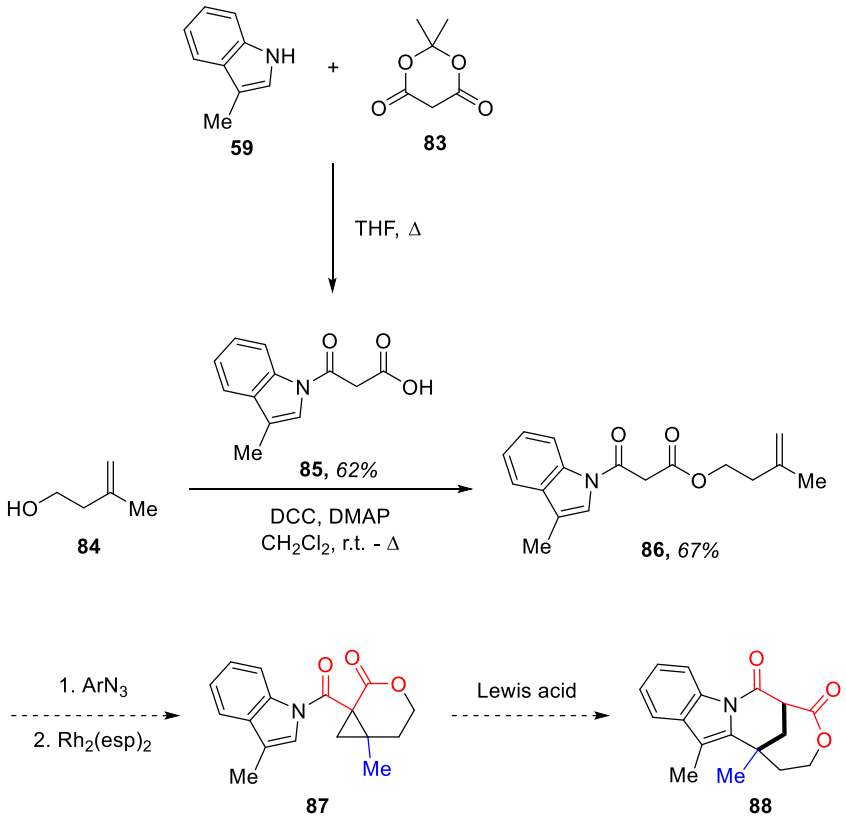

Scheme 4-16: Attempted synthesis of ring-expanded indole-tethered bicyclo[4.1.0]heptane model system.

4.4.3 An Intermolecular, Stepwise Incorporation of the Heteroarene

Considering the challenges associated with the intramolecular ring-opening cyclization, a stepwise, intermolecular incorporation of indole under typical ring-opening cyclization conditions was tested, inspired by Sapeta and Kerr's pioneering work (Scheme 4-17).[14]

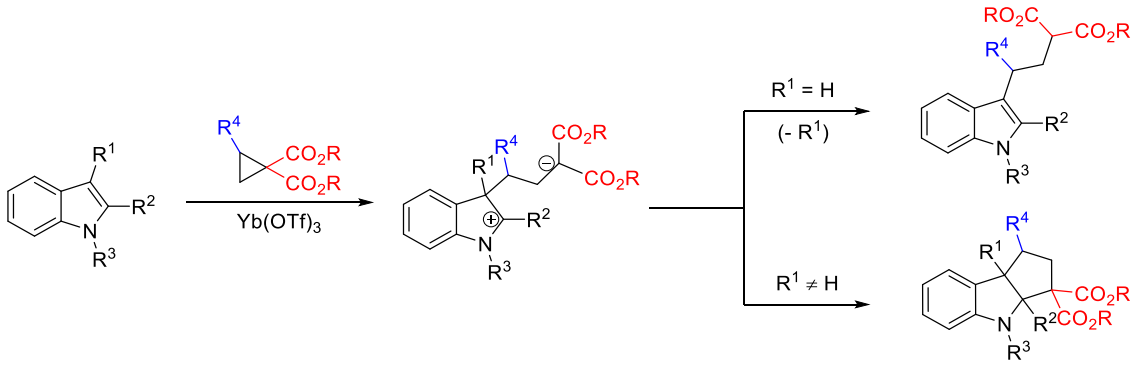

Scheme 4-17: Kerr's intermolecular ring-opening cyclization toward indole-containing tricycles.

A C5-phenyl-substituted donor-acceptor oxabicyclo[3.1.0]hexane model system **89** was readily synthesized to probe this hypothesis (Scheme 4-18). This DACP was selected over its cyclic ketone analogue to promote more effective chelation of the Lewis acid and because the synthesis was more expedient. Alcohol **62** was subjected to nucleophilic addition with methyl malonyl chloride to afford β-ketoester **90** quantitatively. Subsequent diazo transfer and cyclopropanation effected the swift preparations of **91** (86%) and **92** (75%), respectively.

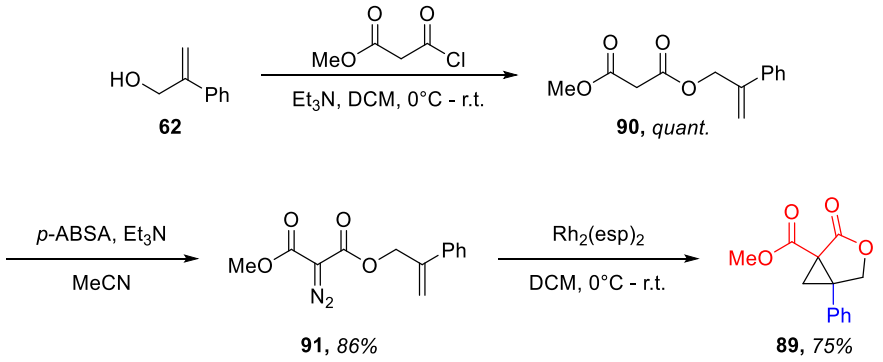

Scheme 4-18: Synthesis of oxabicyclo[3.1.0]hexane intermolecular cycloaddition model system.

DACP **89** was then treated with a Lewis acid (Table 4-11) and, in separate instances, *N*-methylindole and 3-methylindole, in hopes of trapping the carbocation with an external nucleophile. The hypothesized adduct **92** would then be isolated and subjected

to amidation conditions to form bridged bicycle **93**. This Friedel-Crafts-type alkylation was attempted with representative metal triflate $Bi(OTf)_3$ (entries 1-2) and metal chloride $InCl_3$ (entries 3-4), since these catalysts had demonstrated excellent reactivity in the intramolecular ring-opening cyclization study. Consumption of starting material was observed; however, this reaction did not proceed as desired.

Table 4-11: Attempted intermolecular Friedel-Crafts-type alkylation with indoles.

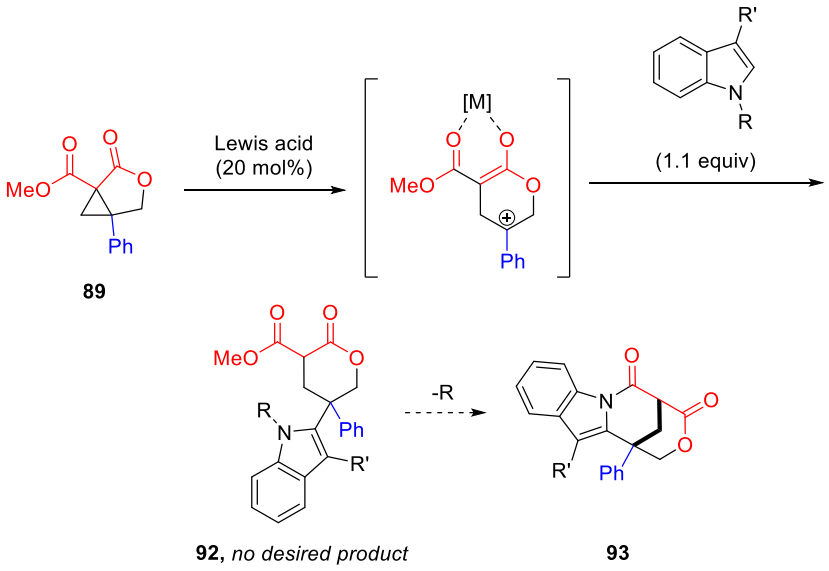

Entry	R, R'	Lewis acid	Result
1	H, Me	$Bi(OTf)_3$	No desired product
2	Me, H	$Bi(OTf)_3$	No desired product
3	H, Me	$InCl_3$	No desired product
4	Me, H	$InCl_3$	No desired product

This hypothesis was tested again with other electron-rich coupling partners (Table 4-12). 2,5-Dimethylfuran showed no reactivity with the D-A bicyclo[3.1.0]hexane (entry

1), so the reaction was repeated with 2,5-dimethylthiophene (entries 2-3). Unfortunately, both $InCl_3$ and $In(OTf)_3$ led to no reaction.

Table 4-12: Attempted intermolecular Friedel-Crafts-type alkylation with 2,5-dimethylfuran and -thiophene.

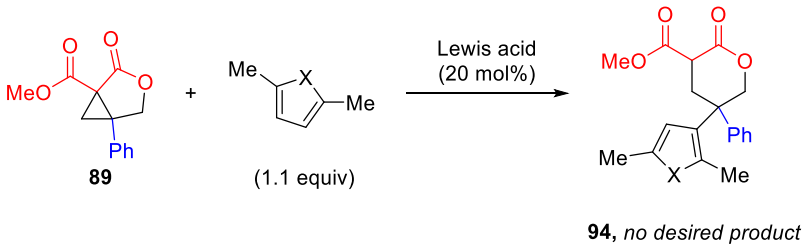

Entry	X	Lewis acid	Result
1	O	$InCl_3$	No reaction
2	S	$InCl_3$	No reaction
3	S	$In(OTf)_3$	No reaction

4.5 Changing Tactics: An Intermolecular Formal [3+2] Cycloaddition

Having exhausted most possibilities toward the hypothesized intramolecular route, and given the challenges with synthesizing alternative model systems (i.e. decarbonylated, ring-expanded), efforts were shifted to an intermolecular formal [3+2] cycloaddition of C5-substituted donor-acceptor bicyclo[3.1.0]hexanes. The operational mindset was that proof of concept of the intramolecular transformation would be streamlined if the system's preferences and limitations could be determined for an analogous polar reaction pathway.

There is no literature precedent for any intermolecular formal cycloaddition from this exact template. However, as early as 1981, Reißig demonstrated sequential $TiCl_4$-catalyzed ring-opening cyclizations of siloxy-substituted DACPs onto ketones to form aldol condensation products, followed by hydroxyl cleavage to yield substituted

dihydrofurans (DHFs).[15] This reaction class has since been broadly expanded with efforts from Johnson,[16] Tomilov,[17] and others.[18] We were particularly inspired by Johnson's method to prepare densely substituted tetrahydrofurans,[16a] which was seminal toward validating the polar ring-opening mechanism of donor-acceptor cyclopropanes. Through a series of competition experiments, Johnson ruled out the possibilities of both electrocyclic and radical mechanisms, and by so doing established a stepwise, polar mechanism for the intermolecular addition between 1,3-dipoles resulting from DACPs and appropriate dipolarophiles such as benzaldehydes (Scheme 4-19).

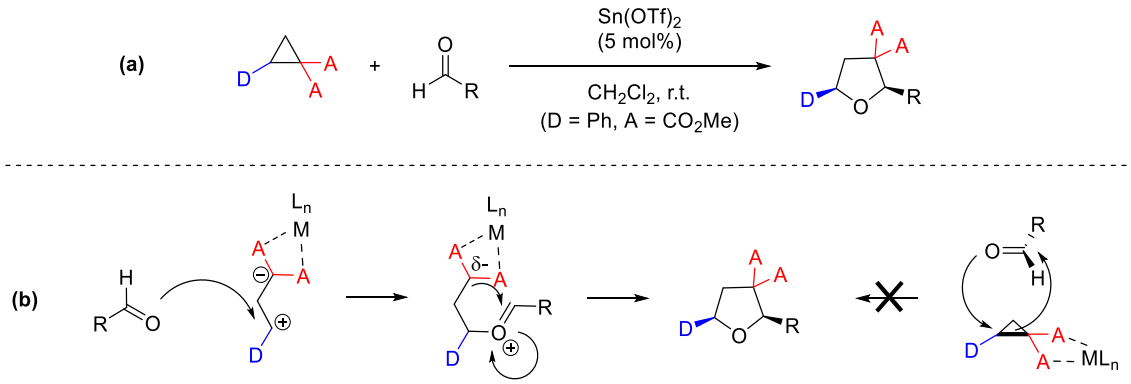

Scheme 4-19: (a) Johnson's intermolecular formal [3+2] cycloaddition of DACPs and aldehydes. (b) Validated polar mechanism.

The first template evaluated in this formal [3+2] cycloaddition was bicyclo[3.1.0]hexane **50a**, using Johnson's preferred catalyst and benzaldehyde as a starting point (Table 4-13). Unfortunately, there was no trace of desired product in any of these reactions, and most of the reactions formed a complex, inseparable mixture of products. The lack of success was attributed to the ability of Lewis acids to deprotect silyl alcohols,[8] as hypothesized for the intramolecular ring-opening cyclization employing the same donor group.

Table 4-13: Lewis acid screen for intermolecular ring-opening cyclization.

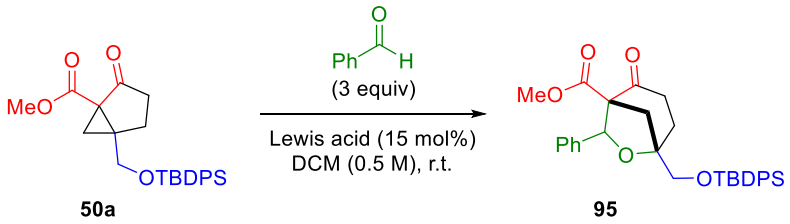

50a **95**

Entry	Lewis acid	Time (h)	Result
1	$Sn(OTf)_2$[a]	4	No reaction
2	$In(OTf)_3$	24	Complex mixture
3	$Zn(OTf)_2$	24	No reaction
4	$Sc(OTf)_3$	6	Complex mixture
5	$Yb(OTf)_3$	24	Not complete
6	$Sn(OTf)_2$	22.5	No desired product
7	$In(OTf)_3$	24	No desired product
8	$Ga(OTf)_3$	2	No desired product
9	$Al(OTf)_3$	22.5	No desired product
10	$Ca(NTf_2)_2$/*n*-Bu_4NPF_6	24	Complex mixture

[a] Used 5 mol% catalyst loading.

Next, oxabicyclo[3.1.0]hexane **89** was evaluated. *p*-Anisaldehyde (**96**, 3 equiv) was selected as the cycloaddition coupling partner, as it was supposed that a more electron-donating benzaldehyde would facilitate nucleophilic trapping of the tertiary carbocation. A Lewis acid screen was conducted, with a catalytic loading of 30 mol%, in DCM at a 0.5 M concentration (Scheme 4-20).

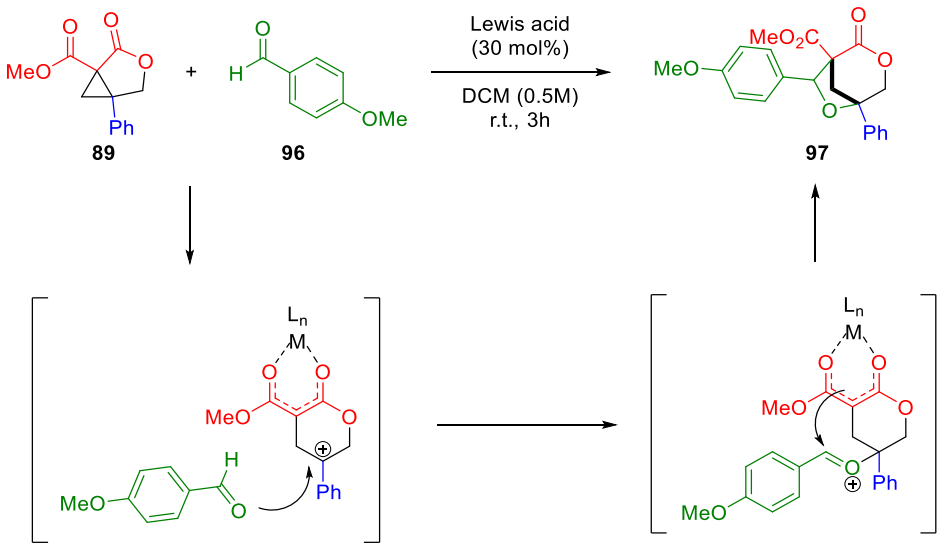

Scheme 4-20: Model intermolecular reaction and proposed mechanism.

Johnson's preferred catalyst, $Sn(OTf)_2$, was ineffective under these conditions, affording only recovered starting material after 3 hours at room temperature (Table 4-14, entries 3-4). Several other Lewis acids yielded the same results (entries 1-2, 6-9); however, slight reactivity was observed in the presence of $Ga(OTf)_3$ (entry 5).

Table 4-14: Conditions screen for model intermolecular reaction.

Entry	Lewis acid	Temp, time	Result
1	$In(OTf)_3$	r.t., 3 h	No reaction[a]
2	$InCl_3$	r.t., 3 h	No reaction[a]
3	$Sn(OTf)_2$	r.t., 3 h	No reaction[a]
4	$Sn(OTf)_2$	r.t., 3 h	No reaction[b]
5	$Ga(OTf)_3$	r.t., 3 h	12% isolated product[b]
6	$Sn(OTf)_2$	Δ, 4 h	No reaction[b]
7	$Bi(OTf)_3$	r.t., 4 h	No reaction[b]
8	$TsOH{\cdot}H_2O$	r.t., 16 h	No reaction[b]
9	$Ca(NTf_2)_2$/*n*-Bu_4NPF_6	r.t., 16 h	No reaction[b]

10	$Ga(OTf)_3$	r.t., 3 h	N/A[c]
11	$Ga(OTf)_3$	r.t., 24 h	26% (q-NMR)[d]
12	$Ga(OTf)_3$	Δ, 24 h	27% isolated product[b]
13	$SnCl_4$	r.t., 24 h	No reaction (q-NMR)[b,d]
14	$Bi(OTf)_3$	Δ, 24 h	No reaction (q-NMR)[b,d]
15	$Sc(OTf)_3$	Δ, 24 h	52% (q-NMR)[b,d]
16	$Ga(OTf)_3$	Δ, 24 h	Degradation[b,e]
17	$Ga(OTf)_3$	Δ, 24 h	Degradation[b,f]
18	$Ga(OTf)_3$	Δ, 24 h	Degradation[b,g]
19	$Ga(OTf)_3$	Δ, 24 h	27% (q-NMR)[b,d]
20	$Sn(OTf)_2$	Δ, 24 h	12% (q-NMR)[b,d]
21	$In(OTf)_3$	Δ, 24 h	52% (q-NMR)[b,d]
22	$Ga(OTf)_3$	Δ, 24 h	Complex mixture[h]
23	$Ga(OTf)_3$	Δ, 24 h	Complex mixture[i]
24	$Ga(OTf)_3$	Δ, 24 h	No desired product[b,j]
25	$Ga(OTf)_3$	Δ, 24 h	No desired product[b,k]
26	$Ga(OTf)_3$	Δ, 6 h	58%[b,d,l]
27	$Ga(OTf)_3$	Δ, 6 h	No desired product[m]
28	$Ga(OTf)_3$	Δ, 24 h	No desired product[n]
29	$InCl_3$	Δ, 24 h	(Not yet performed)
30	$AlCl_3$	Δ, 24 h	(Not yet performed)
31	$Al(OTf)_3$	Δ, 24 h	(Not yet performed)
32	$Ca(NTf_2)_2$/*n*-Bu_4NPF_6	Δ, 24 h	(Not yet performed)
33	$SnCl_4$	Δ, 24 h	(Not yet performed)
34	$FeCl_3$	Δ, 24 h	(Not yet performed)

[a] Filtered reaction mixture through silica for work-up. [b] Purified *p*-anisaldehyde from bottle before use. [c] Control reaction without starting material to observe *p*-anisaldehyde by-product. [d] Evaluated yield by q-NMR. [e] Solvent: THF. [f] Solvent: DCE. [g] Solvent: PhMe. [h] Coupling partner: benzaldehyde. [i] Coupling partner: 2-naphthaldehyde. [j] Used 1 equiv aldehyde. [k] Used 0.8 equiv aldehyde. [l] Used 10 equiv aldehyde. [m] Coupling partner: *p*-methoxystyrene. [n] Coupling partner: *N*-phenylmaleimide.

A small amount of product **97** (12% yield) was isolated by preparatory TLC; and ^{1}H, ^{13}C, and various 2D NMR results were promising. Key differences between the oxabicyclo[3.1.0]hexane starting material and the proposed product are the shifts in the two doublets representing C6 (1.7 & 2.6 ppm in the starting material, 2.8 & 3.4 ppm in the product) and the shifts in the two doublets representing C4 (a pair of doublets at 4.4 ppm in the starting material, independent doublets at 4.5 & 4.6 ppm in the product) (Figure 4-2). Gratifyingly, high-resolution accurate-mass mass spectrometry gave a molecular ion peak that matched the expected mass.

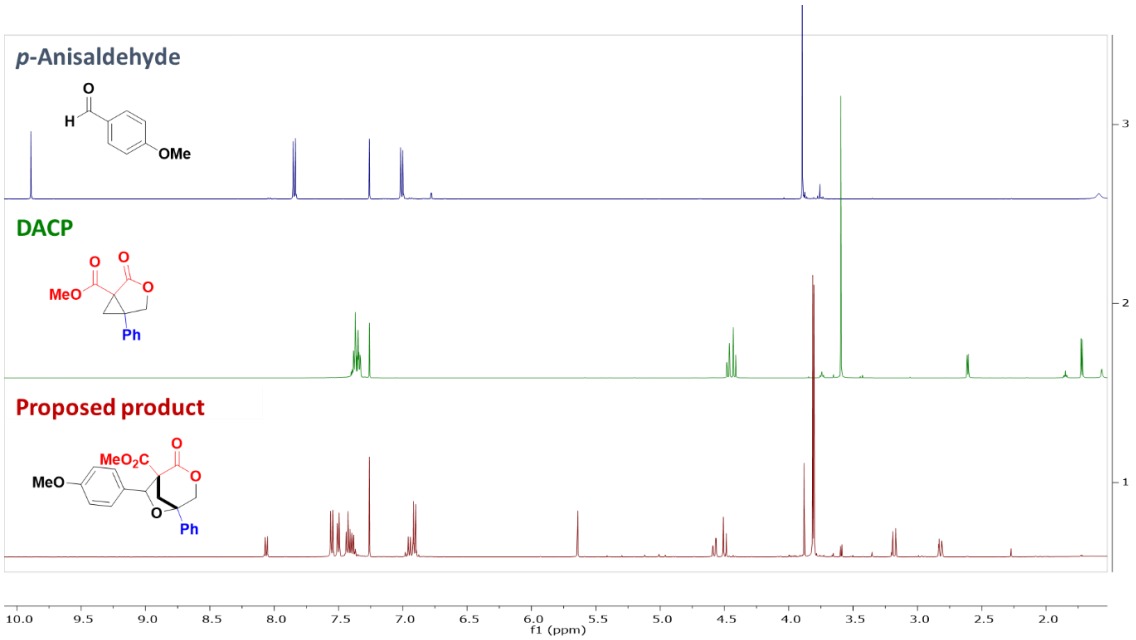

Figure 4-2: ^{1}H NMR overlay for *p*-anisaldehyde, oxabicyclo[3.1.0]hexane starting material, and proposed product.

Eager to validate these results, the $Ga(OTf)_3$ test reaction was replicated and allowed to stir for 24 hours (entry 11). The same product was observed but conversion remained low (26% by q-NMR). Raising the temperature to 40°C allowed for a 27% isolated yield (entry 12), so a short temperature screen was conducted. Unfortunately,

refluxing in higher-boiling solvents such as THF, 1,2-DCE, and toluene (entries 16-18) afforded mostly degradation products.

Instead, the Lewis acid screen initially performed at room temperature for 3 hours was repeated at reflux temperature and allowed to stir for up to 24 hours. The best performing Lewis acids so far, surprisingly, do not include $Ga(OTf)_3$. Rather, $Sc(OTf)_3$ and $In(OTf)_3$ (entries 15 & 21) both yielded 52% of desired product based on quantitative NMR (dimethylterephthalate, DMTP, as the internal standard).

At this stage, several more Lewis acids need to be evaluated for a comprehensive screen (entries 29-34), including $FeCl_3$ and $AlCl_3$, which have been employed in donor-acceptor bicyclo[3.1.0]hexane ring-opening reactions in the literature,[19] and $Ca(NTf_2)_2$/*n*-Bu_4NPF_6, which has proven efficacious for a variety of Lewis acid-mediated chemistries since its publication.[20] Then, several additional parameters such as catalyst loading, solvent, temperature, and concentration must be tested. One series of test reactions that has been pursued altered the loading of *p*-anisaldehyde (entries 24-26); increasing it did not improve yields, and decreasing it was a detriment, so the loading will remain at 3 equivalents.

Additionally, given the success with *p*-anisaldehyde (**96**), different dipolarophiles were evaluated for the formal [3+2] cycloaddition. Two different aromatic aldehydes, benzaldehyde and 2-naphthaldehyde (entries 22-23) were subjected to the $Ga(OTf)_3$ conditions, but NMR results were inclusive. Then, analogous *p*-methoxystyrene was tested as a suitable dipolarophile (entry 27); unfortunately, no desired product was detected. Finally, common cycloaddition partner *N*-phenylmaleimide was evaluated (entry 28), with

similar lack of success. Since the final optimized conditions have yet to be concretely established, these dipolarophiles will likely be revisited.

To round out the study, a crystal is being grown to confirm the novel compound by X-ray analysis. Identification of this substrate would represent a significant advance in the field of DACP polar cycloadditions and rapid access to bridged bicyclic scaffolds.

4.6 Summary

In summary, an intramolecular Friedel-Crafts-type ring-opening cyclization of donor-acceptor C5-substituted bicyclo[3.1.0]hexanes was endeavored for the first time. Targeting tronocarpine for inspiration, an indole-tethered model system was successfully synthesized for Lewis acid screening; however, the desired bridged bicyclic scaffold was never detected. Several additional model syntheses were explored, including benzofuran-tethered, decarbonylated, and ring-expanded donor-acceptor systems, as well as an intermolecular Friedel-Crafts-type addition, with limited or no success. For future work, the syntheses described require optimization to both complete the ring-opening cyclization model systems and prepare sufficient quantities for experimentation.

In addition, an intermolecular formal [3+2] cycloaddition of a donor-acceptor C5-substituted oxabicyclo[3.1.0]hexane was explored for the first time (Section 4.4). Efforts toward this end were more successful: inspired by Johnson's work, a model system was rapidly synthesized and subjected to Lewis acid screening. $Ga(OTf)_3$ initially appeared to be the preferred catalyst, but $Sc(OTf)_3$ and $In(OTf)_3$ outperformed this catalyst according to q-NMR, and further screening of conditions is underway. X-ray analysis of the isolated compound will be accomplished for proof of concept, and lessons learned from this pathway may be applied toward developing the intramolecular methodology.

4.7 Experimental Details

4.7.1 General Information

Chromatographic purification was performed via flash chromatography with Silicycle SiliaFlash P60 silica gel (40-63 μm) or preparative thin-layer chromatography (prep-TLC) with Analtech silica gel F254 (1000 μm) plates and solvents indicated as eluent with 0.1-0.5 bar pressure. For quantitative flash chromatography, technical grades solvents were utilized. Analytical thin-layer chromatography (TLC) was also used to separate and purify reaction products using Silicycle SiliaPlate TLC silica gel F254 (250 μm) TLC glass plates. Products on the TLC plates were visualized under UV light (254 nm).

Proton, and carbon nuclear magnetic resonance spectra (^{1}H NMR and ^{13}C NMR, respectively) were recorded on a Bruker 500 MHz spectrometer. The solvent resonances were used the internal standards (^{1}H NMR: $CDCl_3$ at 7.26 ppm, DMSO-d_6 at 3.50 ppm; ^{13}C NMR: $CDCl_3$ at 77.0 ppm, DMSO-d_6 at 39.5 ppm; ^{19}F NMR: locked to $CDCl_3$ or DMSO-d_6). MestReNova (v. 11.0) was used to analyze NMR spectra. ^{1}H NMR data are reported as follows: chemical shift (ppm), multiplicity (s = singlet, d = doublet, dd = doublet of doublets, dt = doublet of triplets, ddd = doublet of doublet of doublets, t = triplet, m = multiplet, br = broad), coupling constants (Hz), and integration. High-resolution accurate mass-mass spectrometry (HRAM-MS) was performed using a MicroMass Autospec M, run in EI mode at a mass resolution of 10,000 using perfluorokerosene (PFK) as an internal calibrant.

4.7.2 General Procedures

General Mesylation-Bromination Procedure: In a flame-dried flask under N_2, the alcohol (1 equiv) was dissolved in anhydrous THF (0.5 M) and cooled to -42°C. MsCl (1.5 equiv) was added, followed by Et_3N (2 equiv) over 5 minutes. The reaction mixture was allowed to stir for 30 minutes. In a separate flame-dried flask under N_2, LiBr (4 equiv) was suspended in anhydrous THF (1 M) then slow-added to the mesylate solution *via* syringe pump over 15 minutes. The resulting slurry was stirred overnight and allowed to warm to room temperature. When complete, the slurry was poured into H_2O, the aqueous layer was extracted with Et_2O, and the combined organic extracts were washed with saturated aqeuous $NaHCO_3$, dried over anhydrous Na_2SO_4, filtered through celite under reduced pressure, and concentrated by rotary evaporation.

General Acetoacetate Addition Procedure: In a flame-dried flask under N_2, NaH (1.5 equiv, 60% dispersion in mineral oil) was suspended in half the requisite volume of anhydrous THF (0.2 M) and cooled to 0°C. The acetoacetate (1 equiv) was added, the reaction was stirred for 15 minutes, then *n*-BuLi (1.5 equiv, 2.5 M/hexanes) was added slowly. After stirring for 15 minutes, the allyllic bromide (2 equiv) was dissolved in the remaining anhydrous THF and added *via* syringe to the reaction mixture over 10 minutes. After stirring for 1.5 hours, the reaction was quenched with saturated aqueous NH_4Cl, the aqueous layer was extracted with Et_2O, and the combined organic extracts were washed with H_2O and brine, dried over anhydrous Na_2SO_4, filtered through celite under reduced pressure, and concentrated by rotary evaporation. The product was purified by silica flash chromatography.

General TsN_3 Diazo Transfer Procedure: In a flame-dried flask under N_2, the β-ketoester (1 equiv) was dissolved in anhydrous MeCN (0.1 M). Et_3N (1.5 equiv) was added, followed by TsN_3 (1.2 equiv), and the reaction was allowed to stir overnight. The solution was concentrated by rotary evaporation directly onto silica and purified by flash chromatography.

General Intramolecular Cyclopropanation Procedure: $Rh_2(esp)_2$ (0.5 mol%) was charged to a flame-dried flask under N_2, suspended in half the requisite volume of anhydrous DCM (0.02 M), then the suspension was cooled to 0°C. In a separate flame-dried flask under N_2, the α-diazo-β-ketoester (1 equiv) was dissolved in the remaining anhydrous DCM and transferred to the Rh flask *via* syringe in one shot with stirring. After 10 minutes, the solution was allowed to warm to room temperature. After 30 minutes, the reaction was quenched with saturated aqueous thiourea and stirred for an additional 30 minutes. Then, the aqueous layer was extracted with DCM and the combined organic layers were washed with brine, dried over anhydrous Na_2SO_4, filtered through celite under reduced pressure, and concentrated by rotary evaporation. The product was purified by silica flash chromatography.

General Saponification Procedure: The ester (1 equiv) was dissolved in MeOH (1 M) with stirring, then the solution was warmed to 50°C. NaOH (1.2 equiv, 1.7 M/H_2O) was added and the reaction mixture was stirred for 2 hours. Then, the reaction was allowed to cool to room temperature, and 1 M HCl was used to adjust the pH to 3. The aqueous layer was extracted with EtOAc and the combined organic extracts were dried over anhydrous Na_2SO_4, filtered through celite under reduced pressure, and concentrated by rotary evaporation. The product was purified by silica flash chromatography.

General Intramolecular Ring-Opening Cyclization Procedure: The Lewis acid (30 mol%) was charged to a flame-dried flask under N_2, then the bicyclo[3.1.0]hexane (1 equiv) was added as a solution in anhydrous DCM (0.1 M). When complete by TLC or after 24 hours, the reaction mixture was quenched with H_2O, the aqueous layer was extracted with DCM, and the combined organic extracts were dried over anhydrous $MgSO_4$, filtered through celite under reduced pressure, and concentrated by rotary evaporation. The product was purified by silica flash chromatography or prep-TLC.

General Intermolecular Formal [3+2] Cycloaddition Procedure: The Lewis acid (30 mol%) was charged to a flame-dried flask under N_2, followed by *p*-anisaldehyde (3 equiv). Then, the oxabicyclo[3.1.0]hexane (1 equiv) was added as a solution in anhydrous DCM (0.5 M). The reaction mixture was stirred at reflux for 24 h. After cooling to room temperature, the reaction mixture was quenched with H_2O, the aqueous layer was extracted with DCM, and the combined organic extracts were dried over anhydrous $MgSO_4$, filtered through celite under reduced pressure, and concentrated by rotary evaporation. Conversion was determined by quantitative NMR using DMTP as the internal standard, or the product was isolated by silica prep-TLC.

General Reduction Procedure: $LiAlH_4$ (3 or 4 equiv) was charged to a flame-dried flask under N_2, then the carbonyl-containing starting material (1 equiv) was added in anhydrous THF (0.1 M). After stirring overnight, the reaction mixture was quenched with 1 M HCl, the aqueous layer was extracted with Et_2O, and the combined organic extracts were washed with saturated aqueous $NaHCO_3$, dried over anhydrous Na_2SO_4, filtered through celite under reduced pressure, and concentrated by rotary evaporation.

4.7.3 Experimental Procedures

4.7.3.1 Procedures for the First Indole-tethered Model System

*2-(((tert-Butyldiphenylsilyl)oxy)methyl)prop-2-en-1-ol (**55a**).* Following the published procedure:[21] In a flame-dried flask under N_2, NaH (228 mg, 5.67 mmol, 60% dispersion in mineral oil) was suspended in 68 mL of anhydrous THF and cooled to 0°C. 2-Methylene-1,3-propanediol (500 mg, 5.67 mmol) was added dropwise, then the solution was allowed to warm to room temperature and stirred for 45 minutes. TBDPSCl (1.568 g, 5.67 mmol) was added and the mixture stirred for an additional hour. The reaction was quenched with H_2O, the aqueous layer extracted with EtOAc, and the combined organic extracts washed with brine, dried over anhydrous $MgSO_4$, filtered through celite under reduced pressure, and concentrated by rotary evaporation. After purification by silica flash chromatography (25% EtOAc/hexanes, R_f = 0.46), compound **55a** was afforded as a thick, colorless oil (1.550 g, 84% yield). NMR data were consistent with previously reported results.

*Methyl 6-(((tert-Butyldiphenylsilyl)oxy)methyl)-3-oxohept-6-enoate (**57a**).* The general mesylation-bromination and general acetoacetate addition procedures were followed using **55a** (1.123 g, 3.44 mmol), MsCl (0.4 mL, 5.16 mmol), and Et_3N (1 mL, 6.88 mmol) in 7 mL of anhydrous THF, LiBr (1.195 g, 13.76 mmol) in 14 mL of anhydrous THF, then methyl acetoacetate (200 mg, 1.72 mmol), NaH (103 mg, 2.58 mmol), and *n*-BuLi (1.2 mL, 2.58 mmol, 2.5 M/hexanes) in 9 mL of anhydrous THF. After purification by silica flash chromatography (25% EtOAc/hexanes, R_f = 0.57), compound **57a** was afforded as a viscous, light yellow oil (445.4 mg, 71% yield). ^{1}H NMR (300 MHz, $CDCl_3$) δ 7.71 (dd, *J* = 7.7, 1.8 Hz, 4H), 7.49 – 7.37 (m, 6H), 5.21 (s, 1H), 4.88 (d, *J* = 1.3 Hz, 1H),

4.14 (s, 2H), 3.73 (d, *J* = 0.5 Hz, 3H), 3.44 (s, 2H), 2.72 – 2.65 (m, 2H), 2.33 (t, *J* = 7.4 Hz, 2H), 1.10 (s, 9H). ^{13}C NMR (75 MHz, CDCl3) δ 201.71, 167.41, 146.32, 135.41, 133.34, 129.62, 129.60, 127.64, 127.61, 109.45, 66.36, 52.22, 48.83, 41.14, 26.72, 26.09, 19.16.

*Methyl 2-Diazo-3-Oxobutanoate (**60**).* The general TsN_3 diazo transfer procedure was followed using methyl acetoacetate (1 g, 8.61 mmol), TsN_3 (1.5 mL, 10.33 mmol), and Et_3N (1.8 mL, 12.9 mmol) in 48 mL of anhydrous MeCN. After purification by silica flash chromatography (25% EtOAc/hexanes), compound **60** was afforded as a yellow solid (945.3 mg, 77% yield). NMR data were consistent with previously reported results.[22]

*Methyl 6-(((tert-Butyldiphenylsilyl)oxy)methyl)-2-diazo-3-oxohept-6-enoate (**52a**).* The general TsN_3 diazo transfer procedure was followed using **57a** (2.183 g, 6.04 mmol), TsN_3 (1.1 mL, 7.24 mmol), and Et_3N (1.3 mL, 9.06 mmol) in 60 mL of anhydrous MeCN. After purification by silica flash chromatography (25% EtOAc/hexanes, R_f = 0.64), compound **52a** was afforded as a viscous, light yellow oil (2.226 g, 95% yield). ^{1}H NMR (300 MHz, $CDCl_3$) δ 7.73 – 7.66 (m, 4H), 7.44 – 7.35 (m, 6H), 5.21 (s, 1H), 4.92 (s, 1H), 4.15 (s, 2H), 3.83 (s, 3H), 3.05 – 2.97 (m, 2H), 2.36 (t, *J* = 7.6 Hz, 2H), 1.08 (s, 9H). ^{13}C NMR (75 MHz, $cdcl_3$) δ 191.86, 161.64, 146.67, 135.47, 133.51, 129.58, 127.64, 127.61, 127.57, 109.22, 66.39, 52.12, 38.38, 26.76, 19.23.

*Methyl 5-(((tert-Butyldiphenylsilyl)oxy)methyl)-2-oxobicyclo[3.1.0]hexane-1-carboxylate (**51a**).* The general intramolecular cyclopropanation procedure was followed using **52a** (2.226 g, 5.74 mmol) and $Rh_2(esp)_2$ (21.8 mg, 0.0287 mmol) in 287 mL of anhydrous DCM. After purification by silica flash chromatography (25% EtOAc/hexanes, R_f = 0.43), compound **51a** was afforded as an off-white solid (1.844 g, 89% yield). ^{1}H NMR (300 MHz, $CDCl_3$) δ 7.66 – 7.57 (m, 4H), 7.47 – 7.35 (m, 6H), 3.95 (d, *J* = 11.4 Hz,

1H), 3.74 (s, 3H), 3.73 (d, 1H), 2.45 (dd, *J* = 21.5, 10.2 Hz, 1H), 2.35 – 2.15 (m, 2H), 2.05 – 1.90 (m, 2H), 1.43 (d, *J* = 5.2 Hz, 1H), 1.03 (s, 9H). ^{13}C NMR (75 MHz, $CDCl_3$) δ 207.68, 167.82, 135.54, 135.49, 133.15, 133.01, 129.80, 129.79, 127.74, 127.72, 63.67, 52.52, 46.29, 42.43, 33.99, 26.69, 23.77, 23.37, 19.30.

*5-(((tert-Butyldiphenylsilyl)oxy)methyl)-2-oxobicyclo[3.1.0]hexane-1-carboxylic Acid (**58a**).* The general saponification procedure was followed using **51a** (500 mg, 1.39 mmol) and NaOH (1 mL, 1.67 mmol, 1.7 M/H_2O) in 1.4 mL of MeOH. After purification by silica flash chromatography (10% MeOH/DCM, R_f = 0.65), compound **58a** was afforded as a white solid (333.9 mg, 70% yield). ^{1}H NMR (500 MHz, $CDCl_3$) δ 7.67 – 7.61 (m, 4H), 7.46 – 7.37 (m, 6H), 4.13 (d, *J* = 11.4 Hz, 1H), 4.05 (d, *J* = 11.4 Hz, 1H), 2.54 – 2.31 (m, 3H), 2.20 (d, *J* = 4.7 Hz, 1H), 2.09 (ddd, *J* = 12.4, 8.0, 2.0 Hz, 1H), 1.83 (d, *J* = 4.7 Hz, 1H), 1.04 (s, 9H). ^{13}C NMR (126 MHz, $CDCl_3$) δ 215.57, 167.76, 135.64, 135.55, 133.32, 132.78, 129.83, 129.79, 127.74, 62.68, 49.89, 40.53, 32.61, 29.90, 26.77, 23.42, 19.32.

*5-(((tert-Butyldiphenylsilyl)oxy)methyl)-1-(3-methyl-1H-indole-1-carbonyl)bicyclo[3.1.0]hexan-2-one (**50a**).* Following the published procedure:[23] In a flame-dried flask under N_2, **58a** (50 mg, 0.145 mmol) was dissolved in 0.8 mL of andrydrous DCM. Mukaiyama's reagent (44.5 mg, 0.174 mmol) and 3-methylindole (104.7 mg, 0.789 mmol) were subsequently added, then the reaction mixture was stirred at reflux for 1 hour. After cooling the mixture to room temperature, Et_3N (0.04 mL, 0.305 mmol) was added and the mixture stirred at reflux overnight. Then, the mixture was cooled to room temperature and poured into H_2O. The aqueous layer was extracted with DCM, then the combined organic layers were dried over anhydrous Na_2SO_4, filtered through celite

under reduced pressure, and concentrated by rotary evaporation. After purification by silica flash chromatography (25% EtOAc/hexanes, R_f = 0.46), compound **50a** was afforded as a yellow, foamy solid (26.2 mg, 39% yield). ^{1}H NMR (500 MHz, CD_2Cl_2) δ 8.43 (d, *J* = 8.0 Hz, 1H), 7.52 (ddd, *J* = 7.4, 1.4, 0.7 Hz, 1H), 7.42 – 7.28 (m, 8H), 7.22 (t, *J* = 7.6 Hz, 2H), 7.13 – 7.08 (m, 2H), 6.93 (s, 1H), 4.01 (d, *J* = 11.7 Hz, 1H), 3.64 (d, *J* = 11.7 Hz, 1H), 2.58 – 2.40 (m, 3H), 2.20 (d, *J* = 1.3 Hz, 3H), 2.18 – 2.11 (m, 2H), 1.56 (d, *J* = 5.2 Hz, 1H), 0.87 (s, 9H). ^{13}C NMR (126 MHz, CD_2Cl_2) δ 209.37, 165.11, 136.40, 136.04, 135.86, 133.08, 132.98, 132.24, 130.28, 130.18, 128.20, 128.15, 125.57, 124.24, 123.48, 119.35, 118.91, 117.15, 63.82, 47.74, 45.31, 33.89, 26.90, 24.09, 20.78, 19.39, 10.09.

4.7.3.2 Procedures for the Second Indole-tethered Model System

*2-Phenylprop-2-en-1-ol (**55b**).* Following the published Gilman procedure:[9] In a flame-dried flask under N_2, propargyl alcohol (500 mg, 8.92 mmol) and CuI (850 mg, 4.46 mmol) were suspended in 12 mL of anhydrous toluene. After cooling the suspension to -78°C, PhMgBr (27 mL, 26.8 mmol, 1 M/THF) was added dropwise *via* syringe pump. The reaction mixture was allowed to warm slowly to room temperature and stirred overnight. After checking progress of reaction by TLC, the reaction mixture was cooled to 0°C and quenched with saturated aqueous NH_4Cl. The aqueous layer was extracted with Et_2O, then the combined organic extracts were dried over anhydrous Na_2SO_4, filtered through celite under reduced pressure, and concentrated by rotary evaporation. After purification by silica flash chromatography (25% EtOAc/hexanes, R_f = 0.38), compound **55b** was afforded as a thick colorless oil (957.5 mg, 80% yield). NMR data were consistent with previously reported results.

*Methyl 3-Oxo-6-phenylhept-6-enoate (**57b**).* The general mesylation-bromination and general acetoacetate addition procedures were followed using **55b** (756.5 mg, 5.64 mmol), MsCl (0.65 mL, 8.46 mmol), and Et_3N (1.6 mL, 11.3 mmol) in 11 mL of anhydrous THF, LiBr (1.958 g, 22.6 mmol) in 23 mL of anhydrous THF, then methyl acetoacetate (327 mg, 2.82 mmol), NaH (169.1 mg, 4.23 mmol), and *n*-BuLi (1.7 mL, 4.23 mmol, 2.5 M/hexanes) in 14 mL of anhydrous THF. After purification by silica flash chromatography (25% EtOAc/hexanes, R_f = 0.48), compound **57b** was afforded as a thin yellow oil (655.1 mg, 69% yield). ^{1}H NMR (500 MHz, $CDCl_3$) δ 7.41 – 7.36 (m, 1H), 7.36 – 7.31 (m, 1H), 7.30 – 7.26 (m, 1H), 3.72 (s, 1H), 3.42 (s, 1H), 2.85 – 2.80 (m, 1H), 2.70 (dd, *J* = 8.4, 6.4 Hz, 1H).

*Methyl 2-Diazo-3-oxo-6-phenylhept-6-enoate (**52b**).* The general TsN_3 diazo transfer procedure was followed using **57b** (1.098 g, 4.73 mmol), TsN_3 (0.9 mL, 5.67 mmol), and Et_3N (1.0 mL, 7.09 mmol) in 48 mL of anhydrous MeCN. After purification by silica flash chromatography (25% EtOAc/hexanes, R_f = 0.55), compound **52b** was afforded as an off-white, chalky solid (1.187 g, 97% yield). ^{1}H NMR (500 MHz, $CDCl_3$) δ 7.43 – 7.40 (m, 2H), 7.35 – 7.30 (m, 2H), 7.29 – 7.26 (m, 1H), 5.32 (s, 1H), 5.11 (s, 1H), 3.80 (s, 3H), 3.06 – 3.00 (m, 2H), 2.89 – 2.83 (m, 2H).

*Methyl 2-Oxo-5-phenylbicyclo[3.1.0]hexane-1-carboxylate (**51b**).* The general intramolecular cyclopropanation procedure was followed using **52b** (100 mg, 0.387 mmol) and $Rh_2(esp)_2$ (1.5 mg, 1.94 μmol) in 19 mL of anhydrous DCM. After purification by silica flash chromatography (25% EtOAc/hexanes, R_f = 0.75), compound **52b** was afforded as an off-white solid (70.4 mg, 89% yield). ^{1}H NMR (500 MHz, CD_2Cl_2) δ 7.35 (d, *J* = 4.2 Hz, 4H), 7.33 – 7.28 (m, 1H), 3.47 (s, 3H), 2.50 (d, *J* = 5.2 Hz, 1H), 2.42 – 2.33 (m, 4H),

1.75 (d, *J* = 5.2 Hz, 1H). ^{13}C NMR (126 MHz, CD_2Cl_2) δ 206.80, 166.72, 138.65, 128.79, 128.57, 127.92, 51.99, 48.19, 45.77, 34.49, 30.44, 23.27.

*2-Oxo-5-phenylbicyclo[3.1.0]hexane-1-carboxylic Acid (**58b**).* The general saponification procedure was followed using **51b** (456 mg, 1.98 mmol) and NaOH (1.4 mL, 2.38 mmol, 1.7 M/H_2O) in 2 mL of MeOH. After purification by silica flash chromatography (10% MeOH/DCM, R_f = 0.35), compound **58b** was afforded as an off-white foam (428.2 mg, 96% yield). ^{1}H NMR (500 MHz, CDCl3) δ 7.39 – 7.29 (m, 5H), 2.79 (d, *J* = 4.6 Hz, 1H), 2.57 – 2.49 (m, 2H), 2.45 (dd, *J* = 10.6, 4.0 Hz, 2H), 2.15 (d, *J* = 4.6 Hz, 1H). ^{13}C NMR (126 MHz, $CDCl_3$) δ 214.58, 166.24, 136.84, 128.97, 128.76, 128.50, 52.56, 43.72, 33.40, 30.34, 29.41.

4.7.3.3 Procedures for the Third Indole-tethered Model System

*1-(3-Methyl-1H-indol-1-yl)ethan-1-one (**63**).* In a flame-dried flask under N_2, 3-methylindole (100 mg, 0.762 mmol) and *n*-Bu_4NHSO_4 (25.9 mg, 0.0762 mmol) were dissolved in 1.9 mL of anhydrous DCM. Powdered NaOH (76.2 mg, 1.91 mmol) was added, then acetyl chloride (0.08 mL, 1.14 mmol) was added as a solution in 1.2 mL of anhydrous DCM. After 2.5 hours, the reaction mixture was concentrated by rotary evaporation directly onto silica. After purification by silica flash chromatography (25% EtOAc/hexanes), compound **63** was afforded (116.4 mg, 88% yield). NMR data were consistent with previously reported results.[24]

*1-(3-Methyl-1H-indol-1-yl)butane-1,3-dione (**67**).* In a flame-dried flask under N_2, 2,2,6-trimethyl-4*H*-1,3-dioxin-4-one (2 g, 14.1 mmol) and 3-methylindole (1.846 g, 14.1 mmol) were dissolved in 56 mL of anhydrous toluene and the solution heated to reflux overnight. Then, after cooling to room temperature, the reaction mixture was concentrated

by rotary evaporation directly onto silica. After purification by silica flash chromatography (25% EtOAc/hexanes, R_f = 0.46), compound **67** was afforded in a 1.5:1 *keto-enol* mixture as a viscous orange oil (3.029 g, 88% yield). ^{1}H NMR (500 MHz, $CDCl_3$) δ 14.05 (s, 1H), 8.45 (d, *J* = 8.2 Hz, 2H), 7.50 (d, *J* = 7.7 Hz, 3H), 7.40 – 7.27 (m, 5H), 7.22 – 7.19 (m, 1H), 7.09 (s, 1H), 5.66 (s, 1H), 3.99 (s, 3H), 2.37 (s, 4H), 2.28 (dd, *J* = 7.5, 1.3 Hz, 8H), 2.11 (s, 3H).

*6-Methyl-1-(3-methyl-1H-indol-1-yl)hept-6-ene-1,3-dione (**68**).* In a flame-dried flask under N_2, **67** (100 mg, 0.465 mmol) and methallyl bromide (0.07 mL, 0.698 mmol) were dissolved in 4.7 mL of anhydrous THF. After cooling the solution to -15°C (with an ethylene glycol/dry ice bath), LHMDS (1.2 mL, 1.16 mmol, 1 M/THF) was slow-added *via* syringe pump over 10 minutes. After 6 hours, the reaction mixture was quenched with saturated aqueous NH_4Cl and allowed to warm to room temperature. The aqueous layer was extracted with Et_2O, then the combined organic extracts were washed with H_2O and brine, dried over anhydrous Na_2SO_4, filtered through celite under reduced pressure, and concentrated by rotary evaporation. After purification by silica flash chromatography (25% Et_2O/hexanes, R_f = 0.48), compound **68** was afforded in an 8:1 *keto-enol* mixture as a light orange oil (73.8 mg, 59% yield). ^{1}H NMR (500 MHz, $CDCl_3$) δ 8.44 (d, *J* = 8.1 Hz, 1H), 7.50 (ddd, *J* = 7.6, 1.3, 0.7 Hz, 1H), 7.37 (td, *J* = 8.3, 7.9, 1.3 Hz, 1H), 7.32 (td, *J* = 7.5, 1.1 Hz, 1H), 7.11 (s, 1H), 4.74 (s, 1H), 4.67 (s, 1H), 4.01 (s, 2H), 2.84 – 2.79 (m, 2H), 2.35 (t, *J* = 7.5 Hz, 2H), 2.27 (d, *J* = 1.3 Hz, 3H), 1.73 (s, 3H). ^{13}C NMR (126 MHz, $CDCl_3$) δ 202.36, 164.34, 143.85, 125.46, 123.96, 121.76, 119.57, 118.93, 116.70, 110.57, 51.76, 41.15, 31.11, 22.61, 9.73.

*2-Diazo-1-(3-methyl-1H-indol-1-yl)butane-1,3-dione (**70**).* The general TsN_3 diazo transfer procedure was followed using **67** (670 mg, 2.78 mmol), TsN_3 (0.51 mL, 3.33 mmol), and Et_3N (0.58 mL, 4.16 mmol) in 28 mL of anhydrous MeCN. After purification by silica flash chromatography (25% EtOAc/hexanes), compound **70** was afforded (741.8 mg, 99% yield). ^{1}H NMR (500 MHz, $CDCl_3$) δ 8.06 (d, *J* = 8.2 Hz, 1H), 7.54 (d, *J* = 7.8 Hz, 1H), 7.41 – 7.36 (m, 1H), 7.32 (td, *J* = 7.5, 1.1 Hz, 1H), 7.10 (d, *J* = 1.3 Hz, 1H), 2.52 (s, 3H), 2.30 (d, *J* = 1.3 Hz, 3H). ^{13}C NMR (126 MHz, $CDCl_3$) δ 190.06, 158.15, 135.59, 131.49, 125.33, 123.82, 121.42, 119.33, 119.12, 115.12, 28.18, 9.73.

*2-Diazo-6-methyl-1-(3-methyl-1H-indol-1-yl)hept-6-ene-1,3-dione (**66a**).* The general TsN_3 diazo transfer procedure was followed using **68** (70.5 mg, 0.262 mmol), TsN_3 (0.05 mL, 0.314 mmol), and Et_3N (0.05 mL, 0.393 mmol) in 2.6 mL of anhydrous MeCN. After purification by silica flash chromatography (25% EtOAc/hexanes, R_f = 0.65), compound **66a** was afforded as an orange solid (74.6 mg, 96% yield). ^{1}H NMR (500 MHz, $CDCl_3$) δ 8.05 (d, *J* = 8.2 Hz, 1H), 7.54 (d, *J* = 8.1 Hz, 1H), 7.38 (td, *J* = 8.3, 7.8, 1.2 Hz, 1H), 7.32 (td, *J* = 7.5, 1.1 Hz, 1H), 7.09 (q, *J* = 1.3 Hz, 1H), 4.75 (d, *J* = 20.0 Hz, 2H), 3.04 – 2.98 (m, 2H), 2.42 (t, *J* = 7.6 Hz, 2H), 2.30 (s, 3H), 1.76 (s, 3H). ^{13}C NMR (126 MHz, $CDCl_3$) δ 192.33, 158.10, 144.02, 135.58, 131.50, 125.32, 123.80, 121.42, 119.34, 119.09, 115.12, 110.72, 38.51, 32.13, 22.55, 9.74.

*5-Methyl-1-(3-methyl-1H-indole-1-carbonyl)bicyclo[3.1.0]hexan-2-one (**50c**).* The general intramolecular cyclopropanation procedure was followed using **66a** (300 mg, 1.02 mmol) and $Rh_2(esp)_2$ (3.9 mg, 5.08 μmol) in 51 mL of anhydrous DCM. After purification by silica flash chromatography (25% EtOAc/hexanes, R_f = 0.29), compound **50c** was afforded as a light orange solid (255.8 mg, 94% yield). ^{1}H NMR (500 MHz,

$CDCl_3$) δ 8.43 (d, *J* = 8.1 Hz, 1H), 7.49 (ddd, *J* = 7.6, 1.2, 0.7 Hz, 1H), 7.36 (td, *J* = 8.3, 7.8, 1.3 Hz, 1H), 7.31 (td, *J* = 7.5, 1.1 Hz, 1H), 6.80 (s, 1H), 2.38 (td, *J* = 9.5, 8.8, 2.0 Hz, 2H), 2.27 (d, *J* = 1.3 Hz, 4H), 2.25 – 2.19 (m, 1H), 1.93 (d, *J* = 5.1 Hz, 1H), 1.63 (d, *J* = 5.2 Hz, 1H), 1.40 (s, 3H). ^{13}C NMR (126 MHz, $CDCl_3$) δ 208.92, 164.69, 135.80, 131.53, 125.15, 123.72, 121.99, 118.75, 118.73, 116.58, 48.00, 38.78, 33.66, 28.66, 24.59, 19.09, 9.80.

4.7.3.4 Procedures for the Benzofuran-tethered Model System

*2-Phenylallyl Acetate (**72**).* Following the published procedure:[25] In a flame-dried flask under N_2, **55b** (500 mg, 3.73 mmol) was dissolved in 19 mL of anhydrous DCM. The solution was cooled to 0°C, then DIPEA (0.8 mL, 4.47 mmol), DMAP (45.5 mg, 0.373 mmol), and Ac_2O (0.42 mL, 4.47 mmol) were added in sequence. After stirring for 30 minutes, the reaction mixture was quenched with 1% HCl, the aqueous layers were extracted with DCM, and the combined organic extracts were washed with brine, dried over anhydrous Na_2SO_4, filtered through celite under reduced pressure, and concentrated by rotary evaporation. Compound **72** was afforded without further purification (25% EtOAc/hexanes, R_f = 0.69) as a slightly viscous light yellow liquid (586.4 mg, 89% yield). NMR data were consistent with previously reported results.

*2-Phenylallyl 3-(Benzofuran-2-yl)-3-oxopropanoate (**73**).* In a flame-dried flask under N_2, benzofuran-2-carboxylic acid (503.6 mg, 3.11 mmol) was dissolved in 6.2 mL of anhydrous DCM, then the solution was cooled to 0°C. Anhydrous DMF (4 drops) was added, then the flask was equipped with an empty N_2-flushed balloon to vent any HCl vapors. $(COCl)_2$ (0.32 mL, 3.73 mmol) was added slowly. After 15 minutes, the reaction mixture was allowed to warm to room temperature and stirred for 3 hours. The resulting

clear solution was then concentrated by rotary evaporation. Then, in a separate flame-dried flask under N_2, **72** (574.6 mg, 3.26 mmol) was dissolved in 1.6 mL of anhydrous THF. The solution was cooled to -78°C, then LHMDS (6.5 mL, 6.52 mmol, 1M/THF) was added dropwise and the solution stirred for 45 minutes. The prepared benzofuran-2-carboxylic acid chloride was dissolved in 1.7 mL of anhydrous THF and added *via* syringe to the acetate solution, which was stirred for an additional 30 minutes. The reaction mixture was quenched with saturated aqueous NH_4Cl, the aqueous layers extracted with EtOAc, and the combined organic extracts dried over anhydrous Na_2SO_4, filtered through celite under reduced pressure, and concentrated by rotary evaporation. After purification by silica flash chromatography (5% EtOAc/hexanes, R_f = 0.26), compound **73** was afforded in a 10:1 *enol-keto* mixture as an off-white solid (644.3 mg, 65% yield). ^{1}H NMR (500 MHz, $CDCl_3$) δ 11.99 (s, 1H), 7.64 (d, *J* = 7.8 Hz, 1H), 7.50 – 7.45 (m, 3H), 7.38 (td, *J* = 7.4, 1.5 Hz, 3H), 7.35 – 7.32 (m, 1H), 7.31 (d, *J* = 3.7 Hz, 1H), 7.29 – 7.26 (m, 1H), 5.91 (s, 1H), 5.60 (s, 1H), 5.45 – 5.41 (m, 1H), 5.16 – 5.12 (m, 2H). ^{13}C NMR (126 MHz, $CDCl_3$) δ 162.06, 155.41, 142.27, 128.54, 128.14, 126.62, 126.00, 123.53, 122.23, 115.50, 111.59, 108.90, 88.43, 65.69.

*2-Phenylallyl 3-(Benzofuran-2-yl)-2-diazo-3-oxopropanoate (**74**).* In a flame-dried flask under N_2, **73** (639.7 mg, 2.00 mmol) was dissolved in 4 mL of anhydrous MeCN, then Et_3N (0.33 mL, 2.40 mmol) was added. After cooling the solution to 0°C, *p*-ABSA (2.20 mmol) was added. The reaction mixture was allowed to warm to room temperature and stirred overnight. Then, the reaction mixture was filtered through celite under reduced pressure and concentrated by rotary evaporation directly onto silica. After purification by silica flash chromatography (25% EtOAc/hexanes, R_f = 0.52), compound **74** was afforded

as a yellow solid (660.9 mg, 95% yield). ^{1}H NMR (500 MHz, $CDCl_3$) δ 7.81 (s, 1H), 7.70 (d, *J* = 7.9 Hz, 1H), 7.55 (d, *J* = 9.1 Hz, 1H), 7.50 – 7.45 (m, 1H), 7.43 (dd, *J* = 8.2, 1.4 Hz, 2H), 7.39 – 7.29 (m, 4H), 5.60 (s, 1H), 5.43 (s, 1H), 5.21 (s, 2H).

*1-(Benzofuran-2-carbonyl)-5-phenyl-3-oxabicyclo[3.1.0]hexan-2-one (**75**).* The general intramolecular cyclopropanation procedure was followed using **74** (655.2 mg, 1.89 mmol) and $Rh_2(esp)_2$ (7.2 mg, 9.45 μmol) in 94 mL of anhydrous DCM. After purification by silica flash chromatography (25% EtOAc/hexanes, R_f = 0.35), compound **75** was afforded as a yellow solid (363.0 mg, 60% yield). ^{1}H NMR (500 MHz, $CDCl_3$) δ 7.71 (d, *J* = 7.9 Hz, 1H), 7.63 (d, *J* = 9.3 Hz, 1H), 7.55 – 7.50 (m, 2H), 7.36 – 7.31 (m, 1H), 7.28 (dd, *J* = 7.2, 2.5 Hz, 2H), 7.23 (dd, *J* = 5.1, 2.0 Hz, 3H), 4.83 (d, *J* = 10.5 Hz, 1H), 4.59 (d, *J* = 9.8 Hz, 1H), 2.91 (d, *J* = 5.2 Hz, 1H), 1.74 (d, *J* = 5.1 Hz, 1H). ^{13}C NMR (126 MHz, $CDCl_3$) δ 179.55, 172.58, 155.62, 151.97, 132.18, 129.18, 129.03, 129.00, 128.72, 126.94, 124.18, 123.59, 114.29, 112.58, 73.75, 45.72, 42.40, 20.12.

*(Z)-3-(Benzofuran-2-yl(hydroxy)methylene)-5-phenyl-3,6-dihydro-2H-pyran-2-one (**76'**).* The general intramolecular ring-opening cyclization procedure was followed using $Ga(OTf)_3$ (36.6 mg, 0.0708 mmol) and 1-(benzofuran-2-carbonyl)-5-phenyl-3-oxabicyclo[3.1.0]hexan-2-one (75 mg, 0.236 mmol) in 1.2 mL of anhydrous DCM. After work-up, the product was afforded without further purification (25% EtOAc/hexanes, R_f = 0.63) as an orange solid (61.3 mg, 81% yield). ^{1}H NMR (500 MHz, $CDCl_3$) δ 13.38 (s, 1H), 7.80 (t, *J* = 1.4 Hz, 1H), 7.71 – 7.68 (m, 1H), 7.60 – 7.57 (m, 1H), 7.50 (d, *J* = 0.9 Hz, 1H), 7.42 (q, *J* = 3.1 Hz, 5H), 7.37 – 7.31 (m, 2H), 5.46 (d, *J* = 1.5 Hz, 2H).

4.7.3.5 Procedures for the Decarbonylated Model Systems

*1-(Hydroxymethyl)-5-phenylbicyclo[3.1.0]hexan-2-ol (**77**).* The general reduction procedure was followed using **51b** (500 mg, 2.17 mmol) and $LiAlH_4$ (329.6 mg, 8.68 mmol) in 22 mL of anhydrous THF. Compound **77** was afforded without further purification (10% MeOH/DCM, R_f = 0.42) in a 3:1 mixture of diastereomers as a white solid (276.2 mg, 62% yield). ^{1}H NMR (500 MHz, $CDCl_3$) δ 7.35 – 7.28 (m, 2H), 7.27 (d, *J* = 1.8 Hz, 1H), 7.25 (t, *J* = 1.5 Hz, 1H), 7.24 – 7.19 (m, 1H), 4.84 – 4.76 (m, 1H), 3.72 (dd, *J* = 11.5, 4.0 Hz, 1H), 3.32 (dd, *J* = 11.5, 5.3 Hz, 1H), 2.17 (d, *J* = 4.1 Hz, 1H), 2.14 – 1.99 (m, 3H), 1.63 (t, *J* = 5.1 Hz, 1H), 1.34 – 1.21 (m, 2H), 1.00 (d, *J* = 5.3 Hz, 1H). ^{13}C NMR (126 MHz, $CDCl_3$) δ 141.17, 129.23, 128.93, 128.49, 128.44, 126.68, 66.08, 39.27, 37.42, 33.27, 29.26, 13.48.

*Benzofuran-2-ylmethanol (**79**).* The general reduction procedure was followed using benzofuran-2-carboxylic acid (500 mg, 3.08 mmol) and $LiAlH_4$ (351.1 mg, 9.25 mmol) in 31 mL of anhydrous THF. After purification by silica flash chromatography (25% EtOAc/hexanes), compound **79** was afforded as a white solid (235.8 mg, 51% yield). NMR data were consistent with previously reported results.[26]

*2-(Bromomethyl)benzofuran (**80**).* Following the published procedure:[27] In a flame-dried flask under N_2, **79** (100 mg, 0.675 mmol) was dissolved in 2.7 mL of anhydrous THF. The solution was cooled to 0°C, then PBr_3 (0.27 mL, 0.270 mmol, 1 M/DCM) was added dropwise. After stirring for 1 hour, the reaction was quenched with H_2O, the aqueous layer extracted with DCM, and the combined organic extracts dried over anhydrous Na_2SO_4, filtered through celite under reduced pressure, and concentrated by rotary evaporation.

After purification by silica flash chromatography (25% EtOAc/hexanes, R_f = 0.77), compound **80** was afforded as an inseparable mixture with unreacted **79**.

4.7.3.6 Procedures for the Ring-Expanded Model System

*3-(3-Methyl-1H-indol-1-yl)-3-oxopropanoic Acid (**85**).* In a flame-dried flask under N_2, Meldrum's acid (1 g, 6.94 mmol) and 3-methylindole (1.366 g, 10.4 mmol) were dissolved in 28 mL of anhydrous THF. The solution was stirred at reflux overnight. Then, after cooling to room temperature, the reaction mixture was concentrated by rotary evaporation directly onto silica. After purification by silica flash chromatography (10% MeOH/DCM, R_f = 0.18), compound **85** was afforded as an orange solid (938.3 mg, 62% yield). ^{1}H NMR (500 MHz, $CDCl_3$) δ 8.42 (s, 1H), 7.53 – 7.49 (m, 1H), 7.42 – 7.32 (m, 2H), 7.10 (s, 1H), 3.98 (s, 2H), 3.49 (s, 1H), 2.29 (d, *J* = 1.4 Hz, 3H). ^{13}C NMR (126 MHz, $CDCl_3$) δ 168.68, 165.28, 125.90, 124.48, 120.89, 120.70, 119.15, 50.83, 40.91, 9.76.

*3-Methylbut-3-en-1-yl 3-(3-Methyl-1H-indol-1-yl)-3-oxopropanoate (**86**).* In a flame-dried flask under N_2, **85** (100 mg, 0.460 mmol), 3-methyl-3-buten-1-ol (16.5 mg, 0.192 mmol), and DMAP (2.3 mg, 0.0192 mmol) were dissolved in 1.3 mL of anhydrous DCM. Then, DCC (79.2 mg, 0.384 mmol) was added, and the reaction mixture was stirred at reflux for 90 minutes. The reaction mixture was allowed to cool to room temperature then filtered through a pad of celite under reduced pressure, using Et_2O as the eluent. The filtrate was partitioned between Et_2O and H_2O, the aqueous layer was extracted with Et_2O, and the combined organic extracts were washed with H_2O and brine, dried over anhydrous $MgSO_4$, filtered through celite under reduced pressure, and concentrated by rotary evaporation. After purification by silica flash chromatography (25% EtOAc/hexanes, R_f = 0.52), compound **86** was afforded as an orange oil (36.2 mg, 66% yield). ^{1}H NMR (500

MHz, $CDCl_3$) δ 8.43 (s, 1H), 7.50 (d, *J* = 7.6 Hz, 1H), 7.39 – 7.28 (m, 3H), 7.14 (d, *J* = 32.1 Hz, 1H), 4.71 (d, *J* = 24.8 Hz, 2H), 4.31 (t, *J* = 6.8 Hz, 2H), 3.91 (s, 2H), 2.59 (s, 1H), 2.35 (t, *J* = 6.8 Hz, 2H), 2.28 (dd, *J* = 3.7, 1.3 Hz, 4H), 1.71 (s, 3H). ^{13}C NMR (126 MHz, $CDCl_3$) δ 168.23, 166.30, 163.35, 141.05, 135.93, 131.45, 125.41, 125.09, 123.84, 123.31, 122.15, 121.48, 119.40, 118.83, 118.75, 118.31, 116.67, 112.51, 63.88, 43.78, 36.44, 22.25, 9.67, 9.64.

4.7.3.7 Procedures for the Intermolecular Formal [3+2] Cycloaddition

*Methyl (2-Phenylallyl) Malonate (**90**).* In a flame-dried flask under N_2, **62** (1 g, 7.45 mmol) was dissolved in 7.5 mL of anhydrous DCM. After cooling the solution to 0°C, Et_3N (1.2 mL, 8.94 mmol) was added and the reaction was stirred for 15 minutes. Then, methyl malonyl chloride (1 mL, 8.94 mmol) was added slowly. The reaction mixture was allowed to warm to room temperature and stirred for an additional 30 minutes, then quenched with saturated aqueous $NaHCO_3$. The aqueous layers were extracted with DCM and the combined organic extracts were washed with saturated aqueous $NaHCO_3$ and brine, dried over anhydrous Na_2SO_4, filtered through celite under reduced pressure, and concentrated by rotary evaporation. Compound **90** was afforded without further purification (25% EtOAc/hexanes, R_f = 0.52) as a slightly viscous orange liquid (1.822 g, *quant.*). ^{1}H NMR (500 MHz, $CDCl_3$) δ 7.44 – 7.40 (m, 2H), 7.38 – 7.29 (m, 3H), 5.58 – 5.56 (m, 1H), 5.39 (d, *J* = 0.9 Hz, 1H), 5.07 – 5.04 (m, 2H), 3.68 (s, 3H), 3.41 (s, 2H). ^{13}C NMR (126 MHz, $CDCl_3$) δ 166.73, 166.14, 141.84, 137.72, 128.47, 128.11, 125.93, 115.79, 66.68, 52.46, 41.32.

*1-Methyl 3-(2-Phenylallyl) 2-Diazomalonate (**91**).* The general TsN_3 diazo transfer procedure was followed using **90** (200 mg, 0.757 mmol), TsN_3 (0.14 mL, 0.908 mmol),

and Et_3N (0.16 mL, 1.14 mmol) in 7.6 mL of anhydrous MeCN. After purification by silica flash chromatography (25% Et_2O/hexanes, R_f = 0.22), compound **91** was afforded as a yellow solid (203.4 mg, 92% yield). ^{1}H NMR (300 MHz, $CDCl_3$) δ 7.45 – 7.40 (m, 2H), 7.39 – 7.30 (m, 3H), 5.57 (d, *J* = 0.7 Hz, 1H), 5.41 (q, *J* = 1.3 Hz, 1H), 5.14 (dd, *J* = 1.3, 0.6 Hz, 2H), 3.83 (s, 3H). ^{13}C NMR (75 MHz, CDCl3) δ 161.44, 160.55, 141.90, 137.70, 128.51, 128.14, 125.95, 115.61, 66.44, 52.56.

*Methyl 2-Oxo-5-phenyl-3-oxabicyclo[3.1.0]hexane-1-carboxylate (**89**).* The general intramolecular cyclopropanation procedure was followed using **91** (1.657 g, 5.67 mmol) and $Rh_2(esp)_2$ (21.5 mg, 0.0284 mmol) in 113 mL of anhydrous DCM. After purification by silica flash chromatography (25% EtOAc/hexanes, R_f = 0.27), compound **89** was afforded as a white solid (1.160 g, 77% yield). ^{1}H NMR (500 MHz, $CDCl_3$) δ 7.40 – 7.32 (m, 5H), 4.47 (dd, *J* = 9.7, 0.8 Hz, 1H), 4.42 (d, *J* = 9.7 Hz, 1H), 3.60 (s, 3H), 2.61 (d, *J* = 5.0 Hz, 1H), 1.72 (d, *J* = 5.1 Hz, 1H). ^{13}C NMR (126 MHz, $CDCl_3$) δ 170.94, 164.89, 133.02, 129.23, 129.04, 73.21, 52.81, 43.85, 36.53, 22.59.

*Methyl (1R,5S)-7-(4-Methoxyphenyl)-2-oxo-5-phenyl-3,6-dioxabicyclo[3.2.1]octane-1-carboxylate (**97**).* The general intermolecular formal [3+2] cycloaddition procedure was followed using **89** (75 mg, 0.323 mmol), *p*-anisaldehyde (0.12 mL, 0.969 mmol), and $Ga(OTf)_3$ (50.1 mg, 0.0969 mmol) in 0.6 mL of anhydrous DCM. After purification by silica prep-TLC (25% EtOAc/hexanes, R_f = 0.15), compound **97** was afforded as a white solid (9.5 mg, 12% yield). ^{1}H NMR (500 MHz, $CDCl_3$) δ 7.55 (d, *J* = 8.5 Hz, 2H), 7.50 (dd, *J* = 8.3, 1.4 Hz, 2H), 7.40 (dt, *J* = 20.4, 6.7 Hz, 3H), 6.91 (d, *J* = 8.9 Hz, 2H), 4.58 (dd, *J* = 11.7, 1.8 Hz, 1H), 4.50 (d, *J* = 11.6 Hz, 1H), 3.88 (s, 1H), 3.81 (d, *J* = 5.1 Hz, 6H), 3.18 (d, *J* = 11.9 Hz, 1H), 2.82 (dd, *J* = 11.9, 2.1 Hz, 1H). ^{13}C NMR (126

MHz, $CDCl_3$) δ 167.60, 165.57, 159.88, 137.48, 132.31, 128.81, 128.74, 128.04, 127.84, 125.33, 113.76, 113.74, 84.23, 81.30, 79.89, 63.22, 55.20, 52.91, 41.07. HRAM-MS (EI) m/z $[M+Na]^+$ Calcd for $C_{21}H_{20}O_6$ 391.1152; Found 391.1143.

4.8 Copies of NMR Spectra

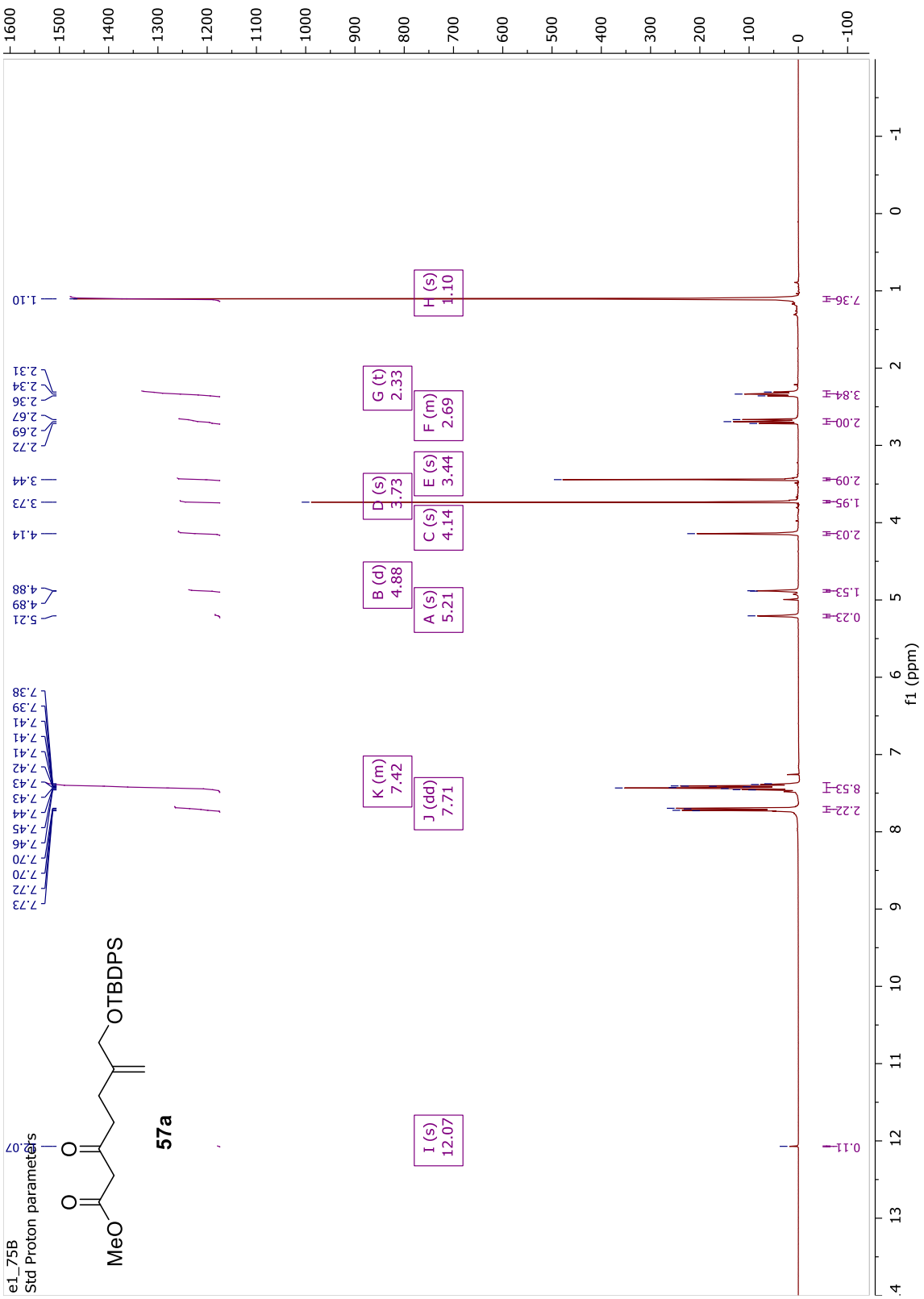
e1_75B
Std Proton parameters
MeO
OTBDPS
57a
I (s) 12.07
J (dd) 7.71
K (m) 7.42
A (s) 5.21
B (d) 4.88
C (s) 4.14
D (s) 3.73
E (s) 3.44
F (m) 2.69
G (t) 2.33
H (s) 1.10
f1 (ppm)

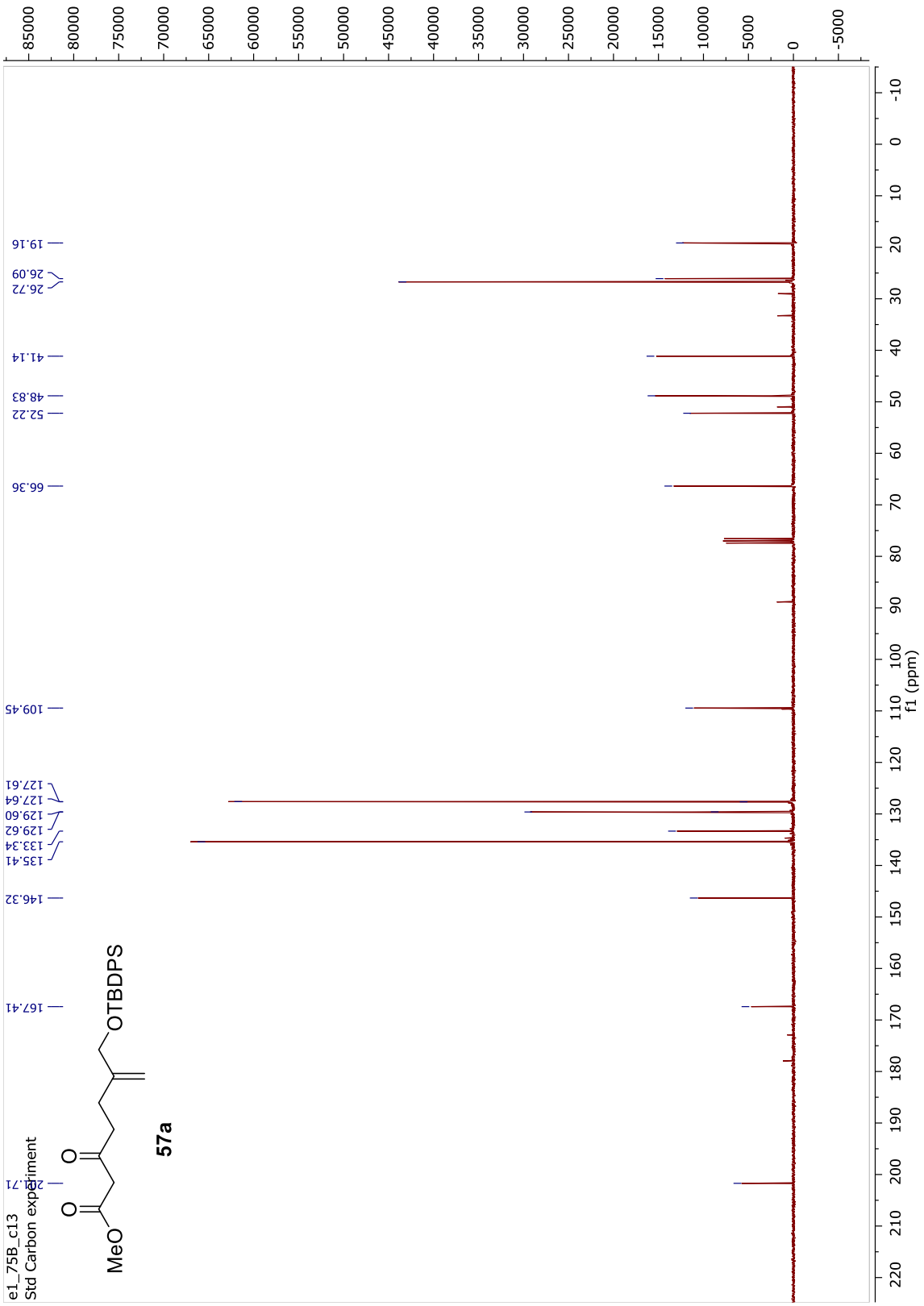
e1_75B_c13
Std Carbon experiment
MeO
O
O
OTBDPS
57a
19.16
26.09
26.72
41.14
48.83
52.22
66.36
109.45
127.61
127.64
129.60
129.62
133.34
135.41
146.32
167.41
172.71
f1 (ppm)

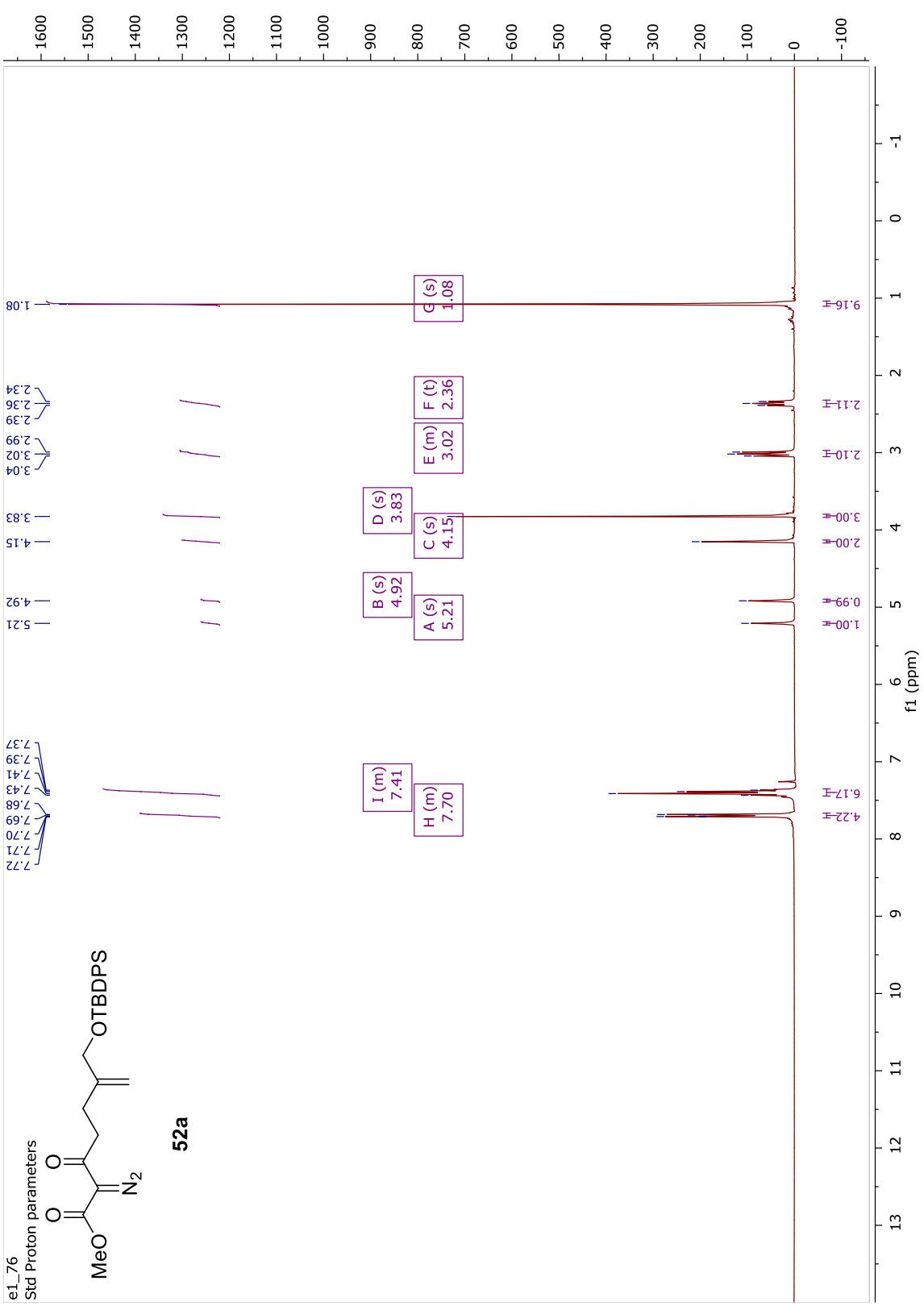
e1_76
Std Proton parameters
MeO
O
O
N2
OTBDPS
52a
f1 (ppm)
A (s) 5.21
B (s) 4.92
C (s) 4.15
D (s) 3.83
E (m) 3.02
F (t) 2.36
G (s) 1.08
H (m) 7.70
I (m) 7.41

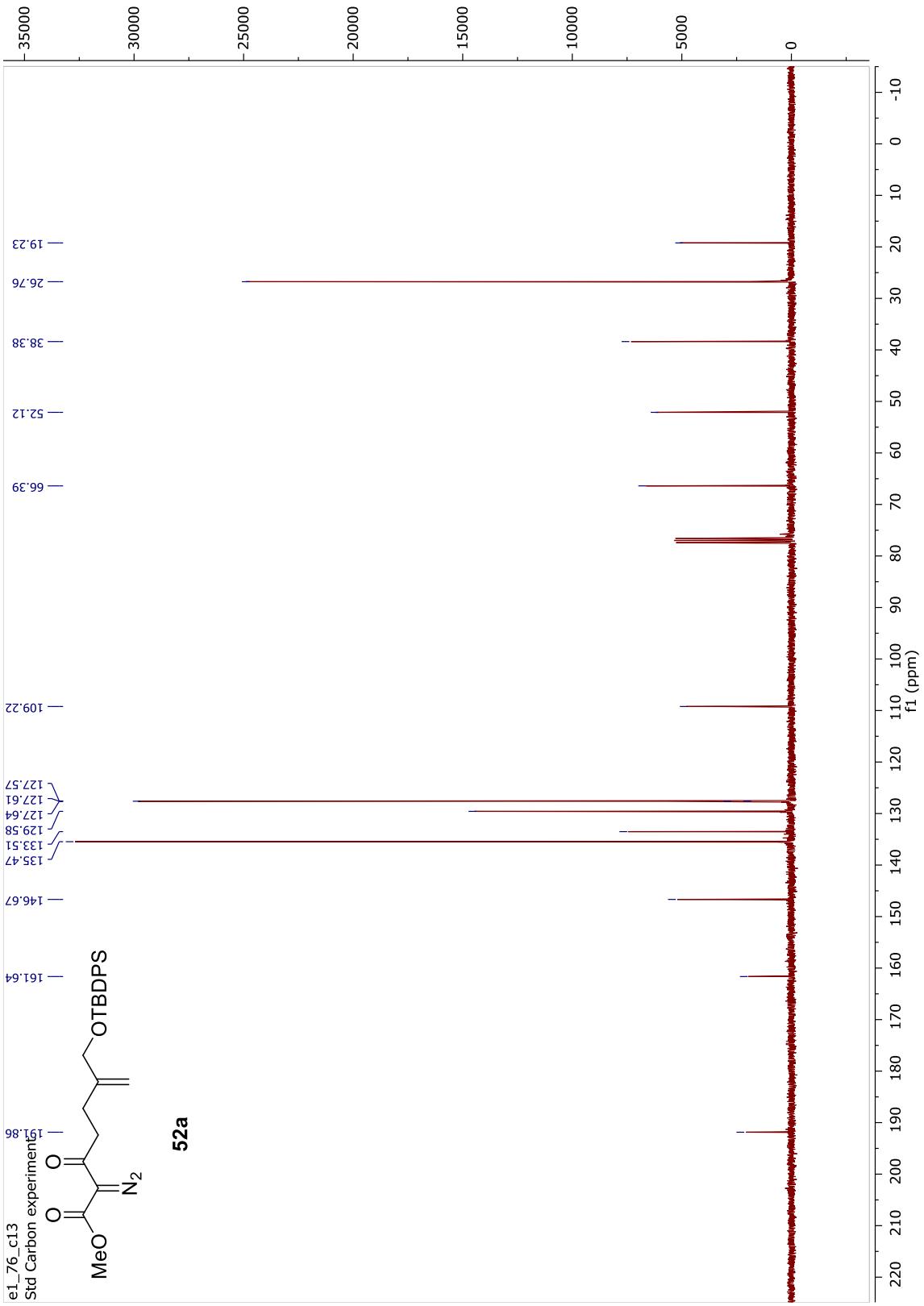
e1_76_c13
Std Carbon experiment
MeO
O
O
N2
OTBDPS
52a
191.86
161.64
146.67
135.47
133.51
129.58
127.64
127.61
127.57
109.22
66.39
52.12
38.38
26.76
19.23
f1 (ppm)

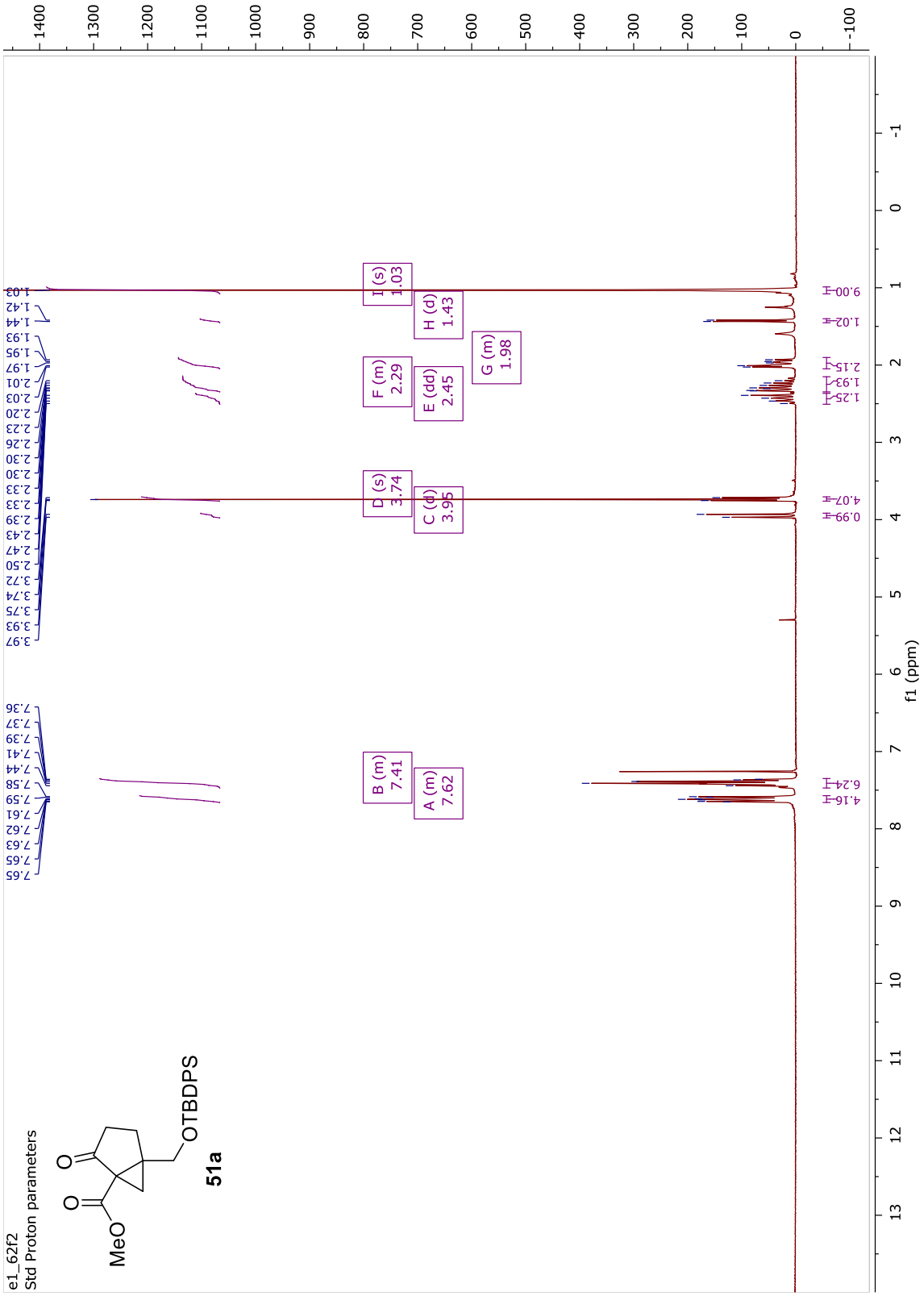
e1_62f2
Std Proton parameters
MeO
O
O
OTBDPS
51a
I (s)
1.03
H (d)
1.43
G (m)
1.98
F (m)
2.29
E (dd)
2.45
D (s)
3.74
C (d)
3.95
B (m)
7.41
A (m)
7.62
f1 (ppm)

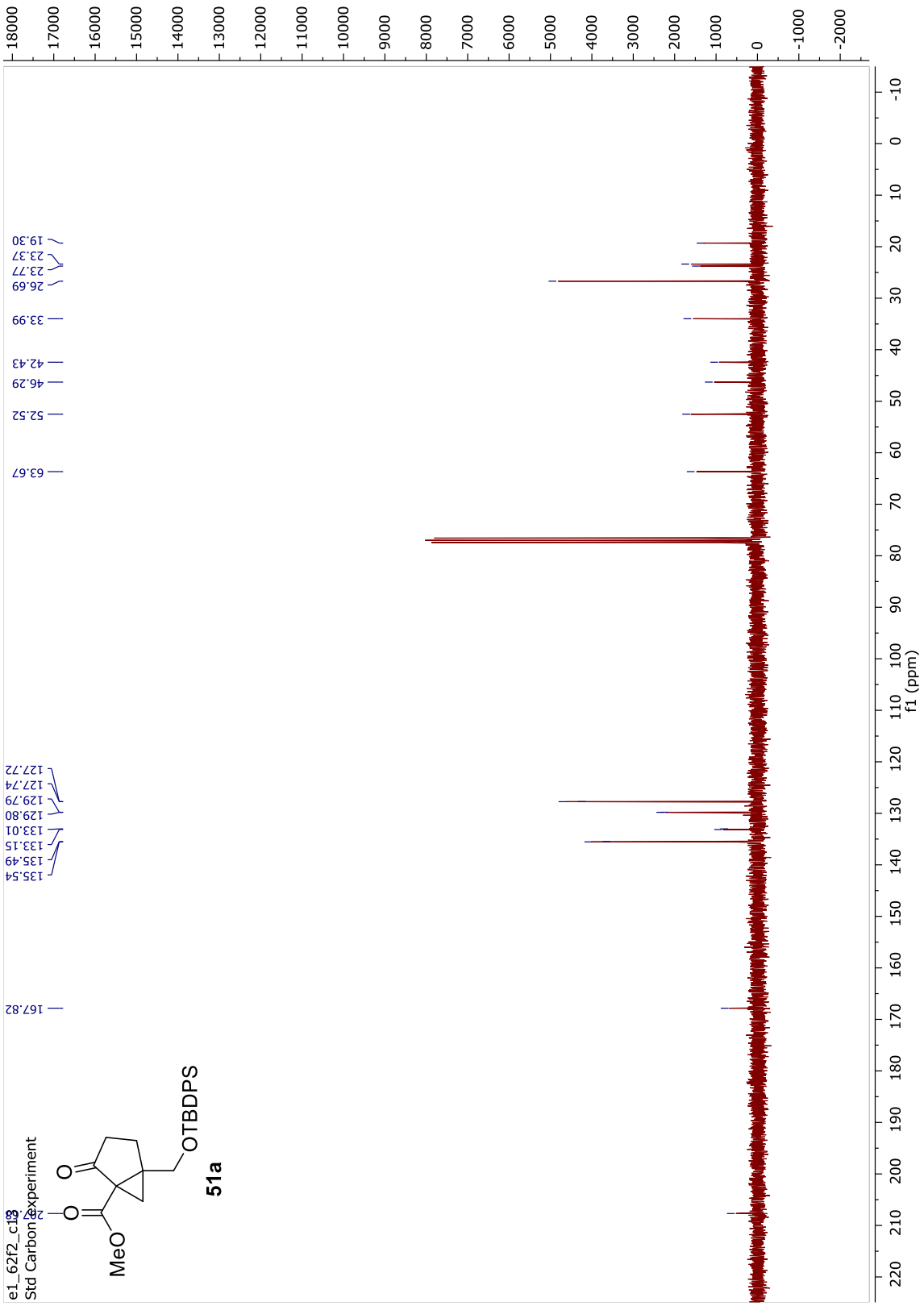
e1_62f2_c13
Std Carbon Experiment
MeO
OTBDPS
51a
167.82
135.54
135.49
133.15
133.01
129.80
129.79
127.74
127.72
63.67
52.52
46.29
42.43
33.99
26.69
23.77
23.37
19.30
f1 (ppm)

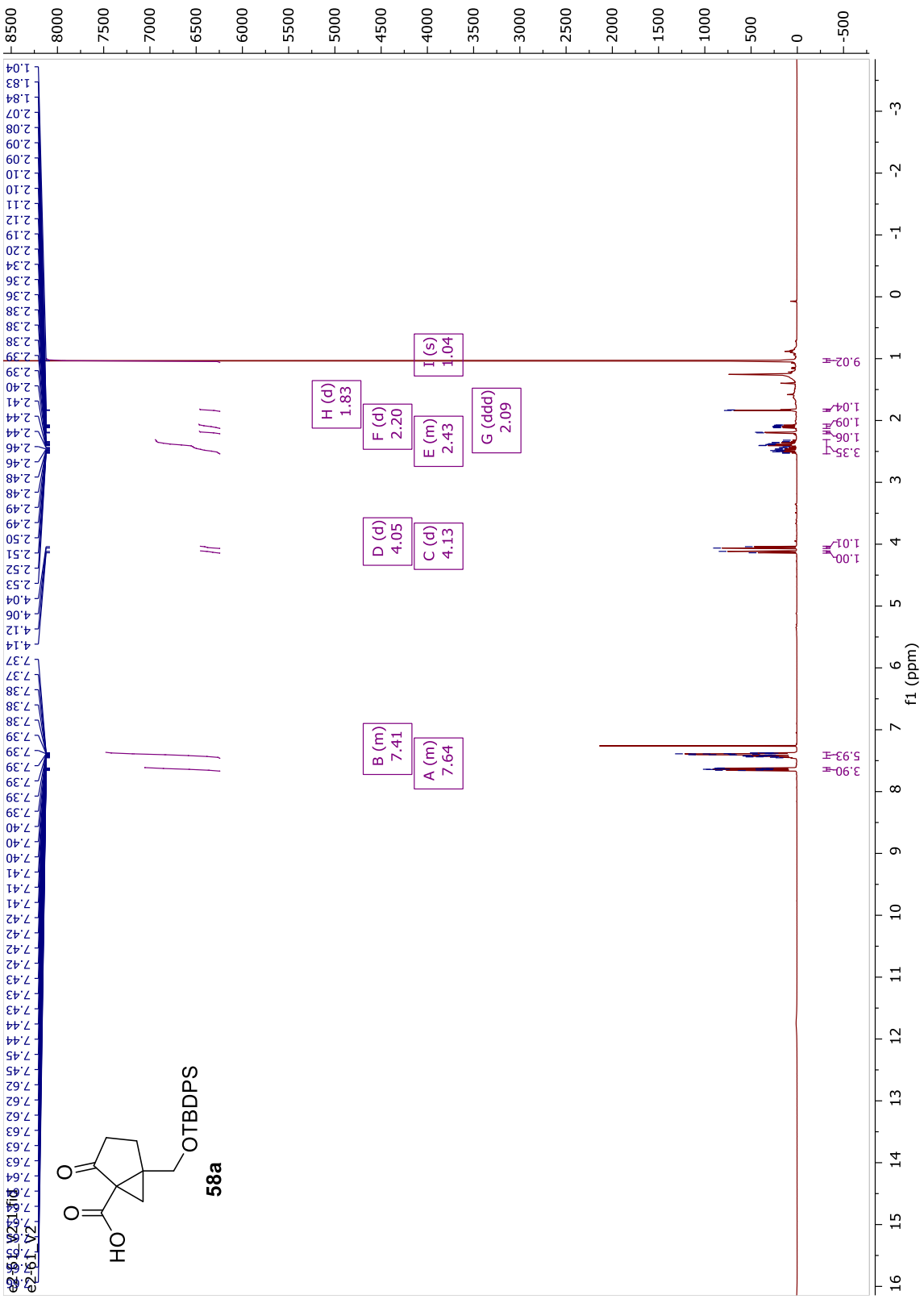
HO
O
O
OTBDPS
58a
A (m) 7.64
B (m) 7.41
C (d) 4.13
D (d) 4.05
E (m) 2.43
F (d) 2.20
G (ddd) 2.09
H (d) 1.83
I (s) 1.04
f1 (ppm)

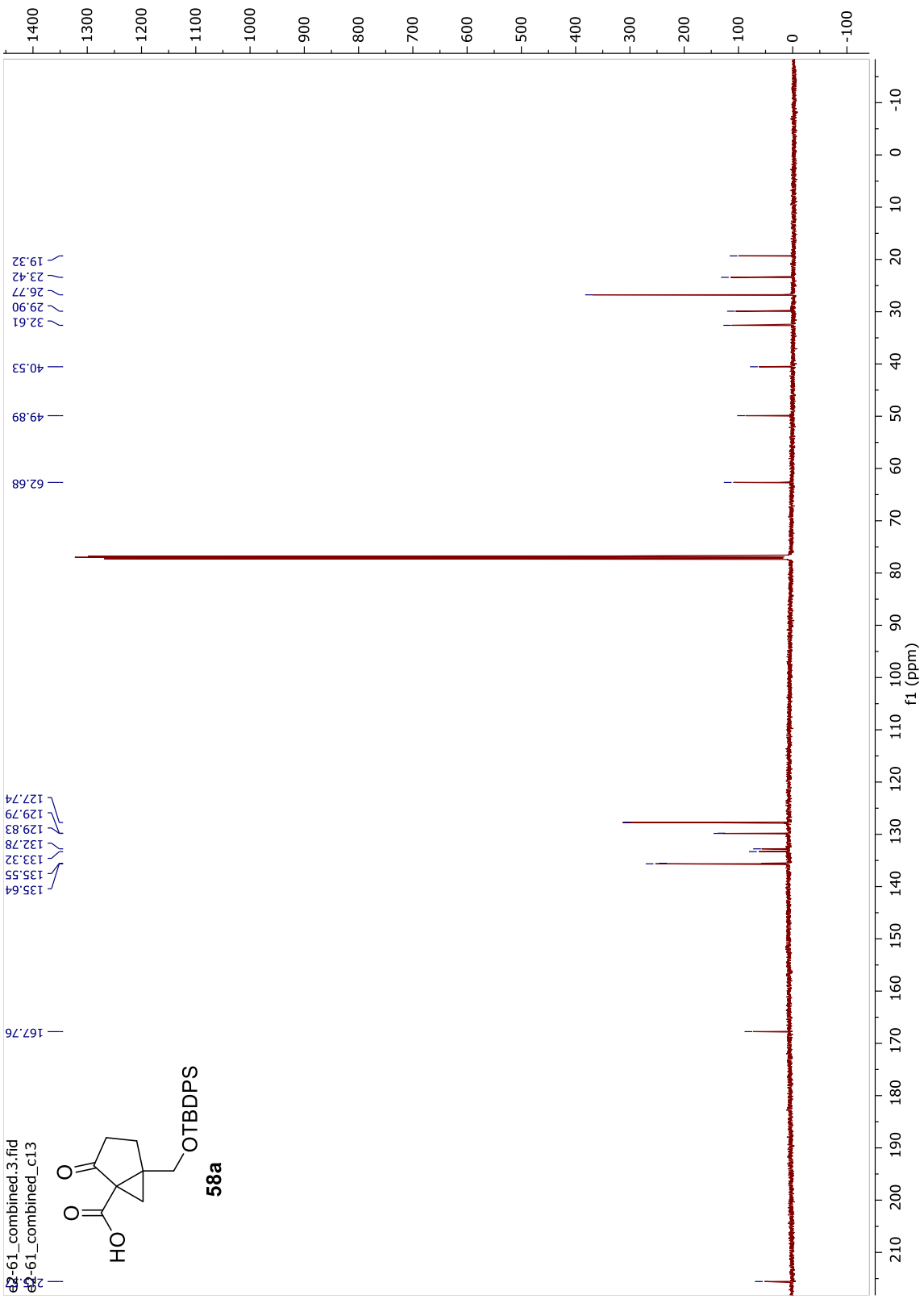
d2-61_combined.3.fid
d2-61_combined_c13
167.76
135.64
135.55
133.32
132.78
129.83
129.79
127.74
62.68
49.89
40.53
32.61
29.90
26.77
23.42
19.32
HO
O
O
OTBDPS
58a
f1 (ppm)

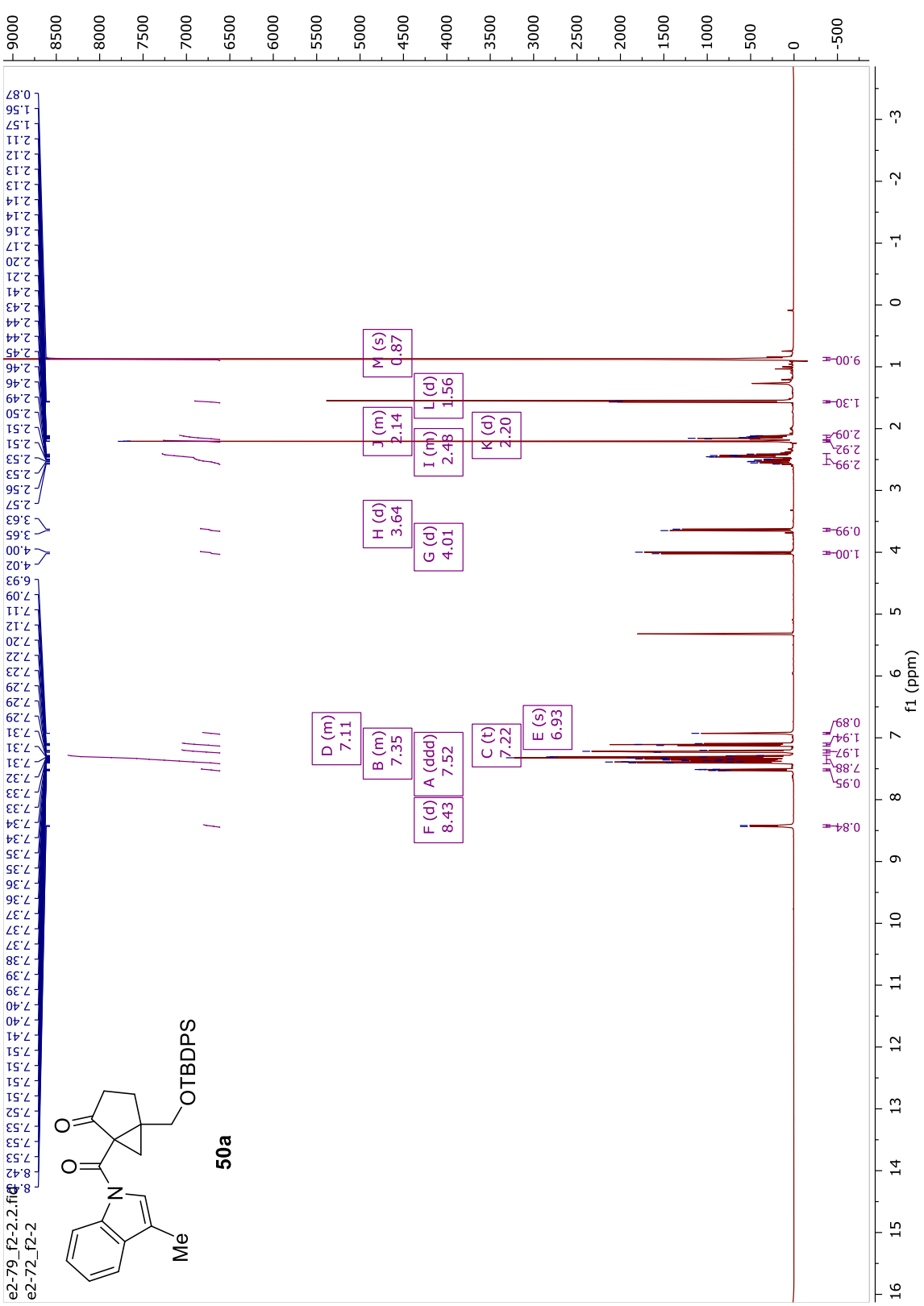
50a
OTBDPS
O
O
N
Me
M (s) 0.87
L (d) 1.56
J (m) 2.14
I (m) 2.48
K (d) 2.20
H (d) 3.64
G (d) 4.01
D (m) 7.11
B (m) 7.35
A (ddd) 7.52
F (d) 8.43
C (t) 7.22
E (s) 6.93
f1 (ppm)
e2-79_f2-2.2.fid
e2-72_f2-2

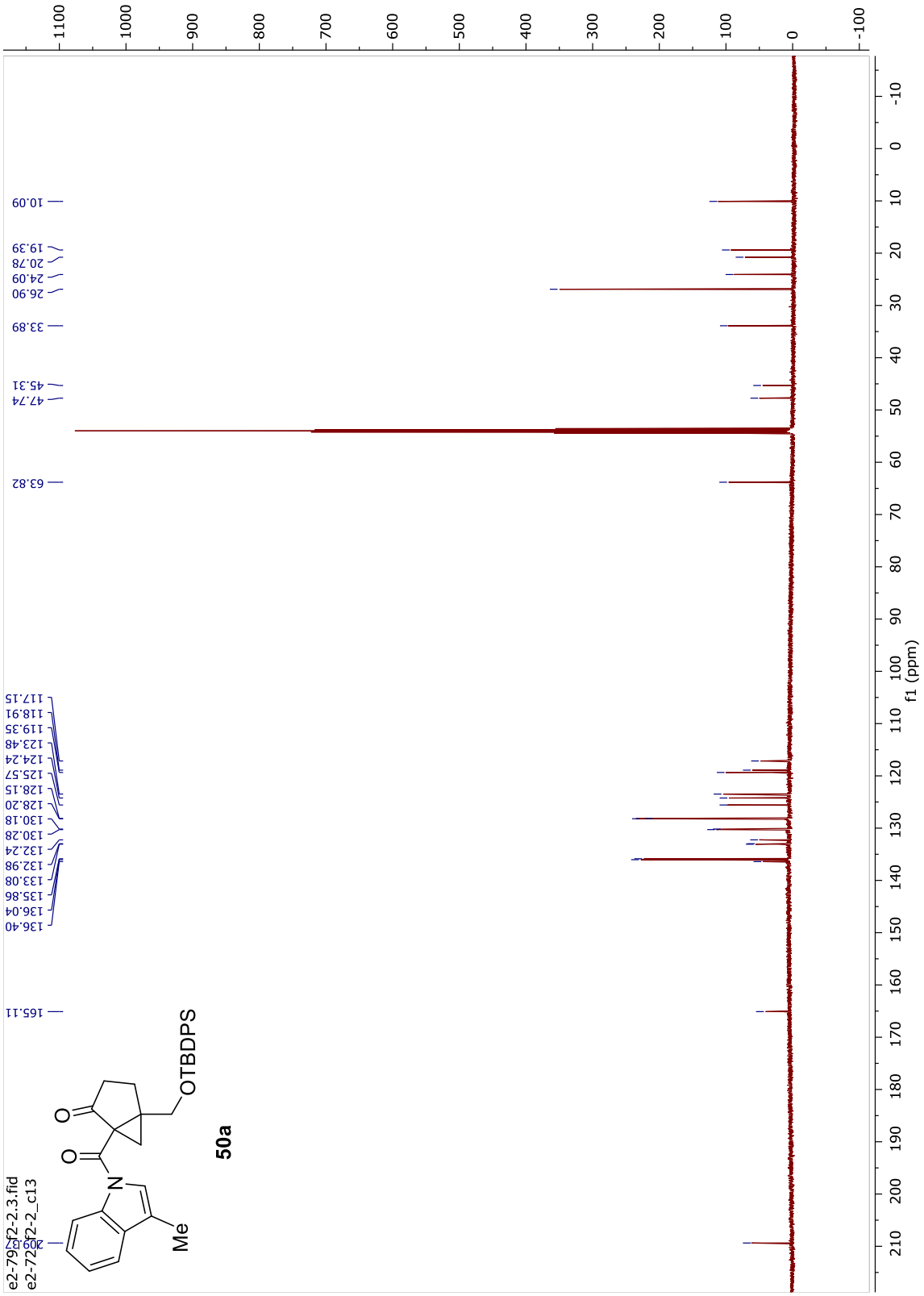
e2-79-f2-2.3.fid
e2-72-f2-2_c13
50a
OTBDPS
Me
O
O
N
209.52
165.11
136.40
136.04
135.86
133.08
132.98
132.24
130.28
130.18
128.20
128.15
125.57
124.24
123.48
119.35
118.91
117.15
63.82
47.74
45.31
33.89
26.90
24.09
20.78
19.39
10.09
f1 (ppm)

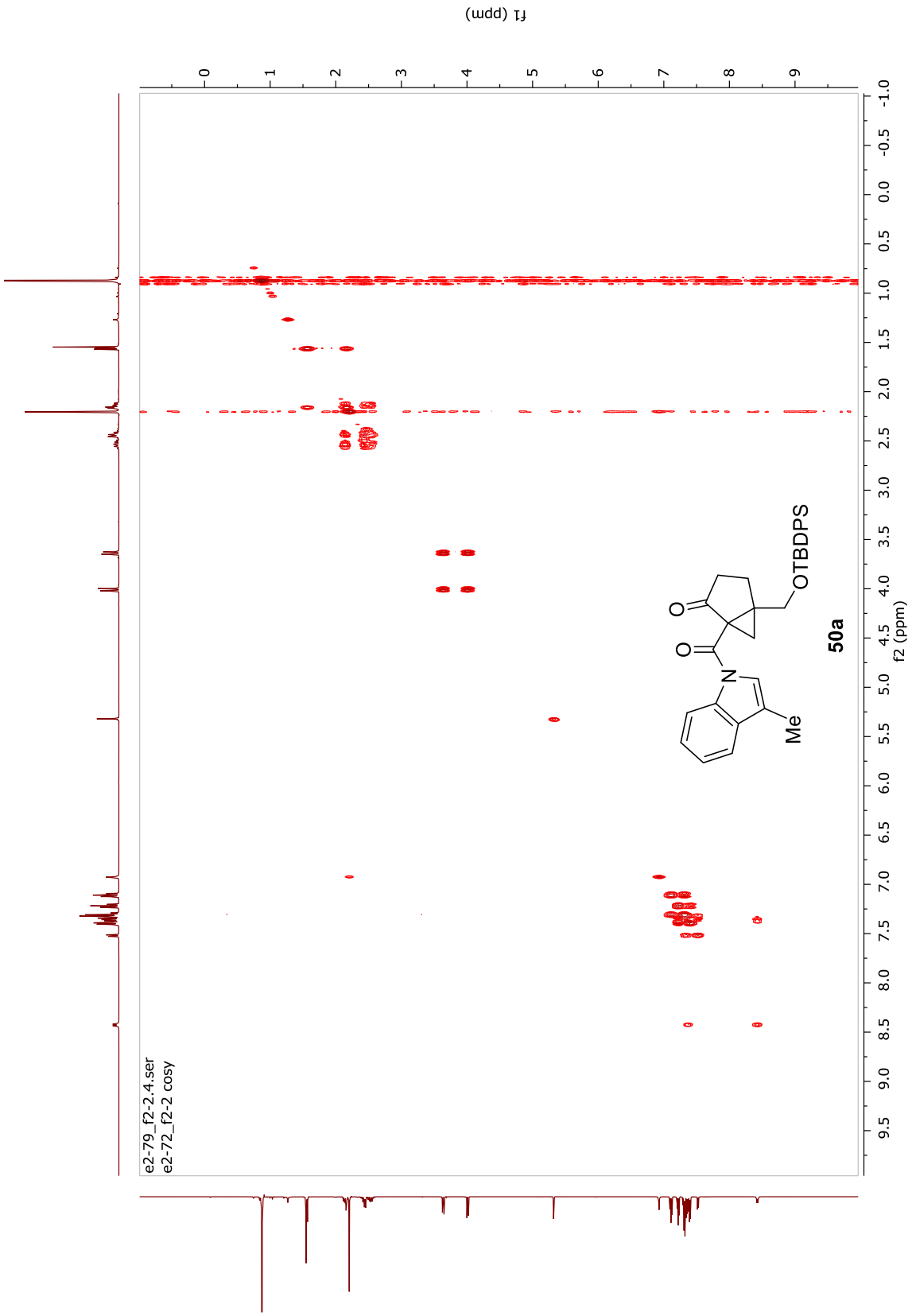
f1 (ppm)
f2 (ppm)
e2-79_f2-2.4.ser
e2-72_f2-2 cosy
OTBDPS
O
O
N
Me
50a

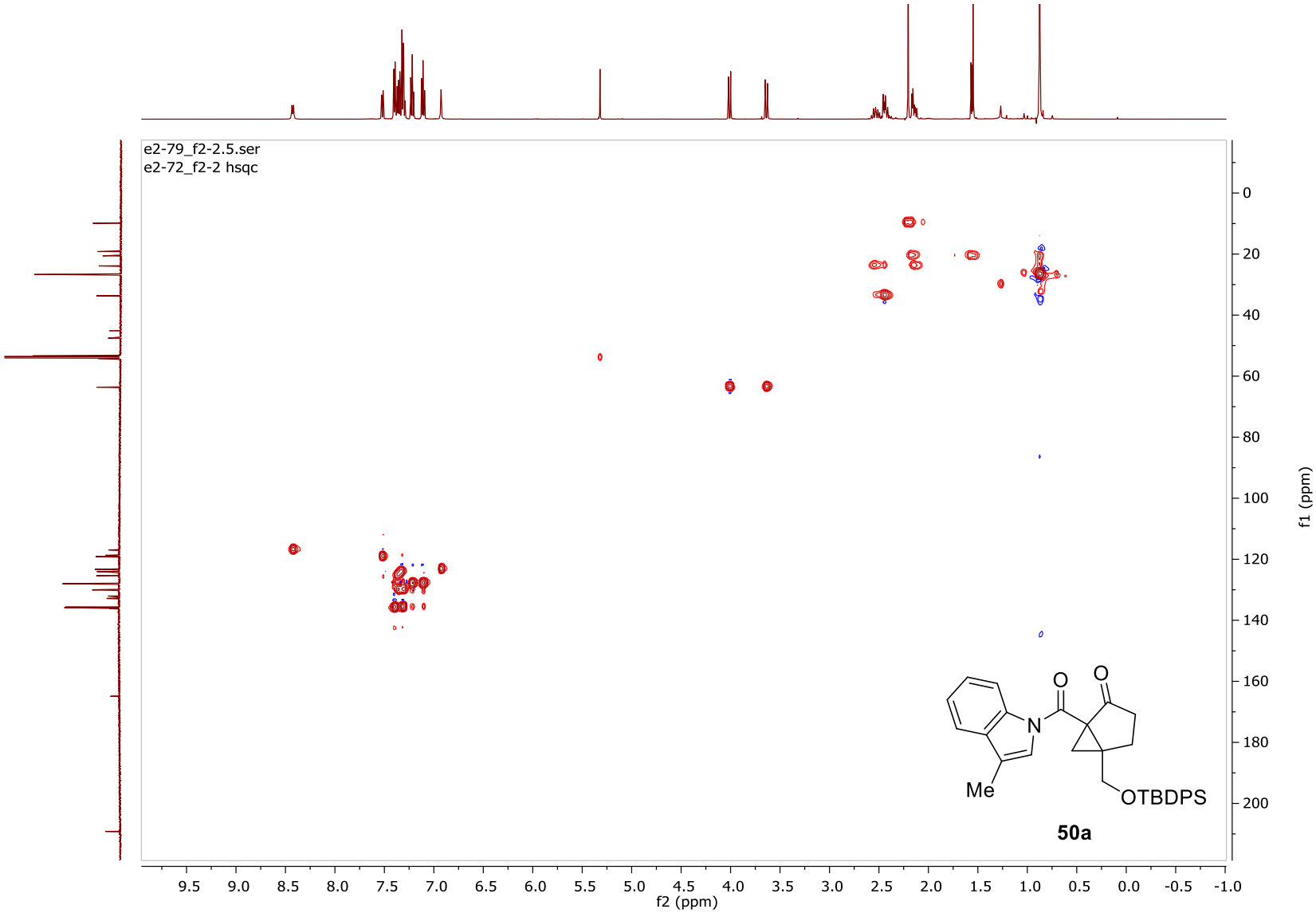
e2-79_f2-2.5.ser
e2-72_f2-2 hsqc
f2 (ppm)
f1 (ppm)
Me
OTBDPS
50a

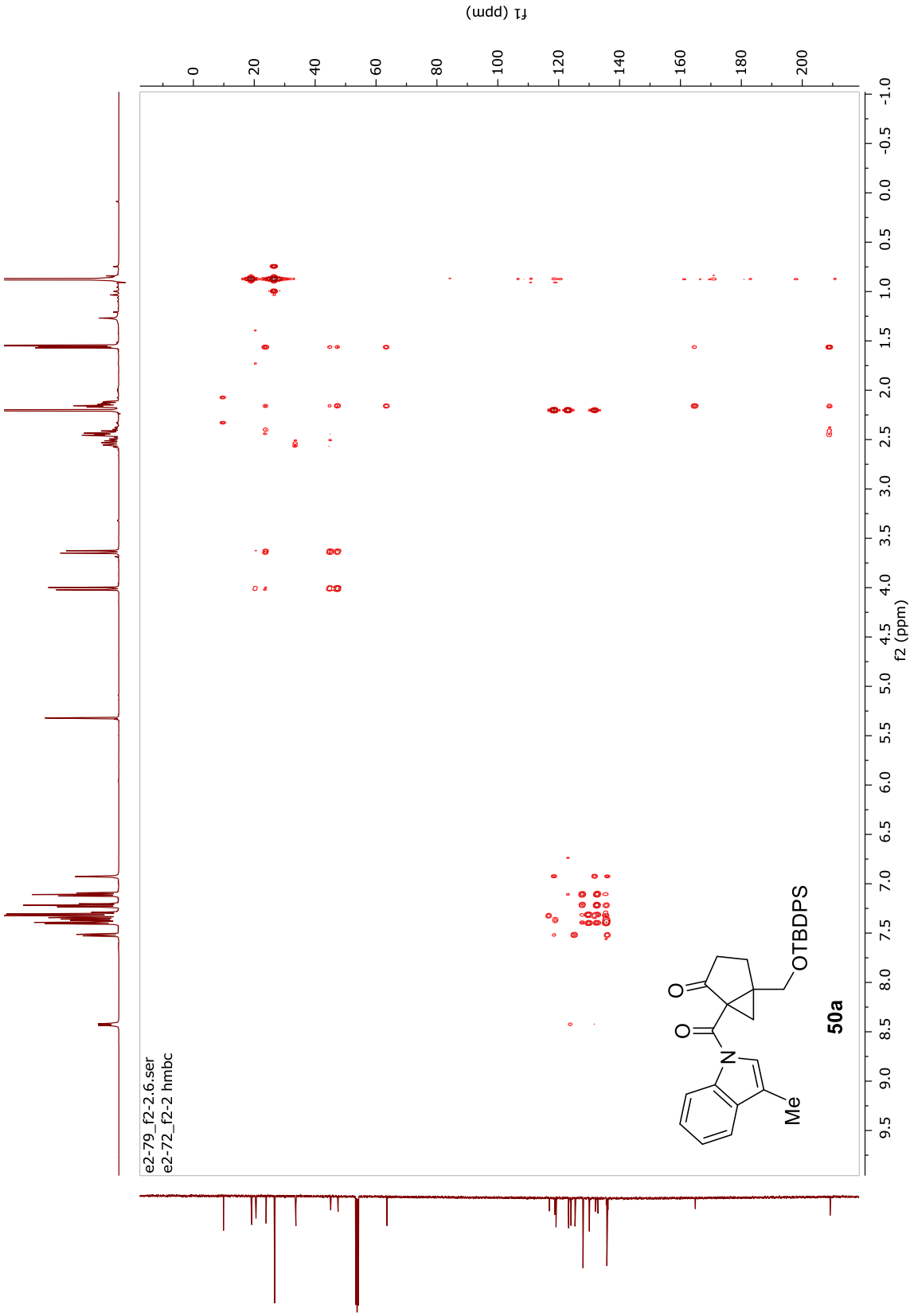
e2-79_f2-2.6.ser
e2-72_f2-2 hmbc
f1 (ppm)
f2 (ppm)
OTBDPS
Me
50a

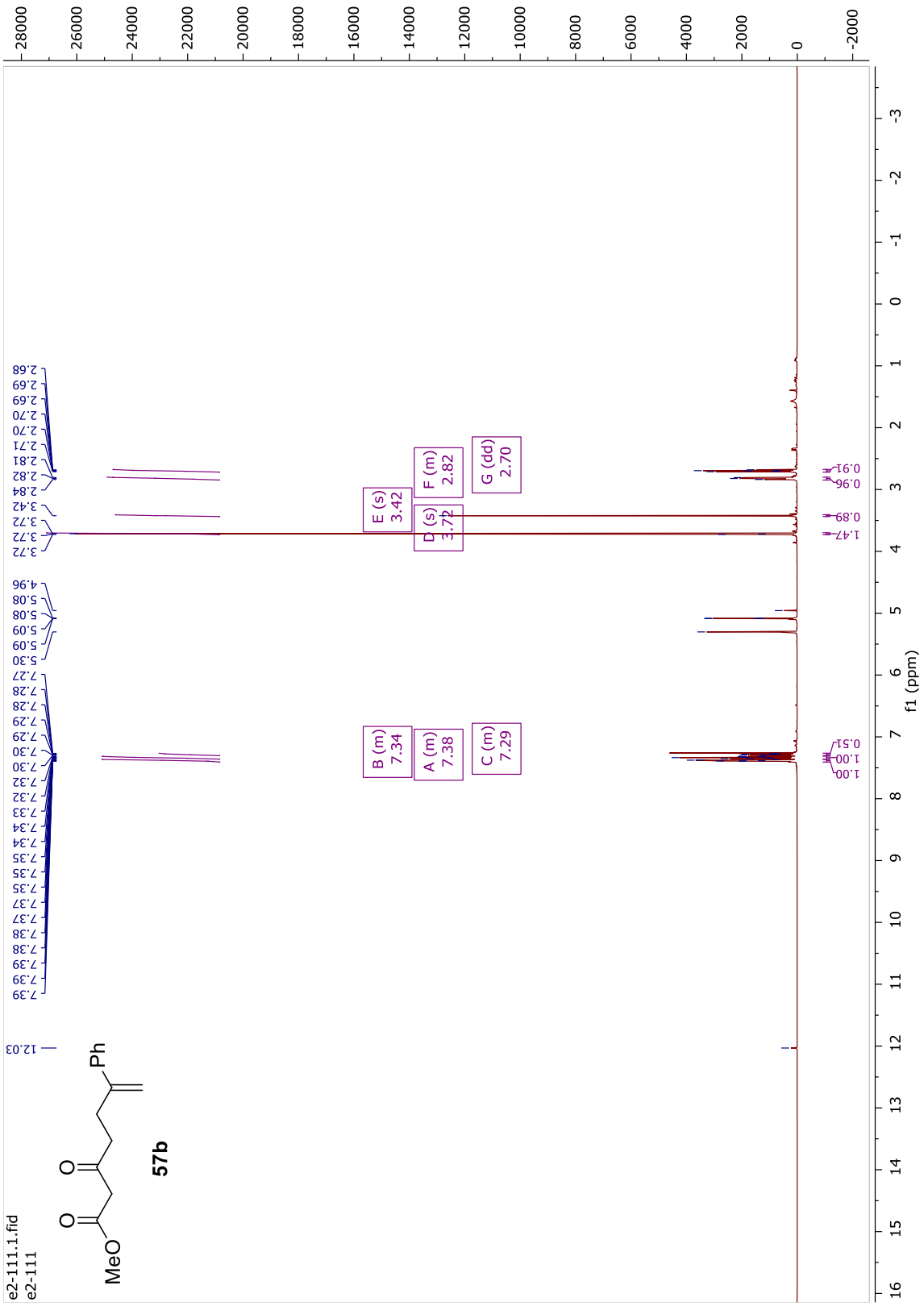
e2-111.1.fid
e2-111
MeO
O
O
Ph
57b
12.03
7.39
7.38
7.37
7.35
7.34
7.33
7.32
7.30
7.29
7.28
7.27
5.30
5.09
5.08
4.96
3.72
3.42
2.84
2.82
2.81
2.71
2.70
2.69
2.68
B (m) 7.34
A (m) 7.38
C (m) 7.29
E (s) 3.42
D (s) 3.72
F (m) 2.82
G (dd) 2.70
1.00
0.51
0.91
0.96
0.89
1.47
f1 (ppm)

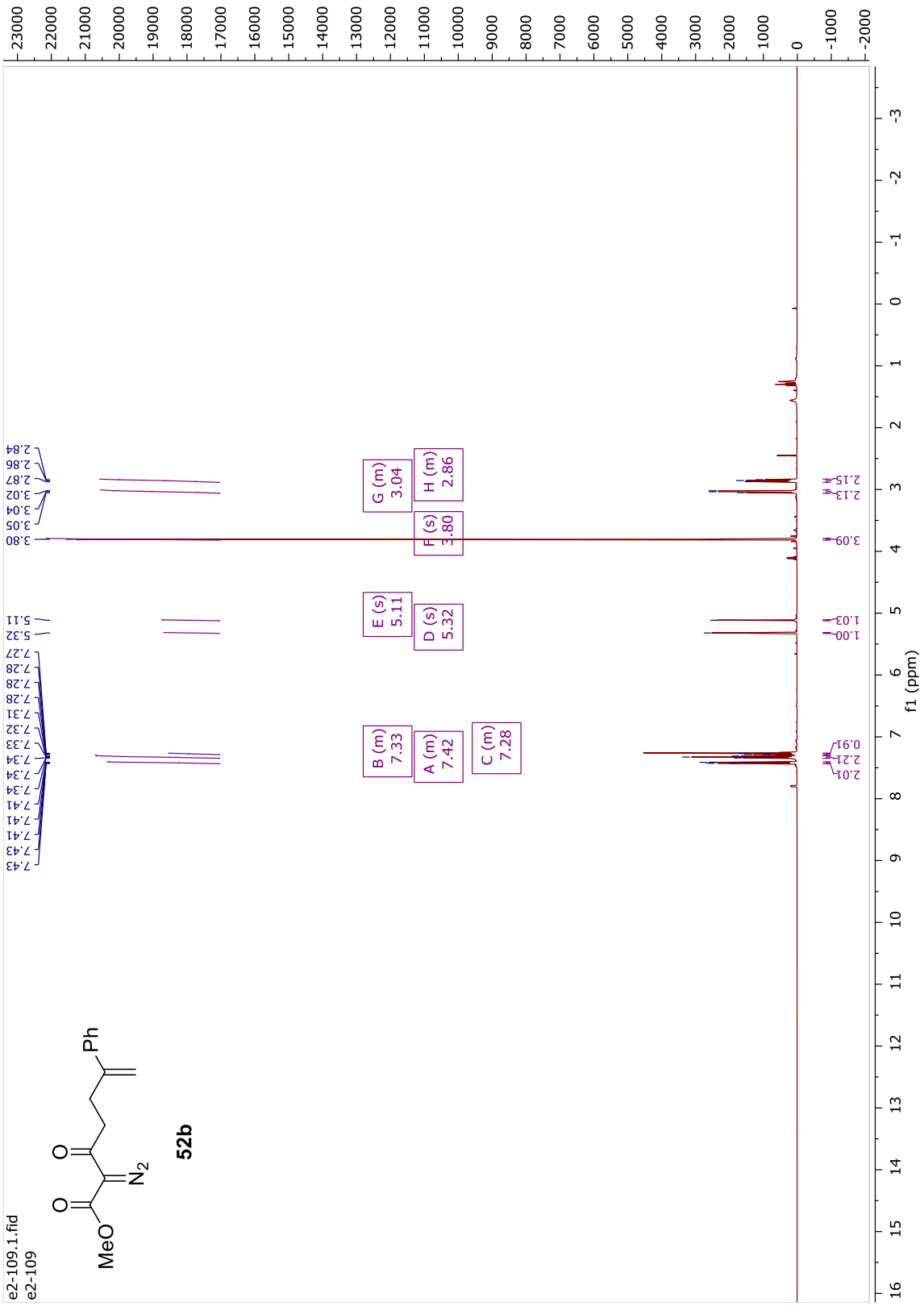
e2-109.1.fid
e2-109
MeO
O
O
N2
Ph
52b
B (m) 7.33
A (m) 7.42
C (m) 7.28
E (s) 5.11
D (s) 5.32
G (m) 3.04
H (m) 2.86
F (s) 3.80
f1 (ppm)

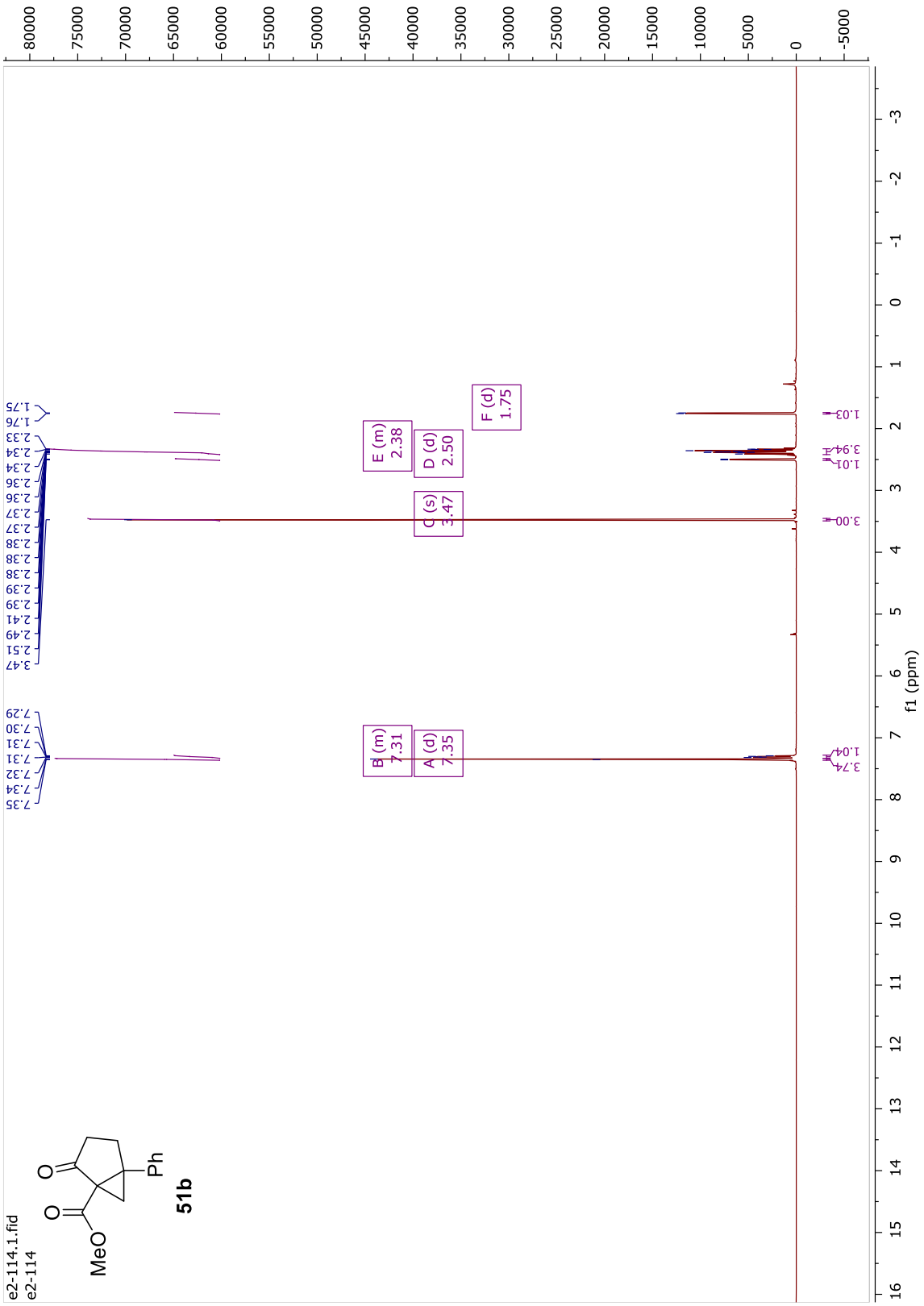
e2-114.1.fid
e2-114
MeO
O
O
Ph
51b
A (d) 7.35
B (m) 7.31
C (s) 3.47
D (d) 2.50
E (m) 2.38
F (d) 1.75
1.04
3.74
3.00
1.01
3.94
1.03
f1 (ppm)

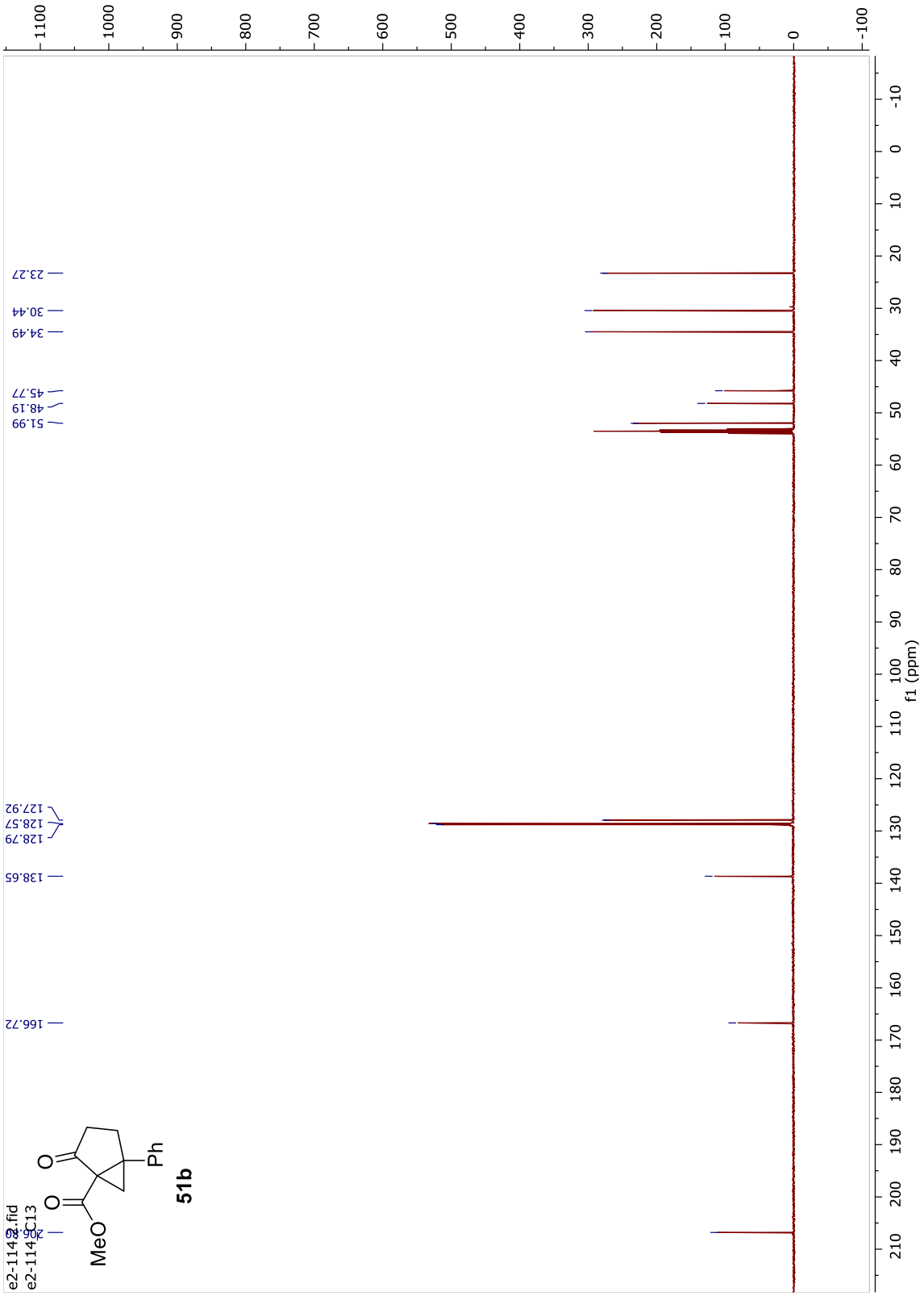
e2-1142.fid
e2-1142C13
MeO
O
O
Ph
51b
206.80
166.72
138.65
128.79
128.57
127.92
51.99
48.19
45.77
34.49
30.44
23.27
f1 (ppm)

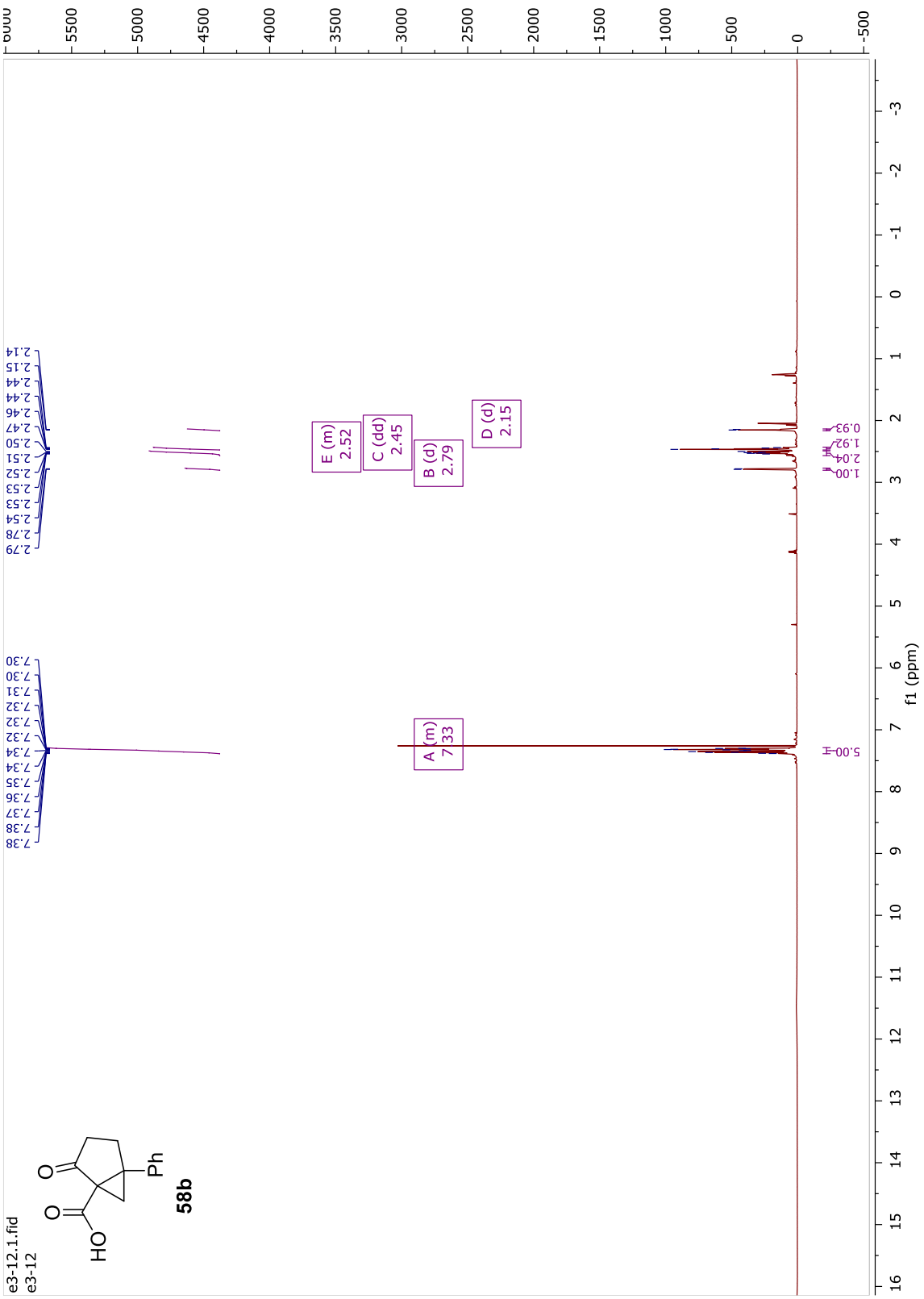
e3-12.1.fid
e3-12
58b
A (m)
7.33
B (d)
2.79
C (dd)
2.45
D (d)
2.15
E (m)
2.52
5.00
1.00
2.04
1.92
0.93
f1 (ppm)

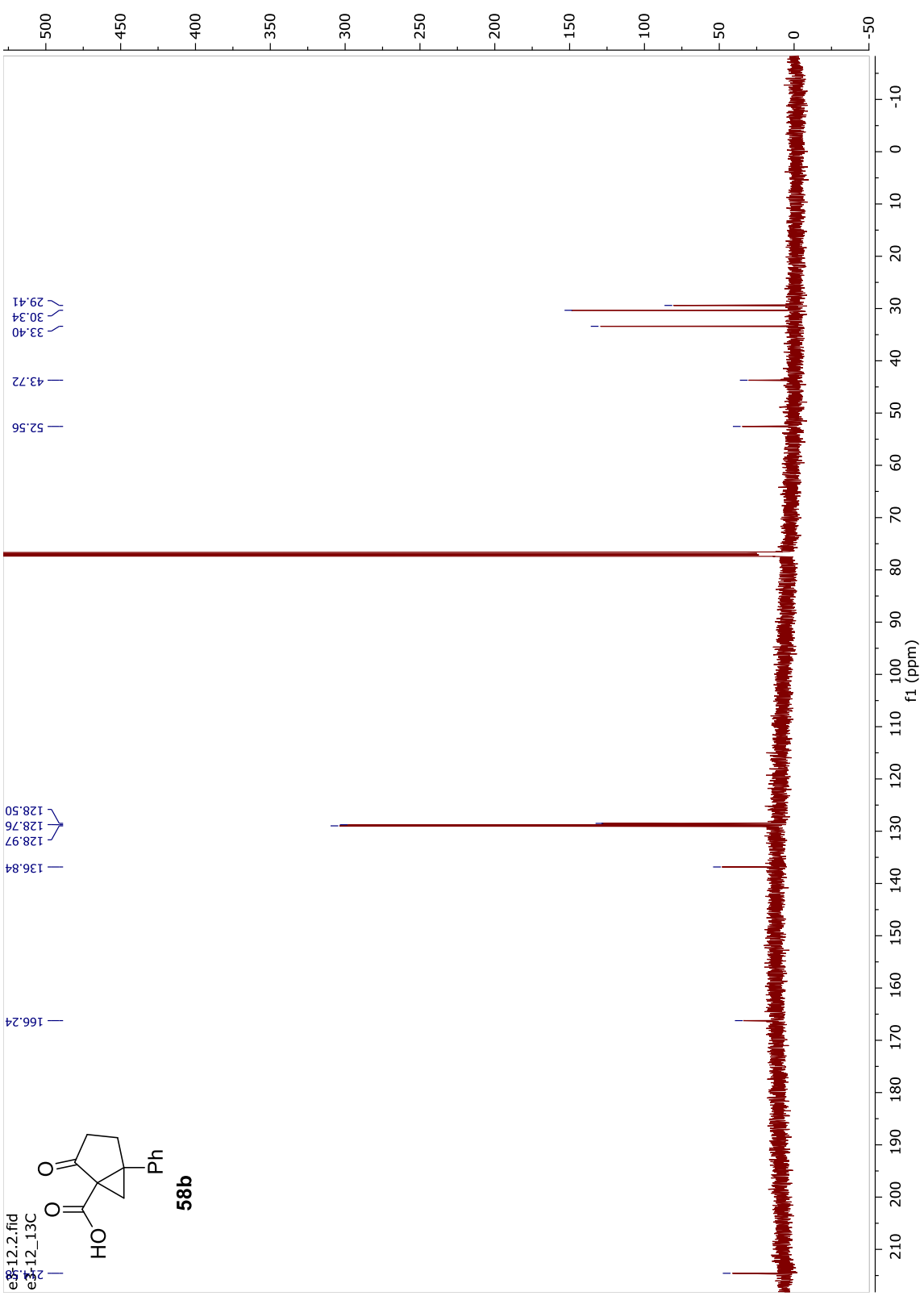
58b
HO
O
O
Ph
166.24
136.84
128.97
128.76
128.50
52.56
43.72
33.40
30.34
29.41
f1 (ppm)

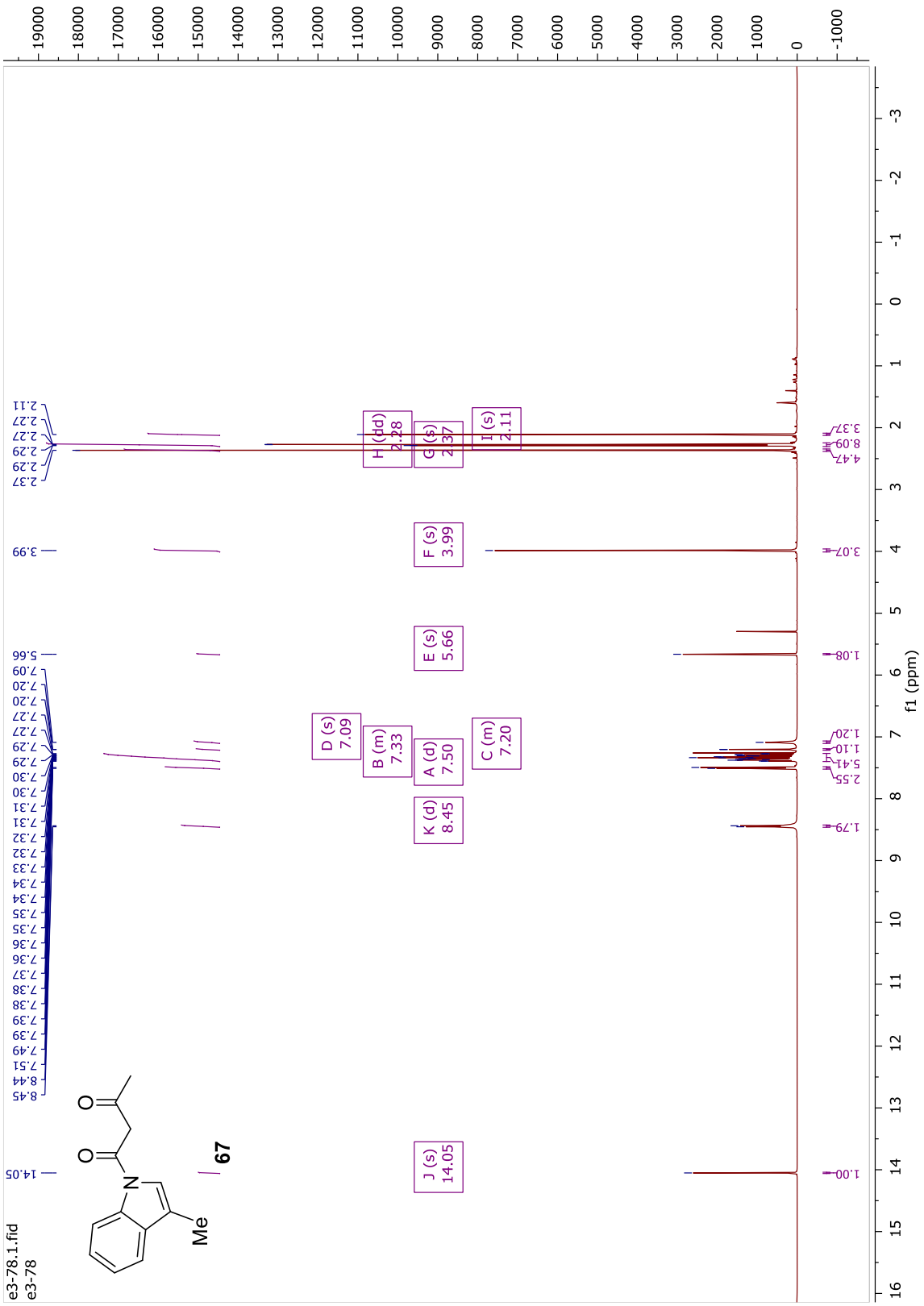
e3-78.1.fid
e3-78
67
Me
O
O
N
J (s) 14.05
K (d) 8.45
A (d) 7.50
B (m) 7.33
C (m) 7.20
D (s) 7.09
E (s) 5.66
F (s) 3.99
G (s) 2.37
H (dd) 2.28
I (s) 2.11
14.05
5.66
3.99
2.37
2.29
2.29
2.27
2.27
2.11
8.45
8.44
7.51
7.49
7.39
7.39
7.38
7.38
7.37
7.36
7.36
7.35
7.35
7.34
7.34
7.33
7.32
7.32
7.31
7.31
7.30
7.30
7.29
7.29
7.27
7.27
7.20
7.20
7.09
1.00
1.79
1.08
3.07
4.47
8.09
3.37
2.55
5.41
1.10
1.20
f1 (ppm)

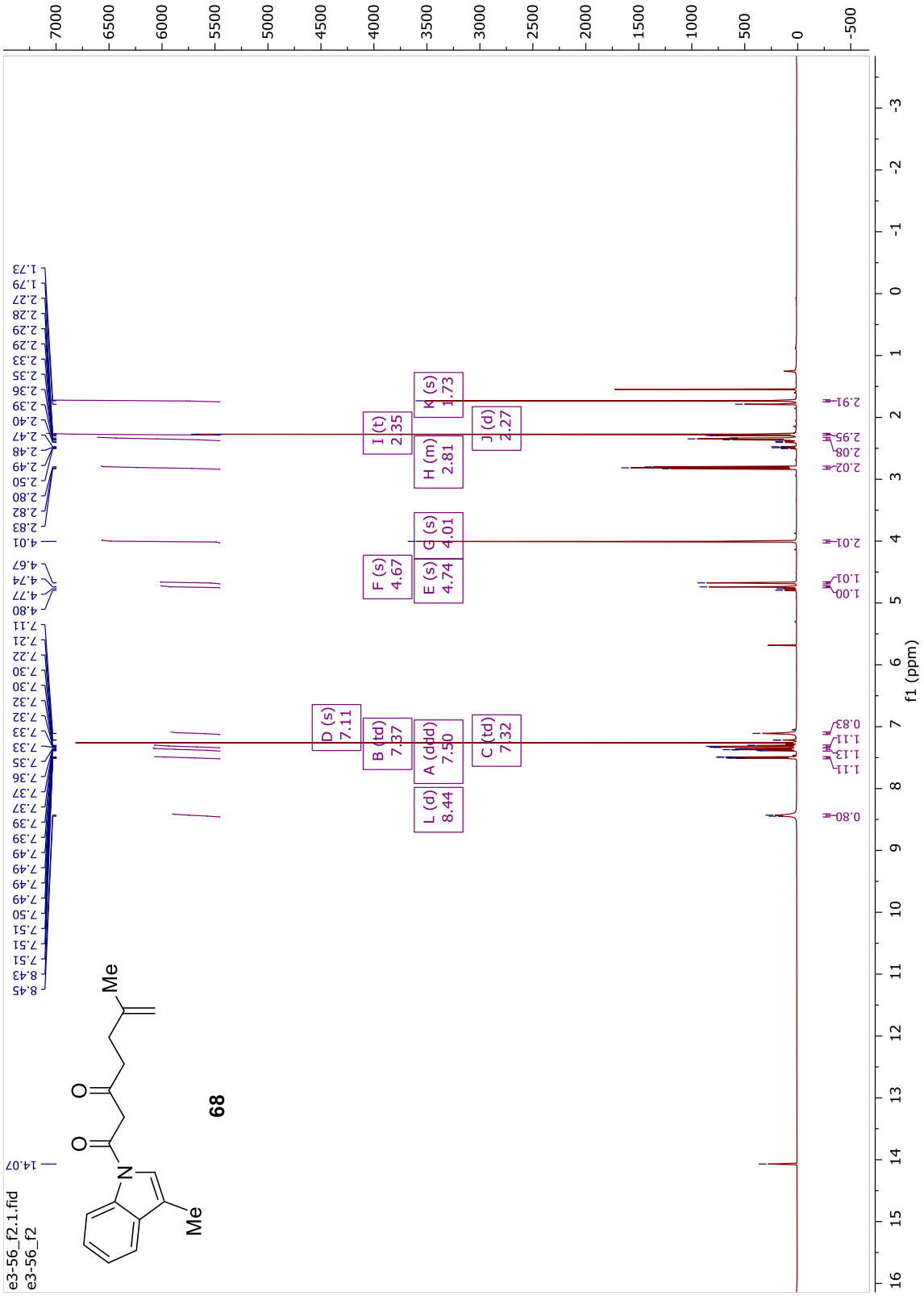
e3-56_f2.1.fid
e3-56_f2
68
Me
Me
O
O
N
L (d) 8.44
A (ddd) 7.50
B (td) 7.37
D (s) 7.11
C (td) 7.32
F (s) 4.67
E (s) 4.74
G (s) 4.01
I (t) 2.35
H (m) 2.81
K (s) 1.73
J (d) 2.27
f1 (ppm)

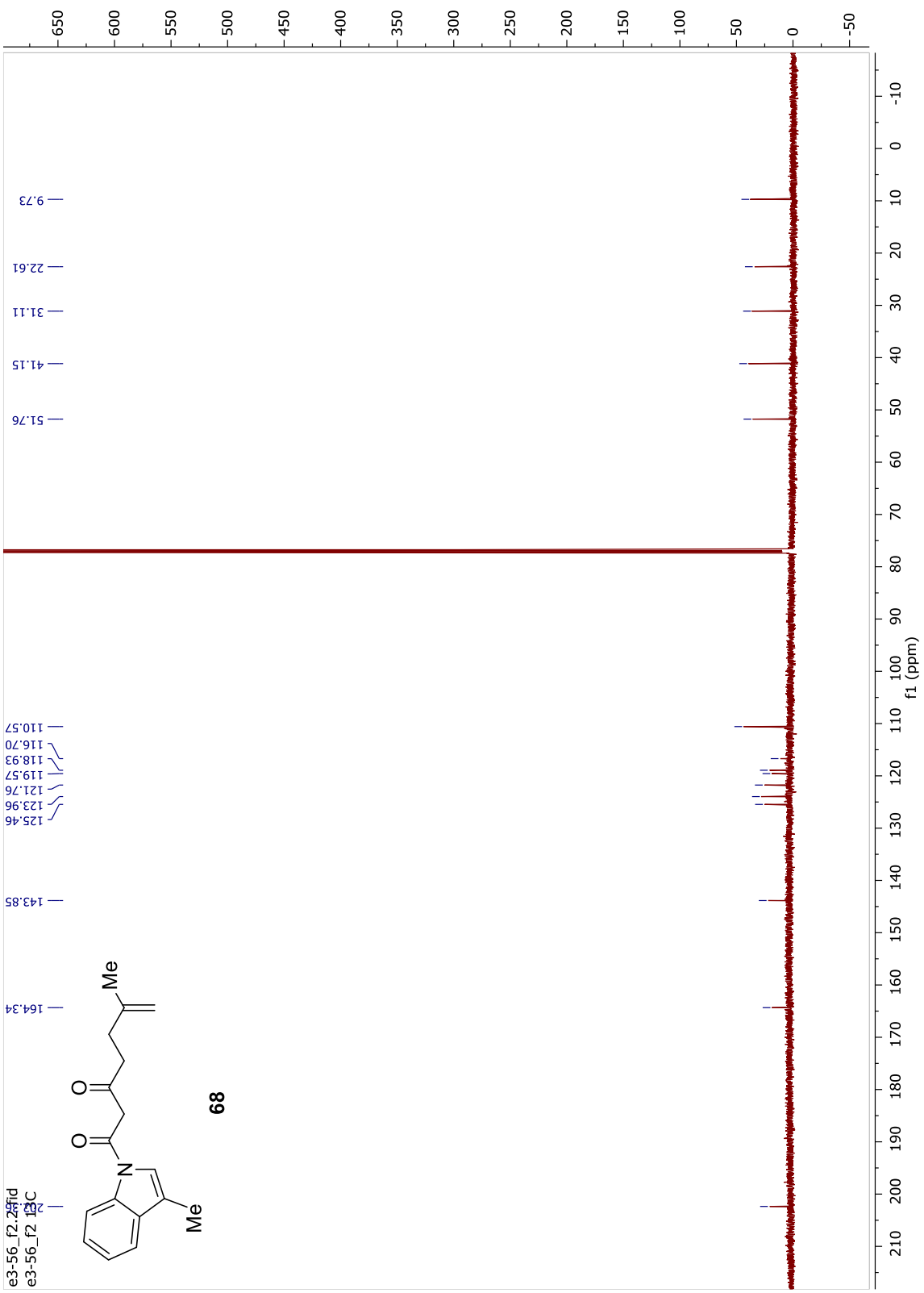
e3-56_f2.2fid
e3-56_f2 13C
9.73
22.61
31.11
41.15
51.76
110.57
116.70
118.93
119.57
121.76
123.96
125.46
143.85
164.34
Me
O
O
N
Me
68
f1 (ppm)

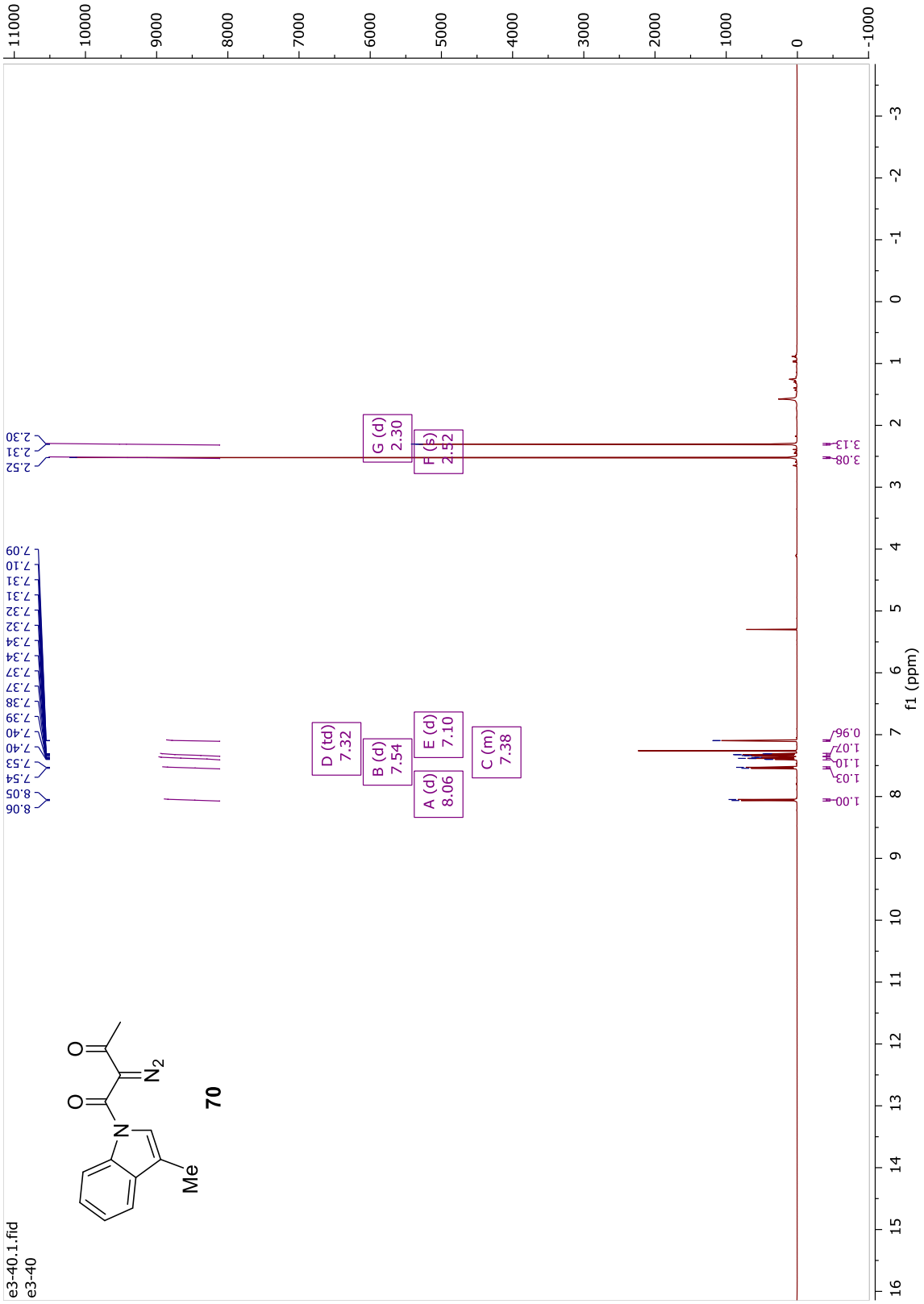
e3-40.1.fid
e3-40
70
Me
N
O
O
N2
A (d) 8.06
B (d) 7.54
C (m) 7.38
D (td) 7.32
E (d) 7.10
F (s) 2.52
G (d) 2.30
8.06
8.05
7.54
7.53
7.40
7.40
7.39
7.38
7.37
7.37
7.34
7.34
7.32
7.32
7.31
7.31
7.10
7.09
2.52
2.31
2.30
3.13
3.08
1.00
1.03
1.10
1.07
0.96
f1 (ppm)

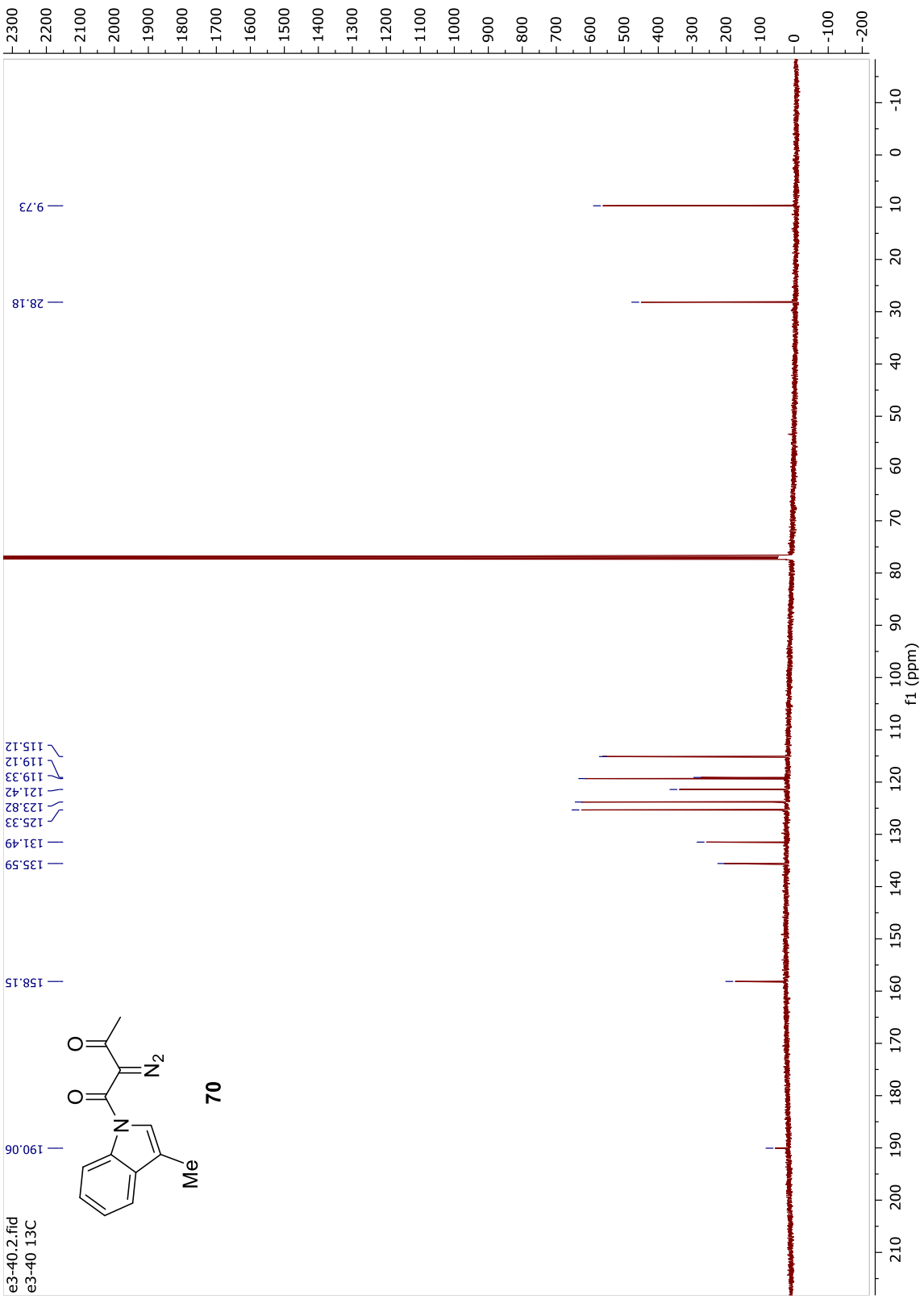
e3-40.2.fid
e3-40 13C
190.06
158.15
135.59
131.49
125.33
123.82
121.42
119.33
119.12
115.12
28.18
9.73
f1 (ppm)
70
Me
N
O
O
N2

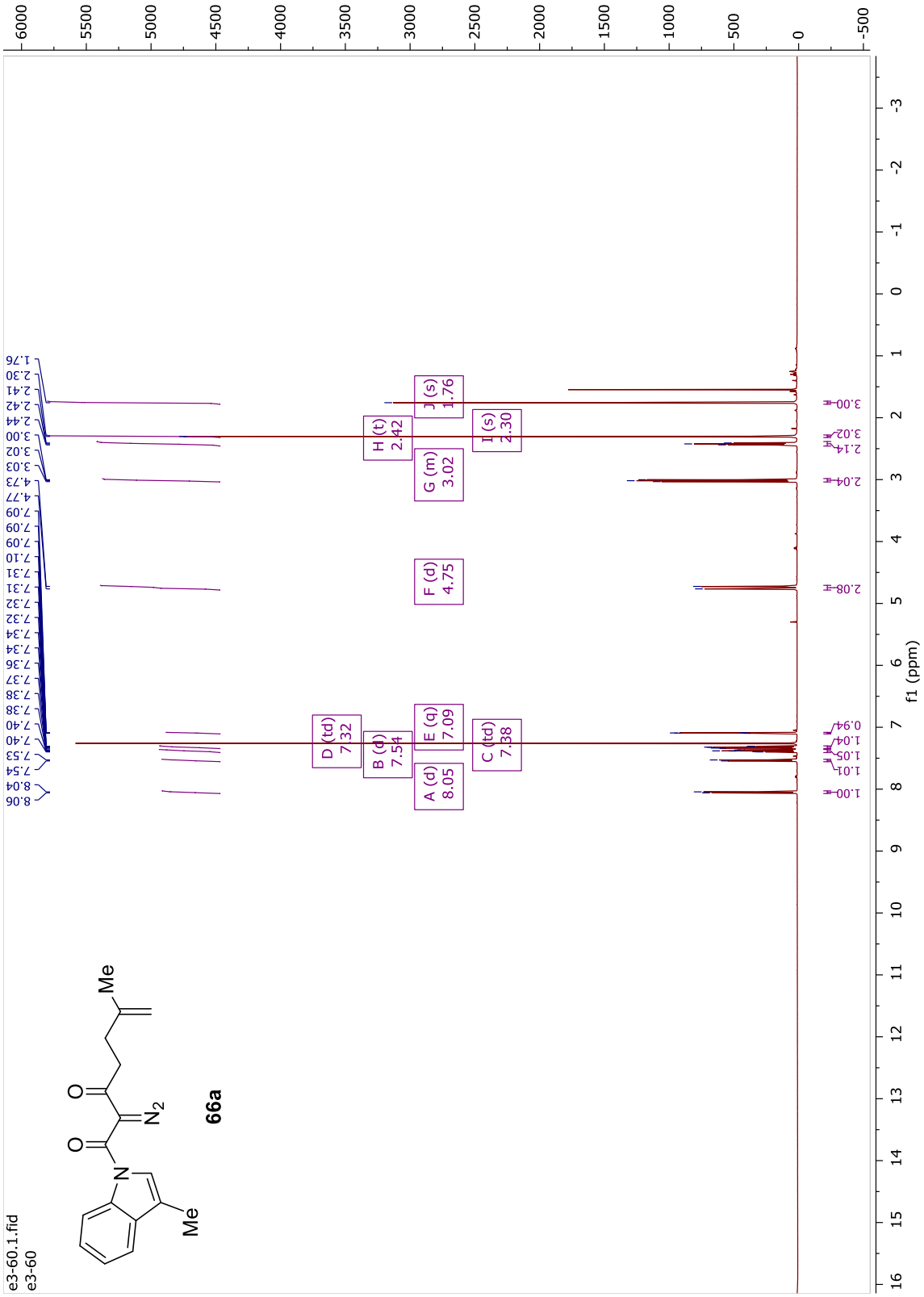
e3-60.1.fid
e3-60
66a
A (d) 8.05
B (d) 7.54
C (td) 7.38
D (td) 7.32
E (q) 7.09
F (d) 4.75
G (m) 3.02
H (t) 2.42
I (s) 2.30
J (s) 1.76
f1 (ppm)

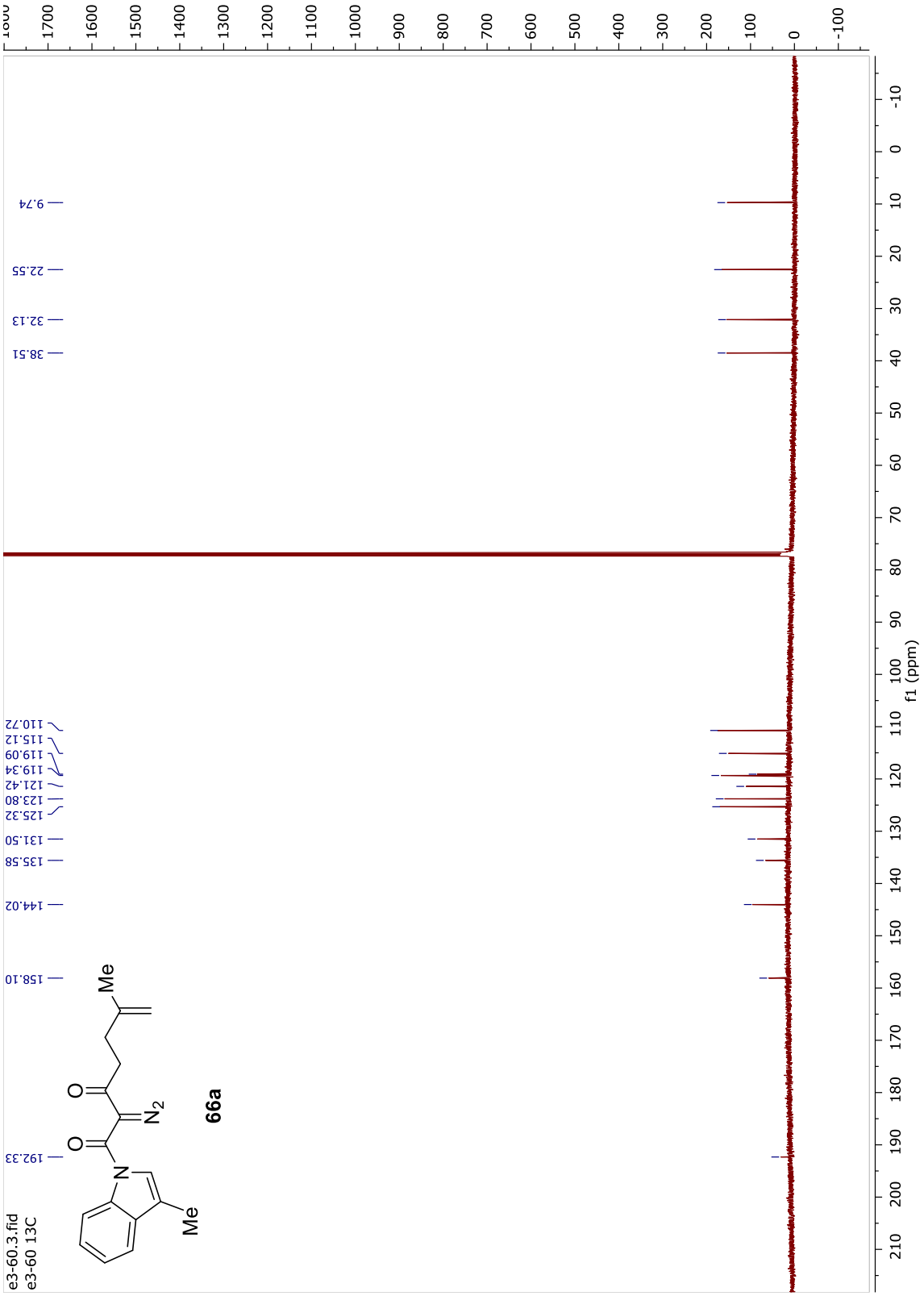
e3-60.3.fid
e3-60 13C
66a
Me
Me
N
O
O
N2
192.33
158.10
144.02
135.58
131.50
125.32
123.80
121.42
119.34
119.09
115.12
110.72
38.51
32.13
22.55
9.74
f1 (ppm)

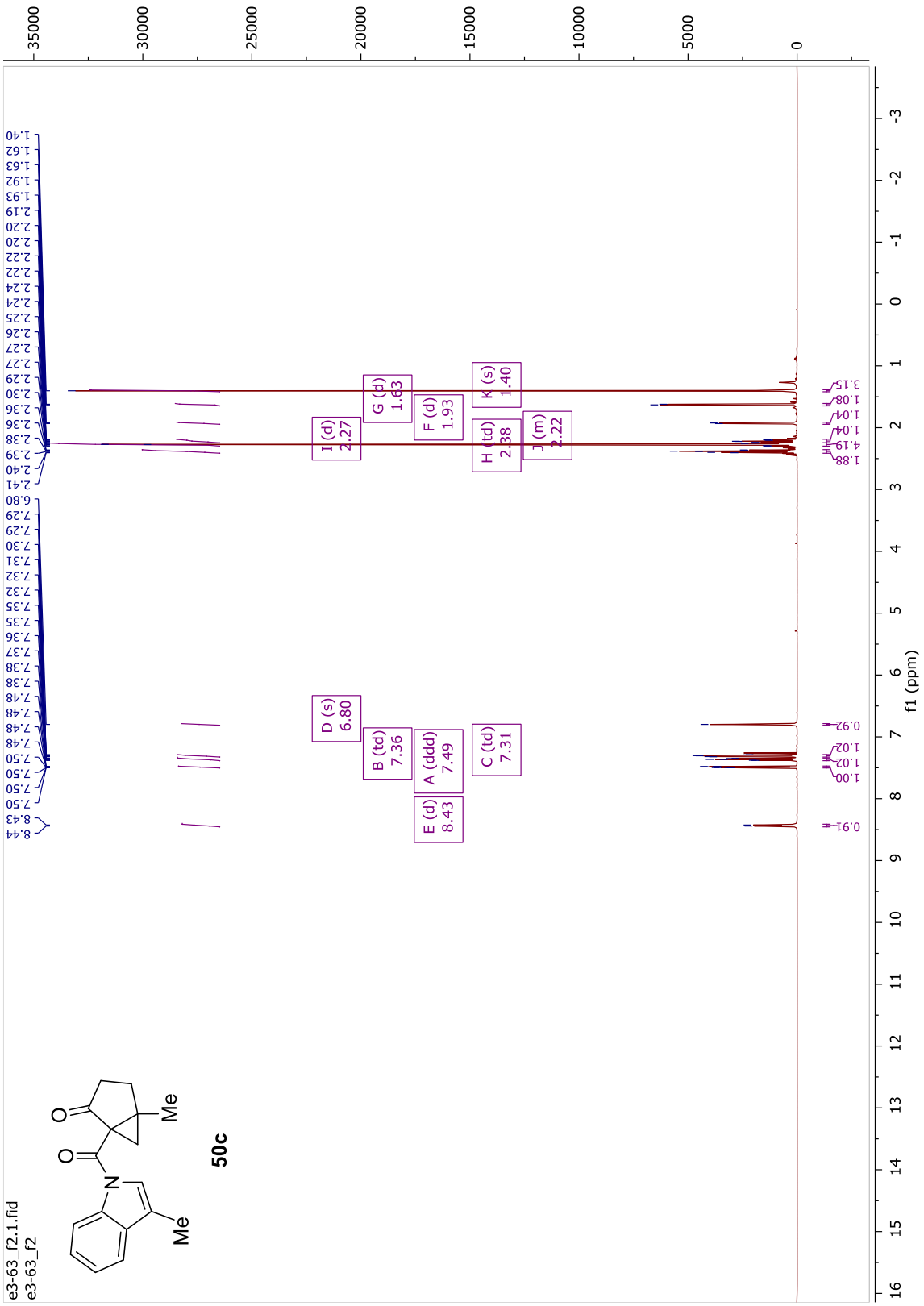
e3-63_f2.1.fid
e3-63_f2
50c
O
O
N
Me
Me
D (s) 6.80
B (td) 7.36
A (ddd) 7.49
E (d) 8.43
C (td) 7.31
I (d) 2.27
G (d) 1.63
F (d) 1.93
H (td) 2.38
J (m) 2.22
K (s) 1.40
f1 (ppm)

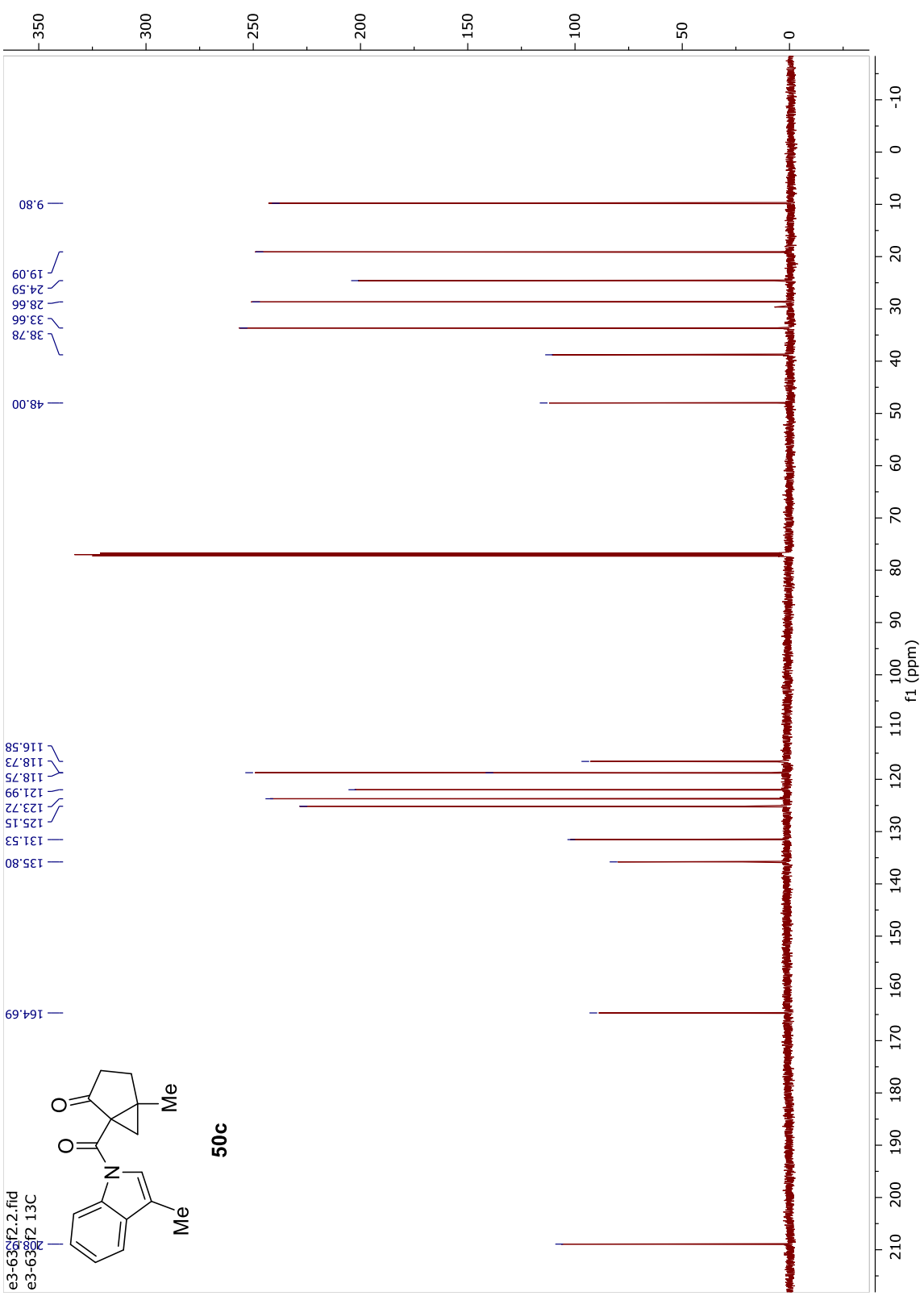
e3-63f2.2.fid
e3-63f2 13C
50c
O
O
N
Me
Me
9.80
19.09
24.59
28.66
33.66
38.78
48.00
116.58
118.73
118.75
121.99
123.72
125.15
131.53
135.80
164.69
208.92
f1 (ppm)

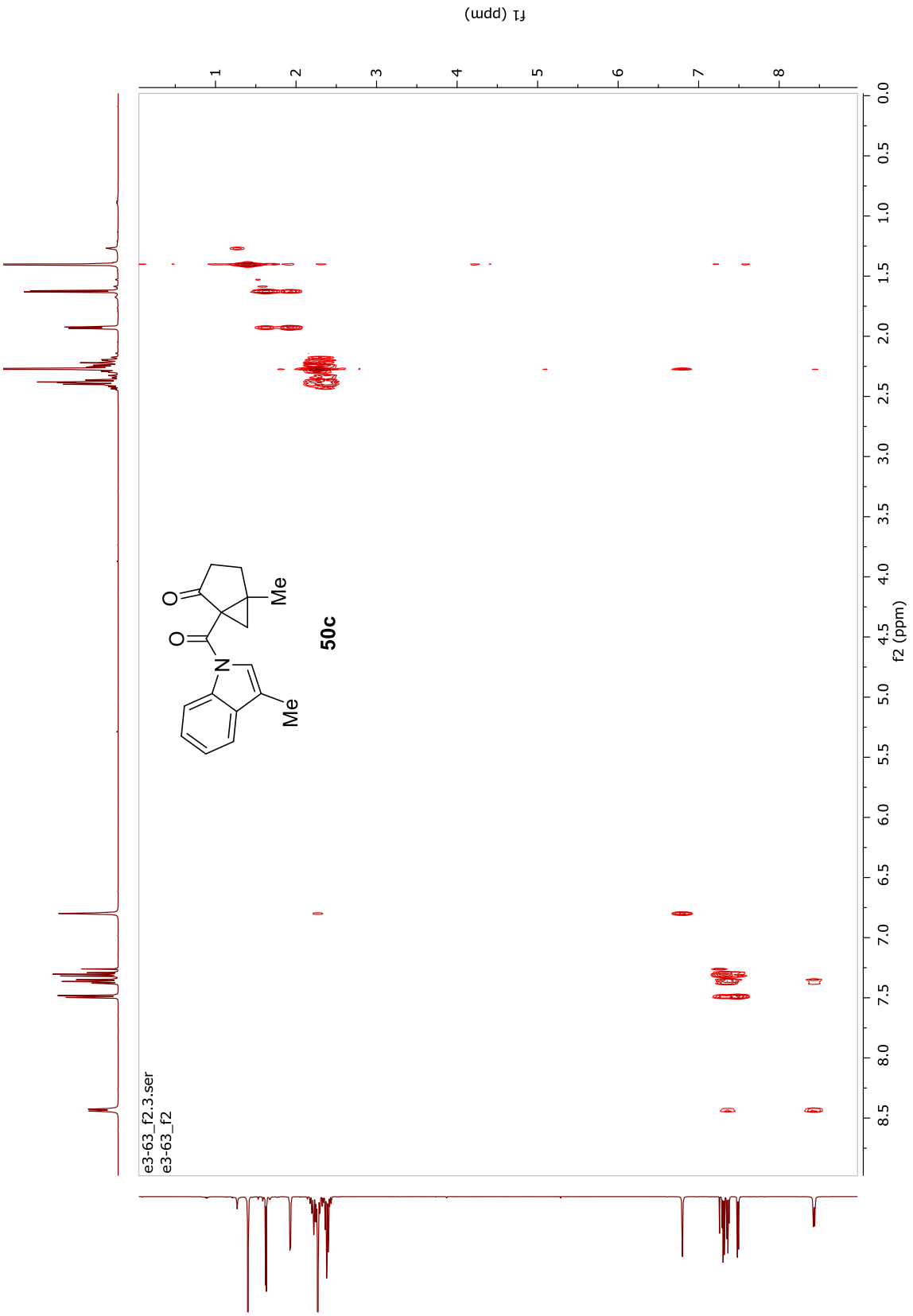
f1 (ppm)
f2 (ppm)
e3-63_f2.3.ser
e3-63_f2
O
O
N
Me
Me
50c

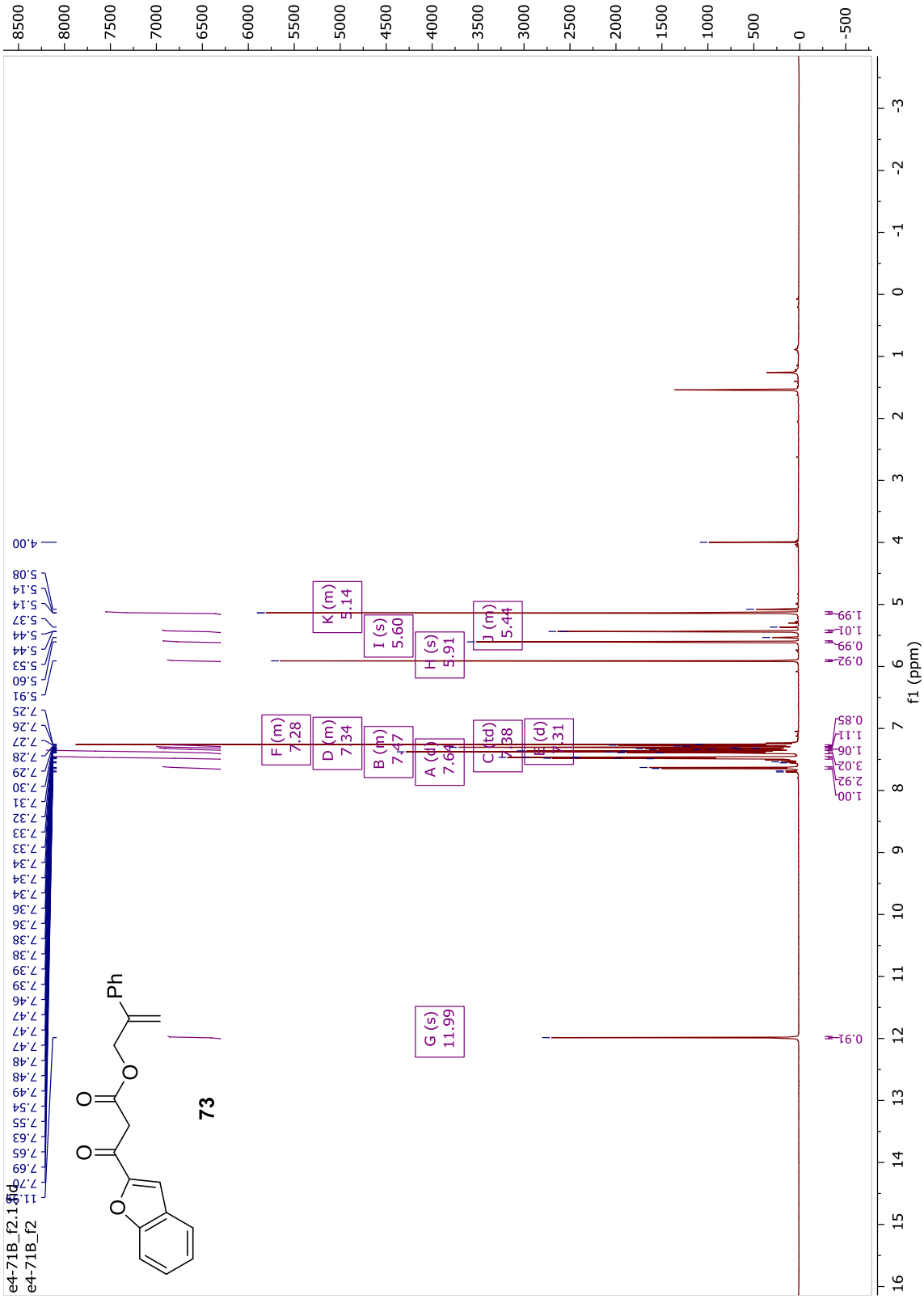
e4-71B_f2.1.fid
e4-71B_f2
73
Ph
O
O
O
O
G (s) 11.99
A (d) 7.64
B (m) 7.47
D (m) 7.34
F (m) 7.28
C (td) 7.38
E (d) 7.31
H (s) 5.91
I (s) 5.60
K (m) 5.14
J (m) 5.44
f1 (ppm)

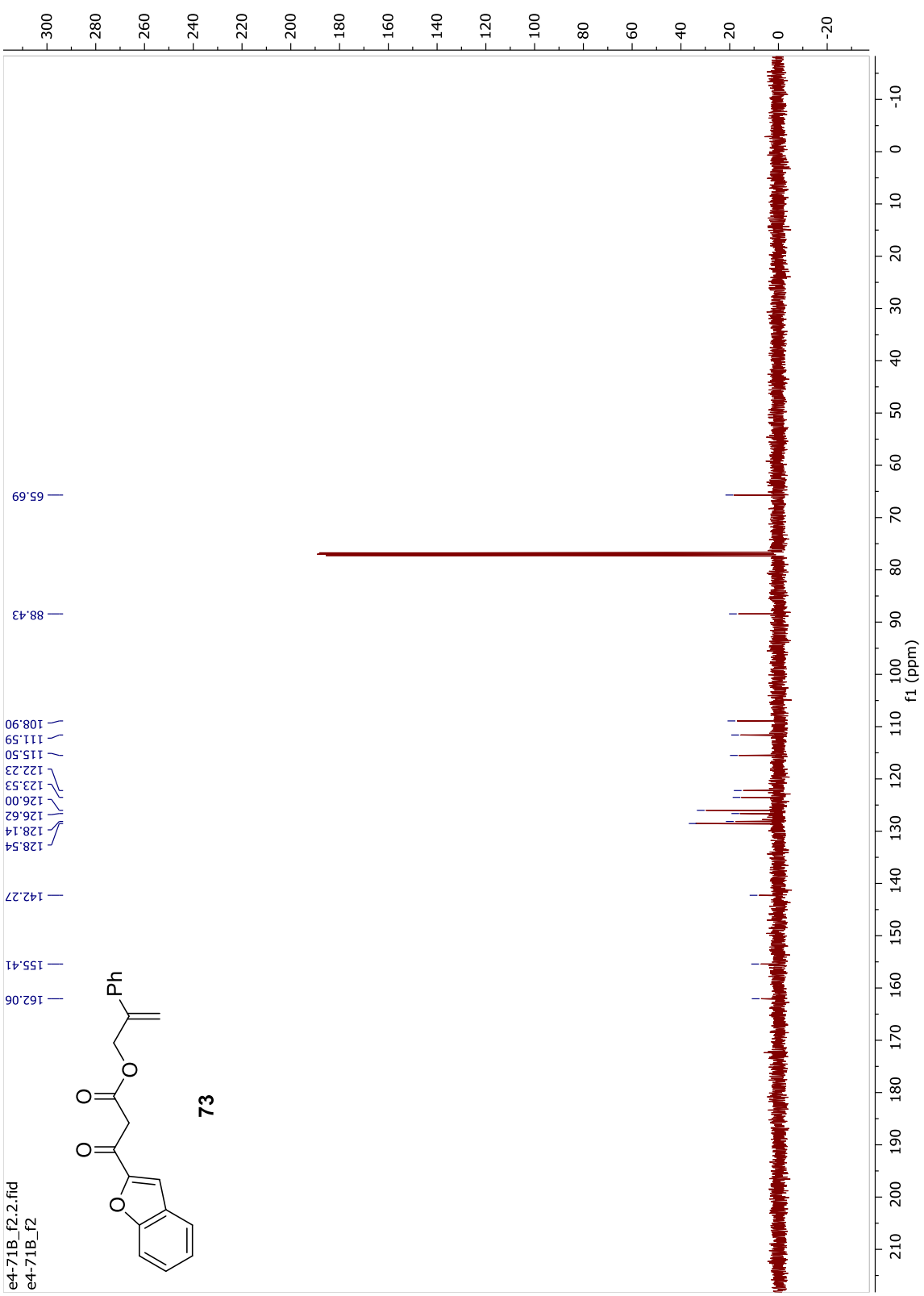
e4-71B_f2.2.fid
e4-71B_f2
73
Ph
O
O
O
O
162.06
155.41
142.27
128.54
128.14
126.62
126.00
123.53
122.23
115.50
111.59
108.90
88.43
65.69
f1 (ppm)

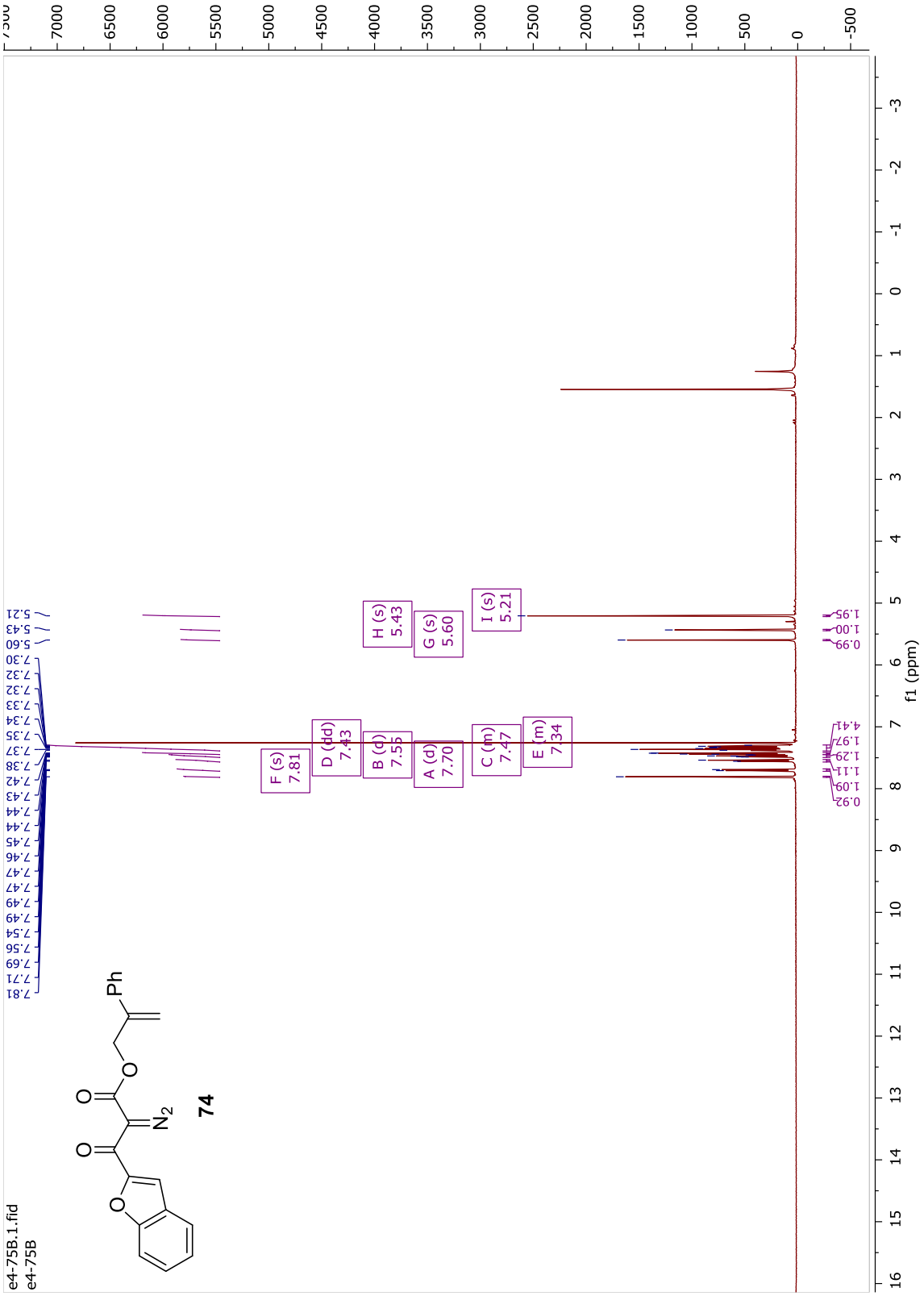
e4-75B.1.fid
e4-75B
74
Ph
O
O
O
O
N2
F (s) 7.81
D (dd) 7.43
B (d) 7.55
A (d) 7.70
C (m) 7.47
E (m) 7.34
H (s) 5.43
G (s) 5.60
I (s) 5.21
f1 (ppm)

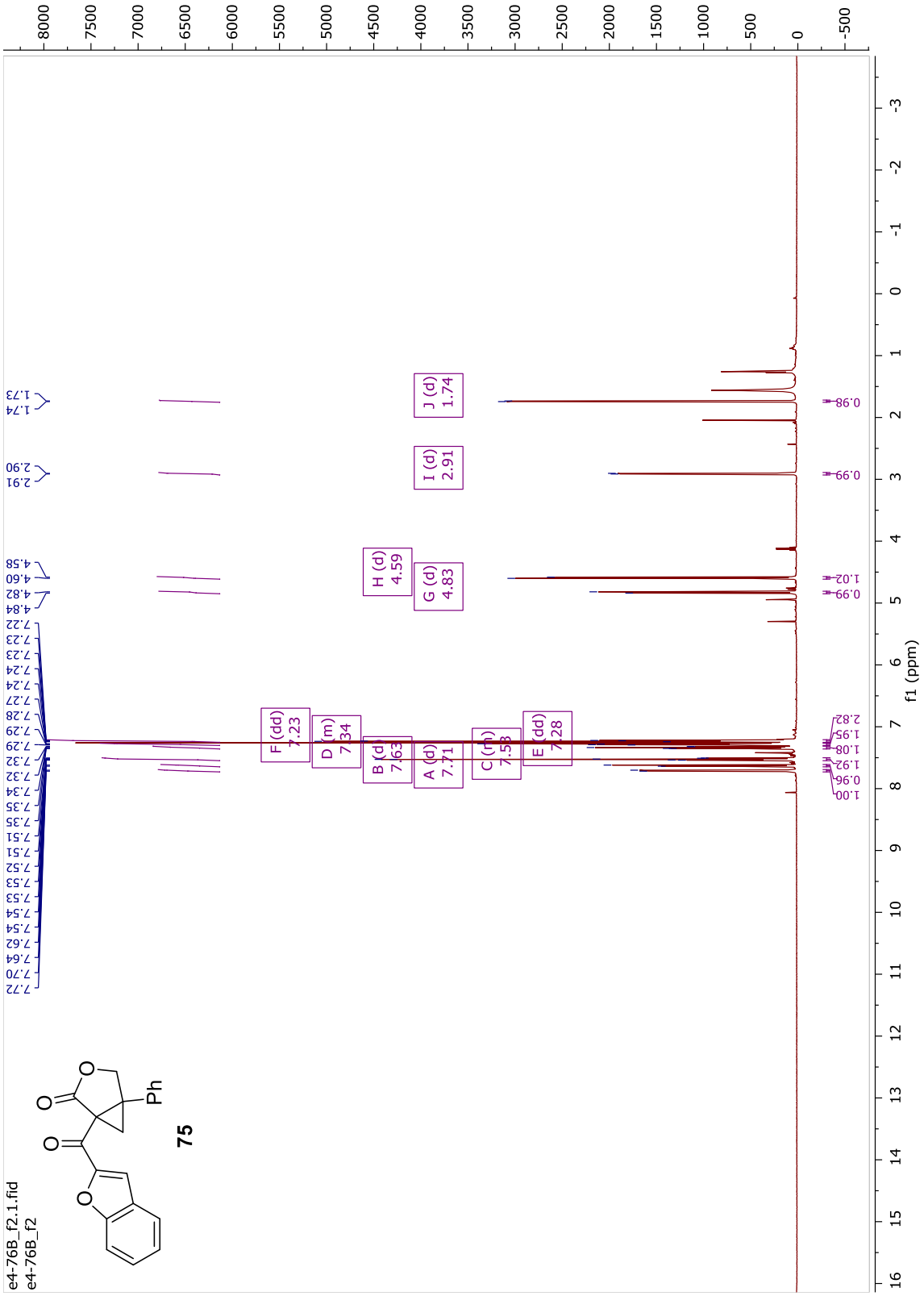
e4-76B_f2.1.fid
e4-76B_f2
75
Ph
O
O
O
A (d) 7.71
B (d) 7.63
C (m) 7.58
D (m) 7.34
E (dd) 7.28
F (dd) 7.23
G (d) 4.83
H (d) 4.59
I (d) 2.91
J (d) 1.74
f1 (ppm)

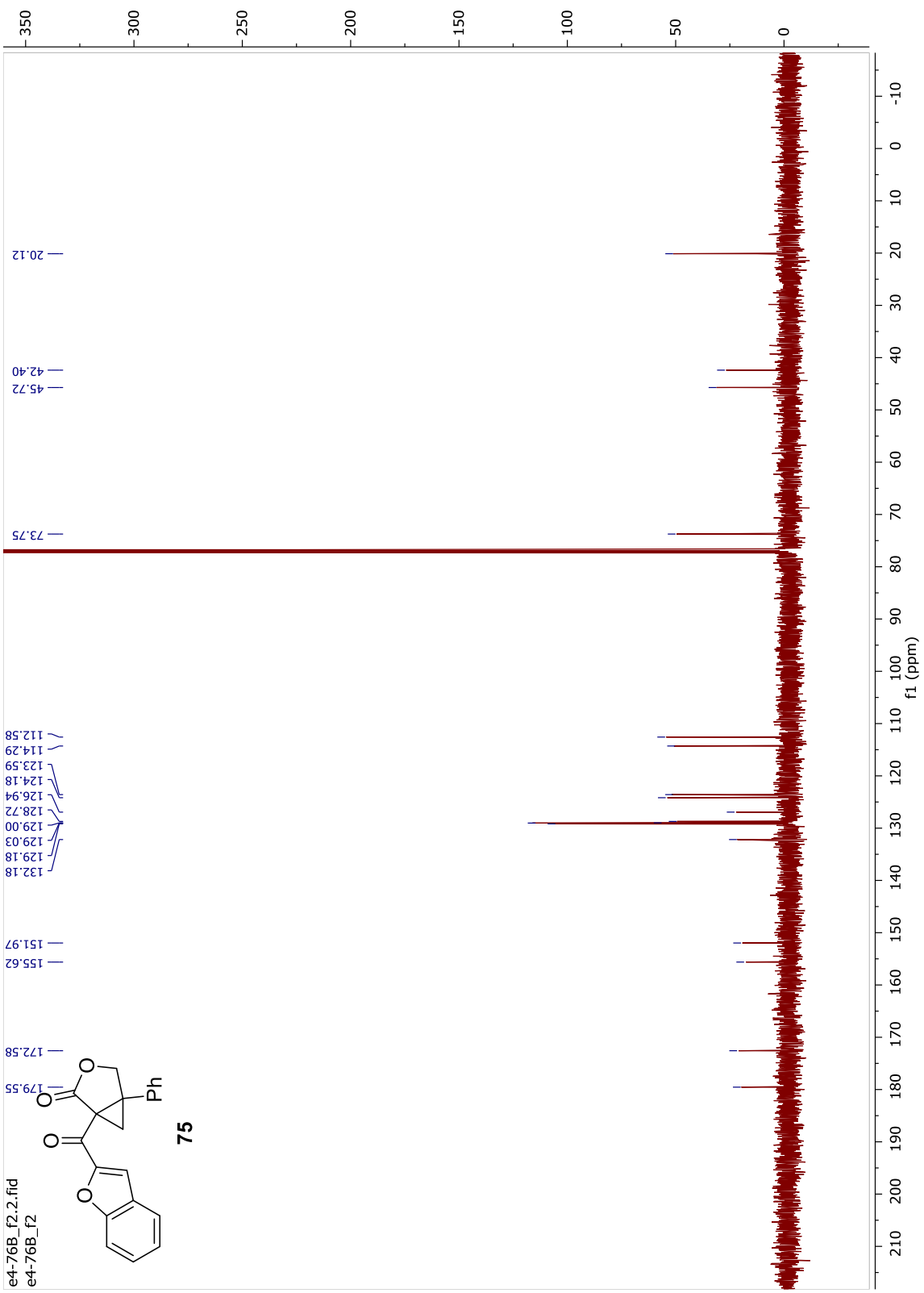
e4-76B_f2.2.fid
e4-76B_f2
75
Ph
O
O
O
O
179.55
172.58
155.62
151.97
132.18
129.18
129.03
129.00
128.72
126.94
124.18
123.59
114.29
112.58
73.75
45.72
42.40
20.12
f1 (ppm)

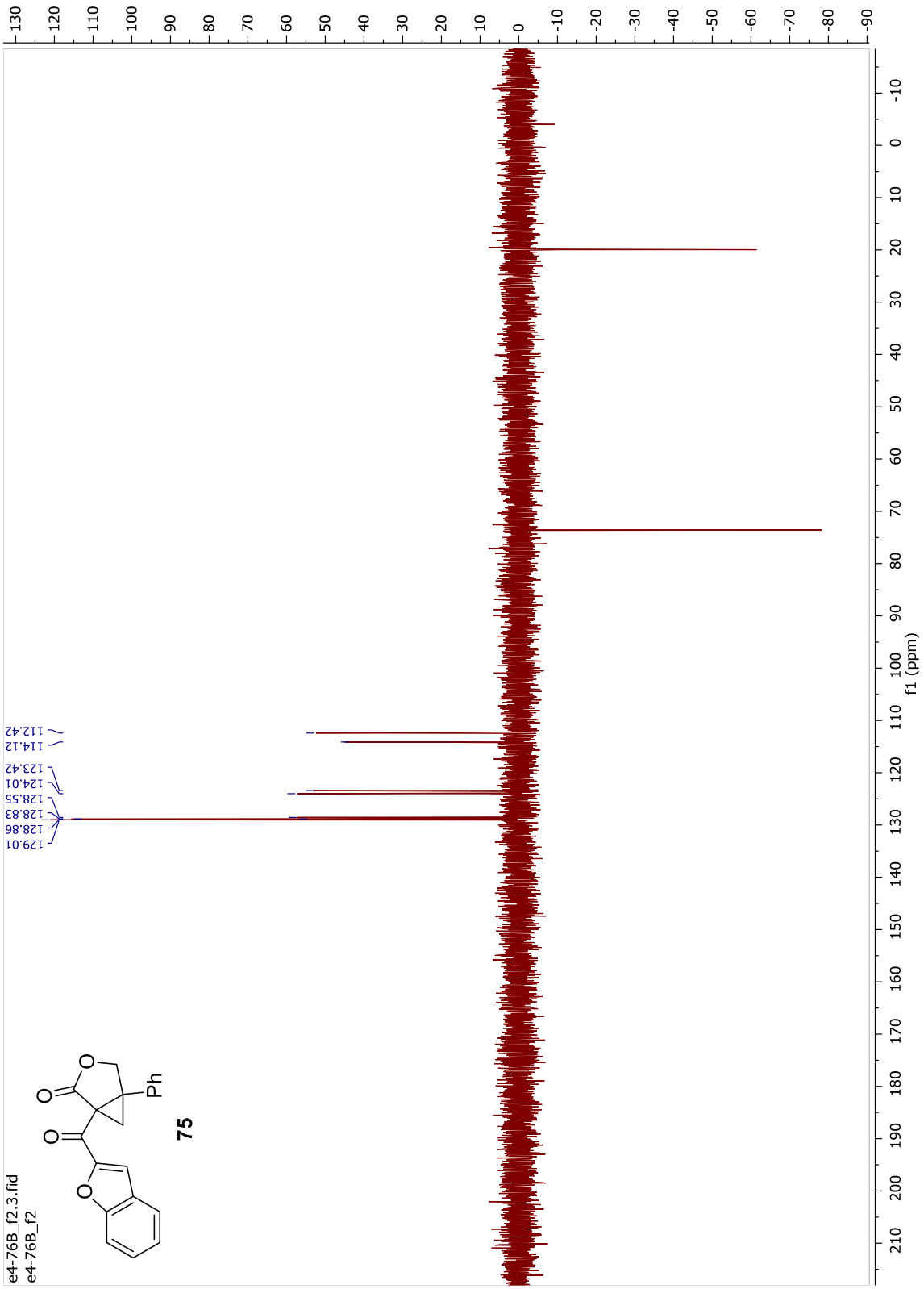
e4-76B_f2.3.fid
e4-76B_f2
129.01
128.86
128.83
128.55
124.01
123.42
114.12
112.42
O
O
O
Ph
75
f1 (ppm)

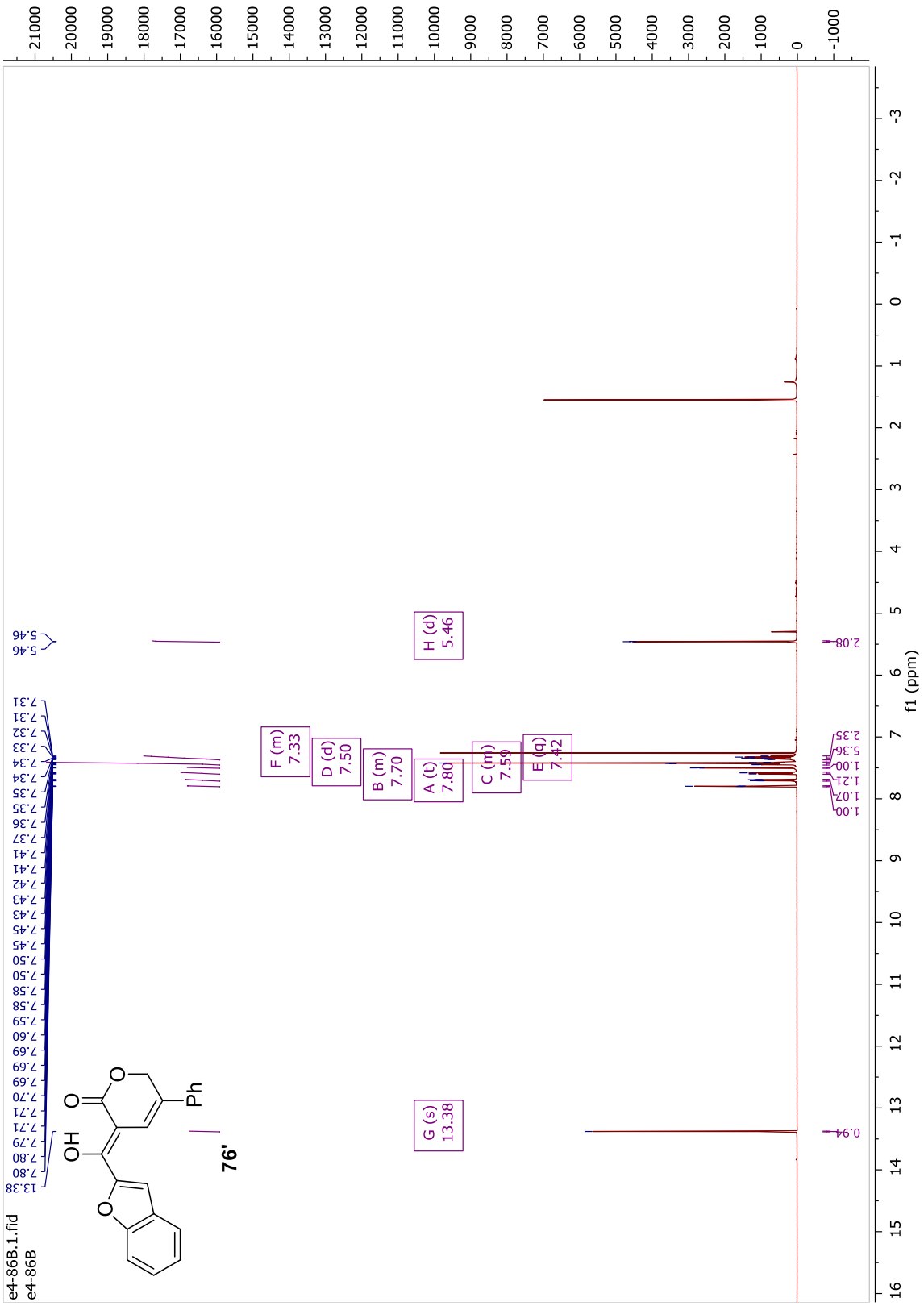
e4-86B.1.fid
e4-86B
76'
OH
O
O
Ph
G (s)
13.38
H (d)
5.46
F (m)
7.33
D (d)
7.50
B (m)
7.70
A (t)
7.80
C (m)
7.59
E (q)
7.42
f1 (ppm)

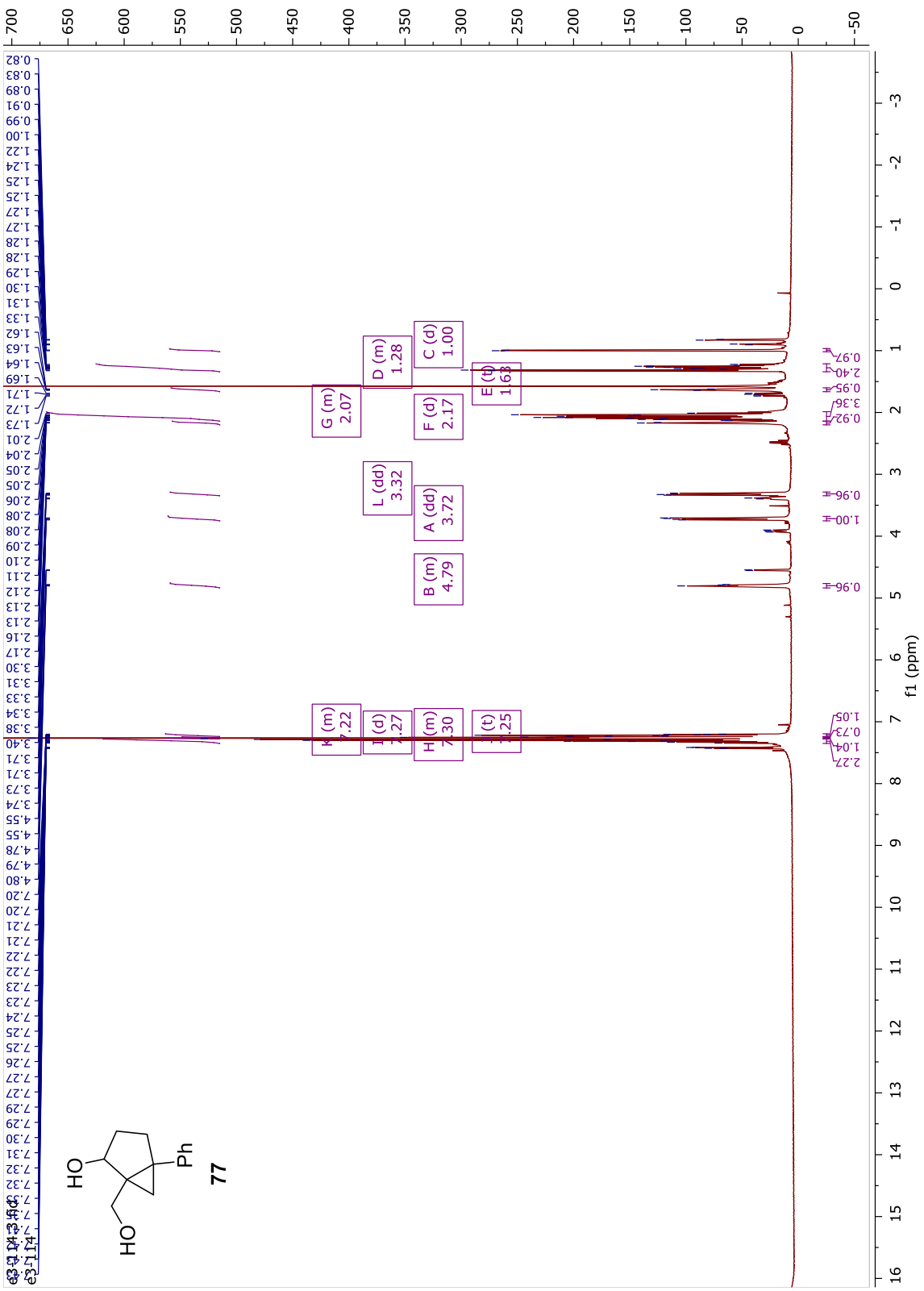
HO
HO
Ph
77
K (m) 7.22
I (d) 7.27
H (m) 7.30
J (t) 7.25
G (m) 2.07
D (m) 1.28
C (d) 1.00
E (t) 1.63
F (d) 2.17
L (dd) 3.32
A (dd) 3.72
B (m) 4.79
f1 (ppm)

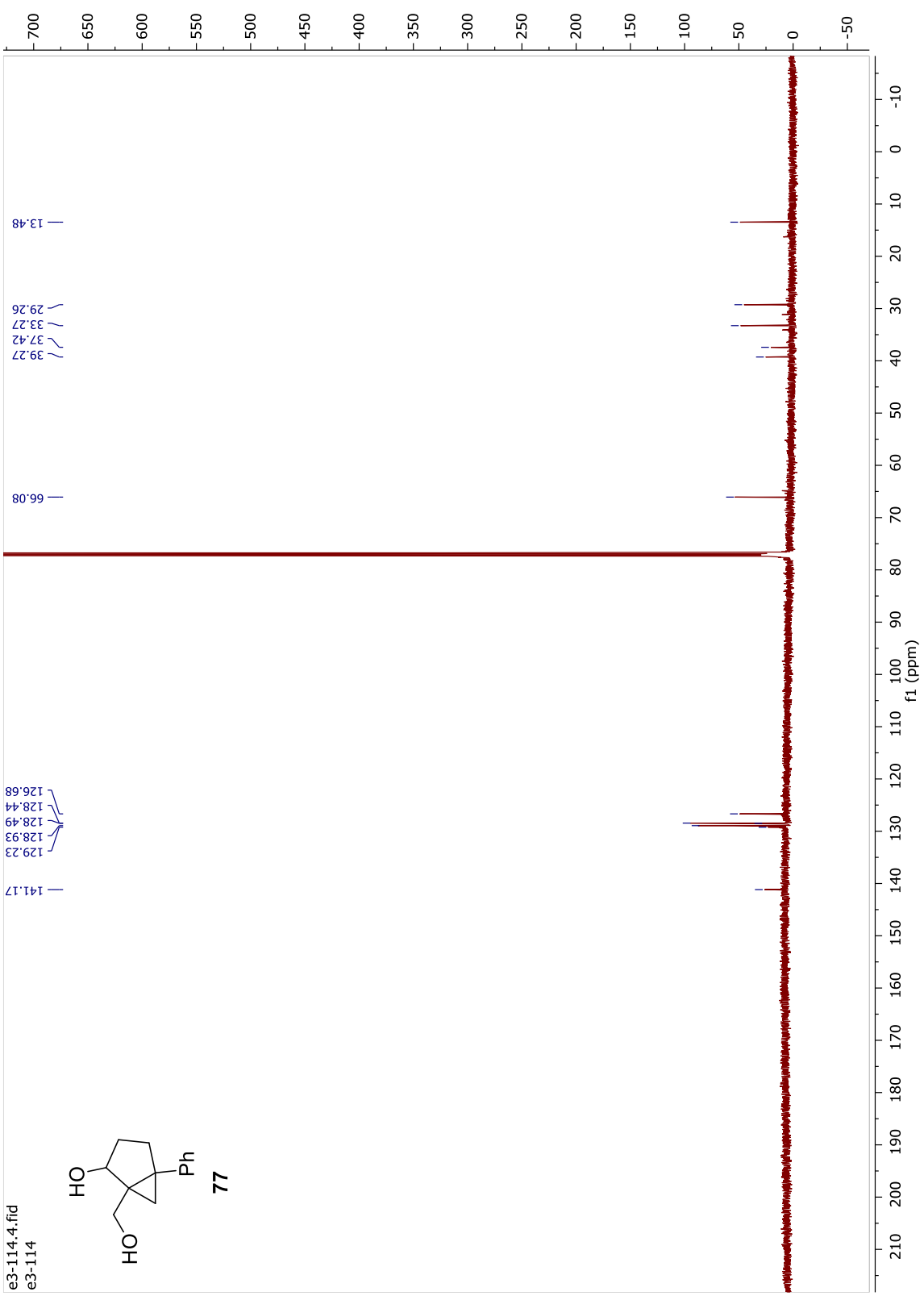
e3-114.4.fid
e3-114
HO
HO
Ph
77
13.48
29.26
33.27
37.42
39.27
66.08
126.68
128.44
128.49
128.93
129.23
141.17
f1 (ppm)

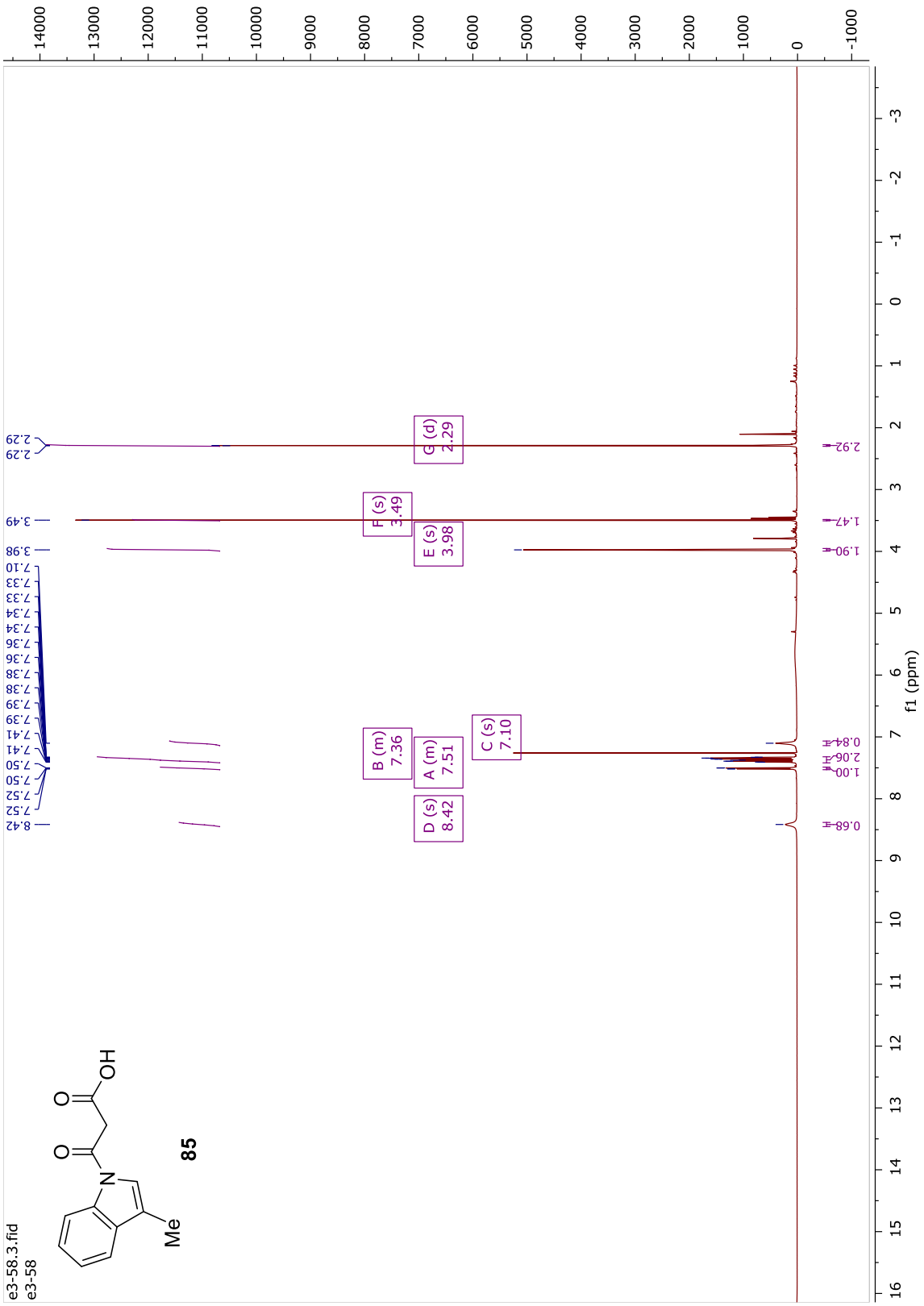
e3-58.3.fid
e3-58
85
Me
N
O
O
OH
A (m) 7.51
B (m) 7.36
C (s) 7.10
D (s) 8.42
E (s) 3.98
F (s) 3.49
G (d) 2.29
f1 (ppm)

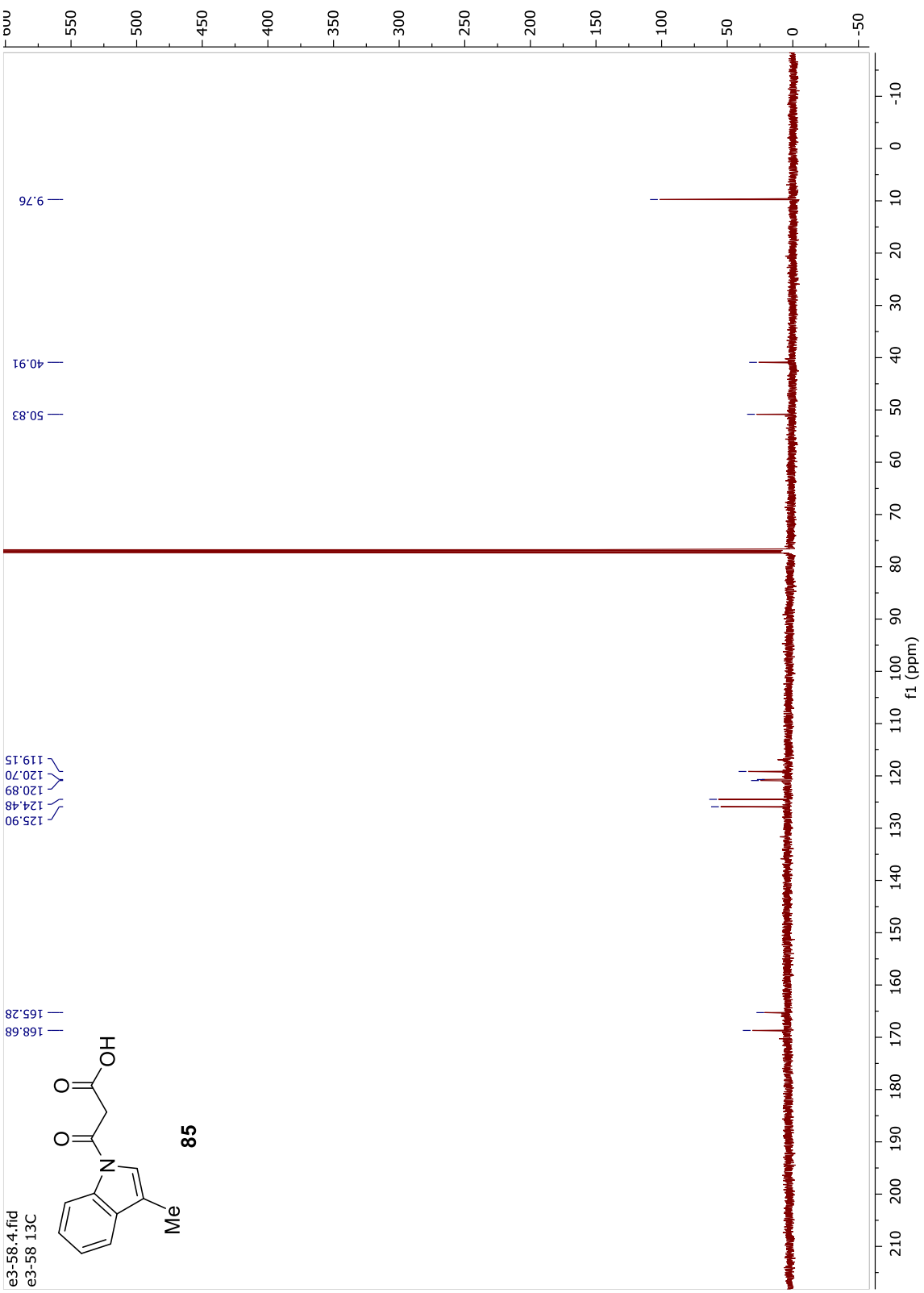
e3-58.4.fid
e3-58 13C
9.76
40.91
50.83
119.15
120.70
120.89
124.48
125.90
165.28
168.68
Me
85
f1 (ppm)

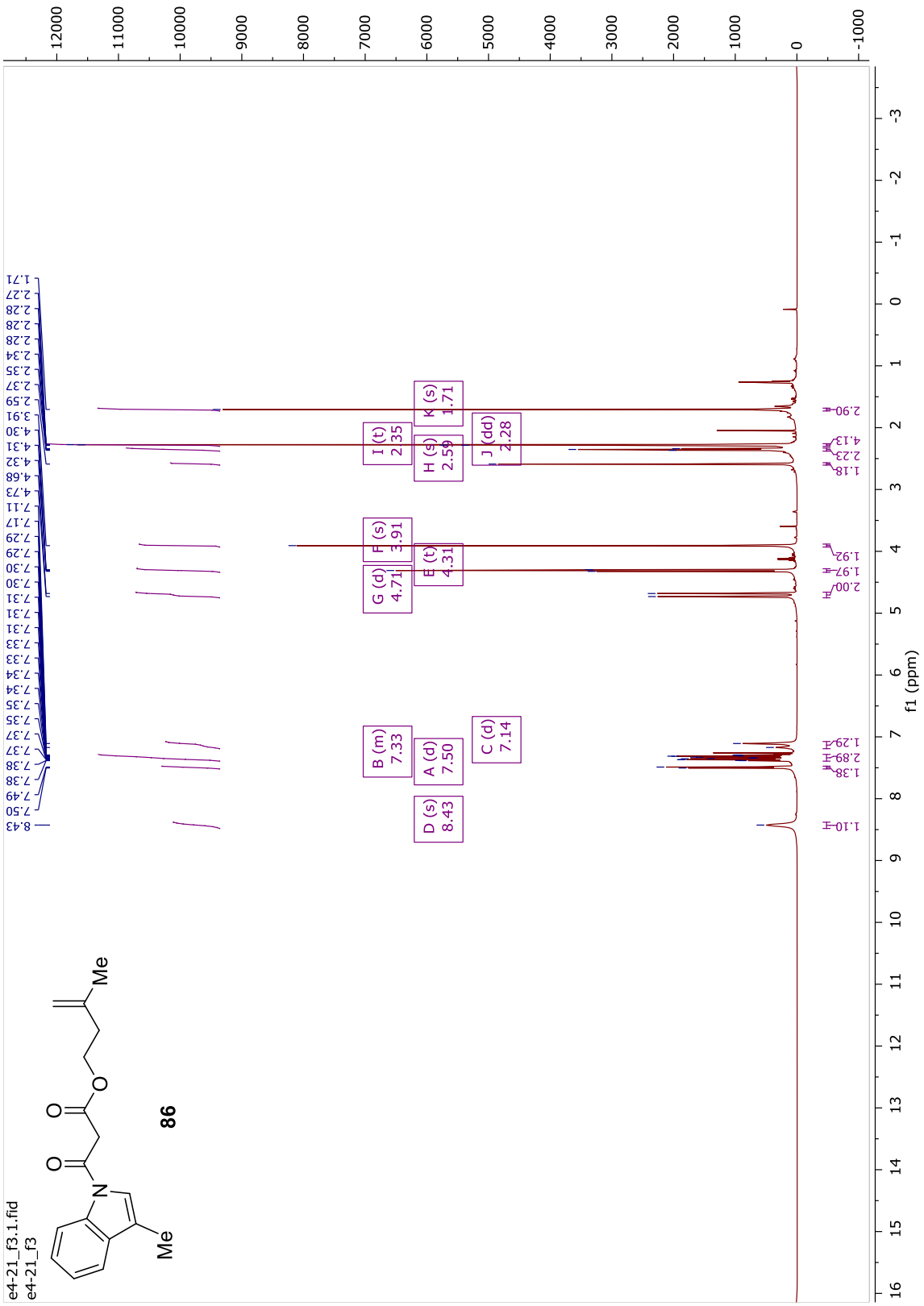
e4-21_f3.1.fid
e4-21_f3
86
Me
Me
O
O
O
N
D (s) 8.43
B (m) 7.33
A (d) 7.50
C (d) 7.14
G (d) 4.71
F (s) 3.91
E (t) 4.31
I (t) 2.35
H (q) 2.59
J (dd) 2.28
K (s) 1.71
f1 (ppm)

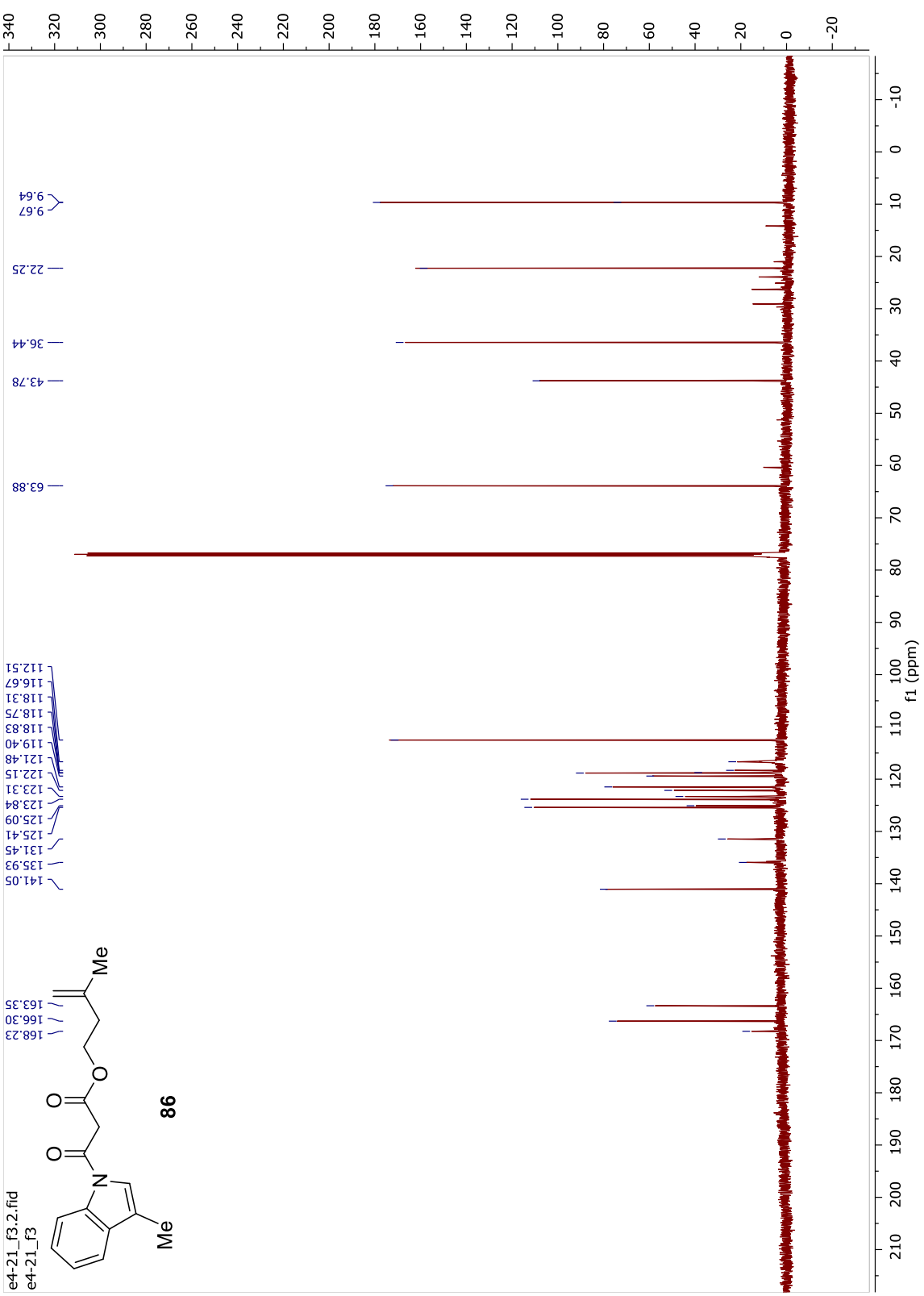
e4-21_f3.2.fid
e4-21_f3
86
Me
Me
O
O
O
N
168.23
166.30
163.35
141.05
135.93
131.45
125.41
125.09
123.84
123.31
122.15
121.48
119.40
118.83
118.75
118.31
116.67
112.51
63.88
43.78
36.44
22.25
9.67
9.64
f1 (ppm)

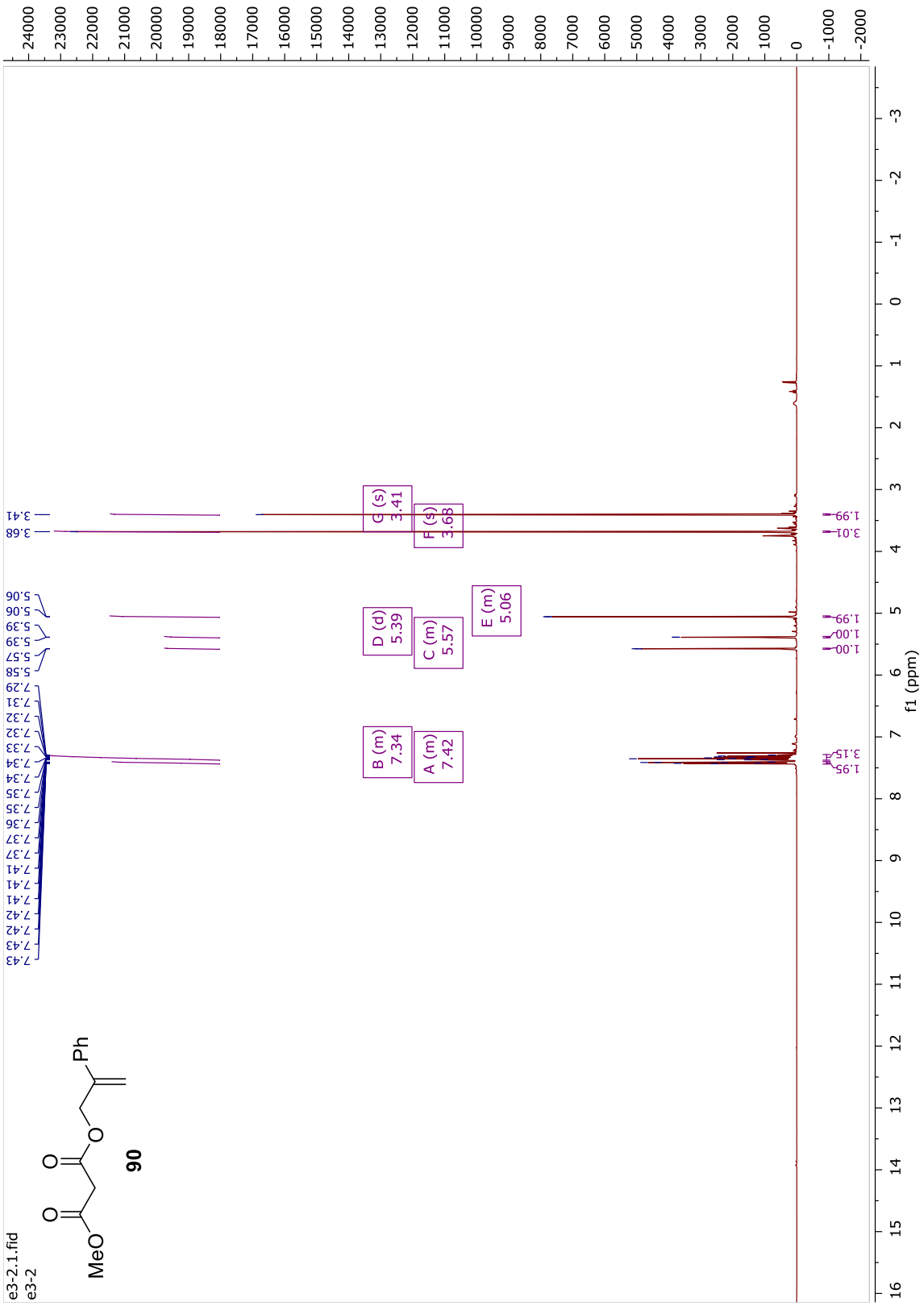
e3-2.1.fid
e3-2
MeO
O
O
O
O
Ph
90
A (m) 7.42
B (m) 7.34
C (m) 5.57
D (d) 5.39
E (m) 5.06
F (s) 3.68
G (s) 3.41
f1 (ppm)

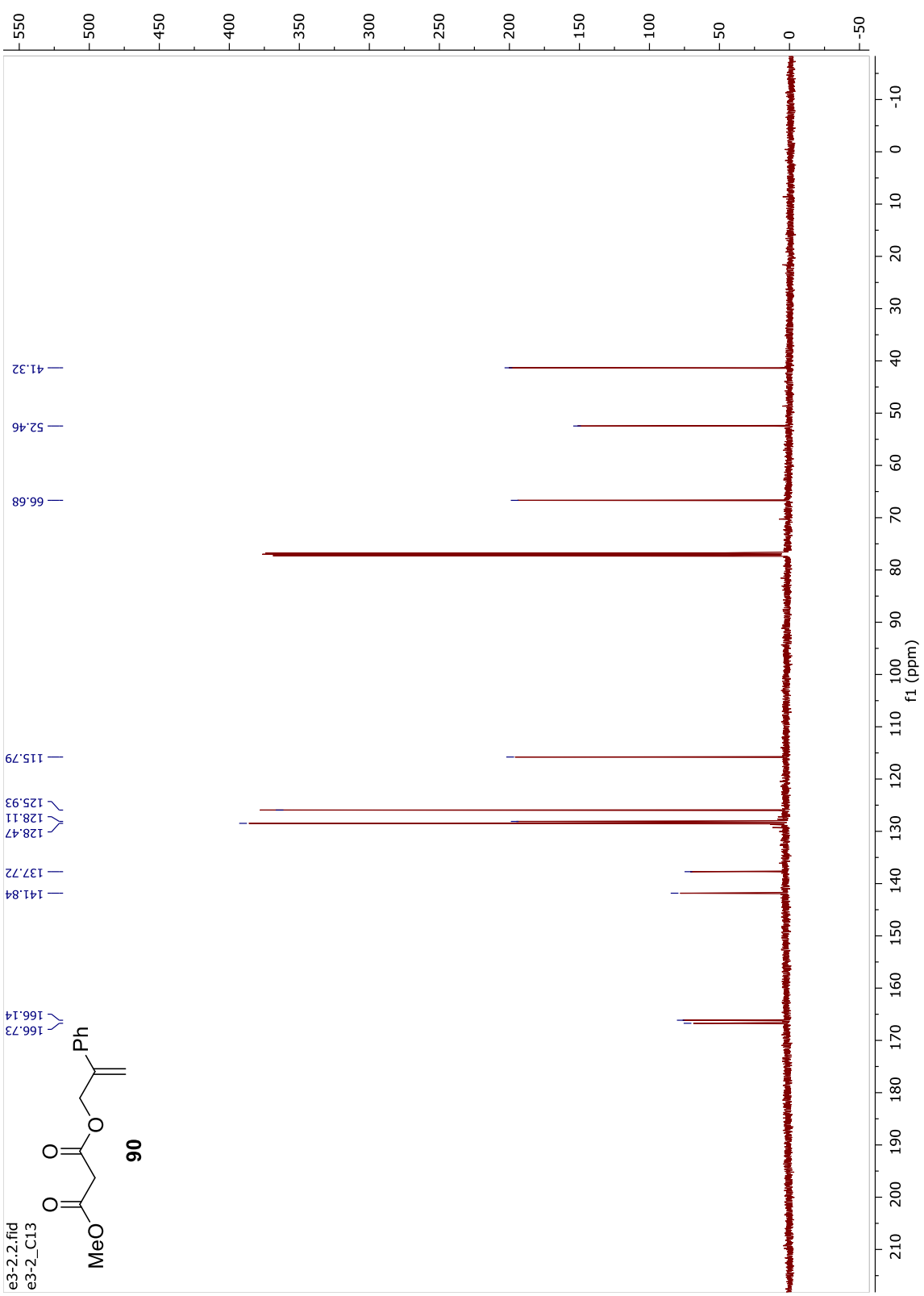
e3-2.2.fid
e3-2_C13
MeO
O
O
O
O
Ph
90
166.73
166.14
141.84
137.72
128.47
128.11
125.93
115.79
66.68
52.46
41.32
f1 (ppm)

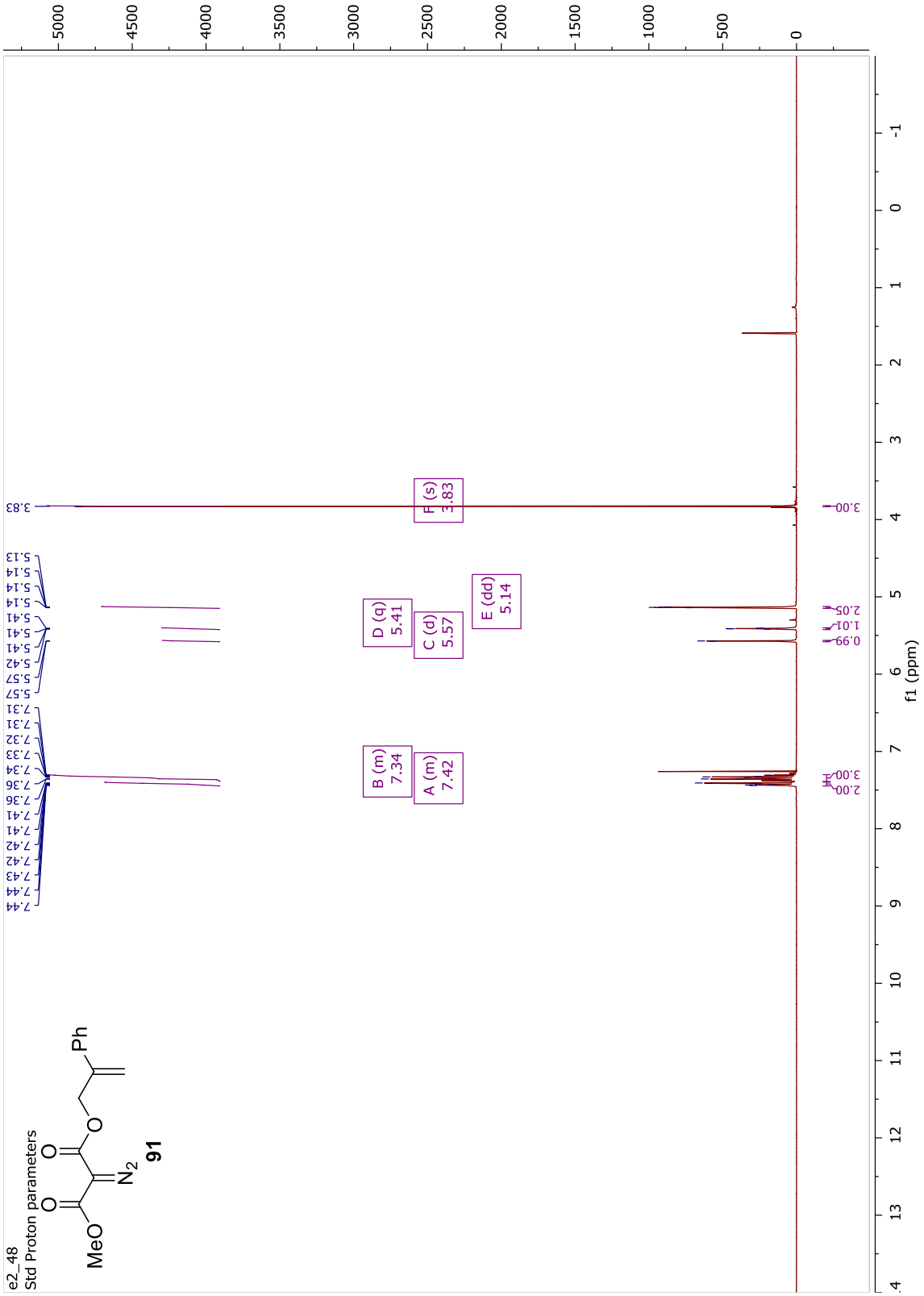
e2_48
Std Proton parameters
MeO
O
O
O
N2
Ph
91
F (s)
3.83
D (q)
5.41
C (d)
5.57
E (dd)
5.14
B (m)
7.34
A (m)
7.42
3.83
5.13
5.14
5.14
5.41
5.41
5.42
5.57
5.57
7.31
7.31
7.32
7.33
7.34
7.36
7.36
7.41
7.41
7.42
7.42
7.43
7.44
7.44
3.00
2.05
1.01
0.99
2.00
3.00
f1 (ppm)

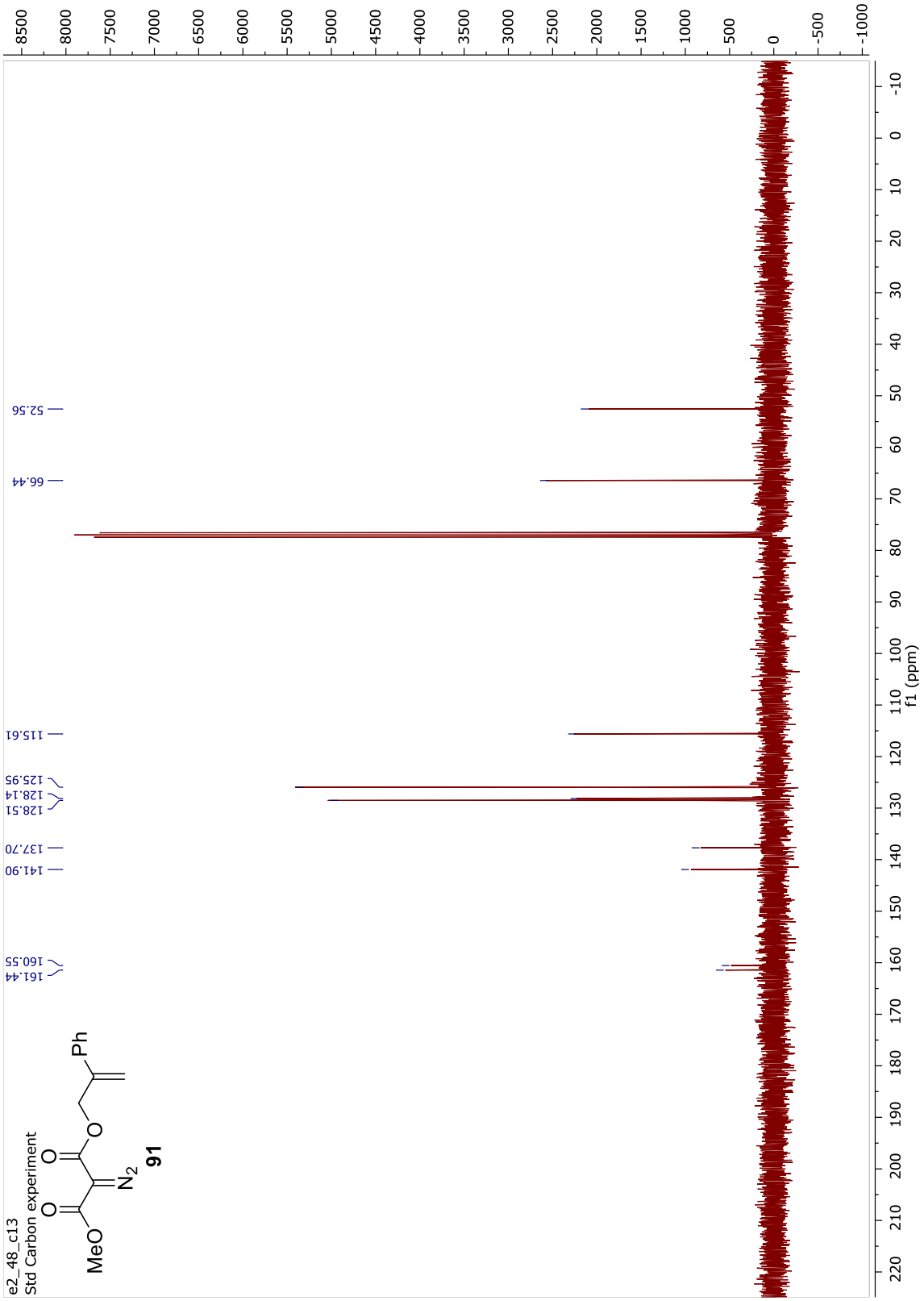
e2_48_c13
Std Carbon experiment
MeO
O
O
O
O
N2
Ph
91
161.44
160.55
141.90
137.70
128.51
128.14
125.95
115.61
66.44
52.56
f1 (ppm)

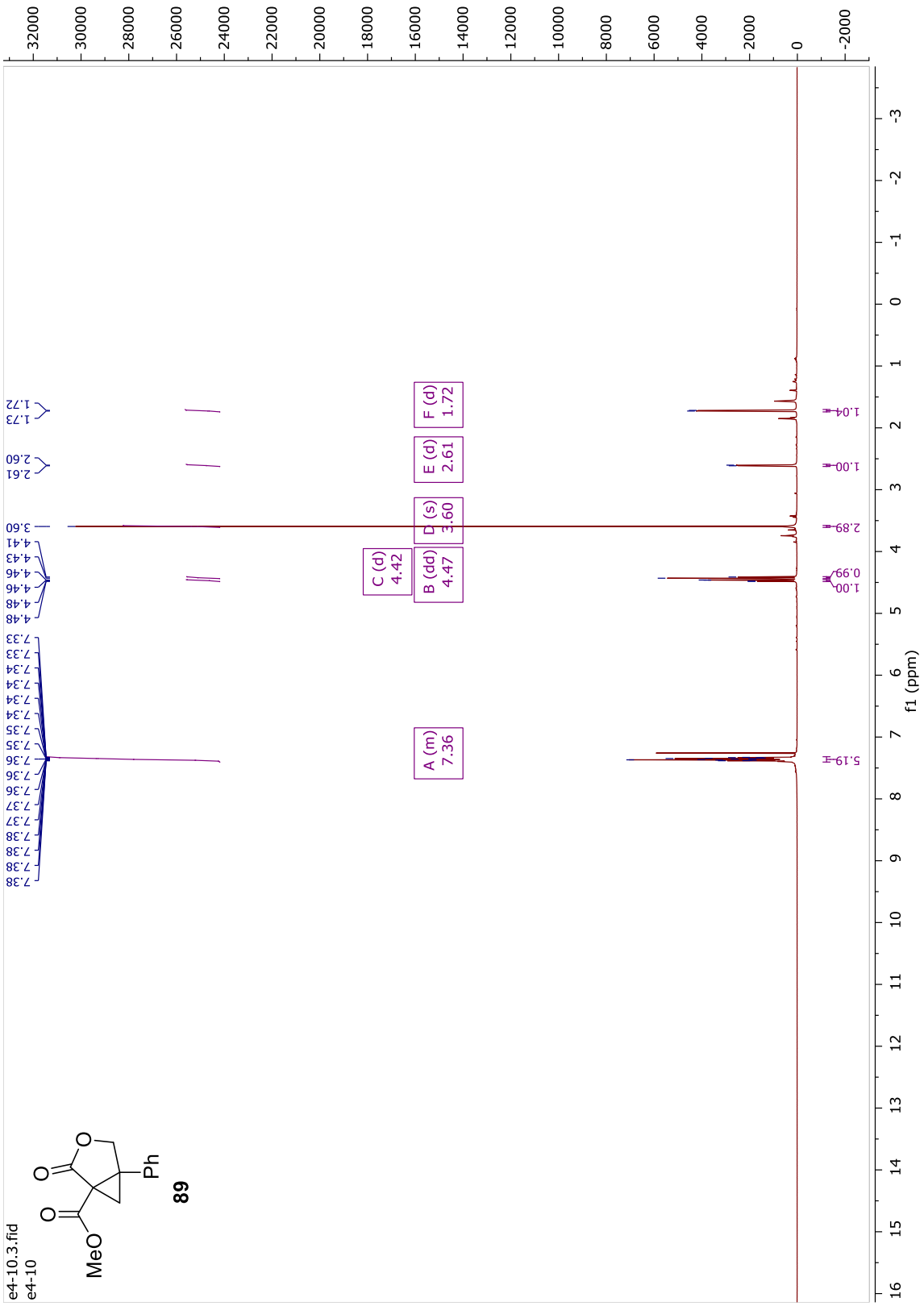
e4-10.3.fid
e4-10
MeO
O
O
O
Ph
89
A (m) 7.36
B (dd) 4.47
C (d) 4.42
D (s) 3.60
E (d) 2.61
F (d) 1.72
f1 (ppm)

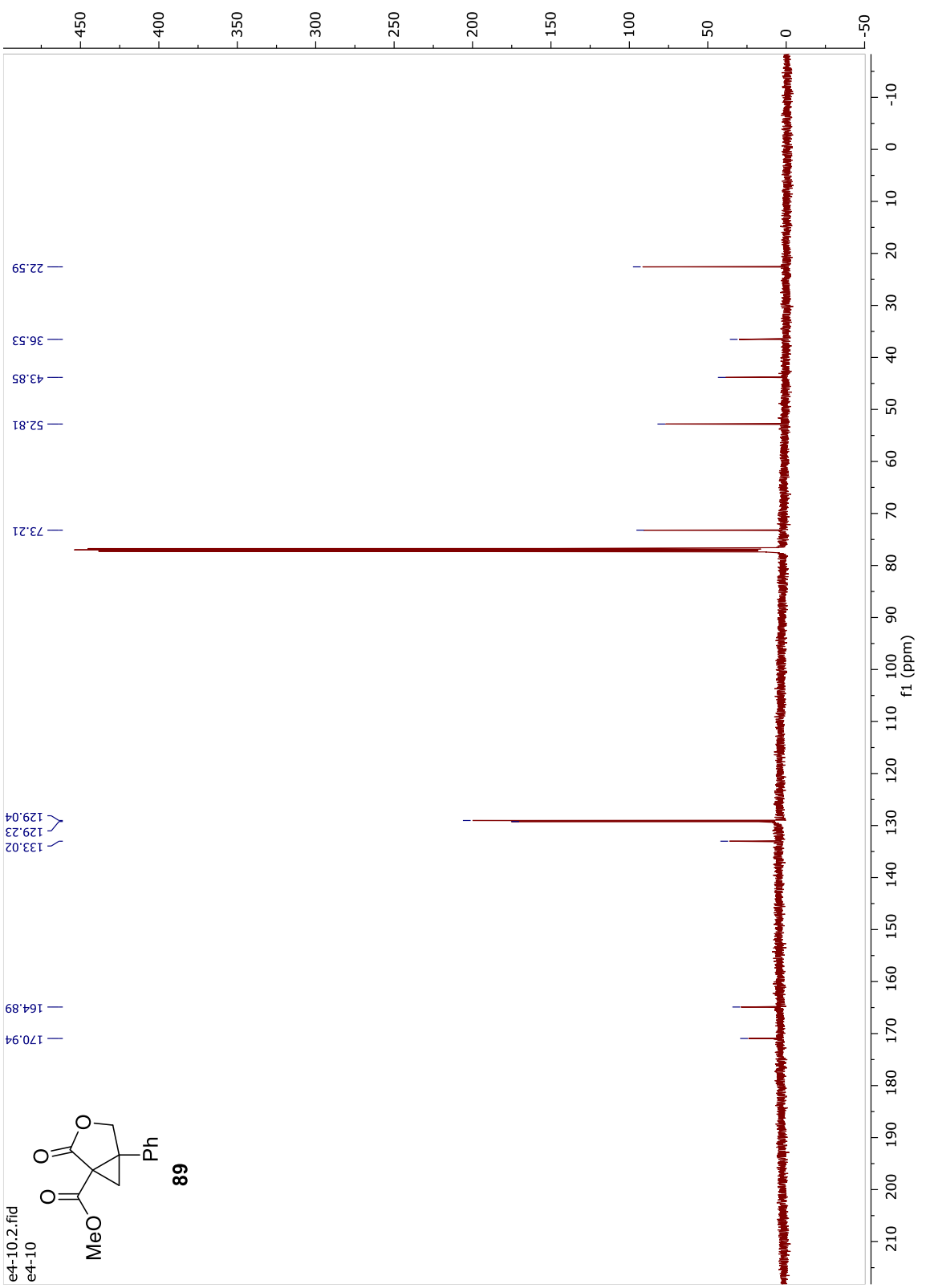
e4-10.2.fid
e4-10
MeO
O
O
O
Ph
89
170.94
164.89
133.02
129.23
129.04
73.21
52.81
43.85
36.53
22.59
f1 (ppm)

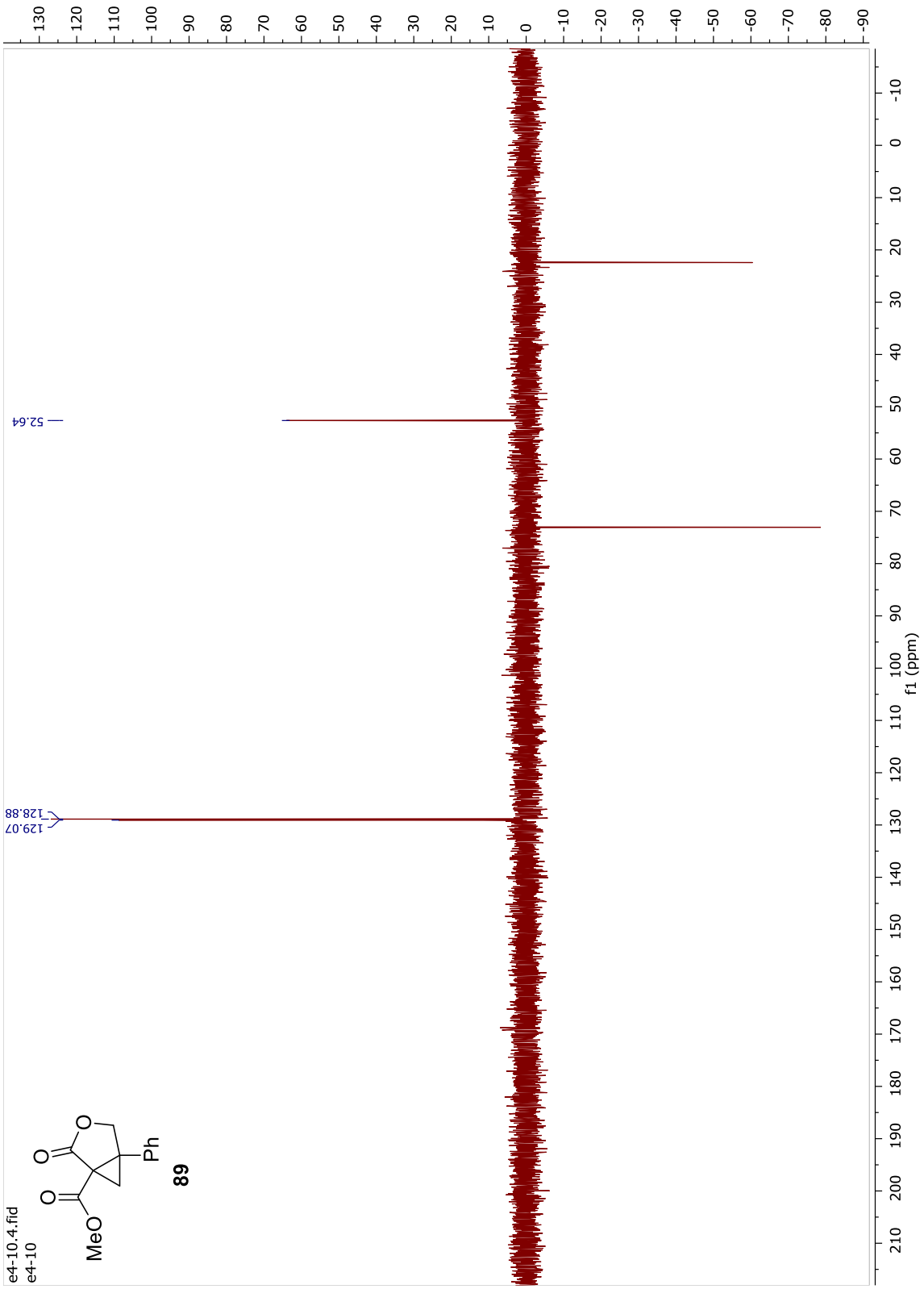
e4-10.4.fid
e4-10
MeO
O
O
O
Ph
89
52.64
129.07
128.88
f1 (ppm)

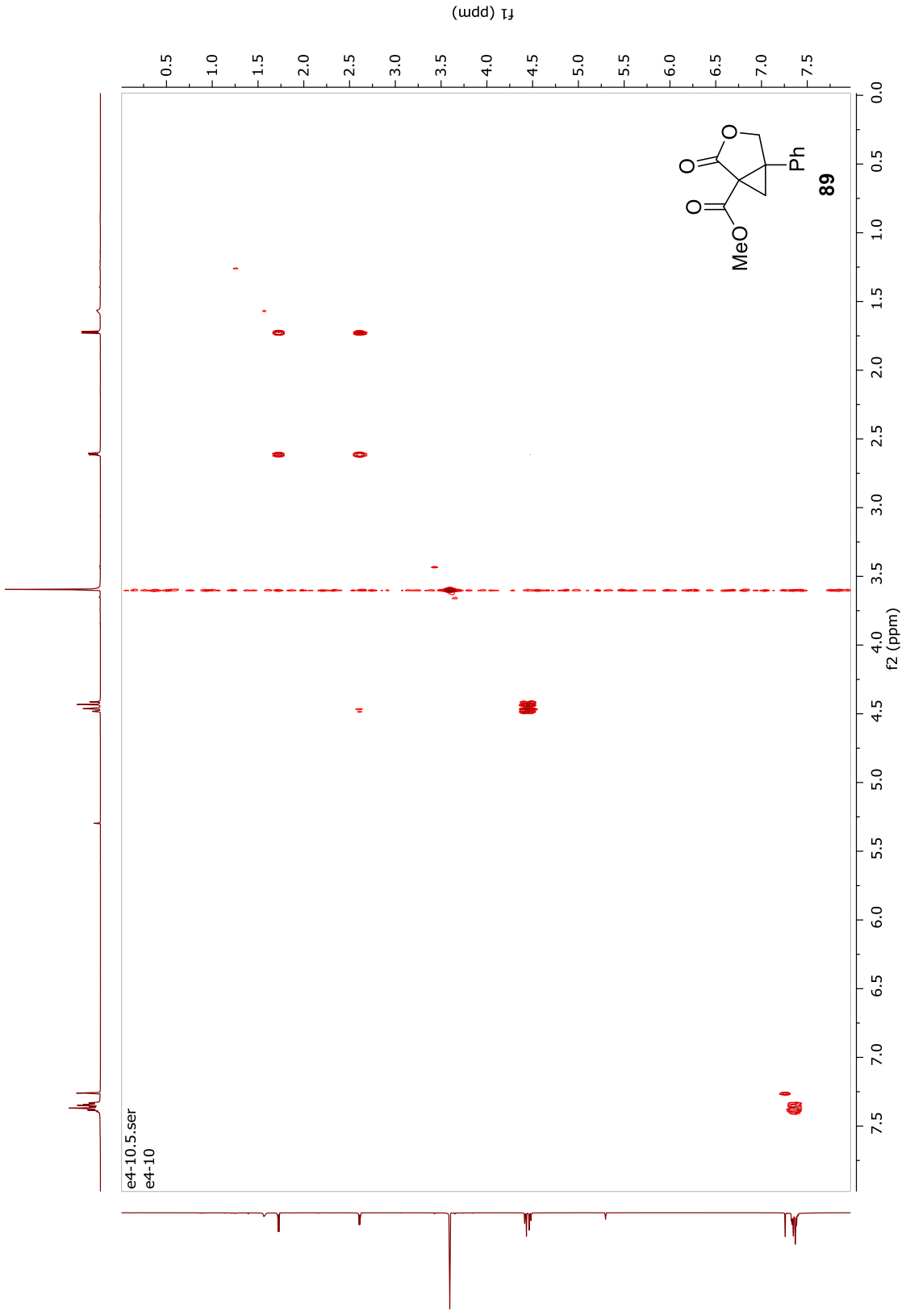
f1 (ppm)
f2 (ppm)
e4-10.5.ser
e4-10
MeO
Ph
89

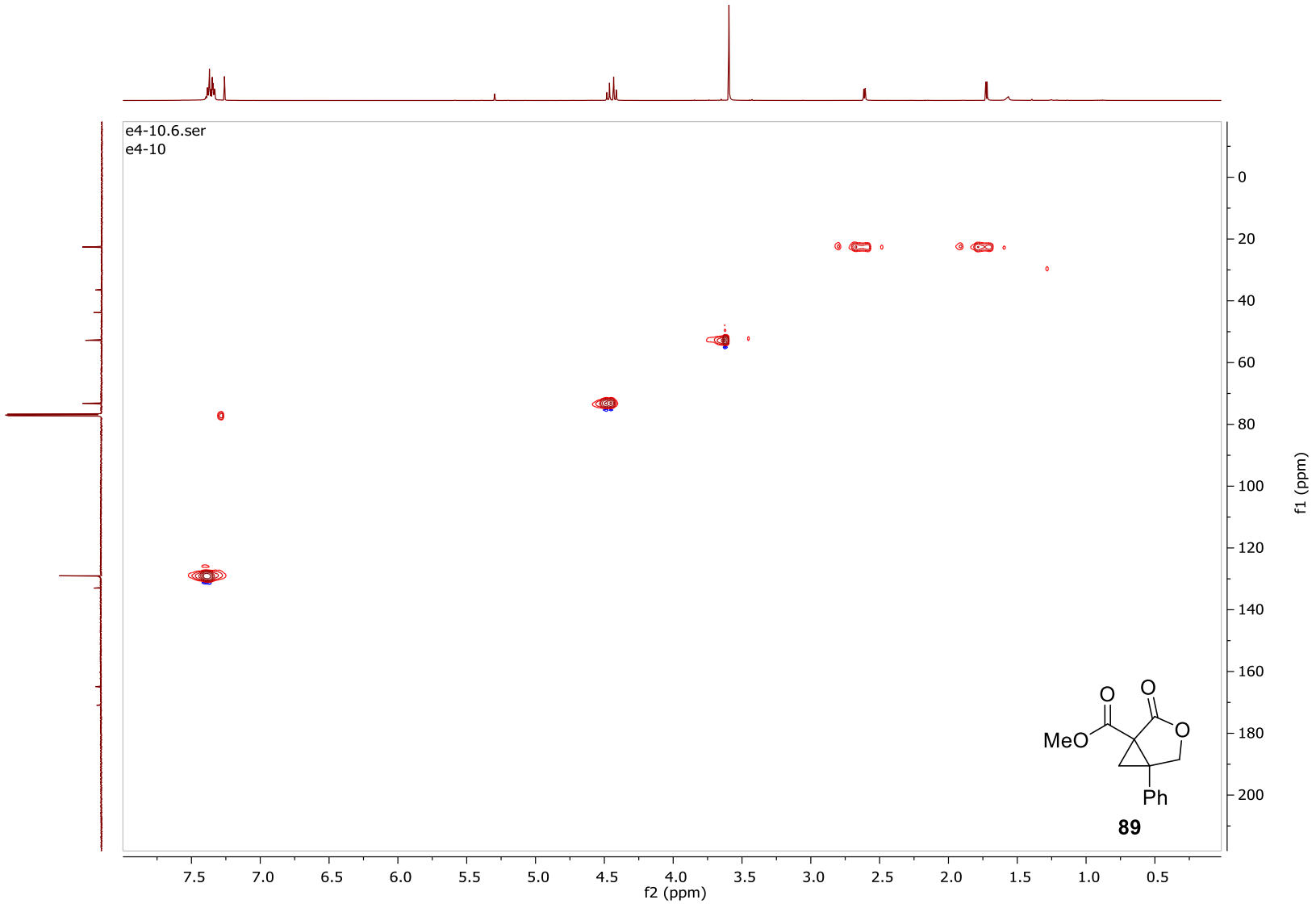
e4-10.6.ser
e4-10
f2 (ppm)
f1 (ppm)
MeO
Ph
89

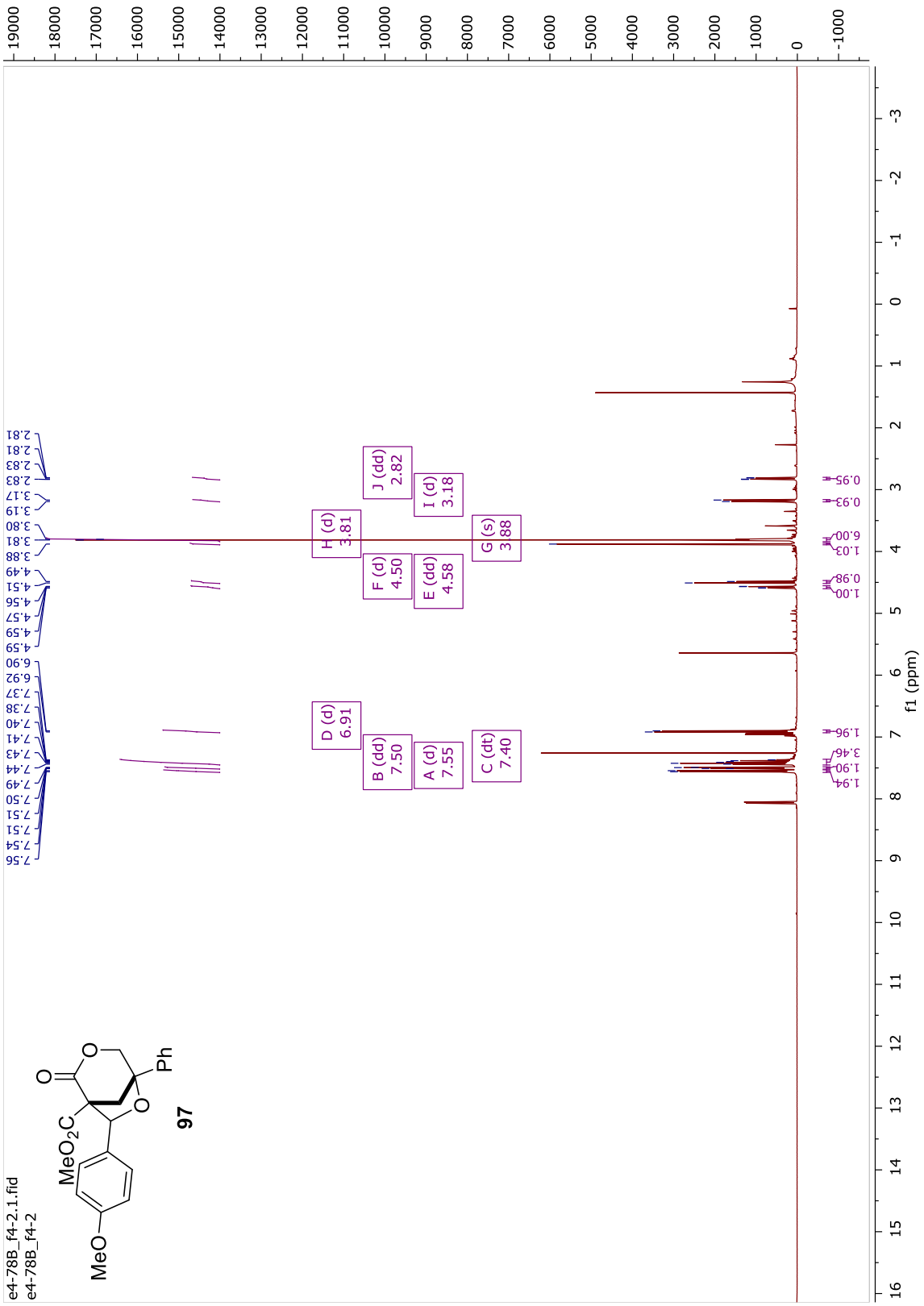
e4-78B_f4-2.1.fid
e4-78B_f4-2
MeO
MeO2C
O
O
O
Ph
97
A (d) 7.55
B (dd) 7.50
C (dt) 7.40
D (d) 6.91
E (dd) 4.58
F (d) 4.50
G (s) 3.88
H (d) 3.81
I (d) 3.18
J (dd) 2.82
f1 (ppm)

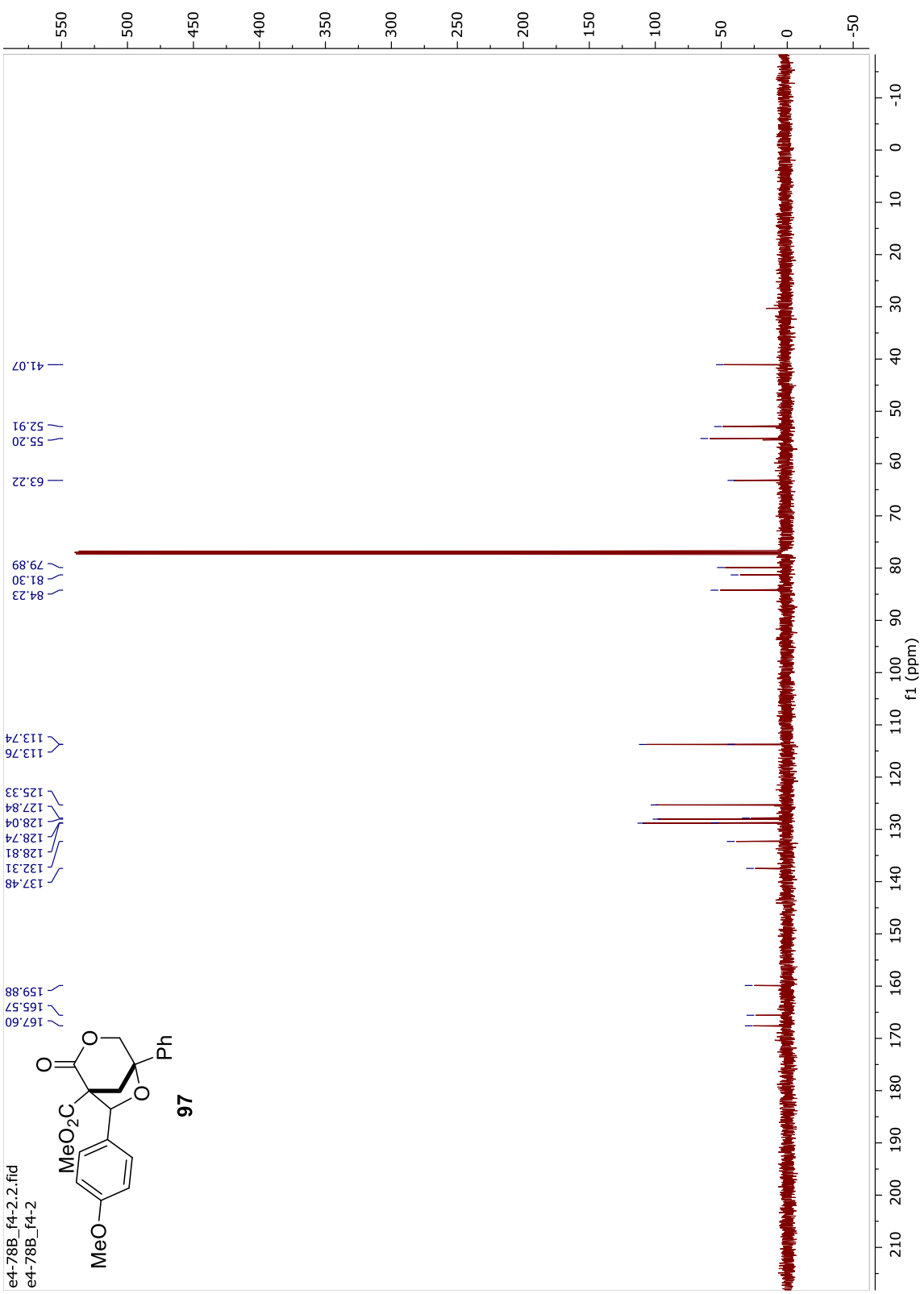
e4-78B_f4-2.2.fid
e4-78B_f4-2
MeO
MeO2C
O
O
O
Ph
97
167.60
165.57
159.88
137.48
132.31
128.81
128.74
128.04
127.84
125.33
113.76
113.74
84.23
81.30
79.89
63.22
55.20
52.91
41.07
f1 (ppm)

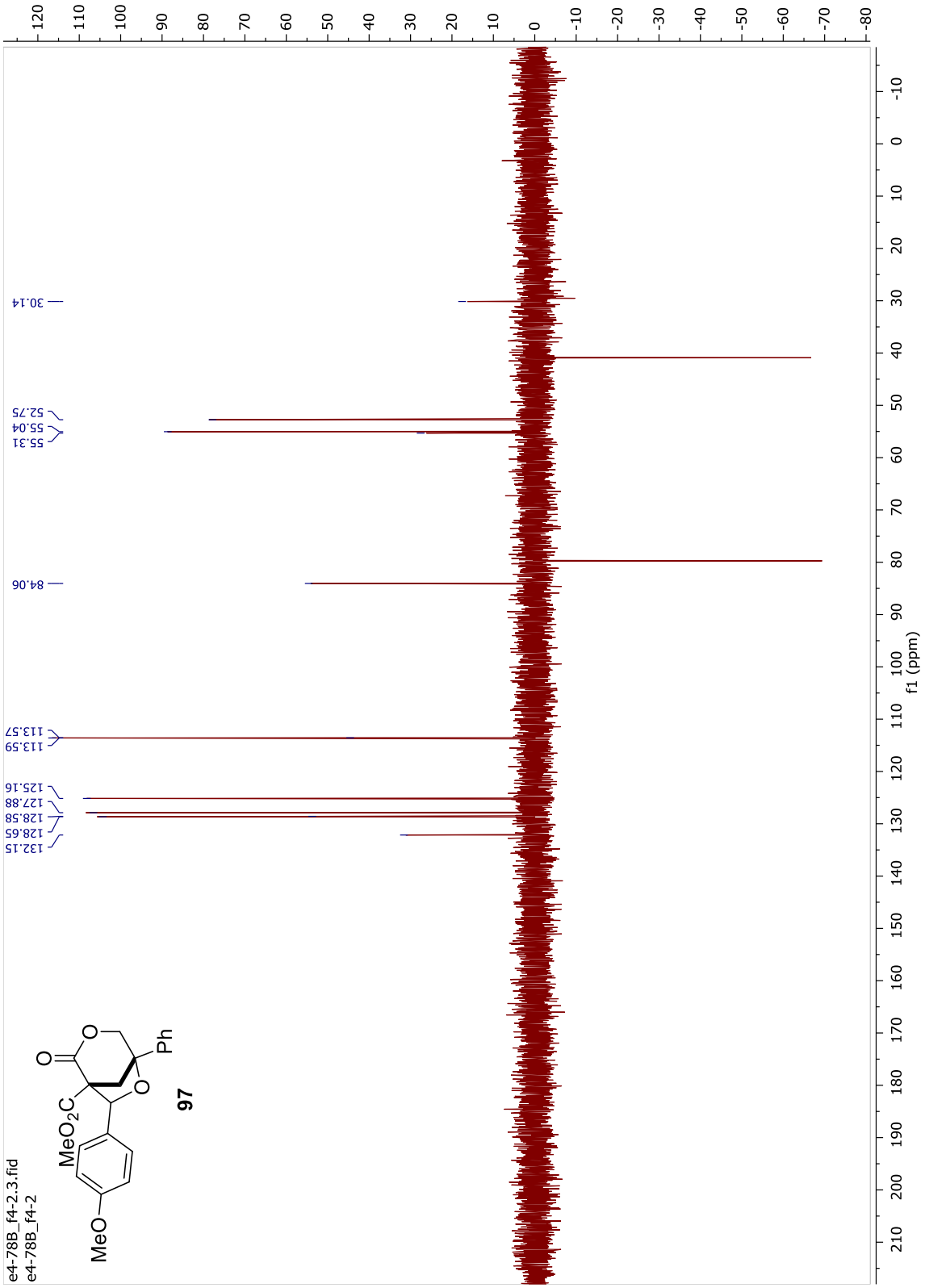
e4-78B_f4-2.3.fid
e4-78B_f4-2
MeO
MeO2C
O
O
O
Ph
97
132.15
128.65
128.58
127.88
125.16
113.59
113.57
84.06
55.31
55.04
52.75
30.14
f1 (ppm)

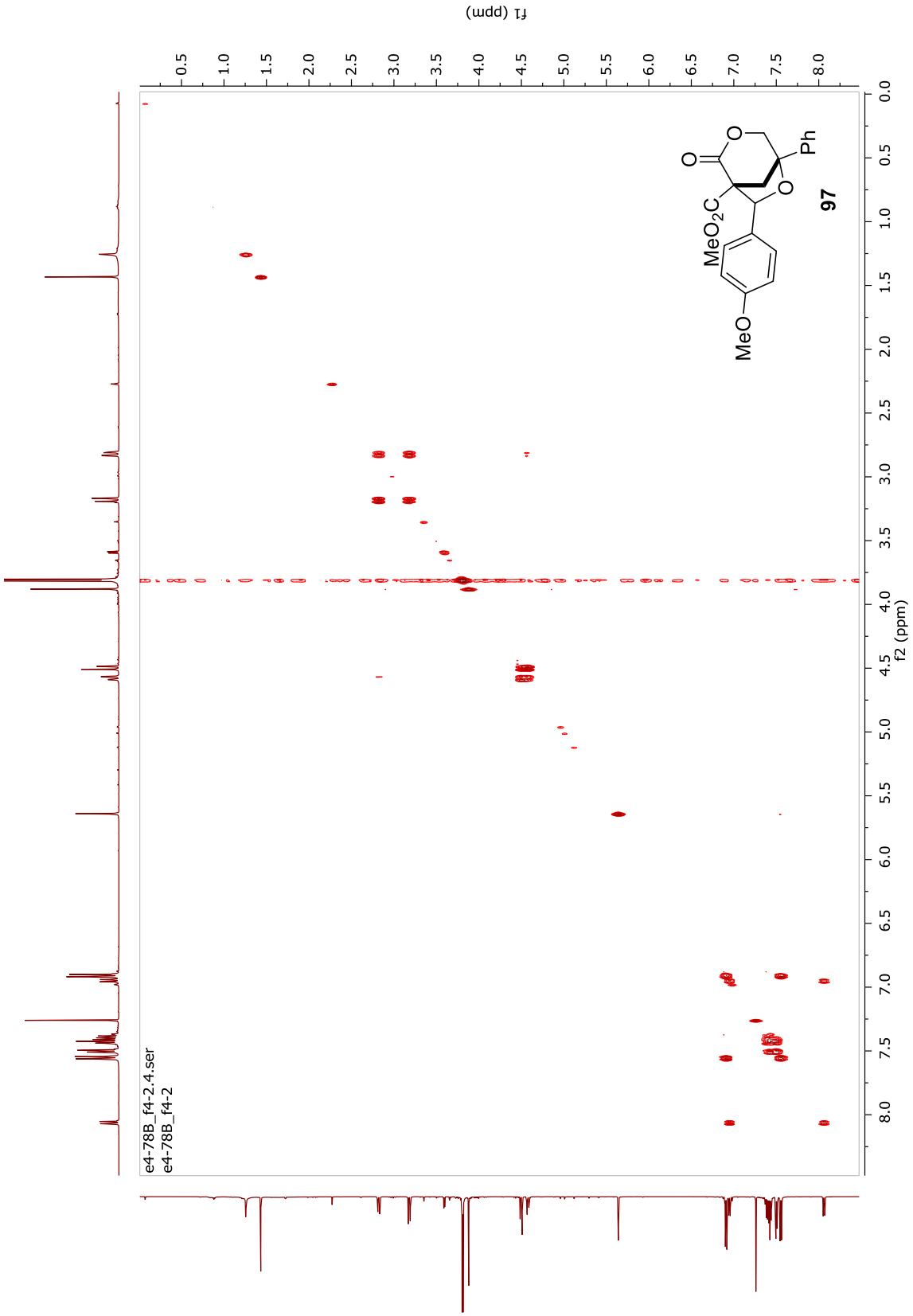
f1 (ppm)
f2 (ppm)
e4-78B_f4-2.4.ser
e4-78B_f4-2
MeO
MeO2C
O
O
O
Ph
97

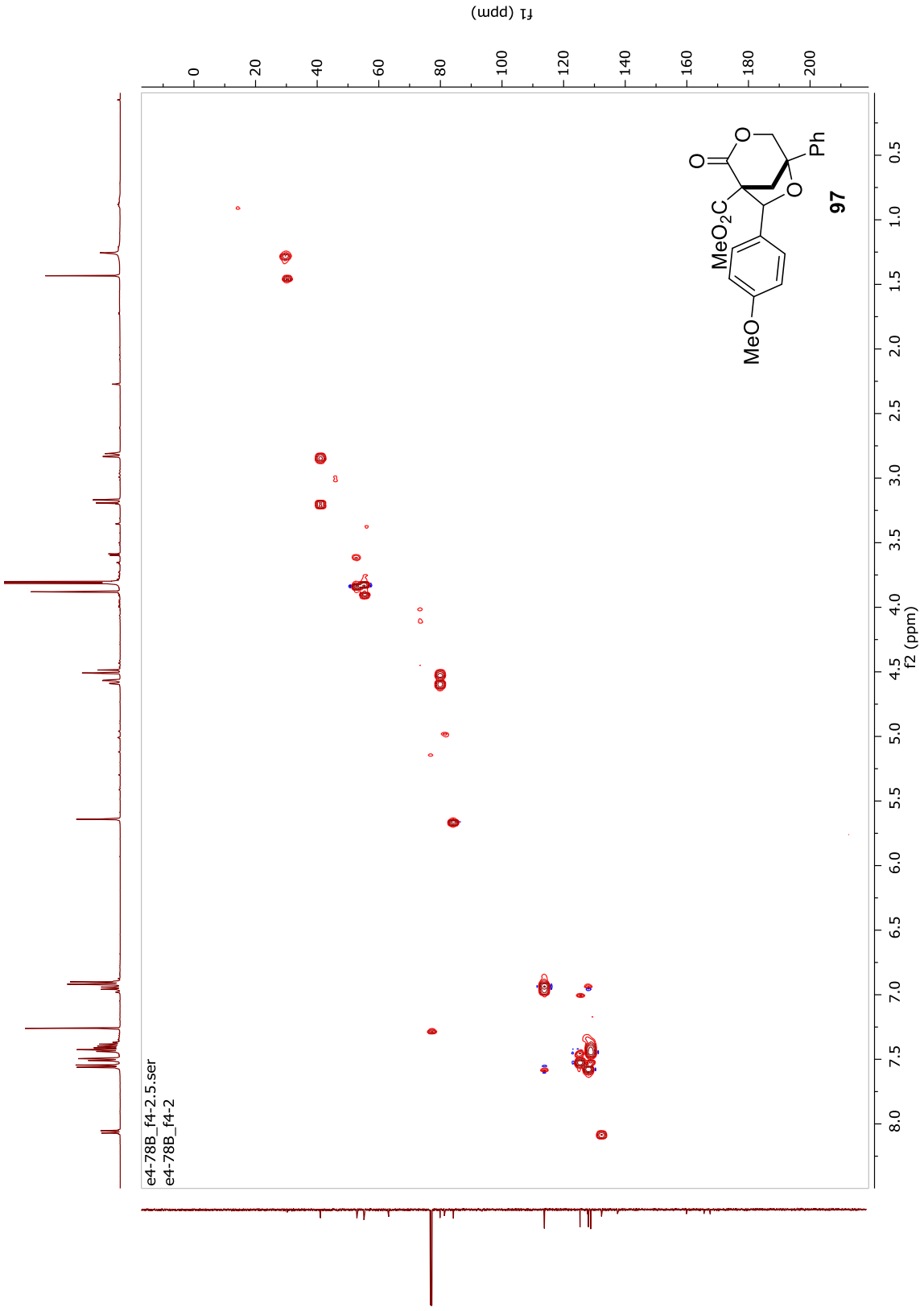
f1 (ppm)
0
20
40
60
80
100
120
140
160
180
200
f2 (ppm)
0.5
1.0
1.5
2.0
2.5
3.0
3.5
4.0
4.5
5.0
5.5
6.0
6.5
7.0
7.5
8.0
e4-78B_f4-2.5.ser
e4-78B_f4-2
MeO
MeO2C
O
O
O
Ph
97

4.9 References

(1) (a) Cavitt, M.A.; Phun, L.H.; France, S.A. Intramolecular donor–acceptor cyclopropane ring-opening cyclizations. *Chem. Soc. Rev.* **2014**, *43*, 804. (b) Schneidere, T.F.; Kaschel, J.; Werv, D.B. A New Golden Age for Donor–Acceptor Cyclopropanes. *Angew. Chem. Int. Ed.* **2014**, *53*, 5504-5523.

(2) (a) Stork, G.; Marx, M. Six-membered rings via olefin participation in the opening of acylcyclopropanes. *J. Am. Chem. Soc.* **1969**, *91*, 2371-2373. (b) Stork, G.; Gregson, M. Aryl participation in concerted cyclization of cyclopropyl ketones. *J. Am. Chem. Soc.* **1969**, *91*, 2373-2374. (c) Stork, G.; Grieco, P.A. Olefin participation in the acid-catalyzed opening of acylcyclopropanes. III. Formation of the bicyclo[2.2.1]heptane system. *J. Am. Chem. Soc.* **1969**, *91*, 2407-2408. (d) Stork, G.; Grieco, P.A. Olefin participation in the acid-catalyzed opening of acylcyclopropanes. IV. Cyclization of 5-methyl-6-endo-(trans-3-pentenyl)bicyclo(3.1.0)hexan-2-one. *Tetrahedron Lett.* **1971**, *12*, 1807-1810. (e) Grieco, P.A.; Finkelhor, R.S. Studies on the acid-catalyzed opening of non-rigid acylcyclopropanes: a dramatic solvent effect. A route to the bicyclo[2.2.1]heptane ring system. *Tetrahedron Lett.* **1974**, *15*, 527-530.

(3) Jiang, X.; Lim, Z.; Yeung, Y.-Y. Studies on the ring-opening of bicyclic cyclopropanes activated by a carbonyl group. *Tetrahedron Lett.* **2013**, *54*, 1798-1801.

(4) Wiseman, J.R.; Chang, H.-F.; Ahola, C.J. Bredt's Rule. II. Synthesis of Bicyclo[4.2.1]non-1(2)-ene and Bicyclo[4.2.1]non-1(8)-ene. *J. Am. Chem. Soc.* **1969**, *91*, 2812-2813.

(5) Trost, B.M.; Fullerton, T.J. New synthetic reactions. Allylic alkylation. *J. Am. Chem. Soc.* **1973**, *95*, 292-294.

(6) Huckin, S.N.; Weiler, L. Alkylaton of Dianions of β-Keto Esters. *J. Am. Chem. Soc.* **1974**, *96*, 1082-1087.

(7) Novosjolova, I. The Mukaiyama Reagent: An Efficient Condensation Agent. *Synlett* **2013,** *24*, 135-136.

(8) Wuts, P.G.M.; Greene, T.W. "Protection for the Hydroxyl Group, Including 1,2- and 1,3-Diols." *Greene's Protective Groups in Organic Synthesis*. John Wiley & Sons, Inc.: Hoboken, NJ. 2007. 4th Ed., pp. 165-221.

(9) Duan, Z.-C.; Hu, X.-P.; Zhang, C. Wang, D.-Y.; Yu, S.-B.; Zheng, Z. Highly Enantioselective Rh-Catalyzed Hydrogenation of β,γ-Unsaturated Phosphonates with Chiral Ferrocene-Based Monophosphoramidite Ligands. *J. Org. Chem*. **2009**, *74*, 9191–9194.

(10) Taber, D.F.; Gleave, D.B.; Herr, R.J.; Moody, K.; Hennessy, M.J. A New Method for the Construction of α-Diazo Ketones. *J. Org. Chem.* **1995**, *60*, 2283-2285.

(11) Baum, J.S.; Shook, D.A.; Davies, H.M.L.; Smith, H.D. Diazotransfer Reactions with *p*-Acetamidobenzenesulfonyl Azide. *Synth. Comm*. **1987**, *17*.

(12) Yu, W.-Y.; Tsoi, Y.-T.; Zhou, Z.; Chan, A.S.C. Palladium-Catalyzed Cross Coupling Reaction of Benzyl Bromides with Diazoesters for Stereoselective Synthesis of (*E*)-α,β-Diarylacrylates. *Org. Lett*. **2009**, *11*, 469 – 472.

(13) Dumas, A.M.; Fillion, E. Meldrum's Acids and 5-Alkylidene Meldrum's Acids in Catalytic Carbon-Carbon Bond-Forming Processes. *Acc. Chem. Res.* **2010**, *43*, 440-454.

(14) Sapeta, K.; Kerr, M.A. Synthesis of Cyclohexanes via [3 + 3] Hexannulation of Cyclopropanes and 2-Chloromethyl Allylsilanes. *Org. Lett*. **2009**, *11*, 2081-2084.

(15) (a) Reißig, H.-U. Lewis-acid-promoted additions of carbonyl compounds to donor-acceptor substituted cyclopropanes: a new synthesis of 2,3-dihydrofurane derivatives. *Tetrahedron Lett.* **1981**, *22*, 2981-2984. (b) Brueckner, C.; Reißig, H.-U. Efficient and flexible syntheses of paraconic esters and other highly substituted furanone derivatives from methyl 2-siloxycyclopropanecarboxylates. *J. Org. Chem.* **1988**, *53*, 2440-2450. (c) Reißig, H.-U.; Holzinger, H.; Glomsda, G. A titanoxycyclopropane as intermediate in a highly stereoselective homoaldol type addition syntheses of cis-substituted tetrahydrofuran derivatives. *Tetrahedron* **1989**, *45*, 3139-3150.

(16) (a) Pohlhaus, P.D.; Sanders, S.D.; Parsons, A.T.; Li, W.; Johnson, J.S. Scope and Mechanism for Lewis Acid-Catalyzed Cycloadditions of Aldehydes and Donor-Acceptor Cyclopropanes: Evidence for a Stereospecific Intimate Ion Pair Pathway. *J. Am. Chem. Soc.* **2008**, *130*, 8642–8650. (b) Smith, A.G.; Slade, M.C.; Johnson, J.S. Cyclopropane−Aldehyde Annulations at Quaternary Donor Sites: Stereoselective Access to Highly Substituted Tetrahydrofurans. *Org. Lett.* **2011**, *13*, 1996-1999. (c) Pohlhaus, P.D.; Johnson, J.S. Highly diastereoselective synthesis of tetrahydrofurans via Lewis acid-catalyzed cyclopropane/aldehyde cycloadditions. *J. Org. Chem.* **2005**, *70*, 1057–1059. (d) Pohlhaus, P.D.; Johnson, J.S. Enantiospecific Sn (II)-and Sn (IV)-Catalyzed Cycloadditions of Aldehydes and Donor−Acceptor Cyclopropanes. *J. Am. Chem. Soc.* **2005**, *127*, 16014–16015. (e) Campbell, M.J.; Johnson, J.S. Asymmetric synthesis of (+)-polyanthellin A. *J. Am. Chem. Soc.* **2009**, *131*, 10370–10371. (f) Sanders, S.D.; Ruiz-Olalla, A.; Johnson, J.S. Total synthesis of (+)-virgatusin via $AlCl_3$ catalyzed [3+2] cycloaddition. *Chem. Commun.* **2009**, 8642–8650.

(17) (a) Novikov, R.A.; Balakirev, D.; Timofeev, V.P.; Tomilov, Y.V. Complexes of Donor–Acceptor Cyclopropanes with Tin, Titanium, and Gallium Chlorides — Mechanism Studies. *Organometallics* **2012**, *31*, 8627-8638. (b) Novikov, R.A.; Tarasova, A.V.; Korolev, V.A.; Timofeev, V.P.; Tomilov, Y.V. A New Type of Donor–Acceptor Cyclopropane Reactivity: The Generation of Formal 1,2- and 1,4-Dipoles. *Angew. Chem. Int. Ed.* **2014**, *126*, 3251-3255. (c) Novikov, R.A.; Tarasova, A.V.; Tomilov, Y.V. Synthesis of substituted naphthalenes by $GaCl_3$-mediated cross-dimerization—fragmentation of 2-arylcyclopropane-1,1-dicarboxylates. *Russ. Chem. Bull*. **2014**, *63*, 2737-2740. (d) Novikov, R.A.; Tarasova, A.V.; Korolev, V.A.; Shulishov, E.V.; Timofeev, V.P.; Tomilov, Y.V. Donor-Acceptor Cyclopropanes as 1,2-Dipoles in $GaCl_3$-Mediated [4+2]-Annulation with Alkenes: Easy Access to the Tetralin Skeleton. *J. Org. Chem*. **2015**, *80*, 8225-8235.

(18) (a) Karadeolian, A.; Kerr, M.A. Total synthesis of (+)-isatisine A. *J. Org. Chem.* **2010**, *75*, 6830–6841. (b) Wang, Z. *Angew. Chem*. **2011**, *123*, 12813–12817. (c) Benfatti, F.; de Nanteuil, F.; Waser, J. Iron-catalyzed [3+2] annulation of aminocyclopropanes with aldehydes: stereoselective synthesis of aminotetrahydrofurans. *Org. Lett.* **2012**, *14*, 386–389.

(19) (a) Yang, G.; Sun, Y.; Shen, Y.; Chai, Z.; Zhou, S.; Chu, J.; Chai, J. *cis*-2,3-Disubstituted Cyclopropane 1,1-Diesters in [3 + 2] Annulations with Aldehydes: Highly Diastereoselective Construction of Densely Substituted Tetrahydrofurans. *J. Org. Chem.* **2013**, *78*, 5393−5400. (b) Yang, G.; Wang, T.; Chai, J.; Chai, Z. $AlCl_3$-Catalyzed [3+2] Annulations of *cis*-2,3-Disubstituted Cyclopropane 1,1-Diesters with Cyclic Ketones: Diastereoselective Construction of Spirotetrahydrofurans. *Eur. J. Org.*

Chem. **2015**, 1040–1046. (c) Feng, M.; Yang, P.; Yang, G.; Chen, W.; Chai, Z. $FeCl_3$-Promoted [3+2] Annulations of γ-Butyrolactone Fused Cyclopropanes with Heterocumulenes. *J. Org. Chem.* **2018**, *83*, 174-184.

(20) Begouin, J.-M.; Niggemann, M. Calcium-Based Lewis Acid Catalysts. *Chem. Eur. J.* **2013**, *19*, 8030-8041.

(21) Russo, F.; Wangsell, F.; Saevmarker, J.; Jacobsson, M; Larhed, M. Synthesis and evaluation of a new class of tertiary alcohol based BACE-1 inhibitors. *Tetrahedron* **2009**, *65*, 10047-10059.

(22) Wada, H.; Williams, H.E.L.; Moody, C.J. Total Synthesis of the Posttranslationally Modified Polyazole Peptide Antibiotic Plantazolicin A. *Angew. Chem. Int. Ed*. **2015**, *54*, 15147–15151.

(23) Bowie, A.L.; Hughes, C.C.; Trauner, D. Concise Synthesis of (±)-Rhazinilam through Direct Coupling. *Org. Lett.* **2005**, *7*, 5207-5209.

(24) Bering, L.; Jeyakumar, K.; Antonchick, A.P. Metal-Free C–O Bond Functionalization: Catalytic Intramolecular and Intermolecular Benzylation of Arenes. *Org. Lett.* **2018**, *20*, 3911 – 3914.

(25) Kelly, P. M.; Parker, D.; Gole, K.; Stephan, H. Selective cation binding with *cis,cis*-1,3,5-trioxycyclohexyl based ligands: application to ion transport and electrochemical detection and assessment of complexation by electrospray mass spectrometry. *J. Chem. Soc., Perkin Trans. 2* **1997**, 59-69.

(26) Tseng, P.-W.; Yeh, S.-W.; Chou, C.-H. Syntheses and Pyrolyses of Benzofuran Analogues of α-Oxo-*o*-quinodimethane. A Study on Vinylcarbene−Cyclopropene Rearrangement. *J. Org. Chem*. **2008**, *73*, 3481–3485.

(27) Martin-Matute, B.; Nevado, C.; Cárdenas, D.J.; Echavarren, A.M. Intramolecular Reactions of Alkynes with Furans and Electron Rich Arenes Catalyzed by $PtCl_2$: The Role of Platinum Carbenes as Intermediates. *J. Am. Chem. Soc*. **2003**, *125*, 5757.

CHAPTER 5. STEREOCHEMICAL IMPLICATIONS OF THE INTRAMOLECULAR FRIEDEL-CRAFTS-TYPE RING-OPENING CYCLIZATION OF DONOR-ACCEPTOR C6-SUBSTITUTED BICYCLO[3.1.0]HEXANES

5.1 Recent Advances in C6-Substituted D-A Bicyclo[3.1.0]hexane Ring-opening Reactions

Of the two classes of D-A bicyclo[3.1.0]hexanes described in Chapter 4, C6-substituted bicyclo[3.1.0]hexanes are more prevalent in the synthetic methodology literature.[1] Primary applications of this template and analogous scaffolds have been formal [3+2] cycloadditions with dipolarophiles (especially aldehydes), intramolecular ring expansions, and intermolecular ring-opening reactions to γ-butyrolactones.

5.1.1 Formal [3+2] Cycloadditions

Johnson presented one of the earliest examples of a formal [3+2] cycloaddition in this class, employing an analogous D-A bicyclo[4.1.0]heptanone and isobutyraldeyde as the dipolarophile (Scheme 5-1a).[2] This study was shortly followed by the total synthesis of (+)-polyanthellin A, featuring this cycloaddition as the first key step (Scheme 5-1b).[3]

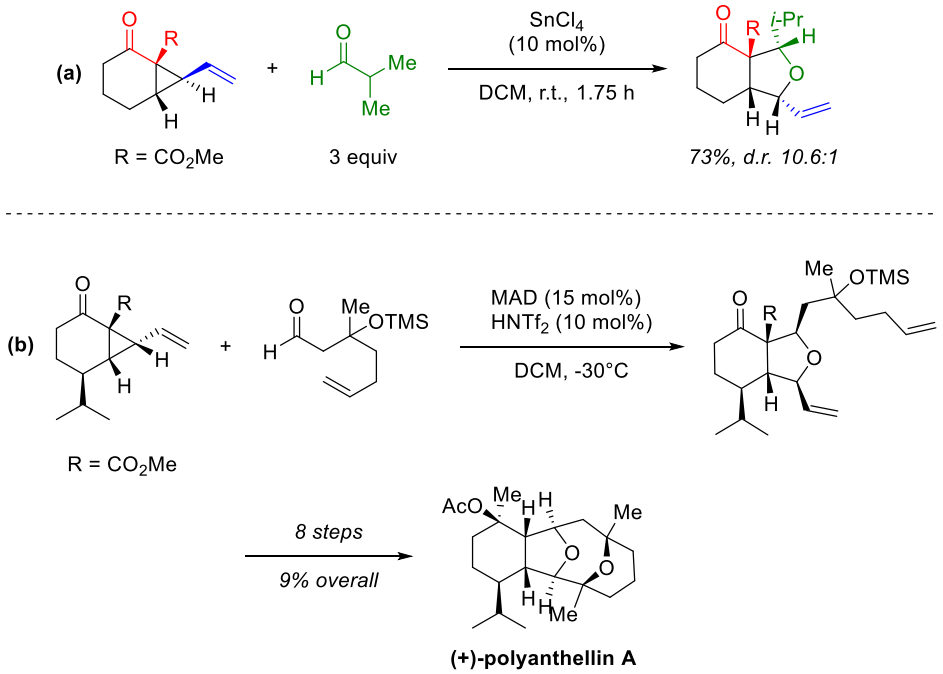

Scheme 5-1: (a) Johnson's formal [3+2] cycladdition of a C6-substituted D-A bicyclo[4.1.0]heptanone. (b) Application in the total synthesis of (+)-polyanthellin A.

In 2011, Johnson further showcased three examples of a D-A bicyclo[3.1.0]hexane formal [3+2] cycloaddition in the presence of catalytic $Sn(OTf)_2$ (5 mol%) or $SnCl_4$ (10 mol%) (Scheme 5-2a).[1a] In the same year, Zhang published one example of this transformation with a C6-phenyl-substituted template, with high stereoselectivity (Scheme 5-2b).[1b] Much more recently, in 2018, Yang reported a formal [3+2] cycloaddition of D-A bicyclo[3.1.0]hexanes with isothiocyanates and carbodiimides, which represent the first examples of employing coupling partners other than aldehydes in (Scheme 5-2c).[1f] This seminal work also represents one of the most efficient methods to date for this type of transformation, as they achieved 53 examples (92-99% yield) with inexpensive $FeCl_3$ (2 equiv) in room-temperature 1,2-DCE.

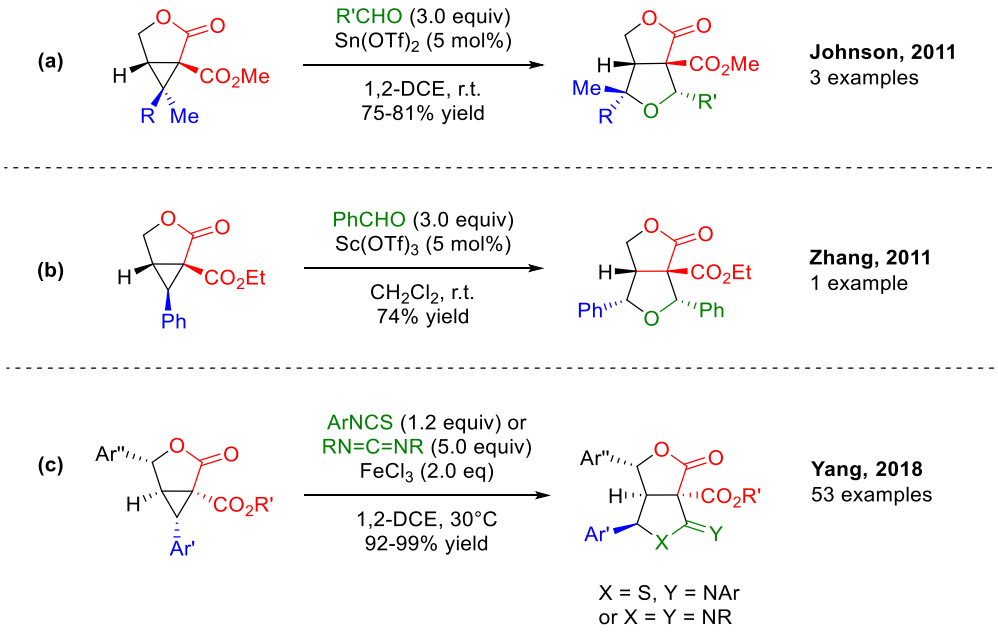

Scheme 5-2: (a) Johnson's formal [3+2] between C6-sub. D-A oxabicyclo[3.1.0]hexanes and aldehydes. (b) Zhang's formal [3+2] between a C6-sub. D-A oxabicyclo[3.1.0]hexane and benzaldehyde. (c) Yang's formal [3+2] between D-A C6-sub. oxabicyclo[3.1.0]hexanes and isothiocyantes or carbodiimides.

It should be noted that Zhang and Yang both observed an inversion of stereochemistry at the donor site with the formal cycloaddition. This result supports a polar mechanism, which is consistent with Johnson's earlier mechanistic findings.[1a]

5.1.2 Intramolecular Ring-Expansions

In 2013, Corey performed a narrow but in-depth study of DACPs contained within highly condensed, polycyclic frameworks and their corresponding intramolecular ring expansions in the presence of TMSOTf and H_2O.[4] Of the small scope, two substrates explicitly examined the influence of a C6-donor on the ring expansions of (oxa)bicyclo[3.1.0]hexanes (Scheme 5-3). Significantly, the second example represents the only literature precedent for a bicyclo[3.1.0]hexane ring-opening reaction in which X = CH_2.

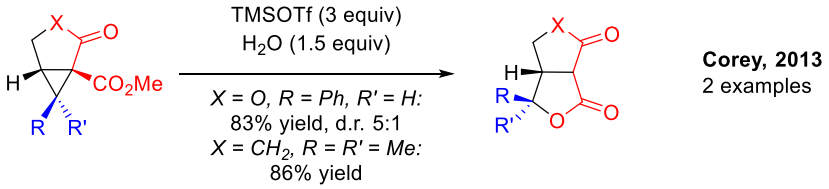

Scheme 5-3: Corey's TMSOTf-promoted ring-expansion of C6-sub. D-A (oxa)bicyclo[3.1.0]hexanes.

5.1.3 Nishii's Manipulations of the D-A Bicyclo[3.1.0]hexane Scaffold

By 2016, studies toward the behavior of this DACP scaffold were beginning to take off, with Nishii leading the charge. Nishii first examined the Lewis acid-mediated oxy-*homo*-Michael addition of alkyl and aryl alcohols onto enantioenriched D-A bicyclo[3.1.0]hexane templates to form γ-butyrolactones (Scheme 5-4a).[5a] Across 14 examples, he observed exclusive preference for inversion of stereochemistry at the site of addition and a *trans* orientation of the α and β hydrogens on the resulting γ-butyrolactone, as well as excellent retention of enantiopurity. This work was quickly followed by the application of this nucleophilic addition to the total synthesis of tupichilignan A[5b] (effecting the key step in 83% yield with 95% *ee*), as well as the syntheses of several 7-benzyloxy dibenzyl lignans lactones.[5c] Next, Nishii expanded the scope by testing Grignard additions onto this scaffold (Scheme 5-4b); across 10 examples (up to 94% yield), the same stereochemical outcomes were favored.[5d] Finally, he explored the effect of hydrogenolysis (Scheme 5-4c); across 7 examples (up to 97% yield), he again observed a *trans*-α,β orientation of the γ-butyrolactone.[5e]

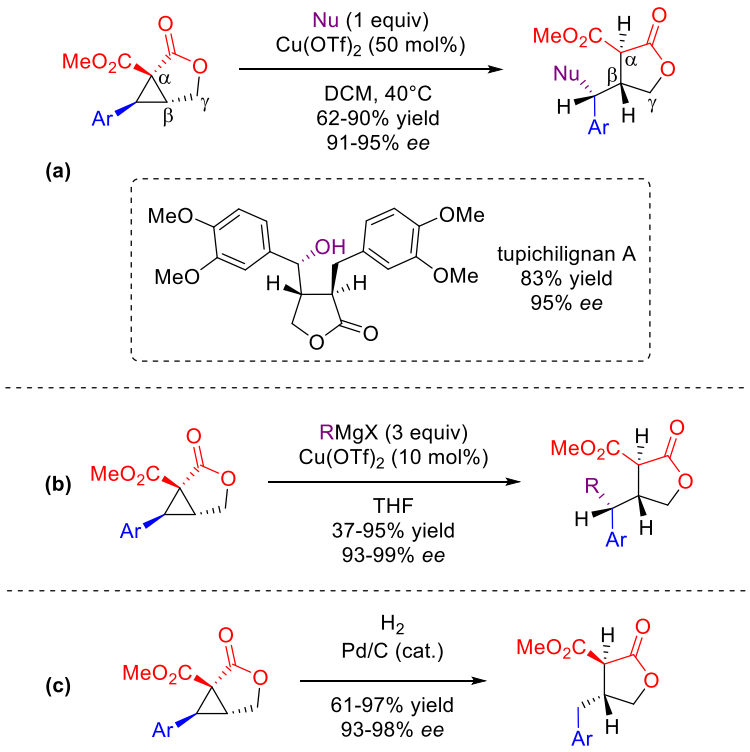

Scheme 5-4: Nishii's synthetic studies toward C6-sub. oxabicyclo[3.1.0]hexane ring-opening reactions. (a) Nucleophilic addition by alcohols. (b) Grignard addition. (c) Hydrogenolysis.

5.2 Opportunity for an Intramolecular Friedel-Crafts-type Ring-opening Cyclization of C6-Substituted D-A Bicyclo[3.1.0]hexanes

Despite recent advances in ring-opening chemistries for this scaffold, intramolecular transformations, such Friedel-Crafts-type ring-opening cyclizations, have not been demonstrated from these synthetic precursors (for the proposed pathway, see Chapter 4). Unlike their C5-substituted analogues, C6-substituted D-A bicyclo[3.1.0]hexanes may be reasonably expected to undergo much more expedient intramolecular ring-opening cyclizations due to more sterically accessible secondary carbocation intermediates and increased flexibility in the resulting fused bicyclic scaffolds.

In 2016, Shenje and France envisioned a synthetic strategy for the total synthesis of propolisbenzofuran B that employed benzofuran-tethered, C6-substituted D-A

oxabicyclo[3.1.0]hexane **98** (Scheme 5-5).[6] As shown from the abbreviated retrosynthetic analysis of truncated model **99**, this DACP would enable a ring-opening cyclization to install the desired tetracycle **100** with *trans* diastereoselectivity, and subsequent functionalizations would open the lactone and afford the final target.

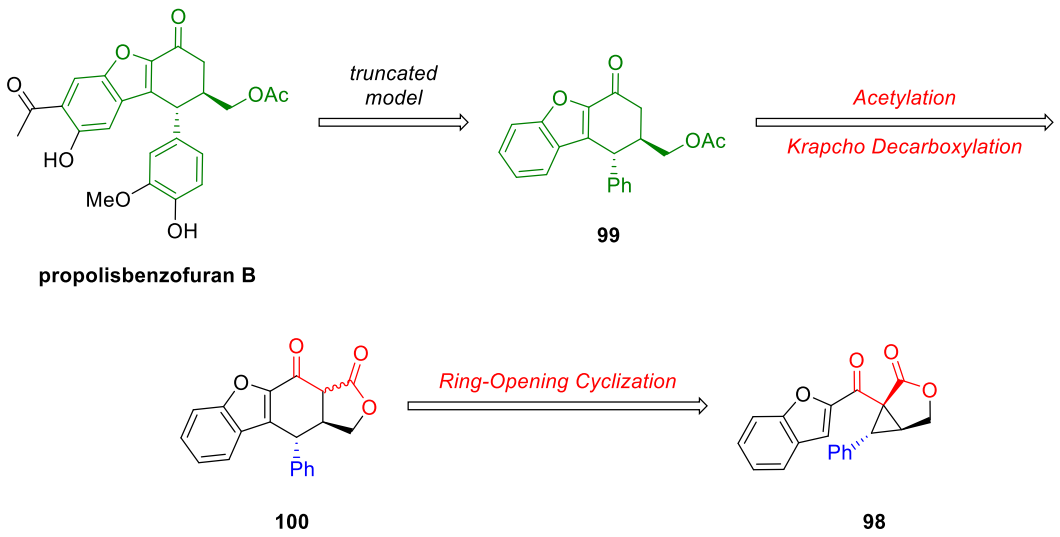

Scheme 5-5: Abbreviated retrosynthetic analysis to truncated model of propolisbenzofuran B.

5.2.1 Previous Literature Regarding Diastereoselectivity

Although this ring-opening cyclization chemistry has not been previously studied, literature for traditional (i.e. non-tethered) DACPs strongly suggests that the intramolecular ring-opening cyclization adduct of a 1,2-disubstituted DACP will possess a *trans* configuration. Waser's seminal report on the catalytic *homo*-Nazarov cyclization of cyclopropyl vinyl ketones supported a polar, stepwise mechanism in which the rate-limiting step was the ring-opening of the cyclopropane, generating a carbocation that could subsequently be trapped.[7] (This is in harmony with Johnson's mechanistic studies for intermolecular formal [3+2] cycloadditions of DACPs, which reached the same conclusion.) The implications of this mechanism are significant, as any stereochemical

information built into the template would be lost with the formation of the carbocation, and the thermodynamic product, most likely *trans*, would be favored. A pericyclic mechanism, in contrast, would be expected to retain stereochemistry.

To date, the only two literature examples of an intramolecular ring-opening cyclization resulting in a *cis*-substituted adduct are from the France group. First, in 2011, thiophene-tethered DACP **101** containing a 1,2-indanyl donor group successfully underwent a Friedel-Crafts-type ring-opening cyclization to afford the 1,2-*cis* adduct **102** as a single diastereomer in 87% yield (Scheme 5-6a).[8] Then, in 2016, cyclopropyl carbinol **103** (also containing a 1,2-indanyl donor) was evaluated, to also afford the 1,2-*cis* adduct **104** (Scheme 5-6b).[9] The stereochemical outcome is not at odds with Waser's findings: although carbocation formation scrambles previous stereoinduction, in this case, the *trans* isomer would cause unwanted strain on the system, therefore the *cis* isomer is preferred.

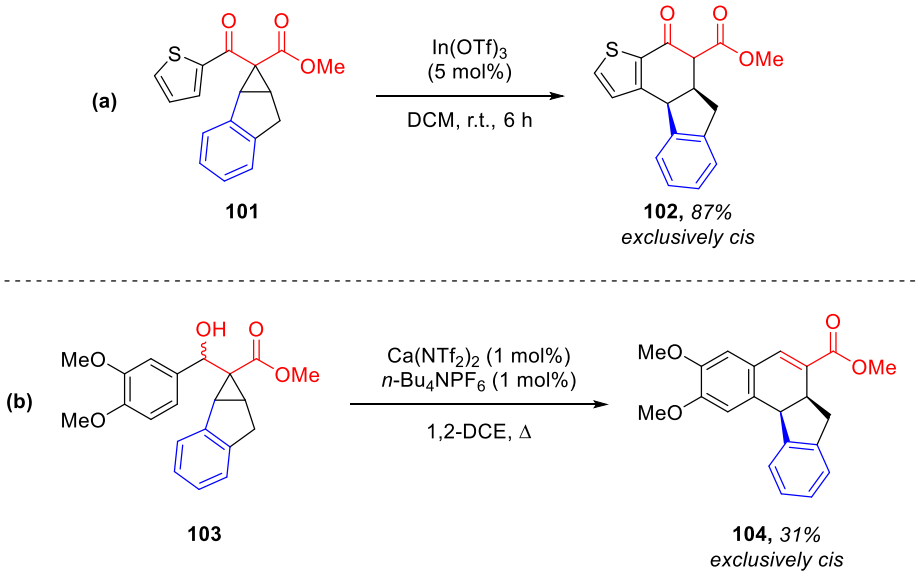

Scheme 5-6: Literature precedent for *cis* diastereoselectivity. (a) France's 1,2-indanyl DACP intramolecular ring-opening cylization. (b) France's 1,2-indanyl cyclopropyl carbinol intramolecular ring-opening cyclization.

Since Shenje's original hypothesis, further studies by Nishii have supported the formation of a *trans*-1,2-disubstituted ring-opening cyclization adduct regardless of the stereochemistry of the DACP precursor. In his 2017 article,[10] Nishii synthesized a variety of enantioenriched and racemic 1,2-*cis*- and -*trans*-disubstituted DACPs, then observed the stereochemical outcomes of the corresponding intramolecular ring-opening cyclizations (Scheme 5-7). (A parallel study was conducted on analogous cyclopropyl carbinols.)[5c] In every case, the *trans* adduct formed preferentially relative to the stereochemistry of the 2-subsituent, which is unaffected by the adjacent carbocation formation. These results led Nishii to conclude that the polar, stepwise, Friedel-Crafts-type mechanism was in fact the mode of action for this transformation.

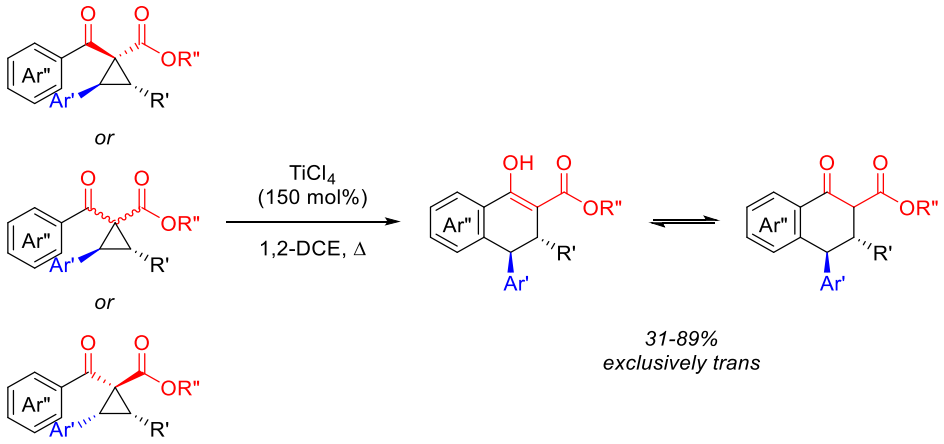

Scheme 5-7: Nishii's ring-opening cyclization of enantioenriched and racemic DACPs to *trans* adducts.

5.2.2 Shenje's Observed Stereochemical Outcome

Surprisingly, and contrary to the proposed retrosynthetic analysis, preliminary results exhibited formation of a single diastereomer in a *cis* configuration at the point of ring fusion (**epi-100**, Scheme 5-8).[6] Though this outcome would render the synthesis of propolisbenzofuran B inviable by this route, this stereochemistry has not been observed in

previous DACP ring-opening cyclizations and would thus serve as a complementary methodology. Additionally, it could open the door to mechanistic studies to better understand and predict the stereochemical outcome of intramolecular ring-opening cyclizations outside the influence of chiral Lewis acid catalysts.

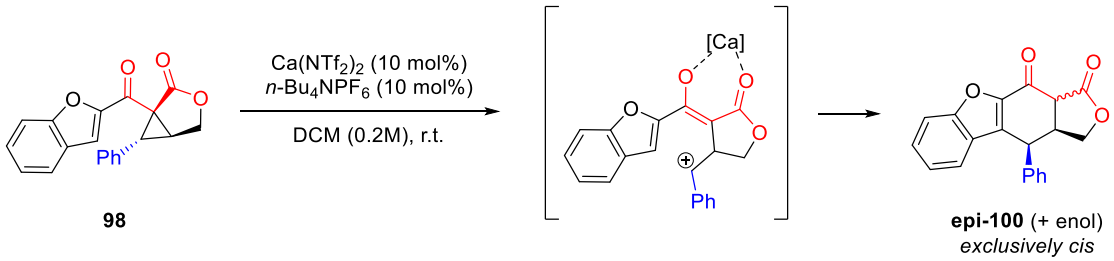

Scheme 5-8: Observed stereochemical outcome of model ring-opening cyclization.

5.3 Further Examination of the *cis*-Exclusive Model Adduct

5.3.1 Optimization of the Ring-opening Cyclization

Desirous to probe this unique transformation further, my first objective was to prepare the model **98** and expand the Lewis acid screen (Table 5-1). Shenje surveyed several catalysts commonly employed for ring-opening cyclizations of DACPs (entries 1-8) and found that 10 mol% $Ca(NTf_2)_2$/*n*-Bu_4NPF_6[11] gave the best yield at 63%. A short but thorough solvent and concentration screen confirmed that his initial conditions of anhydrous DCM at 0.2 M concentration were optimal. Under these parameters, I set about surveying additional catalysts (entries 9-13). Surprisingly, three of the five Lewis acids added to this screen outperformed the $Ca(NTf_2)_2$ catalyst system, including $Sn(OTf)_2$ (Johnson's preferred catalyst,[2] entry 10) and $In(OTf)_3$ (entry 13), which had previously been less successful. It is possible, based on the rapid reaction time for this transformation, that prolonged exposure to $In(OTf)_3$ (i.e. longer than 2-3 hours) led to degradation of the

ring-opening cyclization adduct after it formed (entry 2). Regardless, $Ga(OTf)_3$ was the best-performing catalyst based on this screen (entry 9, 83% yield).

Table 5-1: Lewis acid screen for ring-opening cyclization of 98.

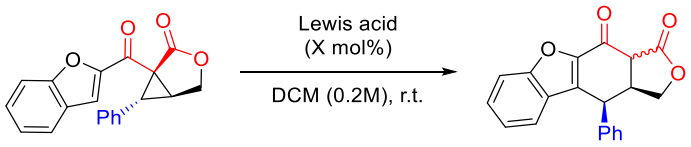

98 **epi-100** (+ enol)

Entry	Lewis acid	X (mol%)	Time (h)	Yield (%)
1[a]	$In(OTf)_3$	5	3	49
2[a]	$In(OTf)_3$	10	4	No desired product
3[a]	$Sc(OTf)_3$	10	4	49
4[a]	$Al(OTf)_3$	10	24	No desired product
5[a]	$Hf(OTf)_4$	10	3	No desired product
6[a]	$Ca(NTf_2)_2$/*n*-Bu_4NPF_6	10	3	63
7[a]	$Ca(NTf_2)_2$/*n*-Bu_4NPF_6	5	13	No desired product
8[a]	$Cu(OTf)_2$	10	24	No desired product
9[b]	$Ga(OTf)_3$	10	2	83
10[b]	$Sn(OTf)_2$	10	18	72
11[b]	$SnCl_4$	10	21	No desired product
12[b]	$Yb(OTf)_3$	10	21	No desired product
13[b]	$In(OTf)_3$	10	2	70

[a] Reactions performed by Shenje. [b] Reactions performed by myself.

5.3.2 Derivatization of the Model Adduct for Further Characterization

Next, inspired by Nishii's recent work, model adduct **epi-100** was capped as *enol* triflate **105** to simplify characterization, since the model ring-opening cyclization adduct exists as a *keto-enol* mixture and may epimerize at the α carbon to yield multiple

diastereomers. After a short conditions screen (Table 5-2), trifluoromethanesulfonic (triflic) anhydride (Tf_2O) was deemed the optimal reagent for this transformation (entries 3 & 4), despite literature precedent for softer triflating agents such as *N*-phenyl-bis(triflimide) (entry 1) and Comins's reagent [*N*-(5-Chloro-2-pyridyl)bis(triflimide)] (entry 2).[12]

Table 5-2: Optimization of enol triflate formation.

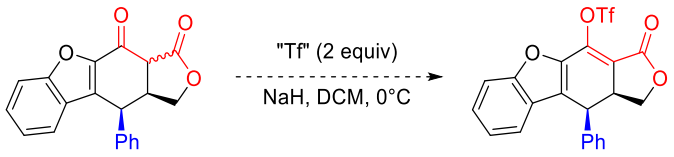

epi-100 **105**

Entry	"Tf"	Result
1	$PhNTf_2$	No desired product
2	Comins's	No desired product
3	Tf_2O	20% desired product + 64% SM[a]
4	Tf_2O	40% desired product + 39% SM

[a] Used crude starting material.

Then, **105** was subjected to rigorous NMR studies. Gratifyingly, this capped adduct was pristine by ^1H NMR (Figure 5-1), and the coupling constants were readily deducible in the aliphatic region (4.5-4.0 ppm). Proton A (9 Hz, 1H) is a triplet that overlaps just slightly with the doublet representing proton B (18 Hz, 1H). Proton C (9 Hz, 1H) is also a triplet, and proton D (18 Hz, 9 Hz, 1H) is a doublet of triplets. COSY analysis shows a proton B correlating only to proton D, whereas protons A, C, and D all correlate with each other. Finally, HSQC confirms that protons A and C are situated on the same carbon. These results support the assignments shown below, and the *J*-values strongly suggest *cis*

orientation among protons B and D, but an X-ray structure would unequivocally confirm this stereochemistry.

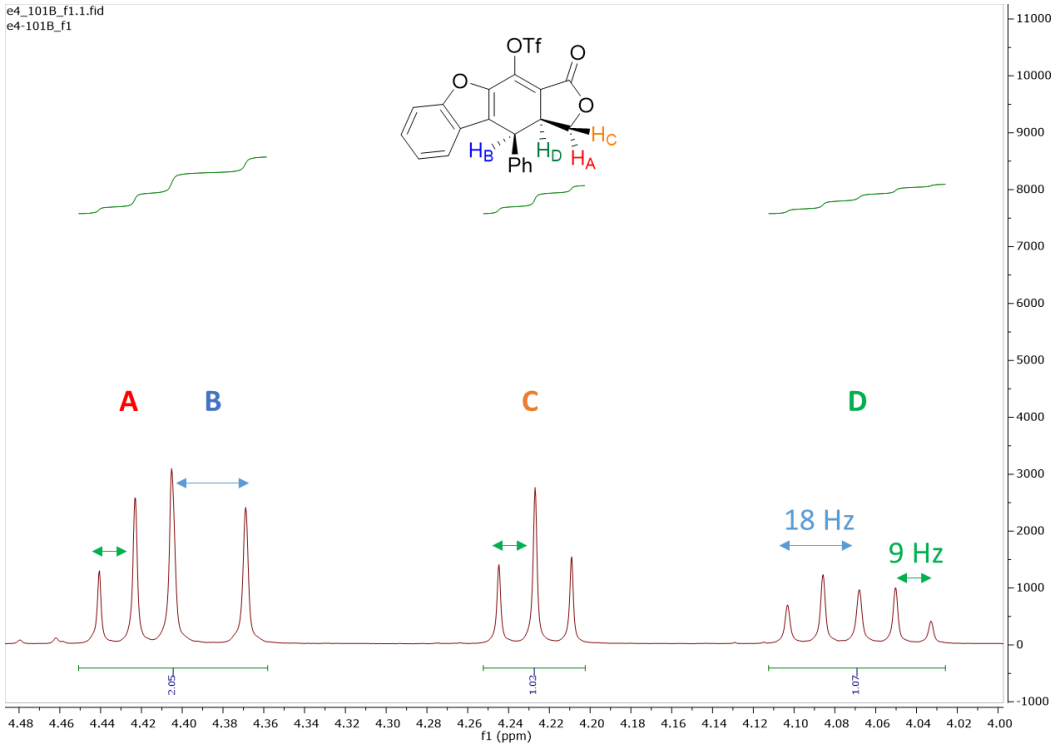

Figure 5-1: ^{1}H NMR results for model *enol* triflate 105.

5.4 Novel Methodology Substrate Scope

5.4.1 Identifying the Desired Targets

As with any synthetic methodology development, several substrates were proposed to test the robustness of the Friedel-Crafts-type ring-opening cyclization (Figure 5-2). Keeping in mind privileged scaffolds of medicinal compounds, various tethered aryl and heteroaryl nucleophiles, including indole, furan, and thiophene were targeted; as the effects of substituent electronics on aryl rings are well-established for Friedel-Crafts substitutions, substrates were intentionally limited to more electron-donating arenes. Then, cyclopropane

donor groups were selected, including diversely substituted arenes, heteroarenes, and β-silylalkanes. Finally, we envisioned three representative substrates to probe the effects of different acceptor groups and ring sizes incorporated into the bicyclo[3.1.0]hexane precursor.

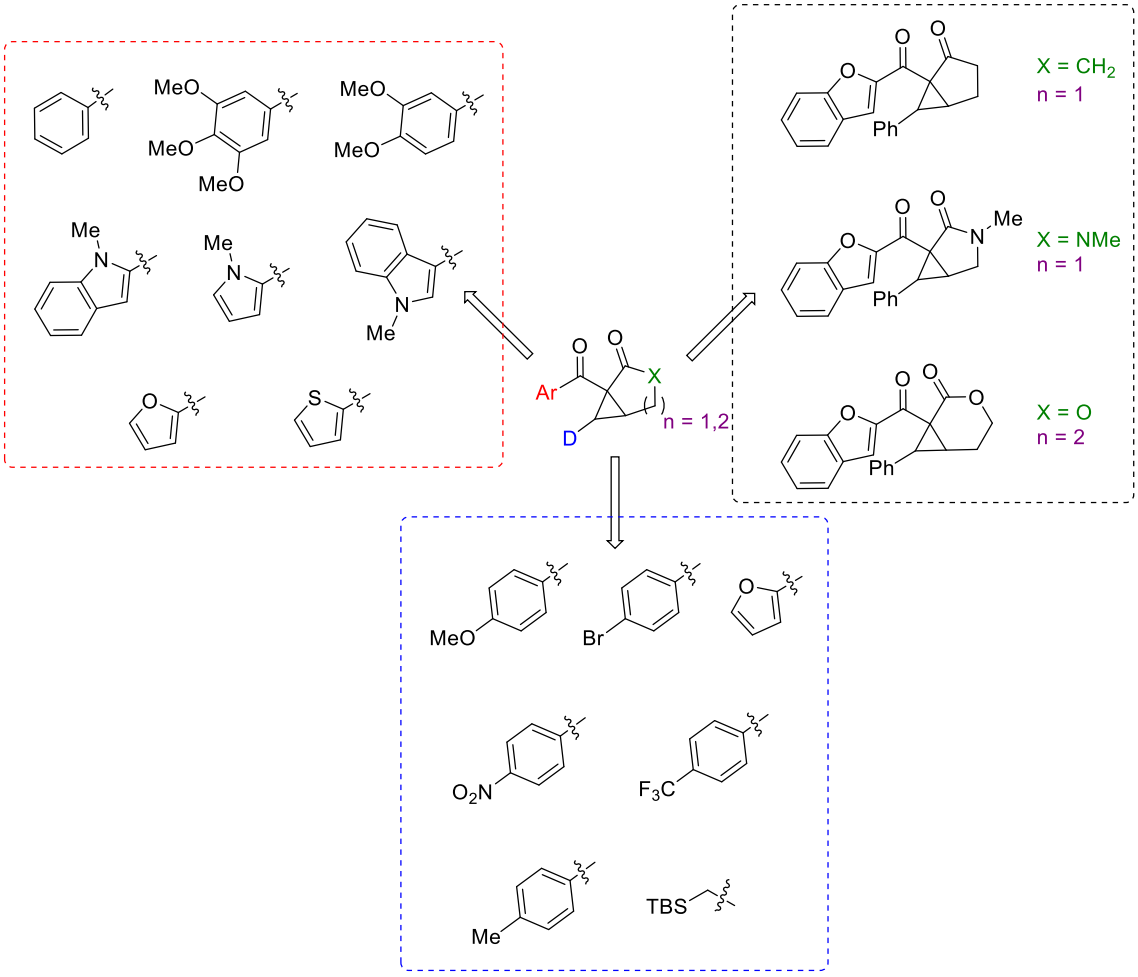

Figure 5-2: Proposed substrate scope.

5.4.2 Progress Toward the Synthesis of the Substrate Scope

To prepare the model adduct, synthesis began with acetylation of cinnamyl alcohol (**106**), which proceeded quantitatively (Scheme 5-9a). Then, the acid chloride of benzofuran-2-carboxylic acid (**71**) was achieved under typical Swern conditions, followed

by α-substitution of cinnamyl acetate (**107**) *via* LHMDS deprotonation to afford the desired β-ketoester **108** in 60% yield (Scheme 5-9b). For the diazo transfer, Shenje applied tosyl azide (TsN_3), as it is readily and inexpensively synthesized on large scale. However, recent literature has highlighted *p*-acetamidobenzenesulfonyl azide (*p*-ABSA)[13] as an exceptionally useful diazo transfer agent due to the facile separation of product from both excess *p*-ABSA and sulfonamide by-product, which is more challenging with TsN_3. Therefore, I attempted this transformation with *p*-ABSA and achieved the β-keto-α-diazoester **109** in 90% yield, an improvement over 80% yield with TsN_3. Subsequent intramolecular cyclopropanation by catalytic $Rh_2(esp)_2$ was effected to afford **98** in 88% yield.

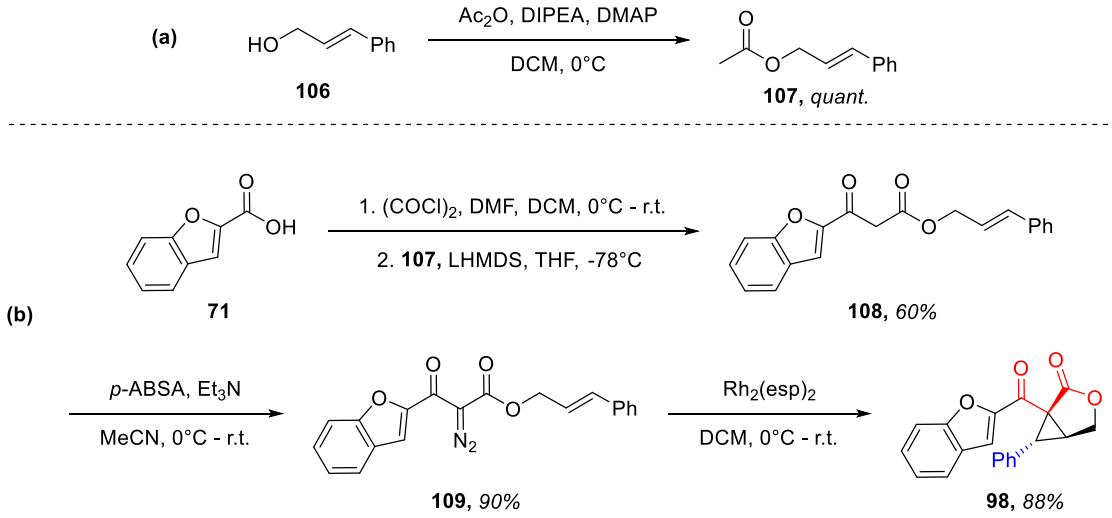

Scheme 5-9: (a) Preparation of cinnamyl acetate. (b) Synthesis of propolisbenzofuran B oxabicyclo[3.1.0]hexane model precursor.

Next, I began synthesizing precursors that varied the tethered arene, as these targets were readily achievable from the route above (Scheme 5-10). Two of the proposed substrates have been prepared through the diazo transfer, while a third (**113b**) has been carried forward to the cyclopropanation, diazo precursor **112b** having been prepared

previously by Sandridge.[14] For **111a**, the LHMDS-mediated addition was effected from commercially available benzoyl chloride.

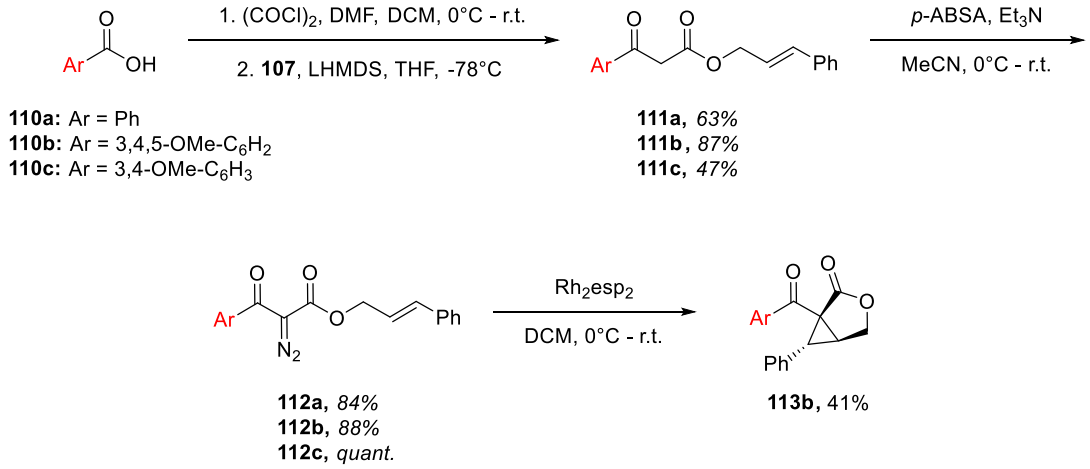

Scheme 5-10: Progress toward synthesis of various aryl-tethered bicyclo[3.1.0]hexanes.

Once the heteroarene precursor syntheses were well underway, synthesis of the precursors with variable donor groups was pursued. As these allyl acetates are not commercially available, a scheme was developed from the corresponding aldehydes (Scheme 5-11). First, a Horner-Wadsworth-Emmons (HWE) reaction was conducted with an α-ester phosphonate, followed by global reduction by diisobutylaluminum hydride (DIBAL-H) and finally acetylation by the conditions previously described. This synthetic route was both high-yielding and practically efficient, as every product (except for **116d**) was pure after work-up.

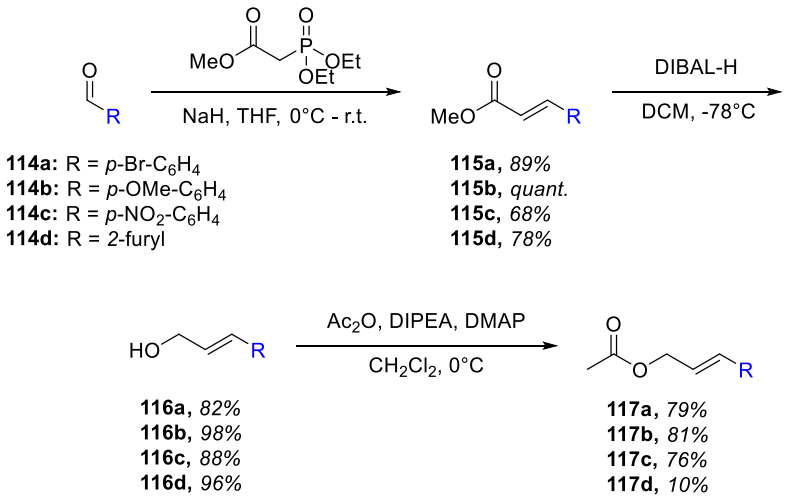

Scheme 5-11: Synthesis of various acetate precursors.

Then, acetates **117a-c** were subjected to LHMDS-mediated addition with benzofuran-2-carboxylic acid chloride (Scheme 5-12). Unfortunately, the *p*-nitrophenyl precursor **118c** did not tolerate the LHMDS conditions, as only degradation products were observed by NMR. Remaining steps include diazo transfer to **119** and cyclopropanation to **120**.

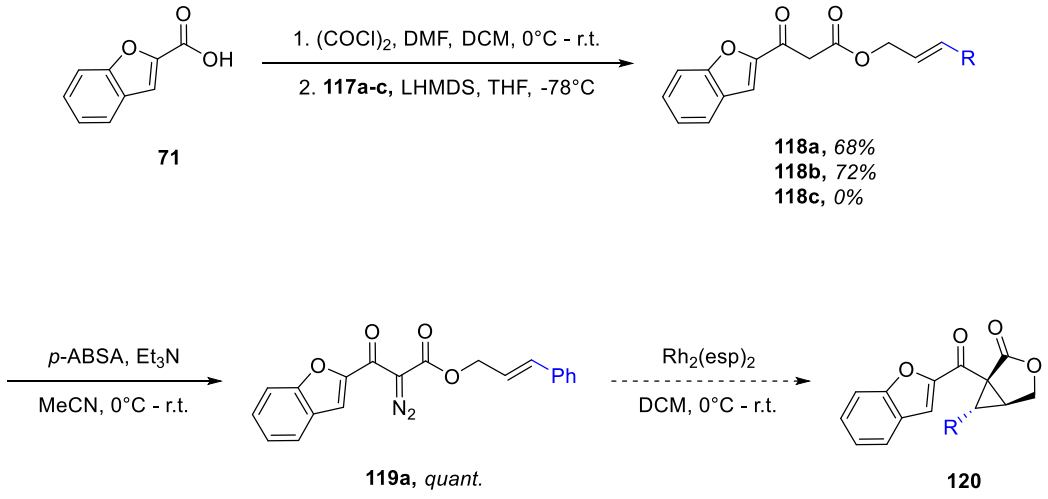

Scheme 5-12: Progress toward synthesis of benzofuran-tethered bicyclo[3.1.0]hexanes with varying donor groups.

5.5 Summary

In summary, an intramolecular Friedel-Crafts-type ring-opening cyclization of a C6-substituted oxabicyclo[3.1.0]hexane was pursued as the key step in a new total synthesis of propolisbenzofuran B. Preliminary results pointed to an unexpected stereochemical outcome, an exclusively *cis* diastereomer when the *trans* isomer was anticipated. Further studies validated the stereochemistry of this ring-opening cyclization adduct. Synthesis of an expanded substrate scope is underway to probe the selectivity of this novel outcome.

5.6 Experimental Details

5.6.1 General Information

Chromatographic purification was performed via flash chromatography with Silicycle SiliaFlash P60 silica gel (40-63 μm) or preparative thin-layer chromatography (prep-TLC) with Analtech silica gel F254 (1000 μm) plates and solvents indicated as eluent with 0.1-0.5 bar pressure. For quantitative flash chromatography, technical grades solvents were utilized. Analytical thin-layer chromatography (TLC) was also used to separate and purify reaction products using Silicycle SiliaPlate TLC silica gel F254 (250 μm) TLC glass plates. Products on the TLC plates were visualized under UV light (254 nm).

Proton, and carbon nuclear magnetic resonance spectra (^{1}H NMR and ^{13}C NMR, respectively) were recorded on a Bruker 500 MHz spectrometer. The solvent resonances were used the internal standards (^{1}H NMR: $CDCl_3$ at 7.26 ppm, DMSO-d_6 at 3.50 ppm; ^{13}C NMR: $CDCl_3$ at 77.0 ppm, DMSO-d_6 at 39.5 ppm; ^{19}F NMR: locked to $CDCl_3$ or DMSO-d_6). MestReNova (v. 11.0) was used to analyze NMR spectra. ^{1}H NMR data are reported as follows: chemical shift (ppm), multiplicity (s = singlet, d = doublet, dd =

doublet of doublets, dt = doublet of triplets, ddd = doublet of doublet of doublets, t = triplet, m = multiplet, br = broad), coupling constants (Hz), and integration. High-resolution accurate mass-mass spectrometry (HRAM-MS) was performed using a MicroMass Autospec M, run in EI mode at a mass resolution of 10,000 using perfluorokerosene (PFK) as an internal calibrant.

5.6.2 General Procedures

General Horner-Wadsworth-Emmons Procedure: In a flame-dried flask under N_2, NaH (1.2 equiv, 60% dispersion in mineral oil) was suspended in anhydrous THF (0.2 M/NaH), then the suspension was cooled to 0°C. Methyl 2-(diethoxyphosphoryl)acetate (1.1 equiv) was added and the solution stirred for 15 minutes, during which time the solution turned clear. Next, the aryl aldehyde (1 equiv) was added in anhydrous THF (3.5 M), and the reaction mixture stirred overnight, warming gradually to room temperature. The reaction mixture was quenched with saturated aqueous NH_4Cl, the aqueous layer was extracted with EtOAc, and the combined organic extracts were washed with brine, dried over anhydrous Na_2SO_4, filtered through celite under reduced pressure, and concentrated by rotary evaporation.

General DIBAL-H Reduction Procedure:[14] In a flame-dried flask under N_2, the methyl acrylate (1 equiv) was dissolved in anhydrous DCM (0.4 M). The solution was cooled to -78°C, then DIBAL-H (3 equiv, 1 M/DCM) was added dropwise. After stirring for 1 hour, the reaction mixture was quenched with saturated aqueous Na_2SO_4, the aqueous layer was extracted with DCM, and the combined organic extracts were washed with saturated aqueous NH_4Cl, dried over anhydrous Na_2SO_4, filtered through celite under reduced pressure, and concentrated by rotary evaporation.

General Acetylation Procedure: In a flame-dried flask under N_2, the alcohol (1 equiv) was dissolved in anhydrous DCM (0.5 M). The solution was cooled to 0°C, then DIPEA (1.2 equiv), DMAP (0.1 equiv), and Ac_2O (1.2 equiv) were added in sequence. After stirring for 30 minutes, the reaction mixture was quenched with 1% HCl, the aqueous layers were extracted with DCM, and the combined organic extracts were washed with brine, dried over anhydrous Na_2SO_4, filtered through celite under reduced pressure, and concentrated by rotary evaporation. The product was afforded without further purification.

General Acid Chloride Procedure: In a flame-dried flask under N_2, the carboxylic acid (1 equiv) was dissolved in anhydrous DCM (0.5 M), then the solution was cooled to 0°C. Anhydrous DMF (cat.) was added, then the flask was equipped with an empty N_2-flushed balloon to vent any HCl vapors. $(COCl)_2$ (1.05 equiv) was added slowly. After 15 minutes, the reaction mixture was allowed to warm to room temperature and stirred for 3 hours. The resulting clear solution was then concentrated by rotary evaporation.

General LHMDS-mediated Addition Procedure: In a flame-dried flask under N_2, the allyl acetate (1.05 equiv) was dissolved in half the requisite volume of anhydrous THF (1 M). The solution was cooled to -78°C, then LHMDS (2.1 equiv, 1M/THF) was added dropwise and the solution stirred for 45 minutes. The acid chloride (1 equiv) was dissolved in the remaining anhydrous THF and added *via* syringe to the acetate solution, which was stirred for an additional 30 minutes. The reaction mixture was quenched with saturated aqueous NH_4Cl, the aqueous layers extracted with EtOAc, and the combined organic extracts dried over anhydrous Na_2SO_4, filtered through celite under reduced pressure, and concentrated by rotary evaporation.

General p-ABSA Diazo Transfer Procedure: In a flame-dried flask under N_2, the β-ketoester (1 equiv) was dissolved in anhydrous MeCN (0.5 M), then Et_3N (1.1 equiv) was added. After cooling the solution to 0°C, *p*-ABSA (1.05 equiv) was added. The reaction mixture was allowed to warm to room temperature and stirred overnight. Then, the reaction mixture was filtered through celite under reduced pressure and concentrated by rotary evaporation directly onto silica.

General Intramolecular Cyclopropanation Procedure for the Synthesis of C6-Substituted Bicyclo[3.1.0]hexanes: $Rh_2(esp)_2$ (0.5 mol%) was charged to a flame-dried flask under N_2, suspended in half the requisite volume of anhydrous DCM (0.02 M), then the suspension was cooled to 0°C. In a separate flame-dried flask under N_2, the α-diazo-β-ketoester (1 equiv) was dissolved in the remaining anhydrous DCM and transferred to the Rh flask *via* syringe in one shot with stirring. After 10 minutes, the solution was allowed to warm to room temperature. After 30 minutes, the reaction was quenched with saturated aqueous thiourea and stirred for an additional 30 minutes. Then, the aqueous layer was extracted with DCM and the combined organic layers were washed with brine, dried over anhydrous Na_2SO_4, filtered through celite under reduced pressure, and concentrated by rotary evaporation. Purification was achieved by silica flash chromatography.

General Intramolecular Ring-opening Cyclization Procedure: The Lewis acid (10 mol%) was charged to a flame-dried flask under N_2, then the oxabicyclo[3.1.0]hexane (1 equiv) was added as a solution in anhydrous DCM (0.2 M). After stirring for 3 hours, the reaction mixture was quenched with H_2O, the aqueous layer was extracted with DCM, and the combined organic layers were washed with brine, dried over anhydrous $MgSO_4$, filtered

through celite under reduced pressure, and concentrated. Purification was achieved by silica flash chromatography.

General Enol Triflation Procedure:[9] In a flame-dried flask under N_2, NaH (2 equiv, 60% dispersion in mineral oil) was suspended in anhydrous DCM (0.1 M/NaH) and the suspension cooled to 0°C. The β-ketoester (1 equiv) was added as a solution in anhydrous DCM (0.1 M/β-ketoester), then the reaction mixture was stirred for 1 hour. Tf_2O (2 equiv) was added, then the reaction was stirred for an additional 30 minutes. The reaction mixture was quenched with saturated aqueous $NaHCO_3$, the aqueous layers extracted with EtOAc, and the combined organic extracts washed with brine, dried over anhydrous Na_2SO_4, filtered through celite under reduced pressure, and concentrated by rotary evaporation. Purification was achieved by silica flash chromatography.

5.6.3 Experimental Procedures

*Cinnamyl Acetate (**107**).* The general acetylation procedure was following using cinnamyl alcohol (2 g, 14.9 mmol), DIPEA (3.1 mL, 17.9 mmol), DMAP (182.2 mg, 1.49 mmol), and Ac_2O (1.7 mL, 17.9 mmol) in 30 mL of anhydrous DCM. Compound **107** was afforded without further purification (25% EtOAc/hexanes, $R_f = 0.6$) as a yellow oil (2.593 g, 99% yield). NMR data were consistent with previously reported results.[16]

*Cinnamyl 3-(Benzofuran-2-yl)-3-oxopropanoate (**108**).* The general acid chloride and LHMDS-mediated addition procedures were followed using benzofuran-2-carboxylic acid (500 mg, 3.08 mmol), DMF (4 drops), and $(COCl)_2$ (0.31 mL, 3.70 mmol) in 6.2 mL of anhydrous DCM, then **107** (570.6 mg, 3.24 mmol) and LHMDS (6.5 mL, 6.48 mmol, 1M/THF) in 3.2 mL of anhydrous THF. After purification by silica flash chromatography (25% EtOAc/hexanes, $R_f = 0.81$), compound **108** was afforded in a 3.3:1 *keto-enol* mixture

(599.9 mg, 61% yield). ^{1}H NMR (500 MHz, $CDCl_3$) δ 7.71 (d, *J* = 7.9 Hz, 1H), 7.61 (s, 1H), 7.56 (d, *J* = 8.4 Hz, 1H), 7.52 – 7.46 (m, 2H), 7.42 (d, *J* = 7.4 Hz, 1H), 7.35 – 7.29 (m, 5H), 6.63 (d, *J* = 15.9 Hz, 1H), 6.25 (dt, *J* = 15.9, 6.4 Hz, 1H), 4.89 (dd, *J* = 6.3, 1.2 Hz, 1H), 4.83 (dd, *J* = 6.4, 1.1 Hz, 2H), 4.03 (s, 2H). ^{13}C NMR (126 MHz, $CDCl_3$) δ 182.85, 166.61, 155.80, 151.69, 135.98, 134.72, 134.36, 128.73, 128.61, 128.56, 128.13, 126.95, 126.64, 126.62, 126.59, 124.13, 123.52, 123.51, 122.85, 122.35, 122.22, 114.11, 112.53, 111.62, 108.86, 88.42, 66.09, 65.03, 45.83.

*Cinnamyl 3-(Benzofuran-2-yl)-2-diazo-3-oxopropanoate (**109**).* The general *p*-ABSA diazo transfer procedure was followed using **108** (200 mg, 0.624 mmol), Et_3N (0.10 mL, 0.686 mmol), and *p*-ABSA (157.4 mg, 0.655 mmol) in 1.2 mL of anhydrous MeCN. After purification by silica flash chromatography (25% EtOAc/hexanes, R_f = 0.43), compound **109** was afforded as an off-white, chalky solid (193.2 mg, 89% yield). ^{1}H NMR (500 MHz, $CDCl_3$) δ 7.85 (d, *J* = 0.8 Hz, 1H), 7.72 (d, *J* = 7.9 Hz, 1H), 7.58 – 7.54 (m, 1H), 7.47 (ddd, *J* = 8.4, 7.2, 1.2 Hz, 1H), 7.42 – 7.38 (m, 2H), 7.37 – 7.27 (m, 4H), 6.72 (d, *J* = 15.9 Hz, 1H), 6.33 (dt, *J* = 15.9, 6.6 Hz, 1H), 4.96 (dd, *J* = 6.6, 1.2 Hz, 2H). ^{13}C NMR (126 MHz, $CDCl_3$) δ 172.30, 160.81, 155.11, 150.61, 135.86, 135.41, 128.65, 128.35, 128.29, 126.92, 126.72, 123.99, 123.41, 122.16, 115.13, 112.29, 66.33.

*1-(Benzofuran-2-carbonyl)-6-phenyl-3-oxabicyclo[3.1.0]hexan-2-one (**98**).* The general intramolecular cyclopropanation procedure was followed using **109** (857 mg, 2.47 mmol) and $Rh_2(esp)_2$ (9.4 mg, 0.0124 mmol) in 120 mL of anhydrous DCM. After purification by silica flash chromatography (25% EtOAc/hexanes, R_f = 0.24), the product was afforded as a white solid (501.4 mg, 63% yield). ^{1}H NMR (500 MHz, $CDCl_3$) δ 7.77 (s, 1H), 7.69 (d, *J* = 7.9 Hz, 1H), 7.49 (d, *J* = 8.4 Hz, 1H), 7.44 (t, *J* = 7.7 Hz, 1H), 7.28 (d,

J = 7.8 Hz, 1H), 7.19 – 7.07 (m, 5H), 4.64 (dd, *J* = 9.4, 4.9 Hz, 1H), 4.50 (d, *J* = 9.4 Hz, 1H), 3.52 (t, *J* = 5.1 Hz, 1H), 3.05 (d, *J* = 5.3 Hz, 1H). ^{13}C NMR (126 MHz, $CDCl_3$) δ 178.19, 170.73, 155.76, 151.34, 131.52, 128.89, 128.58, 128.08, 127.61, 126.83, 123.81, 123.79, 118.57, 112.39, 68.17, 44.45, 38.09, 26.25.

epi-100. The general ring-opening cyclization procedure was followed using $Ga(OTf)_3$ (12.2 mg, 0.0236 mmol) and **98** (75 mg, 0.236 mmol) in 1.2 mL of anhydrous DCM. After purification by silica flash chromatography (25% EtOAc/hexanes, R_f = 0.14), compound **epi-100** was afforded as a yellow foam (62.4 mg, 83% yield). ^{1}H NMR (500 MHz, $CDCl_3$) δ 7.55 (d, *J* = 8.5 Hz, 1H), 7.45 – 7.40 (m, 3H), 7.33 (dd, *J* = 7.4, 2.0 Hz, 2H), 7.19 – 7.12 (m, 1H), 7.07 – 7.02 (m, 1H), 6.59 (d, *J* = 8.0 Hz, 1H), 4.38 – 4.32 (m, 3H), 3.86 (d, *J* = 7.4 Hz, 1H), 3.57 – 3.49 (m, 1H). ^{13}C NMR (126 MHz, $CDCl_3$) δ 176.47, 171.13, 169.72, 156.84, 146.32, 138.99, 135.14, 129.87, 129.46, 129.35, 129.12, 129.01, 128.92, 128.88, 128.70, 128.48, 127.41, 125.93, 125.34, 124.13, 123.94, 123.57, 122.94, 112.88, 112.39, 69.51, 60.35, 51.82, 47.43, 41.30, 21.01, 14.15.

epi-100 *using* $Ca(NTf_2)_2$*/n-*Bu_4NPF_6. The general ring-opening cyclization procedure was followed, with a slight change. $Ca(NTf_2)_2$ (18.9 mg, 0.0314 mmol) was charged to the flask, then *n*-Bu_4NPF_6 (12.2 mg, 0.0314 mmol) was added. The two reagents were suspended in 0.8 mL of anhydrous DCM and stirred for 5 minutes. Then, **98** (100 mg, 0.314 mmol) was added as a solution in 0.8 mL of anhydrous DCM. After purification by silica flash chromatography (25% EtOAc/hexanes, R_f = 0.14), compound **epi-100** was afforded as a yellow foam (64.1 mg, 64% yield).

105. The general enol triflation procedure was followed using **epi-100** (78.8 mg, 0.248 mmol), NaH (19.8 mg, 0.496 mmol, 60% dispersion in mineral oil), and Tf_2O (0.08

mL, 0.496 mmol) in 1.2 mL of anhydrous DCM. After purification by silica flash chromatography (25% EtOAc/hexanes, R_f = 0.44), compound **105** was afforded as a yellow solid (32.1 mg, 28% yield), and unreacted **epi-100** was recovered (31.0 mg, 39%). ^{1}H NMR (500 MHz, $CDCl_3$) δ 7.55 (d, *J* = 8.5 Hz, 1H), 7.50 – 7.33 (m, 6H), 7.09 – 7.03 (m, 1H), 6.49 (d, *J* = 7.9 Hz, 1H), 4.45 – 4.35 (m, 2H), 4.23 (t, *J* = 8.9 Hz, 1H), 4.07 (dt, *J* = 17.6, 8.7 Hz, 1H). ^{13}C NMR (126 MHz, $CDCl_3$) δ 164.50, 156.97, 144.82, 138.15, 137.83, 129.54, 128.66, 127.49, 125.97, 125.56, 124.09, 121.69, 114.66, 112.39, 70.38, 46.70, 45.41.

*Cinnamyl 3-Oxo-3-phenylpropanoate (**111a**).* The LHMDS-mediated addition procedure was followed using benzoyl choride (250 mg, 1.78 mmol), **107** (329.5 mg, 1.87 mmol), and LHMDS (3.7 mL, 3.74 mmol, 1M/THF) in 1.8 mL of anhydrous THF. After purification by silica flash chromatography (25% EtOAc/hexanes, R_f = 0.24), compound **111a** was afforded in a 2.5:1 *keto-enol* mixture (312.5 mg, 63% yield). ^{1}H NMR (500 MHz, $CDCl_3$) δ 7.98 – 7.94 (m, 2H), 7.81 – 7.77 (m, 1H), 7.62 – 7.57 (m, 1H), 7.51 – 7.45 (m, 2H), 7.45 – 7.40 (m, 1H), 7.38 – 7.34 (m, 2H), 7.32 (ddd, *J* = 7.7, 6.7, 1.4 Hz, 2H), 7.29 – 7.23 (m, 2H), 6.63 (d, *J* = 15.9 Hz, 1H), 6.25 (dt, *J* = 15.9, 6.4 Hz, 1H), 4.88 (dd, *J* = 6.4, 1.3 Hz, 1H), 4.82 (dd, *J* = 6.4, 1.3 Hz, 2H), 4.05 (s, 2H). ^{13}C NMR (126 MHz, $CDCl_3$) δ 192.30, 171.79, 167.28, 136.06, 135.96, 134.60, 134.37, 133.78, 131.33, 128.80, 128.61, 128.57, 128.55, 128.52, 128.12, 126.64, 126.09, 123.00, 122.48, 87.17, 65.98, 64.88, 45.94.

*Cinnamyl 3-(3,4-Dimethoxyphenyl)-3-oxopropanoate (**111c**).* The general acid chloride and LHMDS-mediated addition procedures were followed using 3,4-dimethoxybenzoic acid (250 mg, 1.37 mmol), DMF (2 drops), and $(COCl)_2$ (0.14 mL, 1.64

mmol) in 2.7 mL of anhydrous DCM, then **107** (253.8 mg, 1.44 mmol) and LHMDS (2.9 mL, 2.88 mmol, 1M/THF) in 1.4 mL of anhydrous THF. After purification by silica flash chromatography (25% EtOAc/hexanes, R_f = 0.21), compound **111c** was afforded in a 5:1 *keto-enol* mixture (218.6 mg, 47% yield). ^{1}H NMR (500 MHz, $CDCl_3$) δ 7.57 – 7.53 (m, 2H), 7.37 – 7.29 (m, 4H), 6.87 (d, *J* = 8.2 Hz, 1H), 6.62 (d, *J* = 15.9 Hz, 1H), 6.25 (dt, *J* = 15.9, 6.4 Hz, 1H), 4.81 (d, *J* = 7.7 Hz, 2H), 4.01 (s, 2H), 3.93 (d, *J* = 1.1 Hz, 6H). ^{13}C NMR (126 MHz, $CDCl_3$) δ 190.78, 167.49, 153.87, 149.21, 136.06, 134.61, 129.22, 128.58, 128.12, 126.62, 123.59, 122.53, 110.31, 110.04, 65.91, 56.10, 56.00, 45.74.

*Cinnamyl 2-Diazo-3-oxo-3-phenylpropanoate (**112a**).* The general *p*-ABSA diazo transfer procedure was followed using **111a** (308.6 mg, 1.10 mmol), Et_3N (0.17 mL, 1.21 mmol), and *p*-ABSA (277.5 mg, 1.16 mmol) in 2.2 mL of anhydrous MeCN. After purification by silica flash chromatography (25% EtOAc/hexanes), compound **112a** was afforded (283.0 mg, 84% yield). ^{1}H NMR (500 MHz, $CDCl_3$) δ 7.64 (dd, *J* = 8.1, 1.1 Hz, 2H), 7.53 (tt, *J* = 7.0, 1.3 Hz, 1H), 7.43 (t, *J* = 7.6 Hz, 2H), 7.39 – 7.31 (m, 4H), 7.28 (dt, *J* = 8.1, 2.0 Hz, 1H), 6.61 (d, *J* = 15.9 Hz, 1H), 6.24 (dt, *J* = 15.9, 6.5 Hz, 1H), 4.84 (dd, *J* = 6.5, 1.2 Hz, 2H). ^{13}C NMR (126 MHz, $CDCl_3$) δ 160.85, 137.02, 135.87, 135.14, 132.34, 128.65, 128.38, 128.32, 127.92, 126.66, 122.14, 66.02.

*Cinnamyl 2-Diazo-3-(3,4-dimethoxyphenyl)-3-oxopropanoate (**112c**).* The general *p*-ABSA diazo transfer procedure was followed using **111c** (214.7 mg, 0.631 mmol), Et_3N (0.10 mL, 0.694 mmol), and *p*-ABSA (159.1 mg, 0.662 mmol) in 1.3 mL of anhydrous MeCN. After purification by silica flash chromatography (25% EtOAc/hexanes), compound **112c** was afforded (232.3 mg, *quant.*). ^{1}H NMR (500 MHz, $CDCl_3$) δ 7.39 – 7.31 (m, 5H), 7.30 – 7.26 (m, 2H), 6.87 (d, *J* = 8.4 Hz, 1H), 6.64 (d, *J* = 15.9 Hz, 1H), 6.27

(dt, *J* = 15.9, 6.5 Hz, 1H), 4.86 (dd, *J* = 6.5, 1.3 Hz, 2H), 3.91 (d, *J* = 7.4 Hz, 6H). ^{13}C NMR (126 MHz, $CDCl_3$) δ 185.04, 152.87, 148.55, 135.87, 135.16, 129.24, 128.66, 128.33, 126.65, 123.41, 122.22, 111.44, 109.59, 65.98, 55.99.

1-(3,4,5-Trimethoxybenzoyl)-6-phenyl-3-oxabicyclo[3.1.0]hexan-2-one ***(113b)****.* The general intramolecular cyclopropanation procedure was followed using **112b** (250 mg, 0.631 mmol) and $Rh_2(esp)_2$ (2.4 mg, 3.16 μmol) in 6.3 mL of anhydrous DCM. After purification by silica prep-TLC (25% EtOAc/hexanes, R_f = 0.14), compound **113b** was afforded as a white solid (94.6 mg, 41% yield). ^{1}H NMR (500 MHz, $CDCl_3$) δ 7.20 – 7.14 (m, 5H), 7.05 (dd, *J* = 8.0, 1.4 Hz, 2H), 4.61 (dd, *J* = 9.4, 4.9 Hz, 1H), 4.48 (d, *J* = 9.5 Hz, 1H), 3.86 (d, *J* = 15.2 Hz, 9H), 3.42 (t, *J* = 4.8 Hz, 1H), 3.00 (d, *J* = 5.2 Hz, 1H). ^{13}C NMR (126 MHz, $CDCl_3$) δ 188.25, 171.18, 152.53, 143.21, 132.10, 130.50, 128.67, 128.09, 127.31, 107.79, 68.10, 60.88, 56.17, 44.49, 38.01, 26.34.

Methyl (E)-3-(4-Bromophenyl)acrylate ***(115a)****.* The general Horner-Wadsworth-Emmons procedure was followed using NaH (130 mg, 3.24 mmol, 60% dispersion in mineral oil) and methyl 2-(diethoxyphosphoryl)acetate (0.43 mL, 2.97 mmol) in 17 mL of anhydrous THF, then *p*-bromobenzaldehyde (500 mg, 2.70 mmol) in 0.8 mL of anhydrous THF. Compound **115a** was afforded without further purification (580.1 mg, 89% yield). NMR data were consistent with previously reported results.[17]

Methyl (E)-3-(4-Methoxyphenyl)acrylate ***(115b)****.* The general Horner-Wadsworth-Emmons procedure was followed using NaH (176 mg, 4.41 mmol, 60% dispersion in mineral oil) and methyl 2-(diethoxyphosphoryl)acetate (0.59 mL, 4.04 mmol) in 22 mL of anhydrous THF, then *p*-anisaldehyde (500 mg, 3.67 mmol) in 1 mL of anhydrous THF.

Compound **115b** was afforded without further purification (25% EtOAc/hexanes, R_f = 0.47) (705.8 mg, *quant.*). NMR data were consistent with previously reported results.[17]

*Methyl (E)-3-(4-Nitrophenyl)acrylate (**115c**).* The general Horner-Wadsworth-Emmons procedure was followed using NaH (159 mg, 3.97 mmol, 60% dispersion in mineral oil) and methyl 2-(diethoxyphosphoryl)acetate (0.53 mL, 3.64 mmol) in 20 mL of anhydrous THF, then *p*-nitrobenzaldehyde (500 mg, 3.31 mmol) in 1 mL of anhydrous THF. Compound **115c** was afforded without further purification (25% EtOAc/hexanes, R_f = 0.41) (466.3 mg, 68% yield). NMR data were consistent with previously reported results.[18]

*Methyl (E)-3-(Furan-2-yl)acrylate (**115d**).* The general Horner-Wadsworth-Emmons procedure was followed using NaH (300 mg, 6.25 mmol, 60% dispersion in mineral oil) and methyl 2-(diethoxyphosphoryl)acetate (0.83 mL, 5.72 mmol) in 31 mL of anhydrous THF, then 2-furaldehyde (500 mg, 5.20 mmol) in 2 mL of anhydrous THF. Compound **115d** was afforded without further purification (25% EtOAc/hexanes, R_f = 0.59) (628.1 mg, 78% yield). NMR data were consistent with previously reported results.[19]

*(E)-3-(4-Bromophenyl)prop-2-en-1-ol (**116a**).* The general DIBAL-H reduction procedure was followed using **115a** (500 mg, 2.07 mmol), DIBAL-H (6.2 mL, 6.21 mmol, 1 M/DCM) in 5.2 mL of anhydrous DCM. Compound **116a** was afforded without further purification (25% EtOAc/hexanes, R_f = 0.17) as a white solid (363.6 mg, 82% yield). NMR data were consistent with previously reported results.[20]

*(E)-3-(4-Methoxyphenyl)prop-2-en-1-ol (**116b**).* The general DIBAL-H reduction procedure was followed using **115b** (500 mg, 2.60 mmol), DIBAL-H (7.8 mL, 7.80 mmol, 1 M/DCM) in 6.5 mL of anhydrous DCM. Compound **116b** was afforded without further

purification (25% EtOAc/hexanes, R_f = 0.17) as a white solid (420.3 mg, 98% yield). NMR data were consistent with previously reported results.[21]

*(E)-3-(4-Nitrophenyl)prop-2-en-1-ol (**116c**).* The general DIBAL-H reduction procedure was followed using **115c** (400 mg, 1.93 mmol), DIBAL-H (5.8 mL, 5.79 mmol, 1 M/DCM) in 4.8 mL of anhydrous DCM. Compound **116c** was afforded without further purification (25% EtOAc/hexanes, R_f = 0.10) as a white solid (305.7 mg, 88% yield). NMR data were consistent with previously reported results.[21]

*(E)-3-(Furan-2-yl)prop-2-en-1-ol (**116d**).* The general DIBAL-H reduction procedure was followed using **115d** (400 mg, 2.63 mmol), DIBAL-H (7.9 mL, 7.89 mmol, 1 M/DCM) in 6.5 mL of anhydrous DCM. Compound **116d** was afforded without further purification (25% EtOAc/hexanes, R_f = 0.28) as a white solid (303.7 mg, 93% yield). NMR data were consistent with previously reported results.[22]

*(E)-3-(4-Bromophenyl)allyl Acetate (**117a**).* The general acetylation procedure was following using **116a** (250 mg, 1.17 mmol), DIPEA (0.25 mL, 1.41 mmol), DMAP (28.7 mg, 0.235 mmol), and Ac_2O (0.13 mL, 1.41 mmol) in 12 mL of anhydrous DCM. Compound **117a** was afforded without further purification (235.9 mg, 79% yield). NMR data were consistent with previously reported results.[16]

*(E)-3-(4-Methoxyphenyl)allyl Acetate (**117b**).* The general acetylation procedure was following using **116b** (250 mg, 1.52 mmol), DIPEA (0.32 mL, 1.83 mmol), DMAP (37.3 mg, 0.305 mmol), and Ac_2O (0.17 mL, 1.52 mmol) in 15 mL of anhydrous DCM. Compound **117b** was afforded without further purification (253.6 mg, 81% yield). NMR data were consistent with previously reported results.[20]

*(E)-3-(4-Nitrophenyl)allyl Acetate (**117c**).* The general acetylation procedure was following using **116c** (250 mg, 1.40 mmol), DIPEA (0.29 mL, 1.67 mmol), DMAP (34.1 mg, 0.279 mmol), and Ac_2O (0.16 mL, 1.67 mmol) in 14 mL of anhydrous DCM. Compound **116c** was afforded without further purification (25% EtOAc/hexanes, R_f = 0.38) (235.3 mg, 76% yield). NMR data were consistent with previously reported results.[23]

*(E)-3-(Furan-2-yl)allyl Acetate (**117d**).* The general acetylation procedure was following using **116d** (250 mg, 2.01 mmol), DIPEA (0.42 mL, 2.42 mmol), DMAP (49.2 mg, 0.403 mmol), and Ac_2O (0.23 mL, 2.42 mmol) in 20 mL of anhydrous DCM. After purification by alumina flash chromatography (25% EtOAc/hexanes, R_f = 0.70), compound **117d** was afforded (34.1 mg, 10% yield). NMR data were consistent with previously reported results.[24]

*(E)-3-(4-Bromophenyl)allyl 3-(Benzofuran-2-yl)-3-oxopropanoate (**118a**).* The general acid chloride and LHMDS-mediated addition procedures were followed using benzofuran-2-carboxylic acid (125 mg, 0.771 mmol), DMF (1 drop), and $(COCl)_2$ (0.08 mL, 0.925 mmol) in 1.5 mL of anhydrous DCM, then **117a** (206.6 mg, 0.810 mmol) and LHMDS (1.6 mL, 1.62 mmol, 1M/THF) in 0.8 mL of anhydrous THF. After purification by silica flash chromatography (25% EtOAc/hexanes), compound **118a** was afforded in a 2.2:1 *enol-keto* mixture as an off-white, chalky solid (209.1 mg, 68% yield). ^{1}H NMR (500 MHz, $CDCl_3$) δ 12.00 (s, 1H), 7.65 (d, *J* = 7.8 Hz, 1H), 7.50 (d, *J* = 8.9 Hz, 1H), 7.46 (d, *J* = 6.7 Hz, 2H), 7.44 – 7.36 (m, 2H), 7.31 (s, 1H), 7.28 (dd, *J* = 8.2, 2.1 Hz, 2H), 6.65 (d, *J* = 15.9 Hz, 1H), 6.34 (dt, *J* = 15.9, 6.2 Hz, 1H), 5.92 (s, 1H), 4.88 (dd, *J* = 6.2, 1.2 Hz, 2H), 4.81 (dd, *J* = 6.3, 1.2 Hz, 1H). ^{13}C NMR (126 MHz, $CDCl_3$) δ 162.13, 135.08, 132.97, 131.76, 128.15, 127.78, 126.65, 123.74, 123.56, 122.25, 111.63, 108.96, 88.31, 64.75.

*(E)-3-(4-Methoxyphenyl)allyl 3-(Benzofuran-2-yl)-3-oxopropanoate (**118b**).* The general acid chloride and LHMDS-mediated addition procedures were followed using benzofuran-2-carboxylic acid (125 mg, 0.771 mmol), DMF (1 drop), and $(COCl)_2$ (0.08 mL, 0.925 mmol) in 1.5 mL of anhydrous DCM, then **118a** (167.1 mg, 0.810 mmol) and LHMDS (1.6 mL, 1.62 mmol, 1M/THF) in 0.8 mL of anhydrous THF. After purification by silica flash chromatography (25% EtOAc/hexanes), the product was afforded in a 1.8:1 *keto-enol* mixture as a yellow-green oil (194.8 mg, 72% yield). ^{1}H NMR (500 MHz, $CDCl_3$) δ 7.71 (d, *J* = 7.9 Hz, 1H), 7.60 (d, *J* = 0.9 Hz, 1H), 7.58 – 7.54 (m, 1H), 7.52 – 7.46 (m, 1H), 7.36 (d, *J* = 8.8 Hz, 1H), 7.31 (d, *J* = 8.1 Hz, 1H), 7.29 – 7.26 (m, 1H), 6.89 – 6.85 (m, 1H), 6.85 – 6.81 (m, 2H), 6.67 (d, *J* = 15.8 Hz, 1H), 6.58 (d, *J* = 15.8 Hz, 1H), 6.21 (dt, *J* = 15.8, 6.5 Hz, 1H), 6.11 (dt, *J* = 15.8, 6.6 Hz, 1H), 4.87 (dd, *J* = 6.6, 1.2 Hz, 1H), 4.80 (dd, *J* = 6.6, 1.2 Hz, 2H), 4.02 (s, 2H), 3.81 (d, *J* = 4.3 Hz, 3H).

*(E)-3-(4-Nitrophenyl)allyl 3-(Benzofuran-2-yl)-3-oxopropanoate (**118c**).* The general acid chloride and LHMDS-mediated addition procedures were followed using benzofuran-2-carboxylic acid (160 mg, 0.987 mmol), DMF (2 drops), and $(COCl)_2$ (0.10 mL, 1.18 mmol) in 2 mL of anhydrous DCM, then **117c** (229.2 mg, 0.810 mmol) and LHMDS (2.1 mL, 2.07 mmol, 1M/THF) in 1 mL of anhydrous THF. Only degradation products were detected.

*(E)-3-(4-Bromophenyl)allyl 3-(Benzofuran-2-yl)-2-diazo-3-oxopropanoate (**119a**).* The general *p*-ABSA diazo transfer procedure was followed using **118a** (207.1 mg, 0.519 mmol), Et_3N (0.08 mL, 0.571 mmol), and *p*-ABSA (130.9 mg, 0.545 mmol) in 1.5 mL of anhydrous MeCN. After purification by silica flash chromatography (25% EtOAc/hexanes), compound **119a** was afforded as a yellow solid (222 mg, *quant*.). ^{1}H

NMR (500 MHz, $CDCl_3$) δ 7.83 (s, 1H), 7.71 (d, *J* = 7.9 Hz, 1H), 7.57 – 7.52 (m, 1H), 7.50 – 7.43 (m, 3H), 7.35 – 7.29 (m, 1H), 7.28 – 7.23 (m, 2H), 6.65 (d, *J* = 15.9 Hz, 1H), 6.31 (dt, *J* = 15.9, 6.5 Hz, 1H), 4.94 (dd, *J* = 6.5, 1.2 Hz, 2H). ^{13}C NMR (126 MHz, $CDCl_3$) δ 172.16, 160.83, 155.08, 150.62, 134.80, 133.97, 131.77, 128.31, 128.19, 126.87, 124.01, 123.38, 123.01, 122.20, 115.04, 112.26, 66.04.

5.7 Copies of NMR Spectra

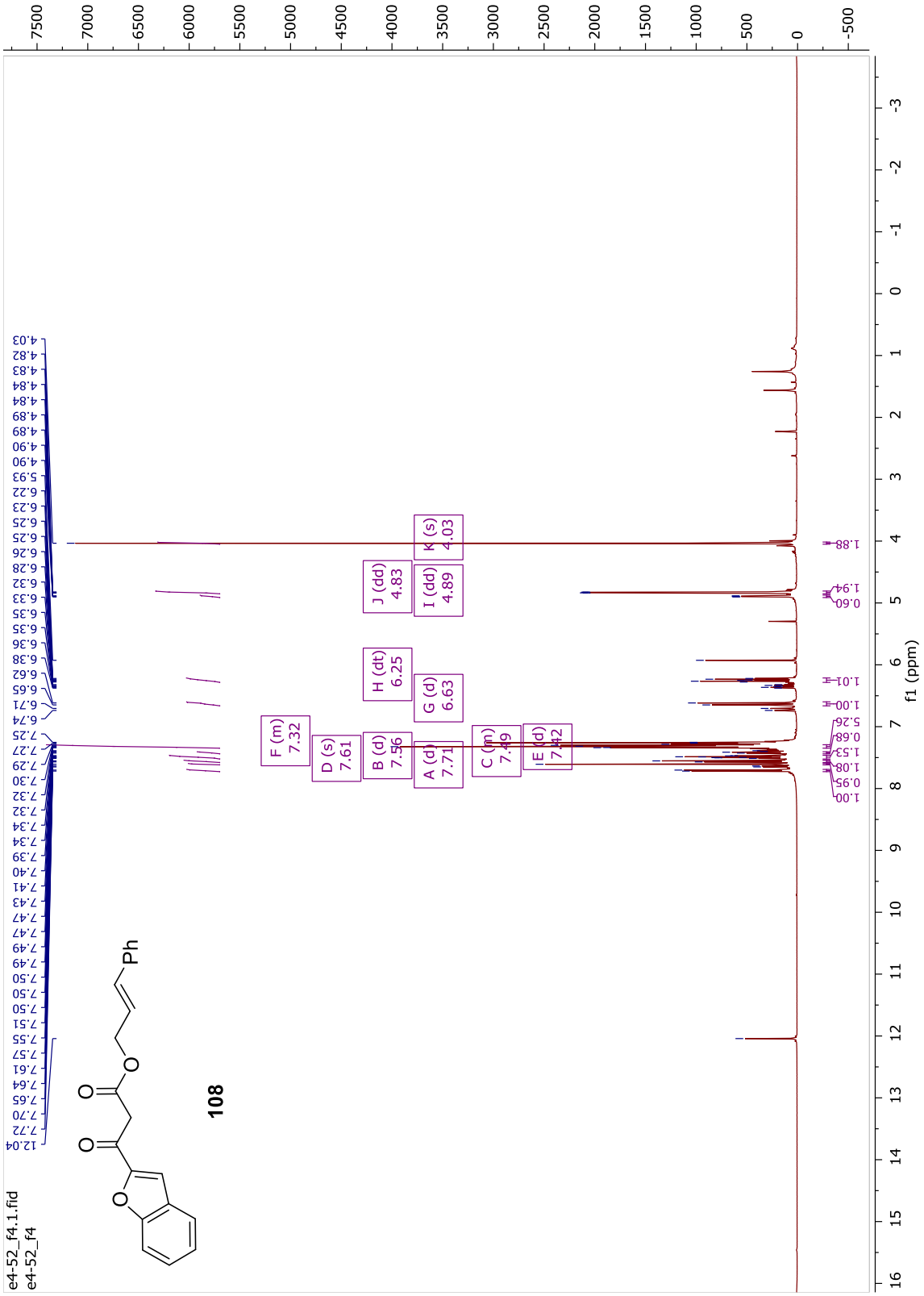
e4-52_f4.1.fid
e4-52_f4
108
Ph
O
O
O
O
A (d) 7.71
B (d) 7.56
C (m) 7.49
D (s) 7.61
E (d) 7.42
F (m) 7.32
G (d) 6.63
H (dt) 6.25
I (dd) 4.89
J (dd) 4.83
K (s) 4.03
f1 (ppm)

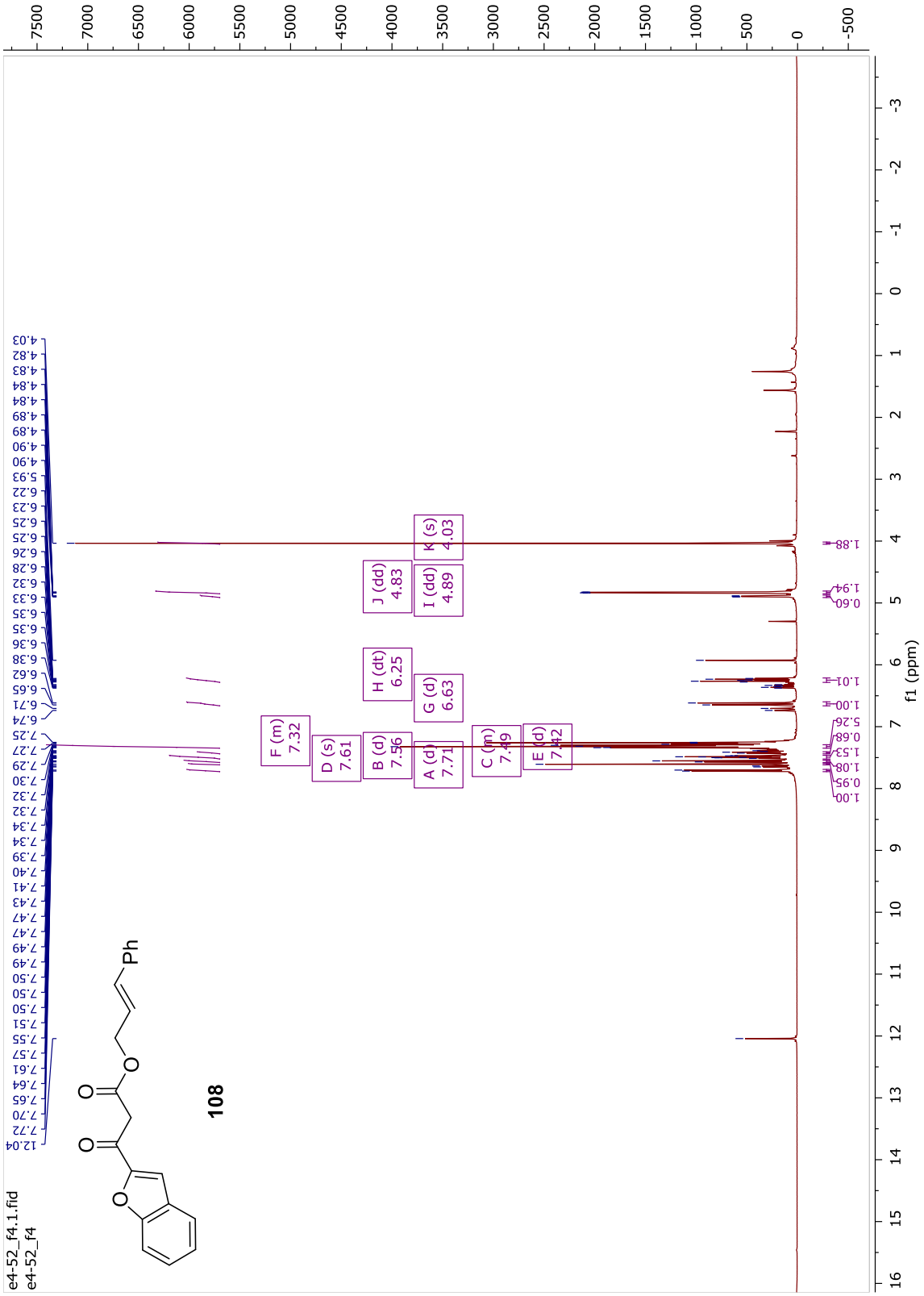
e4-52_f4.1.fid
e4-52_f4
108
Ph
O
O
O
O
A (d) 7.71
B (d) 7.56
C (m) 7.49
D (s) 7.61
E (d) 7.42
F (m) 7.32
G (d) 6.63
H (dt) 6.25
I (dd) 4.89
J (dd) 4.83
K (s) 4.03
1.88
0.60
1.94
1.01
1.00
5.26
0.68
1.53
1.08
0.95
1.00
f1 (ppm)

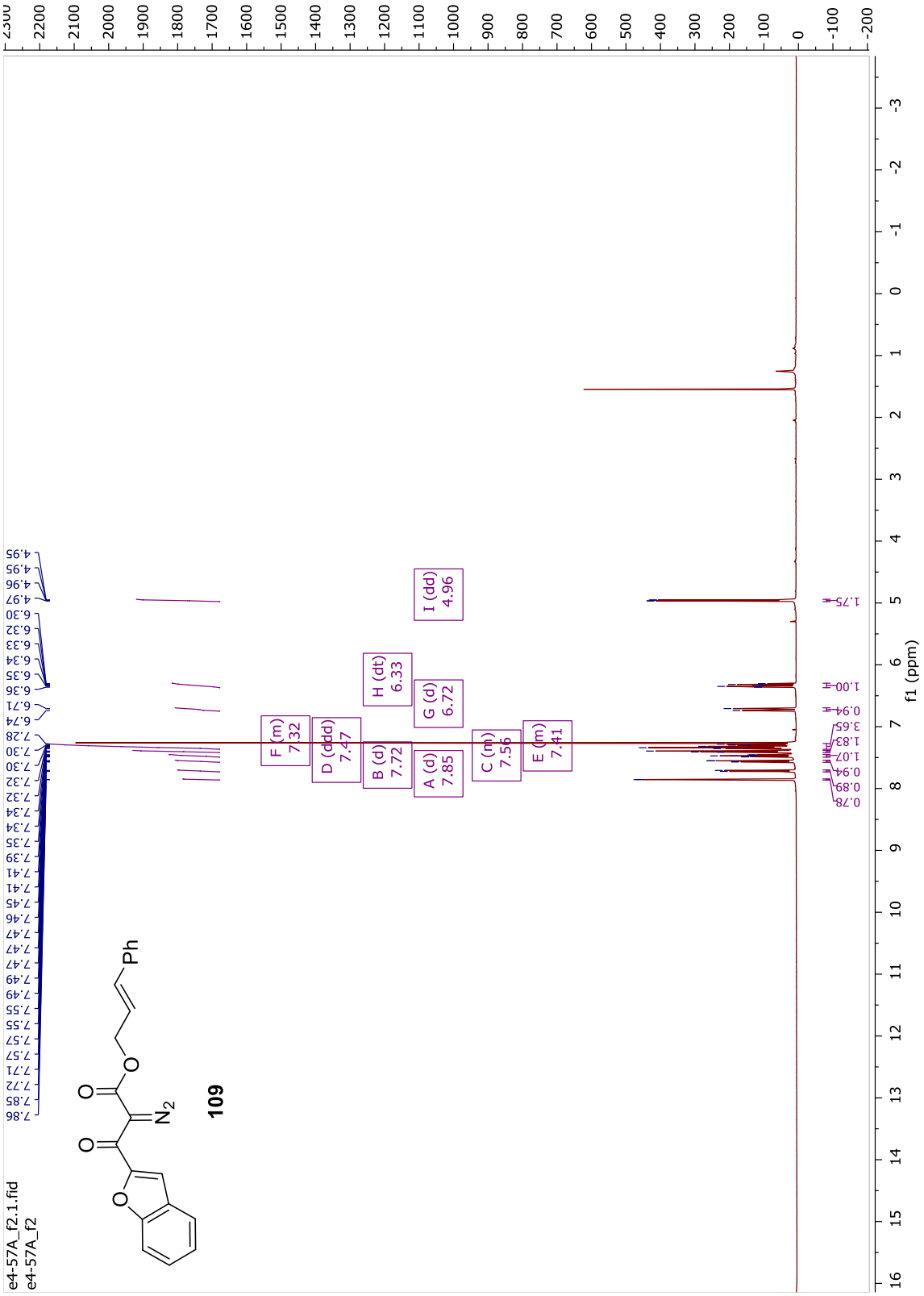
e4-57A_f2.1.fid
e4-57A_f2
109
Ph
O
O
O
O
N2
A (d) 7.85
B (d) 7.72
C (m) 7.56
D (ddd) 7.47
E (m) 7.41
F (m) 7.32
G (d) 6.72
H (dt) 6.33
I (dd) 4.96
1.75
1.00
0.94
3.65
1.83
1.07
0.94
0.89
0.78
f1 (ppm)

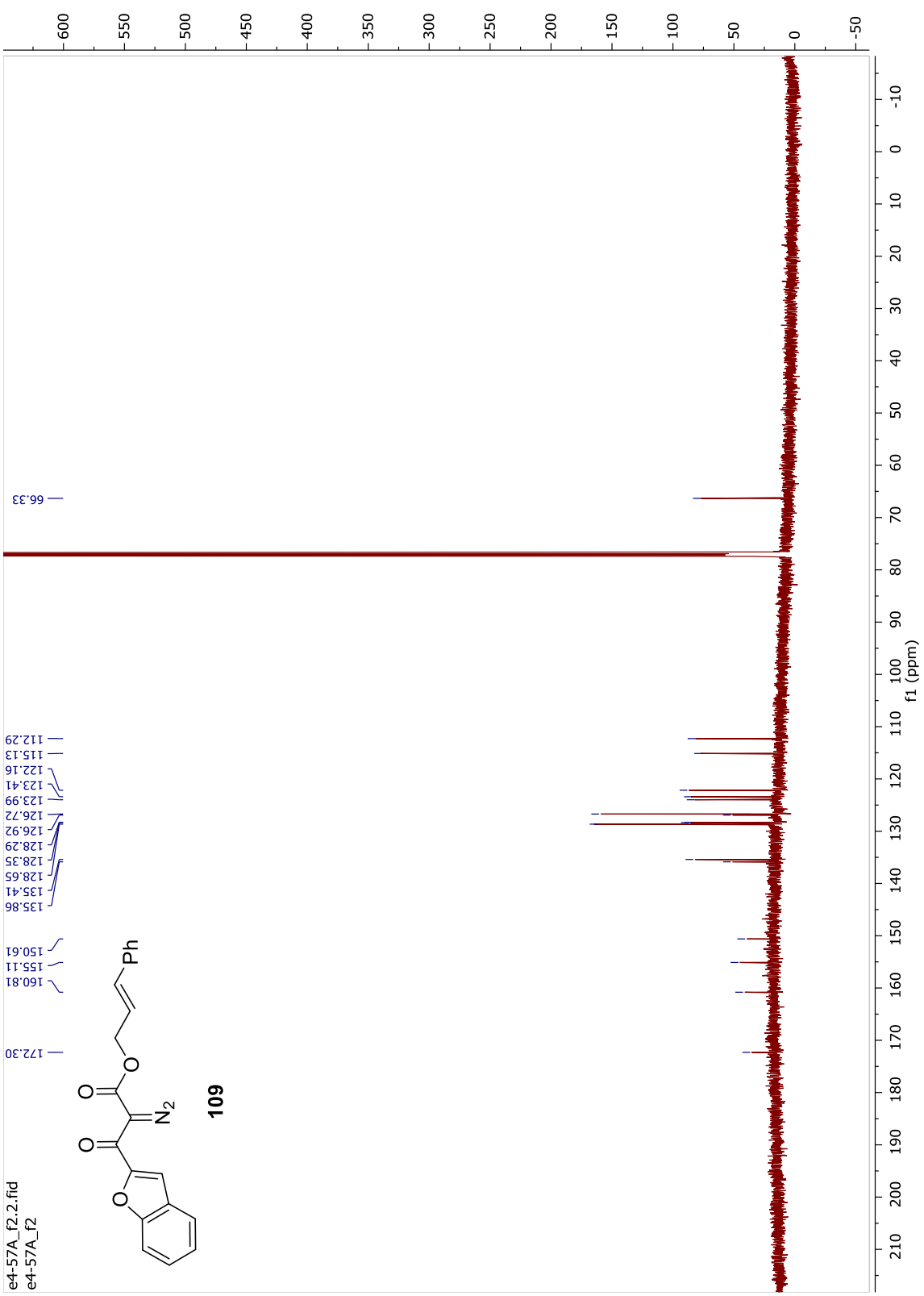
e4-57A_f2.2.fid
e4-57A_f2
109
Ph
O
O
O
O
N_2
172.30
160.81
155.11
150.61
135.86
135.41
128.65
128.35
128.29
126.92
126.72
123.99
123.41
122.16
115.13
112.29
66.33
f1 (ppm)

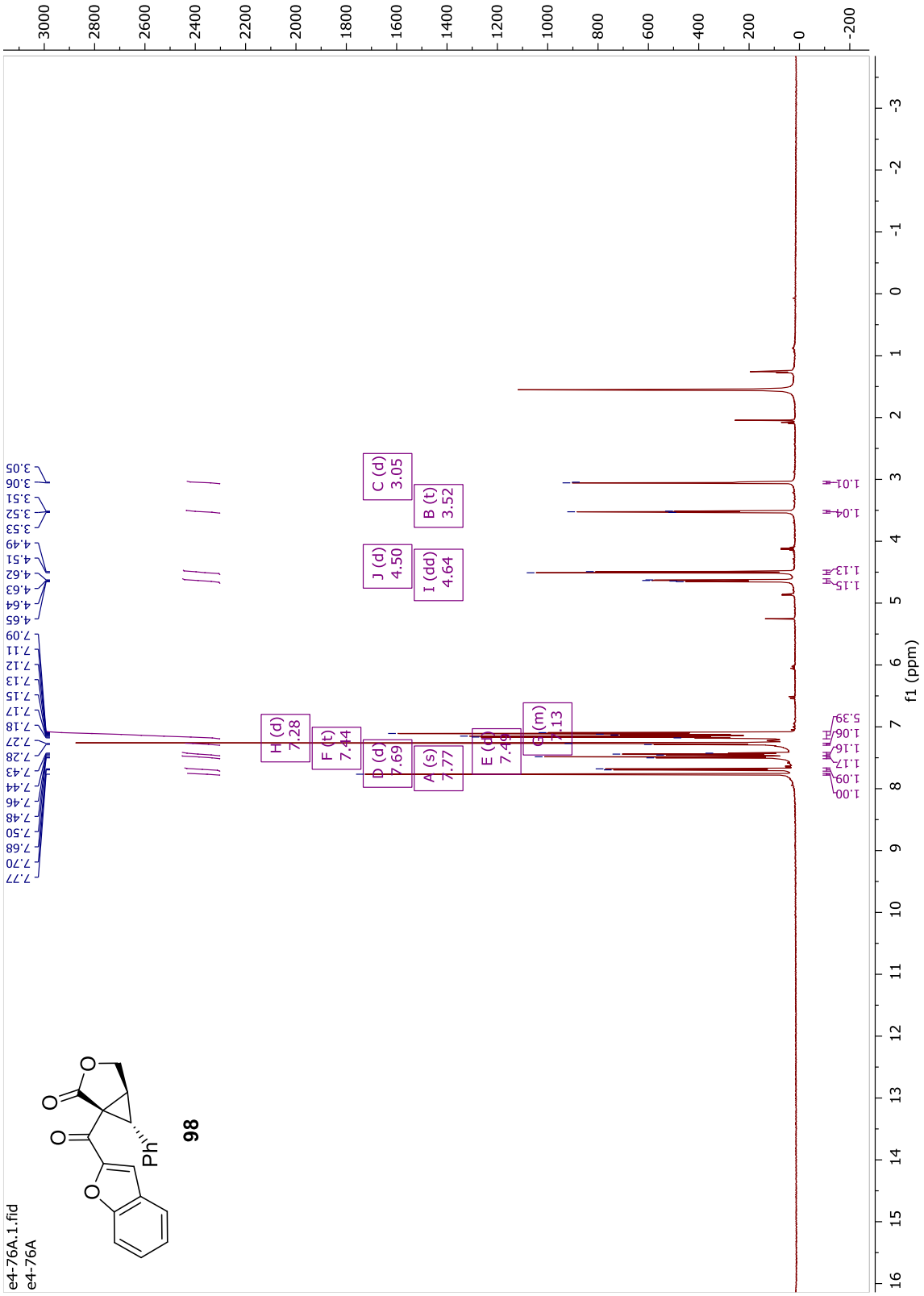
e4-76A.1.fid
e4-76A
98
A (s) 7.77
D (d) 7.69
F (t) 7.44
H (d) 7.28
E (d) 7.49
G (m) 7.13
I (dd) 4.64
J (d) 4.50
B (t) 3.52
C (d) 3.05
f1 (ppm)

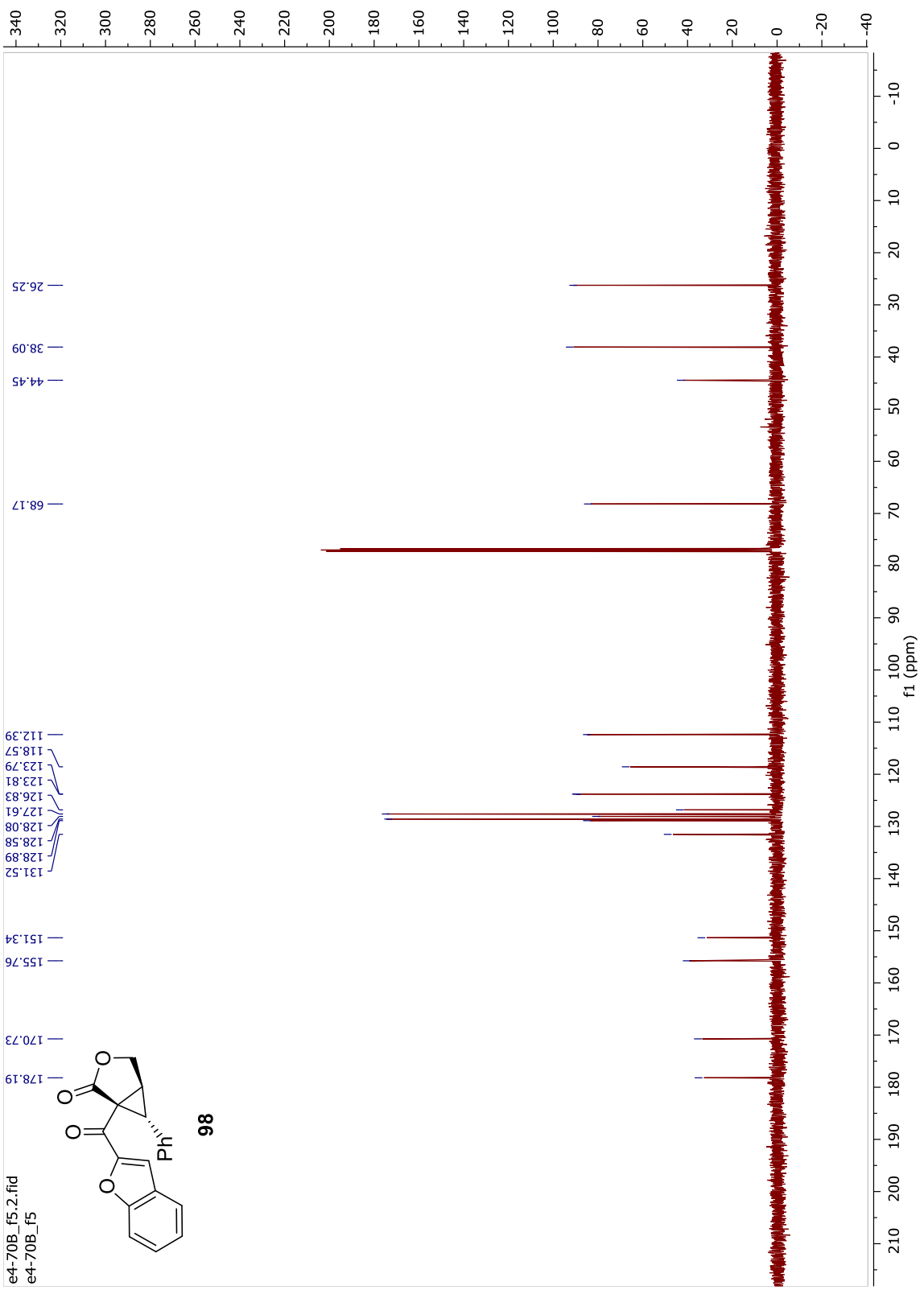
e4-70B_f5.2.fid
e4-70B_f5
178.19
170.73
155.76
151.34
131.52
128.89
128.58
128.08
127.61
126.83
123.81
123.79
118.57
112.39
68.17
44.45
38.09
26.25
Ph
98
f1 (ppm)

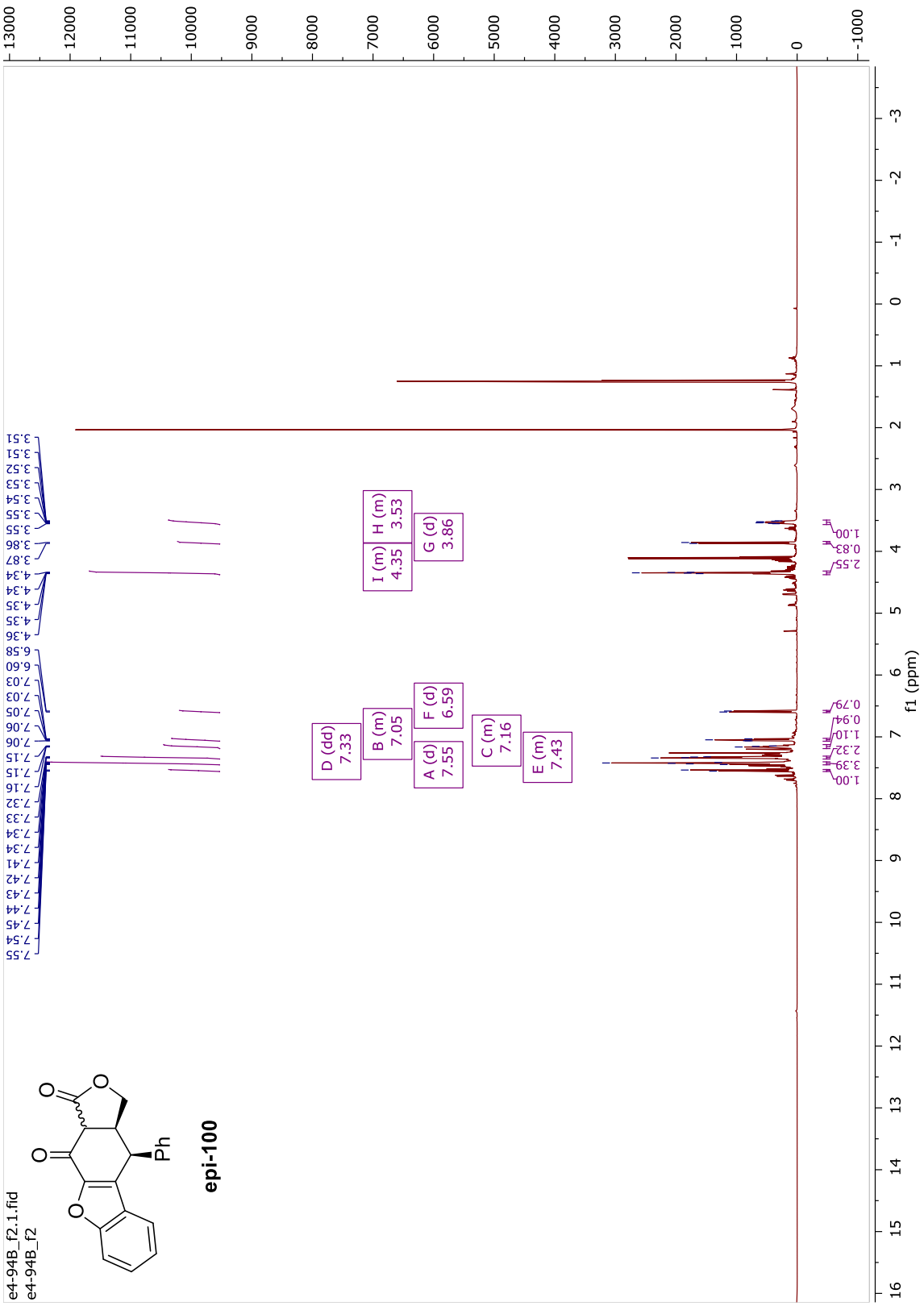
e4-94B_f2.1.fid
e4-94B_f2
epi-100
Ph
D (dd) 7.33
B (m) 7.05
A (d) 7.55
F (d) 6.59
C (m) 7.16
E (m) 7.43
I (m) 4.35
H (m) 3.53
G (d) 3.86
f1 (ppm)

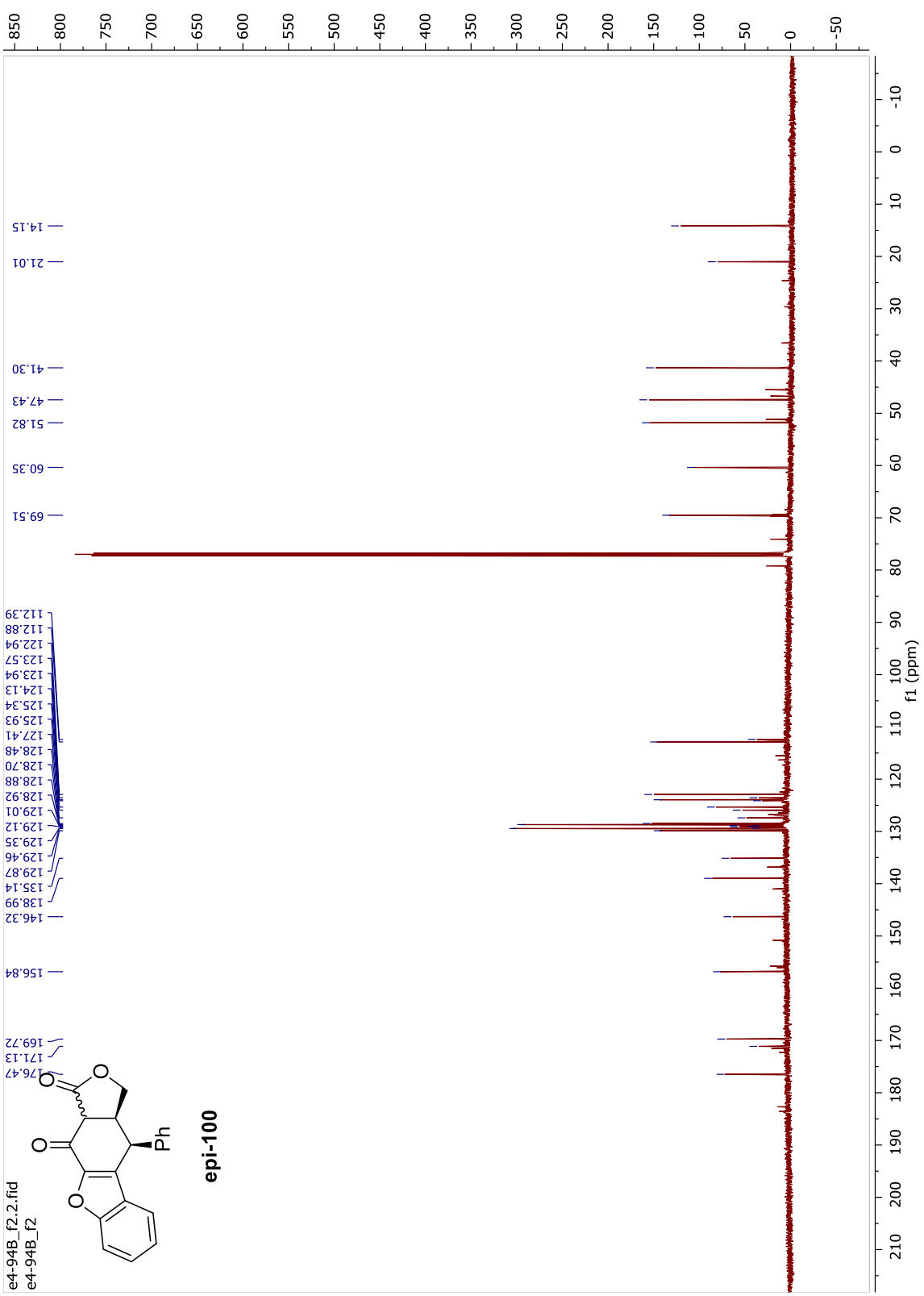
e4-94B_f2.2.fid
e4-94B_f2
epi-100
Ph
f1 (ppm)

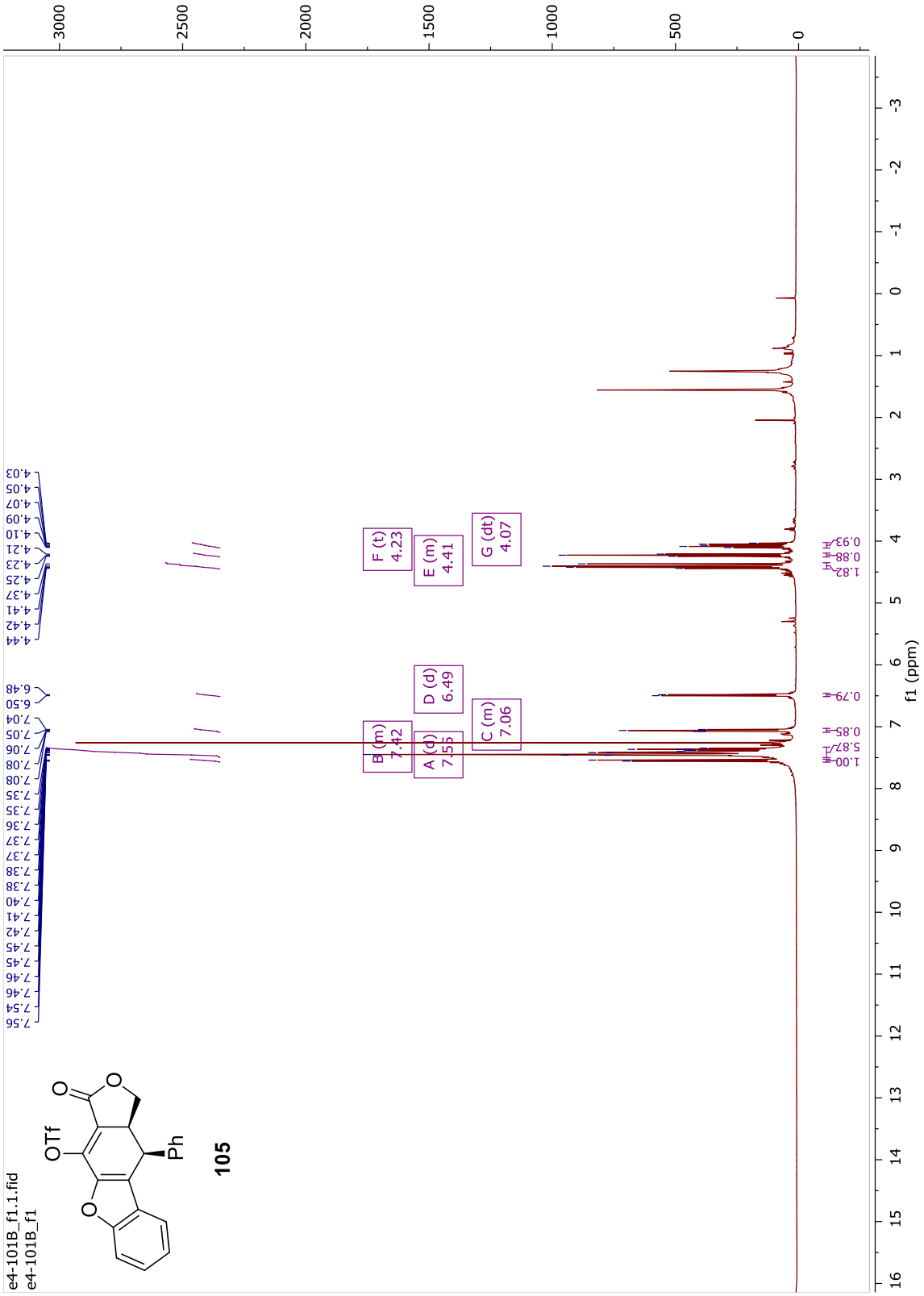
e4-101B_f1.1.fid
e4-101B_f1
105
OTf
Ph
A (d) 7.55
B (m) 7.42
C (m) 7.06
D (d) 6.49
E (m) 4.41
F (t) 4.23
G (dt) 4.07
1.00
5.87
0.85
0.79
1.82
0.88
0.93
f1 (ppm)

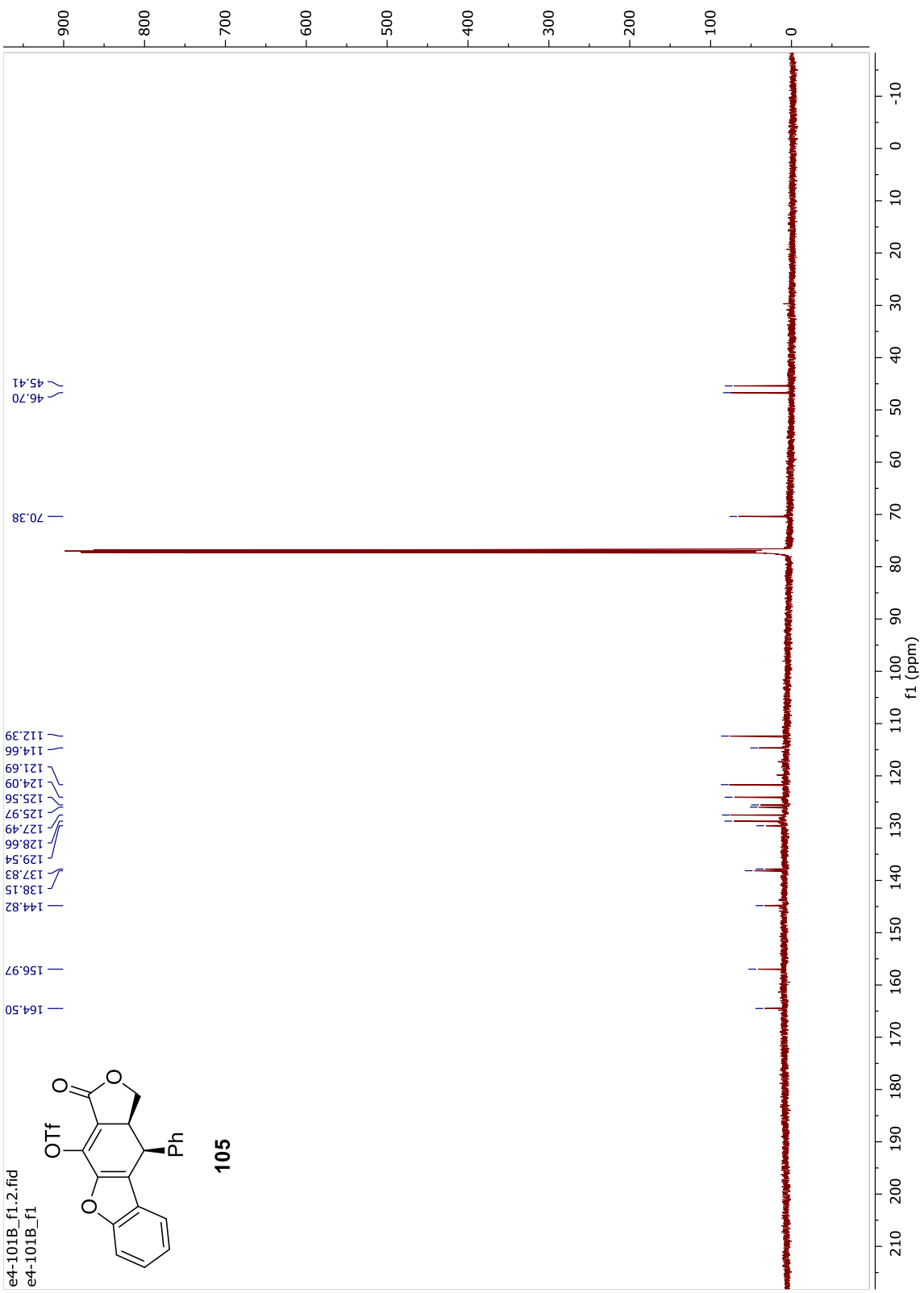
e4-101B_f1.2.fid
e4-101B_f1
105
OTf
Ph
164.50
156.97
144.82
138.15
137.83
129.54
128.66
127.49
125.97
125.56
124.09
121.69
114.66
112.39
70.38
46.70
45.41
f1 (ppm)

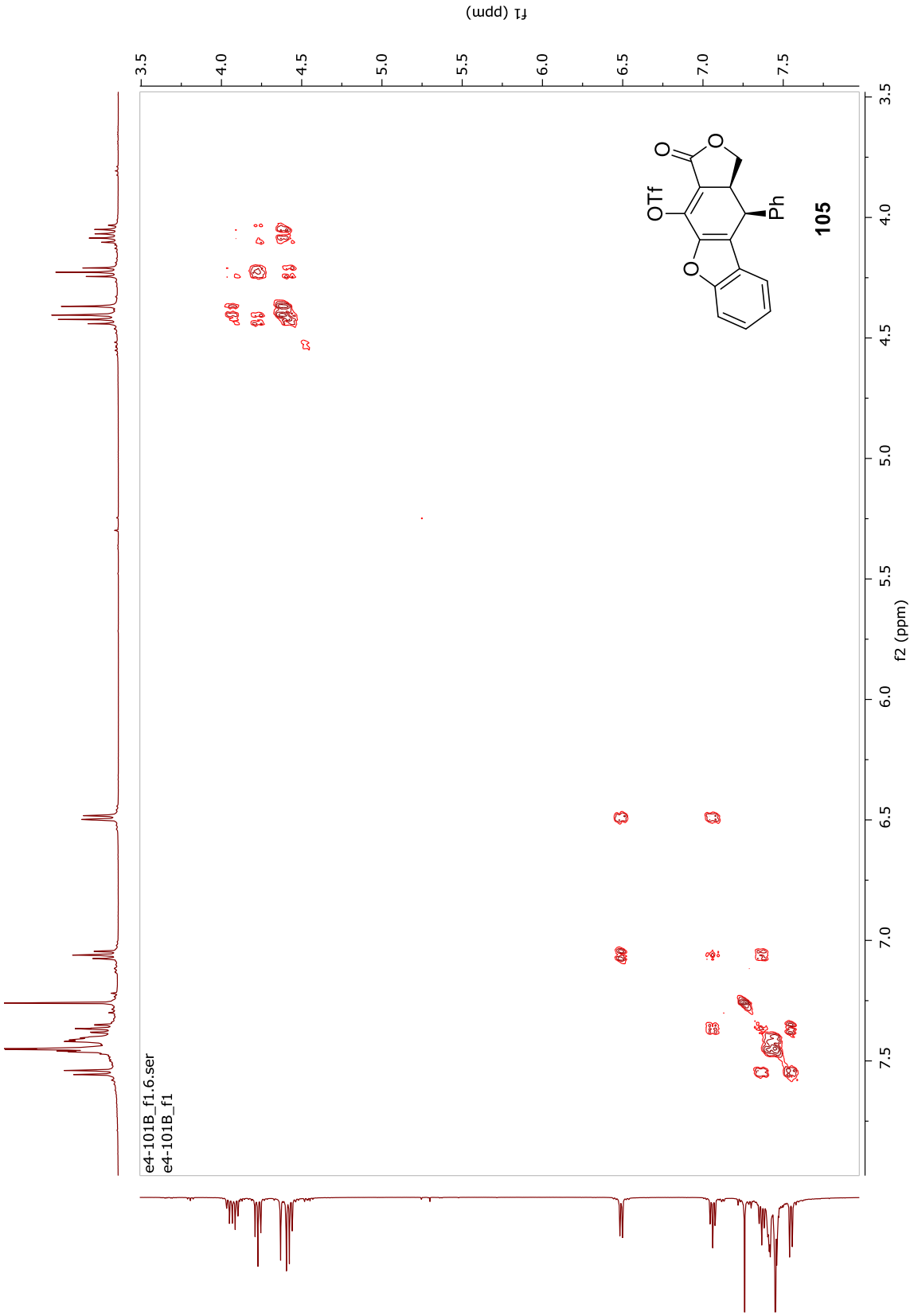
f1 (ppm)
3.5
4.0
4.5
5.0
5.5
6.0
6.5
7.0
7.5
f2 (ppm)
e4-101B_f1.6.ser
e4-101B_f1
OTf
Ph
105

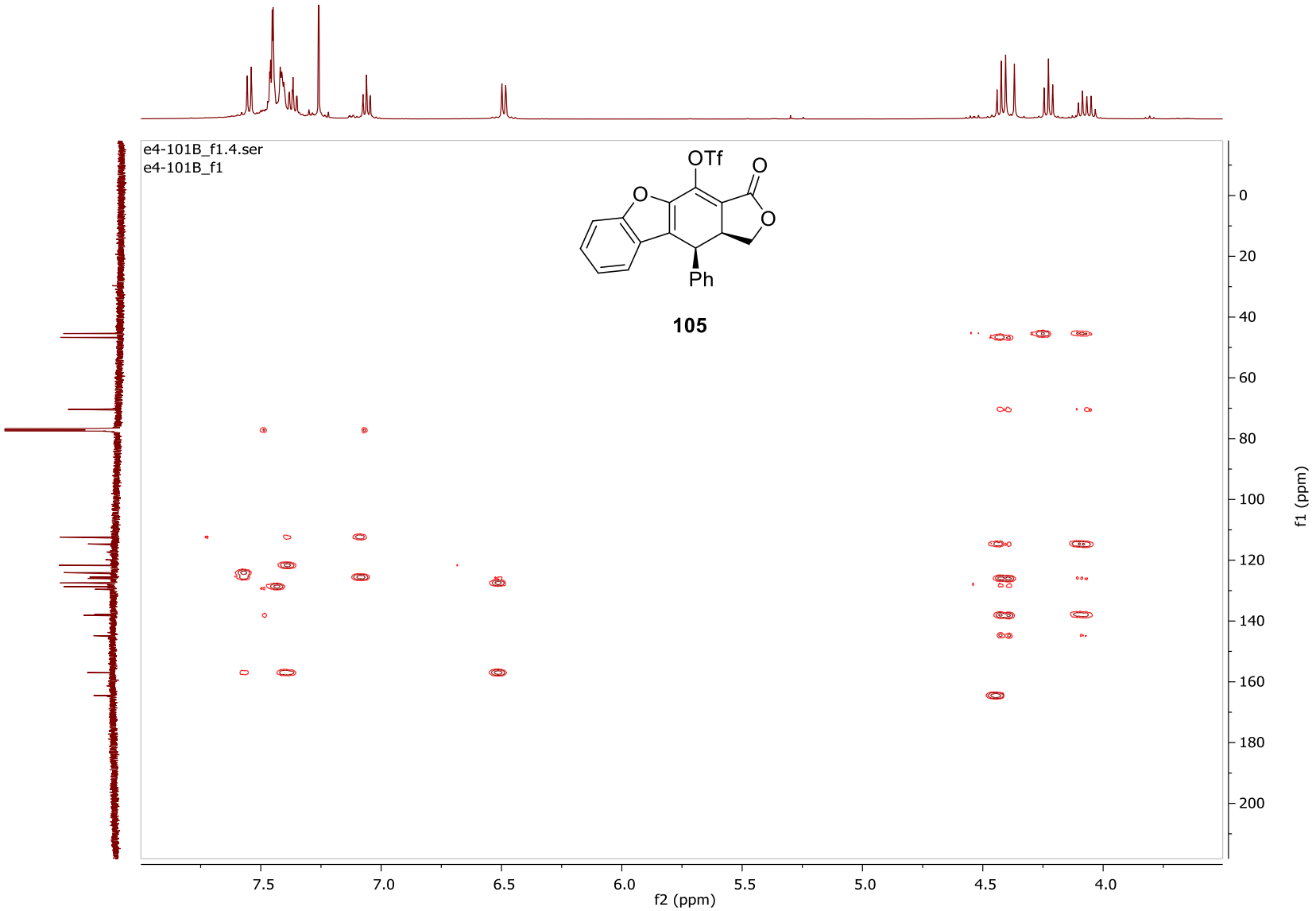
e4-101B_f1.4.ser
e4-101B_f1
OTf
O
O
O
Ph
105
0
20
40
60
80
100
120
140
160
180
200
f1 (ppm)
7.5
7.0
6.5
6.0
5.5
5.0
4.5
4.0
f2 (ppm)

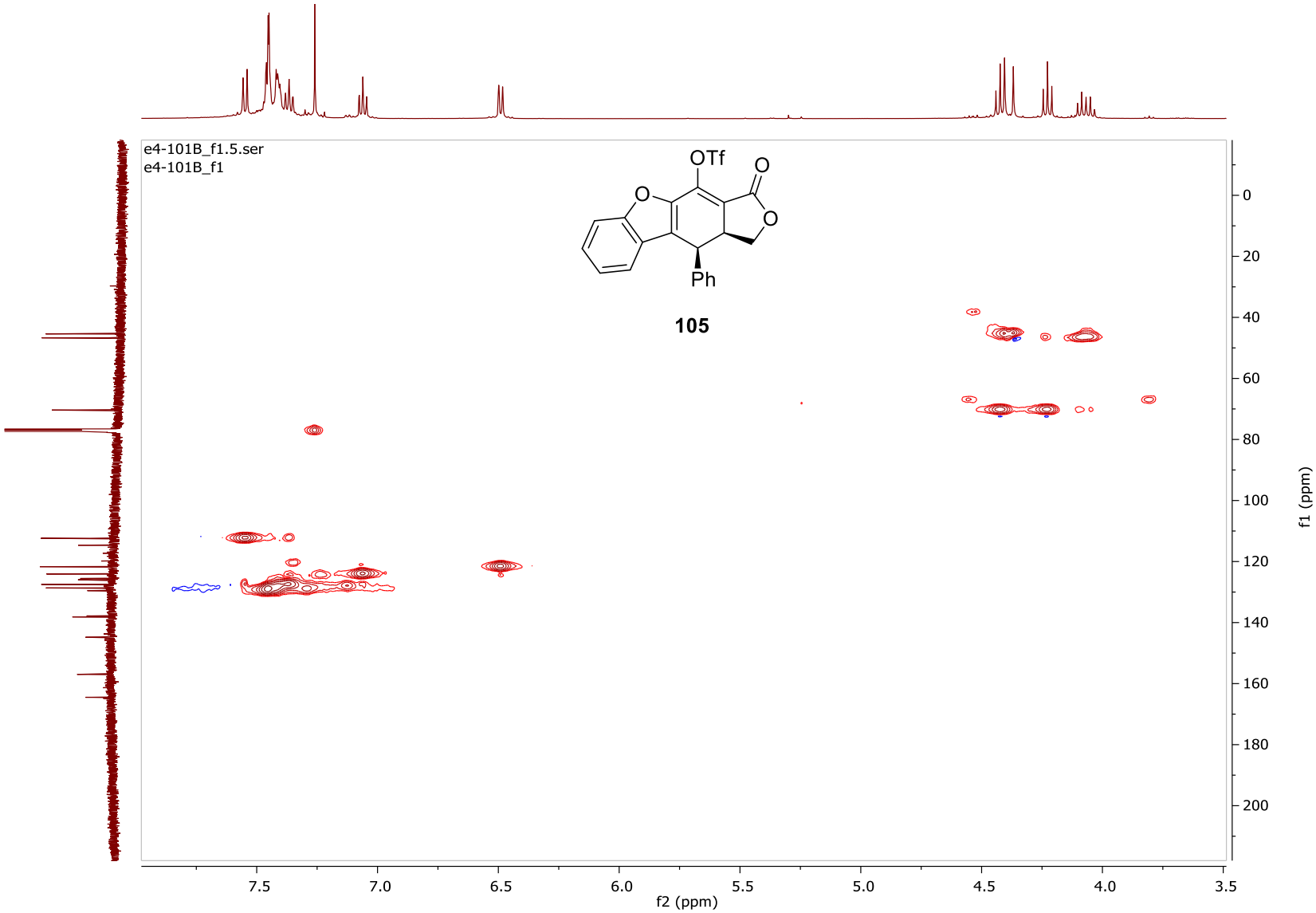
e4-101B_f1.5.ser
e4-101B_f1
OTf
O
O
O
Ph
105
7.5
7.0
6.5
6.0
5.5
5.0
4.5
4.0
3.5
f2 (ppm)
0
20
40
60
80
100
120
140
160
180
200
f1 (ppm)

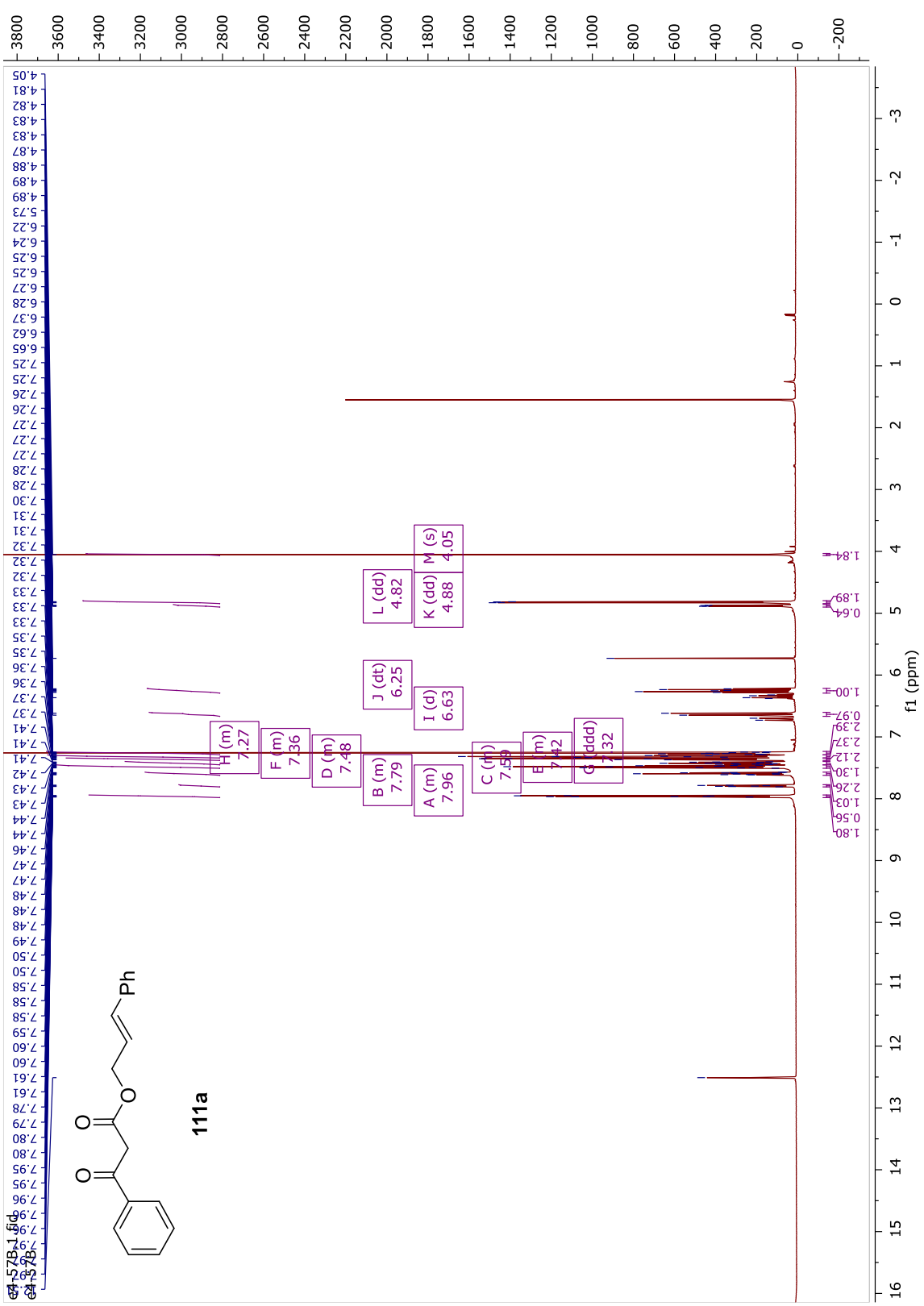
111a
Ph
O
O
O
A (m) 7.96
B (m) 7.79
C (m) 7.59
D (m) 7.48
E (m) 7.42
F (m) 7.36
H (m) 7.27
G (ddd) 7.32
I (d) 6.63
J (dt) 6.25
K (dd) 4.88
L (dd) 4.82
M (s) 4.05
f1 (ppm)

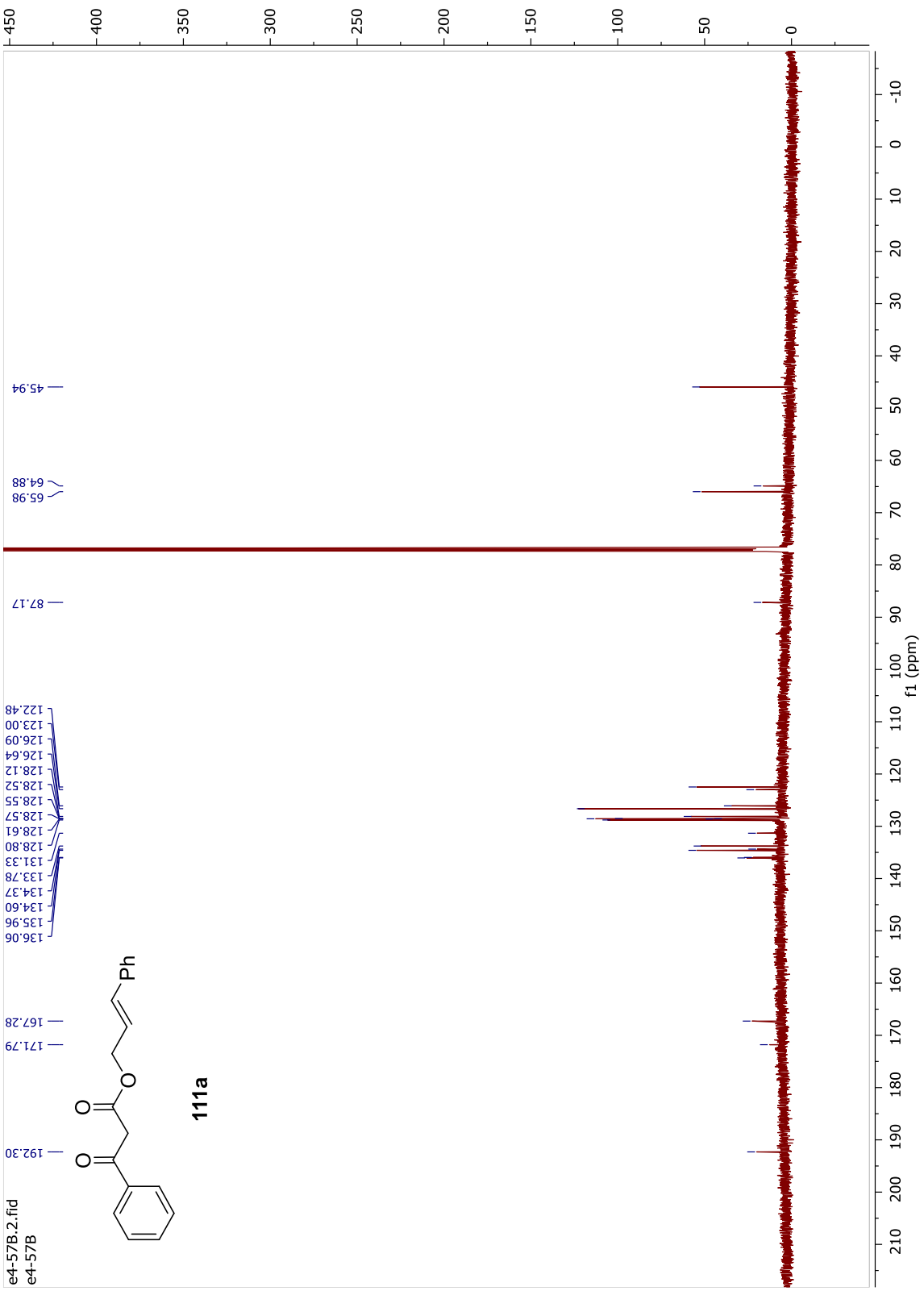
e4-57B.2.fid
e4-57B
192.30
171.79
167.28
136.06
135.96
134.60
134.37
133.78
131.33
128.80
128.61
128.57
128.55
128.52
128.12
126.64
126.09
123.00
122.48
87.17
65.98
64.88
45.94
O
O
O
Ph
111a
f1 (ppm)

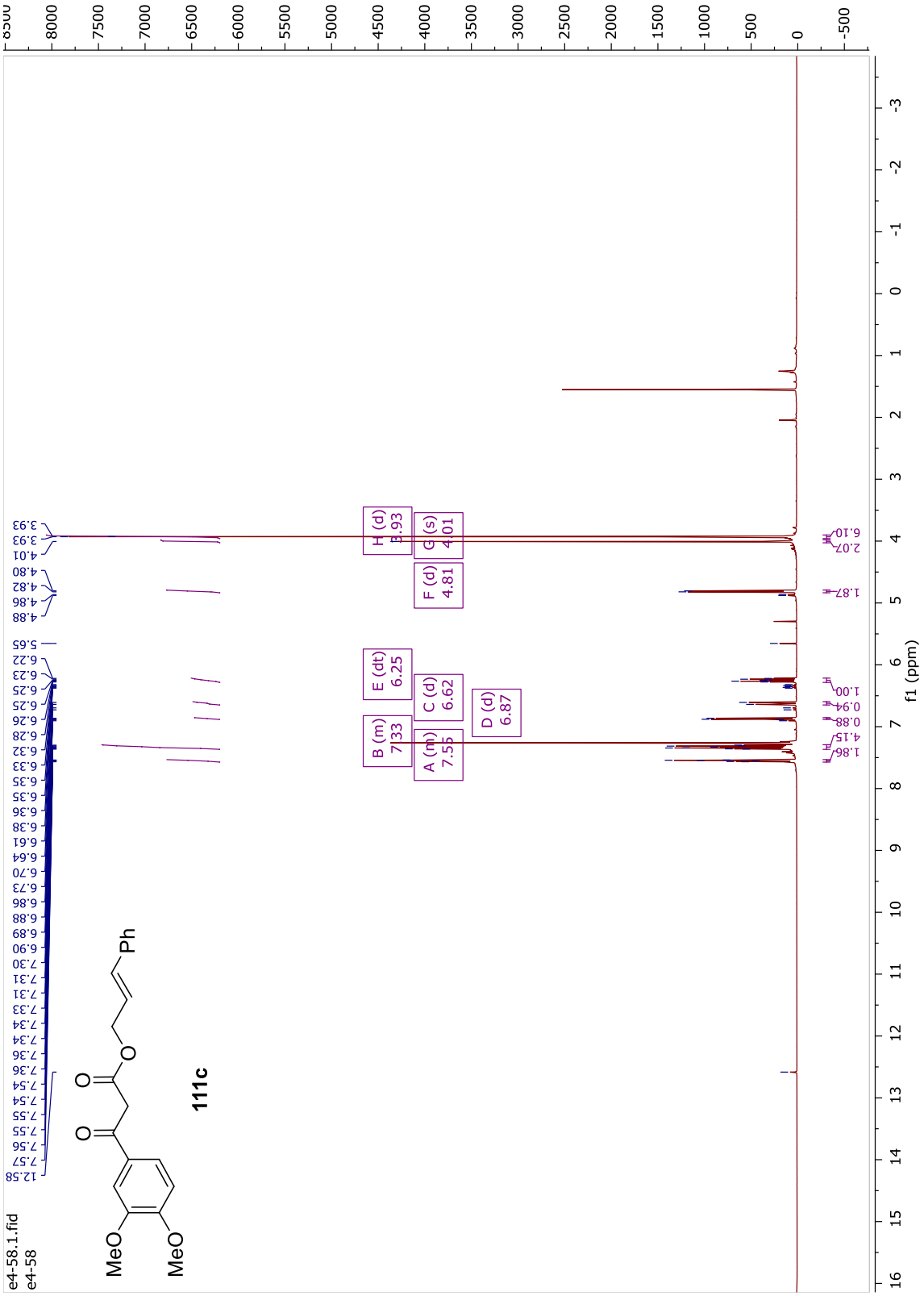
e4-58.1.fid
e4-58
111c
MeO
MeO
O
O
O
Ph
A (m) 7.55
B (m) 7.33
C (d) 6.62
D (d) 6.87
E (dt) 6.25
F (d) 4.81
G (s) 4.01
H (d) 3.93
f1 (ppm)

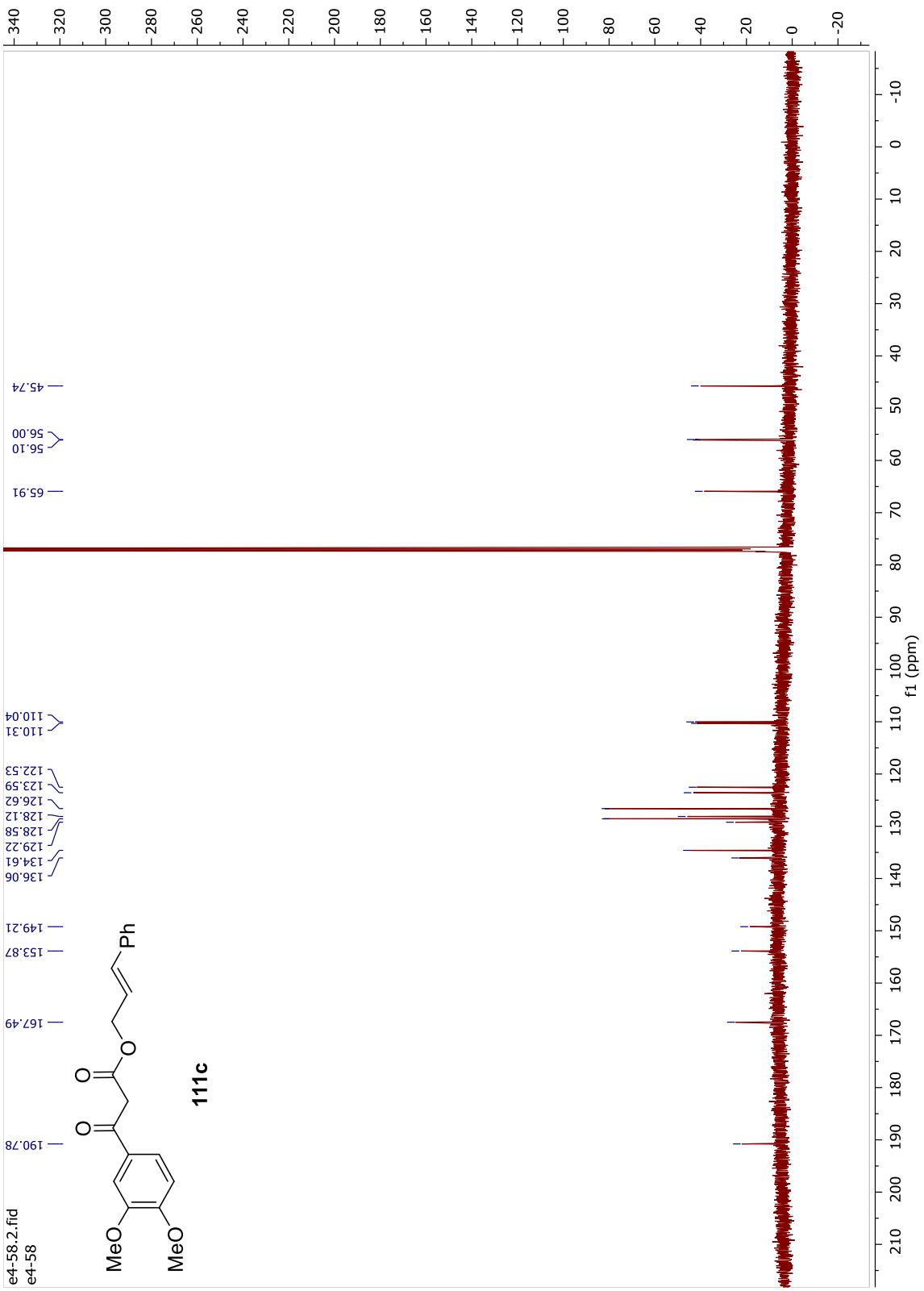
e4-58.2.fid
e4-58
190.78
167.49
153.87
149.21
136.06
134.61
129.22
128.58
128.12
126.62
123.59
122.53
110.31
110.04
65.91
56.10
56.00
45.74
MeO
MeO
O
O
O
Ph
111c
f1 (ppm)

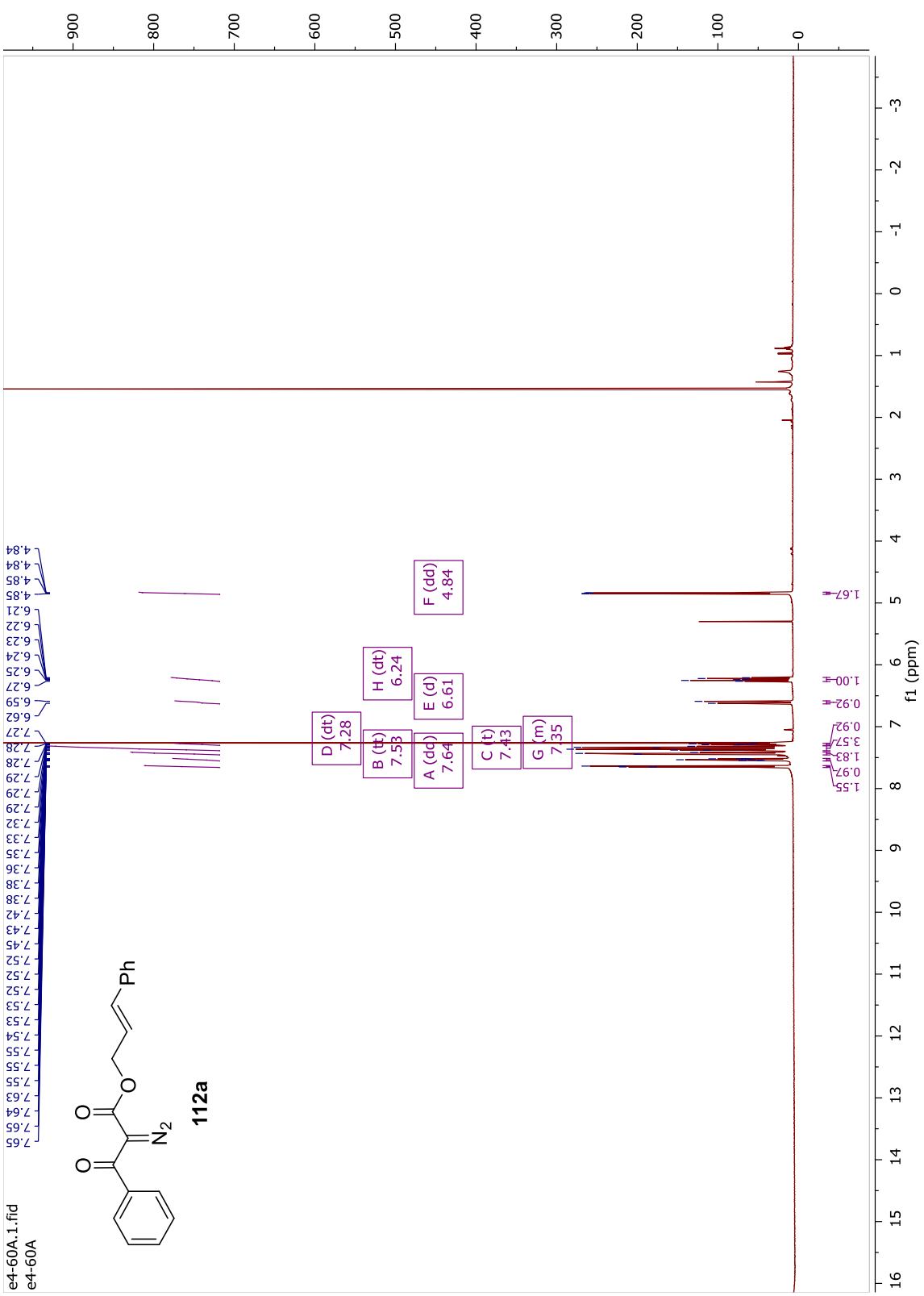
e4-60A.1.fid
e4-60A
112a
A (dd) 7.64
B (tt) 7.53
C (t) 7.43
D (dt) 7.28
E (d) 6.61
F (dd) 4.84
G (m) 7.35
H (dt) 6.24
f1 (ppm)

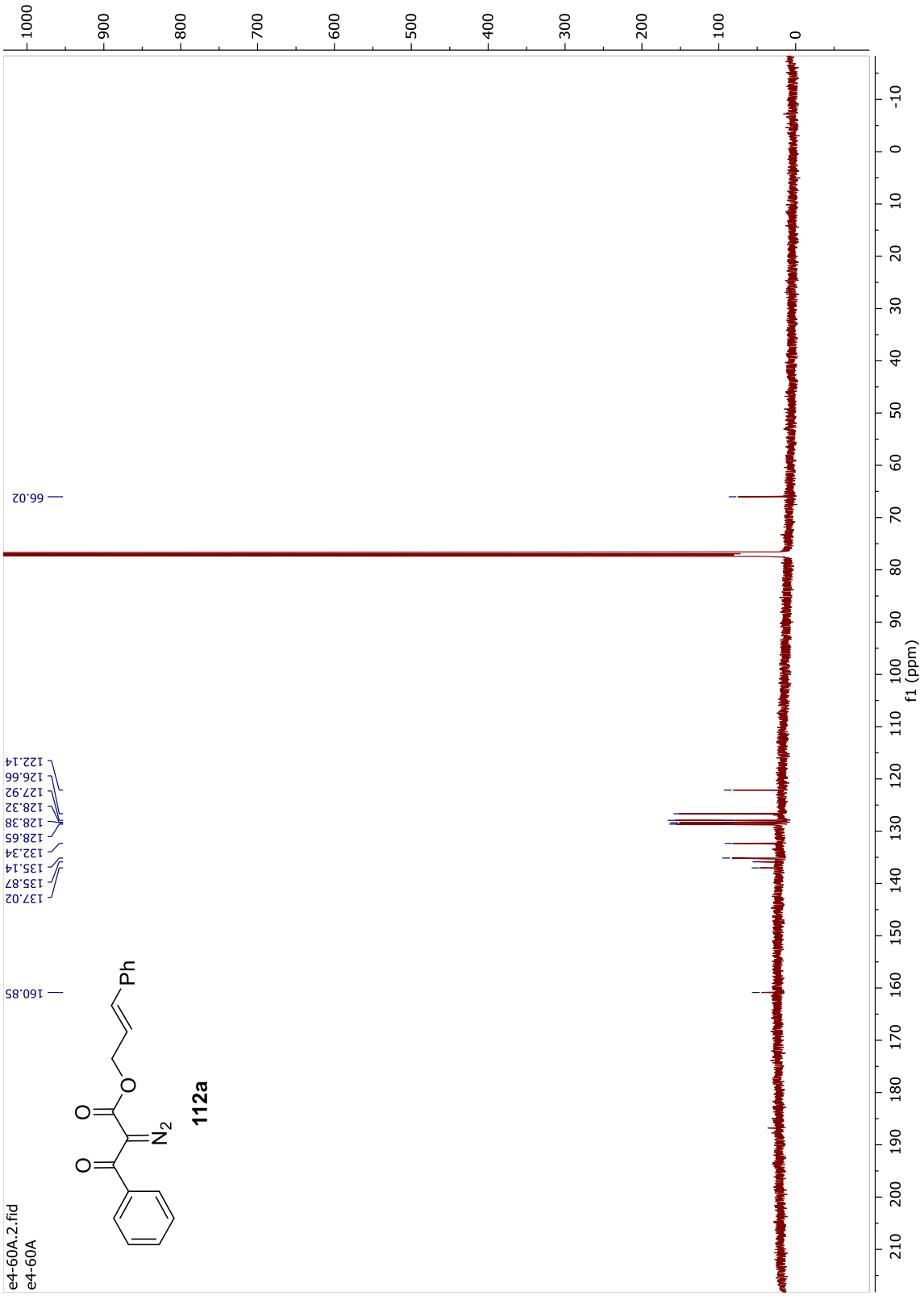
e4-60A.2.fid
e4-60A
112a
Ph
O
O
O
N_2
160.85
137.02
135.87
135.14
132.34
128.65
128.38
128.32
127.92
126.66
122.14
66.02
f1 (ppm)

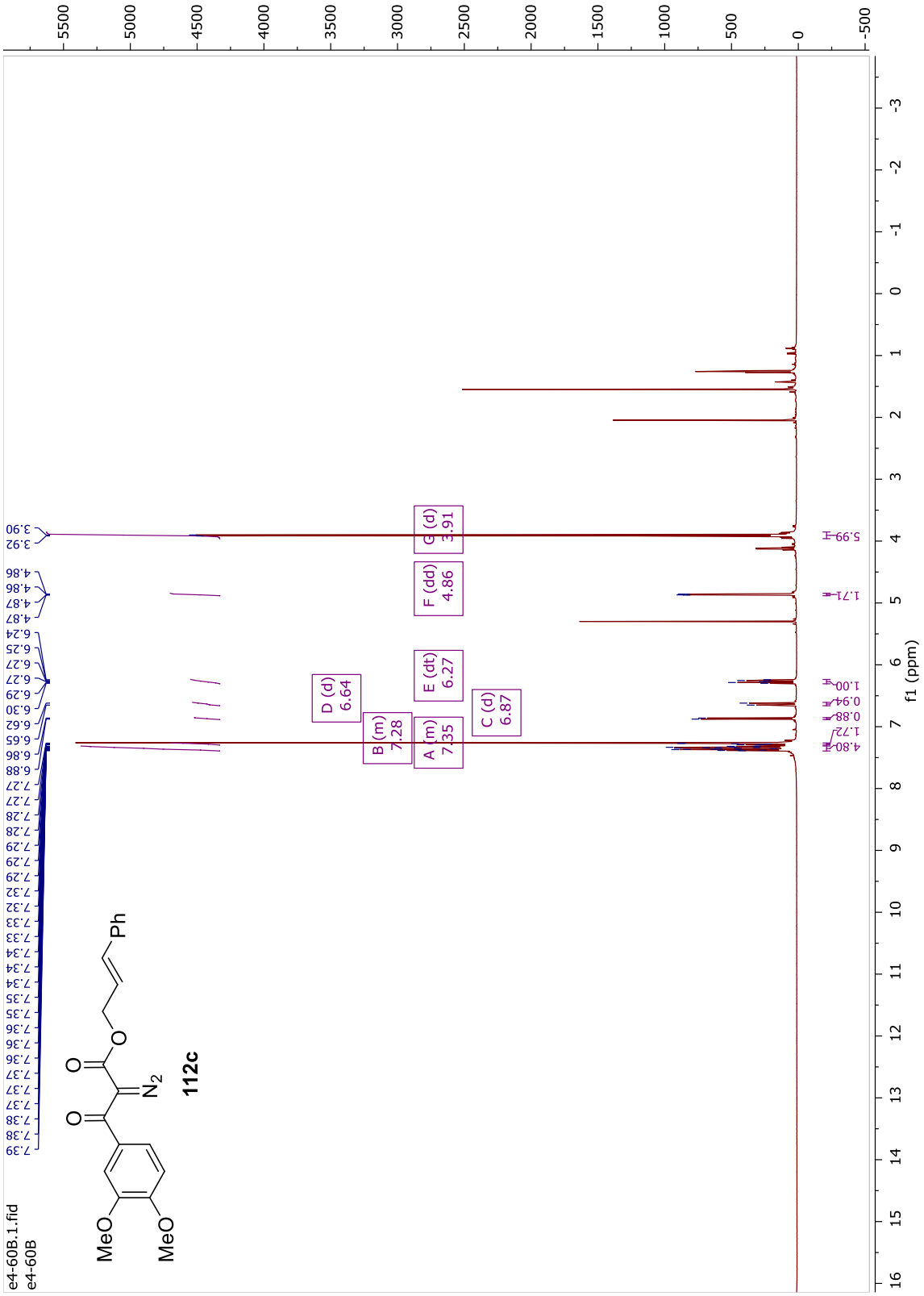
e4-60B.1.fid
e4-60B
MeO
MeO
O
O
O
N2
Ph
112c
A (m) 7.35
B (m) 7.28
C (d) 6.87
D (d) 6.64
E (dt) 6.27
F (dd) 4.86
G (d) 3.91
f1 (ppm)

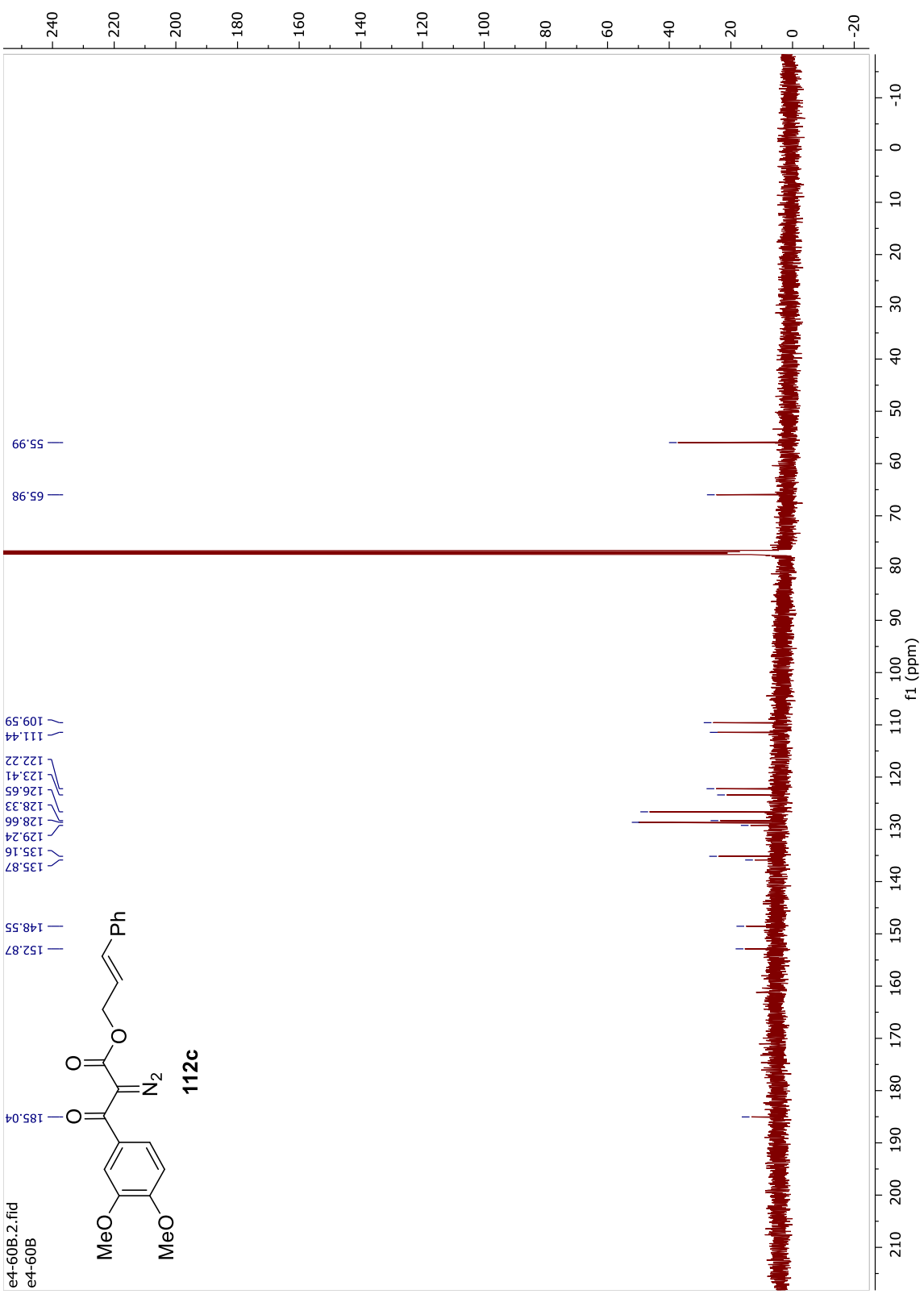
e4-60B.2.fid
e4-60B
185.04
152.87
148.55
135.87
135.16
129.24
128.66
128.33
126.65
123.41
122.22
111.44
109.59
65.98
55.99
MeO
MeO
O
O
O
O
N2
Ph
112c
f1 (ppm)

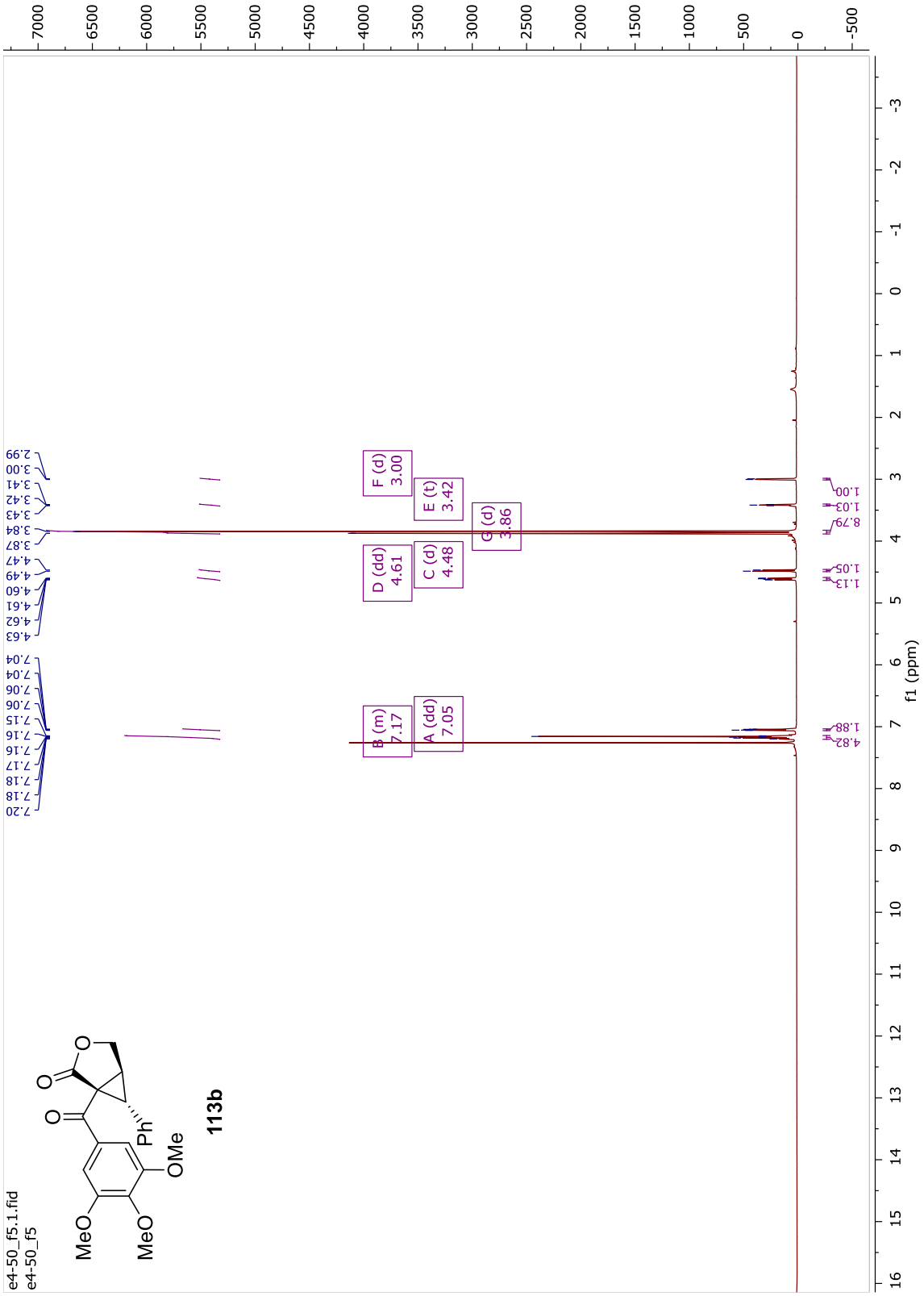
e4-50_f5.1.fid
e4-50_f5
MeO
MeO
OMe
Ph
O
O
O
113b
A (dd) 7.05
B (m) 7.17
C (d) 4.48
D (dd) 4.61
E (t) 3.42
F (d) 3.00
G (d) 3.86
1.88
4.82
1.05
1.13
1.03
1.00
8.79
f1 (ppm)

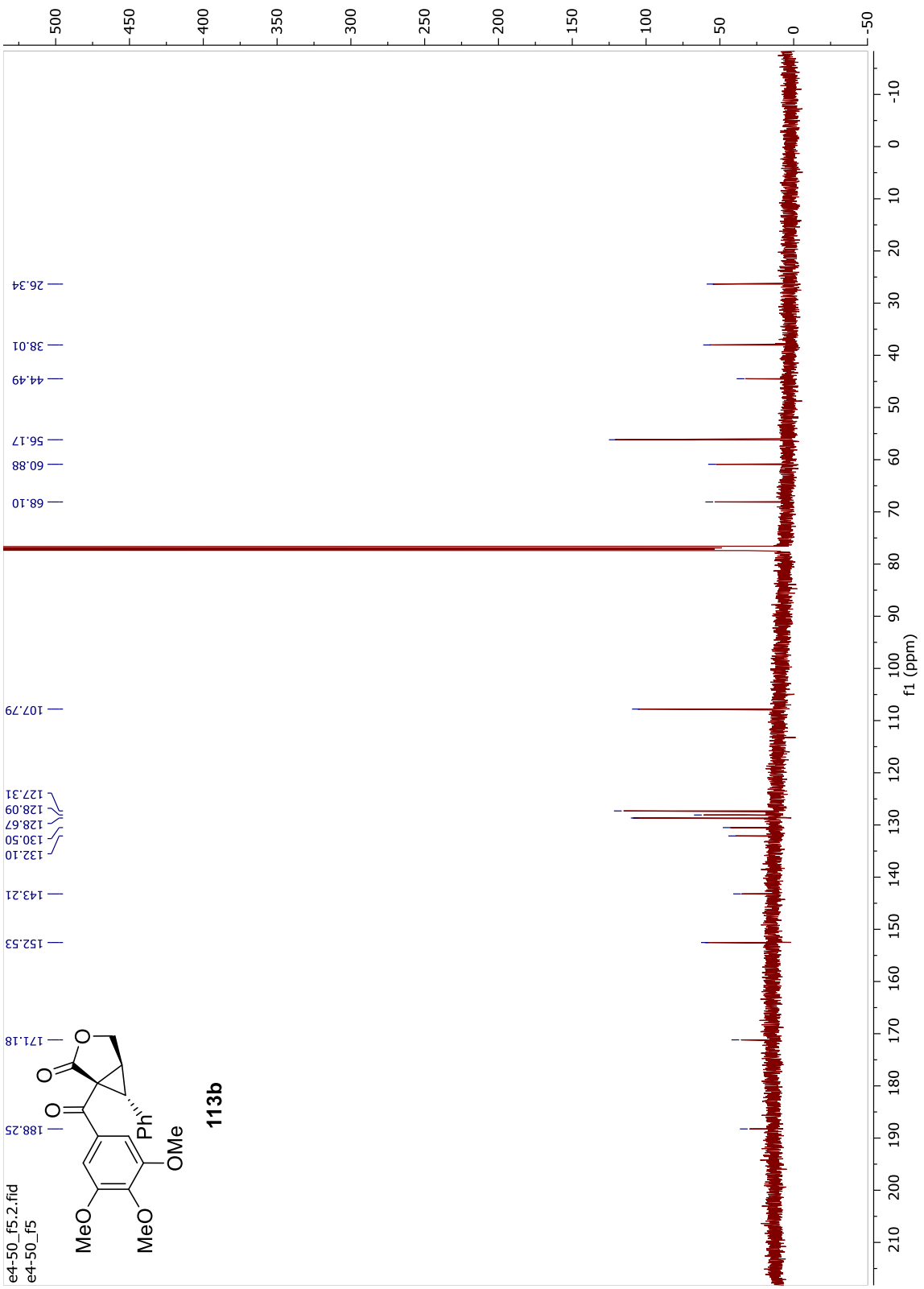
e4-50_f5.2.fid
e4-50_f5
188.25
171.18
152.53
143.21
132.10
130.50
128.67
128.09
127.31
107.79
68.10
60.88
56.17
44.49
38.01
26.34
MeO
MeO
OMe
Ph
O
O
O
113b
f1 (ppm)

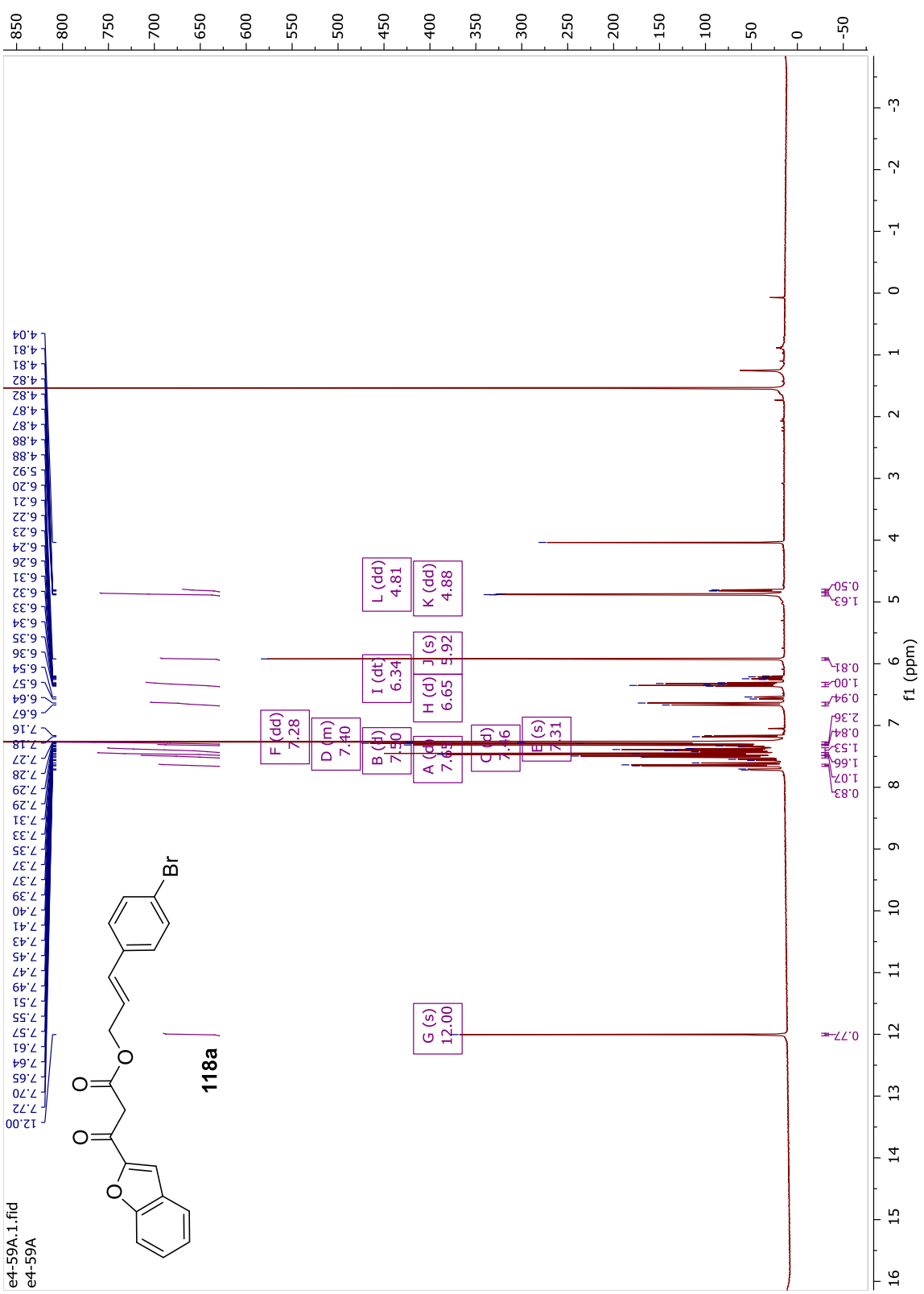
e4-59A.1.fid
e4-59A
118a
Br
O
O
O
O
G (s) 12.00
A (d) 7.63
B (d) 7.50
D (m) 7.40
F (dd) 7.28
I (dt) 6.34
H (d) 6.65
J (s) 5.92
L (dd) 4.81
K (dd) 4.88
f1 (ppm)

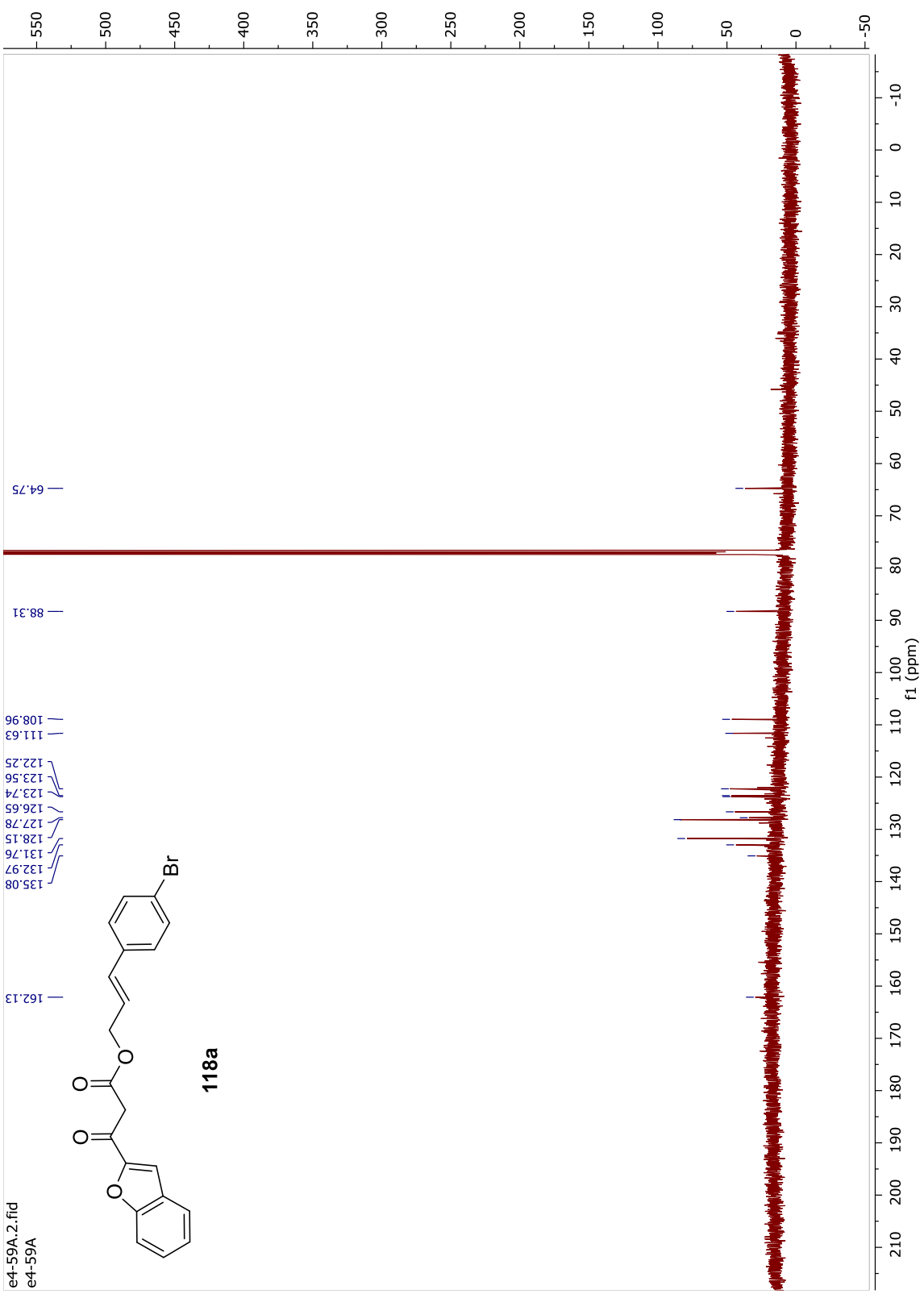
e4-59A.2.fid
e4-59A
118a
Br
O
O
O
O
162.13
135.08
132.97
131.76
128.15
127.78
126.65
123.74
123.56
122.25
111.63
108.96
88.31
64.75
f1 (ppm)

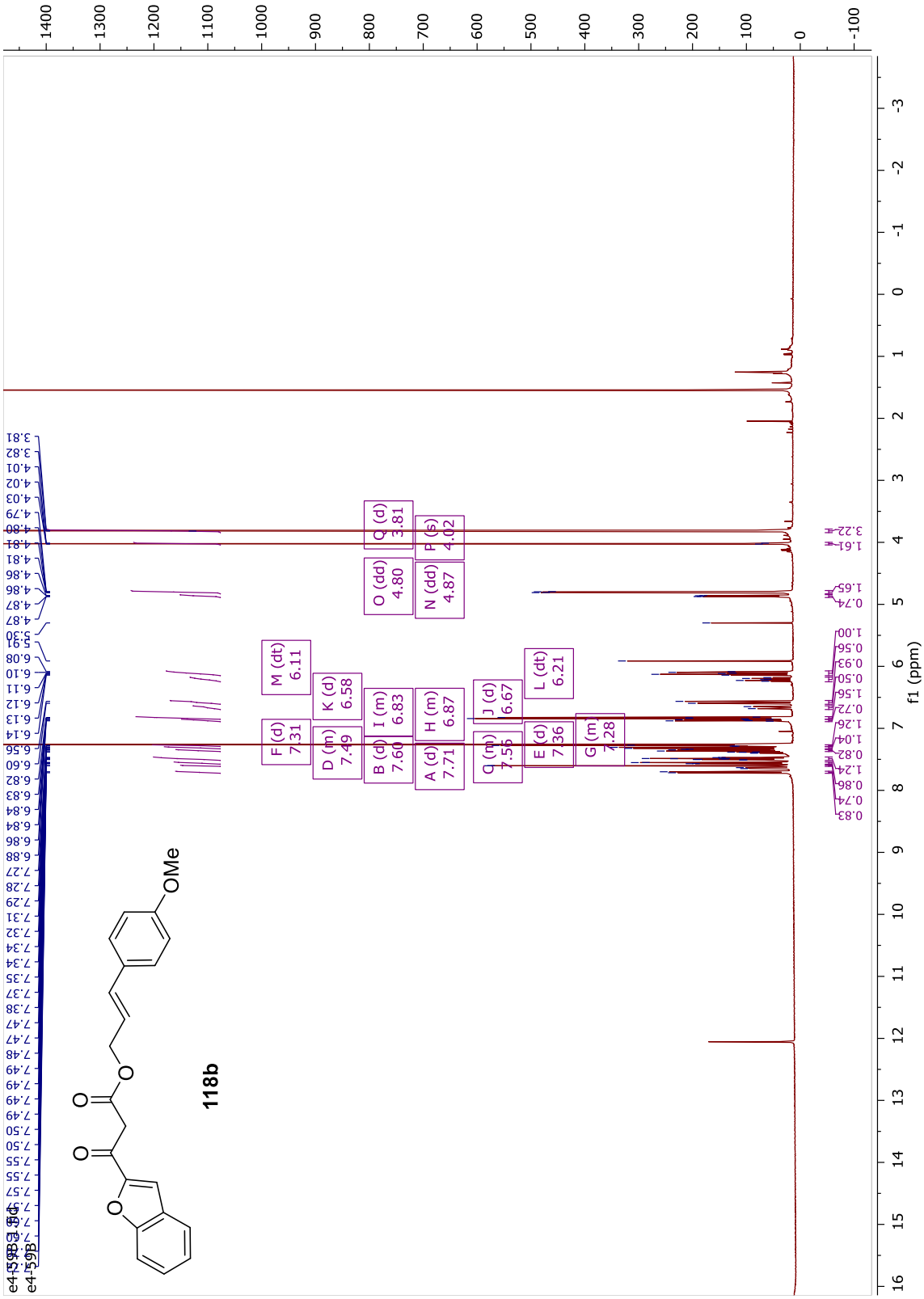
118b
OMe
O
O
O
A (d) 7.71
B (d) 7.60
D (m) 7.49
E (d) 7.36
F (d) 7.31
G (m) 7.28
H (m) 6.87
I (m) 6.83
J (d) 6.67
K (d) 6.58
L (dt) 6.21
M (dt) 6.11
N (dd) 4.87
O (dd) 4.80
P (s) 4.02
Q (d) 3.81
Q (m) 7.56
f1 (ppm)

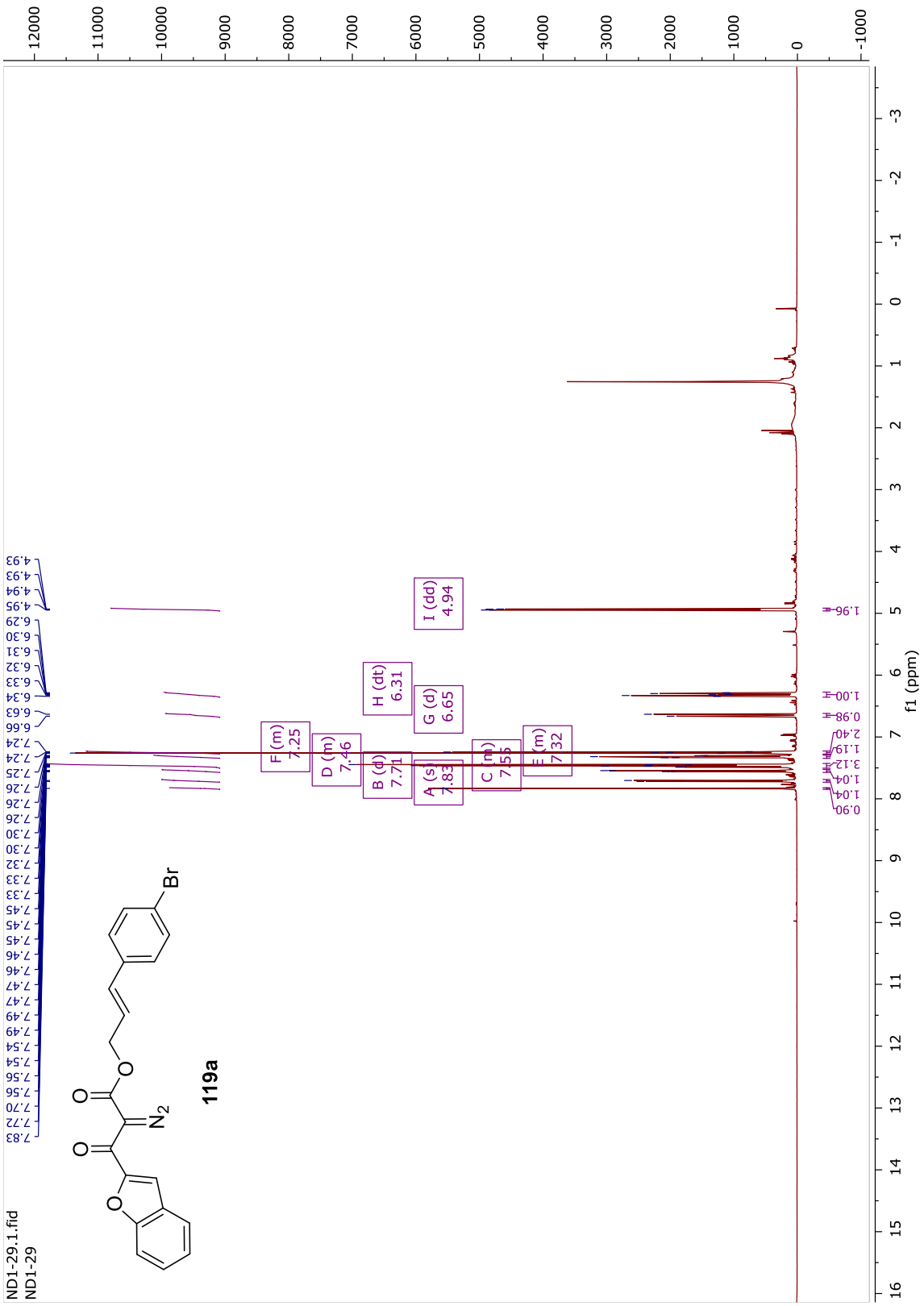
ND1-29.1.fid
ND1-29
119a
A (s) 7.83
B (d) 7.71
C (m) 7.55
D (m) 7.46
E (m) 7.32
F (m) 7.25
G (d) 6.65
H (dt) 6.31
I (dd) 4.94
f1 (ppm)

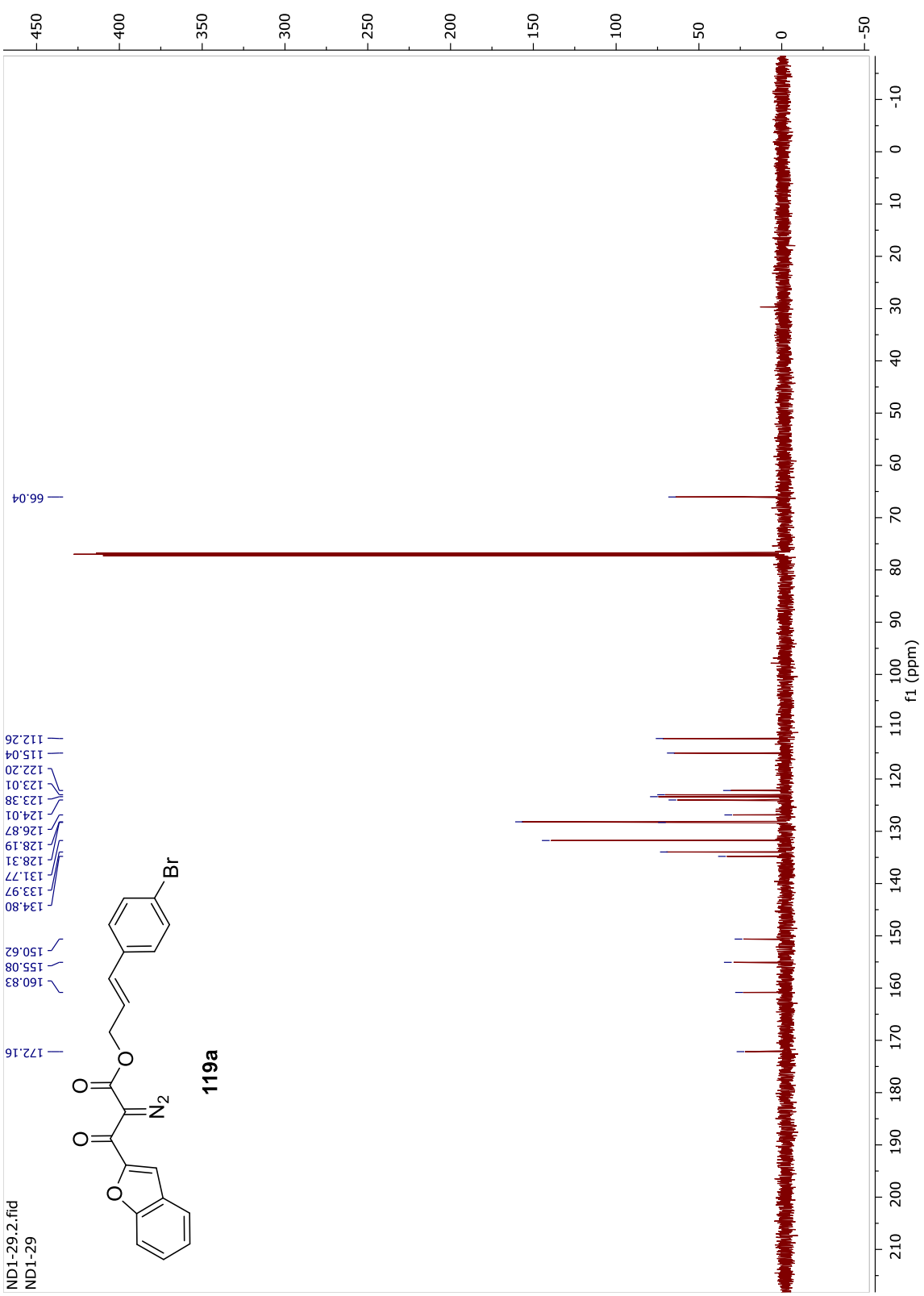
ND1-29.2.fid
ND1-29
119a
Br
O
O
O
O
N2
172.16
160.83
155.08
150.62
134.80
133.97
131.77
128.31
128.19
126.87
124.01
123.38
123.01
122.20
115.04
112.26
66.04
f1 (ppm)

5.8 References

(1) Selected examples: (a) Smith, A.G.; Slade, M.C.; Johnson, J.S. Cyclopropane−Aldehyde Annulations at Quaternary Donor Sites: Stereoselective Access to Highly Substituted Tetrahydrofurans. *Org. Lett.* **2011**, *13*, 1996-1999. (b) Xu, X.; Lu, H.; Ruppel, J.V.; Cui, X.; Lopez de Mesa, S.; Wojtas, L.; Zhang, X.P. Highly Asymmetric Intramolecular Cyclopropanation of Acceptor-Substituted Diazoacetates by Co(II)-Based Metalloradical Catalysis: Iterative Approach for Development of New-Generation Catalysts. *J. Am. Chem. Soc.* **2011**, *133*, 15292-15295. (c) Hung, H.-H.; Liao, Y.-C.; Liu, R.-S. Silver-Catalyzed Stereoselective [3+2] Cycloadditions of Cyclopropyl-Indanimines with Carbonyl Compounds. *Adv. Synth. Catal.* **2013**, *355*, 1545-1552. (d) Takada, S.; Iwata, K.; Yubune, T.; Nishii, Y. Stereoselective oxy-homo-Michael reactions of enantioenriched bicyclic donor–acceptor cyclopropanes to afford optically active *trans*-α,β-disubstituted γ-butyrolactones possessing three serial chiral centers. *Tetrahedron Lett.* **2016**, *57*, 2422-2425. (e) Yang, P.; Shen, Y.; Feng, M.; Yang, G.; Chai, Z. Lewis Acid Catalyzed [3+2] Annulation of γ-Butyrolactone Fused Cyclopropane with Aldehydes/Ketones. *Eur. J. Org. Chem.* **2018**, *2018*, 4103-4112. (f) Feng, M.; Yang, P.; Yang, G.; Chen, W.; Chai, Z. $FeCl_3$-Promoted [3 + 2] Annulations of γ-Butyrolactone Fused Cyclopropanes with Heterocumulenes. *J. Org. Chem.* **2018**, *83*, 174-184. (g) Shen, Y.; Yang, P.; Yang, G.; Chen, W.; Chai, Z. Lewis acid-catalyzed enantiospecific [3 + 2] annulations of γ-butyrolactone fused cyclopropanes with aromatic aldehydes: synthesis of chiral furanolignans. *Org. Biomol. Chem.* **2018**, *16*, 2688-2696.

(2) Pohlhaus, P.D.; Sanders, S.D.; Parsons, A.T.; Li, W.; Johnson, J.S. Scope and Mechanism for Lewis Acid-Catalyzed Cycloadditions of Aldehydes and Donor-Acceptor Cyclopropanes: Evidence for a Stereospecific Intimate Ion Pair Pathway. *J. Am. Chem. Soc.* **2008**, *130*, 8642–8650.

(3) Parsons, A.T.; Johnson, J.S. Catalytic Enantioselective Synthesis of Tetrahydrofurans: A Dynamic Kinetic Asymmetric [3+2] Cycloaddition of Racemic Cyclopropanes and Aldehydes. *J. Am. Chem. Soc.* **2009**, *131*, 3122–3123.

(4) Newhouse, T.R.; Kaib, P.S.J.; Gross, A.W.; Corey, E.J. Versatile Approaches for the Synthesis of Fused-Ring γ-Lactones Utilizing Cyclopropane Intermediates. *Org. Lett.* **2013**, *15*, 1591-1593.

(5) (a) Takada, S.; Iwata, K.; Yubune, T.; Nishii, Y. Stereoselective oxy-homo-Michael reactions of enantioenriched bicyclic donor–acceptor cyclopropanes to afford optically active *trans*-α,β-disubstituted γ-butyrolactones possessing three serial chiral centers. *Tetrahedron Lett*. **2016**, *57*, 2422-2425. (b) Kimura, Y.; Sone, Y.; Saito, T.; Mochizuki, T.; Nishii, Y. An Asymmetric Total Synthesis of Tupichilignan A using Donor–Acceptor Cyclopropanes: A Structural Revision of Tupichilignan A. *Asian J. Org. Chem.* **2017**, *6*, 977-980. (c) Sasazawa, K.; Takada, S.; Yubune, T.; Takaki, N.; Ota, R.; Nishii, Y. Stereochemical Courses and Mechanisms of Ring-opening Cyclization of Donor-Acceptor Cyclopropylcarbinols and Cyclization of 7-Benzyloxy Dibenzyl Lignan Lactones. *Chem. Lett.* **2017**, *46*, 524-526. (d) Takada, S.; Saito, T.; Iwata, K.; Nishii, Y. Copper-Catalyzed 1,5-Addition of Grignard reagents to Enantioenriched Donor–Acceptor Cyclopropanes with Inversion. *Asian J. Org. Chem.* **2016**, *5*, 1225-1229.

(e) Sone, Y.; Kimura, Y.; Ota, R.; Mochizuki, T.; Ito, J.; Nishii, Y. Catalytic Hydrogenolysis of Enantioenriched Donor–Acceptor Cyclopropanes Using H_2 and Palladium on Charcoal. *Eur. J. Org. Chem.* **2017**, *2017*, 2842-2847.

(6) Shenje, R. STRAINED CARBOCYCLES AS GATEWAYS TO POLYCYCLIC MOLECULAR SCAFFOLDS AND NATURAL PRODUCT TARGETS. Doctoral Thesis, **2016.**

(7) De Simone, F.; Andrès, J.; Torosantucci, R.; Waser, J. Catalytic Formal Homo-Nazarov Cyclization. *Org. Lett.* **2009**, *11*, 1023-1026.

(8) Phun, L.H.; Patil, D.V.; Cavitt, M.A.; France, S. A catalytic homo-Nazarov cyclization protocol for the synthesis of heteroaromatic ring-fused cyclohexanones. *Org. Lett.* **2011**, *13*, 1952-1955.

(9) Sandridge, M.J.; France, S. Calcium-Catalyzed, Dehydrative, Ring-Opening Cyclizations of Cyclopropyl Carbinols Derived from Donor−Acceptor Cyclopropanes. *Org. Lett.* **2016**, *18*, 4218−4221.

(10) Takada, S.; Takaki, N.; Yamada, K. Nishii, Y. A formal homo-Nazarov cyclization of enantioenriched donor–acceptor cyclopropanes and following transformations: asymmetric synthesis of multi-substituted dihydronaphthalenes. *Org. Biomol. Chem*. **2017**, *15*, 2443–2449.

(11) Begouin, J.-M.; Niggemann, M. Calcium-Based Lewis Acid Catalysts. *Chem. Eur. J.* **2013**, *19*, 8030-8041.

(12) Comins, D.L.; Dehghani, A. Pyridine-Derived Triflating Reagents: An Improved Preparation of Vinyl Triflates from Metallo Enolates. *Tetrahedron Lett.* **1992**, *33*, 6299–6302.

(13) Baum, J.S.; Shook, D.A.; Davies, H.M.L.; Smith, H.D. Diazotransfer Reactions with *p*-Acetamidobenzenesulfonyl Azide. *Synth. Comm.* **1987**, *17*.

(14) Sandridge, M.J. DEHYDRATIVE CYCLIZATIONS VIA ACID CATALYSIS AS A METHOD FOR MOLECULAR DIVERSITY. Doctoral Thesis, **2018.**

(15) Williams, C.W. NOVEL (HOMO-)NAZAROV APPROACHES TO COMPLEX POLYCYCLES AND APPLICATION TO BIOACTIVE TARGETS. Doctoral Thesis, **2018**.

(16) Huang, X.; Fulton, B.; White, K.; Bugarin, A. Metal-Free, Regio- and Stereoselective Synthesis of Linear (*E*)-Allylic Compounds Using C, N, O, and S Nucleophiles. *Org. Lett.* **2015**, *17*, 2594-2597.

(17) Liu, J.; Dong, K.; Franke, R.; Neumann, H.; Jackstell, R.; Beller, M. Selective Palladium-Catalyzed Carbonylation of Alkynes: An Atom-Economic Synthesis of 1,4-Dicarboxylic Acid Diesters. *J. Am. Chem. Soc.* **2018**, *140*, 10282-10288.

(18) Youn, S.W.; Kim, B.S.; Jagdale, A.R. Pd-Catalyzed Sequential C–C Bond Formation and Cleavage: Evidence for an Unexpected Generation of Arylpalladium(II) Species. *J. Am. Chem. Soc.* **2012**, *134*, 11308-11311.

(19) Ortega, V.; del Castillo, E.; Csákÿ, A.G. Transition-Metal-Free Stereocomplementary Cross-Coupling of Diols with Boronic Acids as Nucleophiles. *Org. Lett.* **2017**, *19*, 6236-6239.

(20) Liu, P.; Yasir, M.; Ruggi, A.; Kilbinger, A.F.M. Heterotelechelic Polymers by Ring-Opening Metathesis and Regioselective Chain Transfer. *Angew. Chem. Int. Ed.* **2018**, *57*, 914-917.

(21) Talwar, D.; Wu, X.; Saldi, O.; Salguero, N.P.; Xiao, J. Versatile Iridicycle Catalysts for Highly Efficient and Chemoselective Transfer Hydrogenation of Carbonyl Compounds in Water. *Chem. Eur. J.* **2014**, *20*, 12835-12842.

(22) Krätzschmar, F.; Kaßel, M.; Delony, D.; Breder, A. Selenium-Catalyzed C(sp^3)-H Acyloxylation: Application in the Expedient Synthesis of Isobenzofuranones. *Chem. Eur. J.* **2015**, *21*, 7030-7034.

(23) Pan, D.; Chen, A.; Su, Y.; Zhou, W.; Li, S.; Jia, W.; Xiao, J.; Liu, Q.; Zhang, L.; Jiao, N. Ligand-Free Pd-Catalyzed Highly Selective Arylation of Allylic Esters with Retention of the Traditional Leaving Group. *Angew. Chem. Int. Ed.* **2008**, *47*, 4729-4732.

(24) Song, T.; Arseniyadis, S.; Cossy, J. Highly Enantioselective, Base-Free Synthesis of α-Quaternary Succinimides through Catalytic Asymmetric Allylic Alkylation. *Chem. Eur. J.* **2018**, *24*, 8076-8080.

CHAPTER 6. EFFORTS TOWARD THE TOTAL SYNTHESES OF RHAZINICINE AND TRONOCARPINE

6.1 Efforts Toward Rhazinicine

As mentioned in Chapter 4, rhazinicine is an anti-tumor natural product that has inspired several total syntheses and tetrahydroindolizine (THI) methodology studies. In 2016, Cavitt and France published a method analogous to the Friedel-Crafts-type ring-opening cyclization of *N*-acyl indole DACPs, whereby *N*-acyl pyrrole DACP **121** ring-opens in the presence of catalytic $Al(OTf)_3$ to form THI scaffold **122** diastereoselectively (Scheme 6-1).[1] This process is significantly milder and greener than previously published conditions. It also represents the culmination of a generalized method to form fused, polycyclic nitrogen-containing heterocycles from *N*-acyl DACPs.

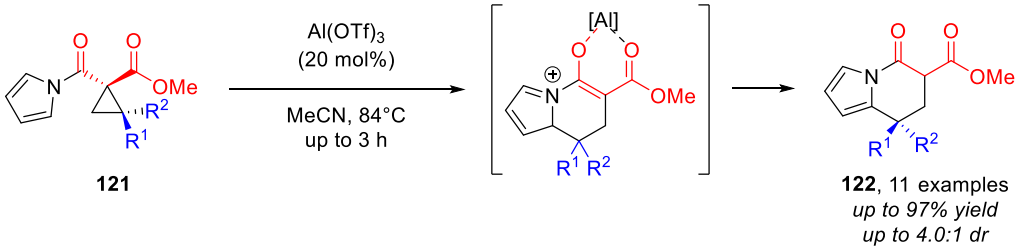

Scheme 6-1: Diastereoselective ring-opening cyclization of *N*-acyl pyrrole DACPs to THIs.

6.1.1 First Synthetic Approach to Rhazinicine

Cavitt's retrosynthetic analysis of rhazicinine is shown in Scheme 6-2.[2] The final step would be a Suzuki cross-coupling to form the 9-membered lactam. 2-Iodoacetanilide precursor **123** would arise from a Krapcho decarboxylation and amidation of the methyl ester moiety in THI **124**, which would be prepared through the ring-opening cyclization of

pyrrole-tethered *N*-acyl DACP **125**. This DACP **125** would be prepared through the cyclopropanation of *N*-acyl diazo precursor **126** and 1,1-disubstituted terminal alkene **127** containing the requisite ethyl and pendant methyl ester functional groups.

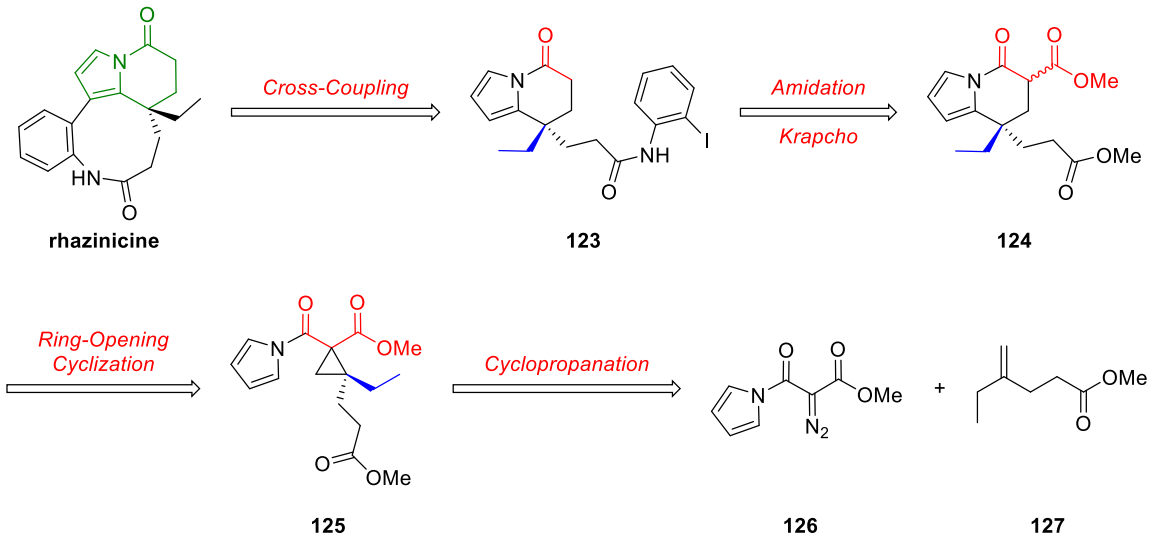

Scheme 6-2: Cavitt's retrosynthetic analysis of rhazinicine.

Early work in the synthesis was promising. Literature protocols furnished efficient routes to both **126** and **127**.[3] Then, the cyclopropanation was extensively optimized by Cavitt to afford **125** in 52% yield, and the subsequent ring-opening cyclization under the published $Al(OTf)_3$ catalysis yielded the desired adduct **124** in 63% yield. The Krapcho decarboxylation to intermediate **128** was achieved at an excellent 90% yield.[2]

6.1.2 Optimizations for First Synthetic Approach to Rhazinicine

Then, I pursued several routes for the subsequent amidation with 2-iodoaniline. First, hydroxy bases were screened for a saponification to acid precursor **129** (Table 6-1). Sodium hydroxide was ultimately selected as the optimal base, despite a modest 61% yield (entries 1, 7).

Table 6-1: Optimization of rhazinicine saponification.

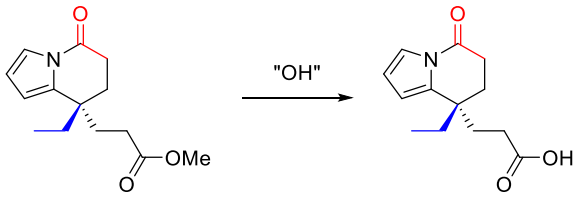

128 **129**

Entry	Base (equiv)	Solvent (conc.)	T (°C)	Result
1	NaOH (1.2)[a]	MeOH (1 M)	50	61%
2	KOH (3)[b]	THF (30%/H_2O)	r.t.	No reaction
3	NaOH (1.5)[a]	MeOH (1 M)	50	Low conversion
4	LiOH·H_2O (8)[c]	MeOH (0.25 M), THF (0.25 M)	r.t.	Low conversion
5	NaOH (1.2)[a]	IPA (1 M)	50	Low conversion
6	TMSI (5)	$CHCl_3$ (0.3 M)	80	Degradation
7	NaOH (1.5)[a]	MeOH (1 M)	50	57%

[a] 1.7 M in H_2O. [b] 85% in H_2O. [c] 2 M in H_2O.

Then, the amidation of acid **129** with 2-iodoaniline (**130**) was attempted (Table 6-2). EDC, a traditional peptide coupling agent, did not afford any desired product (entries 1, 2); however, Mukaiyama's reagent performed well here, and the 2-iodoacetanilide **123** was prepared in 35% yield (entry 3).

Table 6-2: Optimization of rhazinicine amidation.

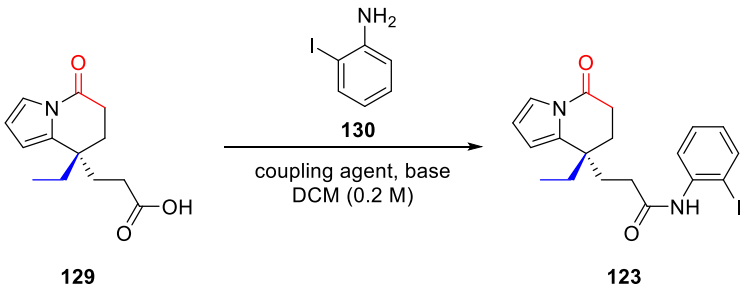

Entry	Aniline equiv	CA (equiv)	Base (equiv)	Result
1	2	EDCI (1.5)	DMAP (0.1)	No reaction
2	2	EDCI·HCl (1.5)	DMAP (0.1)	No reaction
3	5.5	Mukaiyama (1.2)	Et_3N (2.1)	35%

Given the modest yields of the stepwise approach, a direct amidation of methyl ester **128** was attempted (Table 6-3). Unfortunately, Weinreb conditions did not afford any desired amide (entries 1-3), and a literature protocol employing potassium *tert*-butoxide (*t*-BuOK) was similarly ineffective (entry 4).[4]

Table 6-3: Attempts at direct amidation of methyl ester precursor.

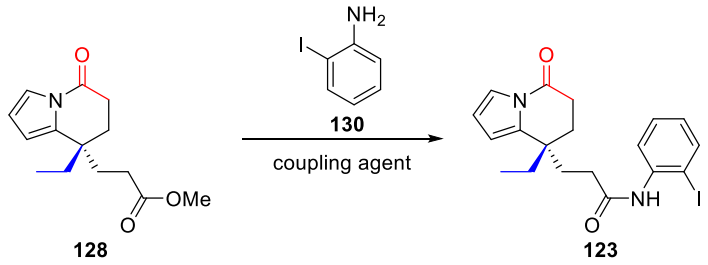

Entry	Aniline equiv	CA (equiv)	Solvent (conc, T)	Result
1	1	Me_3Al (1.2)	PhMe (0.9 M, reflux)	No desired product
2	1	Me_3Al (1.2)	PhMe (0.9 M, reflux)	No desired product[a]
3	1.6	Me_3Al (1.6)	DCE (0.25 M, r.t. to reflux)	Complex mixture
4	1	*t*-BuOK (2)	THF (0.08 M, r.t.)	No desired product

[a] Used a fresh bottle of Me_3Al.

Finally, as it was expected that protection of acetanilide **123** would be necessary to facilitate the final coupling step, several protection protocols employing methoxymethyl chloride (MOMCl, entries 1-3) and benzyl bromide (BnBr, entries 4-6) were attempted with **130** (Table 6-4). All of these, unfortunately, were unsuccessful, which prevented a shorter synthetic route.

Table 6-4: Attempts at 2-iodoaniline protection.

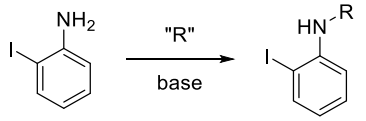

130 **131**

Entry	R-X (equiv)	Base (equiv)	Result
1	MOMCl (1.5)	KH (1.2)[a]	Complex mixture
2	MOMCl (1.1)	DIPEA (6.5)	Complex mixture
3	MOMCl (4)	NaH (4)	Complex mixture
4	BnBr (1.1)	Et_3N (1.2)	No reaction
5	BnBr (1.1)	NaH (1.1)	No reaction
6	BnBr (1.5)	NaH (3)	No reaction

[a] Added TMEDA (1.2 equiv).

At this stage, it was necessary to prepare gram-scale quantities of DACP precursor **125** to push the synthesis to the final coupling step (Table 6-3). Unfortunately, the cyclopropanation yield suddenly plummeted from 50% to 5%. This was initially attributed to difficulties purifying alkene precursor **127**, so sequential distillations were performed to make the alkene as clean as possible. Despite ^{1}H NMR validation that there were no residual impurities in **127**, and despite careful monitoring and purification of the reaction in subsequent attempts, the cyclopropanation remained low-yielding.

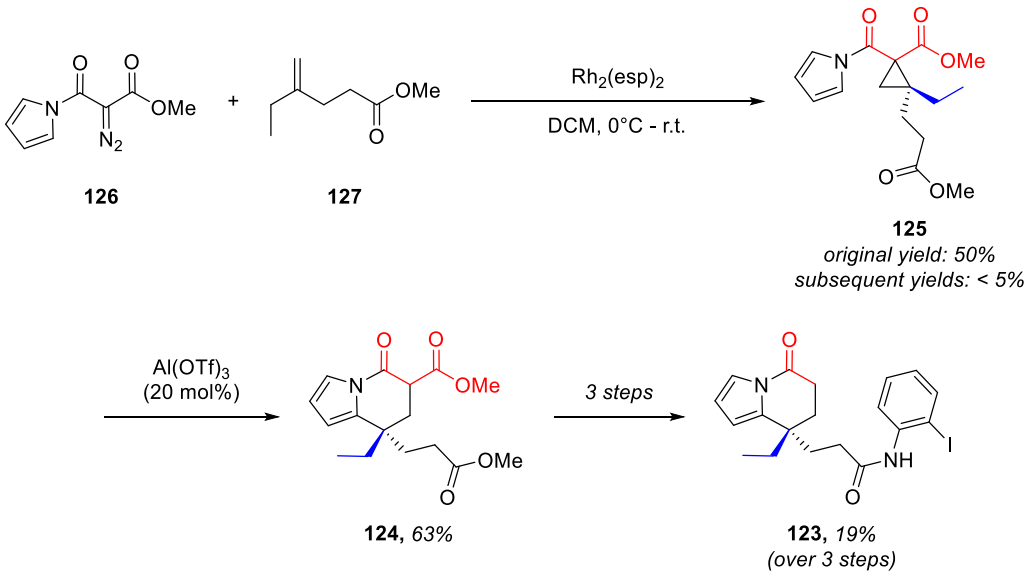

Scheme 6-3: Abbreviated progress toward first synthetic approach to rhazinicine.

6.1.3 Optimizing the Alkene Precursor

Desirous to both improve cyclopropanation yields and avoid any future challenges from the alkene, two different alkene precursors were synthesized. First, a benzyl-protected 2-iodoanilide substrate **132** was evaluated since early incorporation of the aniline moiety would both contribute mass and make the total synthesis more convergent (Scheme 6-4a). Cavitt had previously prepared **132** *via* a two-step route.[5] First, acid precursor **133** was converted to an acid chloride under Swern conditions, followed by a triethylamine-promoted amidation with **130** to prepare intermediate **134** (75% yield). Then, treatment with benzyl bromide furnished **132** (79% yield). Afterwards, I subjected **126** and **132** to typical intermolecular cyclopropanation conditions (Scheme 6-4b), but the resulting reaction mixture was complex and showed no evidence of desired product **135** by NMR.

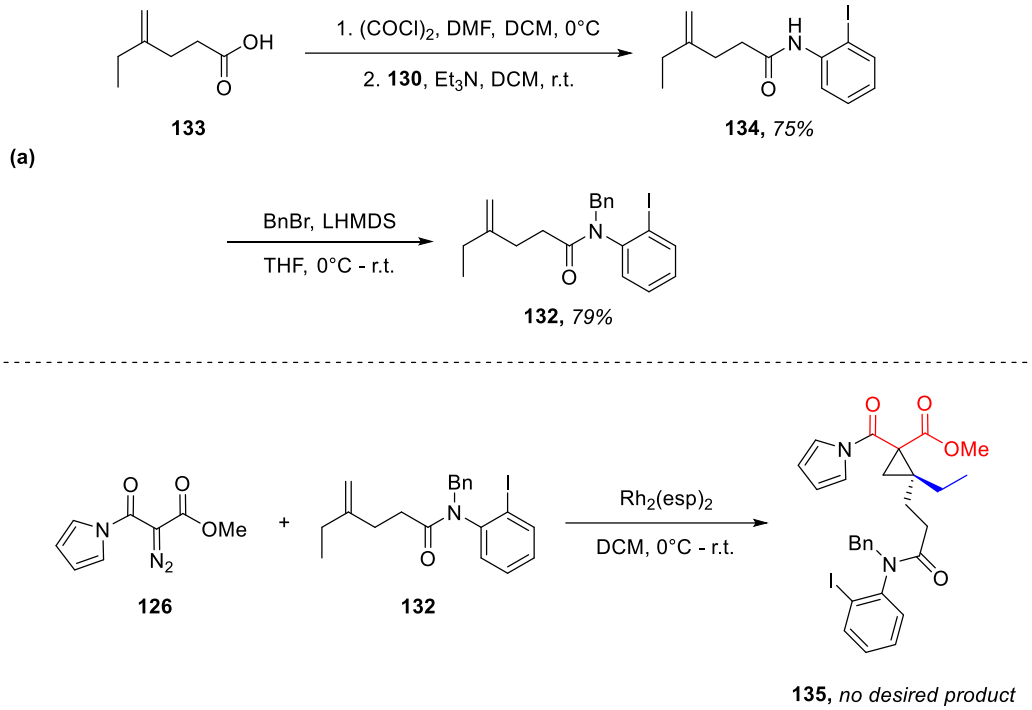

Scheme 6-4: (a) Synthesis of 2-iodoanilide alkene precursor. (b) Failed cyclopropanation.

Next, a benzyl ester precursor **136** was prepared in short order *via* a mixed anhydride synthesis followed by displacement with benzyl alcohol (Scheme 6-5). Initial results were promising, as the esterification was efficient and the product **136**, much more shelf-stable than methyl ester **125**.

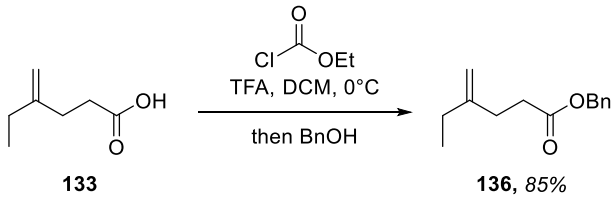

Scheme 6-5: Synthesis of benzyl ester alkene precursor.

Despite extensive optimizations, however, the cyclopropanation yield for DACP **137** was modest (Table 6-5). Temperature displayed prominent influence on the reaction outcome, as reactivity was slow at 0°C but quickly funneled **133** to degradation products

at room temperature (entries 1-3). The first noticeable increase occurred with an increase in loading of **136** (entry 4); slow addition of **133** did not make a positive difference (entry 5). Increasing the loading of **136** continued to drive the yield up (entries 6-8). Finally, it was found that 5 equiv. was a sufficient concentration of **136** to hinder degradation of **133**, and allowing the reaction to stir for 3 hours at room temperature provided the best yield at 39%. Moreover, the stability of **136** on silica column enabled facile recovery of the excess during reaction purification.

Table 6-5: Optimization of rhazinicine cyclopropanation with benzyl ester-functionalized alkene.

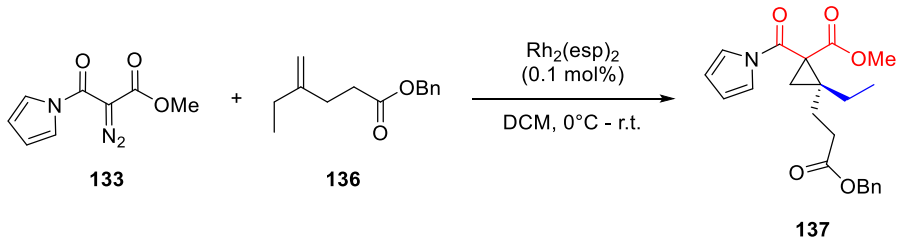

Entry	Alkene equiv	Temp./Time	Yield
1	1.3	0°C 10 min, then r.t. 30 min	9%
2	1.3	0°C 10 min, then r.t. 15 min	13%
3	1.3	0°C 3 h, then r.t. 3 h	10%
4	2	0°C 4 h, then r.t. 30 min	21%
5	1.3	0°C 30 min[a]	11%
6	2	0°C 30 min, r.t. 30 min	19%
7	5	0°C 30 min, r.t. 30 min	33%
8	5	0°C 60 min, r.t. 30 min	33%
9	5	0°C 10 min, r.t. 3 h	39%

[a] Slow-added diazo over 10 min.

Though this cyclopropanation yield was low compared to the original 52% with DACP **125**, the acquired cyclopropane was carried forward to the ring-opening cyclization,

which unfortunately fared little better (Table 6-6). Adduct **138** was ultimately prepared at 37% optimal yield, a far cry from the previously achievable 63%.

Table 6-6: Optimization of rhazinicine ring-opening cyclization from benzyl precursor.

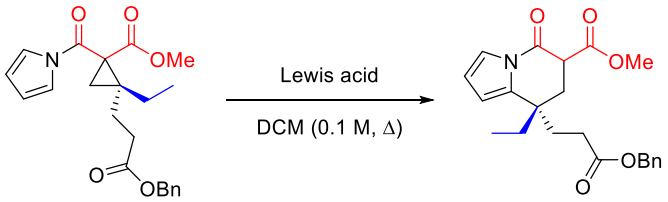

137 **138**

Entry	Lewis acid (X mol%)	Result
1	$In(OTf)_3$ (30)	37%
2	$Al(OTf)_3$ (20)	29%[a]
3	$In(OTf)_3$ (30)	No reaction[b]
4	$Sc(OTf)_3$ (30)	No reaction[b]
5	$In(OTf)_3$ (30)	31%
6	$In(OTf)_3$ (20)	37%
7	$In(OTf)_3$ (10)	No reaction
8	$Bi(OTf)_3$ (20)	7%
9	$Sc(OTf)_3$ (20)	28%
10	$Al(OTf)_3$ (20)	No reaction
11	$InCl_3$ (20)	No reaction
12	$Ca(NTf_2)_2$/*n*-Bu_4NPF_6 (20)	No reaction

[a] Reaction performed in MeCN. [b] Reaction performed at r.t.

As a last-ditch effort, two additional alkenes and one ketone precursor were hypothesized. *t*-Butyl ester **139** was initially selected for its greater mass relative to **127** and for its lower steric profile and potentially simpler saponification compared to **133** (Scheme 6-6a). Traditional esterification conditions, however, did not afford the desired product. Next, perfluorophenyl ester **140** was considered, as recent literature has

showcased its highly electrophilic character, resulting facile cleavage to the acid, and low profile by ^{1}H NMR, but esterification with perfluorophenol (**141**) failed, as well (Scheme 6-6b). Finally, it was envisioned that the geminal di-substituted cyclopropane moiety could be introduced in a stepwise fashion by converting the alkene precursor to a ketone, performing a Knoevenagel condensation, and subsequently preparing the cyclopropane through Simmons-Smith conditions. Unfortunately, oxidative cleavage of **127** to ketone precursor **142** was unsuccessful (Scheme 6-6c).

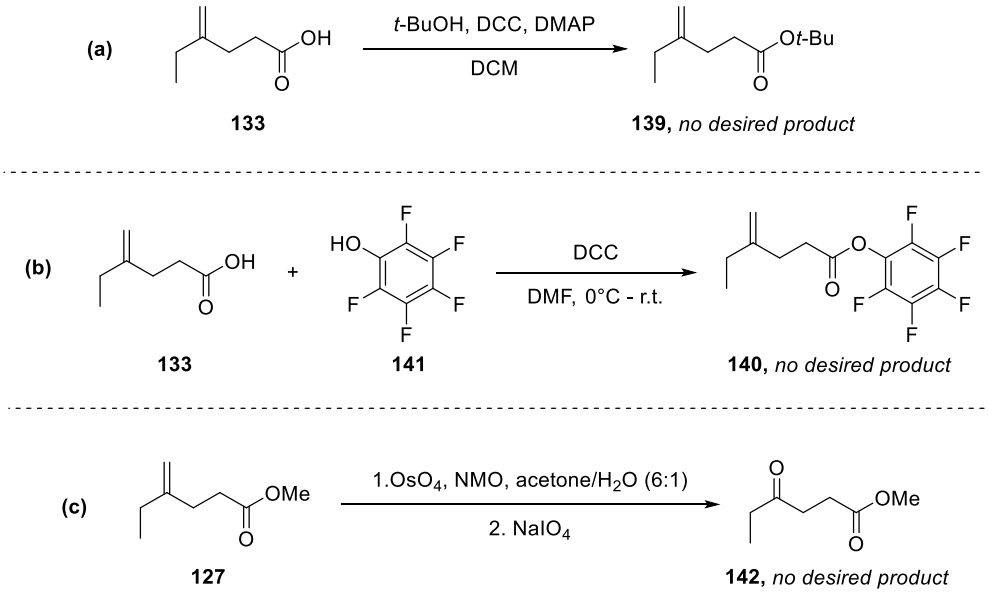

Scheme 6-6: Additional attempted syntheses of cyclopropane precursors. (a) *t*-Butyl ester. (b) Perfluorophenyl ester. (c) Knoevenagel precursor.

6.2 Efforts Toward Tronocarpine

Additional efforts were expended toward a targeted synthesis of tronocarpine that would build the bicyclic moiety incrementally through a key ring-opening cyclization method previously studied by France lab. This is in contrast to the desired pathway that would install the bicylic moiety during the ring-opening cyclization step, but was believed to be workable due to earlier success with Friedel-Crafts-type ring-opening cyclizations of

N-acyl indole-tethered DACPs.[3,6] Two distinct approaches were pursued: first, an intermolecular cyclopropanation with an alkene containing the appropriate functional handles for further annulations; and second, the nucleophilic addition of a 3-substituted indole onto the lactone moiety of a C5-substituted D-A oxabicyclo[3.1.0]hexane. Both approaches would be followed by a Lewis acid-catalyzed ring-opening cyclization to form the hydropyrido[1,2-*a*]indole core of tronocarpine.

6.2.1 Intermolecular Cyclopropanation Approach

The retrosynthetic analysis for the first approach is shown in Scheme 6-7. Tronocarpine would be prepared from a lactamization after deprotecting precursor **143**. Base-mediated annulation would occur from advanced intermediate **144**, which would arise from a Horner-Wadsworth-Emmons (HWE) reaction of aldehyde **145**. The aldehyde would be formed from a deprotection and oxidation of **146**, the Krapcho decarboxylation product of **147**. This adduct would be prepared *via* a ring-opening cyclization of DACP **148**, and cyclopropanation of diazo **149** and alkene **150** would afford the cyclopropane.

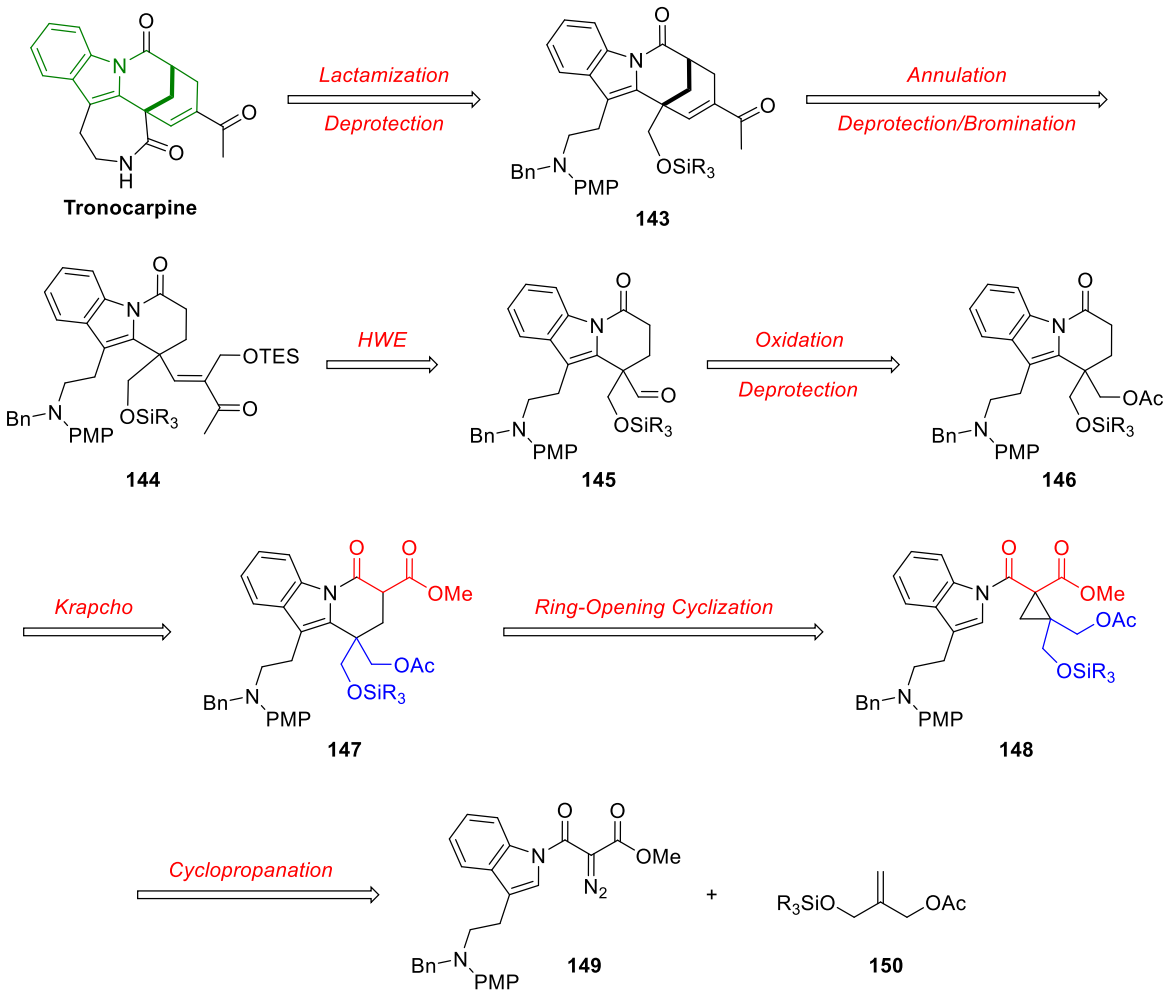

Scheme 6-7: Proposed retrosynthetic analysis for tronocarpine.

To model this process, 3-methylindole (**59**) was selected for the *N*-acyl-tethered nucleophile. Synthesis of malonate **151** was high-yielding (98%), and the diazo transfer to **152** had excellent yield as expected (93%). Then, two different mono-silyl protections of commercially available 2-methylene-1,3-propanediol (**56**) were effected: TBDPS (**55a**, 89%) and TBS (**153**, 80%). The subsequent acetate protections proceeded in quantitative yield for both (TBDPS: **150a**; TBS: **150b**).

Several cyclopropanation conditions were explored, starting with **152** and **150a** (Table 6-7). Standard conditions afforded a complex mixture of inseparable products,

including diazo starting material (entries 1-2), and it was found early on that increases in temperature decreased the overall reaction time but unfortunately did not clean up the resulting reaction mixture or appreciably generate more desired product (entries 3-5). Hypothesizing that the TBDPS protecting group could be sterically hindering the intermolecular interaction, alkene **150b** was tested under standard conditions (entry 6). Although the reaction mixture remained complex, 6% of desired product **154b** was successfully isolated by silica preparatory TLC.

Table 6-7: Test conditions for intermolecular cyclopropanation.

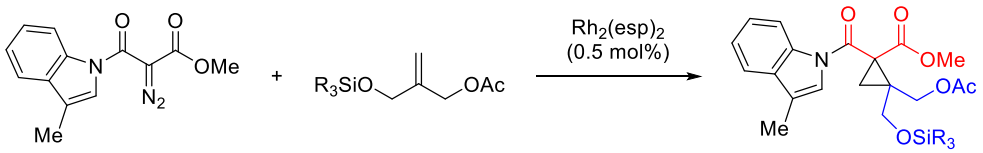

152 **150** **154**

Entry	SiR_3	Solv (conc, T)	Result
1	TBDPS	DCM (0.5 M, 0°C – r.t.)	Complex mixture
2	TBDPS	DCM (0.5 M, 0°C – r.t.)	Complex mixture[a]
3	TBDPS	MeCN (0.2 M, r.t.)	Complete in 24 h, complex mixture
4	TBDPS	MeCN (0.2 M, 50°C)	Complete in 2 h, complex mixture
5	TBDPS	MeCN (0.2 M, Δ)	Complete in 1 h, complex mixture
6	TBS	DCM (0.5 M, 0°C – r.t.)	6% isolated yield
7	TBS	DCM (0.5 M, 0°C – r.t.)	Complex mixture[b]
8	TBS	DCM (0.5 M, 0°C – r.t.)	1% isolated yield[c]

[a] Slow-added solution of diazo starting material. [b] Took forward crude to ring-opening cyclization. [c] Scaled up from 50 mg to 200 mg diazo starting material.

Hoping that perhaps a one-pot method could be feasible for this transformation (since a tandem cyclopropanation/ring-opening cyclization has been demonstrated by France and co-workers),[7] the reaction was duplicated (entry 7) and **154b** taken forward

crude to the ring-opening cyclization step (Scheme 6-8). Unfortunately, no desired cyclization adduct **155b** was detected. Then, the cyclopropanation attempted at a slightly larger scale to attain sufficient product to begin optimizing the ring-opening cyclization (entry 8), but the yield plummeted to trace amounts.

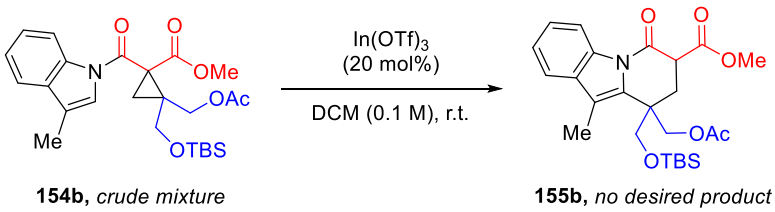

154b, *crude mixture* **155b**, *no desired product*

Scheme 6-8: Test ring-opening cyclization from crude DACP.

6.2.2 Synthetic Attempts Toward a β-Silane Donor Group

At this stage of the tronocarpine study, results from D-A bicyclo[3.1.0]hexane methodology study suggested that the β-silanol donor group proposed for the total synthesis of tronocarpine might not tolerate the Lewis acid-mediated ring-opening cyclization. Thus, the observed poor results from the ring-opening cyclization above could be attributed to this effect. With that possibility in mind, two syntheses toward an allyl β-silane were attempted, as a β-silyl donor group may be converted later in the synthesis to the desired carbonyl functionality through a Fleming-Tamao oxidation to the corresponding alcohol.[8]

First, alcohol **55a** was subjected to the optimized mesylate formation conditions and further treated with lithium chloride (Scheme 6-9). It was envisioned that this allyl chloride could be subsequently converted to a Grignard reagent then add nucleophilically to dimethylphenylsilyl chloride to form the desired allyl β-silane **156**. Unfortunately, this method proved ineffective.

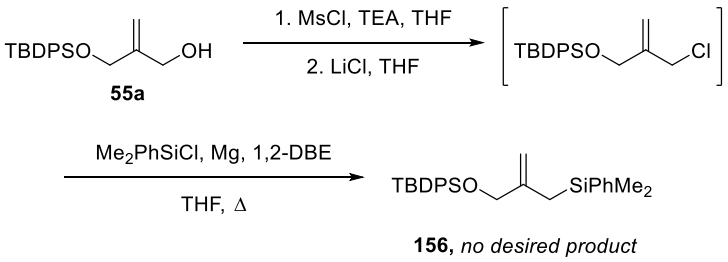

Scheme 6-9: First attempt toward allyl β-silane precursor.

Next, efforts were redirected to a literature Grignard protocol between commercial starting materials (2-(chloromethyl)allyl)dimethyl(phenyl)silane (**157**) and 2-chloroprop-2-en-1-ol (**158**) (Scheme 6-10).[9] This method employed a nickel(II) catalyst to facilitate the cross-coupling, with a reported literature yield of 70% for this product. Unfortunately, this method proved challenging to replicate, and the synthesis was not pursued further.

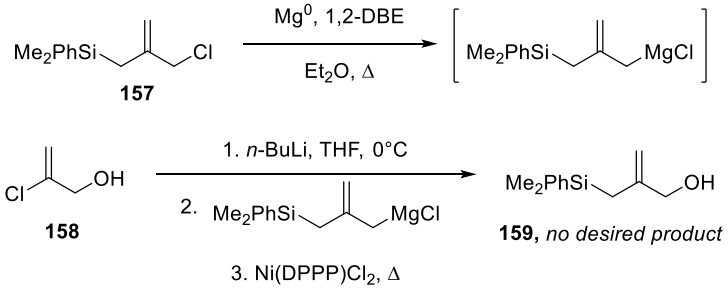

Scheme 6-10: Second attempt toward β-silyl alkene precursor.

6.2.3 Oxabicyclo[3.1.0]hexane Lactone Ring-opening Approach

With the unexpected difficulties encountered in the intermolecular cyclopropanation approach, attention shifted almost exclusively to the second approach. There was hope that this route would be more fruitful given the literature precedent for nucleophilic ring-opening of five-membered lactones and my own previous successes with intramolecular cyclopropanations to prepare oxabicyclo[3.1.0]hexanes (see Chapter 4).

Selecting model **89** as the DACP template and **59** as the nucleophile, various temperatures and loadings of NaH were evaluated to promote nucleophilic addition at the lactone to form DACP **160** (Table 6-8). Unfortunately, almost all conditions led to either no reaction or complete decomposition of **89**. Using excess **89** and 2 equiv. of NaH, a complex mixture resulted, both at high and low temperature (entries 1-2). Decreasing the loading of **89**, removing the base, and promoting the reaction through reflux, however, showed no consumption of starting material (entries 3-5). Reintroducing the NaH and increasing the loading of **59**, unfortunately, also led to degradation of **89** (entry 6).

Table 6-8: Test nucleophilic addition of 3-methylindole onto oxabicyclo[3.1.0]hexane model.

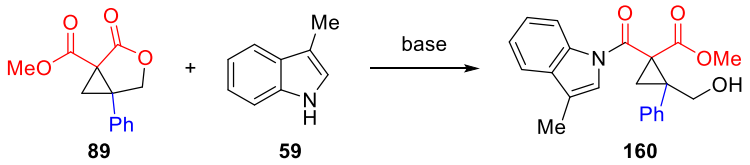

Entry	DACP:Indole	NaH equiv	Solvent (conc, temp)	Result
1	2:1	2	PhMe (0.1 M, 0°C – reflux)	Complex mixture
2	2:1	2[a]	THF (0.1 M, 0°C)	Complex mixture
3	1:1	0	DCE (0.25 M, r.t. – Δ)	No reaction
4	1:1	0	PhMe (0.25 M, r.t. – Δ)	No reaction
5	1:1	0	DMF (0.25 M, Δ)	No reaction
6	1:2	2	THF (0.2 M, 0°C)	Degradation

[a] Added 15-crown-5 (0.2 equiv). [b] NMR showed evidence of cyclopropane or ring-opening cyclization adduct.

One surprising result was detected in the presence of trimethylaluminum (Me_3Al) (Scheme 6-11). It has been demonstrated that various amines, including anilines, may be treated with Me_3Al to form a Weinreb nucleophile that is significantly more reactive in amidation reactions with esters.[10] There was no literature precedent to suggest that indoles

could complex with Me_3Al in this manner, but a test reaction under the classical Weinreb conditions afforded a single isolated product in 22% yield.

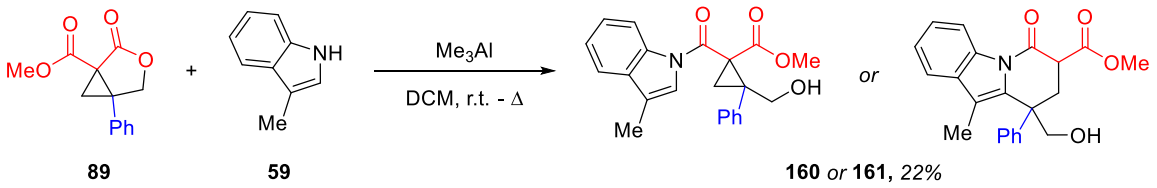

Scheme 6-11: Test Weinreb amidation and proposed products.

Extensive NMR studies and mass analysis were indicative of one of two adducts: the anticipated cyclopropane **160**, or the ring-opening cyclization product **161**. (Both adducts have the same molecular weight). ^{1}H NMR accounts for the methyl ester and methyl peaks, and a broad singlet at 3.49 ppm is highly indicative of an alcohol O-H. However, the aromatic region features only nine aromatic protons: the five from the phenyl substituent, and four from the indole moiety. This result strongly supports ring-opening cyclization adduct **161**, otherwise a fifth proton from indole would be present.

The aliphatic region is even more challenging to decipher, in large part due to the chemical shifts that are more downfield than expected and the presence of one additional proton (Table 6-9). Offering tentative assignments, protons G and K correlate only to each other and are in the appropriate region to be adjacent to an alcohol. That leaves protons J, H, M, and N to assign. By COSY, protons J and H correlate, and protons M and N correlate, with no additional overlap. Moreover, by HSQC, protons J and H share the same carbon, as do protons M and N, and by DEPT, there are two CH_2 moieties, which is consistent with both proposed structures.

Table 6-9: ^{1}H NMR aliphatic region for test Weinreb amidation product.

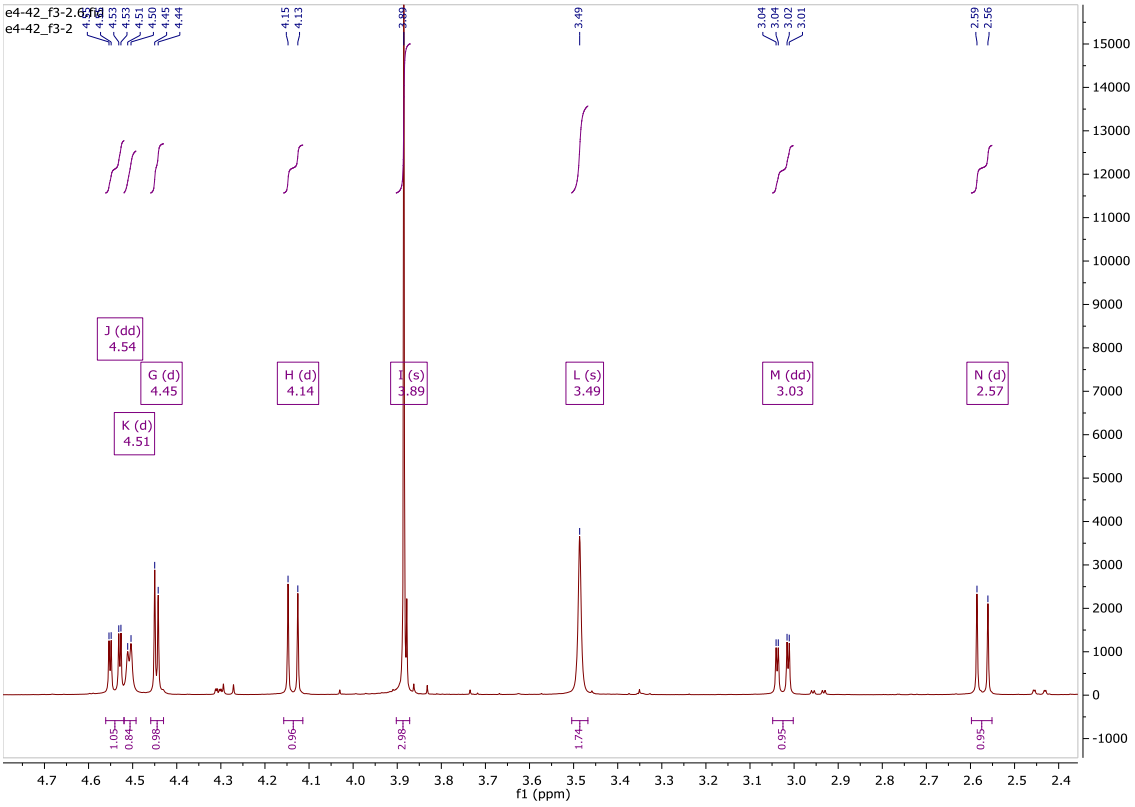

Peak Label	Chemical Shift (Multiplicity, J-Value, Integration)	Correlations
J	4.54 (dd, *J* = 11.1, 2.4 Hz, 1H)	H
K	4.51 (d, *J* = 3.8 Hz, 1H)	G
G	4.45 (d, *J* = 4.0 Hz, 1H);	K
H	4.14 (d, *J* = 11.1 Hz, 1H)	J
M	3.03 (dd, *J* = 12.4, 2.5 Hz, 1H)	N
N	2.57 (d, *J* = 12.4 Hz, 1H)	M

Crystallization is underway to perform X-ray analysis, hopes of solving this mystery. If either of these products is detected, further efforts toward the total synthesis of tronocarpine may be pursued.

6.3 Summary

In summary, the total synthesis of rhazinicine was endeavored *via* a novel ring-opening cyclization of an *N*-acyl pyrrole-tethered DACP. Despite precedent for this Friedel-Crafts-type reaction as well as early success toward the natural product synthesis, the alkene precursor proved unreliable with scale-up. 2-Iodoanilide and benzyl ester alkenes were successfully prepared and evaluated, without notable improvement in yield. Ultimately, the total synthesis of rhazinicine was abandoned because the proposed synthetic route did not improve upon previous published approaches.

Additionally, the first total synthesis of tronocarpine was attempted but ultimately not accomplished by the avenues pursued in this chapter. The primary limitations from the first approach were the failed synthesis of an adequate alkene precursor for the intermolecular cyclopropanation, as well as difficulties effecting the cyclopropanation in sufficiently high yields to move forward in the synthesis. The second approach of introducing the indole moiety through nucleophilic attack onto an oxabicyclo[3.1.0]hexane was more promising, and further work must be done to validate the product's structure. This approach could also open the door to a new methodology study, as Weinreb-type amidations with indole precursors are unprecedented in synthetic literature.

6.4 Experimental Details

6.4.1 General Information

Chromatographic purification was performed via flash chromatography with Silicycle SiliaFlash P60 silica gel (40-63 μm) or preparative thin-layer chromatography (prep-TLC) with Analtech silica gel F254 (1000 μm) plates and solvents indicated as eluent

with 0.1-0.5 bar pressure. For quantitative flash chromatography, technical grades solvents were utilized. Analytical thin-layer chromatography (TLC) was also used to separate and purify reaction products using Silicycle SiliaPlate TLC silica gel F254 (250 μm) TLC glass plates. Products on the TLC plates were visualized under UV light (254 nm).

Proton, and carbon nuclear magnetic resonance spectra (^{1}H NMR and ^{13}C NMR, respectively) were recorded on a Bruker 500 MHz spectrometer. The solvent resonances were used the internal standards (^{1}H NMR: $CDCl_3$ at 7.26 ppm, DMSO-d_6 at 3.50 ppm; ^{13}C NMR: $CDCl_3$ at 77.0 ppm, DMSO-d_6 at 39.5 ppm; ^{19}F NMR: locked to $CDCl_3$ or DMSO-d_6). MestReNova (v. 11.0) was used to analyze NMR spectra. ^{1}H NMR data are reported as follows: chemical shift (ppm), multiplicity (s = singlet, d = doublet, dd = doublet of doublets, dt = doublet of triplets, ddd = doublet of doublet of doublets, t = triplet, m = multiplet, br = broad), coupling constants (Hz), and integration. High-resolution accurate mass-mass spectrometry (HRAM-MS) was performed using a MicroMass Autospec M, run in EI mode at a mass resolution of 10,000 using perfluorokerosene (PFK) as an internal calibrant.

6.4.2 General Procedures

General Intermolecular Cyclopropanation Procedure:[11] $Rh_2(esp)_2$ (0.1 mol%) was charged to a flame-dried flask under N_2, suspended in half the requisite volume of anhydrous DCM (0.5 M), then the suspension was cooled to 0°C. The alkene (1.3 equiv) was added to the Rh flask and stirred. In a separate flame-dried flask under N_2, the α-diazo-β-amidoester (1 equiv) was dissolved in the remaining anhydrous DCM and transferred to the Rh flask *via* syringe in one shot with stirring. After 10 minutes, the solution was allowed to warm to room temperature. After 30 minutes, the reaction was quenched with saturated

aqueous thiourea and stirred for an additional 30 minutes. Then, the aqueous layer was extracted with DCM and the combined organic layers were washed with brine, dried over anhydrous Na_2SO_4, filtered through celite under reduced pressure, and concentrated by rotary evaporation. The product was purified by silica flash chromatography.

General Intramolecular Ring-Opening Cyclization Procedure: The Lewis acid (20 mol%) was charged to a flame-dried flask under N_2, then the cyclopropane (1 equiv) was added as a solution in anhydrous DCM or MeCN (0.1 M). When complete by TLC or after 24 hours, the reaction mixture was quenched with H_2O, the aqueous layer was extracted with DCM, and the combined organic extracts were dried over anhydrous $MgSO_4$, filtered through celite under reduced pressure, and concentrated by rotary evaporation. The product was purified by silica flash chromatography or prep-TLC.

General Krapcho Decarboxylation Procedure:[2] In a flask equipped with a reflux condenser, the indolizine (1 equiv), LiCl (2.338 equiv), and H_2O (cat.) were dissolved in anhydrous DMSO (0.2 M). The reaction was stirred at 150°C under N_2 for 2 h. After cooling to room temperature, the reaction was poured into H_2O, the aqueous layer extracted with Et_2O, and the combined organic extracts dried over anhydrous Na_2SO_4, filtered through celite under reduced pressure, and concentrated by rotary evaporation.

General Saponification Procedure: The ester (1 equiv) was dissolved in MeOH (1 M) with stirring, then the solution was warmed to 50°C. NaOH (1.5 equiv, 1.7 M/H_2O) was added and the reaction mixture was stirred for 2 hours. Then, the reaction was allowed to cool to room temperature, and 1 M HCl was used to adjust the pH to 3. The aqueous layer was extracted with EtOAc and the combined organic extracts were dried over

anhydrous Na_2SO_4, filtered through celite under reduced pressure, and concentrated by rotary evaporation. The product was purified by silica flash chromatography.

General N-Acylation Procedure: In a flame-dried flask under N_2, the indole (1 equiv) was dissolved in anhydrous 1,2-DCE (1 M). Methyl malonyl chloride (1.5 equiv) was added, then the reaction was stirred at reflux. After 3 hours, the reaction mixture was concentrated by rotary evaporation directly onto silica and purified by silica flash chromatography.

General TsN_3 Diazo Transfer Procedure:[12] In a flame-dried flask under N_2, the β-amidoester (1 equiv) was dissolved in anhydrous MeCN (0.1 M). Et_3N (1.5 equiv) was added, followed by TsN_3 (1.2 equiv), and the reaction was allowed to stir overnight. The solution was concentrated by rotary evaporation directly onto silica and purified by flash chromatography.

General Mono-Silylation Procedure: Following the published procedure:[13] In a flame-dried flask under N_2, NaH (1.2 equiv, 60% dispersion in mineral oil) was suspended in anhydrous THF (0.5 M) and cooled to 0°C. 2-Methylene-1,3-propanediol (1 equiv) was added dropwise, then the solution was allowed to warm to room temperature and stirred for 45 minutes. R_3SiCl (1 equiv) was added and the mixture stirred for an additional hour. The reaction was quenched with H_2O, the aqueous layer extracted with EtOAc, and the combined organic extracts washed with brine, dried over anhydrous $MgSO_4$, filtered through celite under reduced pressure, and concentrated by rotary evaporation.

General Acetylation Procedure: In a flame-dried flask under N_2, the alcohol (1 equiv) was dissolved in anhydrous DCM (0.5 M). The solution was cooled to 0°C, then DIPEA (1.2 equiv), DMAP (0.2 equiv), and Ac_2O (1.2 equiv) were added in sequence.

After stirring for 30 minutes, the reaction mixture was quenched with 1% HCl, the aqueous layers were extracted with DCM, and the combined organic extracts were washed with brine, dried over anhydrous Na_2SO_4, filtered through celite under reduced pressure, and concentrated by rotary evaporation. The product was afforded without further purification.

6.4.3 Experimental Procedures

6.4.3.1 Procedures for the Original Synthesis of Rhazinicine

*Methyl 2-Ethyl-2-(3-methoxy-3-oxopropyl)-1-(1H-pyrrole-1-carbonyl)cyclopropane-1-carboxylate (**125**).* The general intermolecular cyclopropanation procedure was followed using **126** (400 mg, 2.07 mmol) in 7 mL of anhydrous DCM (slow-added over 4 hours), and **127** (956.6 mg, 6.73 mmol) and $Rh_2(esp)_2$ (5.8 mg, 7.66 μmol) in 8 mL of anhydrous DCM. After purification by silica flash chromatography, compound **125** was afforded as a yellow oil (331.5 mg, 52% yield). NMR data were consistent with previously reported results.[2]

*Methyl 8-Ethyl-8-(3-methoxy-3-oxopropyl)-5-oxo-5,6,7,8-tetrahydroindolizine-6-carboxylate (**124**).* The general intramolecular ring-opening cyclization procedure was followed using **125** (327 mg, 1.06 mmol) and $In(OTf)_3$ (179.2 mg, 0.319 mmol) in 11 mL of anhydrous DCM (0.1 M). After purification by silica flash chromatography, compound **124** was afforded as a brown oil (193.3 mg, 63% yield). NMR data were consistent with previously reported results.[2]

*Methyl 3-(8-Ethyl-5-oxo-5,6,7,8-tetrahydroindolizin-8-yl)propanoate (**128**).* The general Krapcho decarboxylation procedure was followed using **124** (263.3 mg, 0.857 mmol), LiCl (85.0 mg, 2.00 mmol), and H_2O (2 drops) in 4.3 mL of anhydrous DMSO.

Compound **128** was afforded without further purification (193.4 mg, 90% yield). NMR data were consistent with previously reported results.[2]

*3-(8-Ethyl-5-oxo-5,6,7,8-tetrahydroindolizin-8-yl)propanoic Acid (**129**)*. The general saponification procedure was followed using **128** (189 mg, 0.757 mmol) and NaOH (0.67 mL, 1.14 mmol, 1.7 M/H_2O) in 0.8 mL of MeOH. After purification by silica flash chromatography (10% MeOH/DCM), compound **129** was afforded as a white solid (100.9 mg, 57% yield). ^{1}H NMR (500 MHz, MeOD) δ 7.34 (dd, *J* = 3.4, 1.5 Hz, 1H), 6.28 (t, *J* = 3.3 Hz, 1H), 6.07 (dd, *J* = 3.3, 1.5 Hz, 1H), 2.84 (ddd, *J* = 6.9, 6.1, 1.6 Hz, 2H), 2.40 – 2.21 (m, 2H), 2.08 – 1.90 (m, 4H), 1.81 – 1.65 (m, 2H), 0.93 (t, *J* = 7.5 Hz, 3H). ^{13}C NMR (126 MHz, MeOD) δ 177.74, 170.23, 139.90, 117.59, 113.80, 110.82, 38.42, 32.91, 31.86, 31.27, 30.57, 30.21, 8.66.

*3-(8-Ethyl-5-oxo-5,6,7,8-tetrahydroindolizin-8-yl)-N-(2-iodophenyl)propanamide (**123**)*. Following the published procedure:[13] In a flame-dried flask under N_2, **129** (50 mg, 0.213 mmol) was dissolved in 1.1 mL of andrydrous DCM. Mukaiyama's reagent (65.4 mg, 0.256 mmol) and 3-methylindole (256.3 mg, 1.17 mmol) were subsequently added, then the reaction mixture was stirred at reflux for 1 hour. After cooling the mixture to room temperature, Et_3N (0.08 mL, 0.538 mmol) was added and the mixture stirred at reflux overnight. Then, the mixture was cooled to room temperature and poured into H_2O. The aqueous layer was extracted with DCM, then the combined organic layers were dried over anhydrous Na_2SO_4, filtered through celite under reduced pressure, and concentrated by rotary evaporation. After purification by silica flash chromatography (25% EtOAc/hexanes), compound **123** was afforded (32.2 mg, 35% yield). ^{1}H NMR (500 MHz, $CDCl_3$) δ 8.17 (d, *J* = 7.7 Hz, 1H), 7.77 (d, *J* = 7.9 Hz, 1H), 7.40 – 7.30 (m, 3H), 6.84 (t, *J*

= 7.2 Hz, 1H), 6.23 (t, *J* = 3.3 Hz, 1H), 6.03 (s, 1H), 2.82 (td, *J* = 6.6, 3.3 Hz, 2H), 2.39 (ddd, *J* = 28.1, 10.1, 5.6 Hz, 2H), 2.18 – 2.03 (m, 2H), 1.98 (t, *J* = 7.1 Hz, 2H), 1.80 – 1.62 (m, 2H), 0.92 (t, *J* = 7.5 Hz, 3H). ^{13}C NMR (126 MHz, $CDCl_3$) δ 167.74, 138.74, 137.97, 137.69, 129.29, 126.01, 122.01, 116.74, 112.41, 109.39, 36.98, 31.72, 30.63, 30.38, 29.48, 8.10.

6.4.3.2 Procedures for Rhazinicine Synthesis Optimizations

*Benzyl 4-Methylenehexanoate (**136**).* In a flame-dried flask under N_2, **133** (100 mg, 0.780 mmol) was dissolved in 0.8 mL of anhydrous DCM then cooled to 0°C. Et_3N (0.13 mL, 0.936 mmol) was added slowly, then ethyl chloroformate (0.12 mL, 1.01 mmol) was added slowly. After stirring for 30 minutes, BnOH (0.32 mL, 3.12 mmol) was added, and the reaction was allowed to warm to room temperature. After 15 hours, the reaction was quenched with cold H_2O, the aqueous layer extracted with DCM, and the combined organic extracts washed with brine, dried over anhydrous Na_2SO_4, filtered through celite under reduced pressure, and concentrated by rotary evaporation. After purification by silica flash chromatography (25% EtOAc/hexanes, R_f = 0.70), compound **136** was afforded as a colorless liquid (139.0 mg, 82% yield). ^{1}H NMR (500 MHz, $CDCl_3$) δ 7.40 – 7.31 (m, 5H), 5.13 (s, 2H), 4.77 – 4.69 (m, 2H), 2.52 (dd, *J* = 9.1, 6.5 Hz, 2H), 2.41 – 2.35 (m, 2H), 2.04 (q, *J* = 7.4 Hz, 2H), 1.03 (t, *J* = 7.4 Hz, 3H).

*Methyl 2-(3-(Benzyloxy)-3-oxopropyl)-2-ethyl-1-(1H-pyrrole-1-carbonyl)cyclopropane-1-carboxylate (**137**).* The general intermolecular cyclopropanation procedure was followed using **126** (500 mg, 2.59 mmol), **136** (2.826 g, 12.9 mmol), and $Rh_2(esp)_2$ (2.0 mg, 2.59 μmol) in 5.2 mL of anhydrous DCM. After purification by silica flash chromatography (25% EtOAc/hexanes, R_f = 0.33), compound **137** was afforded in a

1.5:1 mixture of diastereomers (410.5 mg, 41% yield). ^{1}H NMR (500 MHz, $CDCl_3$) δ 7.40 – 7.28 (m, 11H), 6.27 (dt, *J* = 3.6, 2.5 Hz, 3H), 5.13 (d, *J* = 1.4 Hz, 1H), 5.08 (s, 2H), 3.66 (d, *J* = 5.1 Hz, 5H), 2.62 – 2.51 (m, 2H), 2.45 – 2.34 (m, 2H), 2.34 – 2.25 (m, 1H), 2.19 – 2.06 (m, 2H), 1.79 (q, *J* = 7.5 Hz, 2H), 1.67 (ddd, *J* = 13.0, 4.9, 1.2 Hz, 2H), 1.54 (dd, *J* = 15.5, 5.0 Hz, 2H), 1.32 (ddd, *J* = 14.5, 9.8, 6.4 Hz, 1H), 0.96 (dt, *J* = 20.7, 7.0 Hz, 6H). ^{13}C NMR (126 MHz, $CDCl_3$) δ 172.63, 172.52, 169.21, 169.12, 165.02, 164.90, 135.78, 135.73, 128.57, 128.54, 128.31, 128.25, 128.22, 119.78, 119.75, 113.15, 66.47, 66.36, 52.93, 40.37, 39.97, 37.75, 37.65, 31.38, 31.31, 28.39, 27.16, 27.02, 26.68, 23.99, 21.91, 10.60, 10.57.

*Methyl 8-(3-(Benzyloxy)-3-oxopropyl)-8-ethyl-5-oxo-5,6,7,8-tetrahydroindolizine-6-carboxylate (**138**).* The general intramolecular ring-opening cyclization procedure was followed using methyl **137** (50 mg, 0.13 mmol) and $In(OTf)_3$ (21.9 mg, 0.0390 mmol) in 1.3 mL of anhydrous DCM, heated to reflux. After purification by silica flash chromatography (25% EtOAc/hexanes, R_f = 0.13), compound **138** was afforded in a 1.3:1 mixture of diastereomers (18.5 mg, 37% yield). ^{1}H NMR (500 MHz, $CDCl_3$) δ 7.39 – 7.30 (m, 6H), 6.23 (dt, *J* = 12.2, 3.3 Hz, 1H), 5.97 (ddd, *J* = 21.7, 3.3, 1.5 Hz, 1H), 5.11 (s, 1H), 5.04 (s, 1H), 3.97 – 3.78 (m, 5H), 2.46 – 2.33 (m, 3H), 2.28 (ddd, *J* = 16.2, 10.6, 5.7 Hz, 1H), 2.11 (ddd, *J* = 14.3, 9.2, 6.9 Hz, 1H), 2.06 – 1.92 (m, 3H), 1.82 (ddd, *J* = 14.0, 10.6, 5.6 Hz, 1H), 1.72 (q, *J* = 7.4 Hz, 1H), 1.62 (dd, *J* = 14.2, 7.3 Hz, 1H), 0.88 (q, *J* = 7.4 Hz, 4H). ^{13}C NMR (126 MHz, $CDCl_3$) δ 173.18, 172.88, 169.72, 128.59, 128.37, 128.35, 128.30, 128.23, 117.28, 117.16, 113.18, 113.00, 110.07, 109.86, 66.54, 66.49, 52.83, 52.80, 46.99, 46.94, 36.90, 36.55, 34.99, 34.32, 31.73, 31.34, 31.26, 29.83, 29.15, 29.07, 8.24, 7.80.

6.4.3.3 Procedures for the Synthesis of Tronocarpine

*Methyl 3-(3-Methyl-1H-indol-1-yl)-3-oxopropanoate (**151**).* The general N-acylation procedure was followed using 3-methylindole (100 mg, 0.762 mmol) and methyl malonyl chloride (0.12 mL, 1.14 mmol) in 0.8 mL of anhydrous 1,2-DCE. After purification by silica flash chromatography (25% EtOAc/hexanes), compound **151** was afforded (173.7 mg, 98% yield). NMR data were consistent with previously published results.[3]

*Methyl 3-(3-Methyl-1H-indol-1-yl)-2-diazo-3-oxopropanoate (**152**).* The general TsN_3 diazo transfer procedure was followed using **151** (174 mg, 0.751 mmol), TsN_3 (0.14 mL, 0.901 mmol), and Et_3N (0.16 mL, 1.13 mmol) in 7.5 mL of anhydrous MeCN. After purification by silica flash chromatography (25% EtOAc/hexanes), compound **152** was afforded as a yellow solid (180.3 mg, 93% yield). NMR data were consistent with previously published results.[3]

*2-(((tert-Butyldiphenylsilyl)oxy)methyl)prop-2-en-1-ol (**55a**).* The general mono-silylation procedure was followed using 2-methylene-1,3-propanediol (500 mg, 5.67 mmol), TBDPSCl (1.568 g, 5.67 mmol), and NaH (228 mg, 5.67 mmol, 60% dispersion in mineral oil) in 68 mL of anhydrous THF. After purification by silica flash chromatography (25% EtOAc/hexanes, R_f = 0.46), compound **55a** was afforded as a thick, colorless oil (1.550 g, 84% yield). NMR data were consistent with previously published results.[13]

*2-(((tert-Butyldimethylsilyl)oxy)methyl)prop-2-en-1-ol (**153**).* The general mono-silylation procedure was followed using 2-methylene-1,3-propanediol (1 g, 11.4 mmol), TBSCl (1.711 g, 11.4 mmol), and NaH (544.7 mg, 13.6 mmol, 60% dispersion in mineral oil) in 23 mL of anhydrous THF. After purification by silica flash chromatography (25%

EtOAc/hexanes, R_f = 0.46), compound **153** was afforded as a thick, colorless oil (1.736 g, 75% yield). NMR data were consistent with previously published results.[15]

*2-(((tert-Butyldiphenylsilyl)oxy)methyl)allyl Acetate (**150a**).* The general acetylation procedure was following using **55a** (500 mg, 1.53 mmol), DIPEA (0.32 mL, 1.84 mmol), DMAP (37.4 mg, 0.306 mmol), and Ac_2O (0.17 mL, 1.84 mmol) in 15 mL of anhydrous DCM. Compound **150a** was afforded without further purification (560 mg, 99% yield). ^{1}H NMR (500 MHz, $CDCl_3$) δ 7.68 (d, *J* = 6.8 Hz, 1H), 7.46 – 7.37 (m, 2H), 4.59 (s, 1H), 4.20 (s, 1H), 2.03 (s, 1H), 1.07 (s, 2H).

*2-(((tert-Butyldimethylsilyl)oxy)methyl)allyl Acetate (**150b**).* The general acetylation procedure was following using **153** (500 mg, 2.47 mmol), DIPEA (0.52 mL, 2.97 mmol), DMAP (60.4 mg, 0.494 mmol), and Ac_2O (0.28 mL, 2.97 mmol) in 25 mL of anhydrous DCM. Compound **150b** was afforded without further purification (565.7 mg, 94% yield). ^{1}H NMR (500 MHz, $CDCl_3$) δ 5.23 (d, *J* = 1.5 Hz, 1H), 5.13 (q, *J* = 1.3 Hz, 1H), 4.58 (s, 2H), 4.16 (s, 2H), 2.08 (s, 3H), 0.91 (s, 10H), 0.07 (s, 6H). ^{13}C NMR (126 MHz, $CDCl_3$) δ 170.69, 143.20, 112.95, 64.67, 63.77, 25.84, 20.91, 18.33, -5.45.

*Methyl 2-(Acetoxymethyl)-2-(((tert-butyldimethylsilyl)oxy)methyl)-1-(3-methyl-1H-indole-1-carbonyl)cyclopropane-1-carboxylate (**154b**).* The general intermolecular cyclopropanation procedure was followed using **152** (100 mg, 0.389 mmol), **150b** (123.7 mg, 0.506 mmol), and $Rh_2(esp)_2$ (3.0 mg, 3.89 μmol) in 0.8 mL of anhydrous DCM. After purification by silica prep-TLC, compound **154b** was afforded (8.7 mg, 6% yield). ^{1}H NMR (500 MHz, $CDCl_3$) δ 8.45 (d, *J* = 8.6 Hz, 1H), 7.49 (d, *J* = 8.8 Hz, 2H), 7.33 (dtd, *J* = 23.8, 7.4, 1.1 Hz, 3H), 4.75 (d, *J* = 11.6 Hz, 1H), 4.50 (d, *J* = 11.6 Hz, 1H), 3.75 (d, *J* = 9.8 Hz, 1H), 3.65 (s, 3H), 3.58 (d, *J* = 10.8 Hz, 1H), 2.27 (d, *J* = 1.3 Hz, 3H), 2.16 (s, 3H),

1.95 (d, *J* = 5.2 Hz, 1H), 1.78 (d, *J* = 5.1 Hz, 1H), 0.69 (s, 9H), -0.22 (d, *J* = 20.8 Hz, 6H). ^{13}C NMR (126 MHz, $CDCl_3$) δ 170.23, 169.28, 164.15, 131.52, 125.02, 123.71, 123.13, 118.63, 118.02, 116.88, 62.98, 62.92, 53.11, 38.43, 36.94, 25.59, 22.41, 20.77, 18.06, 9.92, -5.93, -6.01.

Methyl 9-(Acetoxymethyl)-9-(((tert-butyldimethylsilyl)oxy)methyl)-10-methyl-6-oxo-6,7,8,9-tetrahydropyrido[1,2-a]indole-7-carboxylate ***(155b)****.* The general intramolecular ring-opening cyclization procedure was followed using a crude mixture of **154b** (~184.2 mg, 0.389 mmol) and $In(OTf)_3$ (43.7 mg, 0.778 mmol) in 3.9 mL of anhydrous DCM. After 1.5 hours, TLC showed consumption of starting material, but there was no evidence of desired product by NMR.

6.4.3.4 Procedures for the Oxabicyclo[3.1.0]hexane Lactone Ring-Opening Approach to Tronocarpine

160 *or* ***161***. Following the published procedure:[10] In a flame-dried flask under N_2, 3-methylindole (69.4 mg, 0.529 mmol) was dissolved in 1.9 mL of anhydrous DCM. Trimethylaluminum (0.3 mL, 0.605 mmol, 2 M solution in heptane) was added slowly. After stirring for 20 minutes, **98** (100 mg, 0.378 mmol) was added as a solution in 1.9 mL of anhydrous DCM, then stirred for an additional hour at room temperature. The reaction was heated to reflux. After stirring overnight, the reaction was cooled to room temperature and quenched carefully with dilute HCl, then the aqueous layer was extracted with DCM and the combined organic extracts were dried over anhydrous Na_2SO_4, filtered through celite under reduced pressure, and concentrated by rotary evaporation. After purification by silica prep-TLC, the product was afforded as either the cyclopropane **160** or the cyclopropane ring-opening cyclization adduct **161** (22.0 mg, 16% yield). ^{1}H NMR (500

MHz, $CDCl_3$) δ 7.45 (t, *J* = 7.4 Hz, 2H), 7.38 (ddd, *J* = 8.4, 7.2, 1.4 Hz, 3H), 7.18 (d, *J* = 7.4 Hz, 1H), 7.12 (td, *J* = 7.8, 1.2 Hz, 1H), 6.77 (td, *J* = 7.4, 0.9 Hz, 1H), 6.65 (d, *J* = 7.8 Hz, 1H), 4.54 (dd, *J* = 11.1, 2.4 Hz, 1H), 4.51 (d, *J* = 3.8 Hz, 1H), 4.45 (d, *J* = 4.0 Hz, 1H), 4.14 (d, *J* = 11.1 Hz, 1H), 3.89 (s, 3H), 3.49 (s, 2H), 3.03 (dd, *J* = 12.4, 2.5 Hz, 1H), 2.57 (d, *J* = 12.4 Hz, 1H), 1.05 (s, 3H). ^{13}C NMR (126 MHz, $CDCl_3$) δ 170.35, 167.12, 150.56, 138.51, 130.45, 129.07, 128.88, 127.93, 126.09, 123.91, 118.48, 109.88, 75.13, 62.69, 57.38, 52.96, 51.90, 50.87, 36.00, 27.91. HRAM-MS (EI) m/z $[M+H]^+$ Calcd for $C_{22}H_{22}O_4N$ 364.1453; Found 364.1543.

6.5 Copies of NMR Spectra

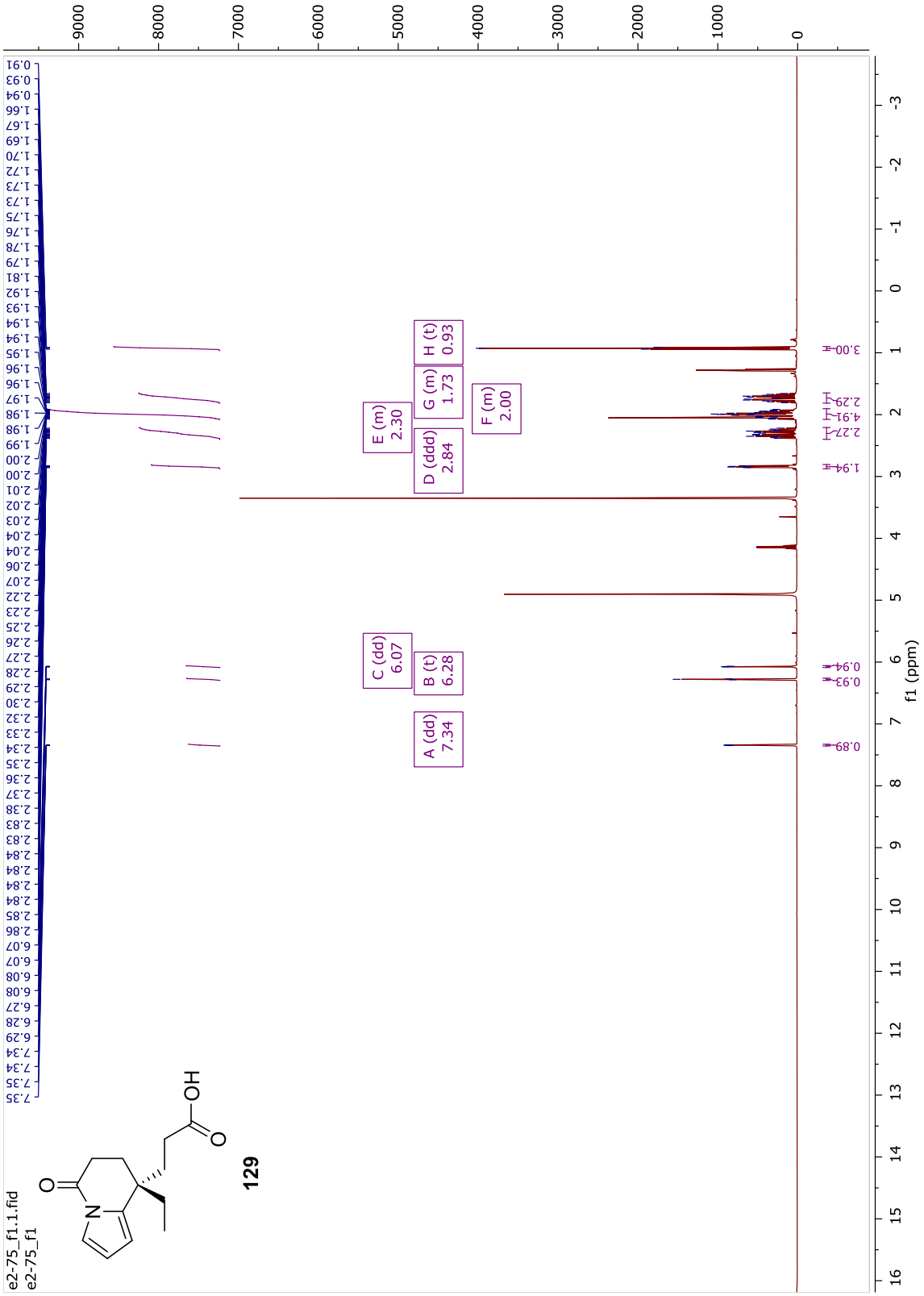
e2-75_f1.1.fid
e2-75_f1
129
A (dd) 7.34
B (t) 6.28
C (dd) 6.07
D (ddd) 2.84
E (m) 2.30
F (m) 2.00
G (m) 1.73
H (t) 0.93
3.00
2.29
4.91
2.27
1.94
0.94
0.93
0.89
f1 (ppm)

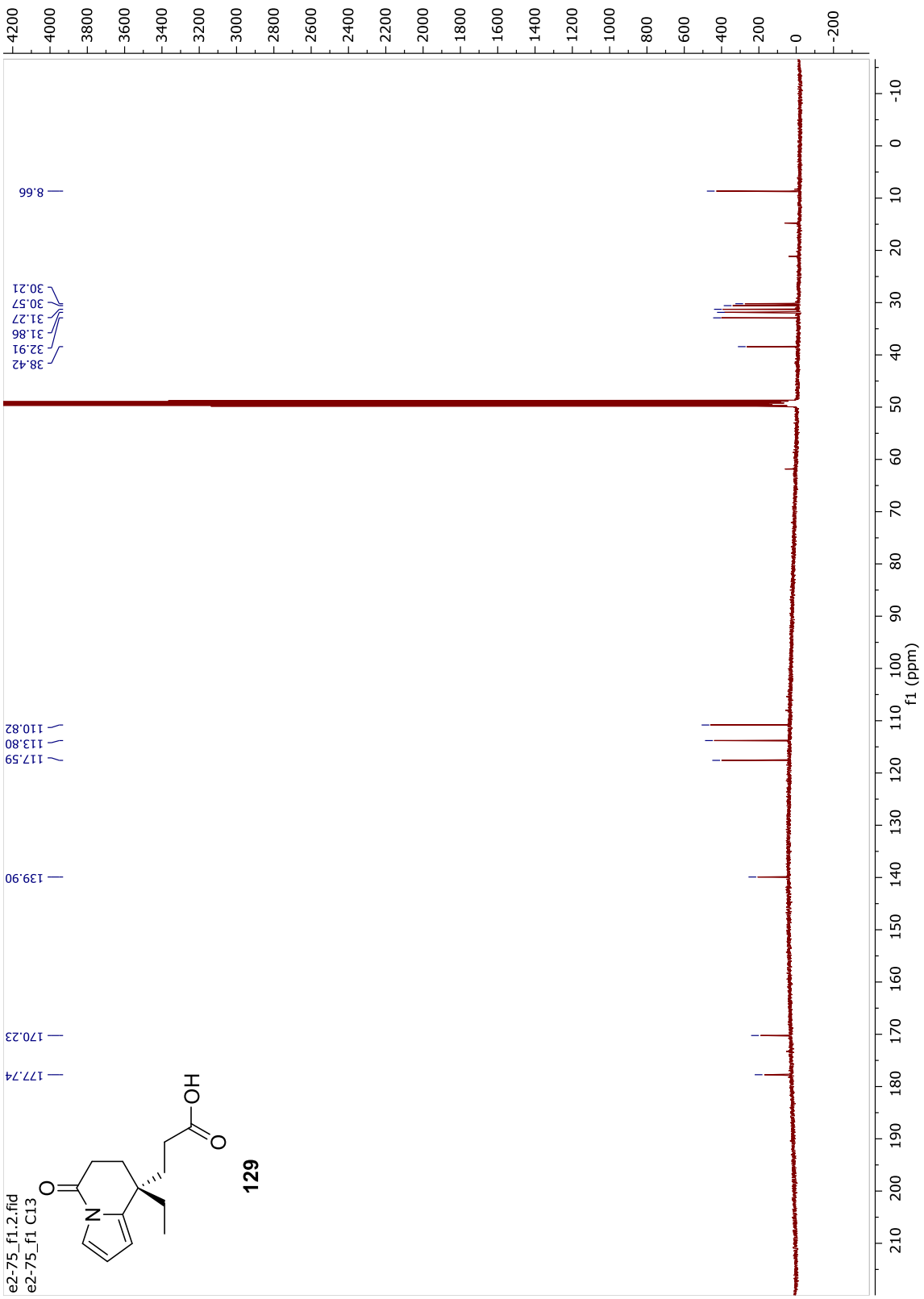
e2-75_f1.2.fid
e2-75_f1 C13
129
177.74
170.23
139.90
117.59
113.80
110.82
38.42
32.91
31.86
31.27
30.57
30.21
8.66
f1 (ppm)

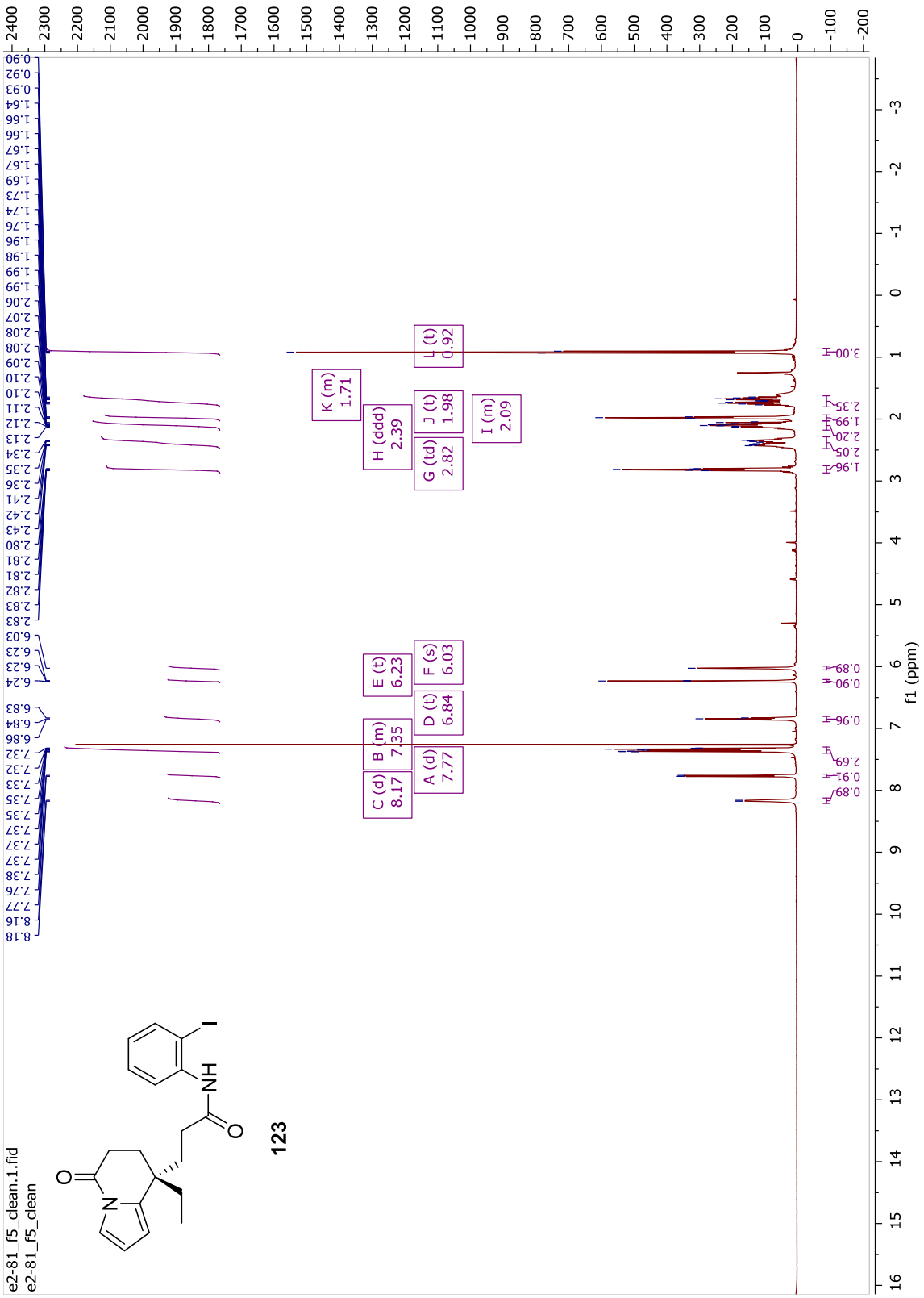
e2-81_f5_clean.1.fid
e2-81_f5_clean
123
f1 (ppm)

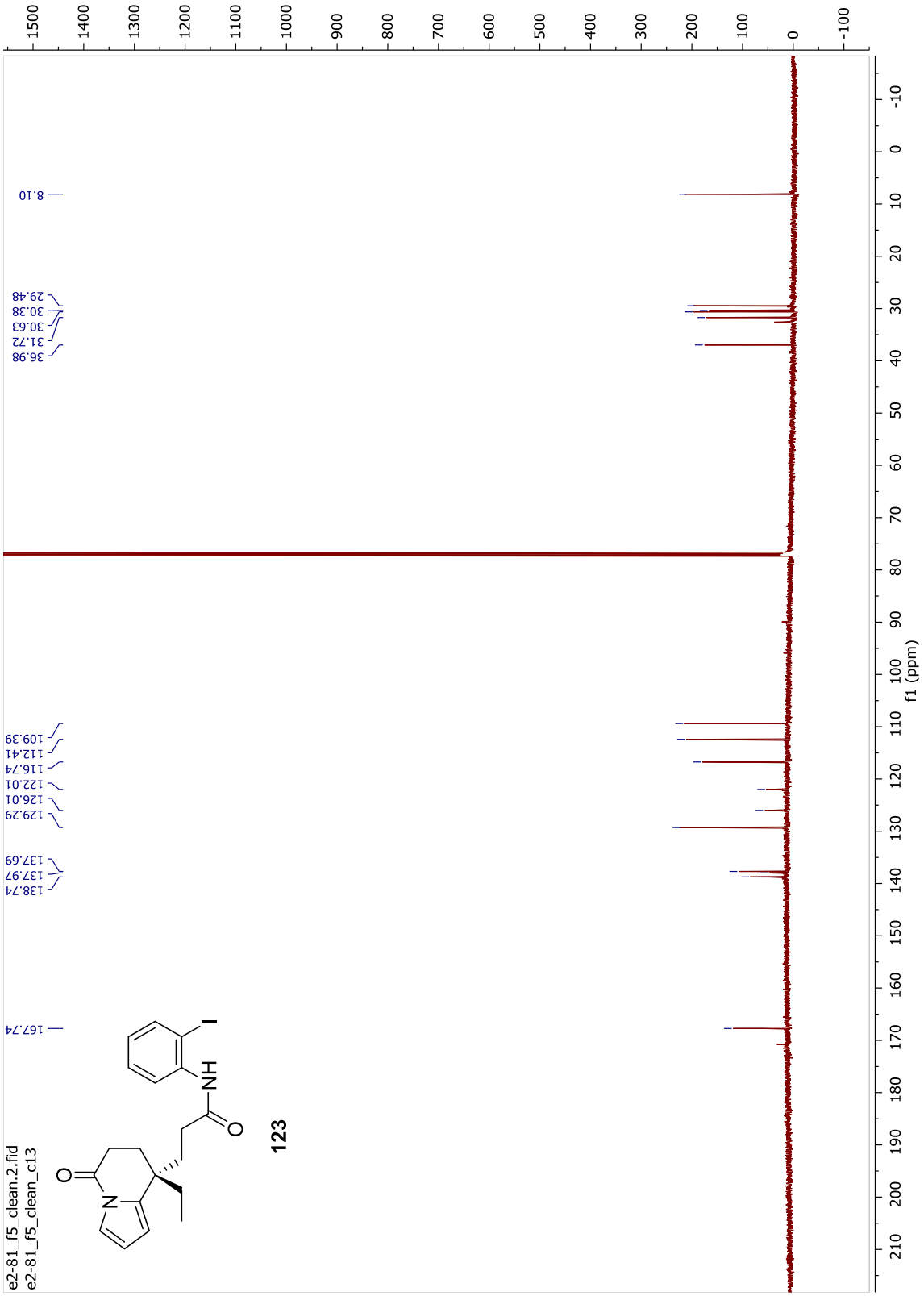
e2-81_f5_clean.2.fid
e2-81_f5_clean_c13
167.74
138.74
137.97
137.69
129.29
126.01
122.01
116.74
112.41
109.39
36.98
31.72
30.63
30.38
29.48
8.10
f1 (ppm)
123

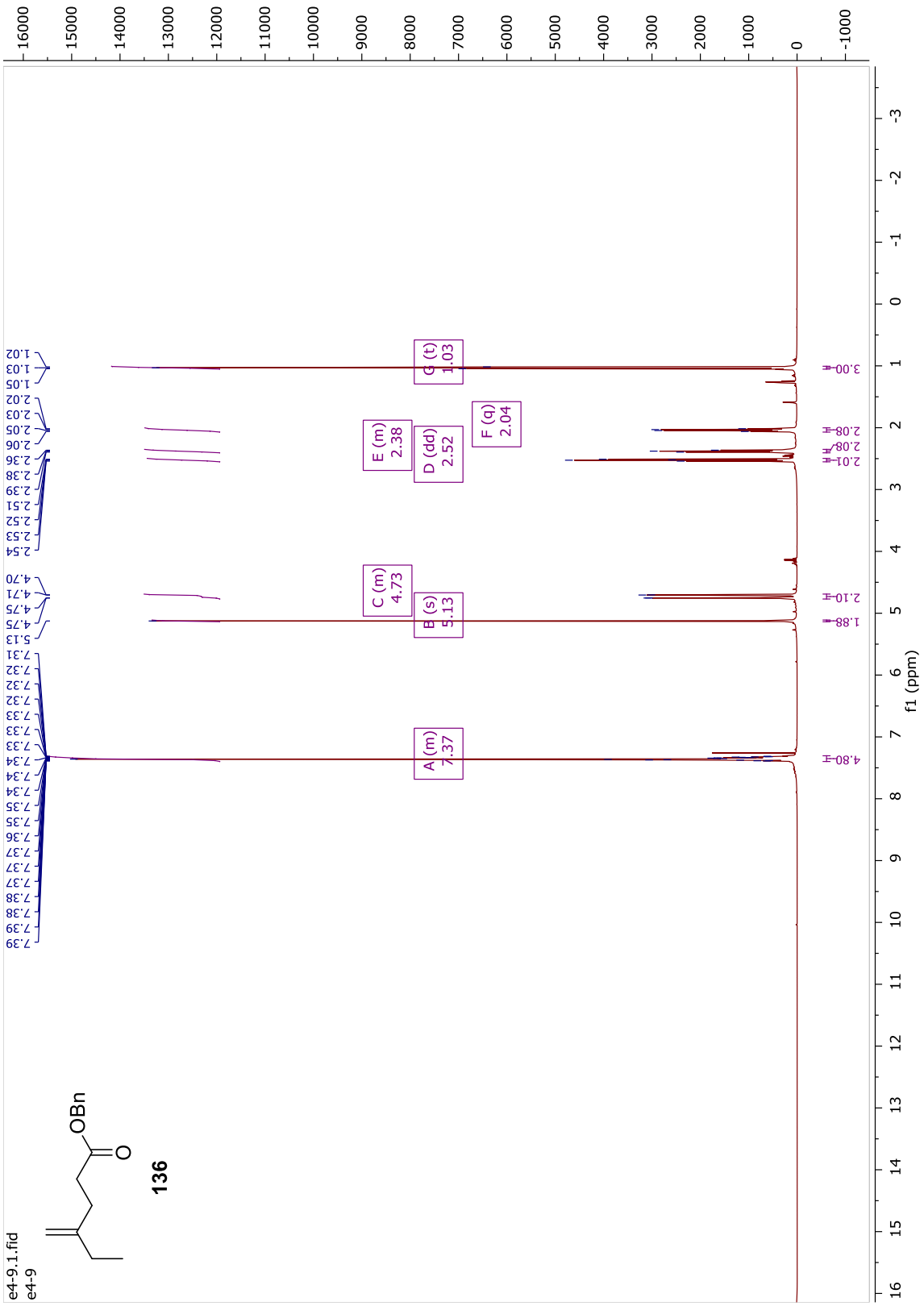
e4-9.1.fid
e4-9
136
OBn
O
A (m) 7.37
B (s) 5.13
C (m) 4.73
D (dd) 2.52
E (m) 2.38
F (q) 2.04
G (t) 1.03
4.80
2.10
1.88
2.08
2.08
2.01
3.00
f1 (ppm)

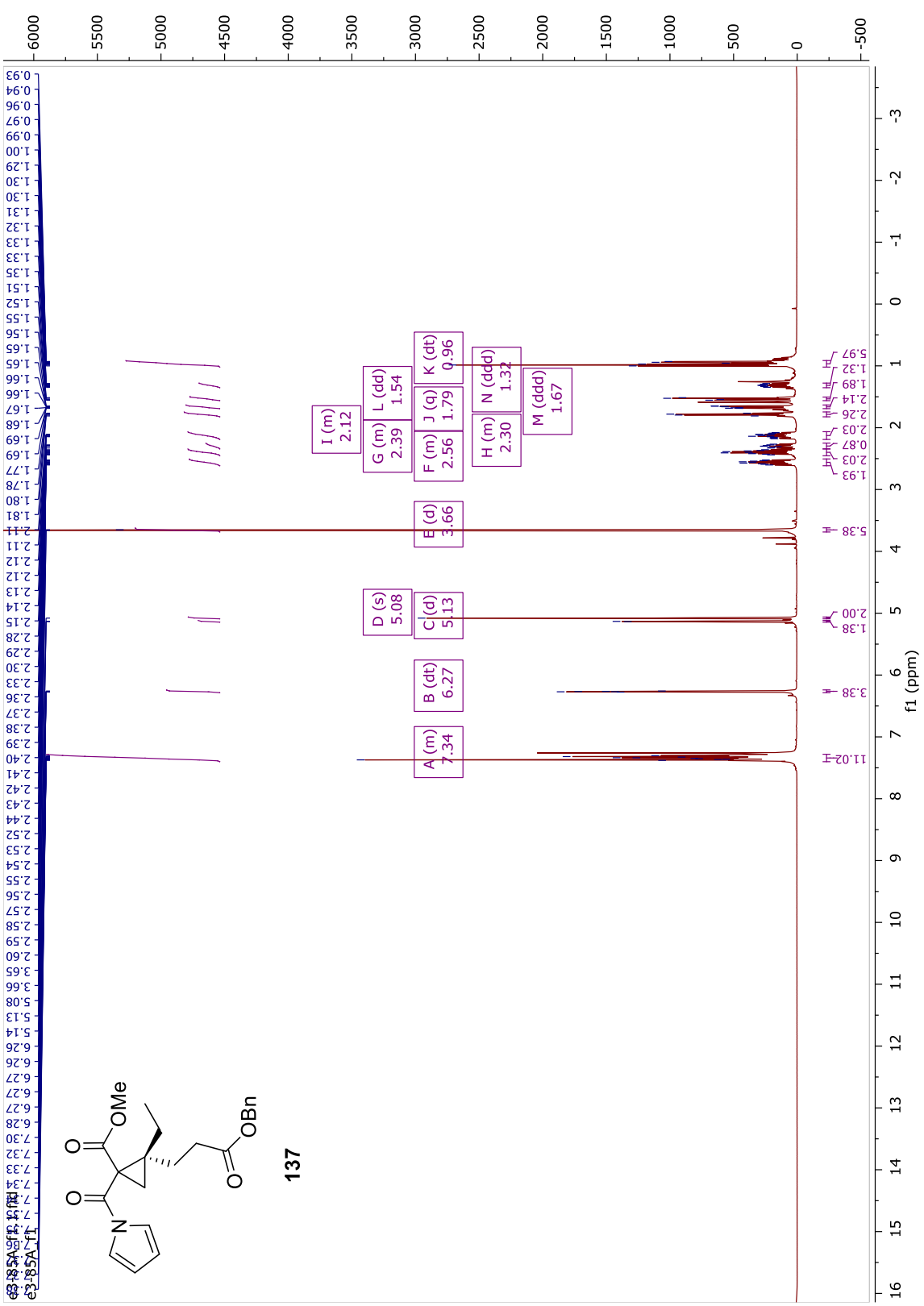
137
OMe
OBn
A (m) 7.34
B (dt) 6.27
C (d) 5.13
D (s) 5.08
E (d) 3.66
F (m) 2.56
G (m) 2.39
H (m) 2.30
I (m) 2.12
J (q) 1.79
K (dt) 0.96
L (dd) 1.54
M (ddd) 1.67
N (ddd) 1.32
f1 (ppm)

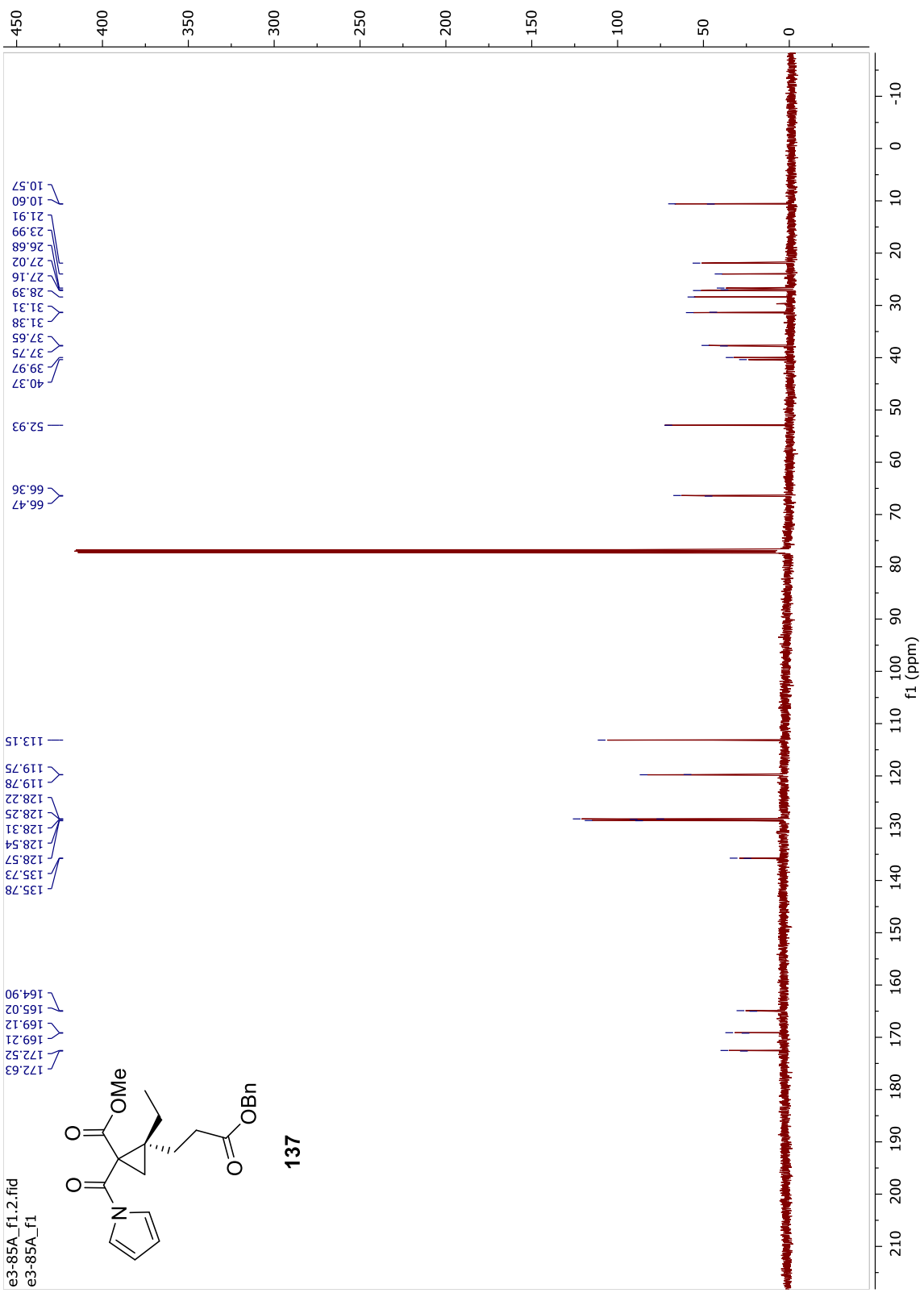
e3-85A_f1.2.fid
e3-85A_f1
172.63
172.52
169.21
169.12
165.02
164.90
135.78
135.73
128.57
128.54
128.31
128.25
128.22
119.78
119.75
113.15
66.47
66.36
52.93
40.37
39.97
37.75
37.65
31.38
31.31
28.39
27.16
27.02
26.68
23.99
21.91
10.60
10.57
OMe
OBn
137
f1 (ppm)

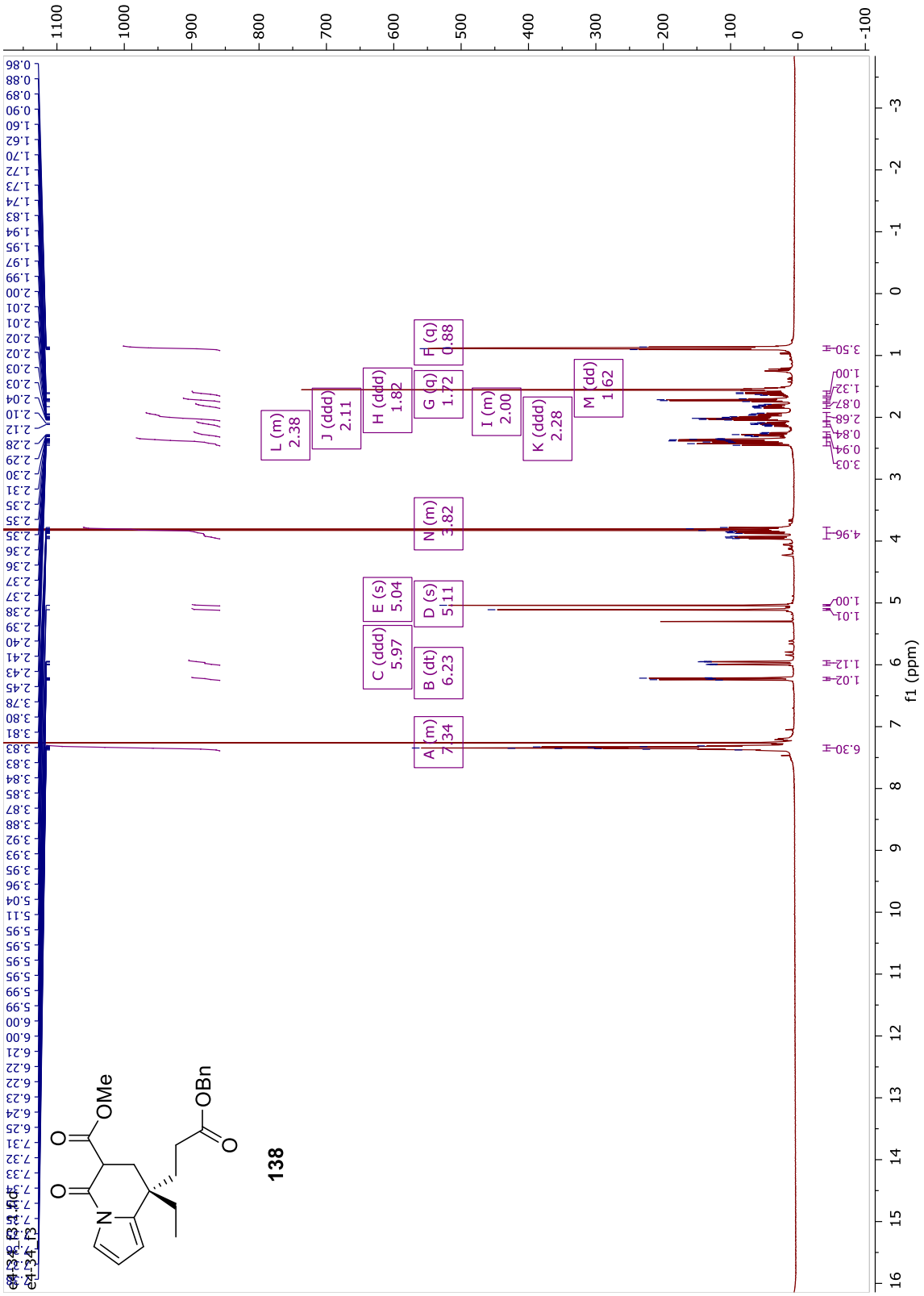
138
A (m) 7.34
B (dt) 6.23
C (ddd) 5.97
D (s) 5.11
E (s) 5.04
N (m) 3.82
L (m) 2.38
J (ddd) 2.11
H (ddd) 1.82
G (q) 1.72
I (m) 2.00
K (ddd) 2.28
M (dd) 1.62
F (q) 0.88
f1 (ppm)

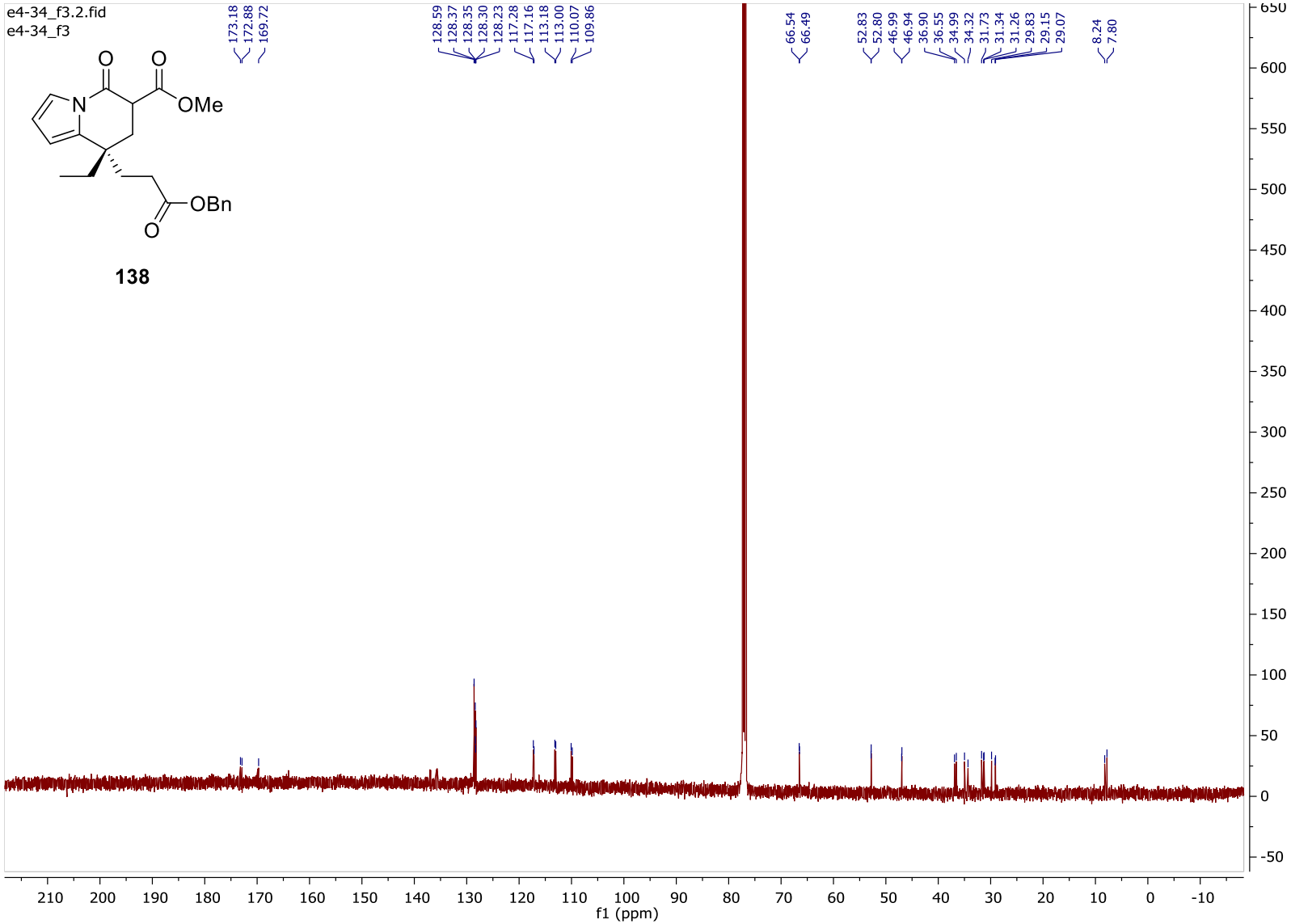
e4-34_f3.2.fid
e4-34_f3
173.18
172.88
169.72
128.59
128.37
128.35
128.30
128.23
117.28
117.16
113.18
113.00
110.07
109.86
66.54
66.49
52.83
52.80
46.99
46.94
36.90
36.55
34.99
34.32
31.73
31.34
31.26
29.83
29.15
29.07
8.24
7.80
O
O
N
OMe
OBn
O
138
f1 (ppm)

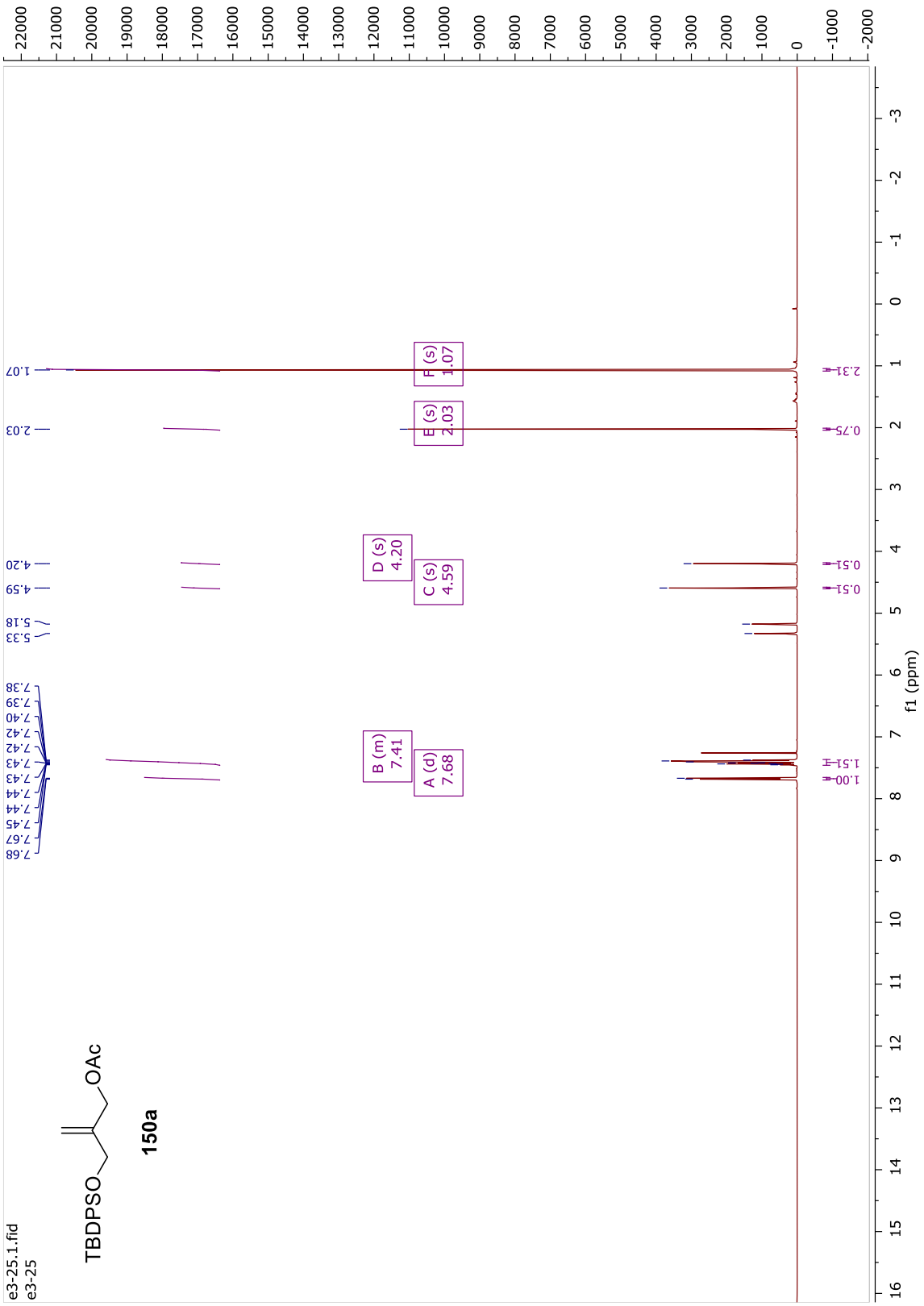
e3-25.1.fid
e3-25
TBDPSO
OAc
150a
A (d) 7.68
B (m) 7.41
C (s) 4.59
D (s) 4.20
E (s) 2.03
F (s) 1.07
f1 (ppm)

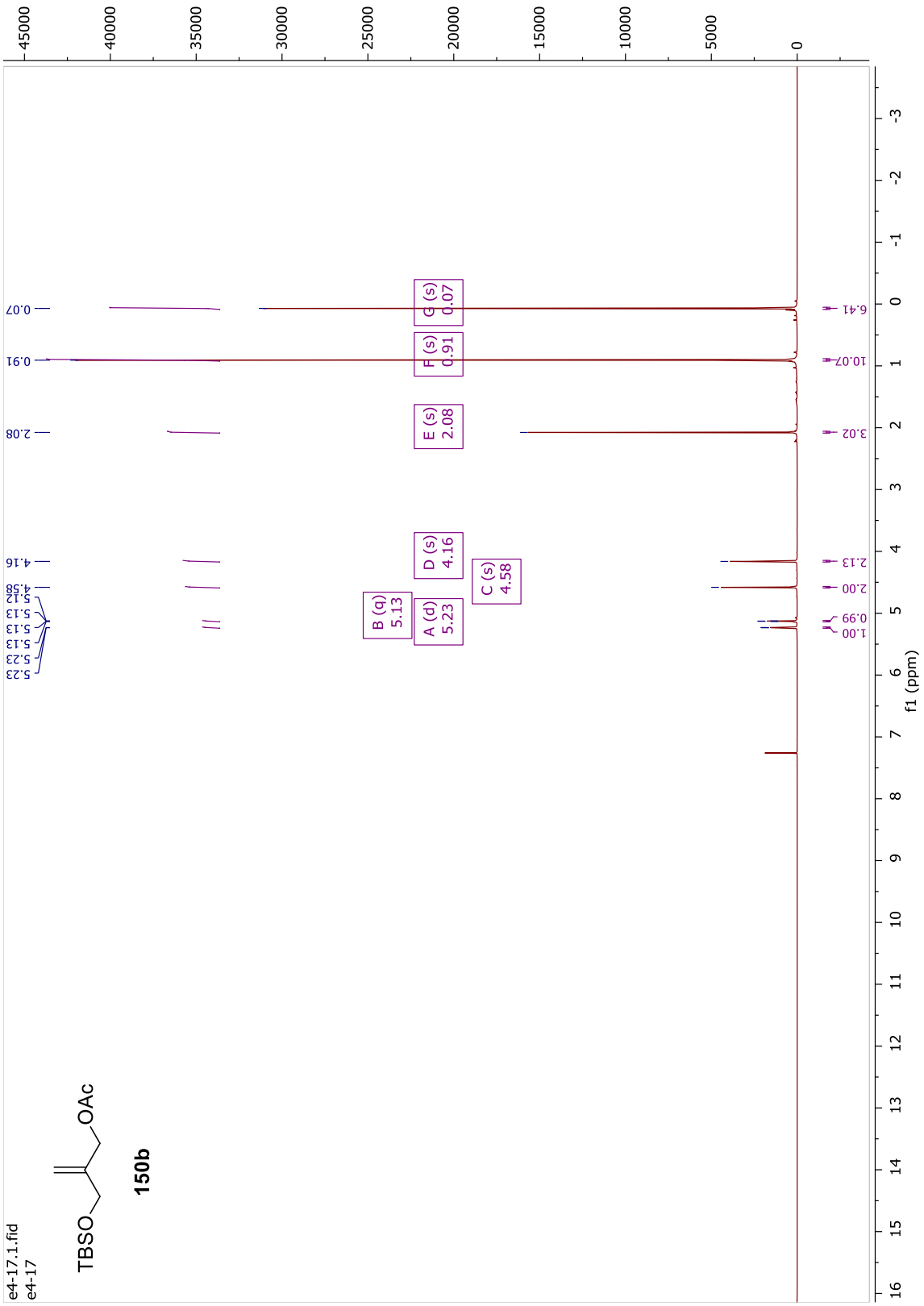
e4-17.1.fid
e4-17
TBSO
OAc
150b
A (d) 5.23
B (q) 5.13
C (s) 4.58
D (s) 4.16
E (s) 2.08
F (s) 0.91
G (s) 0.07
f1 (ppm)

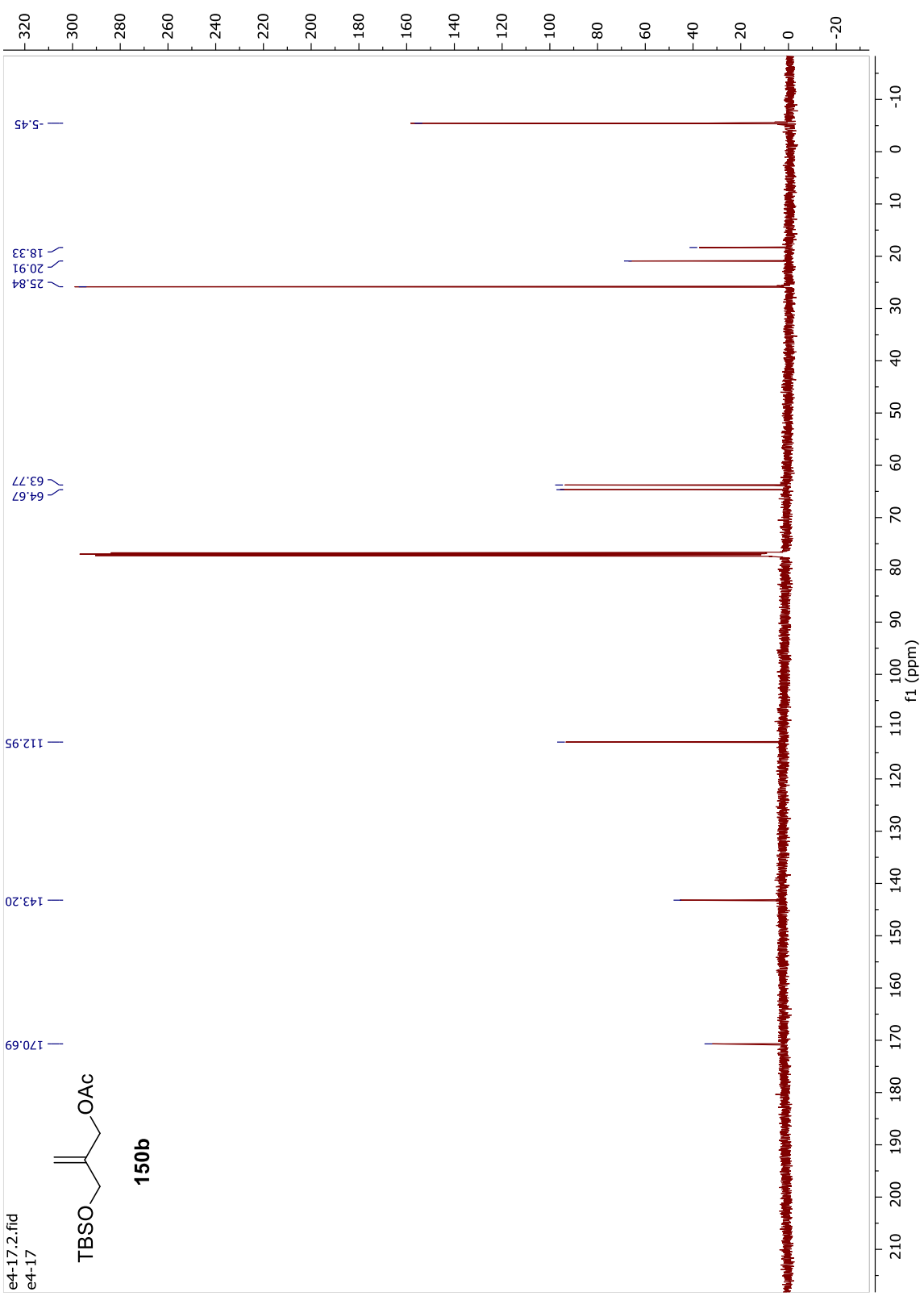
e4-17.2.fid
e4-17
TBSO
OAc
150b
170.69
143.20
112.95
64.67
63.77
25.84
20.91
18.33
-5.45
f1 (ppm)

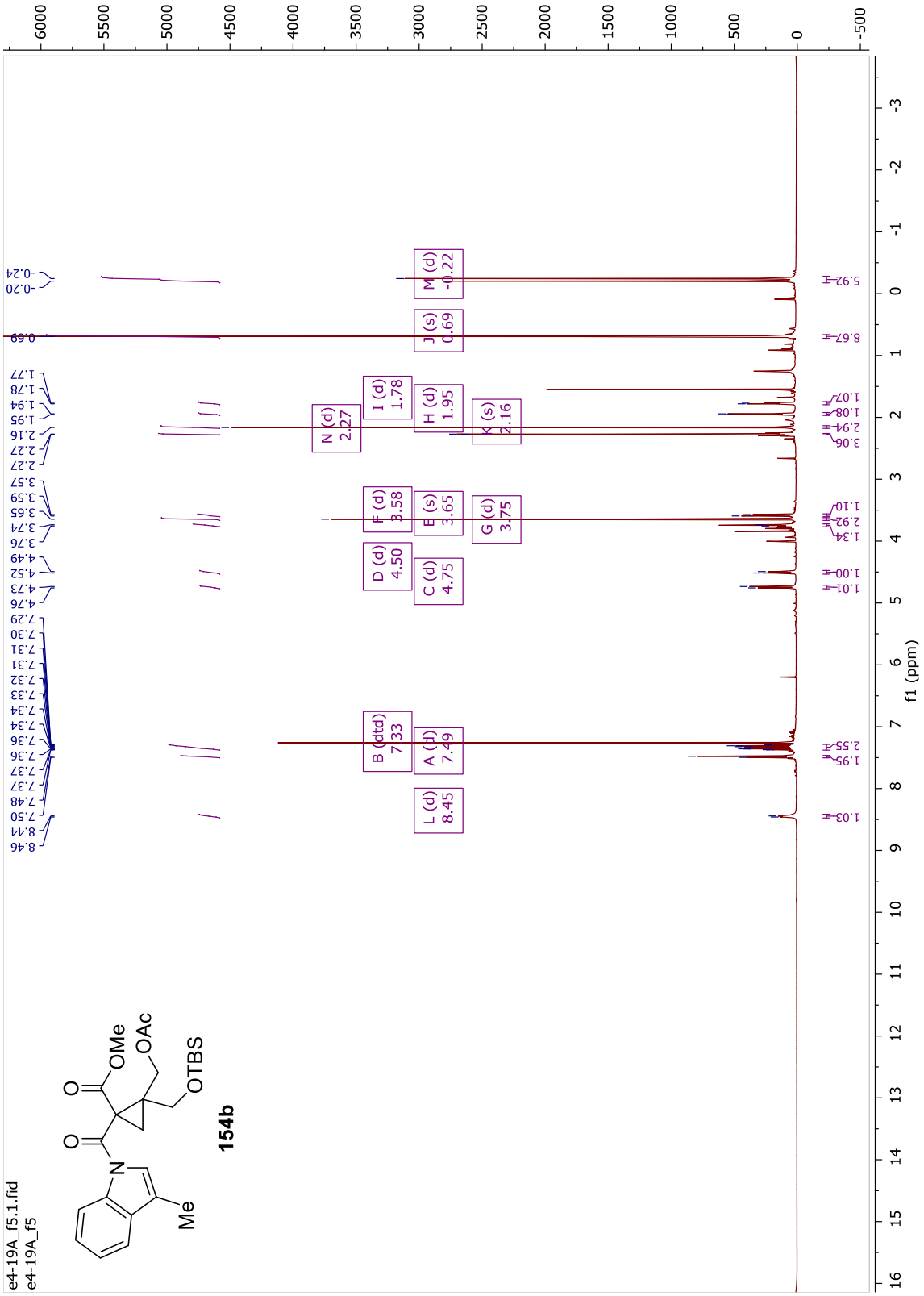
e4-19A_f5.1.fid
e4-19A_f5
154b
OMe
OAc
OTBS
Me
N
O
O
f1 (ppm)
A (d) 7.49
B (dtd) 7.33
C (d) 4.75
D (d) 4.50
E (s) 3.65
F (d) 3.58
G (d) 3.75
H (d) 1.95
I (d) 1.78
J (s) 0.69
K (s) 2.16
L (d) 8.45
M (d) -0.22
N (d) 2.27

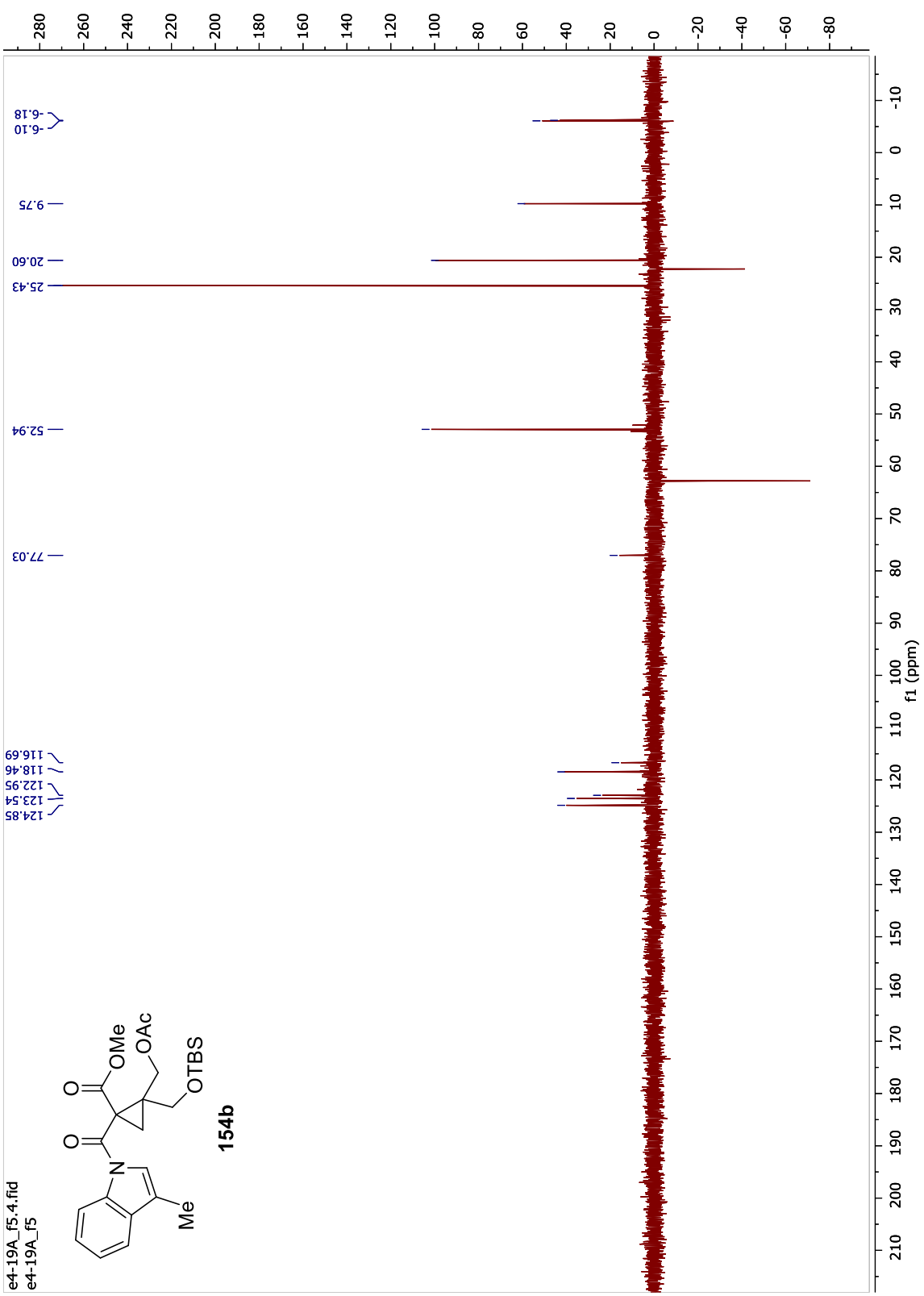
e4-19A_f5.4.fid
e4-19A_f5
-6.18
-6.10
9.75
20.60
25.43
52.94
77.03
116.69
118.46
122.95
123.54
124.85
OMe
OAc
OTBS
O
O
N
Me
154b
f1 (ppm)

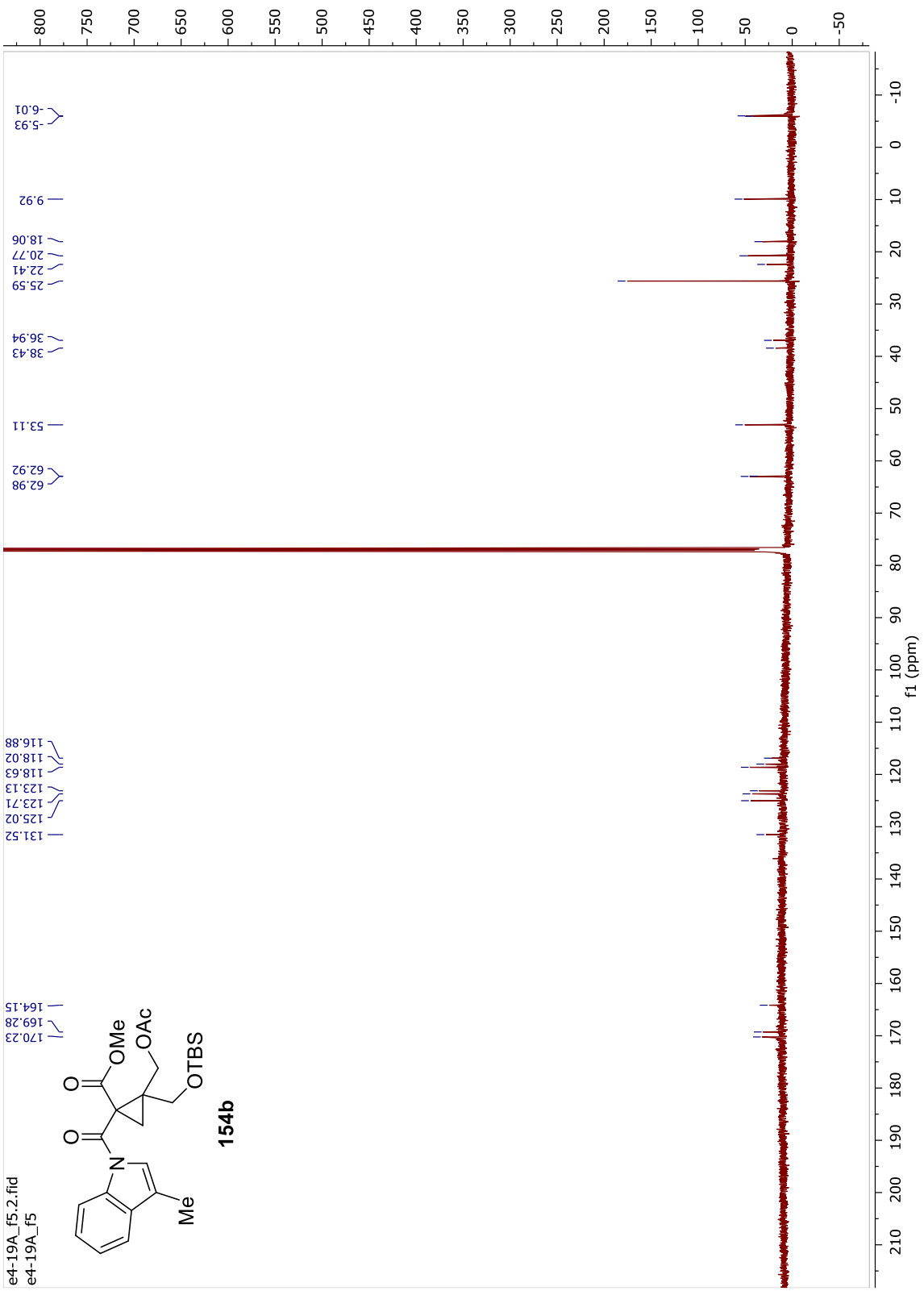
e4-19A_f5.2.fid
e4-19A_f5
154b
OMe
OAc
OTBS
Me
N
O
O
170.23
169.28
164.15
131.52
125.02
123.71
123.13
118.63
118.02
116.88
62.98
62.92
53.11
38.43
36.94
25.59
22.41
20.77
18.06
9.92
-5.93
-6.01
f1 (ppm)

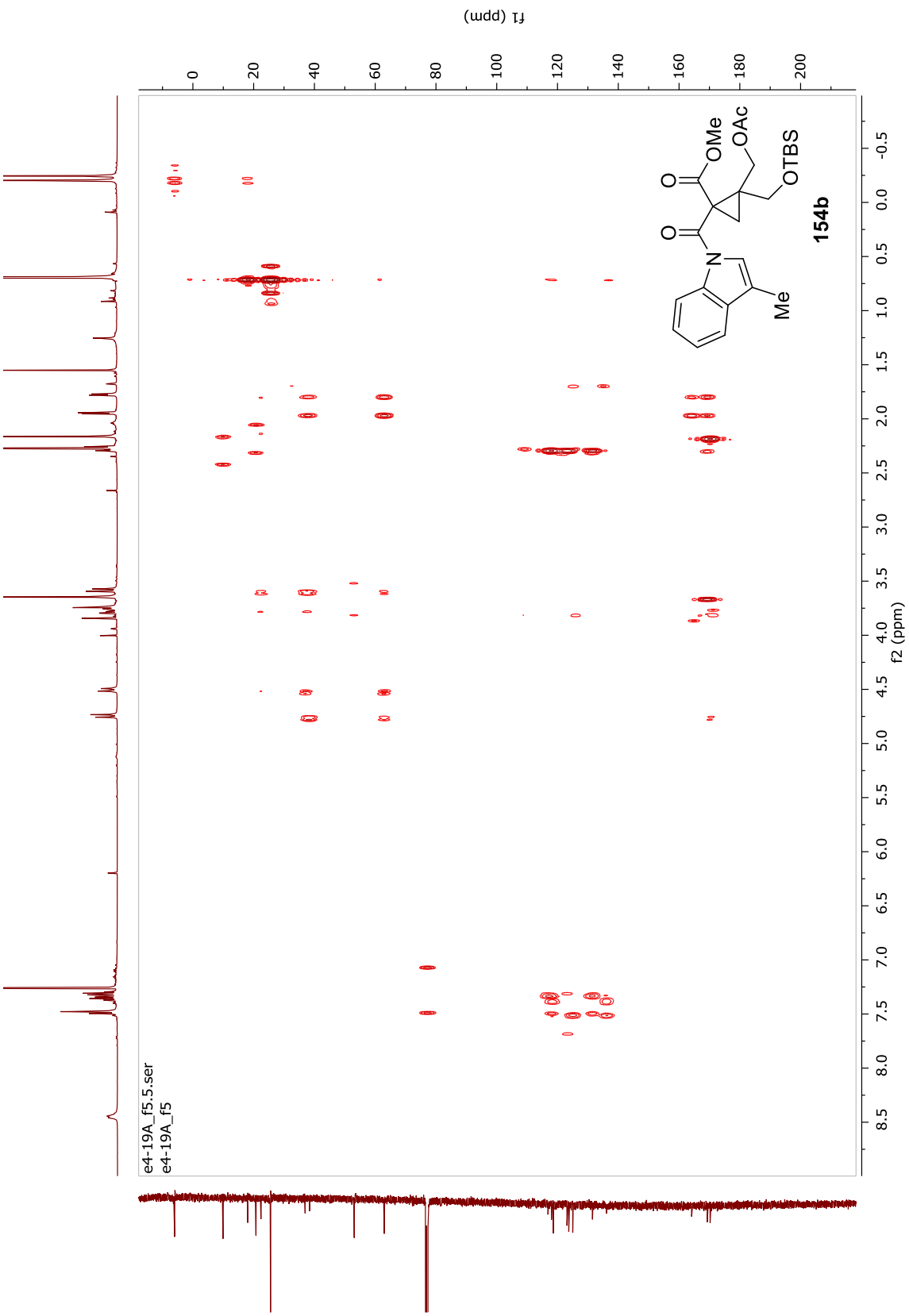
f1 (ppm)
0
20
40
60
80
100
120
140
160
180
200
f2 (ppm)
8.5
8.0
7.5
7.0
6.5
6.0
5.5
5.0
4.5
4.0
3.5
3.0
2.5
2.0
1.5
1.0
0.5
0.0
-0.5
e4-19A_f5.5.ser
e4-19A_f5
OMe
OAc
OTBS
Me
N
O
O
154b

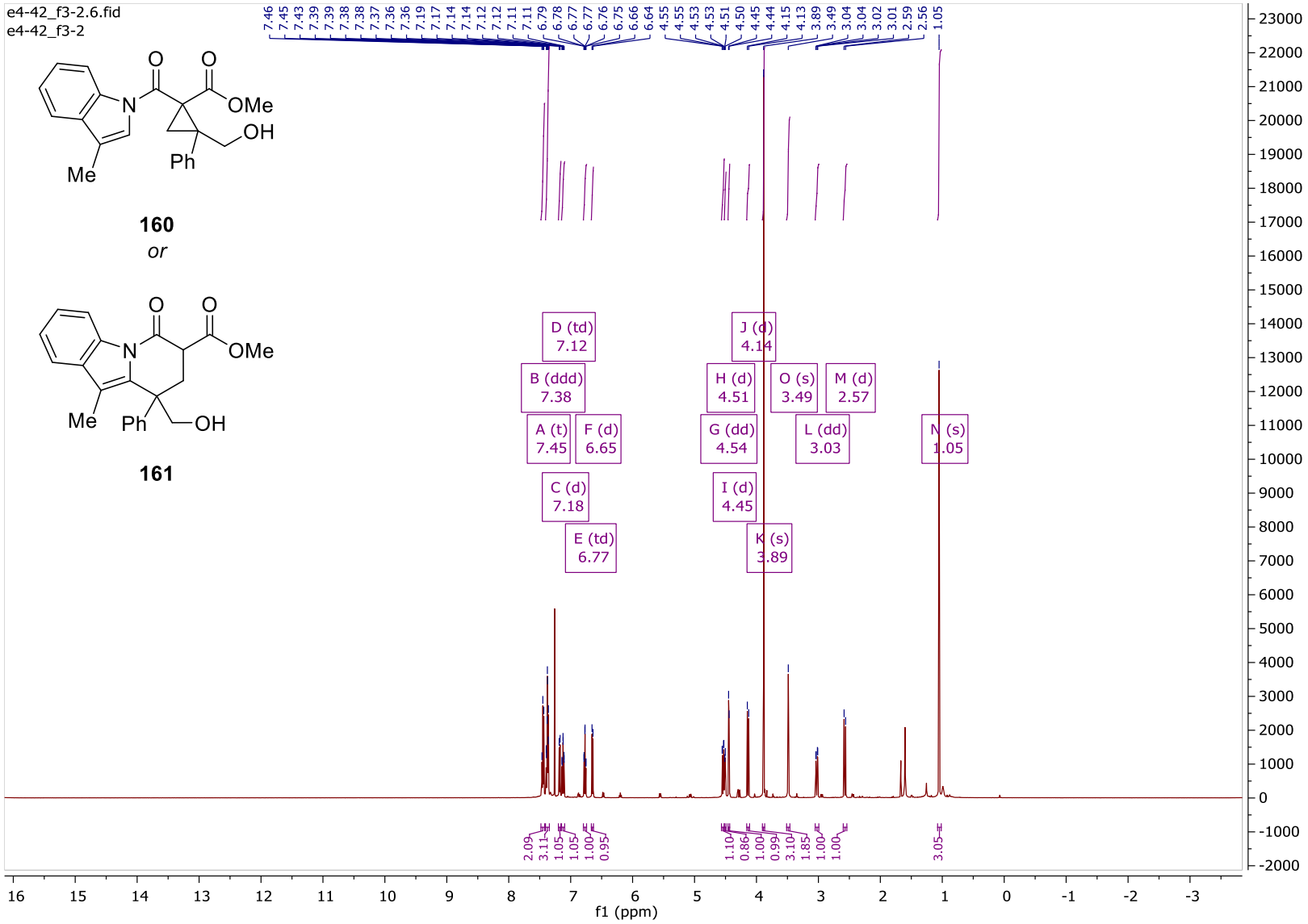
e4-42_f3-2.6.fid
e4-42_f3-2
160
or
161
D (td) 7.12
B (ddd) 7.38
A (t) 7.45
F (d) 6.65
C (d) 7.18
E (td) 6.77
J (d) 4.14
H (d) 4.51
O (s) 3.49
M (d) 2.57
G (dd) 4.54
L (dd) 3.03
N (s) 1.05
I (d) 4.45
K (s) 3.89
f1 (ppm)

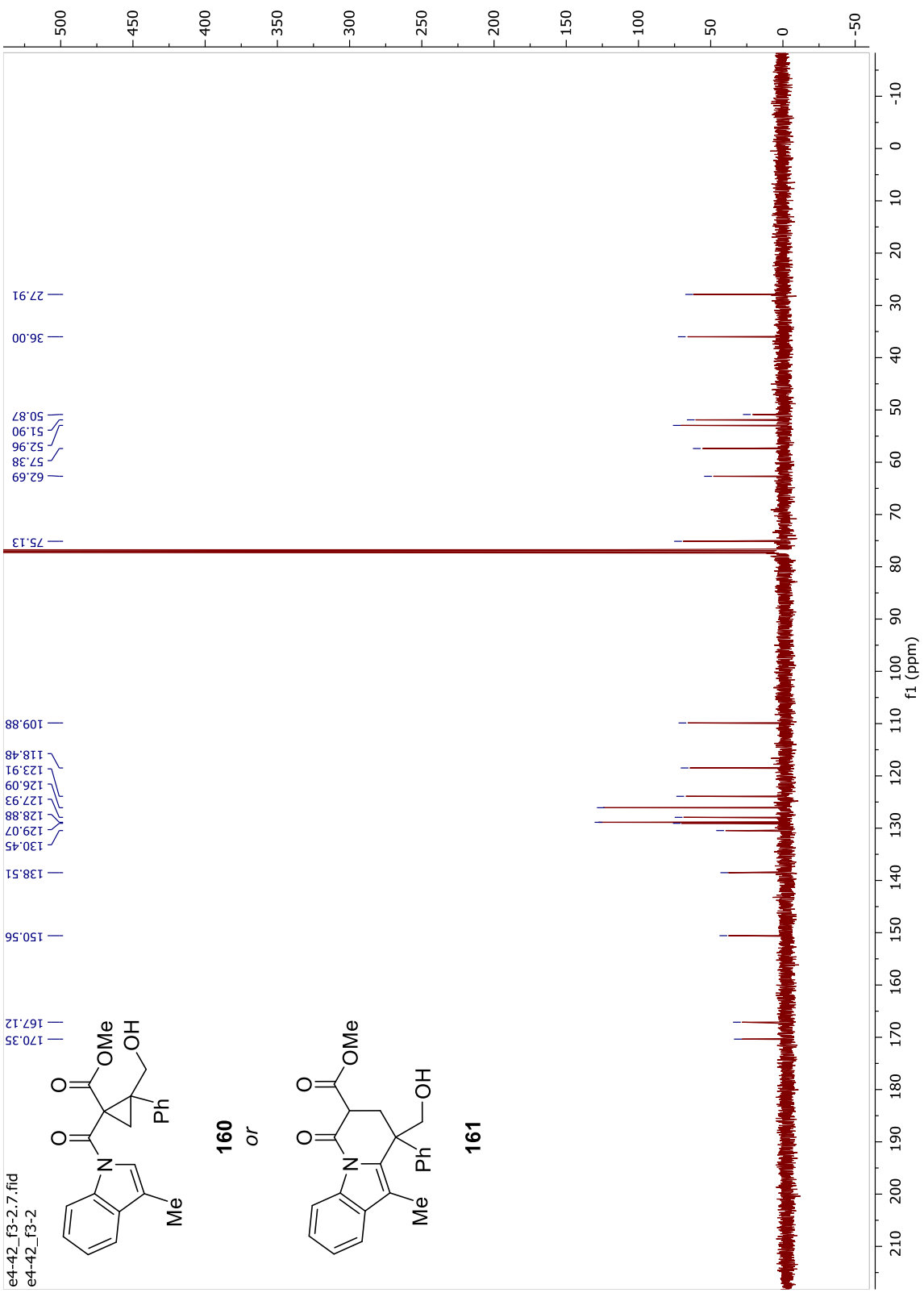
e4-42_f3-2.7.fid
e4-42_f3-2
27.91
36.00
50.87
51.90
52.96
57.38
62.69
75.13
109.88
118.48
123.91
126.09
127.93
128.88
129.07
130.45
138.51
150.56
167.12
170.35
160
or
161
f1 (ppm)

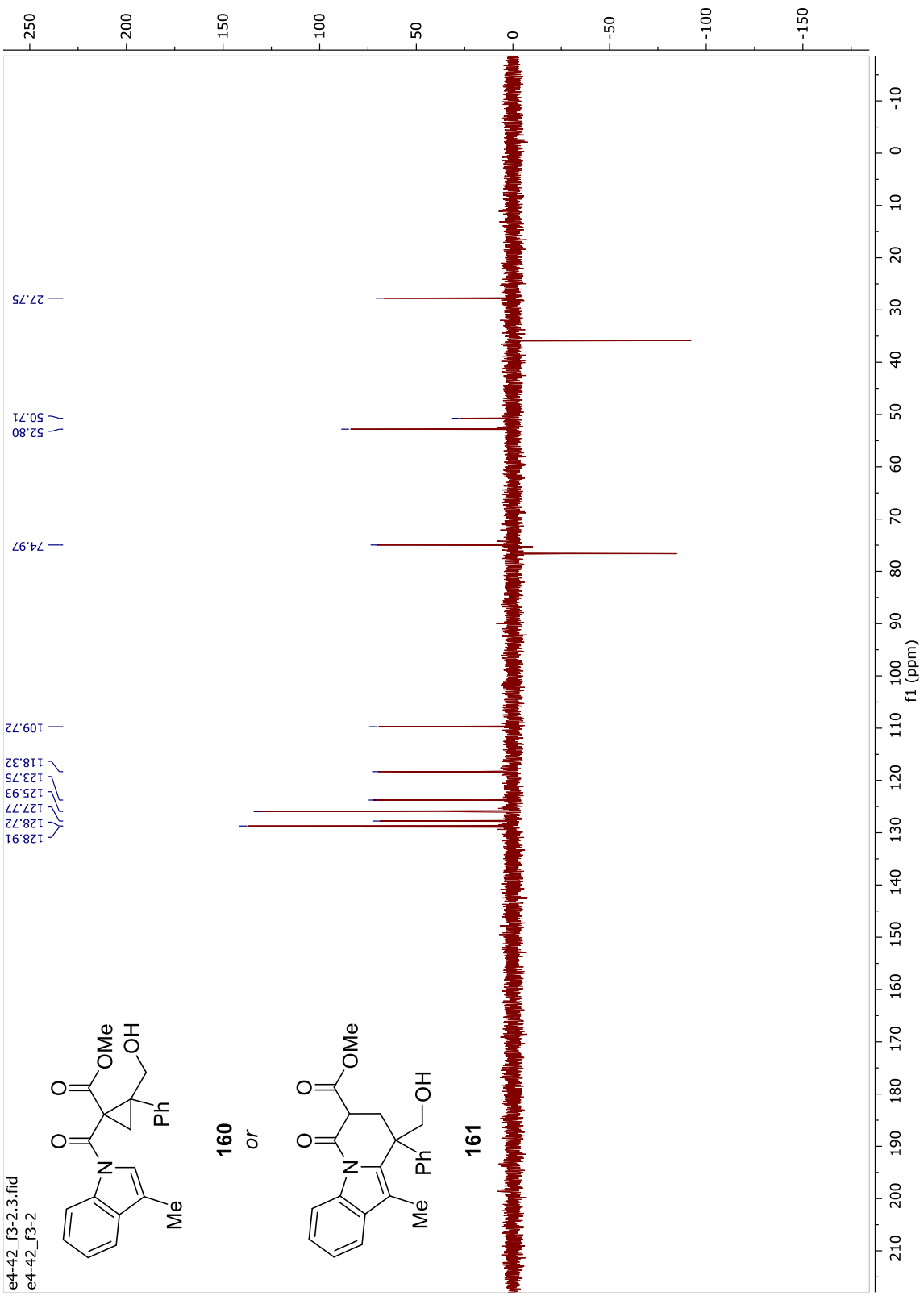
e4-42_f3-2.3.fid
e4-42_f3-2
128.91
128.72
127.77
125.93
123.75
118.32
109.72
74.97
52.80
50.71
27.75
160
or
161
OMe
OH
Ph
Me
f1 (ppm)

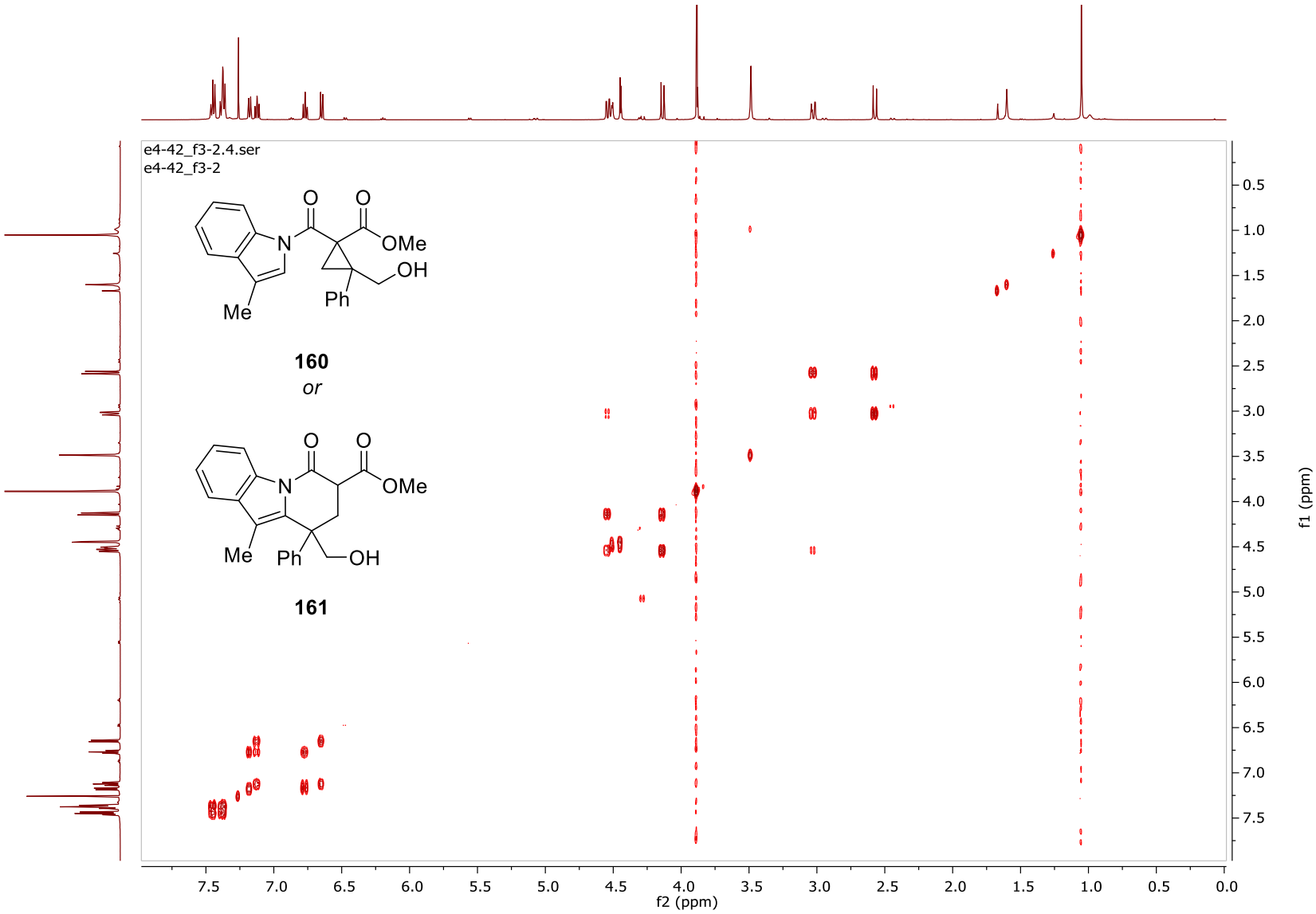
e4-42_f3-2.4.ser
e4-42_f3-2
O
O
N
OMe
OH
Ph
Me
160
or
O
O
N
OMe
Me
Ph
OH
161
7.5
7.0
6.5
6.0
5.5
5.0
4.5
4.0
3.5
3.0
2.5
2.0
1.5
1.0
0.5
0.0
f2 (ppm)
0.5
1.0
1.5
2.0
2.5
3.0
3.5
4.0
4.5
5.0
5.5
6.0
6.5
7.0
7.5
f1 (ppm)

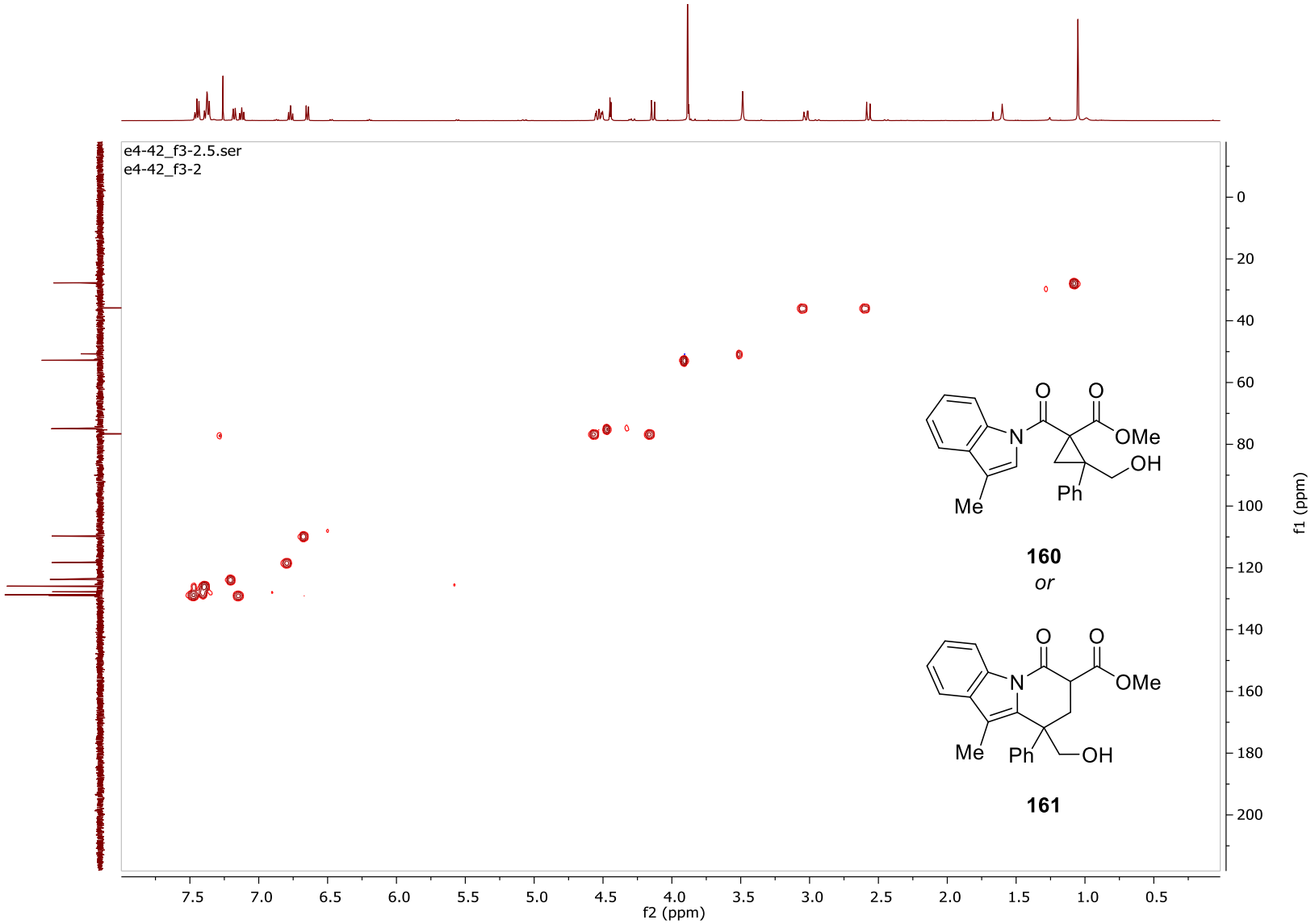
e4-42_f3-2.5.ser
e4-42_f3-2
f2 (ppm)
f1 (ppm)
7.5
7.0
6.5
6.0
5.5
5.0
4.5
4.0
3.5
3.0
2.5
2.0
1.5
1.0
0.5
0
20
40
60
80
100
120
140
160
180
200
O
O
N
OMe
OH
Me
Ph
160
or
O
O
N
OMe
Me
Ph
OH
161

6.6 References

(1) Cavitt, M.A.; France, S. Aluminum(III)-Catalyzed, Formal Homo-Nazarov-Type Ring-Opening Cyclizations toward the Synthesis of Functionalized Tetrahydroindolizines. *Synthesis* **2016**, *48*, 1910-1919.

(2) Cavitt, M.A. STRESS RELIEF: EXERCISING LEWIS ACID CATALYSIS FOR DONOR-ACCEPTOR CYCLOPROPANE RING-OPENING ANNULATIONS, A BASIS FOR NEW REACTION METHODOLOGIES. Doctoral Thesis, **2015**.

(3) Patil, D. V.; Cavitt, M. A.; France, S. Diastereoselective Intramolecular Friedel-Crafts Cyclizations of Substituted Methyl 2-(1*H*-Indole-1-Carbonyl)acrylates: Efficient Access to Functionalized 1*H*-Pyrrolo[1,2-*a*]indoles. *Org. Lett.* **2011**, *13*, 5820–5823.

(4) Kim, B.R.; Lee, H.-G.; Kang, S.-B.; Sung, G.H.; Kim, J.-J.; Park, J.K.; Lee, S.-G.; Yoon, Y.-J. *tert*-Butoxide-Assisted Amidation of Esters under Green Conditions. *Synthesis* **2012**, *44*, 42-50.

(5) Cavitt, M.A. V-MAC-006.

(6) Patil, D.V.; Cavitt, M.A.; Grzybowski, P.; France, S. *Chem. Commun.* **2011**, *47*, 10278.

(7) Patil, D.V.; Cavitt, M.A.; Grzybowski, P.; France, S. *Chem. Commun*. **2012**, *48*, 10337.

(8) (a) Tamao, K.; Ishida, N.; Tanaka, T.; Kumada, M. Silafunctional compounds in organic synthesis. Part 20. Hydrogen peroxide oxidation of the silicon-carbon bond in organoalkoxysilanes. *Organometallics* **1983**, *2*, 1694–1696.

(b) Fleming, I.; Henning, R.; Plaut, H. The phenyldimethylsilyl group as a masked form of the hydroxy group. *J. Chem. Soc., Chem. Commun.* **1984**, *0*, 29-31.

(9) Organ, M.G.; Murray, A.P. Ni-Catalyzed Cross Coupling of Alkoxide-Containing Vinyl Halides with Grignard Reagents. A "One-Pot" Synthesis of 2-[(Trimethylsilyl)methyl]-2-propen-1-yl Acetate. *J. Org. Chem*. **1997**, *62*, 1523-1526.

(10) Basha, A.; Lipton, M.; Weinreb, S.M. A MILD, GENERAL METHOD FOR CONVERSION OF ESTERS TO AMIDES. *Tetrahedron Lett*. **1977**, *48*, 4171-4174.

(11) Gonzalez-Bobes, F.; Fenster, M. D. B.; Kiau, S.; Kolla, L.; Kolotuchin, S.; Soumeillant, M. Rhodium-Catalyzed Cyclopropanation of Alkenes with Dimethyl Diazomalonate. *Adv. Synth. Catal.* **2008**, *350*, 813–816.

(12) Presset, M.; Mailhol, D.; Coquerel, Y.; Rodriguez, J. Diazo Transfer Reactions to 1, 3-Dicarbonyl Compounds with Tosyl Azide. *Synthesis* **2011**, *16*, 2549–2552.

(13) Russo, F.; Wangsell, F.; Saevmarker, J.; Jacobsson, M; Larhed, M. Synthesis and evaluation of a new class of tertiary alcohol based BACE-1 inhibitors. *Tetrahedron* **2009**, *65*, 10047-10059.

(14) Bowie, A.L.; Hughes, C.C.; Trauner, D. Concise Synthesis of (±)-Rhazinilam through Direct Coupling. *Org. Lett.* **2005**, *7*, 5207-5209.

(15) Muriel, B.; Orcel, U.; Waser, J. Palladium-Catalyzed Carboamination of Allylic Alcohols Using a Trifluoroacetaldehyde-Derived Tether. *Org. Lett.* **2017**, *19*, 3548-3551.

CHAPTER 7. CONCLUSIONS AND FUTURE OUTLOOK

7.1 General Conclusions

This dissertation delved deeply into the potential advances and applications of the Friedel-Crafts reaction toward the total syntheses of three medicinal compounds: flubromazepam (and its positional isomers), tronocarpine, and rhazinicine (Figure 7-1). These synthetic and natural products were targeted synthetically for their privileged scaffolds and unique structural features that presented interesting challenges for methodology development.

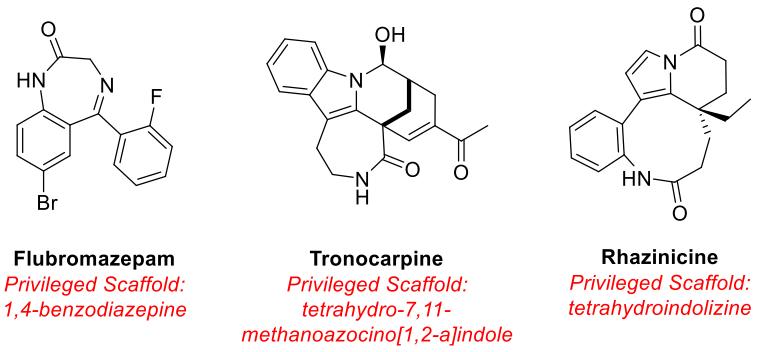

Flubromazepam
Privileged Scaffold: 1,4-benzodiazepine

Tronocarpine
Privileged Scaffold: tetrahydro-7,11-methanoazocino[1,2-a]indole

Rhazinicine
Privileged Scaffold: tetrahydroindolizine

Figure 7-1: Featured medicinal compounds and corresponding privileged scaffolds.

Benzodiazepines, thought prolific in literature, have been limited in scope due in part to the synergistic preferences of Friedel-Crafts acylations to prepare the crucial 2-aminobenzophenone intermediate. This thesis evaluated, and in some cases optimized, known synthetic methods to effect this transformation, Friedel-Crafts and otherwise, and enabled the first total synthesis of eight positional isomers of flubromazepam (plus the parent drug). Key challenges to this synthesis were the relatively labile C-Br bond in

flubromazepam; and steric hindrance in relevant precursors to the (6,X')-flubromazepam isomers, which are the three targets remaining.

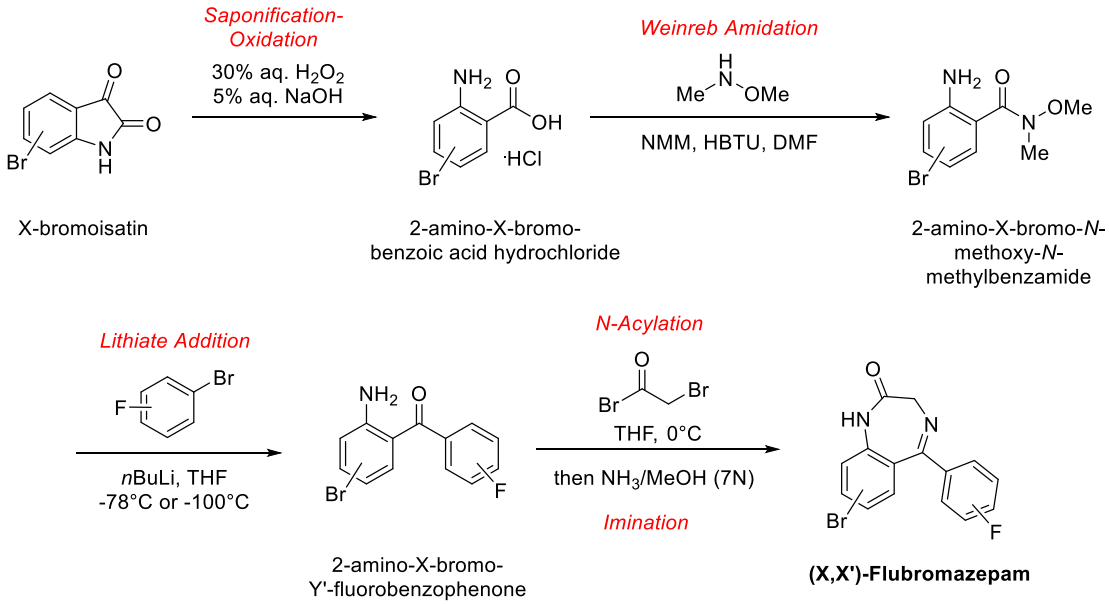

Scheme 7-1: Optimized synthetic route for all except for (6,X')-flubromazepam isomers.

Significantly, this research offers a template for rapid benzodiazepine isomer synthesis, since the key synthetic step, the aryl lithiate addition to Weinreb benzamides, enables a highly convergent synthesis originating from inexpensive, commercially available starting materials. This tool may be an aid to forensic examiners, should a positional isomer of a known designer benzodiazepine be suspected in a case. Furthermore, initial analytical studies show promising evidence that positional isomers of benzodiazepines may be differentiated using currently available forensic techniques. Thus far, IR spectroscopy is the most discriminating method when characterization data are available for comparison.

Tronocarpine, a chippiine-type indole alkaloid, has been the subject of immense interest over the last two decades since its isolation from nature. The bridged bicyclic

moiety embedded in this scaffold is unique even among other members of the chippiine family, as the seven-membered lactam is connected at the bridgehead carbon, and the challenge remaining is how to effect synthesis of the pentacycle with adequate tolerance for functional handles essential to complete the final decorations to the core structure.

Endeavors to solve this issue led to an intensive study of an understudied class of donor-acceptor cyclopropanes (DACPs). D-A bicyclo[3.1.0]hexanes are DACPs with a cyclic tether connecting the acceptor carbon to a vicinal carbon on the cyclopropane. The site of this tether significantly affects the synthetic pathways available: when connected to the donor carbon, a cyclic, tertiary carbocation forms as the reactive intermediate; when connected adjacent to the donor carbon, an exocyclic, secondary carbocation results. Intramolecular Friedel-Crafts-type ring-opening cyclizations of this DACP class have been largely unexplored, and it was envisioned that such a ring-opening cyclization of an *N*-acyl indole-tethered, C5-substituted D-A bicyclo[3.1.0]hexane would efficiently afford the bridged bicyclic moiety of tronocarpine, and that this method could be expanded to additional heterocyclic templates (Scheme 7-2).

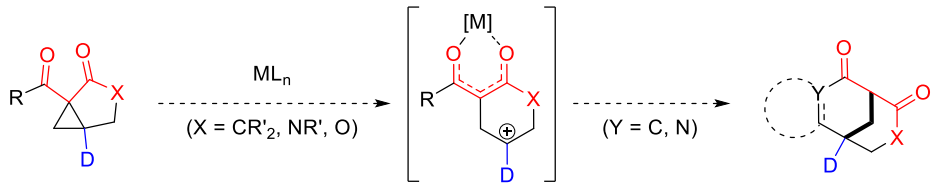

Scheme 7-2: Hypothesized C5-sub. D-A bicyclo[3.1.0]hexane ring-opening cyclization.

Despite extensive optimizations of several model systems, both intramolecular Friedel-Crafts-type ring-opening cyclizations and intermolecular Friedel-Crafts-type additions failed to deliver the desired bridged bicyclic core. Gratifyingly, however, a novel formal [3+2] cycloaddition between a C5-substituted D-A oxabicyclo[3.1.0]hexane and *p*-

anisaldehyde afforded the anticipated oxabicyclo[4.2.1]nonane scaffold (Scheme 7-3). This methodology will be further developed and demonstrates promise toward developing an intramolecular ring-opening cyclization in the future.

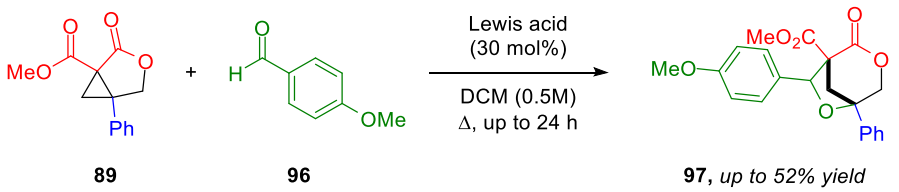

89 **96** **97**, *up to 52% yield*

Scheme 7-3: Successful formal [3+2] cycloaddition of a C5-sub. D-A oxabicyclo[3.1.0]hexane.

Additionally, a benzofuran-tethered C6-substituted D-A oxabicyclo[3.1.0]hexane was employed in an unprecedented intramolecular Friedel-Crafts-type ring-opening cyclization in the pursuit of a new total synthesis of propolisbenzofuran B. A surprising stereochemical outcome was observed: a *cis* ring-opening cyclization adduct in contrast to the expected *trans* based on previous literature (Scheme 7-4). This result was further supported by in-depth NMR analysis simplified by capping the adduct as an *enol* triflate, which opened the door to a methodology study to further probe the stereochemical outcomes of DACPs with cyclic tethers at varying sites on the cyclopropane. Initial efforts toward a substrate scope have been conducted, with the intent of probing substituent effects as well as tether length (i.e. ring size) on diastereoselectivity of the ring-opening cyclization.

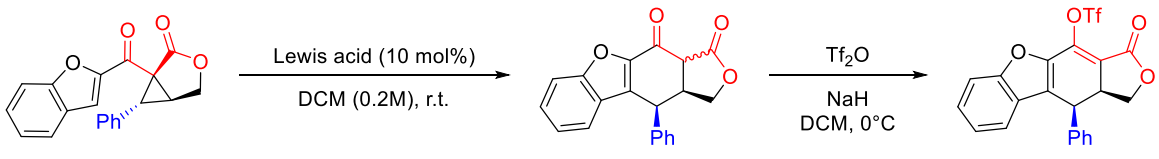

98 **epi-100** *(+ enol)* ***exclusively cis*** **105**

Scheme 7-4: Ring-opening cyclization of a C6-sub. oxabicyclo[3.1.0]hexane to exclusively *cis* adduct.

Finally, the total synthesis of rhazinicine was attempted *via* a recently demonstrated Friedel-Crafts-type ring-opening cyclization of *N*-acyl pyrrole-tethered DACPs. This methodology signaled an important advance in the synthesis of pyrrole-containing compounds, as pyrrole-based starting materials are notoriously difficult to harness in typical heterocyclic synthetic chemistry. Unfortunately, the preceding cyclopropanation step proved unreliable with the more complex alkene precursors required for the total synthesis, despite previous optimizations. Moreover, a similar cyclopropanation strategy employed toward a newly-envisioned total synthesis of tronocarpine also failed to deliver a useful cyclopropane precursor. Gratifyingly, however, in the pursuit of this tronocarpine system, a novel Weinreb-type amidation was observed between 3-methylindole and a C5-substituted D-A oxabicyclo[3.1.0]hexane (Scheme 7-5). This result may signal the advent of a facile nucleophilic introduction of indole scaffolds, often challenging due to the stability of indoles imparted by aromaticity, onto complex DACPs with masked functional handles.

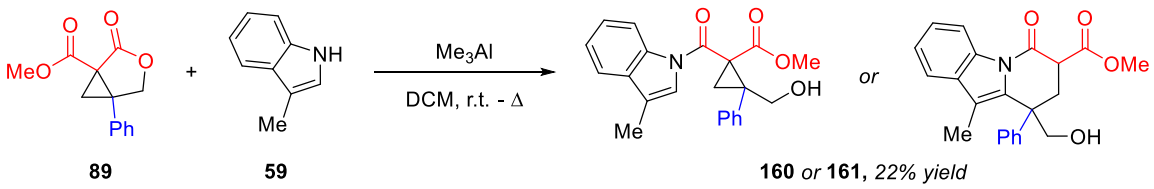

Scheme 7-5: Weinreb-type amidation onto a C5-sub. D-A oxabicyclo[3.1.0]hexane to form potential precursor to tronocarpine.

7.2 Future Outlook for Flubromazepam

Although nine of the twelve positional isomers of flubromazepam were obained by the approach described in Chapter 2, the remaining three isomers have not yet been synthesized. Initial efforts toward the preparation of *N*-benzyl-4-bromo-3-(X-

fluorophenyl)-3-hydroxyoxindoles, however, have been fruitful. The 4-fluorophenyl hydroxyoxindole isomer has been prepared and validated, and the reaction has demonstrated scalability at 500 mg. Remaining steps in the synthesis are benzyl deprotection by hydrogenolysis, oxidative rearrangement, and *N*-acylation/imination under Sternbach conditions. Syntheses of the 2-fluoro and 3-fluoro isomers will be performed in tandem.

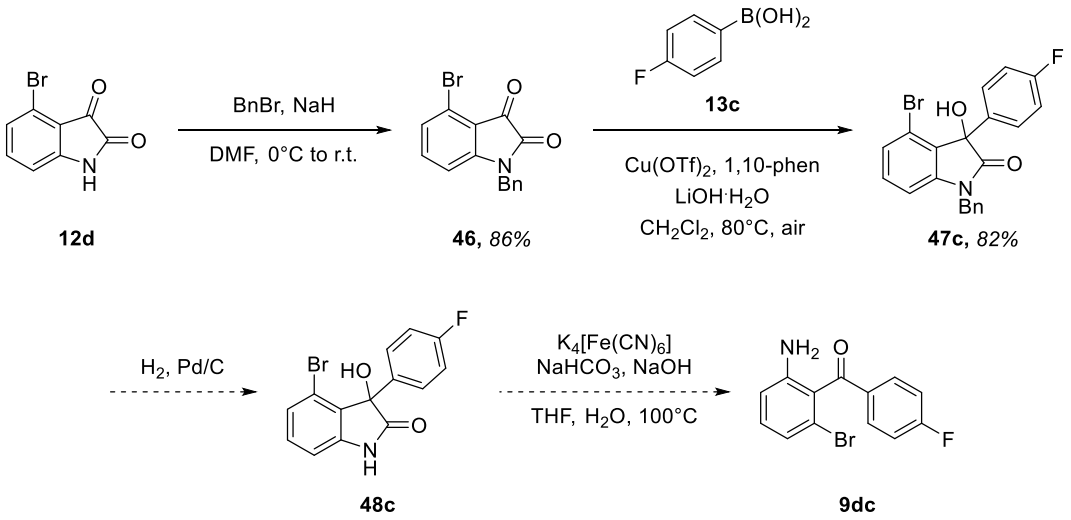

Scheme 7-6: Progress toward synthesis of (6,X')-flubromazepam isomers.

Additionally, the positional isomers of flubromazolam are prime targets due to their facile preparation from flubromazepam and the biological potency displayed by parent flubromazolam. The preparation of these twelve compounds is optimistically expected to be attainable within a two-month period, after which time they will be validated and fully characterized by forensic techniques.

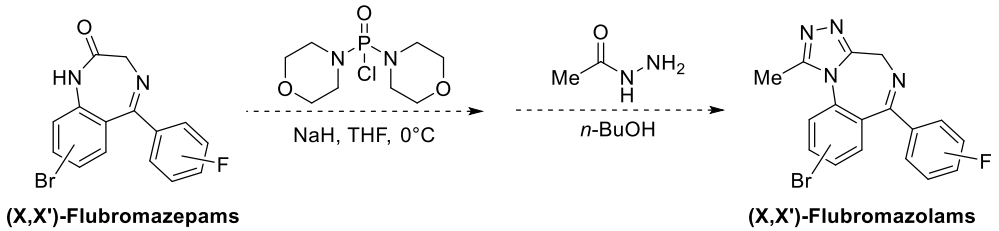

Scheme 7-7: Projected synthesis of (X,X')-flubromazolam isomers.

Furthermore, there is potential to expand this project by subjecting the prepared flubromazepam (and flubromazolam) positional isomers to structure-activity relationship studies; targeting additional benzodiazepines of interest and synthesizing their respective positional isomers; and developing a synthetic route to benzodiazepine-like analogues such as etizolam. Efforts are underway to establish a collaboration for the first aim.

Finally, despite promising analytical results toward positional isomer differentiation, further studies must be conducted to expand the characterization dataset. Each of the flubromazepam isomers will be analyzed by LC-MS, a softer technique than GC-MS, to evaluate potential differentiation by LC retention time and/or mass spectral analysis. Additionally, the pure positional isomers will be subjected to solid-state FTIR to establish a baseline comparison with GC-IR results. Furthermore, to establish reproducibility and a standard deviation, at least three experiments by each of these instrumental techniques will be performed and the data rigorously analyzed by statistical methods. These results will ultimately be published and the data made available to forensic examiners.

7.3 Future Outlook for Donor-Acceptor Bicyclo[3.1.0]hexane Methodologies

No research project is ever truly finished, and the progress made toward the development of novel ring-opening cyclizations of D-A bicyclo[3.1.0]hexanes is only the bright foray into the vast potential this template has to offer. Recommendations will be made herein regarding four individual studies that may be pursued further.

7.3.1 The Intramolecular Friedel-Crafts-type Ring-opening Cyclization of C5-Substituted D-A Bicyclo[3.1.0]hexanes

This research project was disappointingly halted before the realization of an intramolecular ring-opening cyclization to access bridged bicyclic scaffolds. The current leading hypothesis, however, merits deeper investigation: that a heterocyclic-tethered DACP with a decarbonylated linker will facilitate Friedel-Crafts-type addition onto the intermediary carbocation through improved flexibility and proximity. Of the two synthetic routes surveyed, the more promising avenue is likely the benzofuran-tethered system (Scheme 7-8), as the appropriate starting materials are more readily available and the synthesis, more convergent. Also, given the propensity for *N*-acyl indole substituents to dissociate under strongly basic conditions, and the difficulty encountered with introducing indole nucleophilically, the benzofuran model should have greater stability throughout the synthesis and be easier to incorporate.

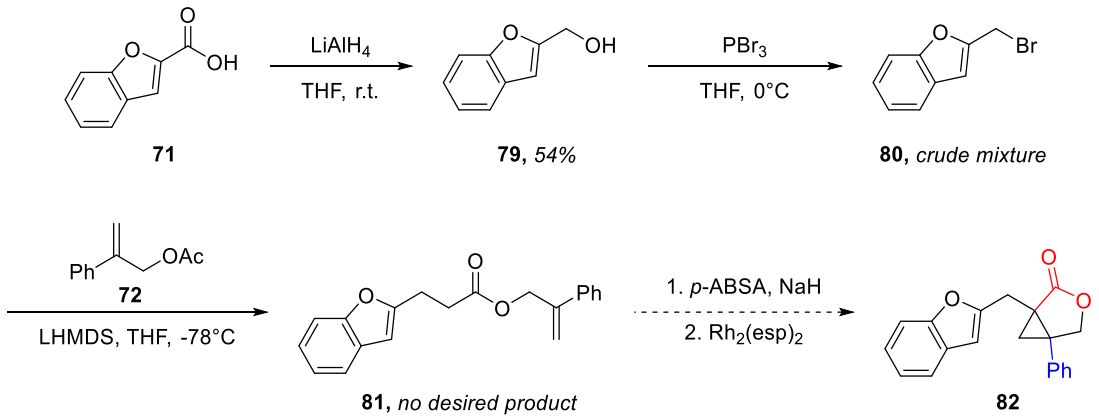

Scheme 7-8: Proposed synthesis of decarbonylated benzofuran-tethered model.

Once the purification issues associated with 2-(bromomethyl)benzofuran are resolved, optimization of the base-promoted substitution may proceed. A temperature screen will be an essential, as this substitution may require higher temperatures than the prescribed -78°C employed for addition onto an acid chloride. The diazo transfer step will likely require NaH or a lithium base for deprotonation, but there should be no competing acidic sites, which will facilitate this transformation. Finally, the cyclopropanation ought to proceed normally but may require optimizations due to removing one of the acceptor groups from the diazo precursor.

The resulting benzofuran-tethered, decarbonylated, C5-substituted oxabicyclo[3.1.0]hexane may then undergo a Lewis acid screen to test the formation of the bridged bicyclic moiety. Elimination products are certainly still plausible, but this undesired pathway may be less thermodynamically favored due to the absence of competing *enol* formation, and the flexibility of the carbon linker bonds should facilitate better proximity to the carbocation intermediate. Following proof of concept, various heterocyclic nucleophiles, donor groups, and ring sizes may be evaluated, and a

determination made as to the viability of this template for the first total synthesis of tronocarpine.

7.3.2 The Intermolecular Formal [3+2] Cycloaddition of C5-Substituted D-A Bicyclo[3.1.0]hexanes

Of the pathways evaluated that employ C5-substituted D-A bicyclo[3.1.0]hexanes, the route that displayed the most distinct promise was most certainly the formal [3+2] cycloaddition with external benzaldehydes. A model adduct has been successfully achieved and validated by NMR and HRAM-MS, and the Lewis acid screen is nearly complete.

Immediate next steps for this project include wrapping up the Lewis acid screen and screening other parameters such as solvent and temperature (though initial tests have shown degradation at temperatures higher than 80°C). It would also be ideal to grow a crystal for X-ray crystallographic analysis, for further confirmation of the observed adduct. Finally, a broad substrate scope will be prepared and surveyed, with various aryl and heteroaryl aldehydes, differing donor groups as well as acceptor groups on the bicyclic tether (e.g. ketones and lactams), and non-aldehyde coupling partners (e.g. maleimides, acrylates, and isothiocyanates).

This study may then be further applied to an intramolecular variant.

7.3.3 The Intramolecular Friedel-Crafts-type Ring-opening Cyclization of C6-Substituted D-A Bicyclo[3.1.0]hexanes

As discussed previously, the implications of this study's preliminary results are astounding. Not only is this Friedel-Crafts-type ring-opening cyclization unprecedented for

C6-substituted D-A bicyclo[3.1.0]hexanes, but the stereochemical outcome of this transformation is in direct contrast to almost all previous studies into the mechanism and diastereoselectivity preferences for *trans* over *cis*. The stage is set to evaluate templates with varying substitutions, tether sites, and tether lengths to offer a more generalized perspective on the stereochemistry of bicyclic DACP ring-opening cyclizations.

This will be a huge undertaking. The immediate next step will be finalizing synthesis of the substrate scope to determine the trends of this particular C6-substituted D-A bicyclo[3.1.0]hexane template. Then, various acceptor groups and ring sizes for the bicyclic tether will be evaluated, which will require strategic synthesis. Finally, a six-membered analogue to the 1,2-indanyl cyclopropane will be prepared, to test the effects of ring size at that site on diastereoselectivity.

7.3.4 Weinreb-type Addition of Indoles to D-A Bicyclo[3.1.0]hexanes

An unexpected but delightful result observed during the pursuit of the total synthesis of tronocarpine was the trimethylaluminum-mediated addition of 3-methylindole to the lactone moiety of an oxabicyclo[3.1.0]hexane, to prepare either an *N*-acyl DACP or the corresponding Friedel-Crafts-type ring-opening cyclization product. This result first needs to be validated, perhaps by X-ray crystallography. Then, two avenues are possible: a short methodology study, and the potential total synthesis of tronocarpine.

The methodology study would survey a small subset of 3-substituted indoles (and possibly pyrroles) and bicyclo[3.1.0]hexane templates, since Weinreb amidations are well established for other amines including anilines. The subsequent total synthesis of tronocarpine would be adapted from the originally hypothesized route involving an

intermolecular cyclopropanation. This new approach, if successful, would actually streamline the synthesis, as the nucleophilic addition to the lactone results in a free alcohol that may be readily oxidized for the HWE step (Scheme 7-9).

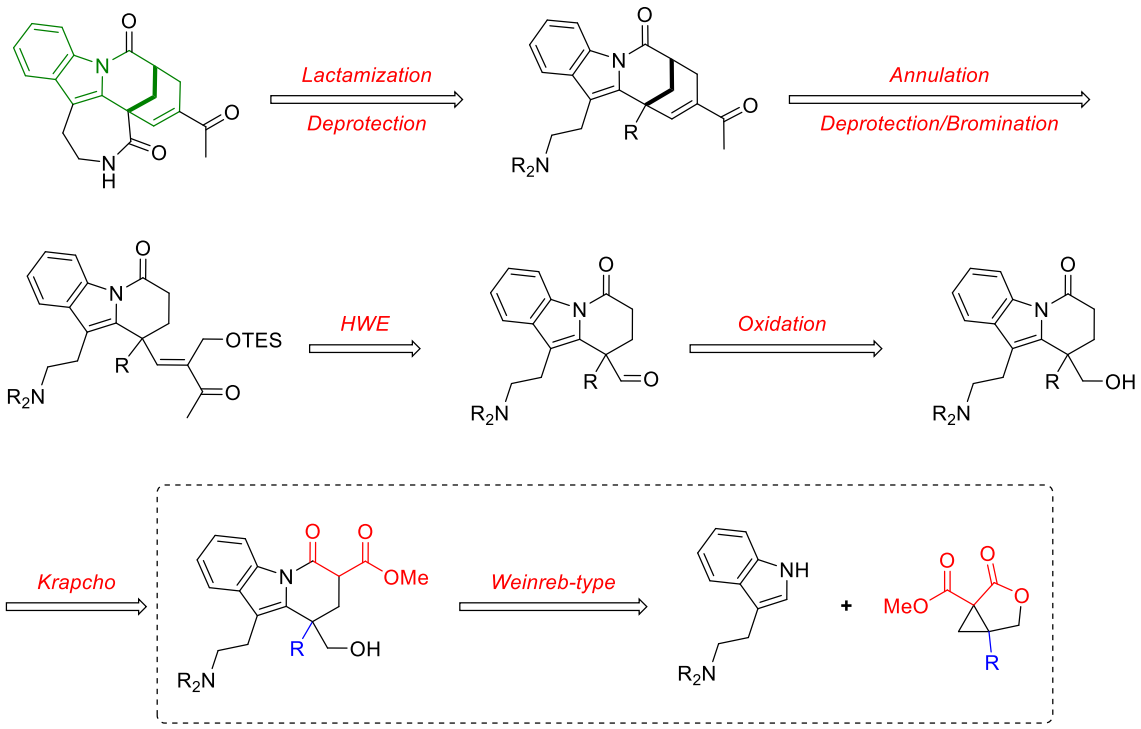

Scheme 7-9: Proposed retrosynthetic analysis of tronocarpine based on successful Weinreb-type amidation.

7.4 Closing Thoughts

The research encompassed by this thesis has been challenging, often frustrating, ultimately rewarding. Methodology development necessarily delves into the unknown, and every research project endeavoured herein exhibited unexpected, sometimes serendipitous, results. There is still so much to be learned from every privileged scaffold and reaction template explored, and as I pass the baton to the next PhD candidate, I look forward to one day reading a paper that solves any one of the mysteries presented.

VITA

Evelyn Shaye Ligon (née Maris) was born in Overland Park, KS, and grew up in Greenville, SC. As a young girl, she displayed an aptitude for mathematics and music, but discovered her passion for chemistry as a sophomore in high school. She attended Wofford College from 2010-2014, during which time she pursued several research opportunities. In the summer of 2012, she participated in the Department of Energy Science Undergraduate Laboratory Internship (DOE SULI) at Pacific Northwest National Laboratory (PNNL), studying lipid distribution in brain tissue by nanospray desorption electrospray ionization (nano-DESI) mass spectrometry. In 2013, she collaborated on a one-month intensive research project toward the synthesis of caprolactone derivatives for ring-opening polymerization, and then served as a part-time research assistant in an atmospheric chemistry lab at the National University of Córdoba in Argentina.

After graduating *summa cum laude* and with Phi Beta Kappa distinction, Evelyn enrolled in the PhD program at Georgia Institute of Technology under the President's Fellowship. Shortly thereafter, she joined the research group of Stefan France and began her research toward tronocarpine and donor-acceptor bicyclo[3.1.0]hexanes. In 2015, she was awarded the Department of Defense Science, Mathematics & Research for Transformation (DoD SMART) Scholarship-for-Service. She plans to pursue a career first with the DoD and then as a professor of undergraduate chemistry.

Evelyn is married to her college sweetheart, George Ligon, J.D., M.Sc. In their rare free time, they enjoy attending the Atlanta Opera as season subscribers, whiskey tasting, and listening to audiobooks together on road trips.